**Alberta
Energy
Regulator**

Directive 034: Gas Well Testing, Theory and Practice

1975

Effective June 17, 2013, the Energy Resources Conservation Board (ERCB) has been succeeded by the Alberta Energy Regulator (AER).

As part of this succession, the title pages of all existing ERCB directives now carry the new AER logo. However, no other changes have been made to the directives, and they continue to have references to the ERCB. As new editions of the directives are issued, these references will be changed.

Some phone numbers in the directives may no longer be valid. Contact AER Inquiries at 1-855-297-8311 or inquiries@aer.ca.

EUB

Theory and Practice of the Testing of Gas Wells

3rd edition, 1975

GUIDE RENAMED AS A DIRECTIVE

As announced in *Bulletin 2004-02: Streamlining EUB Documents on Regulatory Requirements*, the Alberta Energy and Utilities Board (EUB) will issue only "directives," discontinuing interim directives, informational letters, and guides. Directives set out new or amended EUB requirements or processes to be implemented and followed by licensees, permittees, and other approval holders under the jurisdiction of the EUB.

As part of this initiative, this document has been renamed as a directive. However, no other changes have been made. Therefore, the document text continues to have references to "guides." These references should be read as referring to the directive of the same number. When this directive is amended, these references will be changed to reflect their renaming as directives.

Alberta Energy and Utilities Board

THEORY AND PRACTICE

OF THE TESTING OF GAS WELLS

Dimensionless Variable	Flow Geometry	GAS			LIQUID
		p	p^2	ψ	p
x_D	Linear	$\dfrac{x}{x_f}$	$\dfrac{x}{x_f}$	$\dfrac{x}{x_f}$	$\dfrac{x}{x_f}$
r_D	Radial-cylindrical / Radial-spherical	$\dfrac{r}{r_w}$	$\dfrac{r}{r_w}$	$\dfrac{r}{r_w}$	$\dfrac{r}{r_w}$
t_D	Linear	$\dfrac{\lambda\,k\,t}{\phi\,\bar{\mu}\,\bar{c}\,x_f^2}$	$\dfrac{\lambda\,k\,t}{\phi\,\bar{\mu}\,\bar{c}\,x_f^2}$	$\dfrac{\lambda\,k\,t}{\phi\,\mu_i\,c_i\,x_f^2}$	$\dfrac{\lambda\,k\,t}{\phi\,\mu\,c\,x_f^2}$
t_D	Radial-cylindrical / Radial-spherical	$\dfrac{\lambda\,k\,t}{\phi\,\bar{\mu}\,\bar{c}\,r_w^2}$	$\dfrac{\lambda\,k\,t}{\phi\,\bar{\mu}\,\bar{c}\,r_w^2}$	$\dfrac{\lambda\,k\,t}{\phi\,\mu_i\,c_i\,r_w^2}$	$\dfrac{\lambda\,k\,t}{\phi\,\mu\,c\,r_w^2}$
p_D		$\dfrac{p}{p_i\,q_D}$	$\dfrac{p^2}{p_i^2\,q_D}$	$\dfrac{\psi}{\psi_i\,q_D}$	$\dfrac{p}{p_i\,q_D}$
Δp_D		$\dfrac{p_i - p}{p_i\,q_D}$	$\dfrac{p_i^2 - p^2}{p_i^2\,q_D}$	$\dfrac{\psi_i - \psi}{\psi_i\,q_D}$	$\dfrac{p_i - p}{p_i\,q_D}$
q_D	Linear / Radial-cylindrical	$\dfrac{\gamma\,\bar{Z}\,T\,q_{sc}\,\bar{\mu}}{\bar{p}\,k\,h\,p_i}$	$\dfrac{\gamma\,\bar{Z}\,T\,q_{sc}\,\bar{\mu}}{k\,h\,p_i^2}$	$\dfrac{\gamma\,T\,q_{sc}}{k\,h\,\psi_i}$	$\dfrac{\gamma\,B\,q_{sc}\,\mu}{k\,h\,p_i}$
q_D	Radial-spherical	$\dfrac{\gamma\,\bar{Z}\,T\,q_{sc}\,\bar{\mu}}{\bar{p}\,k\,r\,p_i}$	$\dfrac{\gamma\,\bar{Z}\,T\,q_{sc}\,\bar{\mu}}{k\,r\,p_i^2}$	$\dfrac{\gamma\,T\,q_{sc}}{k\,r\,\psi_i}$	$\dfrac{\gamma\,B\,q_{sc}\,\mu}{k\,r\,p_i}$

TABLE 2-3. DEFINITION OF DIMENSIONLESS VARIABLES IN TERMS OF p, p^2 AND ψ
(VALUES FOR λ AND γ MAY BE OBTAINED FROM TABLE 2-4)

		Flow Geometry	GAS			LIQUID
			p	p^2	ψ	p
DARCY UNITS	λ	Linear / Radial-Cylindrical / Radial-Spherical	1	1	1	1
	γ	Linear	$\dfrac{p_{sc}}{T_{sc}}$	$2\dfrac{p_{sc}}{T_{sc}}$	$2\dfrac{p_{sc}}{T_{sc}}$	1
	γ	Radial-Cylindrical / Radial-Spherical	$\dfrac{1}{2\pi}\dfrac{p_{sc}}{T_{sc}}$	$\dfrac{1}{\pi}\dfrac{p_{sc}}{T_{sc}}$	$\dfrac{1}{\pi}\dfrac{p_{sc}}{T_{sc}}$	$\dfrac{1}{2\pi}$
FIELD UNITS	λ	Linear / Radial-Cylindrical / Radial-Spherical	2.637×10^{-4}	2.637×10^{-4}	2.637×10^{-4}	2.637×10^{-4}
	γ	Linear (14.65 psia, 520°R)	4.452×10^5	8.903×10^5	8.903×10^5	887.3
		Radial-Cylindrical / Radial-Spherical (14.65/520)	7.085×10^5	1.417×10^6	1.417×10^6	141.2
	γ	Linear (14.7 psia, 520°R)	4.467×10^5	8.933×10^5	8.933×10^5	887.3
		Radial-Cylindrical / Radial-Spherical (14.7/520)	7.110×10^5	1.422×10^6	1.422×10^6	141.2
METRIC (SI) UNITS	λ	Linear / Radial-Cylindrical / Radial-Spherical	3.601	3.601	3.601	3.601×10^{-3}
	γ	Linear (101.325 kPa, 288°K)	9.624×10^{-2}	1.925×10^{-1}	1.925×10^{-1}	11.57
	γ	Radial-Cylindrical / Radial-Spherical (101.325/288)	1.532×10^{-2}	3.064×10^{-2}	3.064×10^{-2}	1.84

TABLE 2-4. VALUES OF COEFFICIENTS USED IN THE DIMENSIONLESS TERMS

THEORY AND PRACTICE

OF THE TESTING OF GAS WELLS

THIRD EDITION (1975)

ERRATA

JULY 1978

ENERGY RESOURCES CONSERVATION BOARD

603 - 6th AVENUE S.W. · CALGARY, ALBERTA, CANADA · T2P 0T4

Page No.	Location	Error	Correct
ii	heading		add: TO THE THIRD EDITION
xv to xxvi	nomenclature wherever found	$kmol/d$	m^3/d
		μm^2	mD
		hr	h
		$^\circ K$	K
		mol/m^3	−

		Metric (SI) Units	Practical Metric Units
xviii	def. M molecular weight		add: (molar mass in metric units)
xix	def. M_i		add: (molar mass in metric units)
xxi	def. r_w	mm	m
xxi	def. R gas constant	$8.3 \dfrac{m^3 \cdot kPa}{mol \cdot {}^\circ K}$	$8.3\ E\text{-}03\ \dfrac{kJ}{mol \cdot K}$
xxiii	def. V_p	in-place gas volume of a reservoir (Eq. 4-28) MMscf $kmol$	gas-filled pore volume of a reservoir (Eq. 4-29) ft^3 m^3
xxiii	def. V_{pm}	minimum in-place gas volume (Eq. 4-31) MMscf $kmol$	minimum economic V_p (Eq. 4-31) ft^3 m^3
xxvi	def. $\bar{\psi}_R$	incorrect units	" "
xxvi	def. ψ^*		add: " "
xxvii and inside back cover	title		UNIT CONVERSIONS AND PREFIXES
	− wherever found	Metric (SI) Units	Practical Metric Units
	− replace the following lines:		

Field Unit	Multiplying Factor	Practical Metric Unit Name	Symbol
BTU per standard cubic foot (60°F, 14.65 psia)	3.743 225 E+01	kilojoule per cubic metre, at standard conditions	kJ/m^3
cubic foot gas per barrel (60°F, 14.65 psia)	1.772 091 E-01	dimensionless, at standard conditions	−
darcy	9.869 233 E+02	millidarcy	mD
gas constant (10.73)	7.748 75 E-04	kilojoule per mole kelvin	kJ/(mol·K)
McF (thousand cubic foot 60°F, 14.65 psia)	2.817 399 E+01	cubic metre, at standard conditions	m^3
millidarcy	9.869 233 E-01	millidarcy	mD
MMcf (million cubic foot 60°F, 14.65 psia)	2.817 399 E+04	cubic metre, at standard conditions	m^3
standard cubic foot (60°F, 14.65 psia - ideal gas)	2.817 399 E-02	cubic metre, at standard conditions	m^3
Tcf (trillion cubic foot 60°F, 14.65 psia)	2.817 399 E+10	cubic metre, at standard conditions	m^3

Page No.	Location	Error	Correct
2-2	paragraph 2, line 8	microscopic	macroscopic
2-7	def. k (Eq. 2-5)	Darcy's	Darcys
2-16	line 4, following (Eq. 2-26)	spelling	partial
2-36 and inside front cover	Table 2-4 metric coefficients		– replace –

	FLOW GEOMETRY	GAS			LIQUID
		p	p^2	ψ	p
PRACTICAL METRIC UNITS λ	Linear / Radial-Cylindrical / Radial-Spherical	3.600×10^{-3}	3.600×10^{-3}	3.600×10^{-3}	3.600×10^{-6}
γ	Linear (101.325 kPa, 288.15 K)	4.070	8.140	8.140	1.157×10^4
γ	Radial-Cylindrical / Radial-Spherical (101.325/288.15)	6.477×10^{-1}	1.295	1.295	1.842×10^3

Page No.	Location	Error	Correct
2-37	Table 2-5 metric units	μm^2	$^*mD$
		hr	h
		kmol/d	m^3/d
	– after Table 2-5	add:	$^*1mD = 10^{-3}\ \mu m^2$
2-49 to 2-52	Example 2-3 note – this results in errors throughout the example	calculation t_D	$t_D = 853{,}214$
2-68	(Eq. 2-91)	$P_t \equiv$	$\dfrac{\bar{P}_R - P_{wf}}{P_i\ q_D} = \ln \dfrac{r_d}{r_w}$
2-89	Discussion, line 1	spelling	drop
2-114	equation for s	missing subscript, denominator	$\psi_i\ q_{D_1}$
2-122	def. R'_c (Eq. 2-162)	cuft	ft^3
2-128	Fig. 2-25 (b)	scale r.h.s.	same as scale l.h.s.
2-130	line 2, following (Eq. 2-163)	twenty-five	twenty-four
2-134	line 1, following column numbers	column (3)	column (4)
2-137	Fig. 2-27 title	TEMPERATURE	PRESSURE SQUARED
3-11	(Eq. 3-7)	numerator	$\sum \dfrac{\Delta\psi}{q_{sc}} \sum q_{sc}^2 - \sum q_{sc} \sum \Delta\psi$
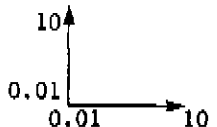
Page No.	Location	Error	Correct

3-13   Fig. 3-3   scales

$$10 \uparrow$$
$$0.01 \quad \longrightarrow$$
$$0.01 \qquad 10$$

3-18   Example 3-1,
     simplified analysis   slope n =   inverse slope n =

     note - this correction applies also to pages 3-22, 3-25, 3-31
          and form EG-33-10-75, App.'E'

3-22   Example 3-2, (LIT ψ)
     flow 4, q^2 calculation   39.7

     extended flow, ψ calculation   115

     note - a_t, a, b, AOF and $\Delta\psi - bq^2$ must be re-calculated

3-23   Fig 3-9   re-calculate and   a × AOF = 218.8 MMpsia²/cp
                   re-plot   a   = 25.44
                                               a_t = 17.624
                                             AOF = 8.6 MMscfd

3-25   Example 3-3, LIT (ψ)   calculation of   flow 1,   14.69
                                     $(\Delta\psi - bq^2)$ flow 2,   17.47
                                                       flow 3,   23.04
                                                        flow 4,   27.25

3-30   (Eq. 3-13)   missing brackets
                             r.h.s.

$$3.263 \times 10^6 \; \frac{T}{k\,h} \left[\log\left(\frac{0.472\, r_e}{r_w} \right) + \frac{s}{2.303} \right]$$

3-45   Fig. 3-19, ordinate   missing heading   add: t_{ws}, hr

3-55   (Eq. 3N-7)   denominator

$$\left(a'\, q_{sc} + b'\, q_{sc}^2 \right) \left(\frac{a' + b'\, q_{sc}}{a' + 2b'\, q_{sc}} \right)$$

3-57   last paragraph, line 2   in Equation (2-83)   is Equation (2-82)

4-3   last paragraph, line 7   reference date   Prats, Hazebroek and
                                                             Strickler, 1962

4-3   last paragraph, line 8   reference date   Prats and Levine, 1963

4-32   line 1   incorrect equation ref.   (4-24)

4-32   line 6   incorrect equation ref.   (4-25)

4-33   Discussion, line 1   incorrect equation ref.   (4-23)

4-33   Discussion, line 2   incorrect equation ref.   (4-25)

4-35   def. V_p (Eq. 4-29) V_p = in-place gas volume V_p = gas-filled pore volume
                                           of the reservoir, MMscf   of the reservoir, ft³

$$V_p \times 10^6 = \pi\, \phi\, h\, r_e^2 \qquad\qquad V_p = \pi\, \phi\, h\, r_e^2$$

4-36   line following   in-place gas volume, V_{pm} economic gas-filled pore
         (Eq. 4-30)   (in MMscf), as   volume, V_{pm} (in ft³, at
                                                                       reservoir conditions), as

Page No.	Location	Error	Correct
4-36	(Eq. 4-31)	$V_{pm} \times 10^6 = \pi \phi h r_{inv}^2$	$V_{pm} = \pi \phi h r_{inv}^2$
4-36	(Eq. 4-32)	numerator	$301.8 \mu_i c_i V_{pm}$
4-53	following (Eq. 4N-9)	$t_0 = q_0 = 1$	$t_0 = q_0 = 0$
4-56	last paragraph, line 1	incorrect equation reference	(2-82)
4-57	second line following (Eq. 4N-21)	$\pi \phi r_e h$	$\pi \phi r_e^2 h$
5-15	line following equation for s'	missing 'x' and power	$1.151 \left[\dfrac{(809.0 - 709.77) \times 10^6}{30.5 \times 10^6} \right.$
5-23	paragraph 2, line 1	spelling	reservoir
5-37	paragraph 1, line 9	spelling	reservoir
5-37	paragraph 2, sentence 3	remove and replace	Whether or not the drawdown preceding the build-up extended into the pseudo-steady state, the desuperposed data plot ($\Delta\psi$ versus log Δt) will give a straight line until $\Delta t = t_s$ at which point deviation will start.
5-37	paragraph 2, sentences 5 & 6	remove	
5-47	last paragraph, line 2	Horner-MDH	Horner-MBH
6-9	def. F_{tf}	add:	$= \sqrt{520/T}$
6-9	def. F_g	add:	$= \sqrt{0.6/G}$
6-9	def. F_{pv}	add:	$= 1/\sqrt{Z}$
7-2	(Eq. 7-2)	missing brackets r.h.s.	$\dfrac{3.263 \times 10^6 \mu Z T}{k h} \left[\log\left(\dfrac{0.472 r_e}{r_w}\right) + \dfrac{s}{2.303} \right]$
7-2	paragraph 1, line 4	may	remove
7-5	Fig. 7-1	Scale inappropriate for use with normal 2×3 cycle log paper. Plot data on transparent paper of same scale.	
7-16	(Eq. 7-14)	denominator	$k^{1/3} \mu r_w h$
A-1	last paragraph, line 1	in	is
A-4	def. R (Eq. A-1)	10.7	10.73
A-4	(Eq. A-2)	numerator	2.699 G p
A-10	def. B (Eq. A-12)	first 'in'	of
B-12	(Eq. B-16)	denominator	$p D^2$
B-18	paragraph 3, line 11	spelling	gradients
B-29	def. D_1 (Eq. B-32)	inside	outside

Page No.	Location	Error	Correct
B-31	(Eq. B-36)	denominator	$(d_2 - d_1)^{1.612} (d_2 + d_1)$
B-31	(Eq. B-37)	denominator	$(d_2 - d_1)^{1.582} (d_2 + d_1)$
C-8	Fig. C-1(g), title	spelling	RECTANGLE
D-3	program BHOLE data input, DIAT	for production through casing replace with effective diameter	remove
EG-34-10-75	critical flow prover		add: $F_g = \sqrt{0.6/G}$
EG-34-10-75	orifice meter		add: $F_g = \sqrt{1.0/G}$
R-3	between Cornett, J.E. and Crawford, G.E. et al.	missing reference	Craft, B.C. and M.F. Hawkins, Jr. (1959). *Applied Petroleum Reservoir Engineering*, Prentice-Hall, Inc., Englewood Cliffs, N.J.
R-10	Prats, Hazebroek and Strickler	reference date	(1962)
R-10	Prats and Levine	reference date	(1963)
R-11	Rawlins and Schellhardt	spelling	*Production*

THEORY AND PRACTICE

OF THE TESTING OF GAS WELLS

THIRD EDITION
1975

ENERGY RESOURCES CONSERVATION BOARD

603 - 6th AVENUE S.W. ● CALGARY, ALBERTA, CANADA ● T2P 0T4

PRICE $25.00

PREFACE

This third edition of the Theory and Practice of the Testing of Gas Wells is a complete updating of the manual originally published by the Oil and Gas Conservation Board (predecessor of the Energy Resources Conservation Board) in 1964. It reflects advances made in the understanding of the flow behaviour of natural gases, both in the reservoir and in the wellbore, since the publication of the second edition in June, 1965. The Board has prepared this edition because of the widespread acceptance of its earlier editions by the oil and gas industry and also by educational institutions.

The emphasis of the previous editions has been altered in that a more detailed review of the theoretical principles underlying the testing of gas wells is now presented. Also, whereas the earlier editions dealt primarily with back pressure tests and related bottom hole pressure calculations, the treatment in this manual is broader and includes a detailed review of deliverability tests, drawdown tests and pressure build-up tests. One of the main objectives is to show how reliable deliverability relationships can be constructed from the different types of tests. Generally, in this edition greater attention is given to more recent and sophisticated methods of testing and interpreting test data. The manual includes a section related to the field conduct of tests but does not treat this matter in detail.

One significant departure in this publication from accepted practice in interpreting gas well tests is the use of pseudo-pressure (sometimes referred to as "the real gas potential") instead of the pressure or pressure-squared terms in gas flow equations. The manual sets out the reasons for this more rigorous treatment of gas flow and although the bulk of the presentation uses pseudo-pressure, the material is presented in a manner to make it possible for the reader to alternatively use the pressure or pressure-squared approaches. Another departure from accepted practice relates to the basic expression of the deliverability equation and the basic deliverability plot. This manual presents the deliverability equation in terms of pseudo-pressures and

also as a logarithmic plot of the pseudo-pressure drop due to laminar
flow effects versus flow rate. Reasons for the adoption of this approach
and other details related to it are given in the manual.

The original preparation of this edition was carried out by
Mr. L. Mattar, formerly on the staff of the Board, and completed by
Mr. G. S. Brar of the Board's Gas Department, under the guidance of a
Committee composed of Dr. K. Aziz of The University of Calgary, Mr. G. J.
DeSorcy, Member of the Board, and myself. Mr. M. E. Mumby of the Board's
Gas Department assisted Messrs. L. Mattar and G. S. Brar in this work.

The units reflected in the manual are generally those in common
use in the North American oil and gas industry. In addition, reference
is made in the theory chapter to the Darcy system and Metric (SI) system
of units. Furthermore, the metric equivalents of various field units
are also included in the nomenclature. The Board intends to convert the
units used throughout its organization to the metric system coincident
with the conversion by the Canadian oil and gas industry. The Board
expects that this would lead to total conversion by approximately the
end of 1978. It has been decided to release this third edition of the
manual at this time reflecting field units, and to issue a fourth
edition in a few years converted to the Metric (SI) system of units.

A concerted effort has been made to bring together all the
relevant theory and to draw appropriately on it in treating the practice
of gas well testing and the interpretation of results. Direct consulta-
tion with industry has so far been only limited, but with the publication
of this third edition, comments and suggestions from industry are
invited. Those involved in the preparation of the manual have
endeavoured to eliminate typographical and other errors but it is
inevitable that some will be found. We hope these will be drawn to our
attention. Both technical comment and notice of errors may be addressed
to the Manager, Gas Department. The fourth edition will incorporate
technical suggestions received from industry.

The manual has been written in a manner such that the suggested
procedures for testing gas wells reflect only the theoretical, practical
and logical considerations, and is not intended as a testing directive

of the Board. The manual does contain an appendix which includes the forms the Board has adopted as standard for the reporting of gas well test data and results. The Board's test requirements are set out in regulations issued under The Oil and Gas Conservation Act which may incorporate by reference parts of this manual.

The Board has been pleased with the acceptance of the previous editions of this manual by industry and believes that this third edition will further serve the objective originally set--that of improving engineering practice in the testing of gas wells and aiding in conservation of resources.

G. W. Govier
Chairman
Energy Resources Conservation Board

September 1975

PREFACE TO THE SECOND EDITION

This second edition of the Theory and Practice of the Testing of Gas Wells has resulted from a detailed review of the first or Discussion Draft carried out during 1964 and 1965. The Board requested the view of the Alberta oil and gas industry on the Discussion Draft through the Alberta Division of the Canadian Petroleum Association. The Association established a special committee, under the chairmanship of Mr. R. L. Taylor of Shell Canada Limited, to review the document and the procedures proposed in it. The other committee members were G. C. Whittaker, Pacific Petroleums Ltd., V. P. Peters, Pan American Petroleum Corporation, J. Hnatiuk, The British American Oil Company Limited, H. S. Simpson, Imperial Oil Limited, and S. M. Thorne, Socony Mobil Oil of Canada, Ltd. This group spent many hours in a detailed study of the Discussion Draft and made many useful suggestions which have been incorporated in the Second Edition. The Board acknowledges this valuable contribution.

In addition, Dr. D. L. Katz of the University of Michigan, Mr. K. Aziz of Rice University and the late Mr. F. K. Beach, Petroleum Consultant, were good enough to send constructive comments for incorporation into the Second Edition. These also are gratefully acknowledged.

Mr. G. J. DeSorcy, Chief Gas Engineer for the Board, accepted the major responsibility for preparing the revisions with Mr. A. S. Telford of the Board's Gas Department giving able assistance.

In addition to introducing the suggestions of the aforementioned, Mr. DeSorcy has made a number of revisions of his own and as suggested by other members of the Board organization.

The Board has been pleased with the acceptance of the Discussion Draft by industry and believes that this Second Edition, incorporating the suggestions received from industry, should serve the objective originally set--that of improving engineering practice in the testing of gas wells and aiding in conservation.

<div style="text-align: right">

G. W. Govier
Chairman
Oil and Gas Conservation Board

June, 1965

</div>

PREFACE TO FEBRUARY 1964 EDITION

This manual on the Theory and Practice of the Testing of Gas
Wells has been prepared to serve a growing need in the Province of
Alberta. It is in what might be called "discussion draft" form. It is
hoped that suggestions for its improvement will be received from industry
during 1964 and it is planned that a revised and improved version will be
published in 1965.

Many advances have been made in the understanding both of the
reservoir and the well bore flow of natural gas since the publication of
the well known "Monograph 7" of the U.S. Bureau of Mines in 1937. Few
of these developments, however, have been incorporated into routine well
testing procedures and the engineer who is not a specialist in the field
may not be familiar with the technical literature describing them.

The manuals published by the Texas Railroad Commission, the
Kansas State Corporation Commission, and recently by the Interstate Oil
Compact Commission have contributed greatly to the precision of
definition of certain of the tests and to a standardization of methods
of calculation. These publications, however, were not intended to
include reviews or criticism of the pertinent theory and except for the
last mentioned they deal only with "stabilized flow" testing.

One of the most significant improvements in the scientific
understanding of gas well testing is in connection with the unsteady
state or unstabilized flow behavior. It seems appropriate to take
advantage of this and other developments and to design well testing
procedures accordingly.

The preparation of the first draft of this manual was carried
out in 1958-59 under my guidance as a class project in the graduate
course, Advanced Natural Gas Engineering, at the University of Alberta,
Edmonton, by graduate students: D. Batcheller, T. Fekete, I. Nielsen,
C. Winter and S. Qayum. Mr. F. Werth, Instructor in Petroleum
Engineering, assisted in the preparation of certain of the tables and
figures. Valuable assistance also was given at this time by Mr. J. G.
Stabback, then Chief Gas Engineer of the Oil and Gas Conservation Board,

and by representatives of the Alberta gas industry, including The British American Oil Company Limited, Northwestern Utilities Limited, Pacific Petroleums Limited, Shell Canada Limited and Imperial Oil Limited. Some of these representatives attended class discussions and many made data from company files available.

The first draft was reworked and revised chiefly by Messrs. J. Pletcher, Assistant Gas Engineer and Mr. S. A. Qayum, Temporary Assistant Gas Engineer of the staff of the Oil and Gas Conservation Board. Mr. K. Aziz, Assistant Professor of Petroleum Engineering, University of Alberta, also gave assistance at this time. This work was carried out intermittently as time permitted during 1961 and 1962. Finally, in mid-1963, Mr. G. J. DeSorcy, Assistant Chief Gas Engineer of the Board was assigned the full time task of preparing a draft suitable for publication and distribution to industry. Mr. DeSorcy and I altered the emphasis of the early draft from one directed to flow tests and related bottom hole pressure calculations to the broader one of the present treatment. Others of the staff of the Board have participated and shared in the checking of calculations.

The manual is being released in its present form not because it is thought to be a finished product but because the Board believes that it will even now be of some value to industry in improving the practice of testing gas wells and, therefore, serve the interests of conservation. Also, in this way, the Board hopes that it will receive suggestions from industry for improvement of the manual.

The manual suggests certain procedures, those which the Board believes best, but it is not intended as a directive with respect to procedures. Following its revision in 1965, however, certain sections of it may be considered suitable for incorporation, by reference, into regulations issued under The Oil and Gas Conservation Act.

G. W. Govier, P. Eng.
Chairman
Oil and Gas Conservation Board

February, 1964

ACKNOWLEDGEMENTS

TABLE OF CONTENTS

CHAPTER

CHAPTER

CHAPTER

CHAPTER

NOMENCLATURE

Symbol	Description	Field Units	Metric (SI) Units
a	length of rectangular drainage area (Fig. 2-18)	ft	m
a	coefficient in the stabilized deliverability equation (Eq. 3-4)	$\dfrac{psia^2}{(cp)(MMscfd)}$	$\dfrac{kPa^2}{(\mu Pa \cdot s)(kmol/d)}$
a_t	coefficient in the transient form of the deliverability equation (Eq. 3-4)	"	"
a'	coefficient in the stabilized deliverability equation (Eq. 3-2)	$\dfrac{psia^2}{MMscfd}$	$\dfrac{kPa^2}{kmol/d}$
a"	coefficient in the stabilized deliverability equation (Eq. 3-3)	$\dfrac{psia}{MMscfd}$	$\dfrac{kPa}{kmol/d}$
A	gross cross-sectional area (Ch. 2, Sec. 2)	–	–
A	drainage area	ft^2	m^2
A	mole fraction ($H_2S + CO_2$) in natural gas (Eq. A-15)	–	–
$A_1, A_2, \ldots, A_8$	coefficients in the Z-factor correlation (Eq. A-13)	–	–
AOF	absolute open flow potential of a well or the deliverability against a zero sandface pressure (Ch. 3)	MMscfd	$kmol/d$
b	coefficient in the stabilized deliverability equation (Eq. (3-4)	$\dfrac{psia^2}{(cp)(MMscfd)^2}$	$\dfrac{kPa^2}{(\mu Pa \cdot s)(kmol/d)^2}$
b	width of rectangular drainage area (Fig. 2-18)	ft	m
b_1	constant dependent on the gas-porous medium system (Eq. 2-13)	–	–
b_3	dimensionless constant (Eq. 2-148)	–	–
b'	coefficient in the stabilized deliverability equation (Eq. 3-2)	$\dfrac{psia^2}{MMscfd^2}$	$\dfrac{kPa^2}{(kmol/d)^2}$
b"	coefficient in the stabilized deliverability equation (Eq. 3-3)	$\dfrac{psia}{MMscfd^2}$	$\dfrac{kPa}{(kmol/d)^2}$
B	formation volume factor	–	–
B	mole fraction H_2S in natural gas (Eqs. A-12 and A-15)	–	–
c	compressibility of a liquid (Ch. 2, Sec. 4.1)	–	–
c	compressibility of any substance	$psia^{-1}$	kPa^{-1}
$\bar{c}$	compressibility of a gas at average conditions	"	"
c_f	formation compressibility	"	"
c_g	gas compressibility	"	"

Symbol	Description	Field Units	Metric (SI) Units
c_o	oil compressibility	$psia^{-1}$	kPa^{-1}
c_r	pseudo-reduced compressibility (Eq. A-19)	–	–
c_t	effective total compressibility (Eq. 2-160)	$psia^{-1}$	kPa^{-1}
c_w	water compressibility	"	"
c_{wf}	gas compressibility corresponding to p_{wf} (Table 2-9)	"	"
c_{ws}	compressibility of wellbore fluids evaluated at the mean wellbore temperature and pressure (Eq. 2-149)	"	"
$c_1, \ldots, c_n$	constants (Eq. (2-116)	–	–
C	coefficient in the deliverability equation (Eq. 3-1)	–	–
C_A	shape factor (Eq. 2-130)	–	–
C_s	wellbore storage constant (Eq. 2-149)	$\dfrac{ft^3}{psia}$	$\dfrac{m^3}{kPa}$
C_{sD}	dimensionless wellbore storage constant (Eq. 2-150)	–	–
C_w	coefficient in the wellhead deliverability equation (Fig. 3-16)	–	–
d	distance between a real well and its image across a no-flow barrier (Ch. 2, Sec. 7.2)	ft	m
d	internal pipe diameter (Eqs. B-18, B-19, B-20, B-21)	in	mm
d_g	average grain diameter (Eqs. 2-1 and 2-2)	–	–
d_H, d_L	distance from a high-rate and a low-rate producing well, respectively, to a no-flow boundary between them (Ch. 5, Sec. 6.5)	ft	m
d_N	distance of the Nth image well from the real well (Eq. 2-121)	"	"
D	IT flow factor (Eq. 2-142)	$MMscfd^{-1}$	$(kmol/d)^{-1}$
D	inside pipe diameter (Eq. B-1)	ft	m
D_{eff}	effective diameter for annular space (Eq. B-32)	"	"
$D(\mu)$	viscosity (or pressure) dependent IT flow factor (Eqs. 2-145 and 2-147)	$MMscfd^{-1}$	$(kmol/d)^{-1}$
e	2.718, base of natural logarithms	–	–
erfc	complimentary error function (Eq. 2-112)	–	–
E	a potential as defined by Hubbert (1940) (Eq. 2-11)	–	–
Ei	exponential integral (Eq. 2-68)	–	–

Symbol	Description	Field Units	Metric (SI) Units
f	Fanning friction factor (App. B)	–	–
f_{CK}	friction factor as defined by Cornell and Katz (1953) (Eq. 2-3)	–	–
f_g	modified Fanning friction factor (Eq. 2-1)	–	–
F	MBH dimensionless pressure function (Eq. 2-129)	–	–
F	factor used in the Cullender and Smith method (Eq. B-24)	–	–
FE	flow efficiency (Eq. 4-13)	–	–
F_r	a factor defined by Equations (B-25) and (B-26) (Table B-2)	–	–
g	gravitational acceleration (Ch. 2)	–	–
g_c	dimension conversion factor	$32.174 \dfrac{lb_m \cdot ft}{lb_f \cdot sec^2}$	–
G	specific gravity of a gas (Eq. A-2)	–	–
G_c	specific gravity of high-pressure separator condensate (Eq. A-25)	–	–
G_{cs}	specific gravity of stock tank condensate (Eq. A-26)	–	–
G_s	specific gravity of a high-pressure separator gas (Eq. A-25)	–	–
g	gravitational vector (Ch. 2)	–	–
h	net formation thickness	ft	m
h_i	thickness of ith layer in a multi-layer reservoir (Eq. 5-35)	"	"
h_D	dimensionless formation thickness (Eq. 4-4)	–	–
I_n	factor used in the Cullender and Smith method (Eqs. B-7 and B-28)	–	–
I_{wf}, I_{mf}, I_{tf}	value of I_n (Eq. B-28) at the bottom, mid-point and wellhead, respectively (App. B)	–	–
I_{ws}, I_{ms}, I_{ts}	value of I_n (Eq. B-7) at the bottom, mid-point and wellhead, respectively (App. B)	–	–
J_0	Bessel function of zero order and first kind (Ch. 2, Sec. 6)	–	–
J_1	Bessel function of first order and first kind (Ch. 2, Sec. 6)	–	–
k	permeability of a medium (Ch. 2, Sec. 2)	–	–
k	reservoir permeability	md	μm^2
k h	permeability thickness of a formation	md·ft	$\mu m^2 \cdot m$

Symbol	Description	Field Units	Metric (SI) Units
$\dfrac{k\,h}{\mu}$	transmissibility of a formation	$\dfrac{md \cdot ft}{cp}$	$\dfrac{\mu m^2 \cdot m}{\mu Pa \cdot s}$
$\overline{k\,h}$	effective permeability of a multi-layer reservoir (Eq. 5-35)	$md \cdot ft$	$\mu m^2 \cdot m$
k_i	permeability of the ith layer of a multi-layer reservoir (Eq. 5-35)	md	μm^2
k_g, k_o, k_w	the permeability of a medium to gas, oil and water, respectively, in multi-phase systems (Eq. 2-159)	"	"
k_L	permeability of the medium to a gas at infinite pressure (Eq. 2-13)	—	—
k_r, k_z	permeability in the radial and vertical directions	md	μm^2
k_{skin}	permeability of a region around the wellbore which is damaged or improved, i.e., $k_{skin} > k$ or $k_{skin} < k$ (Eq. 2-140)	"	"
k_x, k_y, k_z	permeability of the medium in the x, y and z directions (Ch. 2)	"	"
$\left(\dfrac{k}{\mu}\right)_t$	effective total mobility (Eq. 2-159)	$\dfrac{md}{cp}$	$\dfrac{\mu m^2}{\mu Pa \cdot s}$
$\mathbf{k}$	permeability tensor (Ch. 2)	—	—
K	coefficient in the viscosity correlation (Eq. A-24)	—	—
ln	logarithm to the base e	—	—
log	logarithm to the base 10	—	—
L	length of the flow string (App. B)	ft	m
m	value of the integers (Ch. 2, Sec. 7.3) to signify the positions of images relative to the well	—	—
m	slope of the semilog straight line (Chs. 4 and 5)	$\dfrac{psia^2/cp}{cycle}$	$\dfrac{kPa^2/\mu Pa \cdot s}{cycle}$
m'	slope of the straight line plot (Eq. 4-15)	$\dfrac{psia^2/(cp)(MMscfd)}{cycle}$	$\dfrac{kPa^2/(\mu Pa \cdot s)(kmol/d)}{cycle}$
m''	slope of the straight line plot (Eq. 4-28)	$\dfrac{psia^2/cp}{hr}$	$\dfrac{kPa^2/\mu Pa \cdot s}{hr}$
M	molecular weight	$\dfrac{lb_m}{lbmole}$	$\dfrac{kg}{mol}$
M	match point (Ch. 7)	—	—
MBH	abbreviated form of Matthews, Brons and Hazebroek (1954)	—	—
MDH	abbreviated form of Miller, Dyes and Hutchinson (1950)	—	—

Symbol	Description	Field Units	Metric (SI) Units
M_i	molecular weight of any pure component i (App. A)	$\frac{lb_m}{lbmole}$	$\frac{kg}{mol}$
n	value of the integers (Ch. 2, Sec. 7.3) to signify positions of images relative to the well	–	–
n	reciprocal slope of the deliverability line (Eq. 3-1)	–	–
n_w	reciprocal slope of the wellhead deliverability line (Fig. 3-16)	–	–
N	number of data points for least-squares curve fit (Eqs. 3-7, 3-8, 4-19 and 4-20)	–	–
p	pressure	psi	kPa
P_a, P_b, P_c, P_d	pressure drawdown calculated by different methods (Table 2-9)	–	–
P_c	pseudo-critical pressure (Eq. A-6)	psia	kPa
P_{ci}	critical pressure of any pure component i (App. A)	"	"
P_{cs}	static wellhead casing pressure (App. B)	"	"
P_e	pressure at the external boundary of the reservoir	"	"
P_f	flowing reservoir pressure at any position in the reservoir, except at the well and the external boundary	"	"
P_i	initial stabilized shut-in pressure in a new reservoir	"	"
P_i	stabilized shut-in pressure prior to a flow test	"	"
P_{mf}	flowing well mid-point pressure (App. B)	"	"
P_{ms}	static well mid-point pressure (App. B)	"	"
P_r	pseudo-reduced pressure (Eq. A-8)	–	–
$\bar{P}_R$	stabilized shut-in reservoir pressure (Eq. 2-9)	psia	kPa
P_{sc}	standard pressure	14.65 psia	101.325 kPa
P_{tf}	flowing wellhead (top hole) pressure (App. B)	psia	kPa
P_{ts}	static wellhead (top hole) pressure (App. B)	"	"
$\bar{P}_{ts}$	stabilized shut-in wellhead pressure (Fig. 3-16)	"	"
P_{wf}	flowing bottom hole pressure	"	"
P_{ws}	static bottom hole pressure	"	"

Symbol	Description	Field Units	Metric (SI) Units
p_a^2, p_b^2	pressure drawdown (Table 2-9)	-	-
p^0	arbitrary reference pressure (Ch. 2)	-	-
p^*	hypothetical reservoir pressure (Eq. 2-127)	psia	*kPa*
P_t	dimensionless pressure drop at the well excluding skin and inertial-turbulent flow effects (Eq. 2-73)	-	-
Δp	pressure difference	psi	*kPa*
Δp_D	dimensionless pressure drop defined for various systems (Table 2-3)	-	-
$\Delta p_{D\,HOR}$	Horner dimensionless pressure drop (Fig. 5-9)	-	-
$(\Delta p_D)_{IT}$	dimensionless pressure drop due to IT flow effects (Eq. 2-142)	-	-
$\Delta p_{D\,MDH}$	MDH dimensionless pressure drop (Fig. 5-9)	-	-
$(\Delta p_D)_{skin}$	dimensionless pressure drop due to skin (Eq. 2-138)	-	-
q	flow rate (Ch. 2, Sec. 2)	-	-
$\dot{q}$	volumetric flow rate	MMscfd	*kmol/d*
q_A	gas flow rate at well A (Ch. 2, Sec. 7)	"	"
q_B	gas flow rate at well B (Ch. 2, Sec. 7)	"	"
q_{AD}	dimensionless flow rate at well A (Eq. 2-119)	-	-
q_{BD}	dimensionless flow rate at well B (Eq. 2-119)	-	-
q_D	dimensionless flow rate defined for various systems (Table 2-3)	-	-
q_g	production rate of gas in a multi-phase system (Ch. 2, Sec. 9.4)	MMscfd	*kmol/d*
q_H, q_L	high and low flow rates of the wells creating a no-flow boundary between them (Ch. 5, Sec. 6.5)	"	"
q_o	production rate of oil in a multi-phase system (Ch. 2, Sec. 9.4)	bbl/d	*m³/d*
q_{sc}	volumetric flow rate at standard conditions of temperature and pressure	MMscfd	*kmol/d*
q_t	effective total production rate (Eq. 2-161)	"	"
q_{total}	sum of the flow rates of two wells creating a no-flow boundary between them (Ch. 5, Sec. 6.5)	"	"
q_w	production rate of water in a multi-phase system (Ch. 2, Sec. 9.4)	bbl/d	*m³/d*

Symbol	Description	Field Units	Metric (SI) Units
q^*	modified flow rate (Eq. 5-31)	MMscfd	$kmol/d$
Q	production rate (App. B)	"	"
Q_t	dimensionless total production number (Eq. 2-109)	-	-
Q_T	cumulative production (Eq. 2-108)	scf	mol
r	radius	ft	m
r_A	distance of well A from a point P in the reservoir (Ch. 2, Sec. 7)	"	"
r_{AD}	dimensionless value of r_A, r_A/r_w	-	-
r_B	distance of well B from a point P in the reservoir (Ch. 2, Sec. 7)	ft	m
r_{BD}	dimensionless value of r_B, r_B/r_w	-	-
r_d	effective drainage radius (Ch. 2, Sec. 6.4)	ft	m
r_D	dimensionless radius, r/r_w	-	-
r_e	radius of the external boundary	ft	m
r_{eD}	dimensionless external (boundary) radius r_e/r_w	-	-
r_f	fracture radius	ft	m
r_{inv}	radius of investigation (Ch. 2, Sec. 6.4)	"	"
r_{skin}	radius of a hypothetical permeability k_{skin} (Eq. 2-140)	"	"
r_w	well radius	ft	mm
$r_{weffective}$	effective well radius (Eq. 2-141)	ft	m
r, θ, σ	spherical coordinates (Table 2-1)	-	-
r, θ, z	cylindrical coordinates (Table 2-1)	-	-
R	gas constant	$10.7 \frac{ft^3 \cdot psia}{lbmole \cdot {}^oR}$	$8.3 \frac{m^3 \cdot kPa}{mol \cdot {}^oK}$
R	distance from well to the observation point (Table C-1(a) to (n))	ft	m
R_c	gas-condensate ratio (Eq. A-25)	$\frac{scf}{bbl}$	$\frac{mol}{m^3}$
R_{cs}	gas-stock tank condensate ratio (Eq. A-26)	$\frac{scf}{STB}$	$\frac{mol}{m^3}$
R_c'	condensate accumulation in the reservoir per unit volume of gas produced per unit pressure (Eq. 2-162)	$\frac{ft^3}{MMscf \cdot psi}$	$\frac{m^3}{kmol \cdot kPa}$
Re	Reynolds number (Eq. B-19)	-	-
Re_{CK}	Reynolds number as defined by Cornell and Katz (1953) (Eq. 2-3)	-	-

Symbol	Description	Field Units	Metric (SI) Units
Re_g	modified Reynolds number (Eq. 2-2)	–	–
s	skin factor (Eq. 2-138)	–	–
s_c	condensate skin effect (Eq. 2-162)	–	–
s_k	skin due to altered permeability (Ch. 2, Sec. 9.1)	–	–
s_{perf}	skin due to perforations (Ch. 2, Sec. 9.1)	–	–
s_{pp}	skin due to partial penetration (Ch. 2, Sec. 9.1)	–	–
s'	apparent skin factor (Eq. 2-144)	–	–
s_n'	apparent skin factor associated with the flow rate q_n	–	–
S	parameter (Eqs. B-4A and B-22A)	–	–
S_c	hydrocarbon liquid saturation required to reach mobility (fraction of pore volume) (Eq. 2-162)	–	–
SF	stabilized factor (Ch. 7, Sec. 4.3)	–	–
t	time	hr	hr
t_c	corrected time of flow (Eq. 5-30)	"	"
t_D	dimensionless time for various systems (Table 2-3)	–	–
t_{DA}	dimensionless time based on drainage area (Eq. 2-123)	–	–
t_s	time to stabilization (Ch. 2, Sec. 6.4)	hr	hr
t_{ws}	time for wellbore storage effects to become negligible (Eq. 2-154)	"	"
t_{wsD}	dimensionless time for wellbore storage effects to become negligible (Eq. 2-153)	–	–
T	temperature (Ch. 2, Sec. 4)	–	–
T	reservoir temperature	^oR	^oK
T_c	pseudo-critical temperature (Eq. A-5)	"	"
T_{ci}	critical temperature of any pure component i (App. A)	"	"
T_{mf}	flowing well mid-point temperature (App. B)	"	"
T_{ms}	static well mid-point temperature (App. B)	"	"
T_r	pseudo-reduced temperature (Eq. A-7)	–	–
T_{sc}	standard temperature	60^oF	15^oC
T_{tf}	flowing wellhead (top hole) temperature (App. B)	^oR	^oK

Symbol	Description	Field Units	Metric (SI) Units
T_{ts}	static wellhead (top hole) temperature (App. B)	$^\circ R$	$^\circ K$
T_{wf}	flowing bottom hole temperature (App. B)	"	"
T_{ws}	static bottom hole temperature (App. B)	"	"
t_{100}	time required to investigate 100 feet of reservoir (Eq. 3-20)	hr	hr
t^*	modified time (Eq. 5-31)	"	"
t^*	modified time (Eq. 5-36)	–	–
Δt	flowing time for the second rate of a two-rate test (Ch. 4, Sec. 4.2)	hr	hr
Δt	shut-in time (Ch. 5)	"	"
Δt_{DA}	dimensionless pressure drop based on drainage area (Eq. 5-22)	–	–
Δt_{De}	dimensionless shut-in time based on external radius (Eq. 5-20)	–	–
Δt_i	time of intersection of semilog straight lines for a well near a fault (Ch. 5, Sec. 6.5)	–	–
u	superficial velocity (Ch. 2, Sec. 2)	–	–
u	average fluid velocity (App. B)	$\dfrac{ft}{sec}$	$\dfrac{m}{sec}$
u_x, u_y, u_z	superficial velocity in the x, y and z directions (Ch. 2)	–	–
$\mathbf{u}$	velocity vector (Ch. 2)	–	–
v	specific volume of a gas (Eq. A-1)	$\dfrac{ft^3}{lb_m}$	$\dfrac{m^3}{kg}$
V	volume (Ch. 2, Sec. 4.1)	–	–
V_c	condensate vaporizing volume ratio (Eq. A-25)	$\dfrac{scf}{bbl}$	$\dfrac{mol}{m^3}$
V_{cs}	stock tank condensate vaporizing volume ratio (Eq. A-26)	$\dfrac{scf}{STB}$	$\dfrac{mol}{m^3}$
V_1	vaporizing volume of any pure component 1 (App. A)	$\dfrac{scf}{bbl}$	$\dfrac{mol}{m^3}$
V_p	in-place gas volume of a reservoir (Eq. 4-28)	MMscf	$kmol$
V_{pm}	minimum in-place gas volume (Eq. 4-31)	"	"
V_{ws}	volume of wellbore (Eq. 2-149)	ft^3	m^3
W_s	mechanical work done on or by a gas per unit weight of gas (Eq. B-1)	$\dfrac{lb_f \cdot ft}{lb_m}$	$\dfrac{N \cdot m}{kg}$
x	distance	ft	m
x, y, z	rectangular coordinates (Ch. 2)	–	–

Symbol	Description	Field Units	Metric (SI) Units
x_D	dimensionless distance defined for various systems (Table 2-3)	-	-
x_D	dimensionless location of a well in a rectangular drainage area (Table C-1(a) to (n))	-	-
x_e	distance from well to external boundary	ft	m
x_f	fracture half-length or distance from well to fracture perimeter	"	"
x_i	mole fraction of component i in a mixture (App. A)	-	-
X	parameter in the viscosity correlation (Eq. A-24)	-	-
X	Boltzmann transformation (Ch. 2, Sec. 6.1)	-	-
Δx	distance in the x-direction (Ch. 2)	ft	m
y_D	dimensionless location of a well in a rectangular drainage area (Table C-1(a) to (n))	-	-
Y	parameter used in the viscosity correlation (Eq. A-24)	-	-
Y_0	Bessel function of zero order and second kind (Ch. 2, Sec. 6)	-	-
Y_1	Bessel function of first order and second kind (Ch. 2, Sec. 6)	-	-
z	vertical downward direction	ft	m
Z	compressibility factor of a gas (App. A)	-	-
Z_i	compressibility factor at initial conditions	-	-
Z_{wf}	compressibility factor corresponding to p_{wf} (Table 2-9)	-	-
$\bar{Z}$	compressibility factor at average conditions	-	-
α	fraction indicating the position of a well in a rectangular drainage area (Fig. 2-18)	-	-
α_n	roots of Equation (2-80)	-	-
α_n'	roots of Equation (2-84)	-	-
β	fraction indicating the position of a well in a rectangular drainage area (Fig. 2-18)	-	-
β	turbulence factor (Ch. 2, Sec. 2)	-	-
β_n	roots of Equation (2-87)	-	-
γ	coefficient of the dimensionless flow rate q_D, values listed in Table 2-4	-	-
δ	LIT flow correction factor (Ch. 2)	-	-

Symbol	Description	Field Units	Metric (SI) Units
δ	absolute roughness (App. B)	in	mm
δ_x, δ_y, δ_z	value of the LIT flow correction factor in the x, y, and z directions (Ch. 2)	–	–
δ	LIT flow correction tensor (Ch. 2)	–	–
ϵ_3	pseudo-critical temperature adjustment factor (Eq. A-15)	^oF	^oC
η	units conversion coefficient (Eq. 2-150)	–	–
θ	angle between intersecting faults (Ch. 4, Sec. 6.2)	–	–
κ	reciprocal diffusivity (Ch. 2, Sec. 5.6)	–	–
λ	coefficient of the dimensionless time t_D, values listed in Table 2-4	–	–
λ	degree of interporosity flow (Ch. 5, Sec. 6.5)	–	–
λ	a constant in the McKinley (1970) type curves (Ch. 4, Sec. 2.1)	–	–
μ	absolute viscosity (Ch. 2, Sec. 2)	–	–
μ	gas viscosity	cp	$\mu Pa \cdot s$
μ_g	gas viscosity (Ch. 2, Sec. 9.4)	"	"
μ_i	viscosity at initial conditions	"	"
μ_o	oil viscosity (Ch. 2, Sec. 9.4)	cp	$mPa \cdot s$
μ_w	water viscosity (Ch. 2, Sec. 9.4)	"	"
μ_{wf}	gas viscosity corresponding to p_{wf} (Table 2-9)	cp	$\mu Pa \cdot s$
μ_1	gas viscosity at 1 atm. (App. A)	"	"
$\bar{\mu}$	gas viscosity at average conditions	"	"
ξ	dummy variable of integration (Ch. 2)	–	–
π	a constant, 3.1415	–	–
ρ	fluid density	$\dfrac{lb_m}{ft^3}$	$\dfrac{kg}{m^3}$
ρ^0	fluid density at some reference pressure p^0 (Ch. 2)	–	–
ϕ	porosity of the medium (Ch. 2)	–	–
ϕ_t	total porosity (Ch. 2, Sec. 9.4)	–	–
$\dfrac{\phi \mu c}{k}$	diffusity of a gas-porous medium system	$\dfrac{cp}{md \cdot psia}$	$\dfrac{\mu Pa \cdot s}{\mu m^2 \cdot kPa}$
ϕ	an arbitrary scalar (Table 2-1 and Ch. 2, Sec. 5.6)	–	–

Symbol	Description	Field Units	Metric (SI) Units
ϕ	an arbitrary lower limit of integration (Eq. 2-112)	-	-
$\boldsymbol{\phi}$	an arbitrary vector (Table 2-1)	-	-
ψ	pseudo-pressure as defined by Al-Hussainy (1965) (Eq. 2-40)	$\dfrac{psia^2}{cp}$	$\dfrac{kPa^2}{\mu Pa \cdot s}$
ψ_i	pseudo-pressure corresponding to p_i	"	"
ψ_{wf}	pseudo-pressure corresponding to p_{wf}	"	"
ψ_{wfp}	predicted pseudo-pressure (Fig. 5-2)	"	"
ψ_{wf_0}	ψ_{wf} corresponding to p_{wf} at the time of changing the flow rate (Ch. 4, Sec. 4.2)	"	"
ψ_{wf_0}	ψ_{wf} corresponding to p_{wf} at the time of shut-in (Ch. 5, Sec. 4.1)	"	"
ψ_{wf_1}	ψ_{wf} at $\Delta t = 1$ (Ch. 4, Sec. 4.2)	"	"
ψ_{ws}	pseudo-pressure corresponding to p_{ws}	"	"
ψ_{ws_1}	ψ_{ws} at $\Delta t = 1$ (Ch. 5, Sec. 4.1)	"	"
$\bar{\psi}_R$	pseudo-pressure corresponding to $\bar{p}_R$	-	-
ψ^*	pseudo-pressure corresponding to p^*		
ψ'	alternative definition of pseudo-pressure (Eq. 2-45)	$\dfrac{psia^2 \cdot md}{cp}$	$\dfrac{kPa^2 \cdot \mu m^2}{\mu Pa \cdot s}$
$\Delta\psi_D$	dimensionless pseudo-pressure drawdown (Eq. 4-14)	-	-
$(\Delta\psi)_{IT}$	pseudo-pressure drop due to IT flow effects (Eq. 4-11)	$\dfrac{psia^2}{cp}$	$\dfrac{kPa^2}{\mu Pa \cdot s}$
$(\Delta\psi)_{skin}$	pseudo-pressure drop due to skin (Eq. 4-10)	"	"
$(\Delta\psi)_{s'}$	total pseudo-pressure drop due to skin and IT flow effects (Eq. 4-12)	"	"
$\Delta\psi_0$	$(\psi_i - \psi_{wf})/q_n$ corresponding to a value of zero on the abscissa of the plot (Eq. 4-15)	"	"
$\Delta\psi_1$	$(\psi_i - \psi_{wf})$ at $t = 1$ (Ch. 4, Sec. 4.1)	"	"
ω	measure of the capacity (ϕc) of a system (Ch. 5, Sec. 6.5)	-	-
$\nabla, \nabla^2, \nabla\cdot$	gradient operators (Ch. 2)	-	-
∞	infinity	-	-
Boldface	denotes vectors and tensors		

UNITS CONVERSION AND PREFIXES

Conversion of Common Field Units to Metric (SI) Units

Base conditions: Field 60°F   14.65 psia

                    Metric (SI) 15°C, 101.325 kPa

Field Unit	Multiplying Factor	Metric (SI) Unit Name	Symbol
acre	4.046 856 E+03	square metre	m^2
acre	4.046 856 E-01	hectare	ha
acre-foot	1.233 482 E+03	cubic metre	m^3
atmosphere	1.013 25 E+02	kilopascal	kPa
barrel (35 Imp. gal.)	1.589 873 E-01	cubic metre	m^3
BTU per standard cubic foot (60°F, 14.65 psia)	8.799 136 E-01	kilojoule per mole	kJ/mol
centipoise	1.0 E+00	millipascal second	mPa·s
cubic foot	2.831 685 E-02	cubic metre	m^3
cubic foot gas per barrel (60°F, 14.65 psia)	7.494 773 E+00	mole per cubic metre	mol/m^3
darcy	9.869 233 E-01	square micrometre	μm^2
degree Fahrenheit	($^{\circ}$F-32)5/9 E+00	degree Celsius	$^{\circ}$C
degree Rankine	5/9 E+00	kelvin	K
gallon (Cdn)	4.546 09 E-03	cubic metre	m^3
gallon (US)	3.785 412 E-03	cubic metre	m^3
gas constant	8.314 32 E+00	joule per mole kelvin	J/(mol·K)
Mcf (thousand cubic foot 60°F, 14.65 psia)	1.191 574 E+00 2.826 231 E+01	kilo mole cubic metre (API)	kmol m^3API
millidarcy	9.869 233 E-04	square micrometre	μm^2
MMcf (million cubic foot 60°F, 14.65 psia)	1.191 574 E+00 2.826 231 E+04	megamole cubic metre (API)	Mmol m^3API
pound-force per square inch (psi)	6.894 757 E+00	kilopascal	kPa
pound-mass	4.535 924 E-01	kilogram	kg
psi per foot	2.262 059 E+01	kilopascal per metre	kPa/m
section (640 acres)	2.589 988 E+06	square metre	m^2
section (640 acres)	2.589 988 E+02	hectare	ha
standard cubic foot (60°F, 14.65 psia - ideal gas)	1.191 574 E+00 2.826 231 E-02	mole cubic metre (API)	mol m^3API
Tcf (trillion cubic foot 60°F, 14.65 psia)	1.191 574 E+00 2.826 231 E+10	teramole cubic metre (API)	Tmol m^3API
ton (US short - 2000 lb)	9.071 847 E-01	tonne	t
ton (UK long - 2240 lb)	1.016 047 E+00	tonne	t

Prefixes

Multiplying factor			Prefix	Symbol
1 000 000 000 000	=	10^{12}	tera	T
1 000 000 000	=	10^{9}	giga	G
1 000 000	=	10^{6}	mega	M
1 000	=	10^{3}	kilo	k
100	=	10^{2}	hecto	h
10	=	10^{1}	deca	da
0.1	=	10^{-1}	deci	d
0.01	=	10^{-2}	centi	c
0.001	=	10^{-3}	milli	m
0.000 001	=	10^{-6}	micro	μ
0.000 000 001	=	10^{-9}	nano	n
0.000 000 000 001	=	10^{-12}	pico	p
0.000 000 000 000 001	=	10^{-15}	femto	f
0.000 000 000 000 000 001	=	10^{-18}	atto	a

Some Rules Governing the Use of Prefixes

1. Prefix symbols are printed in Roman (upright) type without spacing between prefix symbol and the unit symbol.

2. Only one prefix is applied at one time to a given unit.

   Example:

   nanometre (nm)   not millimicrometre (mμm)

3. In the particular case of the kilogram the <u>root</u> name to which the prefix is applied is <u>gram</u> because only one prefix should be used.

   Examples:

   milligram (mg)   not microkilogram (μkg)

4. The prefix symbol is considered to be combined with the unit symbol which it immediately precedes, forming with it a new symbol. This new symbol can then be raised to a positive or negative power and can be combined with other symbols to form compound symbols.

   Examples:

   $1 \text{ cm}^3 = 1 \text{ (cm)}^3 = (10^{-2}\text{m})^3 = 10^{-6}\text{m}^3$

   $1 \text{ }\mu\text{s}^{-1} = 1 \text{ }(\mu\text{s})^{-1} = (10^{6}\text{s})^{-1} = 10^{6}\text{s}^{-1}$

   $1 \text{ mm}^2/\text{s} = 1 \text{ (mm)}^2/\text{s} = (10^{-3}\text{m})^2/\text{s} = 10^{-6}\text{m}^2 \cdot \text{s}^{-1}$

5. It is recommended that only <u>one</u> prefix should be used in forming decimal multiples or sub-multiples of a derived SI unit. This prefix should be attached to a unit in the numerator. An exception to this occurs when the base unit, kilogram, appears in the denominator.

   Examples:

   μN·m, not mN·mm;   mΩ/m, not Ω/km;   J/kg – showing the exception.

6. The choice of the appropriate multiple (decimal multiple or sub-multiple) of an SI unit is governed by convenience, the multiple chosen for a particular application being the one which will lead to numerical values within a practical range. The use of prefixes representing 10 raised to a power which is a multiple of 3 is recommended.

CHAPTER 1   INTRODUCTION

The ability to analyze the performance and forecast the
productivity of gas wells and to understand the behaviour of gas
reservoirs with a reasonable degree of accuracy is of utmost importance
in today's natural gas industry. One of the most useful aids in
analyzing gas well performance is the flowing well test. A complete
analysis and understanding of the results of an appropriate well test
enables one to determine the stabilized shut-in reservoir pressure,
determine the rate at which a well will flow against a particular pipe-
line "back pressure," predict the manner in which the flow rate will
decrease with depletion and the resulting decline in reservoir pressure,
and estimate the effective reservoir flow characteristics.

The results of well tests are often used by regulatory bodies
in setting maximum gas withdrawal rates. They are also employed by
producing and transporting companies in projecting gas well deliveries,
in the preparation of field development programs, in the design of
gathering and pipeline facilities, in the design of processing plants,
and in the negotiation of gas sale contracts. Other important
applications of well tests and of information gathered during testing
are in the estimation of gas reserves associated with a well or a group
of wells and in making various types of special reservoir studies.

1 HISTORY

In the early days, gas wells were tested by opening a well to
the atmosphere and directly measuring its "absolute open flow" potential.
Such a test was undesirable from a gas conservation and safety viewpoint
so that methods were developed for assessing productive capacity by
conducting well tests at reasonable, controlled rates of flow. The first
such test was the well-known "conventional back pressure test." Later,
more practical methods of testing were developed. These included the
"isochronal test" and the "modified isochronal test." Such tests have

been used extensively by industry. More recently, tests made up of a combination of flow and shut-in periods and involving a greater sophistication with respect to their conduct and interpretation, have been used to determine the flow characteristics of gas wells. Additionally, there has been an increasing awareness of the need for accurate determinations of static reservoir pressures. The history of the flow testing of gas wells is discussed in more detail in Chapter 3.

The understanding, and indeed the development, of the more advanced methods of testing gas wells requires a thorough knowledge of the theory of gas flow within the reservoir. For this reason, this manual includes in Chapter 2, a detailed discussion of the relevant theory. Included are reviews of the fundamental equations related to flow of fluids through porous media. Also included are the solutions of interest for various boundary conditions and reservoir geometries along with example problems to illustrate the use of these equations.

2 TYPES OF TESTS

Basically, there are two types of flow tests conducted on gas wells. The first category involves tests designed primarily to measure the deliverability of gas wells and the second category involves tests designed primarily to yield knowledge of the reservoir.

The conventional back pressure test and the isochronal type tests are examples of tests designed primarily to measure deliverability. These tests are discussed in detail in Chapter 3 of this manual. The chapter includes a review of the theoretical relationships fundamental to deliverability testing. For several types of deliverability tests, various methods of analyzing the test data are presented. Included are appropriate examples illustrating the calculating and plotting essential to the interpretation of tests. Chapter 3 also includes a detailed discussion of some important considerations relative to deliverability tests such as the time necessary to attain stabilized flow and the need for constant flow rates during testing. There is included at the end of Chapter 3, and also at the end of Chapters 4 and 5, a set of "Notes" to the Chapter. These include derivations of equations and other

detailed material which would be of interest to some readers but is not essential to the understanding and use of this manual.

Tests designed primarily to yield knowledge of the reservoir can be further categorized as drawdown tests or build-up tests and can also be used to investigate the deliverability of a well. Drawdown tests are designed primarily to obtain a knowledge of the permeability, sandface effects and other flow characteristics of a reservoir. Such tests are often used to determine the outer limits of a reservoir and may be used to determine the stabilized flow capabilities of gas wells. Drawdown tests are discussed in detail in Chapter 4. The content of the chapter is similar to that of the previous chapter and begins with a presentation of the fundamental theoretical relationships. Different types of drawdown tests, including single and multi-rate tests, are presented along with a discussion of the analysis of the test results. The chapter discusses the duration of and the need for constancy of flow rates and other important considerations related to drawdown testing. It also includes, along with appropriate examples, a description of the methods for calculating, plotting and analyzing data from drawdown tests.

Build-up tests will yield essentially the same knowledge of the flow characteristics of a reservoir as is obtained from drawdown testing but additionally can be used to determine the average stabilized shut-in pressure in the drainage area of a particular well. Chapter 5 deals with build-up testing and is structured in a manner similar to the preceding chapters. The fundamental theoretical relationships are presented for various reservoir geometries, along with a discussion of several alternate methods of analyzing the data. Certain important considerations regarding build-up testing are presented along with examples illustrating the calculating, plotting and interpretation of build-up data.

In addition to determining the flow capabilities of the reservoir through special tests, it is possible to estimate the flow behaviour from limited data obtained from short flow tests, well logs or cores, and estimates of gas properties. Chapter 7 deals with this matter and presents the theoretical basis for such estimates along with appropriate examples.

3 FIELD CONDUCT AND REPORTING OF TESTS

A successful testing program involves, in addition to a thorough understanding of the theory of gas flow in porous media, the knowledge of and adherence to proper procedures in the field conduct of the test. In addition, the results of the test should be reported in a manner which includes all relevant data and provides for maximum utilization of the results. Chapter 6 of this manual provides a detailed discussion of the field conduct and reporting of gas well tests. It includes a discussion of the equipment essential to testing and in particular for the measurement of flow rates and pressures. The chapter also discusses the data which should be gathered and the information which should be included in a report of a test.

In order to measure accurately or to estimate flow rates and pressures, an understanding of the properties of the gas which is being produced is necessary. A detailed discussion of the important properties of natural gas along with examples illustrating how they might be calculated or estimated is presented in Appendix A. Also included in the appendix is a tabulation listing those physical properties of the constituent components of natural gas that are required in carrying out well test calculations.

The accurate measurement of pressures is also of great importance in gas well testing. Since interpretation of back pressure test results must be based on the theory of gas flow in the reservoir, it follows that the important pressure in interpreting the test is the reservoir pressure. Ideally, this pressure should be measured directly through use of an accurate, carefully calibrated bottom hole pressure gauge. There are many types of such gauges available today all of which, when used properly, are quite adequate for obtaining accurate sandface pressures directly. In some instances, due to mechanical difficulties or for other reasons, it is not practical to use a bottom hole pressure gauge. In addition to this, for shallow wells the accuracy of conversion from wellhead pressures to sandface pressures is acceptable, so that bottom hole gauge measurements are unnecessary. In these situations,

wellhead pressures are usually measured and converted to sandface conditions. The highest possible accuracy in wellhead pressure measurement is important, and for best results these pressures should be taken with a dead-weight gauge.

There are many methods of conversion from wellhead to sandface pressures, each having its advantages and disadvantages. Appendix B includes a discussion and the details of one method of determining sandface pressures from wellhead measurements for the case of a single-phase gas. The case where both gas and liquid phases exist in the well is also discussed.

Certain lengthy tables and figures which are referred to in the manual but are not essential to the presentation or understanding of the various chapters are included in Appendix C. Appendix D includes program listings for some of the computer routines mentioned in the manual.

Requirements for the conduct, reporting and analysis of test data vary among different regulatory bodies. The requirements of the Board with respect to Alberta are contained in various parts of the Oil and Gas Regulations and are not included in this manual. Appendix E does contain forms for recording data and reporting test results which the Board is adopting as standard forms for the Province of Alberta.

4 CHOICE AND FREQUENCY OF TESTING

Not only are there two major categories of gas well tests, namely tests designed primarily to determine deliverability, and tests designed primarily to yield knowledge of the reservoir, but there are several types of each category of tests. To illustrate, the conventional, isochronal, modified isochronal, and single-point tests are all types of deliverability tests. One of the most important features of gas well testing is to select the appropriate type of test to be run and also to conduct tests at the right frequency, having regard for the costs of conducting the tests and for the need to understand the flow behaviour of a reservoir over its entire producing life.

The decision regarding whether or not a test should be run and the type of test to be run generally depends on a consideration of the use to which the test results will be put, the markets to be served by the subject well, whether the well is connected to a pipeline system, whether previous tests have been conducted on the well, whether previous tests have been conducted on other wells in the same pool, the workover history of the well, whether water producing problems exist and any available information regarding the producing reservoir. In the conduct of a test, or indeed, in deciding whether or not a test is necessary, the first step is to gather all of the relevant information. A summary sheet should be set up listing all pertinent data regarding the location, the well completion, the probable capability of the well and any other matters affecting the design of a testing program. The material should be carefully reviewed to establish the broad or overall testing program. For example, at this stage it might be decided to conduct extensive tests on some new wells in a pool to obtain information regarding deliverability and the formation characteristics, while at the same time it might be decided to conduct very limited tests on the remaining wells. Having decided on the general program, the next step would be to design each of the tests in a very detailed manner including consideration of the equipment to be used, the approximate flow rates and the duration of flow periods.

The following are guide lines as to the kind of program which might be set up in the testing of gas wells. If the decision regarding a testing program is being made for a new exploratory well recently completed in a new pool, of which little is known, the general rule is that the test should be extensive. In instances such as this, because pipeline and other producing facilities are not usually available, the produced gas must be flared. In fact, the size of the pipeline and production facilities will often be determined on the basis of the results of the initial well test. Since the gas will be flared, care should be taken to obtain the maximum useful information for the amount of gas wasted. If a drill-stem test, log interpretation or other information suggests a reservoir of relatively high flow capacity, the

test can be extensive without the flaring of large volumes of gas. In such instances, it might be appropriate to begin the test with a clean-up flow period followed by a single-rate drawdown test. The drawdown test should be at the minimum flow rate consistent with obtaining useful information and also should be for the minimum time period necessary to obtain a knowledge of the stabilized flow situation. Production and pressure data should be collected during the flow period. An analysis of the drawdown data would indicate the flow capacity of the reservoir and would assist in determining the appropriate size of production facilities and whether production of the well would be economic. The extended flow test would be followed by a pressure build-up, the analysis of which would yield further information regarding formation capacity, but which might also yield some knowledge of reservoir size due to the availability of a new shut-in stabilized reservoir pressure. Following the pressure build-up an appropriate multi-point test might be conducted to establish a back pressure-flow rate relationship. An isochronal type test would be appropriate since the initial extended flow test would be available to position the stabilized deliverability curve.

The preceding type of test is one of the more extensive test procedures that would be employed and if the gas must be flared, it should be used only when testing a new well in a new pool where available information suggests the flow capacity is relatively large. If a drill-stem test or other information suggests that flow capacity is low, the test could be modified to reduce the related flaring. For example, the clean-up period might be extended into a single-rate drawdown test to be followed by a build-up test. The initial flow period would be limited to about ten times the period necessary for clean-up and there would be no multi-point testing. Data from the drawdown and build-up tests would be used to calculate the reservoir characteristics and a back pressure-flow rate relationship, including recognition of stabilized conditions, would also result from such calculations.

The preceding test procedures might apply to new wells in completely new and unknown pools. If new wells are being drilled in

a partially developed pool where some knowledge of the reservoir exists, the complexity of the test might be reduced. For example, if the formation is known to be of high productivity a four-point isochronal type test might be conducted. However, since something is already known of the formation and since flaring of the gas will be necessary, not all of the wells need be tested. In such a case, the stabilized flow point should be delayed until it can be conducted into a pipeline system. In developing pools where the flow capacity is known to be low, a multi-point test would represent an unnecessary waste of gas. Alternatively, a representative portion of the new wells might have their clean-up extended into a drawdown test to be followed by a build-up from which reservoir characteristics could be calculated.

As additional wells are drilled in a pool the new wells require less testing. If the reference is to a new infill well in an almost completely developed pool, no test is normally necessary until it can be run into a pipeline system. At that time, a single-rate or two-rate flow test might be conducted primarily to compare the productivity of the new well to existing wells.

With respect to subsequent test requirements for producing wells, theoretical considerations suggest that only one comprehensive test is required over the life of a well. However, due to shortcomings in the theory, and changes that might occur in reservoir properties, especially near the sandface, at least one additional multi-point test, after four to six years, would seem appropriate. The multi-point tests should be interspersed with occasional single-point tests, with gas flow into pipeline facilities, to determine if changes have occurred in the producing capability of the wells. If changes are indicated, further extensive testing might be warranted. The actual spacing of the tests will be influenced by many factors. The most important factors, and their effect on a properly planned testing program are as follows:

1. A gas well should be extensively tested following any workover or change in production equipment which may significantly change the ability of the well to deliver

gas or if well performance indicates that an appreciable change has taken place in producing characteristics.

2. The number of wells drilled into and producing from the same pool will affect the testing program. Scheduling should be such that sufficient information is available to trace accurately the pressure history for the pool and hence, its deliverability potential.

3. The possibility that damage may occur to a reservoir as a result of excessive producing rates also affects the timing of flow tests. If, for a particular reservoir, strict control of maximum producing rates is necessary to prevent well damage, the frequency of testing should be increased to ensure that adequate information regarding the deliverability behaviour of the wells is available at all times.

4. The ultimate market to which the gas will be delivered is an important factor. If the market being served requires current and highly accurate information regarding the deliverability of the well, then a greater number of tests is necessary.

In summary, a desirable testing program planned to yield the maximum amount of technical information in the most economic manner, should include a series of single-rate, multi-rate, and build-up tests spaced effectively over the life of a pool. If a well happens to be one of the first drilled in a pool, it would most likely have an extensive test including a drawdown and a build-up conducted initially. Thereafter, it might have at least eight to ten single-point tests and one or two multi-point tests conducted over its producing life. The stabilized shut-in reservoir pressure would also be determined every few years. For wells which are drilled in developed pools, initial tests would not be as extensive and in fact the total testing for the well might involve one or two multi-point tests, and a minimum of five to eight stabilized pressure determinations and eight to ten single-point flow tests spaced over the producing life.

The important principles to remember in designing a test program are that sufficient information must be available to properly engineer the production of the gas pool, and the information to be gained from any particular test should be worth the cost of the test including the value of any flared gas. A general observation relative to the testing situation which exists in industry today might be that although fewer tests are required, greater care should be taken with the conduct of the tests, more data should be gathered during the tests and greater use should be made of the methods available to analyze the test data.

CHAPTER 2   THEORETICAL CONSIDERATIONS

1 INTRODUCTION

1.1 Objectives

The theoretical principles underlying the flow and pressure testing of gas wells are developed in this chapter. A detailed understanding of these principles is not mandatory for conducting the tests. However, interpretation of test results is based on theory and, therefore, a thorough knowledge of the theory and its limitations is of great value. Moreover, by suitable mathematical rearrangement of the relevant equations, specific tests can be developed rationally, based on theoretical considerations, and conducted in the field, in order to determine the desired parameters.

The fundamental equations for flow of fluids through porous media are developed and presented, along with solutions of interest for various boundary conditions and reservoir geometries. These solutions are required in the design and interpretation of flow and pressure tests.

Because of their inherent simplicity, dimensionless terms are used wherever expedient. Assumptions and approximations necessary for defining the system and solving the differential equations are clearly stated. The principle of superposition is applied to solve problems involving interference between wells, variable flow rates, and wells located in non-circular reservoirs. The use of numerical solutions of the flow equations is also discussed. Well damage or stimulation, and wellbore storage or unloading are given due consideration. The theory developed in this chapter applies in general to laminar, single-phase flow, but deviations due to inertial and turbulent effects are considered. For well testing purposes two-phase flow in the reservoir is treated analytically by the use of an equivalent single-phase mobility.

2-1

1.2   Continuum Approach

When studying flow through porous media, it is observed that the flow channels in the medium are of widely varying cross section and distribution.   Their orientation is random, often causing channels to end abruptly, resulting in dead-end spaces which contribute to the porosity of the medium but not to its permeability to fluids.   These random characteristics make it difficult to predict the flow behaviour from a geometrical study at the pore level, and only a statistical average result can be of any use in practical applications.   A useful concept in this respect is the continuum approach.   This treats the medium as a continuum which is assigned properties such as porosity, permeability, etc., defined at each point.   These properties reflect the bulk behaviour of the medium.

As an example, consider the porosity of a medium.   From a microscopic examination at each point in the medium, the porosity will alternate between 0 and 1.   Consequently, the average porosity as a function of the volume being considered will behave as is shown in Figure 2-1.   It is seen that if the volume over which the porosity is averaged is less than a certain value, known as the Representative Elementary Volume, microscopic effects dominate, while above this value the medium behaves as a continuum at the microscopic level.   If the
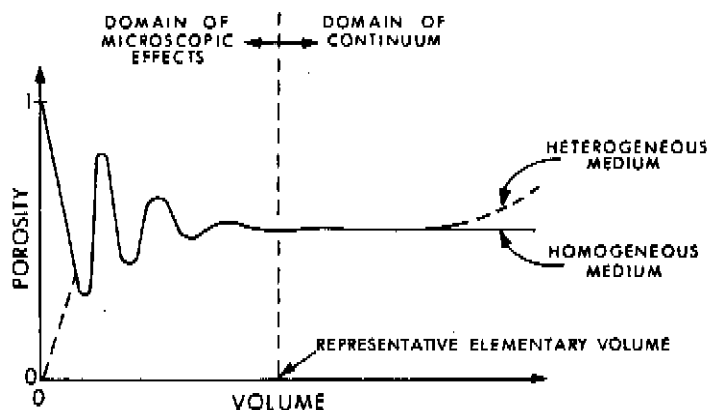
FIGURE 2-1. DEFINITION OF REPRESENTATIVE ELEMENTARY VOLUME

from   Bear (1972, p. 20)

averaging volume is too large and the medium is heterogeneous, the macroscopic variations in porosity will start to show their effect.

Similarly, in practical problems involving fluid flow, the continuum approach is applied to the fluid. Fluids consist of a large number of molecules moving about, colliding with each other and with the walls of the container in which they are placed. A study of fluid flow at the molecular level would present formidable problems which are avoided by treating the fluid as a continuum. As before, a Representative Elementary Volume can be defined as that value of the volume of the fluid below which molecular effects are observable and above which the fluid can be assigned a bulk property, such as density or viscosity. The continuum approach to porous media is discussed extensively in Bear (1972, p. 15) and De Wiest (1969, p. 92).

1.3 Fundamental Equations

The first step towards resolving problems in fluid flow is their expression in mathematical terms through the use of a set of five fundamental equations described below (Govier and Aziz, 1972, p. 119):

1. the constitutive equation, which describes the rheological behaviour of a fluid. It relates the shear stress imposed on a fluid to the resulting shear rate. As is shown in the more detailed treatment in Appendix A, the constitutive equation defines the viscosity of a Newtonian fluid for any given temperature and pressure. For the present development, it is incorporated in the equation of motion, as is discussed in Section 2.1;

2. the momentum equation, which is the application of Newton's second law of motion to a fluid system. This is essentially a force balance on the system;

3. the continuity equation, which is an expression of the law of conservation of mass;

4. the equation of state, which relates the density of a fluid to temperature and pressure;

5. the energy equation, which is an expression of the law of conservation of energy. It takes into account the different types of energy changes and is of greatest interest in non-isothermal flow systems. In the flow of fluids in a gas reservoir, these energy effects may be neglected.

The equations of momentum, continuity, and state, derived from empirical and theoretical considerations, are treated in detail in the sections following. The momentum equation is developed first, followed by the continuity equation. These two are then combined and a relevant equation of state is used to substitute for density in terms of pressure. The result is the basic partial differential equation for flow of fluids through porous media. This equation, in generalized coordinate notation, can be expressed in rectangular, cylindrical, or spherical coordinates, and solved by suitable techniques.

2 MOMENTUM EQUATION

2.1 Theoretical Considerations

The motion of fluids in conduits of arbitrary shapes is described by the Navier-Stokes equations (Bird, Stewart and Lightfoot, 1960, p. 79). These equations are derived by a momentum balance over a differential element in the domain of interest. The equations then reduce to a force balance on a unit volume of the fluid, namely,

$$
\begin{array}{ccc}
\text{mass} \times & \text{pressure} & \text{viscous} & \text{gravitational} \\
\text{acceleration} = & \text{force} + & \text{force} + & \text{force}
\end{array}
$$

The viscous force is due to the shear stress acting on the fluid. This can be expressed in terms of a velocity gradient and viscosity, by using the constitutive equation for the fluid.

For flow in porous media the channels of flow have complex and unknown shapes, and the Navier-Stokes equations can be used only in an average sense. Even then, certain approximations such as laminar flow,

negligible inertial effects, or incompressible fluid may have to be made, or, shape factors related to the assumed geometry of the flow channels may have to be determined empirically. The result of such analyses is similar to Darcy's law or some modification of Darcy's law, depending upon the assumptions made (Hubbert, 1956, Irmay, 1958). In view of these complexities an empirical relationship between pressure gradient and flow velocity is usually resorted to, in order to obtain the momentum equation in a form that can be used practically. Darcy's law, discussed in Section 2-3, is an example of such a relationship.

2.2 Empirical Observations

Steady-state flow of a gas or liquid in the reservoir may be laminar, turbulent, or a combination of both. This was initially demonstrated by Fancher and Lewis (1933) and has since been confirmed by many others. Fancher and Lewis made extensive measurements on the pressure drop-flow rate relationships for the flow of gases through cores of various permeable materials. They expressed their results in terms of a modified Fanning friction factor and a modified Reynolds number (both incorporating the grain diameter) defined respectively as

$$f_g = \frac{g_c \, d_g \, \Delta p}{2 \, u^2 \, \rho \, \Delta x} \tag{2-1}$$

and

$$Re_g = \frac{\rho \, u \, d_g}{\mu} \tag{2-2}$$

where

Δp = pressure difference

g_c = dimension conversion factor

Δx = distance in the x-direction

ρ = fluid density

μ = absolute viscosity

d_g = diameter of an average grain

u = superficial velocity

For each of the porous media investigated, the data of Fancher and Lewis, plotted as f_g versus Re_g on logarithmic coordinates, gave a straight line of slope -1 for low Reynolds numbers. As Re_g became greater than about 1.0, the line began to flatten out due to transition to turbulent flow. Different media were represented by similar curves.

Cornell and Katz (1953) correlated the data for several types of porous media on a single curve, Figure 2-2, by redefining the
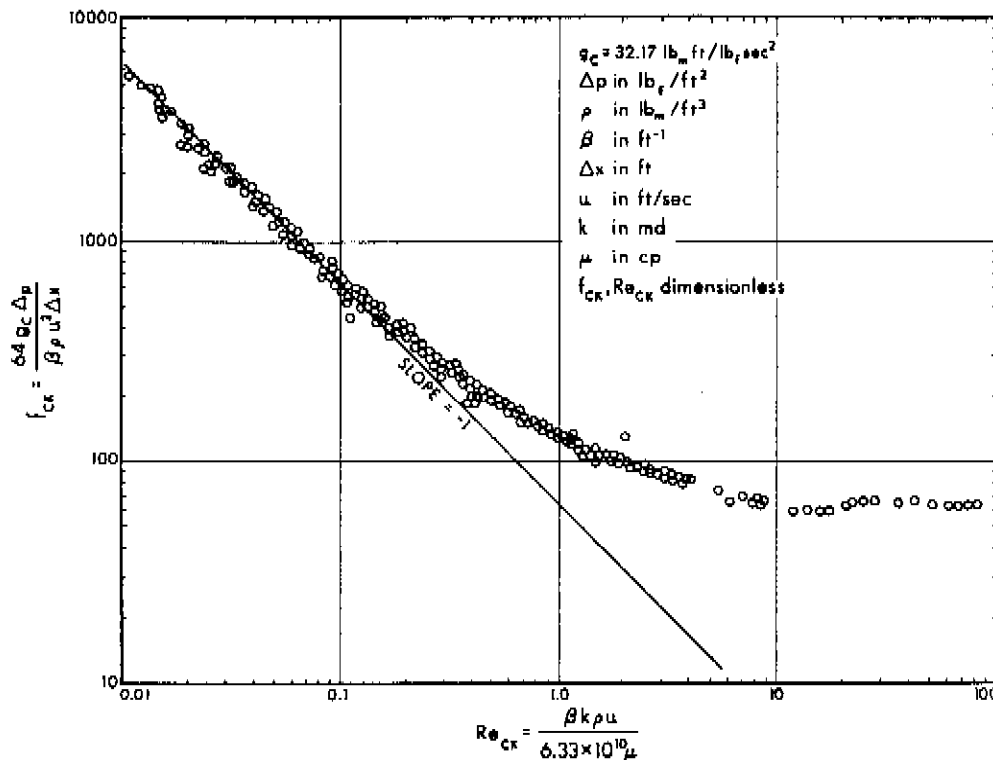
FIGURE 2-2. MODIFIED FRICTION FACTOR FOR FLOW IN POROUS MEDIA
Reprinted with permission from Cornell, D. and D.L.Katz (1953) I.& E.C. 45, 2151
Copyright by the American Chemical Society

friction factor and Reynolds number as follows:

$$f_{CK} = \frac{64\ g_c\ \Delta p}{\beta\ \rho\ u^2\ \Delta x} \qquad (2-3)$$

$$Re_{CK} = \frac{\beta\ k\ \rho\ u}{6.33 \times 10^{10}\ \mu} \qquad (2-4)$$

where

β = a "turbulence factor," which is a constant, characteristic of the porous medium. It may depend on properties such as porosity, tortuousity, permeability, pore shape, and pore size distribution.

k = permeability of the medium

When Figure 2-2 is compared to Figure B-1 for flow of fluids in pipes, the similarity is readily observed; that is, laminar flow at low flow rates gives way, via a transition region, to turbulent flow as the flow rate increases. The transition Reynolds number is different for fluid flow in porous media and for fluid flow in pipes.

Since the characteristics of flow prevailing at low flow rates are different from those at high rates, the equation of motion for each of these flow ranges will be considered separately.

2.3 Low Flow Rates (Laminar Flow Effects)

For one-dimensional steady-state flow of water at a constant rate through a porous medium, Darcy (1856) found from experiments conducted at low and modest flow rates that the pressure drop for a given porous medium was directly proportional to the flow rate. This corresponds to the straight line part, of slope -1, in Figure 2-2. Further experimentation with linear, horizontal flow of different fluids in porous media, led Wyckoff, Botset, Muskat, and Reed (1934) to a form of Darcy's law stated as follows:

$$\frac{q}{A} = u = - \frac{k}{\mu} \frac{dp}{dx} \qquad (2-5)$$

where

q = flow rate

A = gross cross-sectional area

$\frac{dp}{dx}$ = pressure gradient in the x-direction

k = permeability in Darcy's, when q is in cm^3/sec, A is in cm^2, u is in cm/sec, p is in atmospheres, μ is in cp and x is in cm

Equation (2-5) can be expressed as

$$\frac{\mu}{u} = - \frac{k}{u^2} \frac{dp}{dx} \qquad (2\text{-}6)$$

The left-hand side of this equation is proportional to $1/Re_g$ and the right-hand side is proportional to f_g. Thus Equation (2-6) can be written as

$$\frac{1}{Re_g} \propto f_g$$

which shows that a plot of f_g versus Re_g on logarithmic coordinates gives a line of slope -1. This confirms that in Figure 2-2 the straight line portion with slope -1 is equivalent to Darcy's law.

It is possible to generalize the one-dimensional form of Darcy's law given by Equation (2-5). For flow in any direction

$$u = - \frac{k}{\mu} (\nabla p + \rho \, g) \qquad (2\text{-}7)$$

where

u = velocity vector

k = permeability tensor

∇ = gradient operator

g = gravitational vector, $\begin{bmatrix} 0 \\ 0 \\ -g \end{bmatrix}$

g = gravitational acceleration

In the rectangular (Cartesian) coordinate system, the three components of velocity may be expressed as

$$u_x = - \frac{k_x}{\mu} \left(\frac{\partial p}{\partial x} \right) \qquad (2\text{-}8)$$

$$u_y = - \frac{k_y}{\mu} \left(\frac{\partial p}{\partial y} \right) \qquad (2\text{-}9)$$

$$u_z = - \frac{k_z}{\mu} \left(\frac{\partial p}{\partial z} - \rho \, g \right) \qquad (2\text{-}10)$$

In writing the expansion of Equation (2-7), z was assumed to be positive in the vertical downward direction, and the tensor k of the form

$$\begin{bmatrix} k_x & 0 & 0 \\ 0 & k_y & 0 \\ 0 & 0 & k_z \end{bmatrix}$$

The medium was assumed to be anisotropic, hence the permeability was different in the three coordinate directions. The medium is isotropic if, at all points

$$k_x = k_y = k_z = k$$

If throughout the medium the permeability is independent of position, the medium is said to be homogeneous. Otherwise the system is heterogeneous.

A potential, E, may be defined (Hubbert, 1940) as

$$E = \int_{p^0}^{p} \frac{1}{\rho} \, dp - z \, g \qquad (2\text{-}11)$$

where

ρ = density as a function of p

z = vertical downward distance

p^0 = arbitrary reference pressure

Darcy's law in terms of the potential is

$$u = - \frac{k \, \rho}{\mu} \, \nabla E \qquad (2\text{-}12)$$

For liquids flowing in a homogeneous medium, the permeability, k, is found to be independent of the flowing fluid and is, thus, a property of the medium. However, in the case of gas flow, Klinkenberg (1941) observed that when the pores of the medium were of the same order of size as the mean free path of the gas molecules, slippage occurred at the fluid-solid boundary, and the permeability to gas was not constant. Under such conditions, which become significant at low pressures,

$$k = k_L\left(1 + \frac{b_1}{p}\right) \tag{2-13}$$

where

k_L = permeability of the medium to gas at infinite pressure (its value should be equal to the permeability of the medium to a liquid)

b_1 = a constant dependent on the gas-porous medium system

Dranchuk and Flores (1973) indicated that for very low permeability reservoirs (0.1 md), under certain boundary conditions, the Klinkenberg effect is noticeable even at high reservoir pressures (2000 psi).

2.4 High Flow Rates (Inertial and Turbulent Flow Effects)

As the flow velocity is increased, deviations from Darcy's law are observed. Various investigators attributed this to turbulent flow (Fancher and Lewis, 1933, Elenbaas and Katz, 1948, Cornell and Katz, 1953) or inertial effects (Hubbert, 1956, Houpeurt, 1959). The generally accepted explanation (Wright, 1968) is that, as the velocity is increased, initially deviation is due to inertial effects, followed at even higher velocities by turbulent effects. Hubbert (1956) noted deviation from Darcy's law at a Reynolds number of flow of about 1 (based on the grain diameter of unconsolidated media), whereas turbulence was not observed until the Reynolds number approached 600. The transition from purely laminar flow to fully turbulent flow covers a

wide range of flow rates. This range of flow rates, for horizontal steady state flow, is adequately represented by a quadratic equation (Forchheimer, 1901):

$$-\frac{dp}{dx} = \frac{\mu}{k} u + \beta \rho u^2 \tag{2-14}$$

Equation (2-14) which incorporates laminar, inertial, and turbulent (LIT) flow effects is a general momentum balance equation for steady-state flow. It may be rearranged to the form

$$u = -\delta \frac{k}{\mu} \frac{dp}{dx} \tag{2-15}$$

where

$$\delta = 1 \Big/ \left(1 + \frac{\beta \rho k u}{\mu} \right)$$ is the LIT flow correction factor (Govier, 1961, Wattenbarger and Ramey, 1968)

When $\delta = 1.0$, Equation (2-15) is equivalent to Darcy's law.

In an anisotropic medium, δ is different in the x, y, or z directions. Flow through such a medium under conditions where gravitational effects may be neglected is then given by

$$u = -\frac{1}{\mu} k \, \delta \, \nabla p \tag{2-16}$$

where

$$\delta = \begin{bmatrix} \delta_x & 0 & 0 \\ 0 & \delta_y & 0 \\ 0 & 0 & \delta_z \end{bmatrix}$$

It is seen that Equation (2-16) will represent both laminar flow and flow where inertial-turbulent (IT) flow effects are present. It will be referred to as the generalized laminar-inertial-turbulent (LIT) momentum balance equation for steady-state flow.

3 EQUATION OF CONTINUITY

The law of conservation of mass, also called the equation of continuity, states that, for any given system

$$\begin{array}{ccc} \text{rate of mass} \\ \text{accumulation} \end{array} = \begin{array}{c} \text{rate of mass} \\ \text{flow in} \end{array} - \begin{array}{c} \text{rate of mass} \\ \text{flow out} \end{array}$$

By performing a mass balance over a Representative Elementary Volume of the porous medium, the equation of continuity is obtained (Katz et al., 1959, p. 407, Bird, Stewart and Lightfoot, 1960, p. 75, Matthews and Russell, 1967, p. 6) in generalized coordinate notation

$$- \frac{\partial}{\partial t} (\phi \rho) = \nabla \cdot (\rho \mathbf{u}) \tag{2-17}$$

where

$$\phi \qquad = \text{ porosity of the medium}$$
$$\nabla \cdot (\rho \mathbf{u}) = \text{ divergence of } \rho \mathbf{u}$$

The definitions of the ∇ operators are given in Table 2-1, in terms of rectangular, cylindrical, and spherical coordinates (Bird et al., 1960, p. 738).

The term on the left-hand side of Equation (2-17) represents the accumulation of fluid in the pores and equals zero for steady-state conditions. The right-hand side term represents the difference in the mass of fluid leaving and entering the Representative Elementary Volume.

The one-dimensional form of Equation (2.17) is obtained by making appropriate substitutions from Table 2-1. Thus in rectangular coordinates, if flow is assumed to be linear, in the x-direction, the equation of continuity is given by

$$- \frac{\partial}{\partial t} (\phi \rho) = \frac{\partial}{\partial x} (\rho u) \tag{2-18}$$

Similarly, in radial-cylindrical coordinates, if flow is considered to be radial, in the r-direction only, the equation of continuity is given by

THREE-DIMENSIONAL CASE	ONE-DIMENSIONAL CASE

Rectangular Coordinates (x,y,z)

$$(\nabla \cdot \Phi) = \frac{\partial \Phi_x}{\partial x} + \frac{\partial \Phi_y}{\partial y} + \frac{\partial \Phi_z}{\partial z}$$

$$(\nabla \cdot \Phi) = \frac{\partial \Phi_x}{\partial x}$$

$$(\nabla^2 \phi) = \frac{\partial^2 \phi}{\partial x^2} + \frac{\partial^2 \phi}{\partial y^2} + \frac{\partial^2 \phi}{\partial z^2}$$

$$(\nabla^2 \phi) = \frac{\partial^2 \phi}{\partial x^2}$$

Cylindrical Coordinates (r,θ,z)

$$(\nabla \cdot \Phi) = \frac{1}{r} \frac{\partial}{\partial r}(r \, \Phi_r) + \frac{1}{r} \frac{\partial \Phi_\theta}{\partial \theta} + \frac{\partial \Phi_z}{\partial z}$$

$$(\nabla \cdot \Phi) = \frac{1}{r} \frac{\partial}{\partial r}(r \, \Phi_r)$$

$$(\nabla^2 \phi) = \frac{1}{r} \frac{\partial}{\partial r}\left(r \frac{\partial \phi}{\partial r}\right) + \frac{1}{r^2} \frac{\partial^2 \phi}{\partial \theta^2} + \frac{\partial^2 \phi}{\partial z^2}$$

$$(\nabla^2 \phi) = \frac{1}{r} \frac{\partial}{\partial r}\left(r \frac{\partial \phi}{\partial r}\right)$$

Spherical Coordinates (r,θ,σ)

$$(\nabla \cdot \Phi) = \frac{1}{r^2} \frac{\partial}{\partial r}(r^2 \, \Phi_r) + \frac{1}{r \, \sin\theta} \frac{\partial}{\partial \theta}(\Phi_\theta \, \sin\theta) + \frac{1}{r \, \sin\theta} \frac{\partial \Phi_\sigma}{\partial \sigma}$$

$$(\nabla \cdot \Phi) = \frac{1}{r^2} \frac{\partial}{\partial r}(r^2 \, \Phi_r)$$

$$(\nabla^2 \phi) = \frac{1}{r^2} \frac{\partial}{\partial r}\left(r^2 \frac{\partial \phi}{\partial r}\right) + \frac{1}{r^2 \sin\theta} \frac{\partial}{\partial \theta}\left(\sin\theta \frac{\partial \phi}{\partial \theta}\right) + \frac{1}{r^2 \sin^2\theta} \frac{\partial^2 \phi}{\partial \sigma^2}$$

$$(\nabla^2 \phi) = \frac{1}{r^2} \frac{\partial}{\partial r}\left(r^2 \frac{\partial \phi}{\partial r}\right)$$

TABLE 2-1. DEFINITIONS OF ∇-OPERATOR IN VARIOUS COORDINATE SYSTEMS
(Φ IS AN ARBITRARY SCALAR, Φ IS AN ARBITRARY VECTOR)

From Bird, Stewart and Lightfoot (1960, p. 738)

$$-\frac{\partial}{\partial t}(\phi\,\rho) = \frac{1}{r}\frac{\partial}{\partial r}(r\,\rho\,u) \qquad\qquad (2-19)$$

4   EQUATIONS OF STATE

An equation relating the variation of density of a fluid with pressure and temperature is known as an equation of state. Such an equation is needed to combine Equation (2-17), the continuity equation which is in terms of density, with Equation (2-16), the LIT momentum balance equation which is in terms of pressure. Equations of state of various complexities (two to eight parameters) have been proposed, based on theoretical or semi-theoretical considerations. The van der Waal and Redlich-Kwong equations are applicable to gases but give only rough approximations for liquids. The Beattie-Bridgeman equation is suitable for all gases but not for liquids. The Benedict-Webb-Rubin equation is said to be applicable to all gases and saturated liquids, but being an eight parameter equation, implicit in density, it is quite cumbersome for regular everyday use (Govier and Aziz, 1972, p. 69).

4.1   Liquids

For prediction of liquid densities the equations of state mentioned above are so cumbersome and inaccurate that their use is not justified. For a fixed mass of liquid at constant temperature, the compressibility of a liquid is defined as the relative change in volume per unit change in pressure

$$c = -\frac{1}{V}\left.\frac{\partial V}{\partial p}\right|_T \qquad\qquad (2-20)$$

where

c = compressibility of the liquid

V = volume

T = temperature

In terms of the density, Equation (2-20) may be expressed as

$$c = \frac{1}{\rho} \left.\frac{\partial \rho}{\partial p}\right|_T \tag{2-21}$$

For a liquid at constant temperature, c may be considered constant, and Equation (2-21) may be integrated between the limits ρ^0 and ρ to yield:

$$\rho = \rho^0 \, e^{c(p-p^0)} \tag{2-22}$$

where

ρ^0 = density at some reference pressure p^0

This equation, which is the pressure-density relationship for a liquid under isothermal conditions, is applicable to any fluid of constant compressibility.

4.2 Gases

For engineering calculations, the most practical form of the equation of state for a real gas is given by Equation (A-2):

$$\rho = \frac{M}{R\,T}\frac{p}{Z} \tag{2-23}$$

For isothermal conditions,

$$\left.\frac{\partial \rho}{\partial p}\right|_T = \frac{M}{R\,T\,Z} + \frac{M}{R\,T}\, p \left.\frac{\partial}{\partial p}\,(1/Z)\right|_T \tag{2-24}$$

Combining Equations (2-21), (2-23) and (2-24) gives

$$c = \frac{1}{p} + Z \left.\frac{\partial}{\partial p}\,(1/Z)\right|_T$$

$$= \frac{1}{p} - \frac{1}{Z}\left.\frac{\partial Z}{\partial p}\right|_T \tag{2-25}$$

The compressibility factor, Z, is a correction factor which defines the deviation of a real gas from ideal gas behaviour

(Appendix A). It should not be confused with the compressibility, c, which is the coefficient of isothermal compression of any given substance. For an ideal gas Z is constant (=1.0) and $c = \frac{1}{p}$. For a real gas Z may vary with pressure, and $c = \frac{1}{p}$ only in the range of pressures where $\frac{\partial Z}{\partial p} = 0$. The variation of compressibility with temperature and pressure is discussed in Appendix A.

Under certain conditions, p > 2000 psi (Matthews and Russell, 1967, p. 25), a gas can be treated as a fluid of small and constant compressibility, and its pressure-density relationship at constant temperature is adequately represented by Equation (2-22), which is the equation of state for a liquid. Houpeurt (1959) showed that the closer p^0 is chosen to p the more applicable is this equation of state to a gas.

5 THE FLOW EQUATIONS

Combining the continuity Equation (2-17) with the LIT momentum balance Equation (2-16) results in

$$\frac{\partial}{\partial t} (\phi \, \rho) = \nabla \cdot \left[\rho \, \frac{1}{\mu} \, k \, \delta \, \nabla p \right] \tag{2-26}$$

This is a general form of the flow equation relating density, porosity, viscosity, permeability, turbulence factor, time, distance, and pressure. If the appropriate equation of state is introduced into the above equation, a parital differential equation is then obtained which describes the flow of fluids in the system in terms of porosity, viscosity, permeability, LIT flow correction factor, time, distance, and pressure. This equation is non-linear and, without further simplification, it can only be solved by numerical techniques. The simplified forms of the flow equation for a slightly compressible fluid and a highly compressible fluid are given below.

A liquid (or gas at high pressure) at constant temperature may be treated as a fluid of small compressibility. For such a fluid, it is reasonable to assume that c is constant, and that Equation (2-22) is applicable. Substituting for ρ in Equation (2-26) yields

$$\frac{\partial}{\partial t}\left[\phi \rho^0 \, e^{c(p-p^0)}\right] = \rho^0 \, e^{c(p-p^0)} \, \nabla \cdot \left[\frac{1}{\mu} \, k \, \delta \, \nabla p\right]$$

$$+ \left[\frac{1}{\mu} \, k \, \delta \, \nabla p\right] \cdot \nabla \left[\rho^0 \, e^{c(p-p^0)}\right] \qquad (2\text{-}27)$$

which may be rearranged to

$$c \, \phi \, \frac{\partial p}{\partial t} + \frac{\partial \phi}{\partial t} = \nabla \cdot \left[\frac{1}{\mu} \, k \, \delta \, \nabla p\right] + c\left[\frac{1}{\mu} \, k \, \delta \, \nabla p\right] \cdot \nabla p \qquad (2\text{-}28)$$

Ordinarily, a gas is a highly compressible fluid, and Equation (2-23) is applicable. Substituting for ρ in Equation (2-26) gives

$$\frac{\partial}{\partial t}\left(\phi \, \frac{M}{RT} \, \frac{p}{Z}\right) = \nabla \cdot \left[\frac{M}{RT} \, \frac{p}{\mu Z} \, k \, \delta \, \nabla p\right] \qquad (2\text{-}29)$$

which, for isothermal conditions, may be simplified to

$$\frac{\partial}{\partial t}\left(\phi \, \frac{p}{Z}\right) = \nabla \cdot \left[\frac{p}{\mu Z} \, k \, \delta \, \nabla p\right] \qquad (2\text{-}30)$$

5.1 Overall Assumptions

The flow equations given above in generalized form, can usually be solved only by numerical techniques, some of which will be discussed in Section 8. However, by applying a few simplifying assumptions, these equations may be linearized, and, for certain boundary conditions, solved analytically. The assumptions which are applicable throughout the forthcoming theoretical development, are summarized below:

    a.   Isothermal conditions prevail--assumed in developing Equations (2-20), (2-21), (2-22), (2-25), (2-28), and (2-30);

    b.   Gravitational effects are negligible--assumed in developing Equation (2-16);·

c. The flowing fluid is single phase--implicit in the form
of Darcy's law used in this text.

Further simplifying assumptions are

d. The medium is homogeneous, isotropic and incompressible,
and the porosity is constant;

e. Flow is laminar, $\delta = 1$.

The assumption of laminar flow holds well for liquids, but,
under some conditions, not so well for gases. This will be compensated
for, by treating separately, in Section 9.2, the supplementary pressure
drop due to inertial-turbulent (IT) flow effects.

5.2 The Equation for Liquid Flow
(In Terms of Pressure)

In addition to the overall assumptions (a), (b), (c), (d), and
(e), the following will be assumed for the case of slightly compressible
fluids (liquid or a gas at high pressure):

f. Permeability is independent of pressure;

g. Fluid viscosity is constant and independent of pressure;

h. Fluid compressibility is small and constant;

i. Pressure gradients are small.

Assumptions (h) and (i) allow terms like $c(\nabla p)^2$ to be
neglected. When this is done, the second term on the right-hand side of
Equation (2-28) becomes zero.

When assumptions (a) to (i) are applied to Equation (2-28),
the flow equation for a slightly compressible fluid becomes (Collins,
1961, p. 72)

$$\nabla^2 p = \frac{\phi \, \mu \, c}{k} \frac{\partial p}{\partial t} \qquad (2\text{-}31)$$

5.3 An Equation for Gas Flow
(In Terms of Pressure)

By treating a gas as a highly compressible fluid, and applying assumptions (a) to (f), Equation (2-30) may be written as

$$\frac{\partial}{\partial t}\left(\frac{p}{Z}\right) = \frac{k}{\phi} \; \nabla \cdot \left[\frac{p}{\mu Z} \; \nabla p\right] \qquad (2\text{-}32)$$

The left-hand side of this equation may be expanded as

$$\frac{\partial}{\partial t}\left(\frac{p}{Z}\right) = \frac{1}{Z}\frac{\partial p}{\partial t} + p\frac{\partial}{\partial t}\left(\frac{1}{Z}\right)$$

$$= \frac{1}{Z}\frac{\partial p}{\partial t} + p\frac{d}{dp}\left(\frac{1}{Z}\right)\frac{\partial p}{\partial t}$$

$$= \frac{p}{Z}\frac{\partial p}{\partial t}\left[\frac{1}{p} - \frac{1}{Z}\frac{dZ}{dp}\right] \qquad (2\text{-}33)$$

Substituting Equation (2-25) in Equation (2-33) gives

$$\frac{\partial}{\partial t}\left(\frac{p}{Z}\right) = c\,\frac{p}{Z}\frac{\partial p}{\partial t} \qquad (2\text{-}34)$$

Equations (2-32) and (2-34) may be combined and rearranged to yield

$$\nabla^2 p - \frac{d}{dp}\left[\ln\left(\frac{\mu Z}{p}\right)\right](\nabla p)^2 = \frac{\phi\,\mu\,c}{k}\frac{\partial p}{\partial t} \qquad (2\text{-}35)$$

Two different approaches, involving different assumptions, may be followed at this stage to further simplify Equation (2-35). The assumptions to be made here are in addition to (a), (b), (c), (d), and (e)

Case 1. i. Pressure gradients are assumed to be small. This means that $(\nabla p)^2 \to 0$, and Equation (2-35) reduces to

$$\nabla^2 p = \frac{\phi\,\mu\,c}{k}\frac{\partial p}{\partial t} \qquad (2\text{-}36)$$

which is the same as Equation (2-31) for the flow of a
slightly compressible fluid.

Case 2.   j.   The quantity $\frac{p}{\mu Z}$ is assumed to be constant. Under this
condition Equation (2-35) again reduces to Equation (2-36).

5.4 An Equation for Gas Flow (In Terms of Pressure-Squared)

Equation (2-32) may be expanded into several different terms.
In particular, noting that

$$p\ \nabla p = \frac{1}{2}\ \nabla p^2 \qquad \text{and} \qquad p\ \partial p = \frac{1}{2}\ \partial p^2$$

Equations (2-32) and (2-34) may be combined and rearranged to give
(Al-Hussainy, 1967, p. 10)

$$\nabla^2 p^2 - \frac{d}{dp^2}\left[\ln(\mu Z)\right](\nabla p^2)^2 = \frac{\phi\ \mu\ c}{k}\ \frac{\partial p^2}{\partial t} \tag{2-37}$$

In order to simplify this equation further, there are three
different sets of assumptions, in addition to (a), (b), (c), (d), (e),
and (f), that may be made:

Case 1.   k.   The product μZ is assumed to be constant. Then Equation
(2-37) reduces to

$$\nabla^2 p^2 = \frac{\phi\ \mu\ c}{k}\ \frac{\partial p^2}{\partial t} \tag{2-38}$$

Case 2.   i.   Pressure gradients are assumed to be small. This means
that $(\nabla p^2)^2 \to 0$, and Equation (2-37) again reduces to
Equation (2-38).

Case 3.   l.   Ideal gas behaviour is assumed ($Z=1$), and

        g.   Gas viscosity is constant and independent of pressure.
Under these conditions Equation (2-32) reduces to

$$\nabla^2 p^2 = \frac{\phi \mu}{k \, p} \frac{\partial p^2}{\partial t} \tag{2-39}$$

The above equation may also be derived directly from Equation (2-38) by noting that for an ideal gas $c = \frac{1}{p}$.

The additional assumptions (g), (i), (j), (k), and (l), made in Sections 5.3 and 5.4, may cause a significant degree of inaccuracy. For example, the assumption of small pressure gradients leads to errors in estimating pressure distributions for tight formations. Since this assumption is implicit in all of the currently used pressure drawdown and build-up methods, which are based upon ideal gas flow solutions (Equation 2-39) or liquid flow analogies (Equation 2-36), it is desirable to eliminate it and the other assumptions mentioned above. This can be accomplished by the method described in the next section.

5.5 A More Rigorous Equation for Gas Flow
(In Terms of Pseudo-Pressure)

The approximations of the preceding sections may be avoided and a more rigorous treatment applied to gas flow by introducing the concept of a pseudo-pressure, ψ, sometimes called "the real gas potential." Using ψ the variation of μ and Z with pressure can be accommodated, and only the overall assumptions (a), (b), (c), (d), and (e) and assumption (f) are required (assumption (f) can be dispensed with as shown later if the variation of k with pressure is known).

If ψ, the pseudo-pressure, is defined (Al-Hussainy, 1965) as

$$\psi \equiv 2 \int_{p^0}^{p} \frac{p}{\mu Z} \, dp \tag{2-40}$$

where p^0 is some specified reference pressure then

$$\nabla \psi = \frac{\partial \psi}{\partial p} \nabla p = 2 \frac{p}{\mu Z} \nabla p \tag{2-41}$$

and

$$\frac{\partial \psi}{\partial t} = 2 \frac{p}{\mu Z} \frac{\partial p}{\partial t} \qquad (2\text{-}42)$$

Rewriting Equation (2-34) as

$$\frac{\partial}{\partial t}\left(\frac{p}{Z}\right) = \mu \, c \, \frac{p}{\mu Z} \frac{\partial p}{\partial t} \qquad (2\text{-}43)$$

and substituting Equations (2-40), (2-41), (2-42), and (2-43) into
(2-32) gives:

$$\nabla^2 \psi = \frac{\phi \, \mu \, c}{k} \frac{\partial \psi}{\partial t} \qquad (2\text{-}44)$$

This equation is seen to be very similar to Equations (2-36)
and (2-38) except that the pressure and pressure-squared variables are
replaced by ψ, the pseudo-pressure. It must be noted, however, that
Equation (2-44) was derived without making any of the assumptions (g),
(i), (j), (k), or (l).

As mentioned earlier, if the variation of permeability with
pressure is known, an alternative definition of pseudo-pressure
accommodating k can be used.

$$\psi' \equiv 2 \int_{p^0}^{p} k \, \frac{p}{\mu Z} \, dp \qquad (2\text{-}45)$$

Using this definition, an equation similar to Equation (2-44) would
result.

$$\nabla^2 \psi' = \phi \, \mu \, c \, \frac{\partial \psi'}{\partial t}$$

In calculating ψ' not only the gas properties μ and Z, but also the
reservoir parameter k have to be known as functions of pressure. This
is a practical inconvenience when contrasted with calculations of ψ
which involve gas properties alone. Nevertheless, it is clear that

variations of k with pressure may be included in the pseudo-pressure treatment when desired.

Pseudo-Pressure

Transformations similar to the pseudo-pressure function have been used by various authors in fields ranging from heat transfer to hydrology (Al-Hussainy, Ramey and Crawford, 1966). For petroleum engineering applications such transformations were suggested by Carter (1962), Hurst, Goodson and Leeser (1963), and Russell, Goodrich, Perry and Bruskotter (1966). Various names have been used to describe this function. Muskat called the transformation a "potential," while a similar substitution in heat transfer was termed an "effective potential." Russian literature refers to it as the "Leibenzon transformation." Al-Hussainy et al. (1966) originally used the term "real gas potential" but finally decided on "real gas pseudo-pressure." ψ has the unit of (pressure)^2/viscosity and could be called a "modified pressure squared." It is seen then, that no one simple name describes this transformation adequately. Noting that ψ may replace either the "pressure" or "pressure squared" terms of Sections 5.3 and 5.4, the name "pseudo-pressure" will be used for it throughout the text.

In all problems involving the use of ψ, it is recommended that, first, a $\psi - p$ conversion table or plot be constructed (a sample curve is shown in Figure 2-4). Details of how ψ is calculated from p, μ and Z will be given later. Once the $\psi - p$ conversion has been obtained, any pressure is easily converted to ψ and vice versa. Then using ψ as a working variable is as easy as having to calculate p^2. For a given gas, the $\psi - p$ curve is valid only for the temperature for which it was developed. Gas reservoirs are in most cases isothermal, and their fluid composition generally does not vary significantly from well to well. In such cases only one $\psi - p$ curve serves for the entire reservoir. Where either the temperature or the gas composition of a particular reservoir is not uniform throughout, a separate $\psi - p$ curve is required for each well.

It is instructive to see how Equation (2-44) relates to

Equations (2-36) and (2-38), that is, how ψ is related to p and to p^2.
If a plot of (μZ) versus p is drawn for a natural gas, the graph looks
as in Figure 2-3. From the plot it can be seen that for this gas at
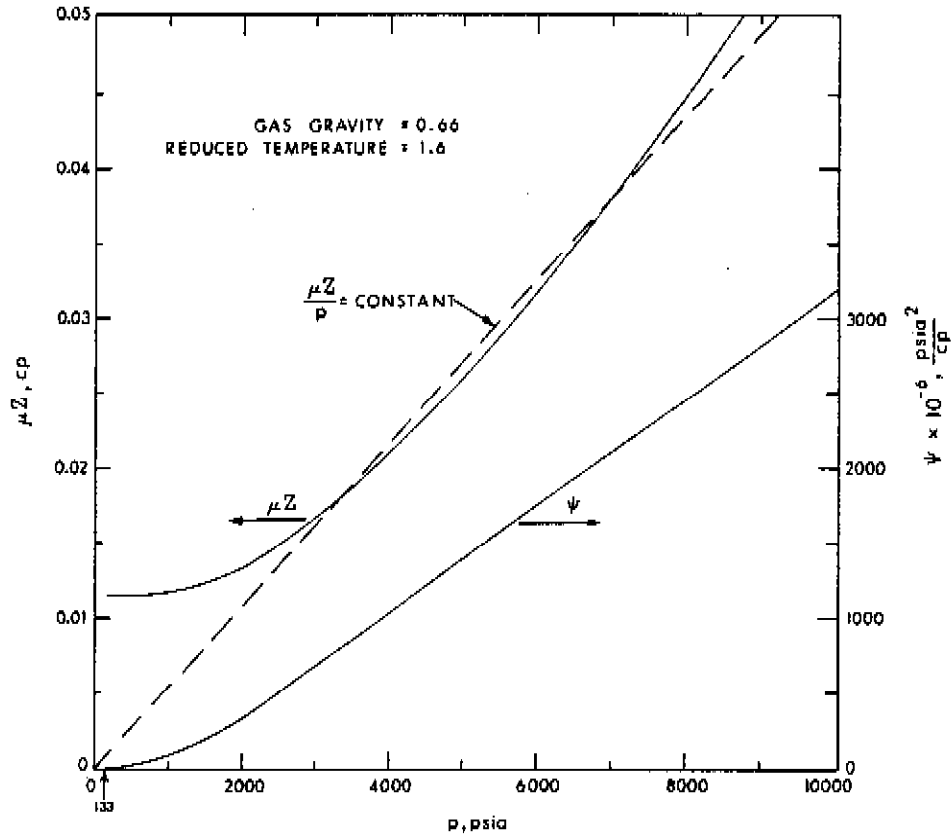
FIGURE 2-3. VARIATION OF ψ AND μZ WITH PRESSURE

From Wattenbarger (1967, p. 99)

low pressure (μZ) is almost constant at ($\mu_i Z_i$), where subscript i
refers to initial conditions, that is,

$$\mu Z = \mu_i Z_i$$

so that

$$\psi = \frac{2}{\mu_i Z_i} \int_{p^0}^{p} p \; dp = \frac{1}{\mu_i Z_i} \, p^2 \qquad \text{for} \quad p^0 = 0$$

This shows that Equation (2-44) reverts to Equation (2-38) and that the flow equation in terms of p^2 is valid for this gas at low pressures, less than about 2000 psia (Wattenbarger, 1967, p. 98).

At the higher pressures, the figure shows that the slope is nearly constant, that is,

$$\frac{p}{\mu Z} = \frac{p_1}{\mu_1 Z_1}$$

so that

$$\psi = \frac{2\ p_1}{\mu_1 Z_1} \int_{p^0}^{p} dp = \frac{2\ p_1}{\mu_1 Z_1}\ p \qquad\qquad \text{for}\quad p^0 = 0$$

This shows that Equation (2-44) reverts to Equation (2-36), and that the flow equation in terms of p applies to this gas flowing at pressures greater than about 2000 psi (Matthews and Russell, 1967, p. 25).

Although the above relationship of ψ to p and p^2 is very enlightening, it has two important drawbacks.

1. The interrelationship of p and μZ is not so simple for most sweet, natural gases since not only the gas composition, but also the temperature of the gas, has a marked effect on this relationship.

2. It lends itself to the generalization that, at low pressures, the p^2 approach is valid and, at high pressures, the p approach is more applicable. This is not always true.

These two points will be explained further in Section 11.2.

To obtain the ψ - p conversion for any gas at a given temperature, the values of $2\ \dfrac{p}{\mu Z}$ are calculated for several values of p, using experimental values of μ and Z whenever possible (otherwise μ and Z may be obtained from the standard generalized correlations given in Appendix A). $2\ \dfrac{p}{\mu Z}$ is plotted versus p and the area under the curve from any convenient reference pressure, p^0, to p is the value of ψ

corresponding to p. Al-Hussainy and Ramey (1966) show how this may be done by simple numerical integration in tabular form. The calculation procedure is shown in Example 2-1 and is applicable to any gas (sweet or sour) provided the correct values of μ and Z are used.

For sweet gases, using the generalized correlations of Carr, Kobayashi and Burrows (1954) for μ and, those of Standing and Katz (1942) for Z, Al-Hussainy, Ramey and Crawford (1966) published tables and plots of $\mu_1\psi/(2p_c^2 T_r)$ in terms of pseudo-reduced properties, arbitrarily choosing $0.2\,p_c$ as the reference pressure. Zana and Thomas (1970) evaluated ψ for sour natural gases using the Robinson, Macrygeorgos and Govier (1960) correction ratios to calculate Z. Their reference pressure was $1.0\,p_c$.

In all problems where the pressure difference and therefore the pseudo-pressure difference is of importance, rather than the pressure itself, the reference pressure used as a base is immaterial. That is $(\psi_1 - \psi_2)$ representing $(p_1 - p_2)$ is the same regardless of the base pressure used. In practice, when calculating ψ, it may be convenient to use zero as the reference pressure. In such a case

$$\left.\frac{p}{\mu Z}\right|_{p=0} \quad \text{is defined as being equal to zero.}$$

In any case ψ may be easily converted from one reference pressure to another; for example,

$$\left[\psi\right]_{p^0}^{p} = \left[\psi\right]_0^{p} - \left[\psi\right]_0^{p^0} \tag{2-47}$$

A computer program for calculating ψ as a function of p is listed in Appendix D. Using this program, the viscosity correlations of Carr, Kobayashi and Burrows (1954), the compressibility factor correlation of Standing and Katz (1942) as computerized by Dranchuk, Purvis and Robinson (1974), and using zero as the reference pressure, a reduced pseudo-pressure tabulation for sweet gases has been prepared and is presented in Table 2-2. The computer program may also be used for calculating ψ for sour gases.

PSEUDO-REDUCED PRESSURE p_r	VALUES OF $\psi_r = \dfrac{\psi \mu_1}{2 p_c^2} = \displaystyle\int_0^{p_r} \dfrac{p_r\, dp_r}{\left(\frac{\mu}{\mu_1}\right)Z}$ FOR PSEUDO-REDUCED TEMPERATURE T_r OF							
	1.05	1.15	1.30	1.50	1.75	2.00	2.50	3.00
0.10	0.0051	0.0051	0.0051	0.0050	0.0050	0.0050	0.0050	0.0050
0.20	0.0208	0.0206	0.0204	0.0202	0.0201	0.0201	0.0200	0.0200
0.30	0.0475	0.0467	0.0461	0.0456	0.0453	0.0452	0.0451	0.0450
0.40	0.0856	0.0839	0.0824	0.0813	0.0807	0.0803	0.0801	0.0800
0.50	0.1355	0.1322	0.1293	0.1272	0.1261	0.1254	0.1250	0.1249
0.60	0.1980	0.1921	0.1869	0.1833	0.1814	0.1803	0.1798	0.1797
0.70	0.2733	0.2637	0.2556	0.2498	0.2468	0.2452	0.2445	0.2443
0.80	0.3620	0.3474	0.3355	0.3266	0.3222	0.3198	0.3189	0.3187
0.90	0.4638	0.4437	0.4262	0.4134	0.4073	0.4039	0.4030	0.4029
1.00	0.5780	0.5529	0.5276	0.5095	0.5019	0.4974	0.4968	0.4967
1.10	0.7053	0.6746	0.6400	0.6154	0.6059	0.6003	0.6004	0.6003
1.20	0.8525	0.8083	0.7638	0.7314	0.7192	0.7131	0.7136	0.7134
1.30	1.0318	0.9539	0.8983	0.8574	0.8416	0.8356	0.8362	0.8360
1.40	1.2392	1.1114	1.0431	0.9930	0.9732	0.9676	0.9681	0.9680
1.50	1.4482	1.2807	1.1978	1.1381	1.1142	1.1091	1.1091	1.1095
1.60	1.6468	1.4616	1.3620	1.2923	1.2645	1.2599	1.2592	1.2602
1.70	1.8359	1.6516	1.5356	1.4557	1.4240	1.4199	1.4183	1.4203
1.80	2.0176	1.8476	1.7182	1.6280	1.5923	1.5887	1.5862	1.5895
1.90	2.1926	2.0472	1.9090	1.8089	1.7695	1.7663	1.7632	1.7679
2.00	2.3619	2.2476	2.1068	1.9982	1.9553	1.9526	1.9492	1.9554
2.10	2.5272	2.4499	2.3109	2.1954	2.1495	2.1472	2.1442	2.1519
2.20	2.6899	2.6546	2.5206	2.3999	2.3519	2.3499	2.3479	2.3575
2.30	2.8500	2.8603	2.7354	2.6116	2.5623	2.5605	2.5602	2.5721
2.40	3.0074	3.0658	2.9549	2.8302	2.7806	2.7788	2.7811	2.7956
2.50	3.1622	3.2701	3.1786	3.0554	3.0067	3.0048	3.0105	3.0280
2.60	3.3143	3.4726	3.4060	3.2872	3.2403	3.2383	3.2482	3.2691
2.70	3.4638	3.6727	3.6367	3.5251	3.4813	3.4792	3.4942	3.5191
2.80	3.6108	3.8701	3.8700	3.7690	3.7297	3.7272	3.7483	3.7776
2.90	3.7553	4.0646	4.1056	4.0185	3.9851	3.9824	4.0106	4.0449
3.00	3.8974	4.2560	4.3429	4.2735	4.2474	4.2444	4.2809	4.3206
3.25	4.2456	4.7260	4.9417	4.9303	4.9299	4.9296	4.9903	5.0465
3.50	4.5859	5.1857	5.5444	5.6102	5.6466	5.6563	5.7459	5.8235
3.75	4.9183	5.6338	6.1461	6.3089	6.3944	6.4224	6.5462	6.6503
4.00	5.2430	6.0700	6.7434	7.0228	7.1705	7.2259	7.3894	7.5257
4.25	5.5622	6.4973	7.3356	7.7491	7.9713	8.0629	8.2745	8.4484
4.50	5.8776	6.9181	7.9228	8.4853	8.7933	8.9296	9.2004	9.4168
4.75	6.1892	7.3324	8.5032	9.2289	9.6339	9.8239	10.1654	10.4297
5.00	6.4972	7.7399	9.0758	9.9772	10.4907	10.7437	11.1682	11.4859
5.25	6.8011	8.1406	9.6400	10.7283	11.3616	11.6870	12.2073	12.5841
5.50	7.1014	8.5345	10.1951	11.4803	12.2446	12.6520	13.2811	13.7232
5.75	7.3980	8.9218	10.7409	12.2318	13.1379	13.6368	14.3883	14.9020
6.00	7.6909	9.3025	11.2773	12.9815	14.0397	14.6399	15.5274	16.1193
6.25	7.9809	9.6780	11.8066	13.7293	14.9488	15.6588	16.6956	17.3731
6.50	8.2688	10.0495	12.3311	14.4749	15.8643	16.6915	17.8901	18.6617
6.75	8.5546	10.4170	12.8504	15.2177	16.7846	17.7366	19.1096	19.9841
7.00	8.8383	10.7805	13.3644	15.9569	17.7087	18.7927	20.3527	21.3390
7.25	9.1198	11.1400	13.8730	16.6917	18.6356	19.8589	21.6184	22.7253
7.50	9.3992	11.4956	14.3760	17.4219	19.5644	20.9337	22.9053	24.1421
7.75	9.6764	11.8473	14.8735	18.1471	20.4942	22.0163	24.2124	25.5882
8.00	9.9516	12.1951	15.3655	18.8669	21.4242	23.1057	25.5386	27.0627
8.25	10.2250	12.5399	15.8527	19.5824	22.3551	24.2007	26.8821	28.5650
8.50	10.4971	12.8826	16.3358	20.2946	23.2874	25.3004	28.2415	30.0944
8.75	10.7678	13.2231	16.8150	21.0033	24.2205	26.4040	29.6156	31.6502
9.00	11.0371	13.5614	17.2901	21.7081	25.1539	27.5107	31.0037	33.2314
9.25	11.3051	13.8976	17.7612	22.4090	26.0869	28.6200	32.4048	34.8371
9.50	11.5718	14.2315	18.2283	23.1057	27.0192	29.7311	33.8182	36.4666
9.75	11.8370	14.5632	18.6914	23.7981	27.9502	30.8437	35.2431	38.1191
10.00	12.1009	14.8928	19.1505	24.4860	28.8797	31.9570	36.6786	39.7937
10.50	12.6258	15.5473	20.0604	25.8522	30.7359	34.1873	39.5759	43.1956
11.00	13.1476	16.1969	20.9615	27.2075	32.5885	36.4211	42.5019	46.6559
11.50	13.6662	16.8412	21.8537	28.5508	34.4352	38.6554	45.4518	50.1691
12.00	14.1816	17.4804	22.7367	29.8815	36.2740	40.8873	48.4215	53.7299
12.50	14.6937	18.1145	23.6105	31.1992	38.1035	43.1147	51.4073	57.3337
13.00	15.2026	18.7435	24.4750	32.5036	39.9223	45.3355	54.4059	60.9761
13.50	15.7081	19.3673	25.3303	33.7943	41.7295	47.5481	57.4142	64.6533
14.00	16.2102	19.9859	26.1763	35.0712	43.5240	49.7510	60.4295	68.3614
14.50	16.7087	20.5993	27.0132	36.3344	45.3055	51.9431	63.4494	72.0971
15.00	17.2039	21.2076	27.8409	37.5837	47.0731	54.1231	66.4718	75.8571

TABLE 2-2. REDUCED PSEUDO-PRESSURE INTEGRAL (ψ_r) AS A FUNCTION OF T_r AND p_r

EXAMPLE 2-1

Introduction   This example illustrates the calculation of ψ by simple numerical integration. Moreover, because the gas is sweet, ψ may also be obtained by using Table 2-2.

Problem   Calculate

$$\psi = 2 \int_0^P \frac{p}{\mu Z} \, dp$$

at various pressures for a dry sweet gas (gravity = 0.61, composition given in Example A-1) at a temperature of $120°$ F, given the following properties:

p (psia)	Z	μ (cp)
0	1.000	--
400	0.955	0.0118
800	0.914	0.0125
1200	0.879	0.0134
1600	0.853	0.0145
2000	0.838	0.0156

also, compare the calculated values to those obtained from Table 2-2, given the following information:

$$P_c = 664 \text{ psia}$$
$$T_c = 357 \text{ }°R$$
$$\mu_1 = 0.0114 \text{ cp}$$

Solution   The calculations are divided into three sections:

Columns ① to ③ represent the data

Columns ④ to ⑧ are the numerical integration (trapezoidal rule)

Columns ⑨ to ⑪ depict the use of Table 2-2

The calculations are presented in tabular form below. The various columns are obtained as follows:

	Column	Term	Units	Source
Data	①	p	psia	given
	②	z	–	given
	③	μ	cp	given
ψ by numerical integration	④	$2\left(\dfrac{p}{\mu z}\right)$	M psia/cp	$2 \times$ ① $\div$ ② $\div$ ③
	⑤	Mean $2\left(\dfrac{p}{\mu z}\right)$	M psia/cp	average of two successive entries of 4
	⑥	Δp	psi	difference of two successive entries of 1
	⑦	Mean $2\left(\dfrac{p}{\mu z}\right)\Delta p$	MM psia²/cp	⑤ $\times$ ⑥
	⑧	ψ	MM psia²/cp	⑦ + previous entry of ⑧
ψ using integral values obtained from Table 2-2	⑨	p_r	–	① $\div p_c$
	⑩	Integral Value	–	from Table 2-2 (by interpolation)
	⑪	ψ	MM psia²/cp	$2 \times p_c^2 \div \mu_1 \times$ ⑩

given			ψ by numerical integration					ψ using Table 2-2		
①	②	③	④	⑤	⑥	⑦	⑧	⑨	⑩	⑪
0			0.0				0.0	0.0	0.0000	0.0
400	0.955	0.0118	70.9	35.5	400	14.2	14.2	0.6	0.1824	14.1
800	0.914	0.0125	140.0	105.5	400	42.2	56.4	1.2	0.7253	56.1
1200	0.879	0.0134	203.8	171.9	400	68.8	125.2	1.8	1.6102	124.5
1600	0.853	0.0145	258.7	231.3	400	92.5	217.7	2.4	2.8054	217.0
2000	0.838	0.0156	306.0	282.4	400	113.0	330.7	3.0	4.2605	329.6

<u>Discussion</u>   Figure 2-4 shows a plot of ψ versus p for the gas in
question.   It will be observed that ψ obtained from numerical
integration, column ⑧ , is essentially identical to ψ obtained from
Table 2-2, column ⑪ and, also to ψ obtained from Figure 2-4. This
is to be expected, as the gas properties μ and Z are represented in all
cases by the same correlations.

    For sour gases ψ must either be calculated by numerical
integration or obtained from the tables of Zana and Thomas (1970).
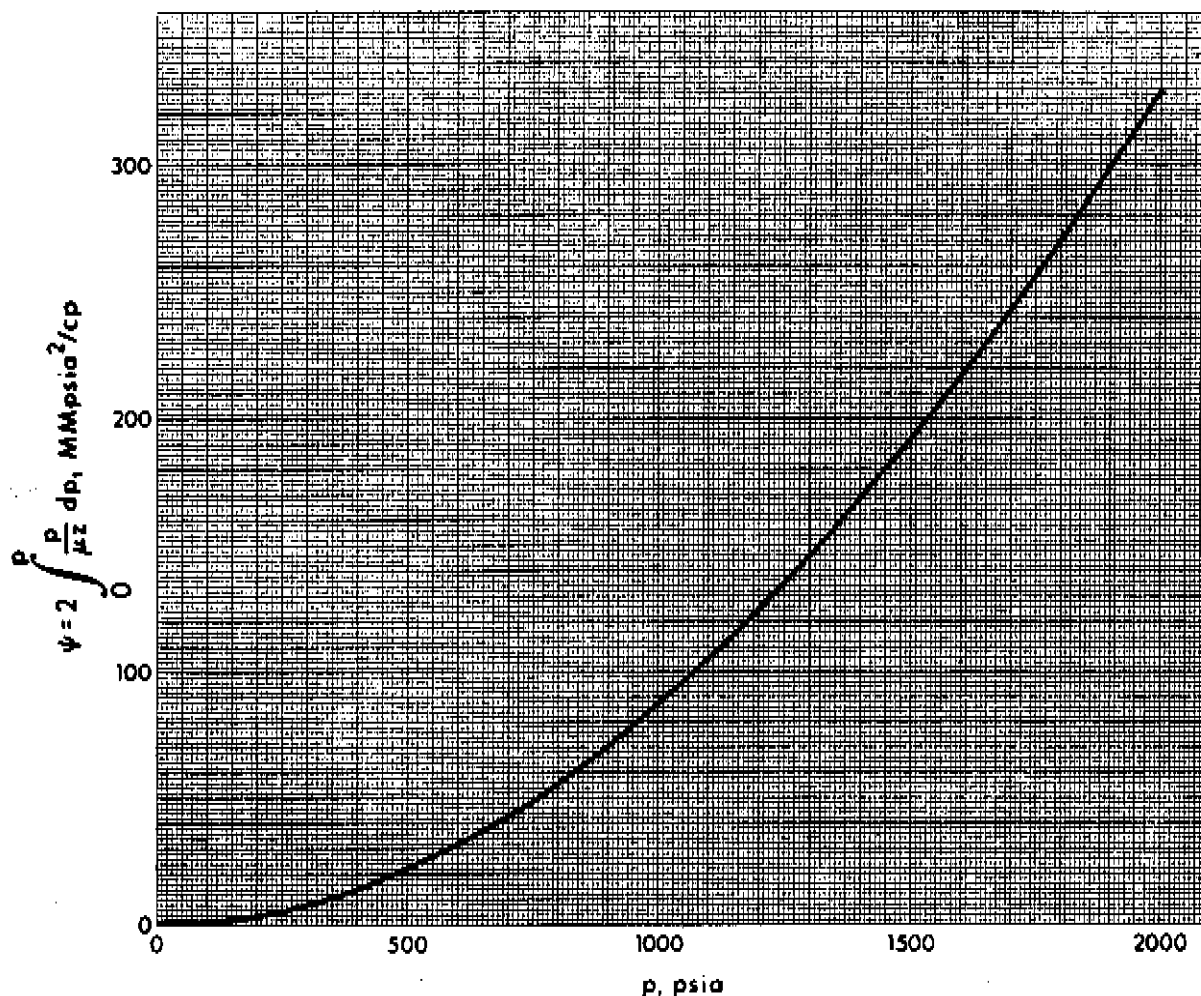
FIGURE 2-4. ψ-p CURVE FOR THE GAS OF EXAMPLE 2-1.

5.6 The General Flow Equation

The equations for the "pressure," "pressure-squared," and "pseudo-pressure" treatments already presented may be combined into one general equation of the form

$$\nabla^2 \Phi = \frac{1}{\kappa} \frac{\partial \Phi}{\partial t} \qquad (2\text{-}48)$$

where Φ and κ have the following interpretations for the different cases,

	Φ	κ
pressure case	p	$\dfrac{k}{(\phi \, \bar{\mu} \, \bar{c})}$
pressure-squared case	p^2	$\dfrac{k}{(\phi \, \bar{\mu} \, \bar{c})}$
pseudo-pressure case	ψ	$\dfrac{k}{(\phi \, \mu_i c_i)}$

The pressure and pressure-squared cases use average gas properties, evaluated at an arithmetic average pressure (Russell, Goodrich, Perry, and Bruskotter, 1966) or at the root-mean-square (rms) pressure (Carter, 1962). Another method of averaging, for example, $\bar{c} = (c_i + c)/2$, has been used in the illustrative Examples 2-2 and 2-3. The pseudo-pressure case uses properties evaluated at initial conditions for production (Al-Hussainy et al., 1966) and injection (Wattenbarger and Ramey, 1968) of gas. It is shown in Section 11 that these conventional approaches may be in considerable error under certain conditions and the indiscriminate use of such generalized approaches should be avoided.

Equation (2-48) may be expressed, as desired, in terms of rectangular, cylindrical, or spherical coordinates. The one-dimensional cases of these coordinate systems will be considered. It should be made clear that the expression "one-dimensional" refers to a specified coordinate system. For example, one-dimensional flow in the r-direction,

in cylindrical coordinates, may be expressed in rectangular coordinates as two-dimensional flow in the x- and y-directions.

Linear Flow

Often fractures exist naturally in the reservoir, or they are caused by hydraulically fracturing the formation in the vicinity of the well. In such cases flow towards the fracture is linear, that is, the flow lines are parallel and the cross-sectional area of flow is constant. Linear flow is illustrated in Figure 2-5(a) and is represented by Equation (2-49), which in the rectangular coordinate system, is the one-dimensional form of Equation (2-48).

$$\frac{\partial^2 \Phi}{\partial x^2} = \frac{1}{\kappa} \frac{\partial \Phi}{\partial t} \qquad (2\text{-}49)$$

PLAN

ELEVATION

(a) Linear   (b) Radial - Cylindrical   (c) Radial - Spherical
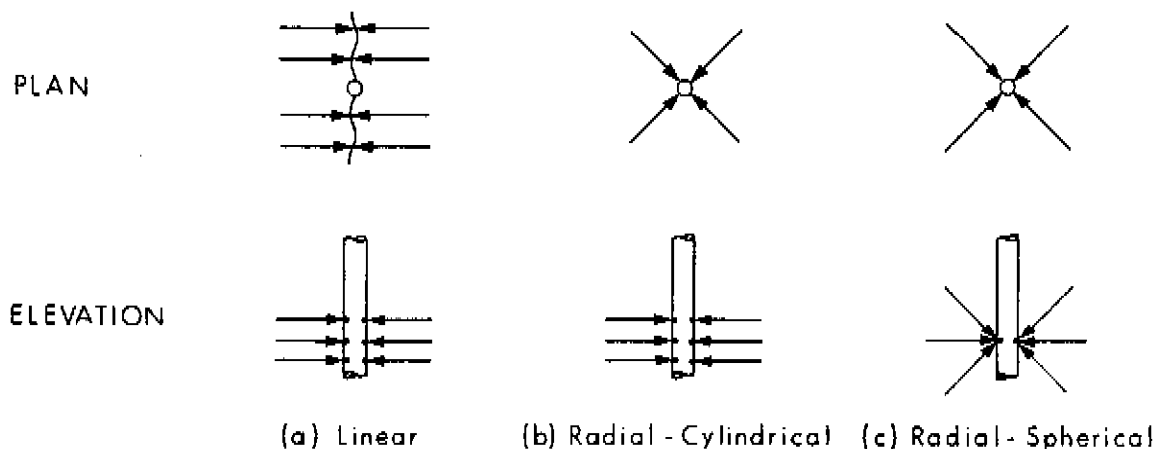
FIGURE 2-5. FLOW GEOMETRIES

Radial-Cylindrical Flow

In petroleum engineering the reservoir is often idealized by considering it to be circular and of constant thickness, h, with a well opened over the entire thickness. Flow is considered to take place in the radial direction only, that is, flow lines converge towards a

central point in each plane, and the cross-sectional area of flow
decreases as the centre is approached. Thus flow is directed towards a
common axial (central) line referred to as a line-sink (or line-source
in the case of an injection well). This flow model is called radial-
cylindrical flow, but in the petroleum literature it is often simply
called radial flow. It is illustrated in Figure 2-5(b) and the
applicable equation of flow, in the cylindrical coordinate system is
the one-dimensional form of Equation (2-48), given by

$$\frac{1}{r} \frac{\partial}{\partial r} \left(r \frac{\partial \Phi}{\partial r} \right) = \frac{1}{\kappa} \frac{\partial \Phi}{\partial t} \qquad (2\text{-}50)$$

Radial-Spherical Flow

For thick reservoirs (h is very large) in which the well is
not open to the entire producing formation, or for the measurement of
vertical permeability, the one-dimensional form of Equation (2-48), in
the spherical coordinate system, is of interest. It is called the
radial-spherical flow equation and is given by

$$\frac{1}{r^2} \frac{\partial}{\partial r} \left(r \frac{\partial \Phi}{\partial r} \right) = \frac{1}{\kappa} \frac{\partial \Phi}{\partial t} \qquad (2\text{-}51)$$

Radial-spherical flow implies flow from all directions towards one
common central point, that is, a point sink (or source). It is
depicted in Figure 2-5(c) and is usually referred to simply as
spherical flow.

5.7 Dimensionless Form of the General Flow Equation

It is convenient to express the flow Equation (2-48) and the
relevant boundary conditions in dimensionless terms as

$$\nabla^2 \left(\Delta p_D \right) = \frac{\partial}{\partial t_D} \left(\Delta p_D \right) \qquad (2\text{-}52)$$

where the subscript D means dimensionless, and the dimensionless terms

are defined in Table 2-3 for the various modes of flow. Expression in this form achieves three main objectives:

1. By suitable definition of Δp_D, t_D, and q_D as in Table 2-3, the "pressure," "pressure-squared" and "pseudo-pressure" cases can all be represented by Equation (2-52). Thus, the solution of only one equation will serve the three cases.

2. The number of parameters upon which the solution depends is minimized. For example, instead of having the problem dependent on p, p_i, c, q, μ, k, h, r, r_w, ϕ, and t individually, only Δp_D, q_D, and t_D need be treated—an obvious reduction in the number of variables. (Subscript w refers to conditions at the well.)

3. Equation (2-52) is equivalent to a standard equation in the field of heat conduction (Carslaw and Jaeger, 1959, p. 29) for which solutions have been obtained for various relevant boundary conditions. These solutions may be applied directly to the present problem of flow of fluids through porous media.

It will be observed in Table 2-3 that t_D and q_D have the coefficients λ and γ, respectively. These factors take on different values for the different systems of Darcy, Field and Metric (SI) units. They include coefficients like 2 and π, units conversion factors, and the numerical values of p_{sc} and T_{sc} that may be inherent in the definitions of the dimensionless terms. Subscript sc means standard conditions; two commonly used standards are 14.65 psia and 60°F in Alberta, Canada, and 14.70 psia and 60°F in many states of the U.S.A. Values of λ and γ for various systems are tabulated in Table 2-4. The different systems of units are given in Table 2-5.

The factor B which occurs in Table 2-3 is the formation volume factor, defined as

$$B = \frac{\text{volume occupied by unit mass of fluid at reservoir conditions}}{\text{volume occupied by unit mass of fluid at standard (surface) conditions}}$$

$$= \frac{q}{q_{sc}} = \frac{p_{sc}}{p} \frac{T}{T_{sc}} Z$$

DIMENSIONLESS VARIABLE	FLOW GEOMETRY	GAS			LIQUID
		p	p^2	ψ	p
x_D	Linear	$\dfrac{x}{x_f}$	$\dfrac{x}{x_f}$	$\dfrac{x}{x_f}$	$\dfrac{x}{x_f}$
r_D	Radial-cylindrical Radial-spherical	$\dfrac{r}{r_w}$	$\dfrac{r}{r_w}$	$\dfrac{r}{r_w}$	$\dfrac{r}{r_w}$
t_D	Linear	$\dfrac{\lambda\,k\,t}{\phi\,\bar{\mu}\,\bar{c}\,x_f^2}$	$\dfrac{\lambda\,k\,t}{\phi\,\bar{\mu}\,\bar{c}\,x_f^2}$	$\dfrac{\lambda\,k\,t}{\phi\,\mu_i\,c_i\,x_f^2}$	$\dfrac{\lambda\,k\,t}{\phi\,\mu\,c\,x_f^2}$
t_D	Radial-cylindrical Radial-spherical	$\dfrac{\lambda\,k\,t}{\phi\,\bar{\mu}\,\bar{c}\,r_w^2}$	$\dfrac{\lambda\,k\,t}{\phi\,\bar{\mu}\,\bar{c}\,r_w^2}$	$\dfrac{\lambda\,k\,t}{\phi\,\mu_i\,c_i\,r_w^2}$	$\dfrac{\lambda\,k\,t}{\phi\,\mu\,c\,r_w^2}$
p_D		$\dfrac{p}{p_i\,q_D}$	$\dfrac{p^2}{p_i^2\,q_D}$	$\dfrac{\psi}{\psi_i\,q_D}$	$\dfrac{p}{p_i\,q_D}$
Δp_D		$\dfrac{p_i-p}{p_i\,q_D}$	$\dfrac{p_i^2-p^2}{p_i^2\,q_D}$	$\dfrac{\psi_i-\psi}{\psi_i\,q_D}$	$\dfrac{p_i-p}{p_i\,q_D}$
q_D	Linear Radial-cylindrical	$\dfrac{\gamma\,\bar{Z}\,T\,q_{sc}\,\bar{\mu}}{\bar{p}\,k\,h\,p_i}$	$\dfrac{\gamma\,\bar{Z}\,T\,q_{sc}\,\bar{\mu}}{k\,h\,p_i^2}$	$\dfrac{\gamma\,T\,q_{sc}}{k\,h\,\psi_i}$	$\dfrac{\gamma\,B\,q_{sc}\,\mu}{k\,h\,p_i}$
q_D	Radial-spherical	$\dfrac{\gamma\,\bar{Z}\,T\,q_{sc}\,\bar{\mu}}{\bar{p}\,k\,r\,p_i}$	$\dfrac{\gamma\,\bar{Z}\,T\,q_{sc}\,\bar{\mu}}{k\,r\,p_i^2}$	$\dfrac{\gamma\,T\,q_{sc}}{k\,r\,\psi_i}$	$\dfrac{\gamma\,B\,q_{sc}\,\mu}{k\,r\,p_i}$

TABLE 2-3. DEFINITION OF DIMENSIONLESS VARIABLES IN TERMS OF p, p^2 AND ψ

(VALUES FOR λ AND γ MAY BE OBTAINED FROM TABLE 2-4)

	FLOW GEOMETRY	GAS			LIQUID
		p	p^2	ψ	p
DARCY UNITS λ	Linear / Radial - Cylindrical / Radial - Spherical	1	1	1	1
γ	Linear	$\dfrac{P_{sc}}{T_{sc}}$	$2\,\dfrac{P_{sc}}{T_{sc}}$	$2\,\dfrac{P_{sc}}{T_{sc}}$	1
γ	Radial - Cylindrical / Radial - Spherical	$\dfrac{1}{2\pi}\dfrac{P_{sc}}{T_{sc}}$	$\dfrac{1}{\pi}\dfrac{P_{sc}}{T_{sc}}$	$\dfrac{1}{\pi}\dfrac{P_{sc}}{T_{sc}}$	$\dfrac{1}{2\pi}$
FIELD UNITS λ	Linear / Radial - Cylindrical / Radial - Spherical	2.637×10^{-4}	2.637×10^{-4}	2.637×10^{-4}	2.637×10^{-4}
γ	Linear (14.65 psia, 520°R)	4.452×10^{6}	8.903×10^{6}	8.903×10^{6}	887.3
	Radial - Cylindrical / Radial - Spherical (14.65/520)	7.085×10^{5}	1.417×10^{6}	1.417×10^{6}	141.2
γ	Linear (14.7 psia, 520°R)	4.467×10^{6}	8.933×10^{6}	8.933×10^{6}	887.3
	Radial - Cylindrical / Radial - Spherical (14.7/520)	7.110×10^{5}	1.422×10^{6}	1.422×10^{6}	141.2
METRIC (SI) UNITS λ	Linear / Radial - Cylindrical / Radial - Spherical	3.601	3.601	3.601	3.601×10^{-3}
γ	Linear (101.325 kPa, 288°K)	9.624×10^{-2}	1.925×10^{-1}	1.925×10^{-1}	11.57
γ	Radial - Cylindrical / Radial - Spherical (101.325/288)	1.532×10^{-2}	3.064×10^{-2}	3.064×10^{-2}	1.84

TABLE 2-4. VALUES OF COEFFICIENTS USED IN THE DIMENSIONLESS TERMS

PARAMETER	DARCY	FIELD	METRIC
r,h	cm	ft	m
k	darcy	md	μm^2
t	s	hr	hr
μ	cp	cp	$\mu Pa \cdot s$ (gas) $mPa \cdot s$ (oil)
p	atm	psia	kPa
V	cm^3	ft^3	m^3
q(oil)	cm^3/s	bbl/d	m^3/d
q(gas)	cm^3/s	MMcf/d	kmol/d

TABLE 2-5. DEFINITION OF UNITS

The last column in Table 2-3 is included to show that the treatment for gas flow using "pressure" as the variable is similar to that used for liquid flow. The dimensionless terms in both cases are the same, but B is replaced for gas by $p_{sc} \bar{Z} T/(T_{sc}\bar{p})$. The values of γ (from Table 2-4) for these two cases are different. The reasons for this difference are that oil flow is measured in barrels per day whereas gas flow is measured in millions of standard cubic feet per day, and also, that γ for gas includes the values of p_{sc} and T_{sc}, which are known constants.

Dimensionless Form of the Radial-Cylindrical Flow Equation

To illustrate where the definitions of the dimensionless terms of Table 2-3 come from, the one-dimensional radial-cylindrical flow equation, Equation (2-50) with Φ interpreted as p for the "pressure" case, will be considered along with the boundary and initial conditions. The case of a well producing at a constant rate, q from an infinite reservoir will be treated. The equation governing flow is:

$$\frac{1}{r}\frac{\partial}{\partial r}\left(r\frac{\partial p}{\partial r}\right) = \frac{\phi\,\mu\,c}{k}\frac{\partial p}{\partial t} \tag{2-53}$$

with the following boundary and initial conditions:

    a. <u>Inner boundary condition</u>: The flow rate q at the wellbore is constant. (q is positive for production.) From Darcy's law

$$\left.\frac{q}{2\pi r h}\right|_{well} = \left.\frac{k}{\mu}\frac{\partial p}{\partial r}\right|_{well} \qquad \text{for} \quad t > 0 \tag{2-54}$$

that is

$$\left.r\frac{\partial p}{\partial r}\right|_{well} = \frac{q\,\mu}{2\pi k h} \tag{2-55}$$

and in terms of standard conditions,

$$\left.r\frac{\partial p}{\partial r}\right|_{well} = \frac{q_{sc}\,\mu}{2\pi k h}\frac{p_{sc}}{\bar{p}}\frac{T\,\bar{Z}}{T_{sc}} \tag{2-56}$$

    b. <u>Outer boundary condition</u>: At all times, the pressure at the outer boundary (radius=infinity) is the same as the initial pressure, p_i, that is,

$$p \to p_i \qquad \text{as} \qquad r \to \infty \qquad \text{for all } t$$

    c. <u>Initial condition</u>: Initially, the pressure throughout the reservoir is constant, that is,

$$p = p_i \qquad \text{at} \qquad t = 0 \qquad \text{for all } r$$

At this stage, the variables which affect the solution of Equation (2-53) are p, p_i, c, r, r_w, q, μ, k, h, ϕ, and t. Let

$$r_D = \frac{r}{r_w} \quad \ldots \ldots \text{ dimensionless radius}$$

$$\Delta p = p_i - p$$

$$(\Delta p_D)' = \frac{p_i - p}{p_i}$$

Then Equation (2-56) becomes

$$r_D \frac{\partial}{\partial r_D} (\Delta p_D)' \bigg|_{r_D=1} = \frac{-1}{p_i} \frac{q_{sc}}{2 \pi k h} \frac{\mu}{\bar{p}} \frac{p_{sc}}{T_{sc}} \frac{T \bar{Z}}{} \qquad (2\text{-}57)$$

Let

$$q_D = \frac{1}{p_i} \frac{q_{sc}}{2 \pi k h} \frac{\mu}{\bar{p}} \frac{p_{sc}}{T_{sc}} \frac{T \bar{Z}}{} \quad \ldots \ldots \ldots \text{ dimensionless flow rate}$$

then Equation (2-57) becomes

$$r_D \frac{\partial}{\partial r_D} \left[\frac{(\Delta p_D)'}{q_D} \right] \bigg|_{r_D=1} = -1 \qquad (2\text{-}58)$$

Let

$$\Delta p_D = \frac{(\Delta p_D)'}{q_D}$$

$$= \frac{p_i - p}{p_i q_D} \quad \ldots \ldots \ldots \text{ dimensionless pressure drop}$$

then Equation (2-58) becomes

$$r_D \frac{\partial}{\partial r_D} (\Delta p_D) \bigg|_{r_D=1} = -1 \qquad (2\text{-}59)$$

Equation (2-53) becomes

$$\frac{1}{r_D} \frac{\partial}{\partial r_D} \left[r_D \frac{\partial}{\partial r_D} (\Delta p_D) \right] = \frac{\phi \mu c r_w^2}{k} \frac{\partial}{\partial t} (\Delta p_D) \qquad (2\text{-}60)$$

Let

$$t_D = \frac{k \, t}{\phi \, \mu \, c \, r_w^2} \quad \ldots \ldots \ldots \text{ dimensionless time}$$

Equation (2-53), the radial-cylindrical flow equation, may now be expressed in dimensionless terms by

$$\frac{1}{r_D} \frac{\partial}{\partial r_D} \left[r_D \frac{\partial}{\partial r_D} (\Delta p_D) \right] = \frac{\partial}{\partial t_D} (\Delta p_D) \tag{2-61}$$

with the boundary and initial conditions as below:

a. $\quad r_D \dfrac{\partial}{\partial r_D} (\Delta p_D) \Big|_{r_D = 1} = -1 \quad$ for $\quad t_D > 0 \qquad (2\text{-}62)$

b. $\quad \Delta p_D \to 0 \quad$ as $\quad r_D \to \infty \quad$ for all t_D

c. $\quad \Delta p_D = 0 \quad$ at $\quad t_D = 0 \quad$ for all r_D

The solution of Equation (2-61), which is the dimensionless form of Equation (2-53), now involves only Δp_D, t_D, and r_D. The dimensionless terms as defined in Table 2-3 for the other flow systems, in terms of p, p^2, or ψ, may be obtained in a manner similar to that of this section.

EXAMPLE 2-2

Introduction   This example illustrates the calculation of some dimensionless quantities. Normally, before starting to solve a problem any one of the three treatments, p, p^2, or ψ, is chosen and all calculations are performed in terms of that variable. However, for the sake of illustration, each of these treatments will be used in this example, but in every case radial-cylindrical flow will be assumed.

Problem   A well in a dry sweet gas reservoir (gas composition given in

Example A-1) was produced at a constant rate, q_{sc}, of 7 MMscfd for a time, t, of 36 hours. The sandface pressure, p_{wf}, at that time was 1600 psia. General data pertinent to the test are as follows:

h	= 39 ft	M	= 17.7	z_i	= 0.838
ϕ	= 0.15 fraction	p_c	= 664 psia	z_{1600}	= 0.853
k	= 20 md	T_c	= 357°R	$\bar{z}$	= 0.846
p_i	= 2000 psia	μ_i	= 0.0158 cp	c_i	= 0.00053
r_w	= 0.4 ft	μ_{1600}	= 0.0146 cp	c_{1600}	= 0.00069
T	= 580°R	$\bar{\mu}$	= 0.0152 cp	$\bar{c}$	= 0.00061

Calculate t_D, q_D, and Δp_D using the p, p^2, and ψ treatments.

Solution

Pressure treatment

From Table 2-3 and Table 2-4

$$t_D = \frac{\lambda\ k\ t}{\phi\ \bar{\mu}\ \bar{c}\ r_w^2}\ , \qquad \lambda = 2.637 \times 10^{-4}$$

$$\therefore \quad t_D = \frac{2.637 \times 10^{-4}\ (20)(36)}{(0.15)(0.0152)(0.00061)(0.4)^2} = 853{,}214$$

From Table 2-3 and Table 2-4

$$q_D = \frac{\gamma\ \bar{z}\ T\ q_{sc}\ \bar{\mu}}{\bar{p}\ k\ h\ p_i}\ , \qquad \gamma = 7.085 \times 10^5$$

$$\therefore \quad q_D = \frac{7.085 \times 10^5\ (0.846)(580)(7)(0.0152)}{(1800)(20)(39)(2000)} = 0.01317$$

From Table 2-3

$$\Delta p_D = \frac{p_i - p}{p_i\ q_D}$$

$$\therefore \quad \Delta p_D = \frac{2000 - 1600}{2000(0.01317)} = 15.2$$

Pressure-squared treatment

From Table 2-3 and Table 2-4

$$t_D = \frac{\lambda \, k \, t}{\phi \, \bar{\mu} \, \bar{c} \, r_w^2} \, , \qquad \lambda = 2.637 \times 10^{-4}$$

$$\therefore \quad t_D = \frac{2.637 \times 10^{-4} \, (20)(36)}{(0.15)(0.0152)(0.00061)(0.4)^2} = 853,214$$

From Table 2-3 and Table 2-4

$$q_D = \frac{\gamma \, \bar{Z} \, T \, q_{sc} \, \bar{\mu}}{k \, h \, p_i^2} \, , \qquad \gamma = 1.417 \times 10^6$$

$$\therefore \quad q_D = \frac{1.417 \times 10^6 \, (0.846)(580)(7)(0.0152)}{(20)(39)(2000)^2} = 0.02371$$

From Table 2-3

$$\Delta p_D = \frac{p_i^2 - p^2}{p_i^2 \, q_D}$$

$$\therefore \quad \Delta p_D = \frac{(2000)^2 - (1600)^2}{(2000)^2 \, (0.02371)} = 15.2$$

Pseudo-pressure treatment

The $\psi - p$ curve is first constructed by the method of Example 2-1. Since the gas for this problem has the same composition and temperature as the gas in Example 2-1, the graph of Figure 2-4 is the applicable $\psi - p$ curve.

From Table 2-3 and Table 2-4

$$t_D = \frac{\lambda \, k \, t}{\phi \, \mu_i \, c_i \, r_w^2} \, , \qquad \lambda = 2.637 \times 10^{-4}$$

$$\therefore \quad t_D = \frac{2.637 \times 10^{-4} \, (20)(36)}{(0.15)(0.0158)(0.00053)(0.4)^2} = 944,710$$

From Table 2-3 and Table 2-4

$$q_D = \frac{\gamma \, T \, q_{sc}}{k \, h \, \psi_i} \, , \qquad\qquad \gamma = 1.417 \times 10^6$$

$$p_i = 2000 \leftrightarrow \psi_i = 3.30 \times 10^8 \quad \text{(Figure 2-4)}$$

$$\therefore \quad q_D = \frac{1.417 \times 10^6 \ (580)(7)}{(20)(39)(3.30 \times 10^8)} = 0.02235$$

From Table 2-3

$$\Delta p_D = \frac{\psi_i - \psi}{\psi_i \, q_D}$$

$$p = 1600 \leftrightarrow \psi = 2.18 \times 10^8 \quad \text{(Figure 2-4)}$$

$$\therefore \quad \Delta p_D = \frac{3.30 \times 10^8 - 2.18 \times 10^8}{(3.30 \times 10^8)(0.02235)} = 15.2$$

Discussion   The values obtained for the dimensionless quantities depend on the treatment used, p, p^2, or ψ. The calculated dimensionless pressure drops for the p and p^2 treatments are exactly identical since the average values for μ and Z were taken to be the same in both cases. The equivalence of these methods when using similar average gas properties will be demonstrated analytically in Section 11. For this particular example, the ψ treatment also gives the same dimensionless pressure drop. As will be explained in Section 11, deviation between the various treatments depends on a number of parameters like drawdown, pressure level, etc. For large drawdown, the results would be sensitive to the method used for averaging reservoir gas properties.

The pressure drop of 400 psia was due to a combination of laminar, inertial-turbulent and skin effects. Calculation of pressure drop due to laminar effects alone will be demonstrated in Example 2-3.

6 DIRECT ANALYTICAL SOLUTIONS OF THE FLOW EQUATIONS

The equations of flow derived so far may be solved analytically only for a limited number of flow geometries, and for some initial and boundary conditions. One case that is capable of solution is of particular interest in gas well testing. This is the radial-cylindrical flow equation. Accordingly, this equation will be treated in much greater detail than either the linear or the radial-spherical flow equations.

Usually, a constant flow rate is stipulated at the well along with one of the following outer boundary conditions:

1. Infinite reservoir;
2. Finite circular reservoir, with no flow across the outer boundary;
3. Finite circular reservoir with constant pressure at the outer boundary.

Solutions for reservoirs with regular straight boundaries, for example, rectangular, polygonal, and so forth, with the wells located on or off centre are obtainable from the infinite reservoir case. This is done by applying the "principle of superposition" in space, in the form of the "method of images." This procedure will be described in detail in Section 7.

Solutions for reservoirs with irregular boundaries are obtained either by fitting approximately reasonable straight line boundaries and treating the problem by image wells, or by numerical techniques such as finite-difference procedures.

For gas well testing purposes, the condition of constant flow rate at the wellhead is the most useful. This situation will be referred to as the constant production rate case. However, a varying flow rate, as in the case of production with constant pressure being maintained at the well, may be studied by the superpostion principle, as shown later.

6.1 Radial-Cylindrical Flow, Constant Production Rate, Infinite Reservoir

As mentioned above, radial-cylindrical flow geometry is of greatest interest in gas well testing. The flow equation for this situation was developed in terms of dimensionless variables in Section 5.6, after some simplifying assumptions had been made in previous sections. It is Equation (2-61) and is repeated below.

$$\frac{1}{r_D} \frac{\partial}{\partial r_D} \left[r_D \frac{\partial}{\partial r_D} (\Delta p_D) \right] = \frac{\partial}{\partial t_D} (\Delta p_D) \tag{2-63}$$

The problem to be solved now is that of radial-cylindrical flow of gas into a well, at constant production rate, from a reservoir of infinite extent. The boundary and initial conditions for this situation are:

a. The flow rate at the well is constant (Equation 2-59).

$$r_D \frac{\partial}{\partial r_D} (\Delta p_D) \bigg|_{r_D = 1} = -1 \qquad \text{for} \quad t_D > 0 \tag{2-64}$$

As a simplification which yields practically identical results (Mueller and Witherspoon, 1965), the well of radius r_w is replaced by a line-sink. The boundary condition above then becomes

$$\lim_{r_D \to 0} r_D \frac{\partial}{\partial r_D} (\partial p_D) = -1 \qquad \text{for} \quad t_D > 0 \tag{2-65}$$

b. At all times the pressure at the boundary is the same as the initial formation pressure, that is,

$$\Delta p_D \to 0 \quad \text{as} \quad r_D \to \infty \quad \text{for all } t_D$$

c. Initially the pressure throughout the reservoir is uniform

$$\Delta p_D = 0 \quad \text{at} \quad t_D = 0 \quad \text{for all } r_D$$

The Boltzman transformation $X = r_D^2/(4t_D)$ is applied to Equation (2-63) to reduce it to an ordinary differential equation (Matthews and Russell, 1967, Appendix A). This is then solved by separating the variables and integrating, with the above three conditions applying. The result is:

$$\Delta p_D = - \frac{1}{2} \, Ei\left(- \frac{r_D^2}{4 \, t_D}\right)$$

(2-66)

$$= - \frac{1}{2} \, Ei\left(- \frac{\phi \, \mu \, c \, r^2}{4 \, \lambda \, k \, t}\right)$$

(2-67)

where Ei is the exponential integral and is defined by

$$Ei(-X) = \int_{\infty}^{X} \frac{e^{-\xi}}{\xi} \, d\xi$$

(2-68)

where ξ is a dummy variable of integration. The exponential integral may be obtained from Tables of Mathematical Functions (Jahnke and Emde, 1945) but it can be expressed in convenient form by a series expansion (Craft and Hawkins, 1959, p. 314):

$$Ei(-X) = \ln(1.781 \, X) - X + \frac{X^2}{2 \, 2!} - \frac{X^3}{3 \, 3!} + \frac{X^4}{4 \, 4!} - \dots$$

$$\dots + \frac{(-X)^n}{n \, n!} \dots$$

$$= \ln(1.781 \, X) + \sum_{n=1}^{\infty} \frac{(-X)^n}{n \, n!}$$

(2-69)

The number of terms required depends upon the magnitude of X and the desired accuracy. For values of X less than 0.01 the exponential integral is closely approximated by

$$Ei(-X) = \ln(1.781 \, X) \qquad for \qquad X < 0.01$$

(2-70)

For X > 5 the exponential integral is closely approximated by zero. A plot of the Ei function is shown in Figure 2-6.
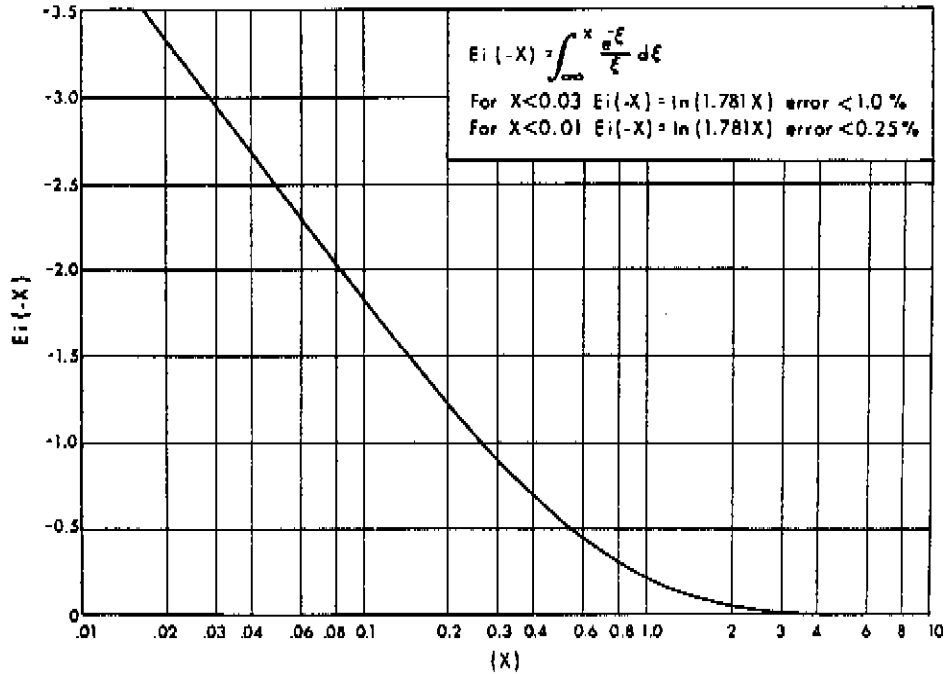
FIGURE 2-6. EXPONENTIAL INTEGRAL FUNCTION - EQUATION (2-68)

Thus for X < 0.01, i.e., $\frac{1}{X} > 100$, Equation (2-66) becomes

$$\Delta p_D = \frac{1}{2} \ln\left(\frac{4\ t_D}{1.781\ r_D^2}\right) \qquad \text{for} \quad \frac{4\ t_D}{r_D^2} > 100 \qquad (2\text{-}71)$$

$$= \frac{1}{2}\left[\ln\left(\frac{t_D}{r_D^2}\right) + 0.80907\right] \qquad \text{for} \quad \frac{t_D}{r_D^2} > 25 \qquad (2\text{-}72)$$

Substitutions for the dimensionless variables Δp_D and t_D may be made from the applicable entry in Table 2-3 in terms of p, p^2, or ψ, as desired. A plot of Equation (2-66) for various values of r_D is shown in Figure 2-7. This equation gives the dimensionless pressure-radius-time relationship for the whole reservoir. Usually, the place of primary interest is at the well, where $r = r_w$ ($r_D = 1$). At this

location the solution to the radial-cylindrical flow equation, Equation (2-63), has been given a special name, P_t. P_t is expressed in dimensionless terms and is the value of Δp_D at the well (excluding inertial-turbulent and skin effects). P_t varies with the boundary
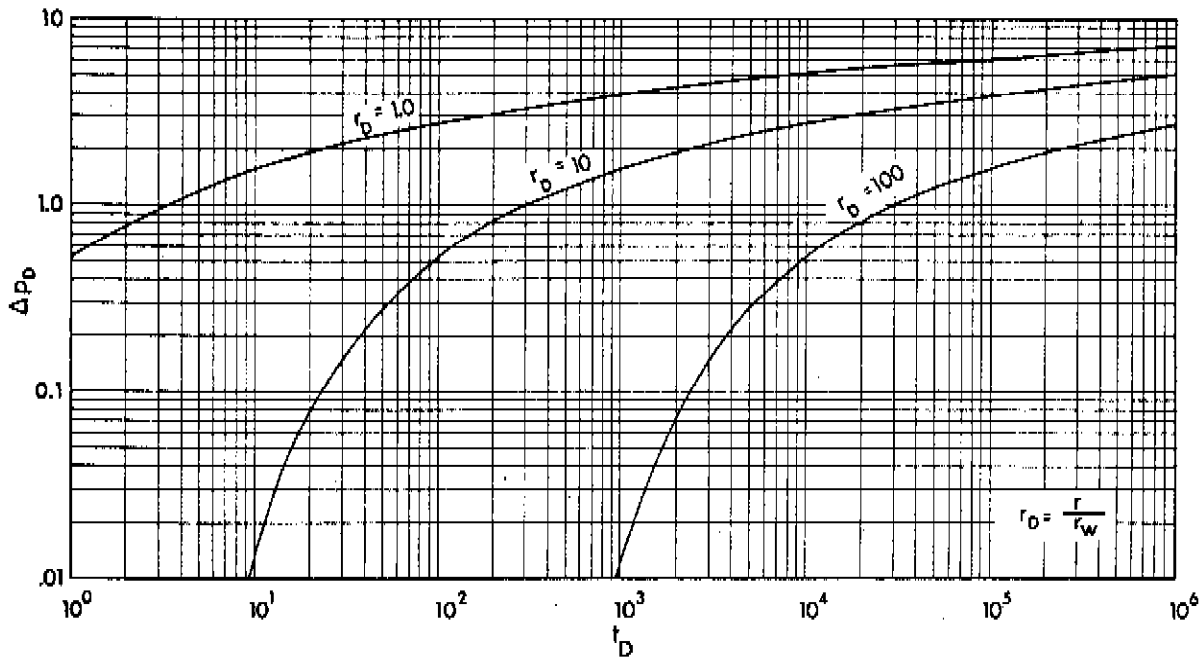
FIGURE 2-7. VALUES OF Δp_D AT VARIOUS DIMENSIONLESS RADII, FOR AN INFINITE RESERVOIR — EQUATION (2-66)

conditions, but for the case of constant production rate from an infinite reservoir, P_t is given by

$$P_t = \Delta p_D \big|_{well} \qquad (2\text{-}73)$$

$$= -\frac{1}{2} \text{Ei}\left(-\frac{1}{4\ t_D}\right) \qquad (2\text{-}74)$$

In terms of the logarithmic approximation, from Equation (2-72)

$$P_t = \frac{1}{2}(\ln\ t_D + 0.809) \qquad \text{for} \quad t_D > 25 \qquad (2\text{-}75)$$

It is evident that P_t for an infinite-acting reservoir is identical to the $r_D = 1$ curve of Figure 2-7. The P_t function is discussed more fully in Section 6.4, but it may be worth noting that it represents the effects of laminar flow alone. The effects of skin, inertial-turbulent flow, etc., are treated later.

EXAMPLE 2-3

Introduction This example illustrates the calculation of the flowing pressure at the well, in an infinite-acting reservoir, due to laminar flow. Once again, the pressure, pressure-squared, and pseudo-pressure treatments will be used to demonstrate the use of each of these techniques. However, in any problem solving situation, only one of these treatments is necessary. Consequently, all subsequent examples will use the pseudo-pressure treatment alone.

Problem A well in an infinite-acting reservoir (gas composition given in Example A-1) was produced at a constant rate of 7 MMscfd. The pressure, p_i, throughout the reservoir prior to the test was 2000 psia. General data pertinent to the test are the same as in Example 2-2. Calculate the flowing sandface pressure, p_{wf}, after 36 hours of flow, using the p, p^2, and ψ treatments.

Solution

Pressure treatment

The flowing sandface pressure, p_{wf}, must actually be known before average values of μ, Z, and c, which are required for the determination of p_{wf} itself, can be calculated. For simplification, this portion of the trial and error procedure will be omitted, and it will be assumed that $\bar{\mu}$, $\bar{Z}$, and $\bar{c}$ are constant at the values given in Example 2-2.

From Example 2-2

$$t_D = \frac{2.637 \times 10^{-4} \; k \; t}{\phi \; \bar{\mu} \; \bar{c} \; r_w^2} = 669,970$$

From Equation (2-75), since $t_D > 25$

$$P_t = \frac{1}{2} (\ln t_D + 0.809)$$

$$= \frac{1}{2} (\ln 669{,}970 + 0.809) = 7.11$$

Alternatively, P_t may also be obtained from Figure 2-7, $r_D = 1.0$ curve.

<u>First trial</u>

Assume $\bar{p} = p_i$

From Table 2-3 and Table 2-4

$$q_D = \frac{7.085 \times 10^5 \ \bar{Z} \ T \ q_{sc} \ \bar{\mu}}{\bar{p} \ k \ h \ p_i}$$

$$= \frac{7.085 \times 10^5 \ (0.867)(580)(7)(0.0144)}{(2000)(20)(39)(2000)} = 0.0115$$

From Table 2-3 and Equation (2-73)

$$P_t = \Delta p_D \bigg|_{well} = \frac{p_i - p}{p_i \ q_D}$$

$$\therefore \ p = p_i - p_i \ P_t \ q_D$$

$$= 2000 - 2000 \ (7.11)(0.0115) = 1836$$

<u>Second trial</u>

Assume $\bar{p} = \dfrac{p_i + p}{2} = \dfrac{2000 + 1836}{2} = 1918$

$$q_D = \frac{7.085 \times 10^5 \ (0.867)(580)(7)(0.0144)}{(1918)(20)(39)(2000)} = 0.0120$$

$$p = 2000 - 2000 \ (7.11)(0.0120) = 1829$$

<u>Third trial</u>

Assume $\quad \bar{p} = \dfrac{p_i + p}{2} = \dfrac{2000 + 1829}{2} = 1915$

$q_D = \dfrac{7.085 \times 10^5 \ (0.867)(580)(7)(0.0144)}{(1915)(20)(39)(2000)} = 0.0120$

$p = 2000 - 2000 \ (7.11)(0.0120) = 1829$

$P_{wf} = 1829 \ psia$

<u>Pressure-squared treatment</u>

As for the pressure treatment, $\bar{\mu}$, $\bar{Z}$, and $\bar{c}$ will be assumed constant at the values given in Example 2-2. Therefore,

$P_t = 7.11$

From Table 2-3 and Table 2-4

$q_D = \dfrac{1.417 \times 10^6 \ \bar{Z} \ T \ q_{sc} \ \bar{\mu}}{k \ h \ p_i^2}$

$= \dfrac{1.417 \times 10^6 \ (0.867)(580)(7)(0.0144)}{(20)(39)(2000)^2} = 0.0230$

From Table 2-3 and Equation (2-73)

$P_t = \Delta p_D \Big|_{well} = \dfrac{p_i^2 - p^2}{p_i^2 \ q_D}$

$\therefore \quad p = \left(p_i^2 - p_i^2 \ P_t \ q_D \right)^{0.5}$

$= \left[(2000)^2 - (2000)^2 \ (7.11)(0.0230) \right]^{0.5} = 1829$

$P_{wf} = 1829 \ psia \quad$ (same as the result from the pressure treatment)

Pseudo-pressure treatment

No assumptions are necessary concerning μ, Z, and c. Since the gas is the same as that of Example A-1, the ψ-p curve already constructed (Figure 2-4) is applicable to this problem.

From Example 2-2

$$t_D = \frac{2.637 \times 10^{-4} \, k \, t}{\phi \, \mu_i \, c_i \, r_w^2} = 944,710$$

From Equation (2-75), since $t_D > 25$

$$P_t = \frac{1}{2} (\ln t_D + 0.809)$$

$$= \frac{1}{2} (\ln 944,710 + 0.809) = 7.28$$

From Example 2-2

$$q_D = \frac{1.417 \times 10^6 \, T \, q_{sc}}{k \, h \, \psi_i} = 0.0224$$

From Table 2-3 and Equation (2-73)

$$P_t = \Delta p_D \Big|_{well} = \frac{\psi_i - \psi_{wf}}{\psi_i \, q_D}$$

$$\therefore \psi_{wf} = \psi_i - \psi_i \, P_t \, q_D$$

$$= 3.30 \times 10^8 - 3.30 \times 10^8 \, (7.28)(0.0224) = 2.76 \times 10^8$$

$$\psi = 2.76 \times 10^8 \leftrightarrow p = 1815 \qquad \text{(Figure 2-4)}$$

$$\therefore p_{wf} = 1815 \text{ psia}$$

<u>Discussion</u> The values of p_{wf} calculated by the p, p^2, and ψ treatments are 1829, 1829, and 1815 psia, respectively. The reason for the similar results of the p and p^2 treatments has been explained in Example 2-2.

The ψ treatment gives a slightly different result since it involves different assumptions. However, the fairly good agreement of these methods is on account of the particular pressure range used in the problem. This aspect will be elaborated upon in Section 11.

The calculated pressure drawdown, by the ψ treatment, at the well was 185 psi. A well similar to that of Example 2-2 experienced an actual pressure drawdown of 400 psi. This consisted of 185 psi due to laminar flow effects, and the remaining pressure loss was mostly due to skin and partly due to inertial-turbulent effects. These latter effects will be considered in detail in Section 9.

EXAMPLE 2-4

Introduction   This example illustrates the calculation of the flowing pressure, due to laminar flow, at some distance from the well in an infinite-acting reservoir.

Problem   A well situated in an infinite-acting reservoir (gas composition given in Example A-1) was produced at a constant rate of 7 MMscfd. The pressure, p_i, throughout the reservoir prior to the test was 2000 psia. General data pertinent to the test are the same as in Example 2-2.

Using the pseudo-pressure treatment calculate the flowing pressure, p_f, in the reservoir at a radius of 40 feet from the well, after 36 hours of production.

Solution   Since the gas is the same as that of Example A-1, the $\psi - p$ curve already constructed (Figure 2-4) is applicable to this problem. From Example 2-2

$$t_D = \frac{2.637 \times 10^{-4} \, k \, t}{\phi \, \mu_i \, c_i \, r_w^2} = 944{,}710$$

$$r_D = \frac{r}{r_w}$$

$$= \frac{40}{0.4} = 100$$

From Equation (2-72), since $\dfrac{t_D}{r_D^2} > 25$

$$\Delta p_D \Big|_{r_D} = \frac{1}{2} \left[\ln\left(\frac{t_D}{r_D^2} \right) + 0.80907 \right]$$

$$\Delta p_D \Big|_{r_D = 100} = \frac{1}{2} \left[\ln\left(\frac{944{,}710}{10{,}000} \right) + 0.80907 \right] = 2.679$$

From Example 2-2

$$q_D = \frac{1.417 \times 10^6 \, T \, q_{sc}}{k \, h \, \psi_i} = 0.0224$$

From Table 2-3

$$\Delta p_D = \frac{\psi_i - \psi}{\psi_i \, q_D}$$

$$\therefore \quad \psi = \psi_i - \psi_i \, \Delta p_D \, q_D$$

$$\psi = 3.30 \times 10^8 - 3.30 \times 10^8 \, (2.679)(0.0224) = 3.10 \times 10^8$$

$$\psi = 3.10 \times 10^8 \longleftrightarrow p = 1933 \qquad \text{(Figure 2-4)}$$

$$p_f \Big|_{r=40'} = 1933 \text{ psia}$$

Discussion   The flowing pressure at 40 feet from the centre of the well is 1933 psia. This compares to a pressure at the well of 1815 psia, calculated in Example 2-3, and indicates that the larger part of the pressure drawdown in a reservoir occurs near the well (in the first 40 feet the pressure drop is 118 psi compared to 67 psi in the rest of the reservoir).

It should be noted that in calculating Δp_D, the exponential integral of Equation (2-66) should be used rather than the logarithmic

approximation given by Equation (2-72). The reason is that at large values of r_D the modulus of the argument of the exponential integral may not be less than 0.01 and the logarithmic approximation may not then be applicable.

6.2 Radial-Cylindrical Flow, Constant Production Rate, Finite Circular Reservoir With No Flow at Outer Boundary

The problem under consideration is that of radial flow from a finite cylindrical reservoir (with sealed upper and lower surfaces) at a constant production rate. The inner boundary is the well. The reservoir is volumetric, that is, the outer boundary is sealed. The boundary and initial conditions for this situation are:

a. The flow rate at the well is constant. With no need to introduce the line-sink concept, the inner boundary condition is the same as Equation (2-59):

$$r_D \frac{\partial}{\partial r_D} (\Delta p_D) \bigg|_{r_D=1} = -1 \qquad \text{for } t_D > 0 \qquad (2\text{-}76)$$

b. The flow at the outer boundary is zero at all times; that is, the pressure gradient at the boundary is zero

$$\therefore \ \frac{\partial p}{\partial r} \bigg|_{r_e} = 0 \qquad \text{for all } t$$

where r_e is the radius of the external boundary. In dimensionless terms

$$\frac{\partial}{\partial r_D} (\Delta p_D) \bigg|_{r_{eD}} = 0 \qquad \text{for all } t_D \qquad (2\text{-}77)$$

where

$$r_{eD} = \frac{r_e}{r_w}$$

c. Initially the pressure throughout the reservoir is uniform

$$\Delta p_D = 0 \quad \text{at} \quad t_D = 0 \quad \text{for all} \quad r_D$$

Equation (2-61), the applicable partial differential equation, can be written as follows:

$$\frac{\partial^2}{\partial r_D^2}(\Delta p_D) + \frac{1}{r_D}\frac{\partial}{\partial r_D}(\Delta p_D) = \frac{\partial}{\partial t_D}(\Delta p_D) \tag{2-78}$$

Using the Laplace Transform (Matthews and Russell, 1967, Appendix A), the following solution is obtained:

$$\Delta p_D = \frac{2}{r_{eD}^2 - 1}\left(\frac{r_D^2}{4} + t_D\right)$$

$$- \frac{r_{eD}^2 \ln r_D}{r_{eD}^2 - 1} - \frac{\left(3r_{eD}^4 - 4r_{eD}^4 \ln r_{eD} - 2r_{eD}^2 - 1\right)}{4\left(r_{eD}^2 - 1\right)^2}$$

$$+ \pi \sum_{n=1}^{\infty} \frac{e^{-\alpha_n^2 t_D} J_1^2(\alpha_n r_{eD})\left[J_1(\alpha_n) Y_o(\alpha_n r_D) - Y_1(\alpha_n) J_o(\alpha_n r_D)\right]}{\alpha_n\left[J_1^2(\alpha_n r_{eD}) - J_1^2(\alpha_n)\right]}$$

$$\tag{2-79}$$

where α_n are the roots of

$$J_1(\alpha_n r_{eD}) Y_1(\alpha_n) - J_1(\alpha_n) Y_1(\alpha_n r_{eD}) = 0 \tag{2-80}$$

J_1 and Y_1 being Bessel functions of the first and second kind, respectively and both of order one. α_n may be obtained from Tables of Mathematical Functions or from a series solution given by Abramowitz and Stegun (1964, p. 374). For the range of α_n not readily available

from this source, the roots of Equation (2-80) may be obtained by iterative numerical procedures.

P_t, which is the solution at the well, is obtained by evaluating Equation (2-79) at $r_D = 1$.

$$P_t \equiv \Delta p_D \Big|_{well}$$

$$= \frac{2t_D}{r_{eD}^2} + \ln r_{eD} - \frac{3}{4} + 2 \sum_{n=1}^{\infty} \frac{e^{-\alpha_n^2 t_D} J_1^2(\alpha_n r_{eD})}{\alpha_n^2 \left[J_1^2(\alpha_n r_{eD}) - J_1^2(\alpha_n) \right]} \quad (2-81)$$

For values of $t_D < 0.25 \, r_{eD}^2$, P_t is equivalent to Equation (2-75); that is the outer boundary effects are insignificant and the reservoir behaves as if it were infinite. As t_D increases, the summation term in Equation (2-79) becomes negligibly small (because of e^{-t_D}) and may safely be ignored for large values of t_D. Thus for $r_e \gg r_w$, which is usually the case, the pressure at the well is expressed by

$$P_t = \frac{2t_D}{r_{eD}^2} + \ln r_{eD} - \frac{3}{4} \qquad \text{for } \frac{t_D}{r_{eD}^2} > 0.25 \qquad (2-82)$$

This equation is easily expressed in terms of p, p^2, or ψ by substitution from Table 2-3 for Δp_D.

Muskat (1937, p. 657) has shown that if the well radius can be assumed to be vanishingly small, that is, a line-sink, then the solution is given by

$$\Delta p_D = - \left[\frac{3}{4} + \ln \frac{r}{r_e} - \frac{1}{2} \left[\left(\frac{r}{r_e} \right)^2 + 4t_D \left(\frac{r_w}{r_e} \right)^2 \right] \right.$$

$$\left. + 2 \sum_{n=1}^{\infty} \frac{J_0(\alpha_n' r) \, e^{-\alpha_n'^2 t_D r_w^2}}{\alpha_n'^2 r_e^2 J_0^2(\alpha_n' r_e)} \right] \qquad (2-83)$$

where α_n' are the roots of

$$J_1(\alpha_n' \, r_e) = 0 \qquad\qquad (2\text{-}84)$$

and are readily available from the Tables of Mathematical Functions already mentioned. For large times and where $r_w \ll r_e$ the solution at the well reduces, as before, to Equation (2-82).

A plot of Equation (2-81) for various values of r_{eD} is shown in Figure 2-8. It should be noted that at early times the solution
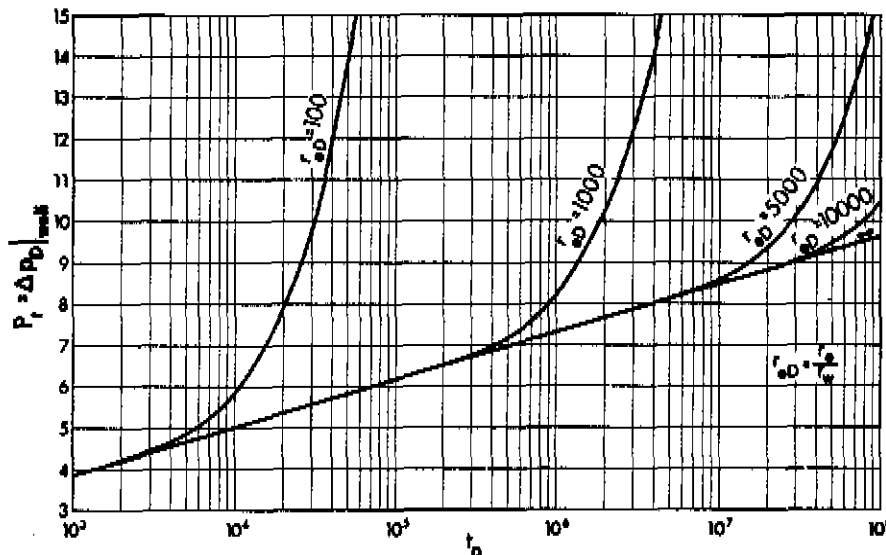
FIGURE 2-8. VALUES OF $P_t(=\Delta p_D|_{well})$ FOR VARIOUS FINITE CIRCULAR RESERVOIRS WITH NO FLOW AT THE EXTERNAL BOUNDARY - EQUATION (2-82)

corresponds to the $r_D = 1$ line of the infinite reservoir case of Figure 2-7. At large times the solution is represented by Equation (2-82). The transition from infinite to finite behaviour occurs at $t_D \simeq 0.25 \, r_{eD}^2$.

EXAMPLE 2-5

Introduction   The previous two examples treated flow from an infinite-acting reservoir. This example treats flow from a finite closed

reservoir, and illustrates that at short times of flow, the reservoir is essentially infinite-acting, whereas at longer flow times, the boundary effects are dominant.

Problem   A well in a closed (no flow across boundary) reservoir (r_e = 2000 feet) was produced at a constant rate of 7 MMscfd. The pressure, p_i, throughout the reservoir prior to the test, was 2000 psia. The gas in the reservoir is the same as that of Example A-1. General data pertinent to the test are the same as in Example 2-2.

Calculate the flowing sandface pressure, p_{wf}, after 36 hours and after 1800 hours of production.

Solution   Since the gas is the same as that of Example A-1, the $\psi - p$ curve already constructed (Figure 2-4) is applicable to this problem.

t = 36

From Example 2-2

$$t_D = \frac{2.637 \times 10^{-4} k\ t}{\phi\ \mu_i\ c_i\ r_w^2} = 944,710$$

$$q_D = \frac{1.417 \times 10^6\ T\ q_{sc}}{k\ h\ \psi_i} = 0.0224$$

From Figure 2-8 (for t_D = 944,710; $r_{eD} = \frac{2000}{0.4} = 5000$)

$$P_t = \Delta p_D \Big|_{well} = 7.30$$

alternatively, since $t_D < 0.25\ r_{eD}^2$ (which equals 6,250,000), P_t is given by Equation (2-75)

$$P_t = \frac{1}{2}\ (\ln t_D + 0.809)$$

$$= \frac{1}{2}\ (\ln 944,710 + 0.809) = 7.28$$

From Table 2-3 and Equation (2-73)

$$P_t = \Delta p_D \Big|_{well} = \frac{\psi_i - \psi_{wf}}{\psi_i \, q_D}$$

$$\therefore \quad \psi_{wf} = \psi_i - \psi_i \, P_t \, q_D$$

$$= 3.30 \times 10^8 - 3.30 \times 10^8 \, (7.28)(0.0224) = 2.76 \times 10^8$$

$$\psi = 2.76 \times 10^8 \leftrightarrow p = 1815 \qquad \text{(Figure 2-4)}$$

$$P_{wf} = 1815 \text{ psia}$$

<u>t = 1800</u>

From Table 2-3 and Example 2-2

$$t_D = \frac{2.637 \times 10^{-4} \, k \, t}{\phi \, \mu_i \, c_i \, r_w^2}$$

$$= \frac{2.637 \times 10^{-4} \, (20)(1800)}{(0.15)(0.0158)(0.00053)(0.4)^2} = 47,235,491$$

$$q_D = \frac{1.417 \times 10^6 \, T \, q_{sc}}{k \, h \, \psi_i} = 0.0224$$

From Figure 2-8 (for $t_D = 47,235,491$; $r_{eD} = 5000$)

$$P_t = \Delta p_D \Big|_{well} = 11.6$$

alternatively, since $t_D > 0.25 \, r_{eD}^2$ (which equals 6,250,000), P_t is given by Equation (2-82)

$$P_t = \frac{2t_D}{r_{eD}^2} + \ln r_{eD} - \frac{3}{4}$$

$$= \frac{2(47,235,491)}{(5000)^2} + \ln 5000 - \frac{3}{4} = 11.5$$

$$\therefore \quad \psi_{wf} = \psi_i - \psi_i \; P_t \; q_D$$

$$= 3.30 \times 10^8 - 3.30 \times 10^8 \; (11.5)(0.0224) = 2.45 \times 10^8$$

$$\psi = 2.45 \times 10^8 \longleftrightarrow p = 1703 \qquad \text{(Figure 2-4)}$$

$$\therefore \quad p_{wf} = 1703 \text{ psia}$$

<u>Discussion</u> The pressure at the well after 36 hours of flow is
1815 psia, the same value as in Example 2-3. In fact, the reservoir is
still infinite-acting and the boundary effects have not yet been felt.

After 1800 hours of flow, the pressure is 1703 psia, compared
with 1770 psia for an infinite-acting reservoir. Boundary effects are
significant at this stage, and the rate of pressure decline throughout
the reservoir, $\partial p / \partial t$, is constant.

<p align="center">6.3 Radial-Cylindrical Flow, Constant Production Rate,
Finite Circular Reservoir With Constant
Pressure at Outer Boundary</p>

In this situation radial flow takes place from a finite
cylindrical reservoir, with sealed upper and lower surfaces, at constant
production rate. The pressure at the outer boundary remains constant,
due to either natural or artificial pressure maintenance at that
location. The boundary and initial conditions for this situation are:

a. Flow rate at the well is constant. As before, this is
Equation (2-59)

$$r_D \frac{\partial}{\partial r_D} (\Delta p_D) \bigg|_{r_D=1} = -1 \qquad \text{for} \quad t_D > 0 \qquad (2\text{-}85)$$

b. The pressure at the boundary is constant at all times

$$P_e = P_i \qquad \text{for all t}$$

In dimensionless terms:

$$\Delta p_D = 0 \qquad \text{at} \quad r_D = r_{eD} \qquad \text{for all } t_D$$

c. Initially the pressure throughout the reservoir is uniform

$$\Delta p_D = 0 \qquad \text{at} \quad t_D = 0 \qquad \text{for all } r_D$$

By the use of the Laplace transform, and the above boundary conditions, the solution is found to be (Carslaw and Jaeger, 1959, p. 334)

$$\Delta p_D = \ln\left(\frac{r_{eD}}{r_D}\right) +$$

$$\pi \sum_{n=1}^{\infty} \frac{e^{-\beta_n^2 t_D} J_o^2(r_{eD}\,\beta_n)\left[J_o(r_D\,\beta_n)\,Y_1(\beta_n) - Y_o(r_D\,\beta_n)\,J_1(\beta_n)\right]}{\beta_n\left[J_1^2(\beta_n) - J_o^2(r_{eD}\,\beta_n)\right]} \tag{2-86}$$

where β_n are the roots of

$$J_1(\beta_n)\,Y_o(r_{eD}\,\beta_n) - Y_1(\beta_n)\,J_o(r_{eD}\,\beta_n) = 0 \tag{2-87}$$

and are obtainable from the same sources as α_n in the previous section. P_t is obtained by evaluating Equation (2-86) at $r_D = 1$. For $r_D = 1$

$$P_t \equiv \Delta p_D\Big|_{\text{well}}$$

$$= \ln r_{eD} - 2 \sum_{n=1}^{\infty} \frac{e^{-\beta_n^2 t_D} J_o^2(r_{eD}\,\beta_n)}{\beta_n^2\left[J_1^2(\beta_n) - J_o^2(r_{eD}\,\beta_n)\right]} \tag{2-88}$$

which may be written, as desired, in terms of p, p^2, or ψ.

As t_D increases, the summation term decreases (due to e^{-t_D}) and Equation (2-88) reduces to

$$P_t = \ln r_{eD} \qquad \text{for} \quad t_D > 1.0\, r_{eD}^2 \quad \text{(approximately)} \tag{2-89}$$

This equation may also be obtained directly by the integration of Darcy's law for a radial system.

A plot of Equation (2-88) for various values of r_{eD} is shown in Figure 2-9. It is observed that in the early part of the production period the well acts as if it were in an infinite reservoir. After a certain time however, $(t_D > 0.25 \; r_{eD}^2)$, boundary effects become noticeable, and a transition period precedes the steady-state condition represented by Equation (2-89).
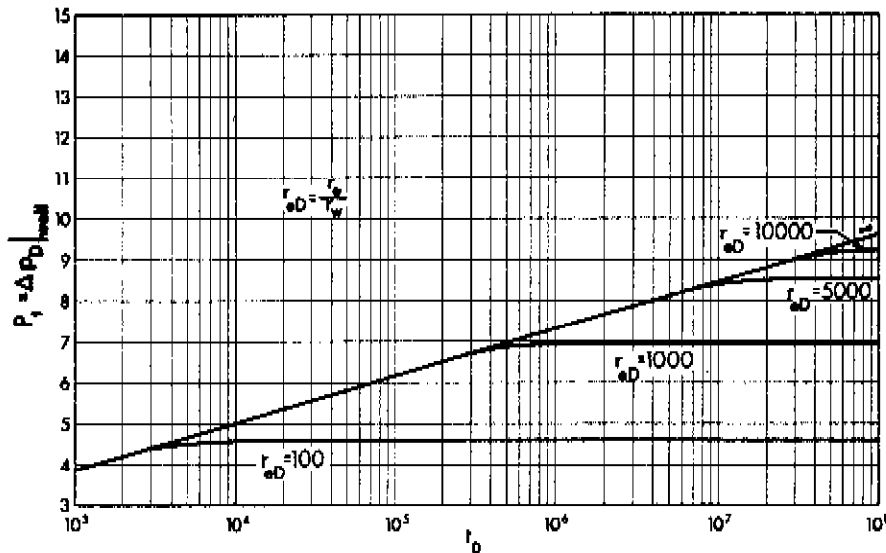
FIGURE 2-9. VALUES OF $P_i (=\Delta p_D|_{well})$ FOR VARIOUS FINITE CIRCULAR RESERVOIRS WITH CONSTANT PRESSURE AT THE EXTERNAL BOUNDARY - EQUATION (2-88)

EXAMPLE 2-6

Introduction   This example shows that a constant-pressure-outer-boundary reservoir behaves initially as an infinite-acting one. After long producing time, true steady state (and not just pseudo-steady state) is achieved.

Problem   A well in a circular reservoir in which constant pressure is being maintained at the outer boundary (r_e = 2000 feet) was produced at

a constant rate of 7 MMscfd. The pressure, p_i, throughout the reservoir prior to the test was 2000 psia. The gas in the reservoir is the same as that of Example A-1. General data pertinent to the test are the same as in Example 2-2.

Calculate the flowing sandface pressure, p_{wf}, after 36 hours and after 1800 hours of production.

Solution   Since the gas is the same as that of Example A-1, the ψ - p curve already constructed (Figure 2-4) is applicable to this problem.

t = 36

From Example 2-2

$$t_D = \frac{2.637 \times 10^{-4} \, k \, t}{\phi \, \mu_i \, c_i \, r_w^2} = 944,710$$

$$q_D = \frac{1.417 \times 10^6 \, T \, q_{sc}}{k \, h \, \psi_i} = 0.0224$$

From Figure 2-8 (for t_D = 944,710; r_{eD} = 5000)

$$P_t = \Delta p_D \Big|_{well} = 7.30$$

alternatively, since $t_D < 0.25 \, r_{eD}^2$ (which equals 6,250,000), P_t is given by Equation (2-75)

$$P_t = \frac{1}{2} \, (\ln t_D + 0.809)$$

$$= \frac{1}{2} \, (\ln 944,710 + 0.809) = 7.28$$

From Table 2-3 and Equation (2-73)

$$P_t = \Delta p_D \Big|_{well} = \frac{\psi_i - \psi_{wf}}{\psi_i \, q_D}$$

$$\therefore \quad \psi_{wf} = \psi_1 - \psi_1 \, P_t \, q_D$$

$$= 3.30 \times 10^8 - 3.30 \times 10^8 \, (7.28)(0.0224) = 2.76 \times 10^8$$

$$\psi = 2.76 \times 10^8 \leftrightarrow p = 1813 \qquad \text{(Figure 2-4)}$$

$$\therefore \quad P_{wf} = 1815 \text{ psia}$$

$\underline{t = 1800}$

From Example 2-5

$$t_D = \frac{2.637 \times 10^{-4} \, k \, t}{\phi \, \mu_1 \, c_1 \, r_w^2} = 47{,}235{,}491$$

$$q_D = \frac{1.417 \times 10^6 \, T \, q_{sc}}{k \, h \, \psi_1} = 0.0224$$

From Figure 2-9 (for $t_D = 47{,}235{,}491; \quad r_{eD} = 5000$)

$$P_t = \Delta p_D \Big|_{well} \simeq 8.5$$

alternatively, since $t_D > 1.0 \, r_{eD}^2$ (which equals 25,000,000) P_t is given by Equation (2-89)

$$P_t = \ln r_{eD} = \ln 5000 = 8.5$$

$$\therefore \quad \psi_{wf} = \psi_i - \psi_i \, P_t \, q_D$$

$$= 3.30 \times 10^8 - 3.30 \times 10^8 \, (8.5)(0.0244) = 2.62 \times 10^8$$

$$= 2.62 \times 10^8 \leftrightarrow p = 1765 \qquad \text{(Figure 2-4)}$$

$$\therefore \quad P_{wf} = 1765 \text{ psia}$$

Discussion   The pressure at the well after 36 hours of flow is 1815 psia.   In fact, the reservoir is infinite-acting and it does not

matter what conditions (no flow or constant pressure) prevail at the boundary. The answer for this part of the problem is the same as for the closed reservoir of the previous example.

The pressure at the well after 1800 hours of flow is 1765 psia, compared with 1770 psia for an infinite-acting reservoir. The reservoir has now reached steady-state and the pressure does not decline any further. At steady-state conditions the gas being produced is replaced at the outer boundary where a constant pressure is being maintained.

6.4 Radial-Cylindrical Flow, Constant Production Rate, Infinite and Finite Circular Reservoirs, Solutions at the Well (P_t)

In the foregoing sections, the solutions to the dimensionless form of the partial differential equation of flow, Equation (2-61), have been given for the three boundary conditions of interest, by Equations (2-67), (2-79), and (2-86). These can be evaluated at various values of r and t. The solutions at $r = r_w$ which are of the greatest interest have, for ease of reference, been termed P_t. Thus P_t is, by definition, the solution of Equation (2-61) at $r_D = 1$. The reason for introducing the pressure function P_t is that the actual pressure function at the wellbore $\Delta p_D\big|_{well}$ will be shown in Sections 9 and 10 to vary with skin and inertial-turbulent effects. It is convenient therefore to have a precisely defined pressure function, P_t, which is the analytical solution to the partial differential equation and is independent of extraneous effects like skin, wellbore storage, IT flow effects, and so forth.

A plot of P_t versus log t_D is shown in Figure 2-10 for various values of r_{eD}. This is in fact a combined graphical representation of the solutions at the wellbore for the infinite reservoir, circular reservoir with no flow at the outer boundary, and circular reservoir with constant pressure at the outer boundary. That is, it is a combined plot of Equations (2-74), (2-81), and (2-88) and results from putting together the graphs of Figures 2-8 and 2-9. These curves have been
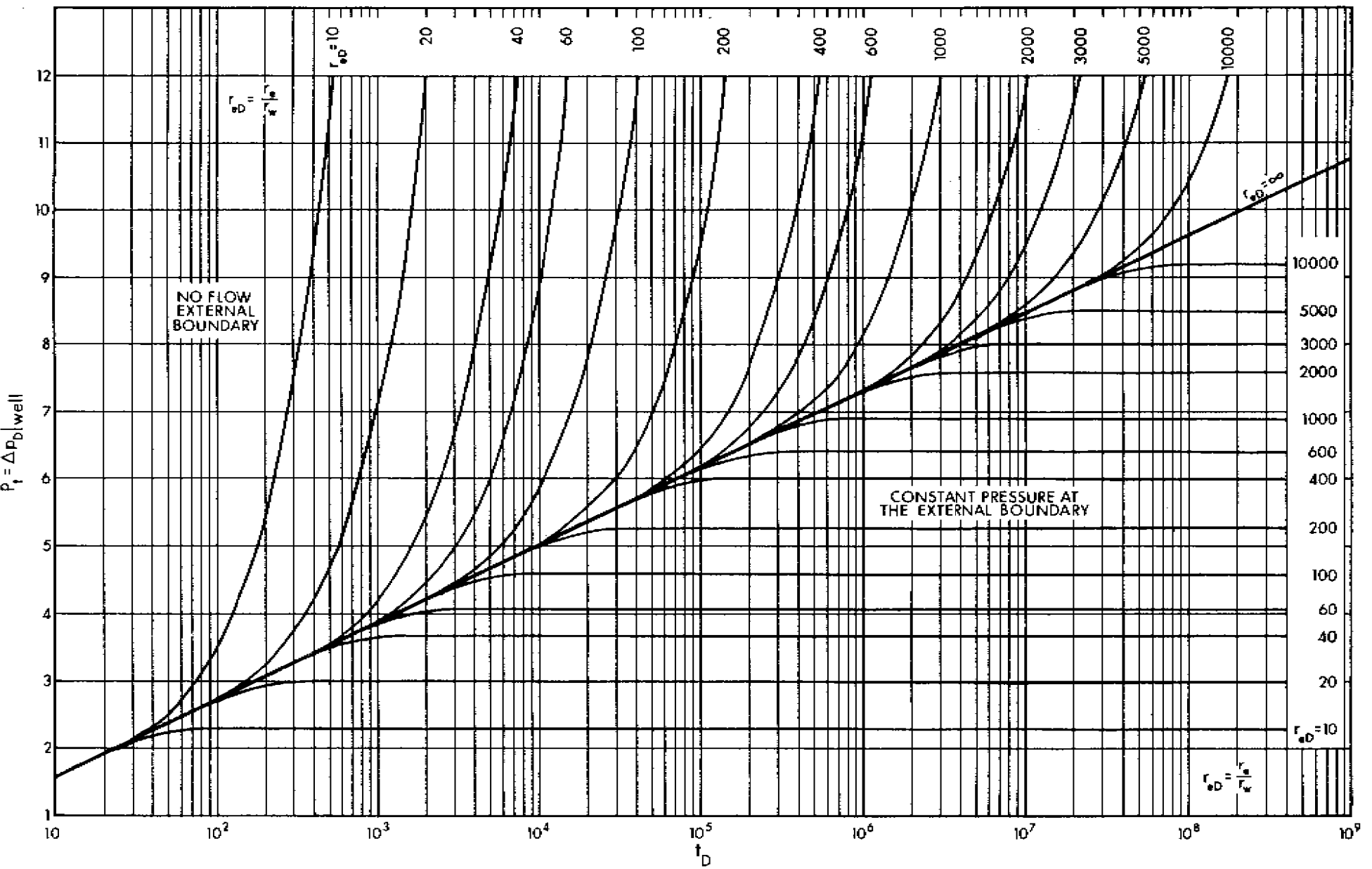
FIGURE 2-10. VALUES OF $P_t(=\Delta p_D|_{well})$ FOR INFINITE RESERVOIRS, FOR FINITE CIRCULAR RESERVOIRS WITH NO FLOW AT THE EXTERNAL BOUNDARY AND FOR FINITE CIRCULAR RESERVOIRS WITH CONSTANT PRESSURE AT THE EXTERNAL BOUNDARY

From Aziz and Flock (1963)

2-67

recalculated but are similar to those of Aziz and Flock (1963).

The P_t functions for the infinite and for the finite circular reservoir cases may be used together to determine time to stabilization for any circular reservoir. This time is the time required for the radius of investigation to become equal to the radius of the outer boundary. The P_t functions may also be expressed in steady-state form by introducing the idea of an effective drainage radius. This concept, together with the concepts of radius of investigation and time to stabilization, is discussed in detail below.

Effective Drainage Radius

Equation (2-89) is seen to be the formula for the steady-state flow of fluids. It applies to stabilized radial-cylindrical flow at a constant rate from a reservoir with constant pressure, p_i, at the outer boundary, r_e. In terms of p it is expressed as

$$P_t \equiv \frac{p_i - p_{wf}}{p_i \, q_D} = \ln \frac{r_e}{r_w} \tag{2-90}$$

In the case of flow from an infinite reservoir, and also of flow from a closed outer boundary reservoir, steady-state flow is never achieved. It is still useful, however, to express the flow from such systems by a formula similar to the steady-state Equation (2-90). Such an equation was given by Aronofsky and Jenkins (1954) and may be written as follows:

$$P_t \equiv \frac{\bar{p}_R - p_{wf}}{p_i \, q_D} = \ln \frac{r_d}{r_w} \tag{2-91}$$

In other words, this steady-state equation is forced to represent the transient behaviour of p_{wf} by suitable definition of the terms $\bar{p}_R$ and r_d.

Let $\bar{p}_R$ be defined as the pressure that would ultimately be obtained upon shut-in of the well. In an infinite reservoir, or in a constant-pressure outer boundary one, $\bar{p}_R$ is equal to the initial pressure, p_i. For a well in a closed outer boundary reservoir $\bar{p}_R$ is the volumetric average reservoir pressure, and is related by a material

balance to the initial formation pressure, p_i, and the amount of depletion. The term r_d is the effective drainage radius and is defined as the radius required to force the steady-state Equation (2-91) to represent the transient solution. This is illustrated in Figure 2-11.
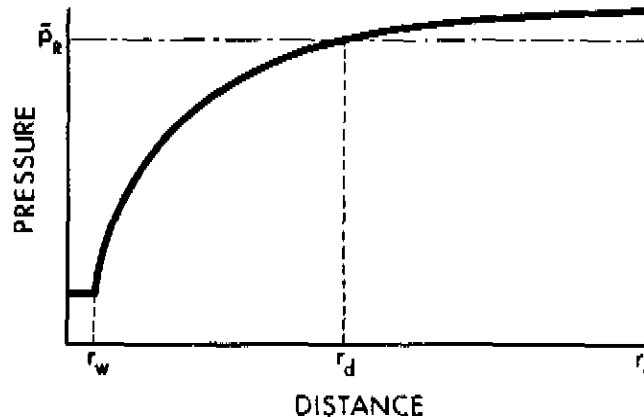
FIGURE 2-11. EFFECTIVE DRAINAGE RADIUS (r_d)

r_d should not be confused with r_D, the dimensionless radius which equals $\frac{r}{r_w}$.

Flow from the closed reservoir, as described in Section 6.2, will be expressed in terms of the effective drainage radius. It was shown that at early times $P_t = \frac{1}{2} (\ln t_D + 0.809)$. Since the reservoir is still infinite acting and there has been no significant depletion, $P_i \simeq \bar{P}_R$ and

$$\ln \frac{r_d}{r_w} = \frac{1}{2} (\ln t_D + 0.809) \tag{2-92}$$

This shows that, initially, the effective radius of drainage starts off near the wellbore and increases independently of the outer boundary radius. As pointed out this situation holds up to a value of $t_D < 0.25 \ r_{eD}^2$. At larger values of t_D boundary effects dominate. This is illustrated in Figure 2-12(a). Figures 2-12(a) and 2-12(b) are derived from Aronofsky and Jenkins (1954) and modified as shown in the light of the figure published by Al-Hussainy (1967, p. 26).
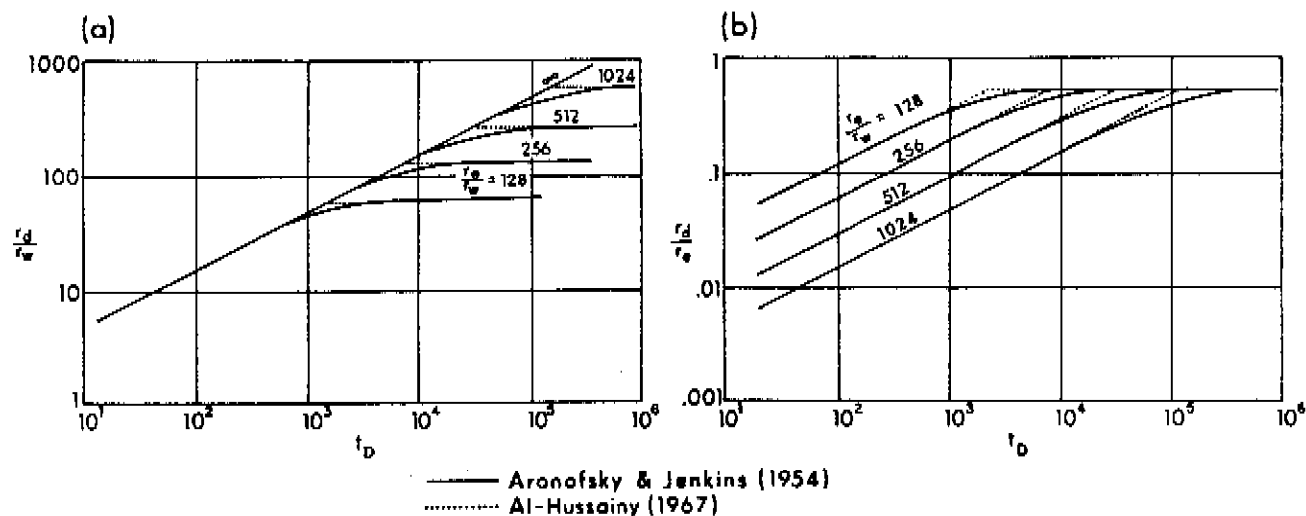
FIGURE 2-12. EFFECTIVE DRAINAGE RADIUS AS A FUNCTION OF TIME

For values of $t_D > 0.25 \, r_{eD}^2$, the amount of depletion must be accounted for. This is done by a simple material balance:

$$P_i - \bar{P}_R = \text{depletion term}$$

$$= \frac{q \, t}{\pi \, r_e^2 \, h \, \phi \, \bar{c}} \qquad (2\text{-}93)$$

$$= \frac{2 \, q_D \, t_D \, P_i}{r_{eD}^2} \qquad (2\text{-}94)$$

$$\therefore \quad \frac{P_i - \bar{P}_R}{P_i \, q_D} = \frac{2 \, t_D}{r_{eD}^2} \qquad (2\text{-}95)$$

from Equation (2-83)

$$\frac{P_i - P_{wf}}{P_i \, q_D} = \frac{2 \, t_D}{r_{eD}^2} + \ln r_{eD} - \frac{3}{4} \qquad (2\text{-}96)$$

subtracting Equation (2-95) from Equation (2-96) gives

$$\frac{\bar{P}_R - P_{wf}}{P_i \, q_D} = \ln r_{eD} - \frac{3}{4} \qquad (2-97)$$

$$= \ln \frac{r_d}{r_w} \quad \text{by definition of } r_d \qquad (2-98)$$

$$\therefore \quad \frac{\ln r_d}{r_w} = \ln r_{eD} - \frac{3}{4} \qquad (2-99)$$

$$= \ln \frac{0.472 \, r_e}{r_w} \qquad (2-100)$$

$$\therefore \quad r_d = 0.472 \, r_e \qquad (2-101)$$

This shows that during the later life of the reservoir the effective drainage radius is no longer dependent on the well radius but only on the exterior radius, r_e. Figure 2-12(b) illustrates this point.

If the results for early and later times are combined it is easily seen that the effective drainage radius increases with time initially, but then it finally stabilizes at approximately one half the outer radius (actually $0.472 \, r_e$). It must be emphasized that r_d is a hypothetical quantity and has no physical reality, and that drainage takes place from the entire reservoir.

Aronofsky and Jenkins (1954) showed that this concept is equally applicable to the flow of ideal gas, and the results obtained using the effective radius of drainage concept apply directly to the "pressure-squared" treatment for gas flow. Al-Hussainy, Ramey and Crawford (1966) confirmed that these same equations for effective radius of drainage also apply to flow of real gases when the "pseudo-pressure" treatment is used. The appropriate equations are given below:

$$\text{"pressure-squared":} \quad \frac{\bar{p}_R^2 - p_{wf}^2}{p_i^2 \, q_D} = \ln \frac{r_d}{r_w} \qquad (2-102)$$

"pseudo-pressure": $\quad \dfrac{\bar{\psi}_R - \psi_{wf}}{\psi_i \, q_D} = \ln \dfrac{r_d}{r_w}$ $\qquad\qquad$ (2-103)

It is instructive to summarize the possible expressions for the effective drainage radius for various systems:

Reservoir Type	Time Limit
Infinite	$t_D > 25$
Closed outer boundary	$25 < t_D < 0.25 \, r_{eD}^2$
Constant pressure outer boundary	$25 < t_D < 0.25 \, r_{eD}^2$

$\ln \dfrac{r_d}{r_w} = \dfrac{1}{2} \, (\ln t_D + 0.809)$

$\qquad\qquad\qquad$ (2-92)

Reservoir Type	Time Limit	
Closed outer boundary	$t_D > 0.25 \, r_{eD}^2$	$r_d = 0.472 \, r_e \qquad$ (2-101)
Constant pressure outer boundary	$t_D > 1.0 \, r_{eD}^2$	$r_d = r_e$

Radius of Investigation

Some confusion often exists between the concepts of the effective radius of drainage and the radius of investigation. This latter radius is a measure of the radial distance over which there is a significant influence due to production at the well. Although the term "radius of influence" is a more appropriate definition, the widespread use of radius of investigation suggests its continued usage. This concept is illustrated in Figure 2-13.
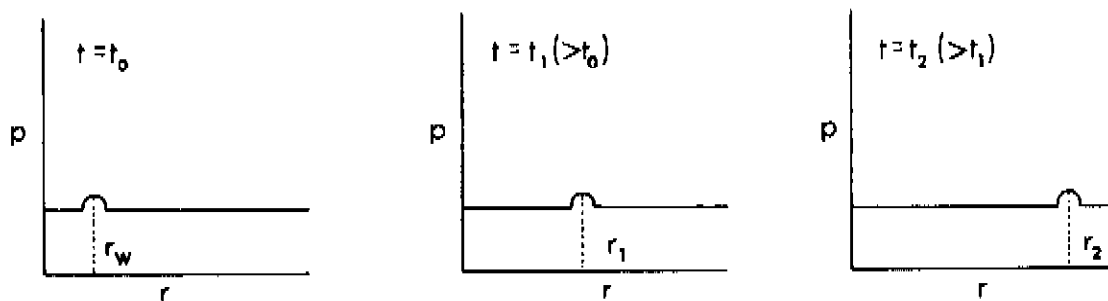
FIGURE 2-13. IDEALIZED TRAVEL OF AN IMPULSE,
TO ILLUSTRATE RADIUS OF INVESTIGATION

If an impulse is applied at the well ($t = t_0$, $r = r_w$) the transient thus created will travel throughout the formation. At any instant of time (t_1 or t_2) the maximum effect of this impulse will be experienced at a certain radius (r_1 or r_2), known as the radius of investigation.

According to the idealized reservoir model adopted in Sections 5 and 6, and the applicable flow equation, a pressure disturbance at the wellbore is instantaneously transmitted to all parts of the reservoir. Even at the outer boundary radius the effect is immediate. However, at any particular time, prior to stabilization, there is a corresponding radial distance beyond which instruments cannot detect the effect of the disturbance. This distance is usually called the radius of investigation. Some authors define it as that radius at which one per cent of the pressure drop occurs, while others fix it according to the limits of accuracy of their pressure measuring instruments. Because of these varying definitions a number of expressions exist for radius of investigation as a function of time. Van Poolen (1964) presented a review of the various definitions and advised caution in their use. Each of these expressions has some degree of arbitrariness and results, at best, in an estimate of the depth of investigation. The definition adopted in this manual is best understood by reference to Figure 2-11. The point of interest is that at which a closed reservoir deviates from an infinite acting system. If the relationship between t_D and r_{eD} at that point is plotted as shown in Figure 2-14, the points fall approximately on the straight line which has the equation

$$t_D = 0.25 \ r_{eD}^{\ 2} \tag{2-104}$$

This line represents the time at which a limited reservoir of radius r_e no longer behaves like an infinite reservoir. Conversely, r_e is the radius of the closed finite reservoir which starts showing the effects of the boundary at dimensionless time t_D. It is clearly seen that as far as pressure behaviour at the well is concerned, an infinite reservoir may be considered to be a limited reservoir with a closed outer boundary at r, provided r is allowed to increase with t_D according
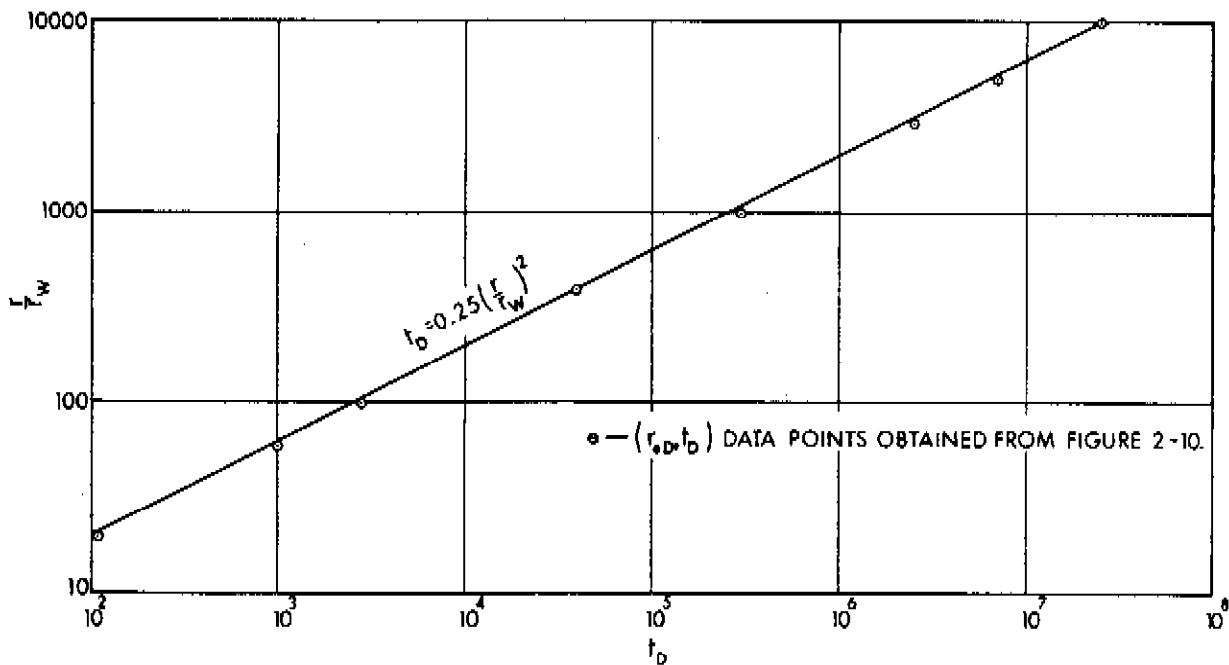
FIGURE 2-14. DIMENSIONLESS RADIUS OF INVESTIGATION AT t_D

to the graph of Figure 2-14. This changing value of r is defined as the radius of investigation r_{inv}, that is

$$\left(\frac{r_{inv}}{r_w}\right)^2 \simeq 4\, t_D$$

$$\therefore \quad r_{inv} = 2\left[\frac{\lambda\, k\, t}{\phi\, \mu\, c}\right]^{0.5} \quad \text{for } r_{inv} \leq r_e \qquad (2-105)$$

If the value of r_{inv} obtained from Equation (2-105) is greater than r_e, then the radius of investigation is taken to be r_e. This is a physical limitation as the maximum value that r_{inv} can attain is the external radius of the reservoir, r_e. This should be contrasted with the maximum value of the effective drainage radius, r_d, which is 0.472 r_e for a closed boundary circular reservoir.

Time to Stabilization

When the radius of investigation has reached the outer boundary, the well is said to be stabilized. Accordingly, the time to stabilization

was shown to be given approximately by Equation (2-104) repeated below

$$t_D \cong 0.25 \ r_{eD}^2 \tag{2-106}$$

For a closed outer boundary reservoir, Katz and Coats (1968) defined the time to stabilization as that time at which the slope of the P_t curves for the infinite-acting and finite-acting reservoirs are equal.

$$\frac{\partial}{\partial t_D} (P_t)_{\text{Equation (2-75)}} = \frac{\partial}{\partial t_D} (P_t)_{\text{Equation (2-82)}}$$

$$\frac{\partial}{\partial t_D} \left[\frac{1}{2} (\ln t_D + 0.809) \right] = \frac{\partial}{\partial t_D} \left[\frac{2 \ t_D}{r_{eD}^2} + \ln r_{eD} - \frac{3}{4} \right]$$

$$\frac{1}{2 \ t_D} = \frac{2}{r_{eD}^2}$$

from which

$$t_D = \frac{1}{4} \ r_{eD}^2$$

which corresponds to Equation (2-106) above. This results in a time to stabilization t_s, given by

$$t_s = \frac{1}{4} \ \frac{\phi \ \mu \ c \ r_e^2}{\lambda \ k} \tag{2-107}$$

Pitzer (1964) confirmed that at $t = t_s$ the values obtained for P_t from Equations (2-75), (2-82), or (2-89) agreed to within 0.5 per cent for $r_{eD} \geq 100$.

6.5 Radial-Cylindrical Flow, Constant Well Pressure, Infinite Reservoir, and Finite Circular Reservoir With No Flow at External Boundary

In production situations, the well is usually producing against a fixed back pressure (constant pressure at the well). In such cases the flow rate is not constant but declines continuously in the manner depicted by Fetkovich (1973). The cumulative production is given by Katz et al. (1959, p. 414) and may be written as

$$Q_T = 2 \pi \phi c r_w^2 h \frac{T_{sc}}{T} \frac{P_i}{P_{sc}} (P_i - P_{wf}) Q_t \qquad (2\text{-}108)$$

where

$$Q_t = \frac{\int_0^{t_D} \left. \frac{\partial p}{\partial r_D} \right|_1 d t_D}{P_i - P_{wf}} \qquad (2\text{-}109)$$

Q_T = total production from time $t_D = 0$ to t_D

Q_t = dimensionless total production number which has been tabulated by Katz et al. (1959, Tables 10-4 and 10-8) for certain boundary conditions.

The pressure distribution in an infinite reservoir with production at constant well pressure is (Carslaw and Jaeger, 1959, p. 335, Van Everdingen and Hurst, 1949)

$$p^2\{r,t\} = p_{wf}^2 - \left[\frac{2}{\pi} (P_i - P_{wf}) \right.$$

$$\left. \int_0^\infty e^{-\xi^2 t_D} \frac{J_0(\xi r) Y_0(\xi r_w) - Y_0(\xi r) J_0(\xi r_w)}{J_0^2(\xi r_w) + Y_0^2(\xi r)} \frac{d\xi}{\xi} \right]$$

$$(2\text{-}110)$$

where

$$J_0, Y_0 = \text{Bessel functions of zero order of the first and}$$
second kinds, respectively

$$\xi = \text{dummy variable of integration}$$

6.6 Linear Flow, Constant Production Rate, Infinite Reservoir

Where linear flow exists, as in flow in the vicinity of a fracture (of length $2\,x_f$) the pressure at any distance x from the sandface ($x \neq 0$) is given by Katz et al. (1959, p. 411) as

$$\Delta p_D = \frac{2}{\sqrt{\pi}} \left(\frac{t_D}{x_D^2} \right)^{\frac{1}{2}} \exp\left(-\frac{x_D^2}{4\,t_D} \right) - \text{erfc}\left[\frac{1}{2} \left(\frac{x_D^2}{t_D} \right)^{\frac{1}{2}} \right] \qquad (2\text{-}111)$$

where t_D, x_D, and q_D are defined for linear flow in Table 2-3 and erfc is the complimentary error function defined as

$$\text{erfc} \, (\Phi) \equiv \frac{2}{\sqrt{\pi}} \int_{\Phi}^{\infty} e^{-\xi^2} \, d\xi \qquad (2\text{-}112)$$

ξ being a dummy variable of integration and Φ an arbitrary function.

At the sandface, $x_D = 0$, the flowing pressure is given by (Carslaw and Jaeger, 1959, p. 75)

$$P_t = \left(\frac{t_D}{\pi} \right)^{\frac{1}{2}} \qquad (2\text{-}113)$$

which upon substituting for the dimensionless variables in terms of p, results in (Katz et al., 1959, p. 411)

$$P_i - P_{wf} = \frac{q}{x_f \, h} \left(\frac{\mu \, t}{k \, \phi \, c \, \pi} \right)^{\frac{1}{2}} \qquad (2\text{-}114)$$

6.7 Radial-Spherical Flow, Constant Production Rate, Infinite Reservoir

The pressure function at any radius, r, is given by (Carslaw and Jaeger, 1959, p. 261)

$$\Delta p_D = \frac{1}{2} \, \text{erfc} \left(\frac{r_D^2}{4 \, t_D} \right)^{\frac{1}{2}} \tag{2-115}$$

where t_D and q_D are defined for radial-spherical flow in Table 2-3. In thick formations, radial-spherical flow may exist in the vicinity of the well when only a limited portion of the formation is opened to flow (as in the case of limited perforation of the casing).

7   FURTHER ANALYTICAL SOLUTIONS OF THE FLOW EQUATIONS

7.1 Principle of Superposition

When the differential equations and boundary conditions describing flow are linear, the mathematical principle of superposition can be used to reduce complex solutions into a number of relatively simple ones. Basically, the principle states that:

If Φ is the desired solution to a homogeneous, linear, partial differential equation and Φ_1, Φ_2, and so forth, are known particular solutions then

$$\Phi = c_1 \, \Phi_1 + c_2 \, \Phi_2 + \ldots \tag{2-116}$$

c_1, c_2 . . . and so forth being constants required to satisfy the boundary conditions.

When the boundary conditions are time independent (say constant production rate), the principle shows that the presence of one boundary condition does not affect the response due to other boundary or initial conditions; that is, there are no interactions among the responses. The total effect, therefore, is the sum of each of the

individual effects.

When the boundary conditions are time dependent (say variable production rate) an extension of the principle of superposition, known as Duhamel's theorem, is used. These principles are usually discussed in mathematical texts under the headings: "Principle of Superposition, Duhamel's Theorem or Faltung Integral" (for instance, Carslaw and Jaeger, 1959, p. 29, Wiley, 1960, p. 335, Bear, 1972, p. 298).

Superposition may be considered to be a problem-solving philosophy in which the pressure behaviour at any point at any time is the sum of the histories of each of the effects that may be considered to affect the solution at that point. Particular applications of superposition which are important in the analysis of pressure test data are discussed in the following sections.

Superposition in Time

The principles enunciated above enable us to analyze changing rates of production from the solution for a constant rate case. Consider, for example, the case of a well flowing at a constant rate q_1 for time t_1, and thereafter at a constant rate q_2 for time t_2.

During the first time interval, the pressure at the well is given (in terms of p) by

$$P_i - P_{wf} = P_i \, q_{D_1} \, P_t\{t_D\}$$

Note that p may be replaced by p^2 or ψ as appropriate, and that the brackets $\{ \}$ mean "which is a function of."

This solution applies until time t_1 is reached. From then on, the solution is made up of two parts:

1. that due to the original rate q_{D_1}, since time $t = 0$
2. that due to the change in rate $(q_2 - q_1)_D$, since time $t = t_1$

Thus for $0 \leq t < t_1$

$$P_i - P_{wf} = P_i \, q_{D_1} \, P_t\{t_D\} \tag{2-117}$$

for $t_1 < t < t_2$

$$P_i - P_{wf} = P_i \, q_{D1} \, P_t\{t_D\} + P_i(q_2 - q_1)_D \, P_t\{(t - t_1)_D\} \qquad (2\text{-}118)$$

The same reasoning may be applied to any number of variable rates, even if some of them are total well shut-ins (zero flow rate). The pressure behaviour is obtained by simply superposing the basic solutions, each of which becomes operative at the time the new flow rate begins, the basic solutions being based on the change in flow rates.

The principle is illustrated in Figure 2-15. The pressure at any time t less than t_1 is that which would be obtained from flowing at q_1, for time t. The pressure at any time t, between t_1 and t_2, is that
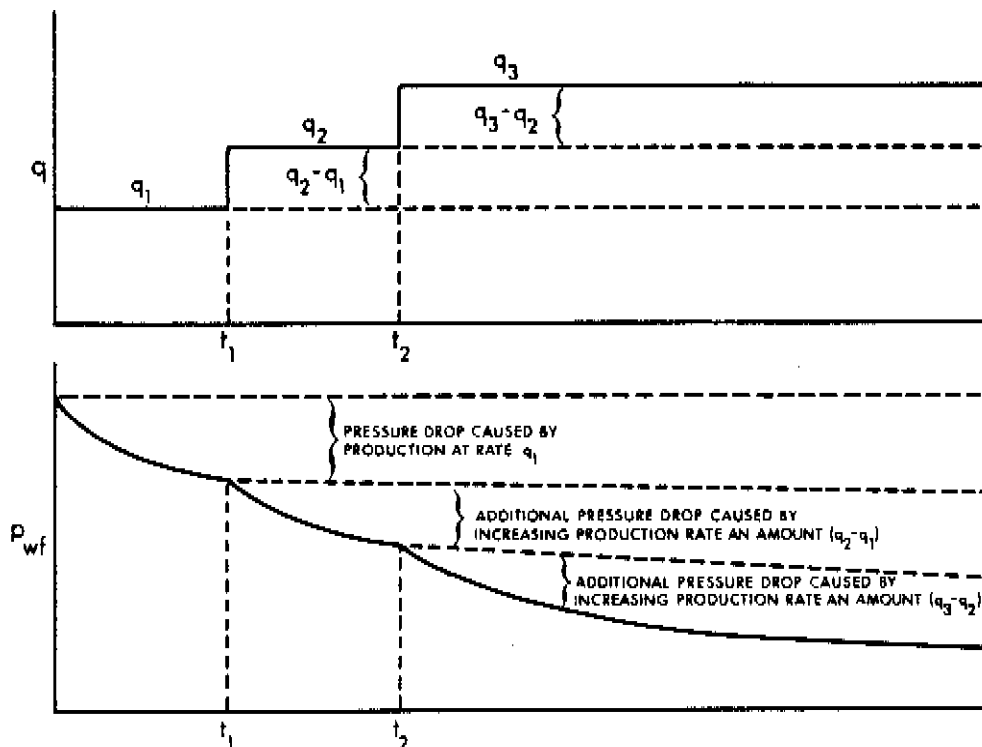
FIGURE 2-15. SUPERPOSITION

which would be obtained from flowing at q_1, for time t, plus that which would be obtained from flowing at $(q_2 - q_1)$ for time $(t - t_1)$. The pressure at any time t greater than t_2 is that which would be obtained from flowing at q_1, for time t, plus that which would be obtained from

flowing at $(q_2 - q_1)$ for time $(t - t_1)$, plus that which would be obtained by flowing at $(q_3 - q_2)$ for time $(t - t_2)$.

The above is the basis for analyzing tests such as "pressure build-up" and "multi-rate flow." These tests will be discussed in detail in appropriate chapters.

EXAMPLE 2-7

<u>Introduction</u>   This example illustrates the principle of superposition in time as applied to the pressure drawdown due to two different flow rates. The method may be extended to any number of changing flow rates.

<u>Problem</u>   A well situated in an infinite-acting reservoir (gas composition given in Example A-1) was produced at a constant rate of 7 MMscfd for 36 hours at which time the flow rate was changed to 21 MMscfd. The stabilized shut-in pressure, $\bar{p}_R$, prior to the test was 2000 psia. General data pertinent to the test are the same as in Example 2-2.

Using the principle of superposition in time calculate the flowing sandface pressure, p_{wf}, after 72 hours of production at the increased flow rate, that is, 108 hours of total production time.

<u>Solution</u>   Since the gas is the same as that of Example A-1, the $\psi - p$ curve already constructed (Figure 2-4) is applicable to this problem.

Noting that $t = 108$, $t_1 = 36$, $q_1 = 7$, $q_2 = 21$
From Table 2-3 and Table 2-4

$$t_D = \frac{2.637 \times 10^{-4} \; k \; t}{\phi \; \mu_i \; c_i \; r_w^2}$$

$$\therefore \; t_{D_1} = \frac{2.637 \times 10^{-4} \; (20)(108)}{(0.15)(0.0158)(0.00053)(0.4)^2} = 2,834,129$$

$$t_{D_2} = \frac{2.637 \times 10^{-4} \; (20)(72)}{(0.15)(0.0158)(0.00053)(0.4)^2} = 1,889,420$$

From Table 2-3 and Table 2-4

$$q_D = \frac{1.417 \times 10^6 \; T \; q_{sc}}{k \; h \; \psi_i}$$

$$\therefore \quad q_{D_1} = \frac{1.417 \times 10^6 \; (580)(7)}{(20)(39)(3.30 \times 10^8)} = 0.0224$$

$$(q_2 - q_1)_D = \frac{1.417 \times 10^6 \; (580)(14)}{(20)(39)(3.30 \times 10^8)} = 0.0447$$

Since the reservoir is infinite-acting, Equation (2-75) applies, so that

$$P_t\Big|_{q_1} = \frac{1}{2}\left[\ln t_{D_1} + 0.809\right]$$

$$= \frac{1}{2}\left[\ln 2,834,129 + 0.809\right] = 7.83$$

$$P_t\Big|_{q_2 - q_1} = \frac{1}{2}\left[\ln t_{D_2} + 0.809\right]$$

$$= \frac{1}{2}\left[\ln 1,889,420 + 0.809\right] = 7.63$$

Equation (2-118) may be written in terms of pseudo-pressure as

$$\psi_{wf} = \psi_i - \psi_i \; P_t\Big|_{q_1} q_{D_1} - \psi_i \; P_t\Big|_{q_2 - q_1} (q_2 - q_1)_D$$

$$= 3.30 \times 10^8 - 3.30 \times 10^8 \; (7.83)(0.0224)$$

$$- 3.30 \times 10^8 (7.63)(0.0447) = 1.60 \times 10^8$$

$$\psi = 1.60 \times 10^8 \; \leftrightarrow \; p = 1362 \qquad \text{(Figure 2-4)}$$

$$\therefore \quad P_{wf} = 1362 \text{ psia}$$

<u>Discussion</u>   Considerable error would result if the continuing effect of
the first rate were ignored and if the effects of each flow rate were
only considered over their respective time intervals. It may be
instructive to note that such a calculation would result in a p_{wf} of
1076 psia which is considerably lower than the correct value of 1362 psia.

Superposition in Space

When more than one well is producing from a common reservoir,
say well A at rate q_A and well B at rate q_B, the pressure at any point
is affected by each of the producing wells. Thus the pressure at a
point P in the reservoir is obtained by superposing (adding) the
solution at point P due to well A to that at point P due to well B.
Each of these solutions is independent of the other and, to obtain it,
the pressure behaviour at any point, r, in the reservoir is required;
that is, the general solution of the partial differential equation and
not just the solution at the well. Thus

$$\Delta p \bigg|_{\text{point P}} = \Delta p \bigg|_{\text{evaluated at P due to flow } q_A \text{ in well A}}$$

$$+ \Delta p \bigg|_{\text{evaluated at P due to flow } q_B \text{ in well B}}$$

$$= p_i \, q_{AD} \left[- \frac{1}{2} \, Ei \left(- \frac{r_{AD}^2}{4 \, t_D} \right) \right]$$

$$+ p_i \, q_{BD} \left[- \frac{1}{2} \, Ei \left(- \frac{r_{BD}^2}{4 \, t_D} \right) \right] \qquad (2\text{-}119)$$

where

$$r_A \quad = \quad \text{distance from point P to well A}$$

$$r_{AD} \quad = \quad r_A / r_w$$

$$r_B \quad = \quad \text{distance from point P to well B}$$

$$r_{BD} \quad = \quad r_B / r_w$$

This is the basis of "interference" type tests used to determine reservoir characteristics such as inter-well porosity. In such a test, point P is really an observation well and the interference of other producing wells is measured at P.

Method of Images

When two wells are producing at the same rate, from an infinite reservoir, there exists, halfway between them, a no-flow boundary. If one well is producing while the other is injecting, the half-way location is a constant pressure boundary. This suggests that the effect of a boundary may be simulated by suitably replacing the boundary by an "image" well. The method of images is in fact a particularly useful application of the principle of superposition for the case of a well situated near a boundary. Using this technique, the boundary is replaced by an odd or even image well, depending on the boundary condition, and the solutions of the real well and the image well are superposed to simulate the boundary conditions (Bear, 1972, p. 304). Superposition employing the method of images proves to be very useful in solving the equations of flow for non-circular reservoirs and for wells situated near a fault.

Odd Image

If $\Phi\{x,y,t\}$ is the solution to a partial differential equation, in rectangular coordinates, satisfying the boundary condition

$$\Phi\{x,0,t\} = 0$$

then

$$\Phi\{x,y,t\} = -\Phi\{x,-y,t\}$$

is the solution of the differential equation for $y < 0$.

This means that a _producing_ well in a semi-infinite reservoir on one side of a constant pressure boundary may be treated simply by superposing on the other side of the boundary, at an equal distance, an image well _injecting_ at the same flow rate, Figure 2-16.
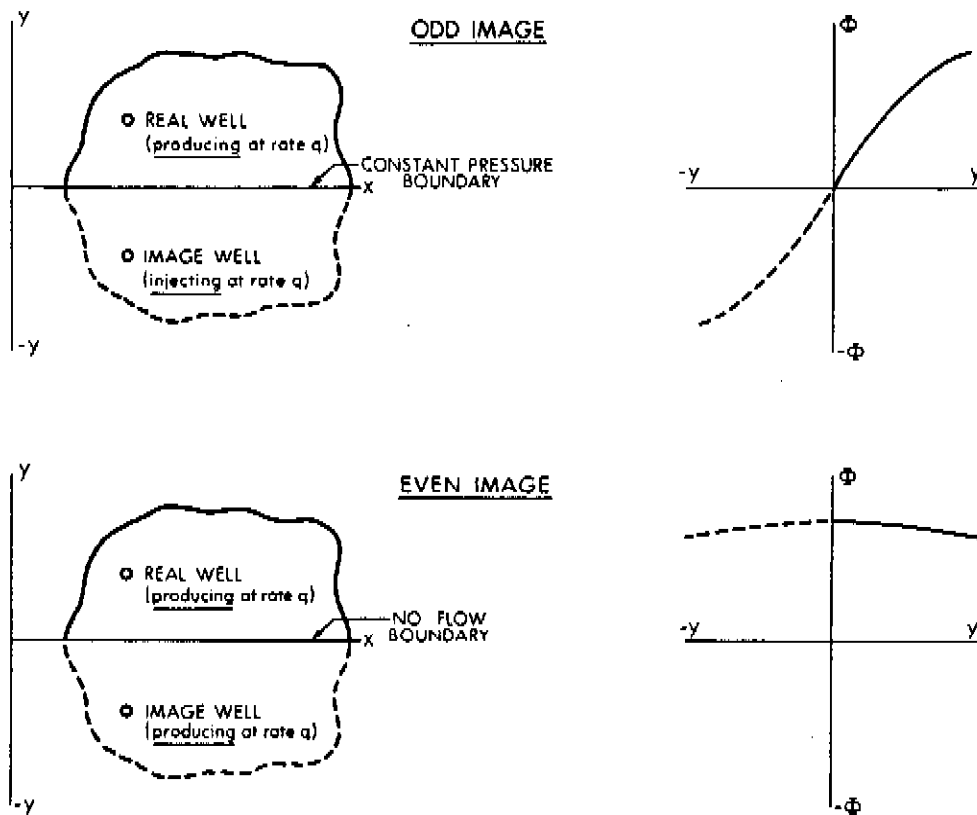
FIGURE 2-16. ODD AND EVEN IMAGES

Even Image

If the boundary condition to be satisfied is

$$\frac{\partial}{\partial x} \ \Phi\{x,0,t\} \ = \ 0$$

then

$$\Phi\{x,y,t\} \ = \ \Phi\{x,-y,t\}$$

is the solution of the differential equation for y < 0.

This means that a producing well on one side of a no-flow boundary may be treated simply by superposing, on the other side of the boundary, at an equal distance, an image well producing at the same flow rate, Figure 2-16.

Simultaneous Superposition
  in Time and Space

Solutions may be superposed both in space and time. For instance, the observation well in an interference test could have pressure effects persisting from its former history, say the pressure was building up after shut-in. Another example could be that of a well located near a boundary, and producing at changing rates. In either case, superposition, in space and time, of the individual effects due to location and flow rate history, will give the resulting behaviour at the observation point.

Consider the case of two wells, A and B, located in the same pool. Well A has produced at rate q_{A_1} for time t_A and the rate was then changed to q_{A_2}. Well B has produced at rate q_{B_1} for time t_B and the rate was then changed to q_{B_2}. The pressure at any point P in the reservoir, at time t, is then given by

$$\Delta p \Big|_P = \Delta p \Big|_{\text{evaluated at P, caused by } q_{A_1} \text{ for } t}$$

$$+ \Delta p \Big|_{\text{evaluated at P, caused by } (q_{A_2} - q_{A_1}) \text{ for } (t - t_A)}$$

$$+ \Delta p \Big|_{\text{evaluated at P, caused by } q_{B_1} \text{ for } t}$$

$$+ \Delta p \Big|_{\text{evaluated at P, caused by } (q_{B_2} - q_{B_1}) \text{ for } (t - t_B)}$$

Desuperposition

Sometimes the only effect that is directly measurable is the superposed effect, as for example, when the build-up pressure is being measured at time $t + \Delta t$ in a well that has been shut-in since time t. The shut-in pressure is in fact the superposed sum of two components, the one due to flow q for a time $t + \Delta t$, and the other due to the change in flow of $(0 - q)$ for time Δt. If one of these components is known, then the other may be obtained by desuperposing the known

component from the measured effect. One important application of this technique is that it enables pressure build-ups to be analyzed by pressure drawdown techniques.

7.2 Well Near a Barrier

Consider a well, A, situated at a distance, $\frac{d}{2}$, from a no-flow barrier and producing at constant rate. This system can be treated by replacing the barrier by an imaginary well A' identical to the real well but situated at a distance, d, from it, as shown in Figure 2-17.
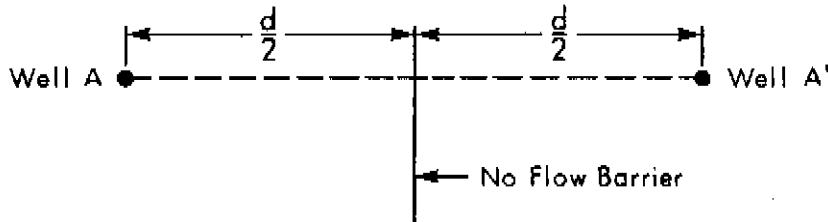
FIGURE 2-17. IMAGE WELL FOR A NO-FLOW BARRIER

Thus the pressure history of the well will be that of an infinite-acting well at A, plus the effect at point A of an infinite-acting well at A', that is

$$\Delta p \Big|_{well} = P_i \, q_D \left[\underbrace{- \frac{1}{2} \, Ei \left(- \frac{\phi \, \mu \, c \, r_w^2}{4 \, \lambda \, k \, t} \right)}_{\text{caused by A}} + \underbrace{\left[- \frac{1}{2} \, Ei \left(- \frac{\phi \, \mu \, c \, d^2}{4 \, \lambda \, k \, t} \right) \right]}_{\text{effect of A' at A}} \right]$$

(2-120)

The first Ei term may be approximated by Equation (2-75) because the argument is usually less than 0.01 for all practical times. However, the same is not true of the second Ei term because of the presence of d^2 (usually a large number) in the argument.

$$\therefore \quad \Delta p = p_i \; q_D \left[\frac{1}{2} \left(\ln t_D + 0.809 \right) - \frac{1}{2} \; Ei \left(- \frac{\phi \; \mu \; c \; d^2}{4 \; \lambda \; k \; t} \right) \right] \qquad (2\text{-}121)$$

EXAMPLE 2-8

Introduction   This example illustrates the principle of superposition in space as applied to the simulation of no-flow barriers within a reservoir.

Problem   A well situated 100 feet from a barrier in an otherwise infinite-acting reservoir (gas composition given in Example A-1) was produced at a constant rate of 7 MMscfd. The stabilized shut-in reservoir pressure, $\bar{p}_R$, prior to the test was 2000 psia. General data pertinent to the test are the same as in Example 2-2. The well/barrier configuration is shown in the figure below.

Using the principle of superposition in space calculate the flowing sandface pressure, p_{wf}, after 36 hours of production.
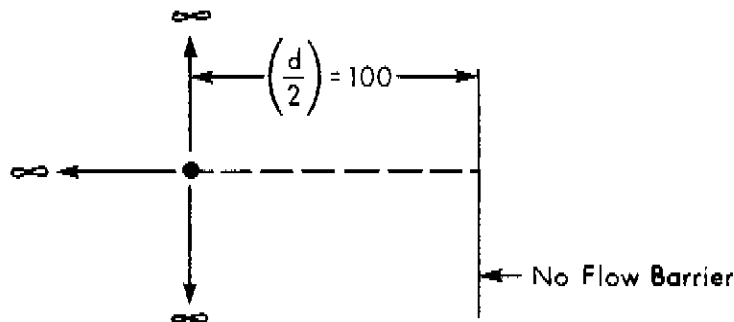
Solution   Since the gas is the same as that of Example A-1, the $\psi - p$ curve already constructed (Figure 2-4) is applicable to this problem. From Example 2-2

$$t_D = \frac{2.637 \times 10^{-4} \; k \; t}{\phi \; \mu_i \; c_i \; r_w^2} = 944,710$$

$$q_D = \frac{1.417 \times 10^6 \; T \; q_{sc}}{k \; h \; \psi_i} = 0.0224$$

Equation (2-121) may be written in terms of pseudo-pressure as:

$$\psi_{wf} = \psi_i - \psi_i \, P_t \, q_D$$

where

$$P_t = \frac{1}{2} (\ln t_D + 0.809) - \frac{1}{2} Ei \left(- \frac{\phi \, \mu_1 \, c_1 \, d^2}{4 \, \lambda \, k \, t} \right)$$

$$= \frac{1}{2} (\ln 944,710 + 0.809)$$

$$- \frac{1}{2} Ei \left(- \frac{(0.15)(0.0158)(0.00053)(200)^2}{4(2.637 \times 10^{-4})(20)(36)} \right)$$

$$= 7.28 - \frac{1}{2} Ei \, (-0.066) = 7.28 + \frac{1}{2} (2.2) \quad \text{(Figure 2.6)}$$

$$= 8.38$$

$$\therefore \quad \psi_{wf} = 3.30 \times 10^8 - 3.30 \times 10^8 \, (8.38)(0.0224)$$

$$= 2.68 \times 10^8$$

$$\psi = 2.68 \times 10^8 \leftrightarrow p = 1787 \quad \text{(Figure 2-4)}$$

$$\therefore \quad P_{wf} = 1787 \text{ psia}$$

<u>Discussion</u> The increased pressure drops at the well due to the presence of a no-flow barrier is observed by comparing the above result to the flowing sandface pressure of 1815 psia from Example 2-3.

<div align="center">

7.3 Well in Rectangular Drainage Area,
No-Flow Boundaries

</div>

For a well with constant production rate, enclosed in a rectangular reservoir with no flow across the boundaries as shown in Figure 2-18, there will be an infinite number of images, because each image will in turn have to be reflected off all the other boundaries (Matthews, Brons and Hazebroek, 1954). Superposing the effect of each
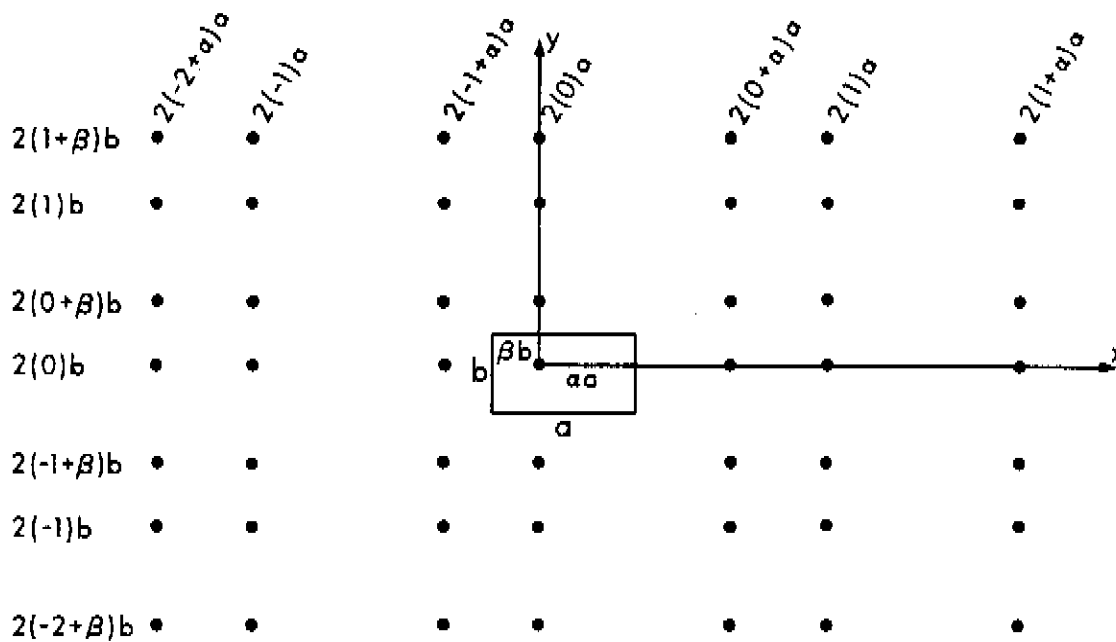
FIGURE 2-18. SOME IMAGES OF A WELL INSIDE A RECTANGLE

From Matthews, Brons and Hazebroek (1954)

of the wells, the pressure drop at the real well is given by

$$\Delta p \bigg|_{well} = p_i \, q_D \left[\frac{1}{2} \, (\ln t_D + 0.809) + \sum_{N=1}^{\infty} - \frac{1}{2} \, Ei \left(- \frac{\phi \, \mu \, c \, d_N^2}{4 \, \lambda \, k \, t} \right) \right]$$

(2-122)

where d_N is the distance of the Nth image well from the real well. d_N is easily calculated from the relative position of the well in the rectangle. Thus, for the well shown in Figure 2-18, the images are located at positions:

$$(2 \, m \, a, \, 2 \, n \, b), \, \left[2 \, (m+\alpha) \, a, \, 2 \, n \, b \right], \, \left[2 \, m \, a, \, 2 \, (n+\beta) \, b \right]$$

and

$$\left[2 \, (m+\alpha) \, a, \, 2 \, (n+\beta) \, b \right] \qquad \text{for} \quad -\infty \leq m,n \leq +\infty$$

An infinite number of image wells is required for an exact representation of the solution. However, in practical problems, the series in Equation (2-122) converges quite rapidly.

7.4 Well in Regular Polygon, No-Flow Boundaries

For a well enclosed in any polygonal drainage area, Equation (2-122) will apply, provided d_N is properly calculated for that shape. The well is not necessarily in the centre of the drainage area. This equation has been evaluated for regular polygons by several authors among whom are Matthews, Brons and Hazebroek (1954), Dietz (1965), Pitzer (1964), Earlougher, Ramey, Miller, and Mueller (1968). For practical applications, the concept of the shape factor, C_A, which depends on the shape of the area and the well position, is quite useful.

Defining a dimensionless time based on drainage area, A, as

$$t_{DA} = \frac{\lambda \, k \, t}{\phi \, \mu \, c \, A} = t_D \frac{r_w^2}{A} \tag{2-123}$$

Equation (2-122) may be rewritten (for $t_D > 25$) as (Ramey, 1967):

$$P_i - P_{wf} = P_i \, q_D \, \frac{1}{2} \left[\ln \left(\frac{4A \, t_{DA}}{1.781 \, r_w^2} \right) + 4 \, \pi \, t_{DA} \right.$$

$$\left. - 4 \, \pi \, t_{DA} - \sum_{N=1}^{\infty} Ei \left(\frac{-1}{4 \, t_{DA}} \frac{d_N^2}{A} \right) \right] \tag{2-124}$$

$$= P_i \, q_D \, \frac{1}{2} \left[\ln \left(\frac{4A \, t_{DA}}{1.781 \, r_w^2} \right) + 4 \, \pi \, t_{DA} - F \right] \tag{2-125}$$

where

$$F = 4 \, \pi \, t_{DA} + \sum_{N=1}^{\infty} Ei \left(\frac{-1}{4 \, t_{DA}} \frac{d_N^2}{A} \right) \tag{2-126}$$

Defining

$$p^* = p_i - \frac{p_i \, q_D}{2} (4 \pi \, t_{DA} - F) \qquad (2\text{-}127)$$

Equation (2-125) becomes

$$\frac{p^* - p_{wf}}{p_i \, q_D} = \frac{1}{2} \ln \left(\frac{4A \, t_{DA}}{1.781 \, r_w^2} \right)$$

$$= \frac{1}{2} (\ln t_D + 0.809) \qquad (2\text{-}128)$$

It is readily seen that Equation (2-128), which represents the pressure at the well in a reservoir of any shape, may be obtained simply by replacing p_i by p^* in Equation (2-75), which is the equation applicable to an infinite reservoir.

Returning to Equation (2-127) and substituting in terms of the average reservoir pressure, $\bar{p}_R$, from the material balance Equation (2-94) gives

$$p^* = \bar{p}_R + \frac{p_i \, q_D}{2} F$$

from which

$$F = 2 \frac{p^* - \bar{p}_R}{p_i \, q_D} = 2 \frac{\psi^* - \bar{\psi}_R}{\psi_i \, q_D} \qquad (2\text{-}129)$$

F is in fact the Matthews, Brons and Hazebroek (1954) dimensionless pressure function which has been evaluated for various reservoir shapes and well locations. In Chapter 5, dealing with pressure build-up analysis, it is shown that p^* may be obtained from the extrapolation to $\left(\frac{t + \Delta t}{\Delta t} \right) = 1$ of the straight line portion of a build-up curve plotted as p_{ws} versus $\log \left(\frac{t + \Delta t}{\Delta t} \right)$, where p_{ws} is the shut-in pressure at the well.

Values of F are tabulated in Table 2-6 for various rectangles (Earlougher et al., 1968), and sample curves of F versus $\log t_{DA}$ are shown in Appendix C, Figures C-1(a) to C-1(g) inclusive (Matthews et al.,

1954). It will be observed from Figures C-1 (a-g) that after a certain t_{DA}, depending on the reservoir shape and the location of the well, pseudo-steady state is reached and the curves become straight lines described by

$$F = \ln \left(\frac{C_A \lambda k t}{\phi \mu c A} \right) = \ln (C_A t_{DA}) \tag{2-130}$$

C_A is a shape factor and is obtained from $\ln C_A$ by extrapolating the straight line portion of F to $t_{DA} = 1$.

Examination of Equation (2-125) shows that for small t_{DA}, that is, the transient region of flow, the well is infinite acting and

$$F = 4 \pi t_{DA} \tag{2-131}$$

and

$$P_t = \frac{1}{2} \ln \left(\frac{4 A t_{DA}}{1.781 r_w^2} \right) \tag{2-132}$$

For large t_{DA}, when all the boundaries have been felt, that is, at pseudo-steady state, Equation (2-130) applies and

$$P_t = \frac{1}{2} \ln \left(\frac{4 A}{1.781 r_w^2 C_A} \right) + 2 \pi t_{DA} \tag{2-133}$$

Ramey and Cobb (1971) consider Equation (2-133) to be a defining equation for C_A, the shape factor. It is easily seen that this is equivalent to the previous definition of C_A. The range of applicability of Equations (2-132) and (2-133) varies with C_A. Table 2-7 obtained from Dietz (1965) gives values for C_A for various systems, and the value of t_{DA} after which Equation (2-133) applies. Similar values of $\ln C_A$ and t_{DA} were evaluated by Earlougher et al. (1968) and also by Earlougher and Ramey (1973). These latter values appear, in Appendix C, at the base of the second columns of Tables C-1(a) to C-1(n), inclusive. Earlougher and Ramey (1968) showed how the shape factor for non-tabulated shapes may be obtained by interpolation from known values of C_A.

DIMENSIONLESS TIME

F=MBH DIMENSIONLESS PRESSURE FUNCTION

t_{DA}	1	1	1	1	2	2	2	2
0.0010	0.0126	0.0126	0.0126	0.0126	0.0126	0.0126	0.0126	0.0126
0.0015	0.0188	0.0188	0.0188	0.0188	0.0188	0.0188	0.0188	0.0188
0.0020	0.0251	0.0251	0.0251	0.0251	0.0251	0.0251	0.0251	0.0251
0.0025	0.0314	0.0314	0.0314	0.0311	0.0314	0.0314	0.0314	0.0314
0.0030	0.0377	0.0377	0.0377	0.0368	0.0377	0.0377	0.0377	0.0377
0.0040	0.0503	0.0503	0.0503	0.0460	0.0503	0.0502	0.0503	0.0502
0.0050	0.0628	0.0628	0.0628	0.0517	0.0628	0.0626	0.0628	0.0626
0.0060	0.0754	0.0754	0.0754	0.0537	0.0754	0.0745	0.0754	0.0745
0.0070	0.0880	0.0880	0.0879	0.0524	0.0880	0.0858	0.0880	0.0858
0.0080	0.1005	0.1005	0.1004	0.0483	0.1005	0.0963	0.1005	0.0963
0.0090	0.1131	0.1130	0.1128	0.0422	0.1131	0.1059	0.1131	0.1059
0.0100	0.1257	0.1254	0.1251	0.0345	0.1257	0.1145	0.1257	0.1145
0.0150	0.1885	0.1854	0.1823	-0.0162	0.1884	0.1449	0.1884	0.1449
0.0200	0.2513	0.2402	0.2287	-0.0700	0.2508	0.1601	0.2505	0.1598
0.0250	0.3141	0.2892	0.2630	-0.1181	0.3119	0.1678	0.3107	0.1663
0.0300	0.3769	0.3333	0.2864	-0.1584	0.3708	0.1723	0.3676	0.1683
0.0400	0.5016	0.4108	0.3087	-0.2166	0.4804	0.1812	0.4686	0.1657
0.0500	0.6237	0.4791	0.3099	-0.2512	0.5785	0.1955	0.5511	0.1593
0.0600	0.7415	0.5413	0.3002	-0.2694	0.6667	0.2169	0.6167	0.1513
0.0700	0.8537	0.5991	0.2856	-0.2766	0.7471	0.2450	0.6683	0.1428
0.0800	0.9597	0.6531	0.2700	-0.2765	0.8217	0.2787	0.7085	0.1346
0.0900	1.0592	0.7038	0.2553	-0.2716	0.8917	0.3167	0.7398	0.1269
0.1000	1.1524	0.7516	0.2427	-0.2633	0.9581	0.3581	0.7642	0.1198
0.1500	1.5364	0.9583	0.2226	-0.1951	1.2524	0.5864	0.8261	0.0954
0.2000	1.8212	1.1314	0.2637	-0.1027	1.4987	0.8106	0.8476	0.0873
0.2500	2.0439	1.2854	0.3412	0.0025	1.7064	1.0104	0.8629	0.0923
0.3000	2.2262	1.4257	0.4365	0.1129	1.8830	1.1841	0.8829	0.1087
0.4000	2.5139	1.6720	0.6400	0.3300	2.1678	1.4674	0.9447	0.1687
0.5000	2.7370	1.8797	0.8321	0.5268	2.3905	1.6899	1.0299	0.2537
0.6000	2.9193	2.0563	1.0028	0.6994	2.5724	1.8722	1.1280	0.3518
0.7000	3.0735	2.2083	1.1527	0.8499	2.7269	2.0263	1.2307	0.4545
0.8000	3.2070	2.3411	1.2847	0.9821	2.8605	2.1599	1.3329	0.5567
0.9000	3.3249	2.4586	1.4019	1.0994	2.9782	2.2776	1.4315	0.6552
1.0000	3.4302	2.5638	1.5070	1.2045	3.0836	2.3830	1.5252	0.7489
2.0000	4.1234	3.2569	2.2000	1.8976	3.7768	3.0762	2.2002	1.4239
4.0000	4.8166	3.9501	2.8933	2.5908	4.4701	3.7695	2.8932	2.1170
8.0000	5.5099	4.6435	3.5867	3.2842	5.1633	4.4627	3.5866	2.8103
10.0000	5.7331	4.8667	3.8098	3.5073	5.3865	4.8859	3.8098	3.0335

DIMENSIONLESS TIME

F=MBH DIMENSIONLESS PRESSURE FUNCTION

t_{DA}	2	2	2	4	4	4	4	5
0.0010	0.0125	0.0126	0.0125	0.0126	0.0126	0.0126	0.0126	0.0126
0.0015	0.0179	0.0188	0.0179	0.0188	0.0188	0.0188	0.0188	0.0188
0.0020	0.0209	0.0251	0.0208	0.0251	0.0251	0.0251	0.0251	0.0251
0.0025	0.0203	0.0314	0.0200	0.0314	0.0311	0.0314	0.0311	0.0314
0.0030	0.0160	0.0377	0.0155	0.0377	0.0368	0.0377	0.0368	0.0377
0.0040	-0.0019	0.0502	-0.0027	0.0503	0.0460	0.0503	0.0460	0.0503
0.0050	-0.0284	0.0626	-0.0295	0.0628	0.0517	0.0628	0.0517	0.0628
0.0060	-0.0596	0.0745	-0.0612	0.0754	0.0537	0.0754	0.0537	0.0753
0.0070	-0.0932	0.0858	-0.0951	0.0879	0.0524	0.0879	0.0524	0.0878
0.0080	-0.1277	0.0962	-0.1298	0.1004	0.0483	0.1004	0.0483	0.1000
0.0090	-0.1620	0.1058	-0.1644	0.1129	0.0422	0.1129	0.0422	0.1119
0.0100	-0.1957	0.1144	-0.1983	0.1251	0.0345	0.1251	0.0345	0.1234
0.0150	-0.3468	0.1445	-0.3502	0.1823	-0.0162	0.1823	-0.0162	0.1713
0.0200	-0.4670	0.1589	-0.4718	0.2291	-0.0701	0.2291	-0.0701	0.2015
0.0250	-0.5615	0.1641	-0.5695	0.2643	-0.1186	0.2643	-0.1187	0.2163
0.0300	-0.6357	0.1633	-0.6507	0.2897	-0.1600	0.2897	-0.1600	0.2200
0.0400	-0.7395	0.1492	-0.7839	0.3197	-0.2231	0.3194	-0.2235	0.2075
0.0500	-0.8012	0.1224	-0.8965	0.3332	-0.2662	0.3315	-0.2682	0.1820
0.0600	-0.8339	0.0862	-0.9989	0.3385	-0.2957	0.3335	-0.3013	0.1516
0.0700	-0.8457	0.0437	-1.0949	0.3399	-0.3158	0.3290	-0.3278	0.1203
0.0800	-0.8422	-0.0028	-1.1859	0.3401	-0.3291	0.3199	-0.3510	0.0899
0.0900	-0.8272	-0.0512	-1.2723	0.3403	-0.3375	0.3072	-0.3727	0.0613
0.1000	-0.8038	-0.1004	-1.3542	0.3412	-0.3421	0.2913	-0.3942	0.0351
0.1500	-0.6223	-0.3322	-1.7021	0.3663	-0.3257	0.1826	-0.5128	-0.0580
0.2000	-0.4138	-0.5189	-1.9613	0.4269	-0.2661	0.0468	-0.6499	-0.0935
0.2500	-0.2196	-0.6580	-2.1508	0.5120	-0.1811	-0.0959	-0.7928	-0.0855
0.3000	-0.0479	-0.7555	-2.2854	0.6102	-0.0829	-0.2344	-0.9312	-0.0477
0.4000	0.2343	-0.8547	-2.4344	0.8152	0.1220	-0.4789	-1.1758	0.0773
0.5000	0.4567	-0.8671	-2.4768	1.0075	0.3143	-0.6712	-1.3681	0.2266
0.6000	0.6389	-0.8284	-2.4564	1.1783	0.4852	-0.8134	-1.5103	0.3753
0.7000	0.7931	-0.7620	-2.4011	1.3282	0.6351	-0.9129	-1.6098	0.5143
0.8000	0.9267	-0.6820	-2.3278	1.4602	0.7670	-0.9775	-1.6744	0.6409
0.9000	1.0444	-0.5969	-2.2469	1.5774	0.8843	-1.0145	-1.7114	0.7555
1.0000	1.1497	-0.5115	-2.1640	1.6825	0.9894	-1.0301	-1.7270	0.8595
2.0000	1.8430	0.1507	-1.5058	2.3755	1.6824	-0.7325	-1.4294	1.5516
4.0000	2.5363	0.8436	-0.8129	3.0688	2.3757	-0.0756	-0.7725	2.2448
8.0000	3.2295	1.5370	-0.1195	3.7623	3.0691	0.6173	-0.0796	2.9381
10.0000	3.4527	1.7601	0.1036	3.9854	3.2922	0.8406	0.1438	3.1615

TABLE 2-6.   MBH DIMENSIONLESS PRESSURE FUNCTIONS FOR VARIOUS CLOSED RECTANGULAR RESERVOIRS

From Earlougher, Ramey, Miller and Mueller (1968)

2-95

Shape	$\ln C_A$	C_A	Stabilized Conditions for $t_{DA}>$		Shape	$\ln C_A$	C_A	Stabilized Conditions for $t_{DA}>$
IN BOUNDED RESERVOIRS					rectangle (dot top), 2	2.38	10.8	0.3
circle (dot center)	3.45	31.6	0.1		rectangle (dot right-center), 2	1.58	4.86	1.0
square (dot center)	3.43	30.9	0.1		rectangle (dot upper-right), 2	0.73	2.07	0.8
hexagon (dot center)	3.45	31.6	0.1		rectangle (dot center), 4	1.00	2.72	0.8
triangle (dot center)	3.32	27.6	0.2		rectangle (dot right-center), 4	-1.46	0.232	2.5
parallelogram 60°	3.30	27.1	0.2		rectangle (dot upper-right), 4	-2.16	0.115	3.0
right triangle 1/3, 1	3.09	21.9	0.4		rectangle (dot top)	1.22	3.39	0.6
rectangle (dot center), 2	3.12	22.6	0.2		rectangle (dot top), 2	1.14	3.13	0.3
rectangle (dot center), 4	1.68	5.38	0.7		rectangle (dot right), 2	-0.50	0.607	1.0
rectangle (dot center), 5	0.86	2.36	0.7		rectangle (dot right), 2	-2.20	0.111	1.2
square 2×2 (dot center)	2.56	12.9	0.6		trapezoid 3,4	-2.32	0.098	0.9
square 2×2 (dot offset)	1.52	4.57	0.5		*IN WATER-DRIVE RESERVOIRS* circle (dot center)	2.95	19.1	0.1
					IN RESERVOIRS OF UNKNOWN PRODUCTION CHARACTER circle (dot center)	3.22	25	0.1

TABLE 2-7   PSEUDO-STEADY STATE SHAPE FACTORS FOR VARIOUS RESERVOIRS

From Dietz (1965)

For wells located centrally in a regular polygon, Equation (2-132) applies up to $t_{DA} = 0.1$. The transition between Equations (2-132) and (2-133) varies with each situation. During this period, the pressure drop function may be obtained from Equation (2-125) provided F is obtained from either Table 2-6 or Figures C-1(a-g).

The equations which have been discussed describe the pressure at the well, but similar expressions may be obtained for the pressure at any point in the formation. Results for various well geometries and for different observation points are shown in Tables C-1(a) to C-1(n) (Earlougher and Ramey, 1973). These tabulations are useful in calculating interference effects and are not limited to use with $\sqrt{A}/r_w = 2000$, except at the well point itself. For $\sqrt{A}/r_w \neq 2000$, the pressure function at the well is obtained by adding to the tabular values the quantity $\left(\ln \dfrac{\sqrt{A}}{r_w} - \ln 2000 \right)$. At any other location, the tabulated values may be used directly.

Graphically, the drawdown curve at the well may be depicted as shown in Figure 2-19. The curve may be represented throughout by
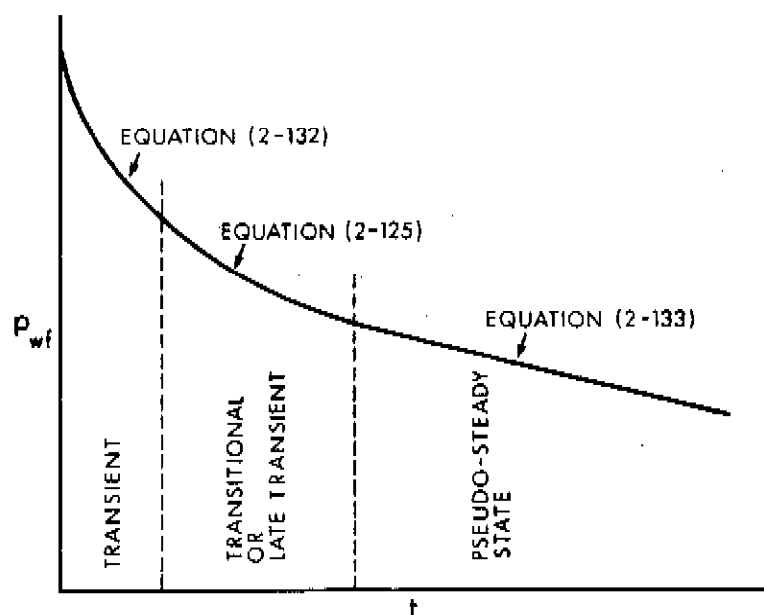
FIGURE 2-19. WELLBORE PRESSURE FOR A WELL PRODUCING AT A CONSTANT RATE FROM A CLOSED RESERVOIR OF GENERAL SHAPE

Equation (2-125). However, for the transient period it simplifies to
Equation (2-132). At the end of the transient period, the boundaries
start to be felt. This gives rise to the late transient or transition
period which can only be represented by Equation (2-125). When the
effect of all the boundaries has been felt, pseudo-steady state starts
and Equation (2-133) applies. As discussed previously, the length of
the transition period depends on the well/reservoir shape situation.
For a well in the centre of a circular or a square reservoir, with no
flow across the boundaries, and where the distance from the well to the
boundaries is more than 100 times the wellbore radius (as is usually the
case for gas reservoirs) there is no discernible transition period
between the transient period and the pseudo-steady state. That is,
the flow equations are Equation (2-132) for the transient state,
followed immediately by Equation (2-133) for the pseudo-steady state.
This was discussed in Section 6.4 along with the time to stabilization,
and is confirmed by Pitzer (1964) and Ramey and Cobb (1971).

Some authors, however (Matthews and Russell, 1967, p. 48,
Jones, 1963, Odeh and Nabor, 1966) indicate that for a circular
reservoir there exists a transition period from $t_{DA} \simeq 0.03$ to $t_{DA} \simeq 0.1$,
between the transient and pseudo-steady states.

EXAMPLE 2-9

Introduction   The analytical solutions discussed in Section 6 were
developed for a radial-cylindrical flow model assuming the existence of
infinite or finite, circular reservoirs. These solutions can be extended
quite easily to account for different reservoir geometries, that is,
regular polygons.

Problem   A well situated in the centre of a regular polygon, as shown
in the figure below (gas composition given in Example A-1) having closed
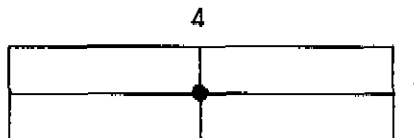
"no-flow" boundaries, and an area, A, of 10×10^6 feet^2, was produced at a constant rate of 7 MMscfd. The stabilized shut-in reservoir pressure, $\bar{p}_R$, prior to the test was 2000 psia. General data pertinent to the test are the same as in Example 2-2.

Calculate the flowing sandface pressure, p_{wf}, after 36 hours and after 1800 hours of production.

Solution   Since the gas is the same as that of Example A-1, the $\psi - p$ curve already constructed (Figure 2-4) is applicable to this problem.

t = 36

From Equation (2-123) and Table 2-4

$$t_{DA} = \frac{2.637 \times 10^{-4} \; k \; t}{\phi \; \mu_i \; c_i \; A}$$

$$= \frac{2.637 \times 10^{-4} \; (20)(36)}{(0.15)(0.0158)(0.00053)(10 \times 10^6)} = 0.0151$$

From Example 2-2

$$q_D = \frac{1.417 \times 10^6 \; T \; q_{sc}}{k \; h \; \psi_i} = 0.0224$$

$$t_{DA} = 0.0151 \quad \leftrightarrow \quad F = 0.1823 \qquad \text{(Table 2-6)}$$

$$\approx 0.2 \qquad \text{(Figure C-1(d))}$$

From Equation (2-125)

$$P_t = \Delta p_D \Big|_{well} = \frac{1}{2} \left[\ln \left(\frac{4A \; t_{DA}}{1.781 \; r_w^2} \right) + 4 \pi \; t_{DA} - F \right]$$

$$= \frac{1}{2} \left[\ln \left(\frac{4 \; (10 \times 10^6)(0.0151)}{1.781 \; (0.40)^2} \right) + 4 \pi \; (0.0151) - 0.1823 \right]$$

$$= 7.29$$

From Table 2-3 and Equation (2-73)

$$P_t = \frac{\psi_i - \psi_{wf}}{\psi_i \, q_D}$$

$$\psi_{wf} = \psi_i - \psi_i \, P_t \, q_D$$

$$= 3.30 \times 10^8 - 3.30 \times 10^8 \, (7.29)(0.0224)$$

$$= 2.76 \times 10^8$$

$$\psi = 2.76 \times 10^8 \quad \leftrightarrow \quad p = 1815 \qquad \text{(Figure 2-4)}$$

$$P_{wf} = 1815 \text{ psia}$$

t = 1800

From Equation (2-123) and Table 2-4

$$t_{DA} = \frac{2.637 \times 10^{-4} \, k \, t}{\phi \, \mu_i \, c_i \, A}$$

$$= \frac{2.637 \times 10^{-4} \, (20)(1800)}{(0.15)(0.0158)(0.00053)(10 \times 10^6)} = 0.7558$$

From Example 2-2

$$q_D = \frac{1.417 \times 10^6 \, T \, q_{sc}}{k \, h \, \psi_i} = 0.0224$$

$$t_{DA} = 0.7558 \quad \leftrightarrow \quad F = 1.4019 \qquad \text{(Table 2-6)}$$

$$\approx 1.4 \qquad \text{(Figure C-1(d))}$$

From Equation (2-125)

$$P_t = \Delta P_D \bigg|_{well} = \frac{1}{2} \left[\ln \left(\frac{4A \, t_{DA}}{1.781 \, r_w^2} \right) + 4 \, \pi \, t_{DA} - F \right]$$

$$= \frac{1}{2} \left[\ln \left(\frac{4 \ (10 \times 10^6)(0.7558)}{1.781 \ (0.40)^2} \right) + 4 \ \pi \ (0.7558) - 1.4019 \right]$$

$$= 13.29$$

$$\therefore \ \psi_{wf} = \psi_1 - \psi_i \ P_t \ q_D$$

$$= 3.30 \times 10^8 - 3.30 \times 10^8 \ (13.29)(0.0224)$$

$$= 2.32 \times 10^8$$

$$\psi = 2.32 \times 10^8 \quad \leftrightarrow \quad p = 1654 \qquad \text{(Figure 2-4)}$$

$$\therefore \ P_{wf} = 1654 \ \text{psia}$$

Alternatively, from Table 2-7, t_{DA} required for stabilization equals 0.7 and $C_A = 5.38$. Since t_{DA} at 1800 hours = 0.7558 > 0.7, Equation (2-133) can be used to evaluate P_t.

From Equation (2-133)

$$P_t = \frac{1}{2} \ln \left(\frac{4A}{1.781 \ r_w^2 \ C_A} \right) + 2 \ \pi \ t_{DA}$$

$$= \frac{1}{2} \ln \left[\frac{4 \ (10 \times 10^6)}{(1.781)(0.4)^2 \ (5.38)} \right] + 2 \ \pi \ (0.7558)$$

$$= 13.29$$

$$\therefore \ \psi_{wf} = \psi_1 - \psi_i \ P_t \ q_D$$

$$= 3.30 \times 10^8 - 3.30 \times 10^8 \ (13.29)(0.0224)$$

$$= 2.32 \times 10^8$$

$$\psi = 2.32 \times 10^8 \quad \leftrightarrow \quad p = 1654 \qquad \text{(Figure 2-4)}$$

$$\therefore \ P_{wf} = 1654 \ \text{psia}$$

<u>Discussion</u>   After 36 hours of flow the reservoir is still infinite-
acting so that the answer is the same as for the infinite reservoir of
Example 2-3.

The pressure at the well after 1800 hours of flow is 1654 psia,
compared with 1680 psia for a well in the centre of a circular reservoir
of equal area. The reservoir has now achieved pseudo-steady state and the
rate of pressure decline, $\partial p/\partial t$, throughout the reservoir is constant.

7.5 Well Enclosed in Mixed No-Flow/Constant-Pressure Boundaries

Wells situated near a large aquifer often possess one or more
constant-pressure boundaries. Situations of this kind, for various
reservoir shapes have been studied in great detail by Ramey, Kumar and
Gulati (1973). Their results, published as an AGA monograph, include a
computer program and cover numerous shapes and mixed (constant-pressure/
no-flow) boundary conditions for water-drive reservoirs. This work
should be consulted for the various well/boundary/reservoir geometries.
The method of superposition is employed, using an even image for a no-
flow boundary and an odd image for a constant-pressure boundary.

7.6 Well in the Centre of a Square Reservoir, Constant-Pressure Outer Boundaries

For a well located centrally in a square with all boundaries
at constant pressure and with the well producing at a constant rate,
three regions of flow may be recognized.

1. Transient region: As before, the dimensionless pressure
   at the well is given by Equation (2-131). However, this
   region extends only up to $t_{DA} \leq 0.05$ (contrast with no-
   flow boundaries, $t_{DA} \leq 0.1$).

2. Steady-state region: True steady state can be achieved
   with constant-pressure boundaries. In this region, the
   governing equation is (Ramey et al., 1973, p. 45)

$$P_t = \frac{1}{2} \ln \left(\frac{16 \ A}{1.781 \ r_w^2 \ C_A} \right) \qquad \text{for} \qquad t_{DA} > 0.25 \qquad (2\text{-}134)$$

This equation may be regarded as a definition of the shape factor, C_A, for a well in a constant-pressure drainage shape.

3. Transition region: This extends from the end of the transient to the beginning of steady-state, that is, from $t_{DA} = 0.05$ to $t_{DA} = 0.25$.

For a well in the middle of a square with constant-pressure outer boundaries, Equation (2-132) may be used up to $t_{DA} = 0.125$ and thereafter Equation (2-134), with a maximum error of about 1.4 per cent (Ramey et al., 1973, p. 46).

8 NUMERICAL SOLUTIONS OF THE FLOW EQUATION

All of the solutions to the partial differential equations discussed so far were obtained from analytical or semi-analytical methods. The simplest example of the analytical solution is Equation (2-72). A semi-analytical procedure is required if the pseudo-pressure concept is used for real gases, since in this case the integral, given by Equation (2-40), must be evaluated numerically. In both of these cases the boundary value problem was linearized by assuming that coefficients of all terms in the partial differential equation are independent of the dependent variable, Δp_D.

Numerical methods must be used for cases where the partial differential equation and its boundary conditions (Boundary Value Problem) cannot be linearized, where the reservoir shape is irregular or where the reservoir is heterogeneous. In some complex situations analytical solutions, even when possible, may be so difficult to apply, that numerical methods are preferred. In this section a brief discussion of the numerical approach is presented along with the types of problems solved by this approach.

8.1 Radial One-Dimensional Models

The transient radial flow of a real gas in a porous medium is expressed by Equations (2-26) or (2-30) as

$$\frac{1}{r}\frac{\partial}{\partial r}\left[r\frac{p}{Z}\left(-\frac{k}{\mu}\delta\frac{\partial p}{\partial r}\right)\right] = -\frac{\partial}{\partial t}\left(\frac{\phi\,p}{Z}\right) \tag{2-135}$$

This equation with appropriate boundary conditions may be solved directly by numerical methods without any further assumptions regarding the properties of the gas or of the porous medium. We note that it is not necessary to assume that the reservoir is homogeneous; k and ϕ may vary with position or pressure. IT flow is accounted for through δ.

The first numerical treatment of this problem reported in the literature was by Bruce, Peaceman, Rachford and Rice (1953). They assumed k, ϕ and Z to be constant and $\delta = 1$. They solved Equation (2-135) and the corresponding linear flow equation for various flow rates and presented their results in dimensionless coordinates. Jones (1961) extended the treatment to include the effect of IT flow. Russell, Goodrich, Perry and Bruskotter (1966) have applied the numerical solution of Equation (2-135) to the prediction of gas well performance (assumptions made by Russell et al. are the same as those made by Bruce et al.). They gave an example of well draining 640 acres in a 25 md-ft formation (8,120 MMSCF in place) at a constant rate of 993 Mscfd. Analysis based on the analytical solutions presented previously, where $(\nabla p)^2$ terms are neglected, shows that the bottom hole pressure will decline from 4000 to 1000 psia in 5.3 years, while the more accurate numerical analysis predicts that the same decline will occur in 8.7 years. Such large difference between the pressures predicted by the analytical and numerical solutions occur only when the pressure drawdown is also large. This aspect is considered in more detail by Aziz, Mattar, Ko and Brar (1975). Their findings are summarized in Section 11 of this chapter. Wattenbarger and Ramey (1968) have numerically solved Equation (2-135) by retaining the IT flow coefficient δ, and with a radial zone of altered permeability (skin) around the well. They also consider the wellbore storage effect.

8.2 Radial Two-Dimensional Models

Where vertical flow is important a two-dimensional radial model must be considered. The equation to be solved in this case is

$$\frac{1}{r} \frac{\partial}{\partial r} \left[r \frac{p}{Z} \left(- \frac{k_r}{\mu} \delta_r \frac{\partial p}{\partial r} \right) \right] + \frac{\partial}{\partial z} \left[\frac{p}{Z} \left(- \frac{k_z}{\mu} \delta_z \frac{\partial p}{\partial z} \right) \right] = - \frac{\partial}{\partial t} \left(\frac{\phi \, p}{Z} \right)$$

$$(2\text{-}136)$$

A computer model that solves the above equation can be used to analyze the effects of certain types of reservoir heterogeneity and anisotropy in addition to the problems mentioned in connection with the solution of the one-dimensional problem. The solution of this equation can only be used for the analysis of single-well problems where every pie-shaped slice of the reservoir is identical to every other slice of the same size. This limits the class of problems that can be investigated by this method. Kazemi and Seth (1969) have used a model of this type to study

1. The combined effects of anisotropy, stratification with crossflow, and restricted flow entry on the transient pressure analysis of drawdown and build-up tests;

2. The feasibility of calculating the horizontal permeabilities of intercommunicating stratified systems; and

3. Pressure interference tests in such systems.

As mentioned previously, it is not possible to account for the horizontal variation of rock properties in this model. Kazemi (1969) has used a similar model to provide certain guidelines for the analysis of transient pressure data from naturally fractured reservoirs with a uniform fracture distribution.

The use of r - z coordinates provides a natural and simple method of obtaining accurate and detailed solutions near the well, where pressure gradients are largest. In the solution of Equations (2-135) and (2-136), production and injection terms are accounted for through the boundary condition at the well.

8.3 Areal Two-Dimensional Models

Extension of single-well models obtained from the solution of Equation (2-135) to multi-well models is possible through the solution of Equation (2-137)

$$\frac{\partial}{\partial x}\left(\frac{p}{Z}\frac{h}{\mu}\frac{k_x}{\delta_x}\frac{\partial p}{\partial x}\right) + \frac{\partial}{\partial y}\left(\frac{p}{Z}\frac{h}{\mu}\frac{k_y}{\delta_y}\frac{\partial p}{\partial y}\right) = \frac{\partial}{\partial t}\left(\frac{\phi\,h\,p}{Z}\right) + q\{x,y,t\}$$

(2-137)

Any areal domain with any number of wells may be considered. The injection or production from different wells is accounted for by the q term. The reservoir shape may be completely arbitrary and different types of boundary conditions (no-flow, constant pressure, and so forth) may be considered on different portions of the boundary. This model can also be used for interference test analysis. Studies of this type for Darcy flow have been reported in the literature, for example, by Carter (1966) and Quon et al. (1966).

8.4 Three-Dimensional Models

The extension of Equations (2-136) or (2-137) to three dimensions is straightforward. Generation of computer models and their use in three dimensions does, however, require a fair amount of human and computer time. Use of three-dimensional models is only justified in rare cases.

At the present time there are no published studies which discuss the application of three-dimensional single-phase models to the analysis of transient pressure data from gas wells. Such models could conceivably be used for the study of completely heterogeneous reservoirs. For single-well problems, the use of cylindrical coordinates provides greater accuracy than the other coordinate systems. For the study of multi-well systems it is usually necessary to use rectangular coordinates with closely spaced grid points near the well.

Models of this type could prove useful for understanding anomalous
results from gas well tests.

8.5 Multiphase Models

More than one fluid may be flowing in the reservoir during
pressure testing of wells. Under such conditions the theory and models
presented so far are not valid, and large errors are possible if the
multiphase flow aspect of the problem is ignored. Some approximate
methods of handling this problem are available (Perrine, 1956). More
accurate results are possible through the use of two or three-phase
models in one, two or three dimensions.

From the point of view of pressure test analysis the most
useful model is a two-dimensional model in r - z coordinates. Such
models are often referred to as coning models (Letkeman and Ridings,
1970, MacDonald and Coats, 1970, Settari and Aziz, 1973, Aziz et al.,
1973). Computer studies with such models have shown that the movement
of water, or any other second phase, within the reservoir can have a
significant effect on the pressure behaviour of a well even before
there is any production of water.

9 DEVIATIONS FROM THE IDEALIZED MODEL

In the derivation of the equations of Section 5 it was
assumed that the medium was homogeneous and isotropic and that flow was
single-phase and obeyed Darcy's law. It was also supposed that opening
and shut-in of the well was done at the sandface. In actual fact these
idealizations, convenient as they are, are not realistic, and deviations
from the ideal model are too frequent and too important to be ignored.
Ways of accounting for skin effects, IT flow, wellbore storage, and
multiphase flow will be treated in the following sections.

9.1 Skin Factor

It is a known fact that the permeability of the formation immediately around the well can be damaged by the well drilling process or improved by fracturing or acidizing the well on completion. To account for this altered permeability a skin factor was defined by Van Everdingen (1953) as

$$(\Delta p_D)_{skin} = s , \qquad \text{a constant} \qquad (2\text{-}138)$$

so that

$$\Delta p_D \Big|_{well} \text{ (including skin)} = P_t + s \qquad (2\text{-}139)$$

This essentially states that there will be an added pressure difference due to the skin effect given by Equation (2-139). This concept of s corresponds to an infinitesimal skin around the well causing an additional or a decreased resistance to flow. s may be considered to be made up of various skin effects, namely: altered permeability, s_k, partial penetration, s_{pp}, and perforations, s_{perf} (Ramey, 1965). The estimation of these effects individually is discussed in Chapter 7. A positive value of s indicates a damaged well, and a negative value an improved well. In the case of negative skin, this concept, which is mathematically correct, leads to some difficulty in physical interpretation (Hurst, Clark and Brauer, 1969). Mathematically, it is equivalent to superposing an injection well on top of the producing well. Hawkins (1956) proposed that the skin be treated as a region of radius r_{skin} with permeability k_{skin}, with the skin factor given by

$$s = \left(\frac{k}{k_{skin}} - 1 \right) \ln \frac{r_{skin}}{r_w} \qquad (2\text{-}140)$$

This concept is valid for both positive skin ($k_{skin} < k$) and negative

skin ($k_{skin} > k$) but there is no unique set of values of k_{skin} and r_{skin} for a particular s. This problem has been handled numerically by Wattenbarger and Ramey (1970).

An alternative treatment of the skin effect is that of an "effective wellbore radius" (Matthews and Russell, 1967, p. 21), defined as that radius which makes the pressure drop in an ideal reservoir equal to that in an actual reservoir with skin. Thus

$$r_{w \text{ effective}} = r_w e^{-s} \qquad (2-141)$$

This is equivalent to taking $k_{skin} = \infty$ in Equation (2-140).

For positive skin, $r_{w \text{ effective}} < r_w$, that is, the fluid must travel through additional formation to cause the observed Δp.

For negative skin $r_{w \text{ effective}} > r_w$. This is a useful concept in hydraulically fractured wells.

The various interpretations of skin effect are illustrated in Figure 2-20. In the practical solution of real problems the infinitesimal skin concept is usually employed as in Equation (2-139).

| ACTUAL PRESSURE DISTRIBUTION SHOWING ZONE OF ALTERED PERMEABILITY | INFINITESIMAL SKIN CONCEPT | EFFECTIVE WELLBORE RADIUS CONCEPT |
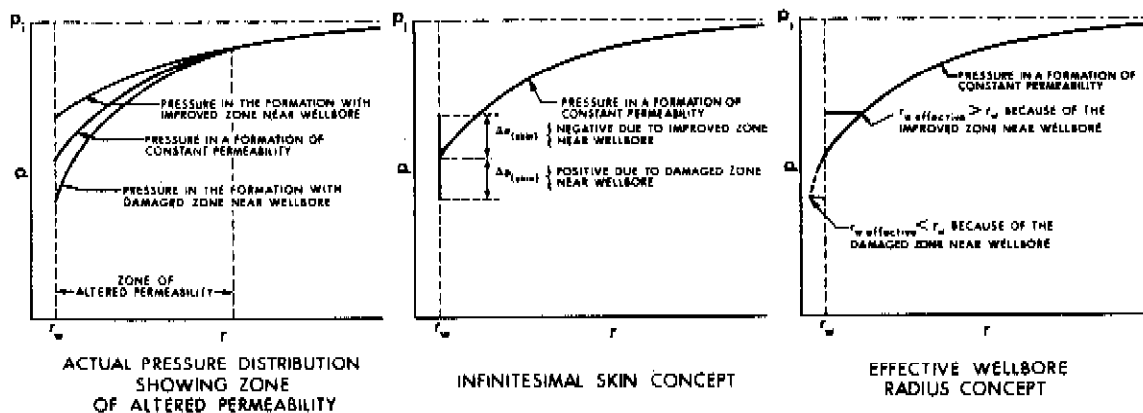
FIGURE 2-20. IDEALIZATION OF SKIN EFFECTS IN A PRODUCING FORMATION

9.2 Inertial-Turbulent Flow Effects

All of the solutions presented so far are based on the assumption that Darcy's law, Equation (2-7), is valid for flow throughout the reservoir and for all times. As shown in previous sections, it is possible to linearize the partial differential equations with suitable assumptions when Darcy flow exists. For gas flow, however, inertial and/or turbulent (IT) flow effects, not accounted for by Darcy's law, are frequently of significance and should not be ignored. If these IT flow effects are taken into consideration in the partial differential equation, the result is Equation (2-28) or Equation (2-30) which, being non-linear, can only be solved by numerical procedures.

Since flow velocity in a radial flow system increases as the well is approached (even for the constant production rate case), IT flow is most pronounced near the well and results in an additional pressure drop similar to the skin effect, except that it is not a constant but varies directly with flow rate (Houpeurt, 1959). Smith (1961) confirmed with actual test results and with numerical solutions that IT flow could be treated as an additional, rate-dependent skin effect

$$(\Delta p_D)_{IT} = D \, q_{sc} \qquad (2-142)$$

where

D = IT flow factor for the system

Consequently, for gas flow in a reservoir, the pressure at the well is given by

$$\Delta p_D \Big|_{well} \text{(including skin and IT flow effects)} = P_t + s + D \, q_{sc}$$

$$(2-143)$$

Since both skin and IT flow effects are concentrated around the well, they will usually be detected as a single effect, the apparent skin factor, s'.

$$s' = (\Delta p_D)_{skin} + (\Delta p_D)_{IT} = s + D q_{sc} \qquad (2\text{-}144)$$

It is important to recognize this and to calculate each effect separately, as the $(\Delta p_D)_{skin}$ can be eliminated by stimulation whereas $(\Delta p_D)_{IT}$ will persist even after stimulation, as it depends on the flow rate. By measuring s' at two different flow rates and by applying Equation (2-144) a pair of simultaneous equations is obtained from which s and D may be evaluated (Swift and Kiel, 1962, Ramey, 1965).

In Equation (2-143), flow in the turbulent region is assumed to be stabilized. Wattenbarger and Ramey (1968) have shown that the IT flow effects do become stabilized at $t_D \simeq 2000$, for various values of q_D and k. Since D depends upon k, it is possible to alter $(\Delta p_D)_{IT}$ by well stimulation which changes the permeability around the well.

Equation (2-143) is an approximate constant-rate solution which does not take into account the variation of gas viscosity with pressure. Wattenbarger (1967, p. 68) integrated the three-dimensional form of the Forchheimer equation, Equation (2-16) with the assumptions:

a. the radius of drainage is sufficiently far from the well, at which point turbulence is negligible;

b. steady-state or pseudo-steady state approximately exists,

to give

$$(\Delta p_D)_{IT} = \left[\frac{2.715 \times 10^{-12} \beta \, k \, M \, P_{sc}}{h \, T_{sc}} \int_{r_w}^{r_d} \frac{1}{\mu \, r^2} \, dr \right] q_{sc} \qquad (2\text{-}145)$$

Since viscosity depends on pressure, which changes with distance from the well, the value of the integral in Equation (2-145) changes with time, even though turbulence is stabilized. Consequently, a more rigorous form of Equation (2-143), proposed by Wattenbarger (1967, p. 70) is

$$\Delta p_D \Big|_{well} = P_t + s + D\{\mu\} q_{sc} \qquad (2\text{-}146)$$

where $D\{\mu\}$ represents the effect of real gas viscosity on turbulence. The dimensionless form of Equation (2-145) can be written as

$$(\Delta p_D)_{IT} = D\{\mu\}q_{sc} = 1.916\times10^{-18}\ \beta k^2\ q_D\left[\frac{\psi_1}{2}\frac{M}{R\,T}\int_{r_w}^{r_d}\frac{1}{\mu\ r^2}\ dr\right] \quad (2\text{-}147)$$

Equation (2-147) shows that $D\{\mu\}q_{sc}$ is proportional to βk^2 for a given q_D. Katz et al. (1959, p. 50) have shown that β is approximately inversely proportional to k. This means that $D\{\mu\}q_{sc}$ is approximately proportional to k for a given q_D. Furthermore, since q_D has k in the denominator, the term $D\{\mu\}q_{sc}$ should depend essentially on the flow rate per unit thickness of formation, almost independently of k.

In conclusion, although the rigorous form of Equation (2-146) should be used for large drawdown to accommodate the variation of viscosity with time, Equation (2-143) is a good approximation for many practical situations.

EXAMPLE 2-10

Introduction   The calculation of pressure drop due to laminar flow effects was illustrated by Example 2-3. This example shows how pressure drop is attributed to laminar flow, skin and IT flow effects. It assumes negligible effects of viscosity on turbulence.

Problem   A well in an infinite-acting reservoir (gas composition given in Example A-1) was produced at a constant rate, q_1, of 7 MMscfd for a time, t_1, of 36 hours. The flowing bottom hole pressure, p_{wf_1}, at that time was 1600 psia.

The same well was produced at a constant rate, q_2, of 10 MMscfd for a time, t_2, of 24 hours. The flowing bottom hole pressure, p_{wf_2}, at that time was 1400 psia.

The stabilized shut-in pressure, $\bar{p}_R$, prior to each of the two flow periods was 2000 psia. General data pertinent to the test are the same as in Example 2-2.

Calculate the skin and IT flow effects, s and D, respectively. Also calculate, for the first flow rate:

1. the pressure drop due to laminar flow effects,
2. the pressure drop due to skin effects,
3. the pressure drop due to IT flow effects.

<u>Solution</u>   Since the gas is the same as that of Example A-1, the $\psi - p$ curve already constructed (Figure 2-4) is applicable to this problem. From Table 2-3 and Table 2-4

$$t_D = \frac{2.637 \times 10^{-4} \, k \, t}{\phi \, \mu_i \, c_i \, r_w^2}$$

$$\therefore \quad t_{D1} = \frac{2.637 \times 10^{-4} \, (20)(36)}{(0.15)(0.0158)(0.00053)(0.4)^2} = 944{,}710$$

$$t_{D2} = \frac{2.637 \times 10^{-4} \, (20)(24)}{(0.15)(0.0158)(0.00053)(0.4)^2} = 629{,}807$$

From Table 2-3 and Table 2-4

$$q_D = \frac{1.417 \times 10^6 \, T \, q_{sc}}{k \, h \, \psi_i}$$

$$\therefore \quad q_{D1} = \frac{1.417 \times 10^6 \, (580)(7)}{(20)(39)(3.30 \times 10^8)} = 0.0224$$

$$q_{D2} = \frac{1.417 \times 10^6 \, (580)(10)}{(20)(39)(3.30 \times 10^8)} = 0.0319$$

Since the reservoir is infinite-acting, Equation (2-75) applies, so that

$$P_{t1} = \frac{1}{2} \left[\ln t_{D1} + 0.809 \right]$$

$$= \frac{1}{2} \left[\ln 944{,}710 + 0.809 \right] = 7.28$$

$$P_{t_2} = \frac{1}{2}\left[\ln t_{D_2} + 0.809\right]$$

$$= \frac{1}{2}\left[\ln 629{,}807 + 0.809\right] = 7.08$$

From Table 2-3

$$\Delta p_D = \frac{\psi_i - \psi_{wf}}{\psi_i \, q_D}$$

From Figure 2-4

$$p = 1600 \quad \leftrightarrow \quad \psi = 2.18 \times 10^8$$

$$p = 1400 \quad \leftrightarrow \quad \psi = 1.68 \times 10^8$$

$$\Delta p_{D_1} = \frac{3.30 \times 10^8 - 2.18 \times 10^8}{3.30 \times 10^8 \, (0.0224)} = 15.15$$

$$\Delta p_{D_2} = \frac{3.30 \times 10^8 - 1.68 \times 10^8}{3.30 \times 10^8 \, (0.0319)} = 15.39$$

From Equation (2-143)

$$\Delta p_D = P_t + s + D \, q_{sc}$$

Substituting the calculated values of Δp_D, P_t and q_{sc} in the above equation, gives

$$15.15 = 7.28 + s + 7 \, D$$

$$15.39 = 7.08 + s + 10 \, D$$

Solving these above equations simultaneously, gives

$$D = \frac{(15.39 - 15.15) - (7.08 - 7.28)}{(10 - 7)} = 0.15$$

$$s = 15.15 - 7.28 - 7 \, (.15) = 6.82$$

For the first production rate, q_1:

pressure drop due to laminar flow effects is given by

$$P_{t_1} = \frac{\psi_i - \psi}{\psi_i \, q_{D_1}}$$

$\therefore \quad \psi = \psi_i - \psi_i \, P_{t_1} \, q_{D_1}$

$\quad = 3.30 \times 10^8 - 3.30 \times 10^8 \, (7.28)(0.0224) = 2.76 \times 10^8$

$\psi = 2.76 \times 10^8 \quad \leftrightarrow \quad p = 1815 \qquad$ (Figure 2-4)

$\therefore \quad \Delta p_{laminar\ flow} = P_i - p = 2000 - 1815 = 185$ psi

pressure drop due to skin effects is given by

$$s = \frac{\psi_i - \psi}{\psi_i \, q_D}$$

$\therefore \quad \psi = \psi_i - \psi_i \, s \, q_{D_1}$

$\quad = 3.30 \times 10^8 - 3.30 \times 10^8 \, (6.82)(0.0224) = 2.80 \times 10^8$

$\psi = 2.80 \times 10^8 \quad \leftrightarrow \quad p = 1829 \qquad$ (Figure 2-4)

$\therefore \quad \Delta p_{skin} = P_i - p = 2000 - 1829 = 171$ psi

pressure drop due to IT flow effects is given by

$$Dq_1 = \frac{\psi_i - \psi}{\psi_i \, q_{D_1}}$$

$\therefore \quad \psi = \psi_i - \psi_i \, Dq_1 \, q_{D_1}$

$\quad = 3.30 \times 10^8 - 3.30 \times 10^8 \, (0.15)(7)(0.0224) = 3.22 \times 10^8$

$$\psi = 3.22 \times 10^8 \quad \leftrightarrow \quad p = 1973 \qquad \text{(Figure 2-4)}$$

$$\therefore \quad \Delta p_{\text{IT flow}} = p_i - p = 2000 - 1973 = 27 \text{ psi}$$

$$\text{Total pressure drop} = \Delta p_{\text{laminar flow}} + \Delta p_{\text{skin}} + \Delta p_{\text{IT flow}}$$

$$= 185 + 171 + 27 = 383 \text{ psi}$$

<u>Discussion</u>   The calculated total pressure drop of 383 psi compares favourably with the actual total pressure drop of 400 psi.   The difference is due to round-off errors in calculating s and D and errors in translating from ψ to p.   In this example the total pseudo-pressure drop, $\Delta\psi = \Delta\psi_{\text{laminar}} + \Delta\psi_{\text{skin}} + \Delta\psi_{\text{IT}} = \left[(3.3 - 2.76) + (3.3 - 2.8) + (3.3 - 3.22)\right] \times 10^8 = 1.12 \times 10^8$.   The actual pseudo-pressure drop, $\Delta\psi = \psi_{2000} - \psi_{1600} = (3.3 - 2.18) \times 10^8 = 1.12 \times 10^8$.   Since the above values of $\Delta\psi$ agree, the errors in this problem are in converting from ψ to p.

9.3   Wellbore Storage/Unloading

When a producing well is shut-in at the surface, flow from the formation does not stop immediately.   Flow of fluid into the well persists for some time after shut-in due to the compressibility of the fluid.   The rate of flow changes gradually from q_{sc} at the time of shut-in to zero during a certain time period.   This effect is known as after-flow or wellbore storage.   For the case of drawdown, the reverse takes place.   On opening the well at surface, the initial flow rate is due to wellbore unloading.   As this gradually decreases to zero, the flow from the formation increases from zero to q_{sc}.   The constant rate maintained at the surface is in effect the sum of two flow rates varying in opposite directions, viz: decreasing wellbore unloading, plus increasing flow from the formation.   This illustrates that the wellbore storage effect is associated with a continuously varying flow rate in the formation.   One solution (Van Everdingen, 1953) is to assume the flow rate in the formation to be given by

$$q = q_{sc}\left(1 - e^{-b_3 t_D}\right)$$ (2-148)

where b_3 is a dimensionless constant derived from observations of casing-head, tubing-head, and bottom hole pressures and from a knowledge of the dimensions of the casing and tubing. This varying flow rate can be accounted for by superposition, as discussed in Section 7.1.

An alternative approach (Van Everdingen and Hurst, 1949) is to assume that the rate of unloading of, or storage in, the wellbore per unit pressure difference is constant. This constant is known as the wellbore storage constant, C_s, and is given by

$$C_s = V_{ws} c_{ws}$$ (2-149)

where

V_{ws} = volume of the wellbore tubing (and annulus, if there is no packer)

c_{ws} = compressibility of the wellbore fluid evaluated at the mean wellbore pressure and temperature, and not at reservoir conditions as is usually the case.

The wellbore storage constant may be expressed in dimensionless terms as

$$C_{sD} = \frac{\eta\, C_s}{\phi\, h\, c\, r_w^2}$$ (2-150)

where

η = a constant

= $\dfrac{1}{2\pi}$, Darcy units

= 0.159, when V_{ws} is in ft^3, Field units

= 0.894, when V_{ws} is in bbl, Field units

The rate of flow of fluid from the formation may then be obtained from

$$q = q_{sc}\left[1.0 - C_{sD}\,\frac{\partial}{\partial t_D}\,(\Delta p_D)\Big|_{wellbore}\right]$$ (2-151)

The latter treatment is more common in the technical literature but both of these approaches exhibit similar results. At early times a deviation from the true constant rate solution is observed. After a certain period of time, t_{ws}, this deviation becomes negligible, and the dimensionless pressure drop function at the well is given by P_t. Ramey (1965) has shown that for various values of C_{sD}, the time for which wellbore storage effects are significant, is given by

$$t_{wsD} = 60\, C_{sD} \qquad (2\text{-}152)$$

By definition (Table 2-3)

$$t_{wsD} = \frac{\lambda\, k\, t_{ws}}{\phi\, \mu\, c\, r_w^2} \qquad (2\text{-}153)$$

Combining Equations (2-152) and (2-153) with Equations (2-149) and (2-150) gives

$$t_{ws} = \frac{60\, \eta\, \mu\, V_{ws}\, c_{ws}}{\lambda\, k\, h} = \frac{\eta}{\lambda}\, 60\, \frac{\mu\, V_{ws}\, c_{ws}}{k\, h} \qquad (2\text{-}154)$$

Inspection of this equation reveals the following interesting trends:

a. wellbore storage effects increase directly with well depth ($\propto V_{ws}$) and inversely with formation flow capacity $\left(\propto \dfrac{1}{k\,h}\right)$;

b. wellbore storage effects decrease with increasing pressure level ($\propto c_{ws}$).

In general, wellbore storage effects are likely to be of importance for tests of short duration, approximately less than one day (Ramey, 1965). The preceding discussion applies to wells with zero skin effect.

Agarwal, Al-Hussainy and Ramey (1970) showed that for all practical purposes, the duration of wellbore storage effects is also

given by $t_{wsD} \geq 60\ C_D$ for either positive or negative skin factors. In particular for $s \geq 0$, they showed that

$$t_{wsD} = (60 + 3.5\ s)\ C_{sD} \qquad (2\text{-}155)$$

They also showed that for positive and for zero skin effects, at very early times

$$\Delta p_D \Big|_{well} \{s,\ C_{sD},\ t_D\} = \frac{t_D}{C_{sD}} \qquad (2\text{-}156)$$

which shows that very early pressure drop performance is controlled entirely by wellbore storage up to a time, t_D, of the order of 0.5 C_{sD} to 1.0 C_{sD}.

EXAMPLE 2-11

Introduction   This example illustrates a simple method of estimating the time required for wellbore storage effects to become negligible. An alternative method which utilizes the type curves of the next section is described in Chapter 4.

Problem   Calculate the time, t_{ws}, required for wellbore storage effects to become negligible for a well with no bottom hole packer, given the following characteristics:

$$
\begin{aligned}
L &= 5000 \text{ ft (well depth)} \\
r_w &= 0.5 \text{ ft} \\
h &= 39 \text{ ft} \\
c_{ws} &= 0.00054 \text{ psia}^{-1} \\
k &= 20 \text{ md} \\
\mu &= 0.0150 \text{ cp}
\end{aligned}
$$

Solution

$$V_{ws} = \pi r_w^2 L = 3927 \text{ ft}^3$$

From Equation (2-154)

$$t_{ws} = \frac{\eta}{\lambda} \frac{60 \; \mu \; V_{ws} \; c_{ws}}{k \; h} \; , \qquad \lambda = 2.637 \times 10^{-4} \quad \text{(Table 2-3)}$$
$$\eta = 0.159 \qquad \text{(Section 9.3)}$$

$$\therefore \quad t_{ws} = \frac{(0.159)(60)(0.0150)(3927)(0.00054)}{(2.637 \times 10^{-4})(20)(39)} = 1.5 \text{ hours}$$

Discussion   After a time of 1.5 hours, wellbore storage effects become negligible and the analytical solutions for transient flow apply.

Boundary Condition Modifications

When solving the radial-cylindrical flow Equation (2-63), appropriate boundary conditions may be written to account for skin and after-flow effects (Agarwal, Al-Hussainy and Ramey, 1970). For early times, the well may be considered to be infinite-acting and the inner boundary conditions, of constant flow rate at the wellhead, in the presence of skin and after flow is given by

$$C_{sD} \frac{\partial}{\partial t_D} (\Delta p_D) \Big|_{\text{wellbore}} - \frac{\partial}{\partial r_D} (\Delta p_D) \Big|_{\text{well}} = 1 \qquad (2\text{-}157)$$

and

$$\Delta p_D \Big|_{\text{wellbore}} = P_t - s \frac{\partial}{\partial r_D} (\Delta p_D) \Big|_{\text{well}} = 1 \qquad (2\text{-}158)$$

Equation (2-157) states that the dimensionless wellbore storage/unloading rate, plus the dimensionless sandface flow rate, equal the dimensionless constant production rate (=1).

Equation (2-158) corrects the dimensionless pressure function by the skin effect.

The infinite reservoir, constant production rate case (Section 6.1) may be solved with the above modifications to the boundary condition, for various skin effects, s, and wellbore storage constants, C_D. The solution may be obtained semi-analytically (Agarwal et al.,

1970), or by finite difference techniques (Wattenbarger and Ramey, 1970).

9.4 Gas-Condensate Flow

Production at the surface is often a multiphase mixture of gas, condensate and water. This could be the result of single-phase flow in the reservoir with subsequent drop-out of liquids in the well-bore due to the prevailing conditions of temperature and pressure. In these instances, the single-phase flow theory previously developed is applicable directly, and corrections for multiphase flow have to be made only for flow in the pipes and not in the formation.

Sometimes, however, condensation occurs in the formation itself, and in these cases single-phase flow theory may be adapted with reasonable success. Often, flow in the reservoir will start as single-phase gas. As the pressure near the well decreases due to flow, retrograde condensation may occur in a zone near the well. This reduces the relative permeability to gas flow and causes an added resistance to flow, which may be treated as a skin. However, this skin is pressure dependent, as the extent of condensation or revaporization depends directly on pressure, for a gas at a given temperature. This changing skin factor affects the long-term deliverability of a well and is one of the factors affecting the frequency of testing of wells.

As was indicated in Section 8, multiphase flow problems in the formation may be treated numerically. The relative permeability of the different phases as a function of time and location in the reservoir must be accounted for. Perrine (1956) suggested that the equations developed previously for single-phase flow may be modified to apply to multiphase situations by substituting some effective total system mobility, compressibility and flow rate for their single-phase equivalents. Martin (1959) gave the theoretical basis of Perrine's analysis. The effective total properties are defined below, where subscripts t, g, o, w, and f refer to total, gas, oil (or condensate), water and formation, respectively. The effective total mobility, $(k/\mu)_t$, is given, in terms of the in situ permeability to each of the

phases by

$$\left(\frac{k}{\mu}\right)_t \;=\; \frac{k_g}{\mu_g} + \frac{k_o}{\mu_o} + \frac{k_w}{\mu_w} \tag{2-159}$$

The in situ permeability to each phase is the product of the permeability of the formation, and the relative permeability to that phase. This latter factor depends on the prevailing saturation conditions.

The effective total compressibility, c_t, is the sum of the fractional compressibilities,

$$c_t \;=\; c_g + c_o + c_w + c_f \tag{2-160}$$

The fractional compressibility of a fluid is its compressibility multiplied by the fraction of the pore volume that it occupies (that is, its saturation).

The effective total production rate is simply the sum of the individual fluid flow rates

$$q_t \;=\; q_g + q_o + q_w \tag{2-161}$$

Substitution of these effective total properties and the total porosity, ϕ_t, for their single-phase equivalents in Equation (2-53), makes it possible to use the solutions of this equation for multiphase problems.

Various forms of pressure integrals, basically similar to ψ' as defined by Equation (2-45), have been suggested to account for multiphase flow (Clegg, 1968, Fussell, 1972). These are useful only if the permeabilities are known as functions of pressure.

Fetkovich (1973) gives an approximate equation for the skin factor caused by condensation around the well, in terms of time and rate. The effect is in fact similar to that of IT flow since both are rate dependent. However, the condensate skin effect, s_c, is also time dependent. It is given approximately, in field units, by

$$s_c = \frac{k - k_{skin}}{2\ k_{skin}}\ \ln\left(\frac{4729.2\ q_{sc}^2\ \mu\ Z\ R_c'\ t}{h^2\ \phi\ k\ \bar{p}\ S_c\ r_w^2}\right) \qquad (2\text{-}162)$$

where

R_c' =   cuft of condensate accumulation in the reservoir per MMscf of total (recombined) gas produced, per psi

S_c =   hydrocarbon liquid saturation required to reach mobility, fraction of pore volume

k_{skin} =   effective permeability to gas in the region of the well which is saturated with condensate

s_c =   skin factor due to condensate drop-out in the reservoir

All of the methods discussed here for the solution of multi-phase problems are very approximate. A more accurate treatment of this problem is possible through the use of reservoir simulation models.

10 GRAPHICAL (TYPE CURVE) SOLUTIONS OF THE FLOW EQUATIONS

The solutions of the flow equations, in particular for radial-cylindrical flow, for various boundary conditions may be obtained analytically as shown in Sections 6 and 7, or numerically as discussed in Section 8. In either case the solutions may be presented graphically and are referred to as type curves. This form of presentation has certain unique advantages in gas well test analyses as is demonstrated in Chapters 4, 5 and 7. Only a limited number of type curves are available at the present time, but as their usefulness increases, type curves covering various other reservoir/well conditions will no doubt be generated and published.

The most generally useful type curves have been selected and are included herein as Figures 2-21, 2-22, 2-23, 2-24, 2-25(a) and 2-25(b).
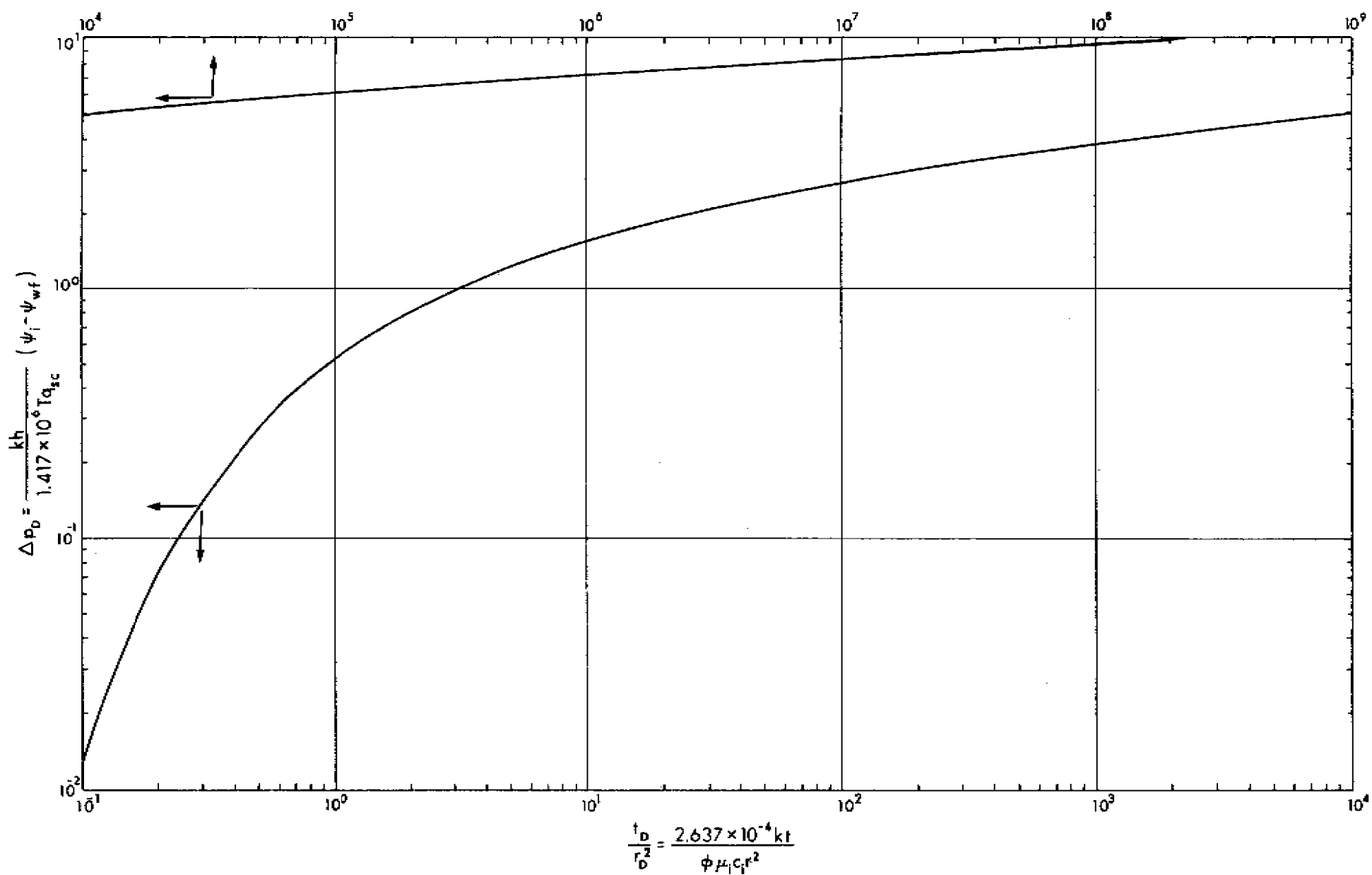
FIGURE 2-21. LINE SOURCE SOLUTION

Courtesy of H.R. Romey, Jr.

The y-axis is labeled:

$$\Delta p_D = \frac{kh}{1.417 \times 10^6 \, Tq_{sc}} (\psi_i - \psi_{wf})$$

The x-axis is labeled:

$$\frac{t_D}{r_D^2} = \frac{2.637 \times 10^{-4} \, kt}{\phi \mu_i c_i r^2}$$

$$\Delta p_D = \frac{kh}{1.417 \times 10^6 \, T q_{sc}} (\psi_i - \psi_{wf})$$

$s = 20$ $C_{sD} = 0$

$s = 10$ $C_{sD} = 0$

$s = 5$ $C_{sD} = 0$

$s = 0$ $C_{sD} = 0$

$C_{sD} = 0$

$s = -5$

$C_{sD} = 10^2$

$C_{sD} = 10^3$

$C_{sD} = 10^4$

$$C_{sD} = \frac{0.159 \, C_s}{\phi \, h c r_w^2}$$

$$C_s = V_{ws} c_{ws}$$

2-124

$$t_D = \frac{2.637 \times 10^{-4} \, kt}{\phi \mu_i c_i r_w^2}$$
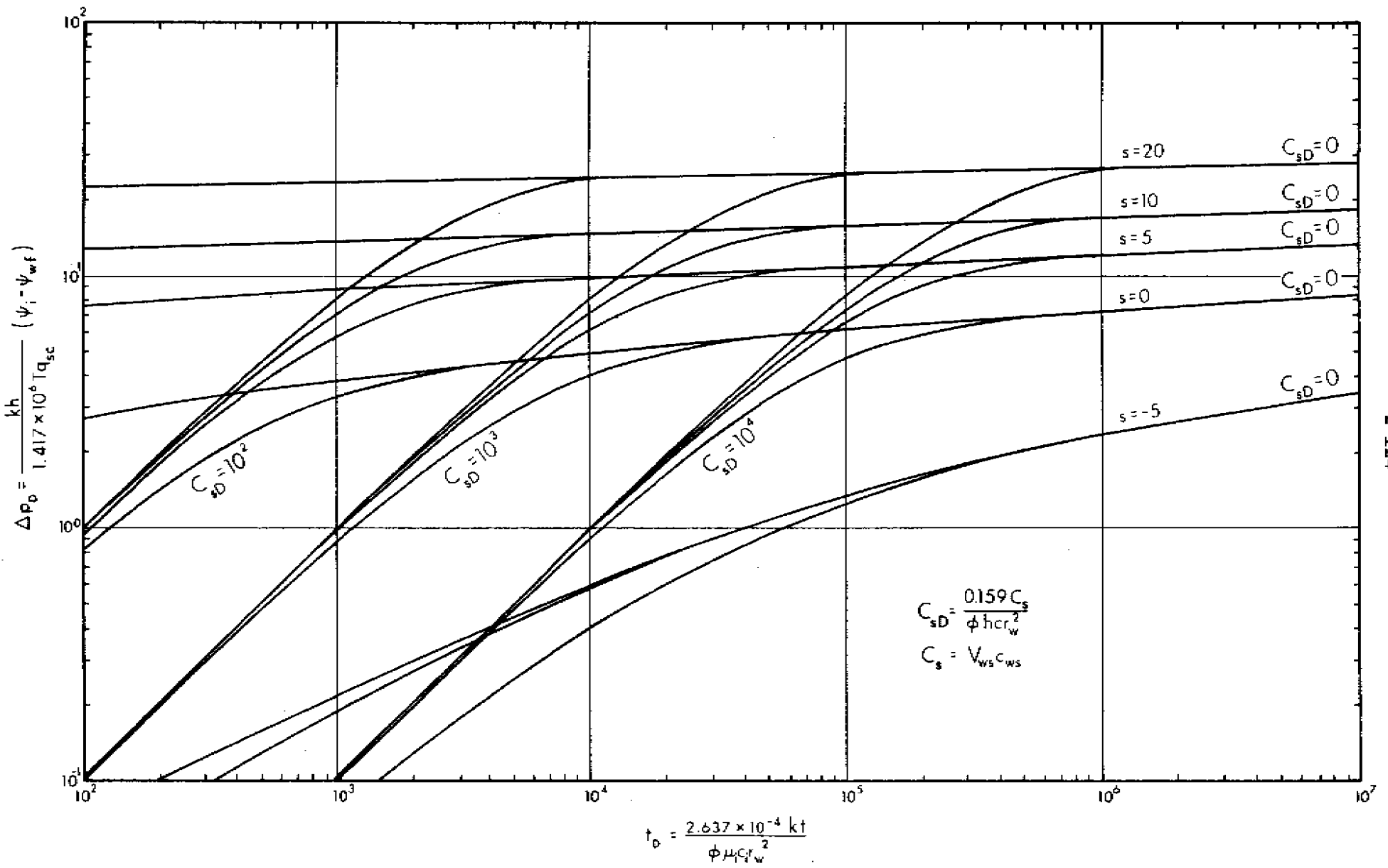
FIGURE 2-22. Δp_D VERSUS t_D, INCLUDING WELLBORE STORAGE AND SKIN EFFECTS

Courtesy of H.R. Ramey, Jr.
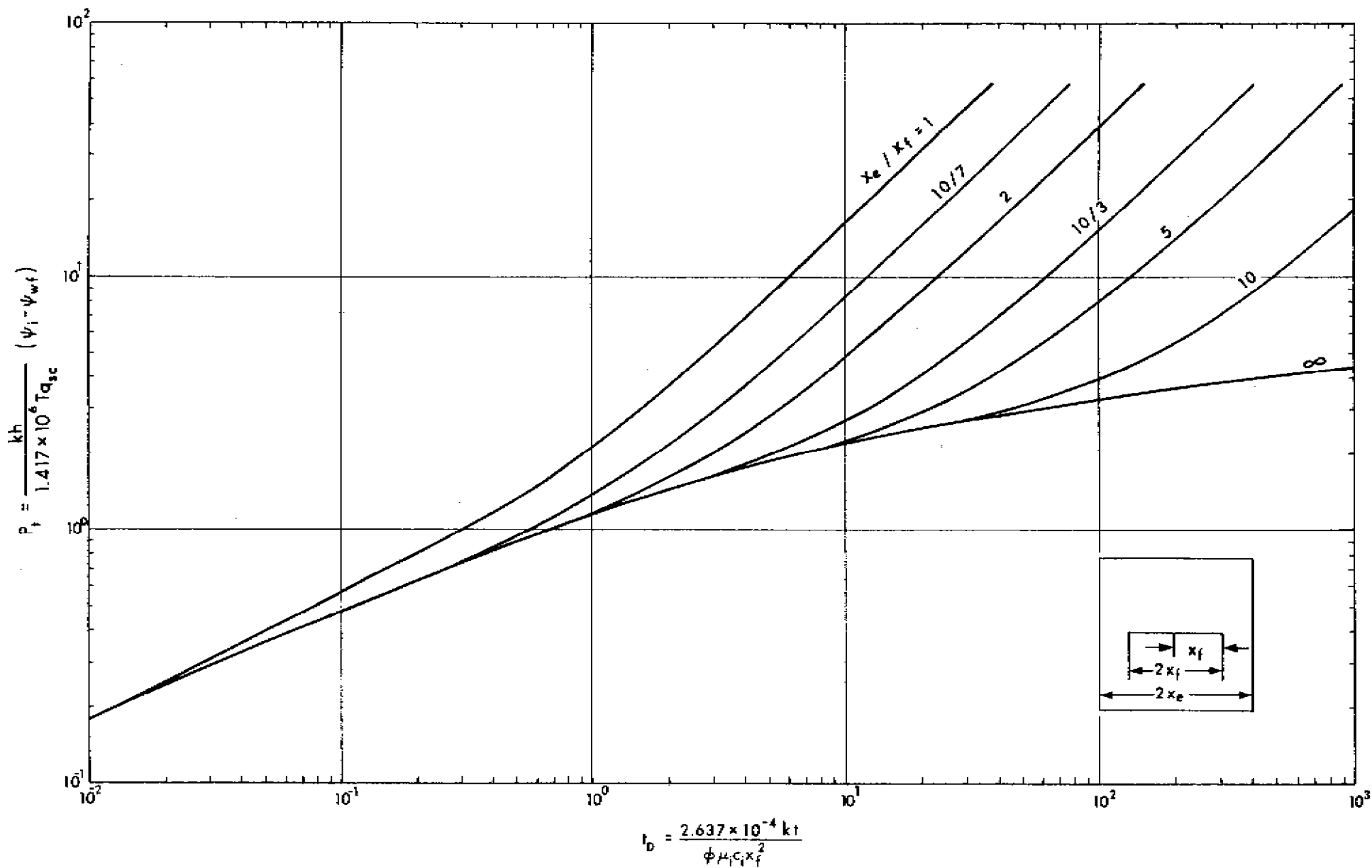
FIGURE 2-23. P_t VERSUS t_D FOR A VERTICALLY FRACTURED WELL (INFINITE FRACTURE CONDUCTIVITY)

Courtesy of H.R. Ramey, Jr.
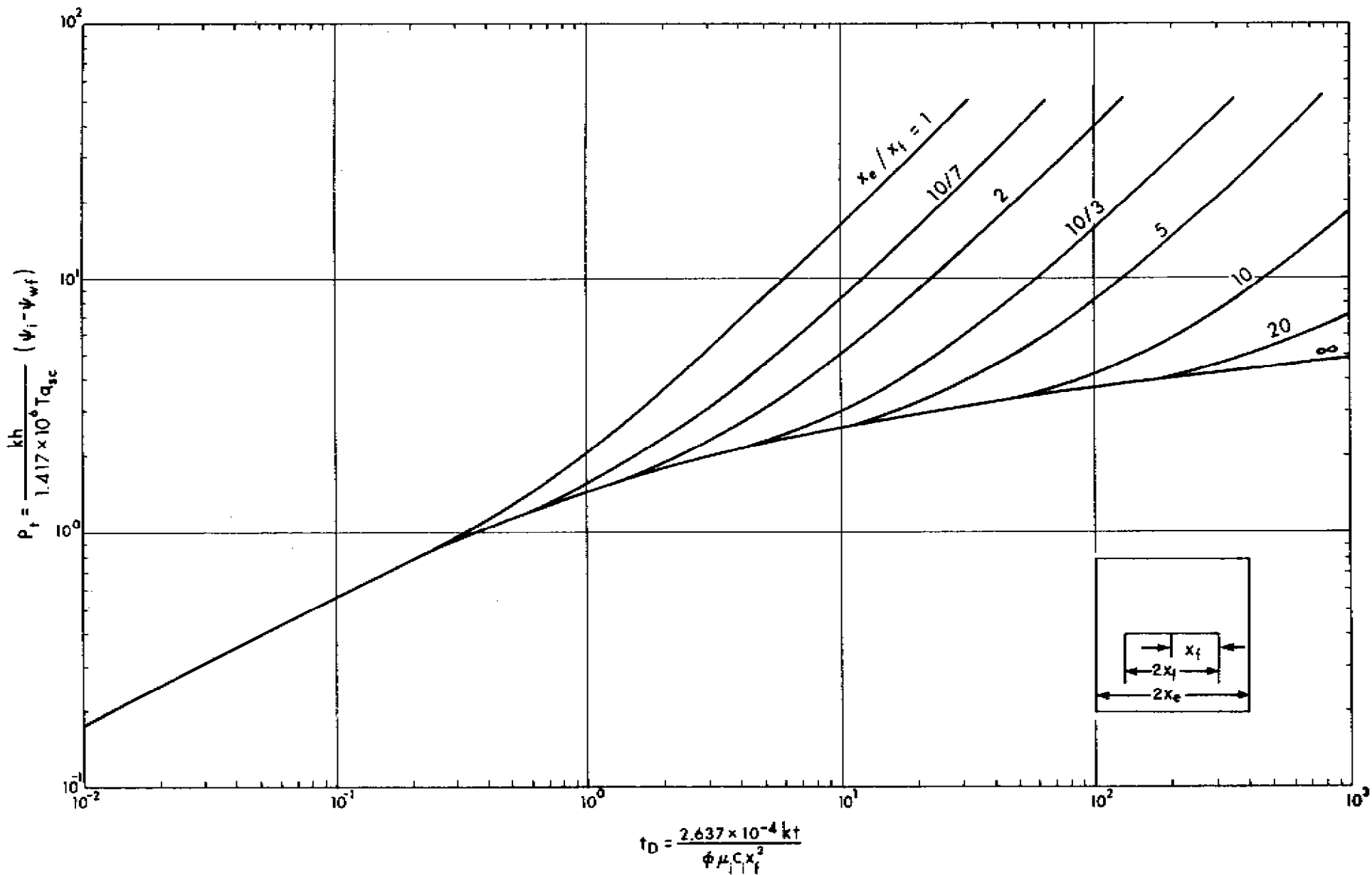
FIGURE 2-24. P_t VERSUS t_D FOR A VERTICALLY FRACTURED WELL (NATURAL FRACTURE)

Courtesy of H.R. Ramey, Jr.

Axis labels:

$$P_t = \frac{kh}{1.417 \times 10^6 \, Tq_{sc}} (\psi_i - \psi_{wf})$$

$$t_D = \frac{2.637 \times 10^{-4} \, kt}{\phi \mu_i C_i x_f^2}$$

Curve labels: $x_e / x_f = 1$, $10/7$, 2, $10/3$, 5, 10, 20, ∞

2-126
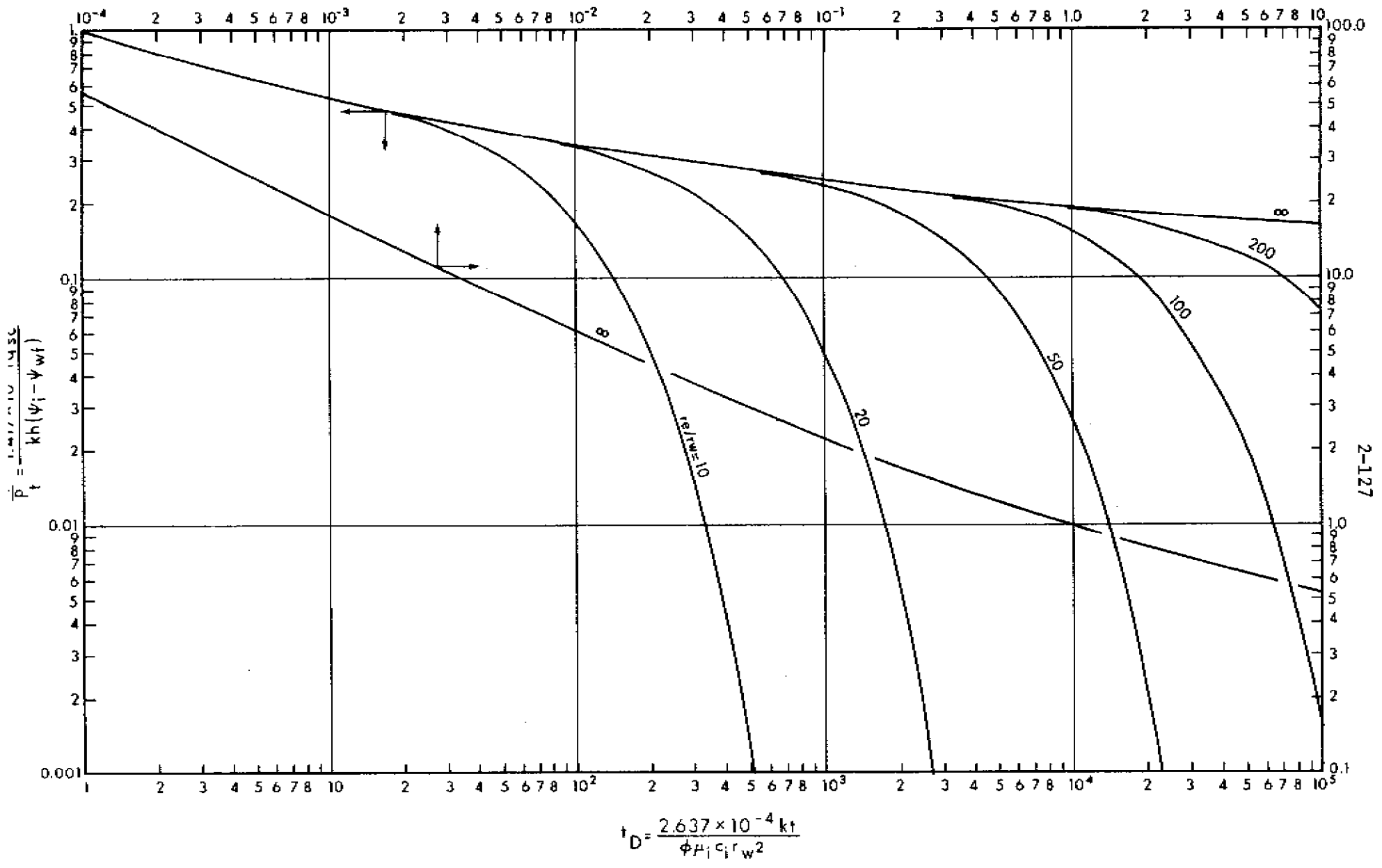
FIGURE 2-25(a). VARIATION OF FLOW RATE WITH TIME, FOR PRODUCTION AT CONSTANT WELL PRESSURE, FROM AN INFINITE RESERVOIR, AND FROM A FINITE CIRCULAR RESERVOIR WITH NO FLOW AT THE EXTERNAL BOUNDARY.

From Fetkovich (1973)
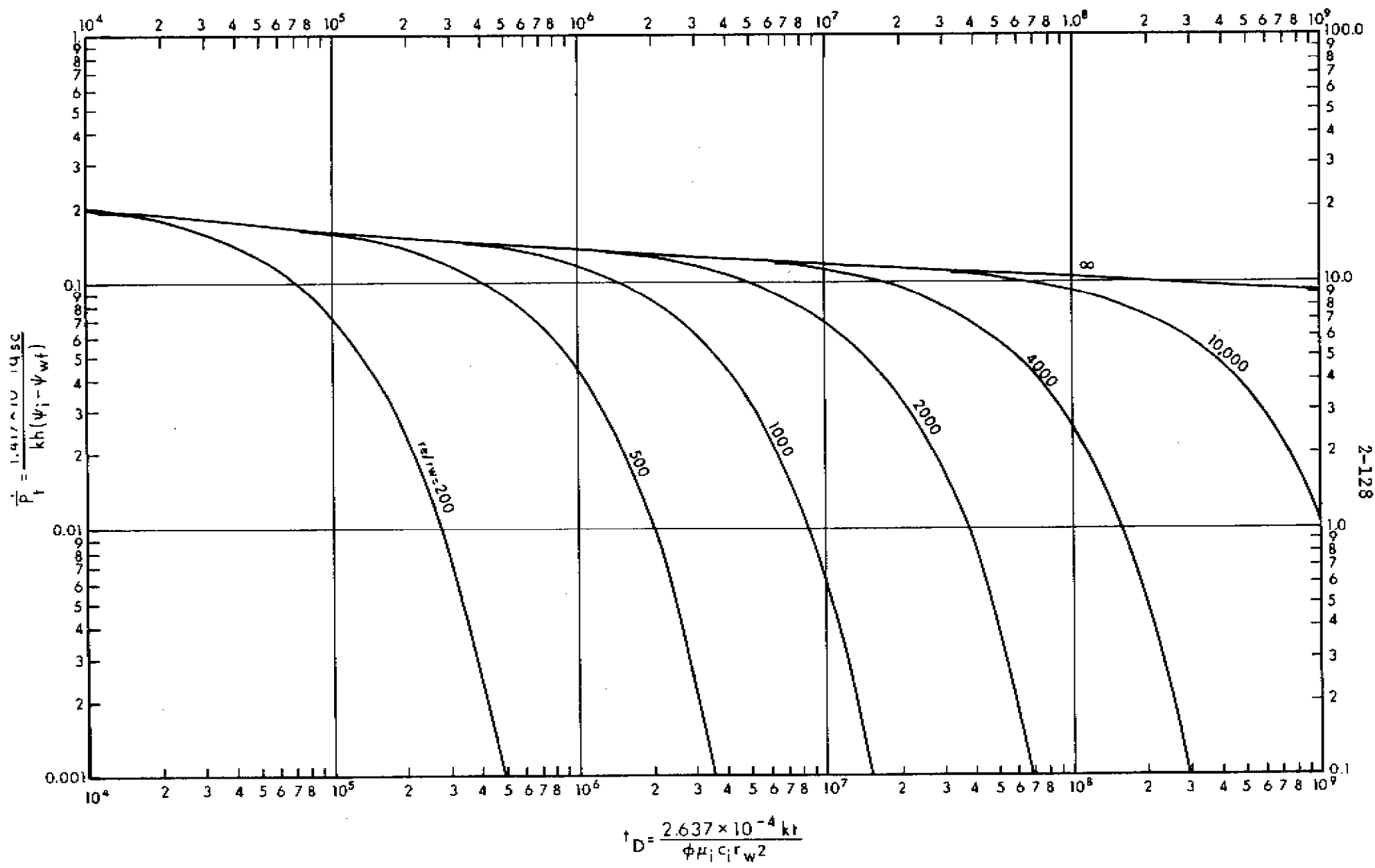
FIGURE 2-25(b). VARIATION OF FLOW RATE WITH TIME, FOR PRODUCTION AT CONSTANT WELL PRESSURE, FROM AN INFINITE RESERVOIR, AND FROM A FINITE CIRCULAR RESERVOIR WITH NO FLOW AT THE EXTERNAL BOUNDARY.

From Fetkovich (1973)

Figure 2-21 represents the Ei function (defined in Section 6.1) and is the solution at any radius for constant-rate production from an infinite-acting reservoir. It is very useful for analyzing interference effects.

Figure 2-22 depicts the effects of skin and wellbore storage on constant-rate drawdown. Since most gas well tests are controlled by surface valves, wellbore storage may be of significance in tests of short duration.

Figure 2-23 represents the condition of constant-rate production for a vertically fractured well. It is a combination of the linear and radial flow equations. Its usefulness is readily seen since the majority of wells receive a hydraulic fracture upon completion. Such fractures are generally vertical and have an infinite conductivity.

Figure 2-24 is more applicable to a vertical fracture of high but not infinite conductivity. The solution assumes a constant flux in the fracture. Such conditions are usually representative of a natural fracture or of a healed hydraulic fracture.

Figures 2-25(a) and 2-25(b) give the variation in flow rate for production at constant well pressure from infinite or finite (no flow boundaries) reservoirs.

A type curve not included in this section is that for constant-rate production from a horizontal fracture (Gringarten and Ramey, 1974). It is of little practical value in the analysis of gas well test data.

All of the type curves presented here are plotted on logarithmic coordinates and will be used for history matching, known as type curve matching, in Chapters 4, 5 and 7. These curves are presented here because they also represent the exact analytical solutions for various conditions in a convenient form.

11 CHOICE OF EQUATION FOR GAS FLOW ANALYSIS
(PRESSURE, PRESSURE-SQUARED OR
PSEUDO-PRESSURE)

In Section 5 of this chapter three different flow equations
are developed using the radial-cylindrical flow model. In Equations
(2-36), (2-38) and (2-44) the dependent variable is pressure, pressure-
squared and pseudo-pressure, respectively. All of these equations may
be written in the dimensionless form of Equation (2-50). This equation
and its associated boundary conditions, in dimensionless form, are
based upon certain assumptions which are different for the pressure,
pressure-squared or pseudo-pressure approaches. Furthermore, it is
possible to use different assumptions for any given approach in order
to linearize the associated non-linear, partial differential equation.
All this is done so that the analytical solution for a linear partial
differential equation may be applied to the non-linear flow equation.
An analysis of this problem has been conducted by Aziz, Mattar, Ko and
Brar (1975). They consider the analytical solution at the well for an
infinite reservoir given by Equation (2-74):

$$P_t = - \frac{1}{2} \, \text{Ei} \left(- \frac{1}{4 \, t_D} \right) \qquad (2\text{-}163)$$

and calculate the sandface pressure from this equation, using different
approaches, for twenty-five different gas well test conditions from
reservoirs in Alberta. The results of the Aziz et al. (1975) study are
summarized here in two parts. In the first part sandface pressures
calculated using the pressure, pressure-squared and pseudo-pressure
approaches are compared with each other and with a more accurate
numerical solution. This shows why the pseudo-pressure approach is
adopted in this manual. In the second part a simple graphical
technique is presented for determining whether or not the pressure or
the pressure-squared approach may be used for a given problem.

11.1 Comparison of Calculated Pressures
by Different Methods

The dimensionless time, t_D, in Equation (2-163) is defined by

$$t_D = \frac{2.637 \times 10^{-4} \ k \ t}{\phi \ r_w^2} \left(\frac{1}{\mu \ c} \right) \qquad (2\text{-}164)$$

in field units for all three approaches. Note that at this stage no distinction is made regarding the conditions at which μc is evaluated.

The definition of P_t, however, is different for each of the three approaches.

For the Pressure Case:

$$P_t = \frac{P_i - P}{\dfrac{7.085 \times 10^5 \ T \ q_{sc}}{k \ h} \left(\dfrac{\mu \ Z}{P} \right)} \qquad (2\text{-}165)$$

For the Pressure-Squared Case:

$$P_t = \frac{P_i^2 - P^2}{\dfrac{1.417 \times 10^6 \ T \ q_{sc}}{k \ h} \ (\mu \ Z)} \qquad (2\text{-}166)$$

For the Pseudo-Pressure Case:

$$P_t = \frac{\psi_i - \psi}{\dfrac{1.417 \times 10^6 \ T \ q_{sc}}{k \ h}} \qquad (2\text{-}167)$$

Equations (2-164) to (2-167) may be derived from Tables 2-3 and 2-4. The quantity $(1/\mu c)$ in Equation (2-164), the quantity $(\mu Z/p)$ in Equation (2-165) and the quantity (μZ) in Equation (2-166) must be assumed constant at some specified conditions before the analytical solution, Equation (2-163), can be used. It is worth noting that no assumptions are involved in the definition of P_t, for the pseudo-pressure case,

by Equation (2-167).

From a comparison of Equations (2-165) and (2-166) it is seen that pressure and pressure-squared approaches become identical, as far as calculating pressure from the analytical solution is concerned, if p in the ($\mu Z/p$) term of Equation (2-165) is evaluated as ($p_i + p$)/2. This is well illustrated by Example 2-3 in Section 6.1 of this chapter.

Table 2-8 provides data on twenty-four different well test conditions in Alberta reservoirs and Table 2-9 provides the predicted flowing pressures calculated by different approaches and different procedures for averaging gas properties. The entries in columns (8) and (10) of Table 2-9 can also be obtained by the pressure-squared approach if averages are defined in the same way as for the pressure approach.

Table 2-9 shows large differences in the pressures computed by different methods for some of the well test conditions. For example, well test conditions (8), (11), and (16) give very different results. In order to get some idea of the accuracy of some of these methods, Aziz et al. (1975) have compared the transient solutions for Test Numbers (8), (11), and (16) with the true solution obtained by numerical methods. A typical comparison of this type is presented in Figure 2-26 for Test Number (8).

From the results of Aziz et al. (1975), as given in Table 2-9, it is possible to draw the following conclusions as far as the calculation of sandface pressure from the analytical solution is concerned:

1. The use of average gas properties in the definition of P_t and t_D results in more accurate solutions than the use of initial conditions. This is true regardless of the approach used. Differences between the solutions by the three approaches are small. Compare columns (4) and (8).

2. The method of averaging gas properties does not have a large influence on the resulting solution. Compare columns (8) and (10).

3. When gas properties must be assumed constant at the initial values, only the pseudo-pressure approach is

No.	P_i psia	Temp °R	Gas Gravity G	P_c psia	T_c °R	k h md-ft	φ h ft	Flow Rate MMscfd	Time hr	Mole Per Cent Sour Gas	
										H_2S	CO_2
1	7208	714	.75	733	412	6165.0	4.0	50.000	20	10.0	2.0
2	5100	674	1.02	707	463	24.0	9.6	4.000	100	12.0	3.0
3	5092	725	.74	801	417	185.0	18.5	20.000	20	18.0	4.0
4	4417	701	.96	794	481	933.0	6.0	13.000	20	19.0	3.0
5	4213	701	.70	791	406	424.0	4.6	25.000	20	-	-
6	4209	643	.74	741	402	300.0	7.0	25.000	70	7.0	6.0
7	3859	670	.67	695	377	520.0	3.0	35.000	20	1.0	4.0
8	3534	630	.71	692	374	29.8	1.9	4.000	20	4.0	7.0
9	3294	641	.76	686	397	104.0	3.0	7.500	50	-	6.0
10	3225	640	.73	687	382	104.0	6.0	10.000	70	-	5.0
11	3136	615	.73	666	399	71.0	.5	7.000	50	-	-
12	2925	680	.67	699	378	970.0	3.4	50.000	20	2.0	4.0
13	2322	614	.73	681	393	12.0	1.2	.500	70	-	-
14	2264	598	.70	676	386	120.0	2.0	2.000	15	-	-
15	1940	608	.73	672	349	1270.0	1.2	4.000	100	-	2.0
16	1877	604	.69	683	384	350.0	2.3	15.000	40	.4	2.6
17	1744	554	.70	699	377	138.0	2.0	1.500	5	-	-
18	1455	588	.66	670	378	56.0	6.0	1.000	100	-	-
19	1397	588	.66	670	377	16.0	4.0	.160	100	-	-
20	1191	602	.63	669	354	440.0	.5	4.000	70	-	-
21	1060	581	.66	666	373	830.0	1.6	3.500	20	-	-
22	658	535	.58	665	339	3.8	.4	.020	100	-	-
23	630	525	.57	668	341	45.0	1.0	.200	100	-	-
24	444	525	.57	690	353	5.0	1.9	.015	100	-	-

TABLE 2-8. RESERVOIR AND GAS DATA FOR THE COMPARISON OF THE p, p^2 AND ψ APPROACHES

From Aziz, Mattar, Ko and Brar (1975)

Test Number	Measured Initial Pressure p_i	Predicted Drawdown $\frac{(1)-(4)}{(1)}$	(μc) Evaluated at p_i	(μc) Evaluated at $\left(\frac{p_i+p_{wf}}{2}\right)$	(μc) and (μZ) Evaluated at p_i	(μc) and (μZ) Evaluated at $\sqrt{\frac{p_i^2+p_{wf}^2}{2}}$	(μc) and (μZ/p) Evaluated at p_i	(μc) and (μZ/p) Evaluated at $\frac{p_i+p_{wf}}{2}$	μ and Z Evaluated at p_i and with $\left(\frac{p_i+p_{wf}}{2}\right)$, $\left(\frac{c_i+c_{wf}}{2}\right)$	Average Values $(μ_i+μ_{wf})/2$, $(c_i+c_{wf})/2$, $(Z_i+Z_{wf})/2$, $(p_i+p_{wf})/2$	Numerical Solution
			ψ Approach		p² Approach		p Approach				
			Predicted Flowing Pressure, p_{wf}								
1	7208	.025	7028	7028	7032	7028	7025	7028	7029	7028	7022
2	5100	.584	1994	2123	*	1876	*	2191	2474	2220	1864
3	5092	.328	3390	3420	3181	3403	3068	3430	3492	3431	3308
4	4417	.067	4119	4120	4118	4119	4108	4120	4123	4120	4098
5	4213	.234	3218	3228	3150	3225	3119	3231	3247	3230	3231
6	4209	.354	2696	2721	2446	2704	2354	2733	2778	2727	2715
7	3859	.329	2572	2591	2430	2582	2377	2599	2626	2594	2616
8	3534	.649	1111	1239	*	1163	*	1339	1333	1287	1257
9	3294	.406	1930	1958	1711	1946	1636	1976	1981	1961	2027
10	3225	.570	1319	1388	796	1355	524	1441	1410	1404	1463
11	3136	.687	862	983	*	913	*	1126	923	948	943
12	2925	.415	1687	1710	1569	1703	1528	1722	1721	1715	1737
13	2322	.320	1568	1579	1511	1580	1498	1586	1568	1577	1584
14	2264	.123	1984	1986	1976	1986	1974	1986	1985	1985	1989
15	1940	.042	1859	1859	1859	1860	1859	1860	1859	1860	1862
16	1877	.674	556	612	350	602	249	651	542	624	630
17	1744	.096	1577	1577	1573	1577	1574	1577	1576	1577	1579
18	1455	.292	1026	1030	1014	1030	1012	1031	1020	1030	1033
19	1397	.154	1181	1183	1177	1183	1178	1183	1180	1183	1185
20	1191	.313	815	818	808	818	806	820	814	818	818
21	1060	.135	917	917	915	917	916	918	916	917	918
22	658	.346	427	431	428	431	426	431	428	431	432
23	630	.351	405	409	408	409	406	409	406	409	412
24	444	.360	280	284	281	282	279	283	281	285	285
Column Number	(1)	(2)	(3)	(4)	(5)	(6)	(7)	(8)	(9)	(10)	(11)

Column (2) gives the predicted drawdown values = $(p_i-p)/p_i$ where p is from column (3).

*Calculated pressure is negative.

TABLE 2-9. COMPARISON OF THE PRESSURES CALCULATED BY THE p, p² AND ψ APPROACHES

From Aziz, Mattar, Ko and Brar (1975)
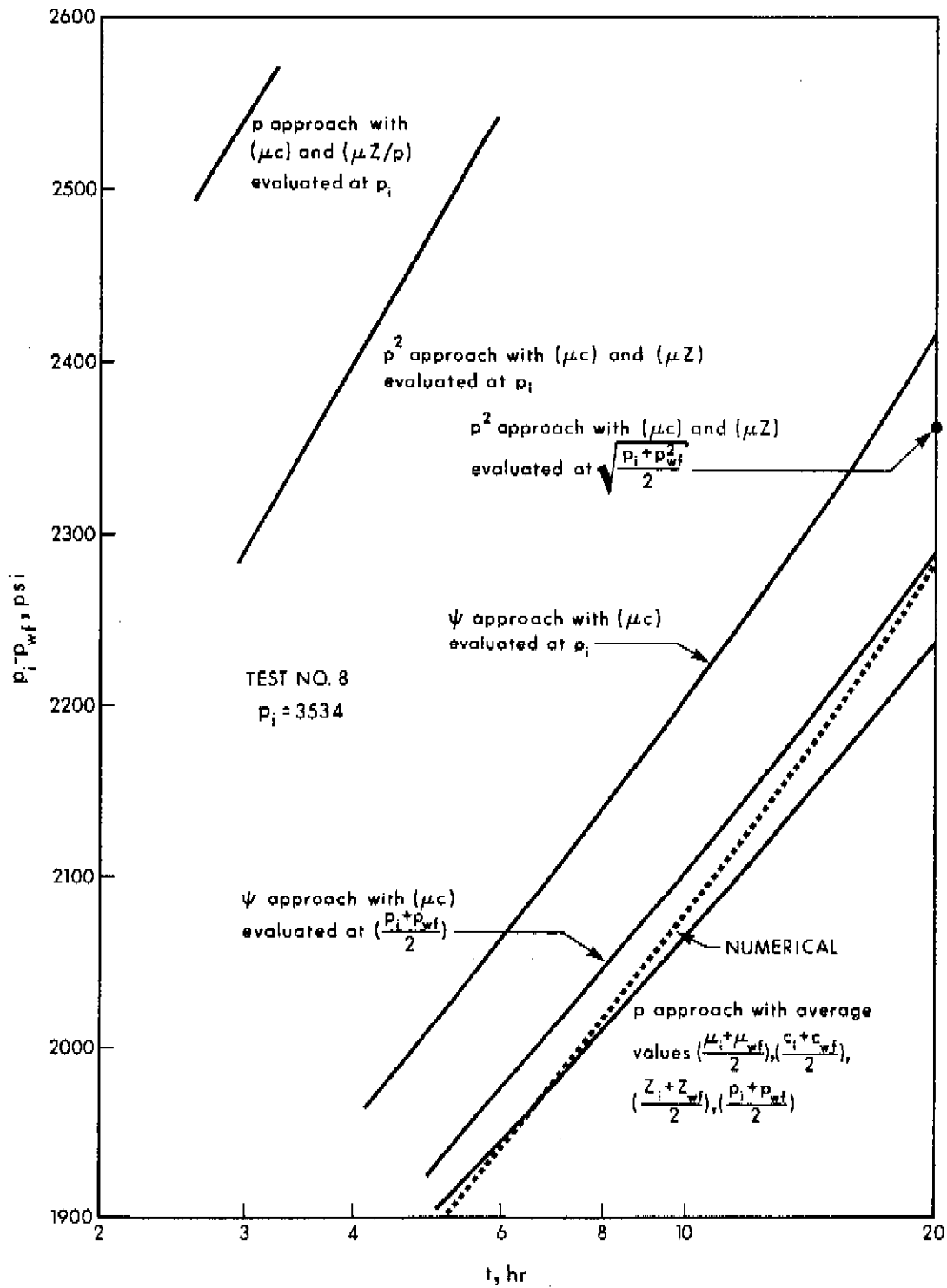
FIGURE 2-26. COMPARISON OF PRESSURE DRAWDOWN CALCULATED BY DIFFERENT METHODS

From Aziz, Mattar, Ko and Brar (1975)

reliable for large drawdowns. The pressure-squared approach using initial properties is usually more accurate than the pressure approach using initial properties. This latter point is considered in more detail in the last part of this section. Compare columns (3), (5), and (7).

4. Any approach may be used when the drawdown is small. This point is also considered in more detail in the last part of this section. Compare the results for well test conditions (1), (4), (14), (15), (17), (20), and (22).

It must be remembered that whenever average properties are used, a trial-and-error (iterative) type of solution becomes necessary. This exemplifies the advantage of using the pseudo-pressure approach, whenever possible, with properties evaluated at initial conditions.

11.2 Range of Validity of the Pressure-Squared or Pressure Approach

It is clear from the above discussion that when the analytical solution is to be applied with gas properties assumed constant at initial conditions, the pseudo-pressure approach will be most reliable. Aziz et al. (1975) have presented a simple method for determining which of the approaches, pressure or pressure-squared, will be closer to the pseudo-pressure approach for a given problem.

The proposed method is based on the observation that if ψ is a linear function of p the pressure approach becomes identical to the ψ approach, and if ψ is a linear function of p^2 then the pressure-squared approach becomes identical to the ψ approach. Aziz et al. (1975) have plotted curves of the reduced pseudo-pressure of Table 2-2 as a function of p_r and p_r^2, with T_r as a parameter. One such plot for $T_r = 1.7$ is shown in Figure 2-27.

As an example of the application of this approach consider Test Number 8 from Table 2-8. The p_r range of interest for this gas is from 1.5 to 5. Figure 2-27 shows that over this range ψ_r is neither a linear function of p_r nor of p_r^2. This is confirmed by Figure 2-26.

Figure 2-27 also shows that the pressure-squared approach is slightly better than the pressure approach for this problem. This too is confirmed by Figure 2-26.

The reduced pseudo-pressure curves for a full range of reduced temperatures are presented in Figures 2-28 and 2-29 as a function of p_r and p_r^2, respectively, with T_r as a parameter. These curves may be used to determine the range of validity of the pressure and pressure-squared approaches.

The reason for exercising caution in the use of the simple interrelationship, based on Figure 2-3, Section 5.5, is well explained by Figure 2-30. In this figure $(\mu/\mu_1)Z$ is plotted versus p_r, with T_r as a parameter. It essentially negates the generalization that the p^2 approach is valid at low pressure while the p approach applies at high pressures. Furthermore, Figures 2-28 and 2-29 show that under some conditions, the p^2 approach may apply at high pressures rather than the p approach.
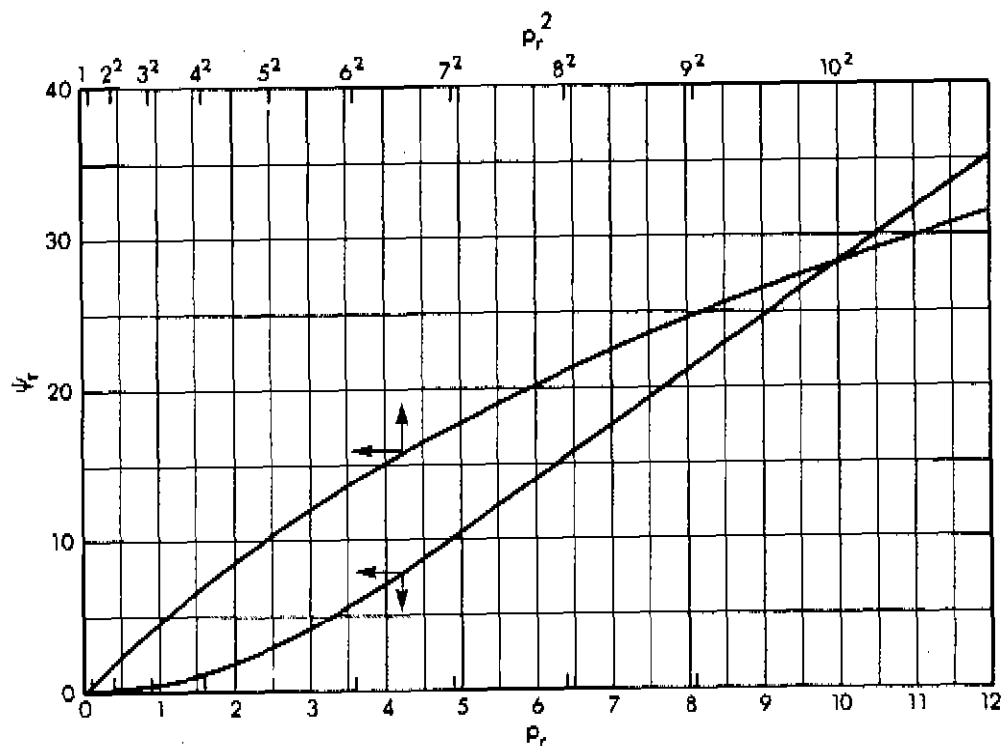
FIGURE 2-27. VARIATION OF REDUCED PSEUDO PRESSURE WITH
REDUCED TEMPERATURE AND PRESSURE ($T_r = 1.7$; $0 \leq p_r \leq 15.0$)

From Aziz, Mattar, Ko and Brar (1975)
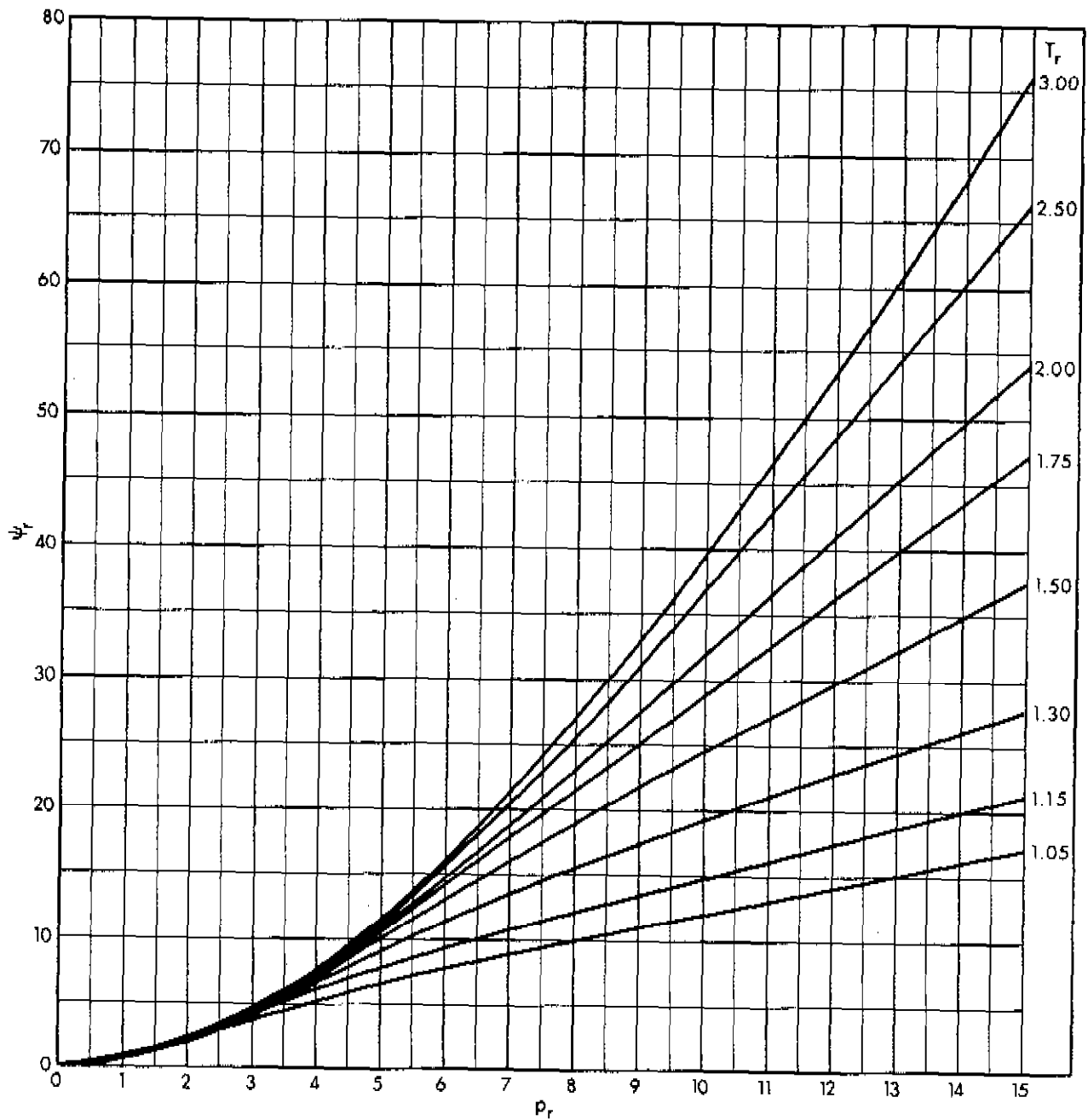
FIGURE 2-28. VARIATION OF REDUCED PSEUDO PRESSURE WITH
REDUCED TEMPERATURE AND PRESSURE ($1.05 \leq T_r \leq 3.0$; $0 \leq p_r \leq 15.0$)
From Aziz, Mattar, Ko and Brar (1975)
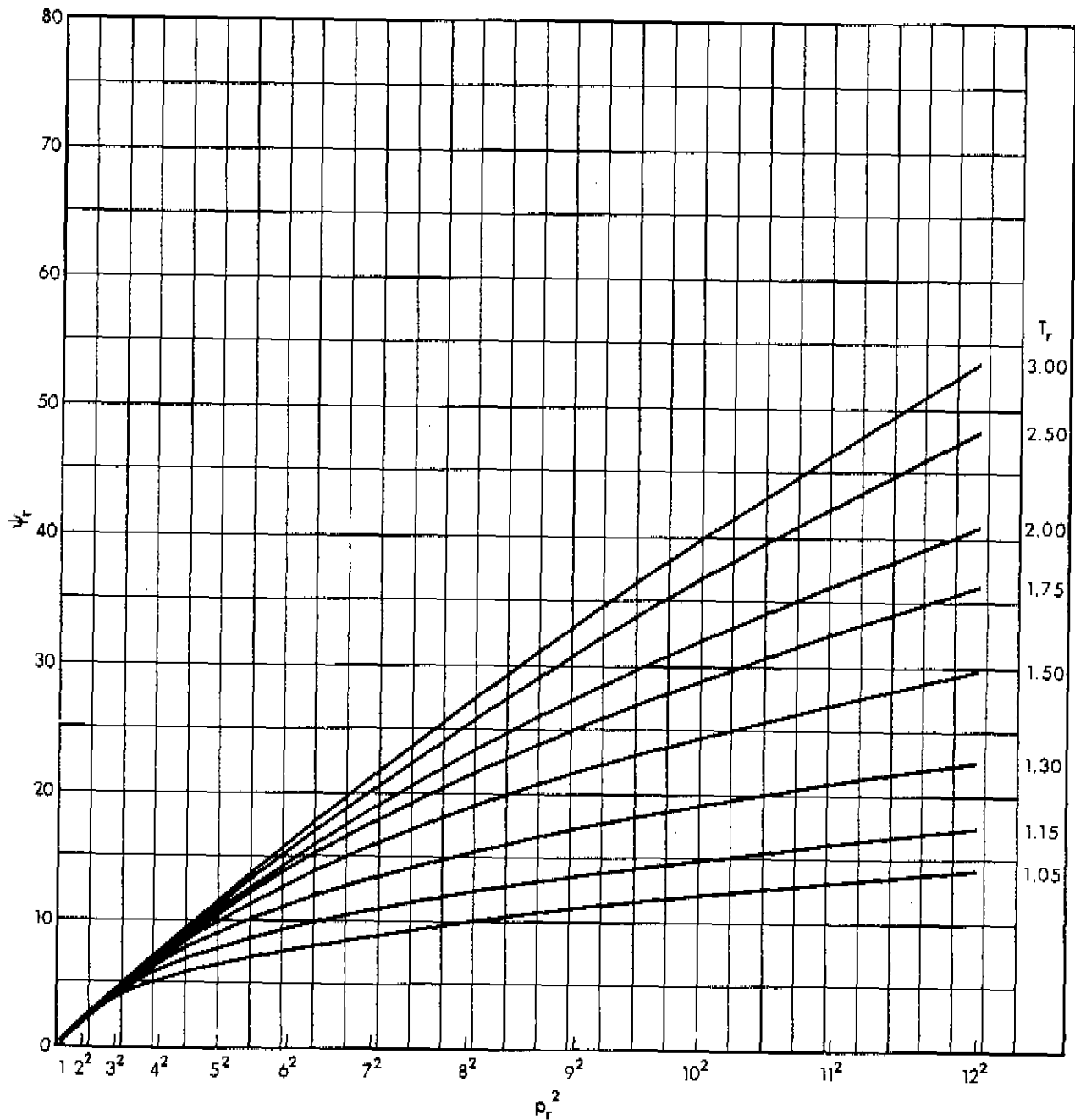
FIGURE 2-29. VARIATION OF REDUCED PSEUDO PRESSURE WITH
REDUCED TEMPERATURE AND PRESSURE SQUARED ($1.05 \leq T_r \leq 3.0$; $0 \leq p_r^2 \leq 12^2$)
From Aziz, Mattar, Ko and Brar (1975)
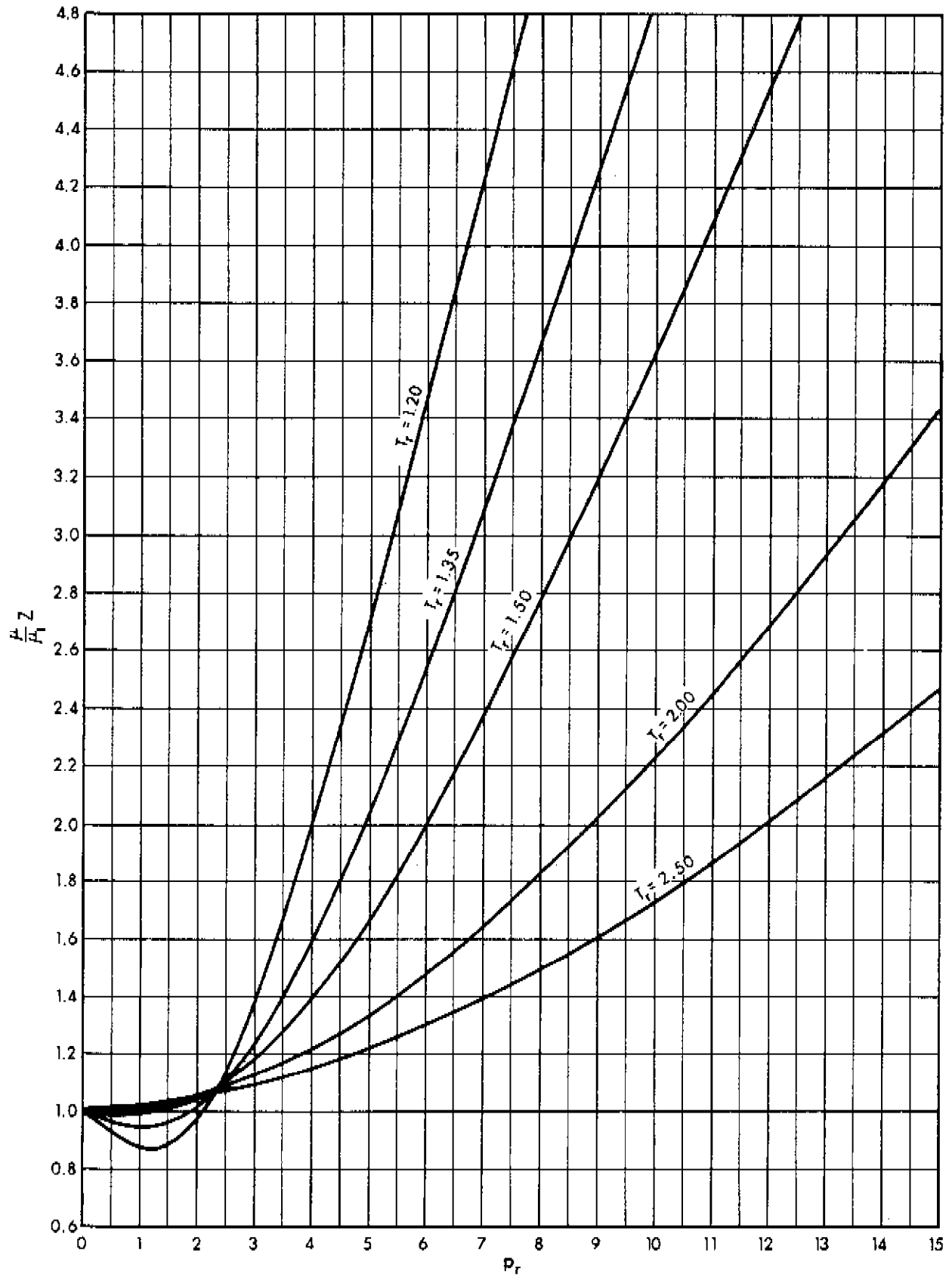
FIGURE 2-30. VARIATION OF $\left(\dfrac{\mu}{\mu_1}\right)Z$ WITH

REDUCED TEMPERATURE AND PRESSURE

From Aziz, Mattar, Ko and Brar (1975)

CHAPTER 3   DELIVERABILITY TESTS

1   INTRODUCTION

Deliverability tests have conventionally been called "back pressure" tests because they make possible the prediction of well flow rates against any particular pipeline "back pressure." Since most flowing well tests are performed to determine the deliverability of a well, the term "deliverability tests" is used in this publication rather than "back pressure tests." The purpose of these tests is to predict the manner in which the flow rate will decline with reservoir depletion.

The Absolute Open Flow (AOF) potential of a well is defined as the rate at which the well would produce against a zero sandface back pressure. It cannot be measured directly but may be obtained from deliverability tests. It is often used by regulatory authorities as a guide in setting maximum allowable producing rates.

1.1   History

It is interesting to note the historical development of deliverability tests. In the early days, a well was tested by opening it fully to the atmosphere and measuring the gas flow rate, which was termed the practical open flow potential. This method was recognized as undesirable because the potential thus obtained depended on the size of the well tubing, and apart from the serious wastage of gas resulting from such practices, wells were often damaged through water coning and attrition by sand particles.

The basic work towards development of a practical test was carried out by Pierce and Rawlins (1929) of the U.S. Bureau of Mines and culminated with the publication of the well-known and widely used Monograph 7 of Rawlins and Schellhardt (1936). Their test, known as the

"conventional back pressure test," consisted of flowing the well at several different flow rates with each flow rate being continued to pressure stabilization. They observed that a plot of the difference between the square of the static reservoir pressure and the square of the flowing sandface pressure versus the corresponding rate of flow would yield a straight line on a logarithmic coordinate plot. They showed that this stabilized deliverability plot could be employed to determine the well capacity at any flowing sandface pressure, including zero, corresponding to absolute open flow conditions, and also showed that it could be used to predict the behaviour of a well with reservoir depletion.

The critical aspect of the Rawlins and Schellhardt conventional deliverability test is that each separate flow rate must be continued to stabilized conditions. In low permeability reservoirs, the time required to achieve pressure stabilization can be very large. As a consequence the actual duration of flow while conducting conventional tests on such reservoirs is sometimes not lengthy enough, and the resulting data can be misleading. Cullender (1955) described the "isochronal test" method which involves flowing the well at several different flow rates for periods of equal duration, normally much less than the time required for stabilization, with each flow period commencing from essentially static conditions. A plot of such pressure and flow rate data, as is described above for the conventional test, gives a straight line or a transient deliverability plot. One flow rate is extended to stabilization and a stabilized pressure-flow rate point is plotted. A line through this stabilized point parallel to that established by the isochronal points gives the desired stabilized deliverability plot. This stabilized deliverability line is essentially the same as that obtained by the conventional test.

Another type of isochronal test was presented by Katz et al. (1959, p. 448). This "modified isochronal test" has been used extensively in industry. The modification requires that each shut-in period between flow periods, rather than being long enough to attain essentially static conditions, should be of the same duration as the

flow period. The actual unstabilized shut-in pressure is used for calculating the difference in pressure squared for the next flow point. Otherwise, the data plot is identical to that for an isochronal test.

1.2 New Approach to Interpreting Gas Well Flow Tests

It is observed that there has been a progressively greater saving of time, and a reduction in flared gas with the evolution of various deliverability tests. Application of the theory of flow of fluids through porous media, as developed in Chapter 2, results in a greater understanding of the phenomena involved. Accordingly more information, and greater accuracy, can result from the proper conduct and analysis of tests.

It will be shown in a later chapter that the analysis of data from an isochronal type test, using the laminar-inertial-turbulent (LIT) flow equation will yield considerable information concerning the reservoir in addition to providing reliable deliverability data. This may be achieved even without conducting the extended flow test which is normally associated with the isochronal tests, thus saving still more time and gas. For these reasons, the approach utilizing the LIT flow analysis is introduced and its use in determining deliverability is illustrated in this chapter. This will set the stage for subsequent chapters where the LIT flow equation will be used to determine certain reservoir parameters.

2 FUNDAMENTAL EQUATIONS

The relevant theoretical considerations of Chapter 2 are developed further in the Notes to this chapter to obtain the equations applicable to deliverability tests. Two separate treatments with varying degrees of approximation may be used to interpret the tests. These will be called the "Simplified analysis" and the "LIT flow analysis."

2.1 Simplified Analysis

This approach is based on the well-known Monograph 7 (Rawlins and Schellhardt, 1936) which was the result of a large number of empirical observations. The relationship is commonly expressed in the form

$$q_{sc} = C \left(\bar{p}_R^2 - p_{wf}^2 \right)^n \equiv C(\Delta p^2)^n \qquad (3\text{-}1)$$

where

q_{sc} = flow rate at standard conditions, MMscfd (14.65 psia, 60°F)

$\bar{p}_R$ = average reservoir pressure obtained by shut-in of the well to complete stabilization, psia

p_{wf} = flowing sandface pressure, psia

Δp^2 = $\left(\bar{p}_R^2 - p_{wf}^2 \right)$

C = a coefficient which describes the position of the stabilized deliverability line

n = an exponent which describes the inverse of the slope of the stabilized deliverability line.

It should be noted that p_{wf} in the above equation is the stabilized flowing sandface pressure resulting from the constant flow rate, q_{sc}. If the pressure is not stabilized, C decreases with duration of flow but eventually becomes a fixed constant at stabilization. Time to stabilization and related matters is discussed in detail in Section 7.1. In the Notes to this chapter, it is shown that n may vary from 1.0 for completely laminar flow in the formation to 0.5 for fully turbulent flow, and it may thus be considered to be a measure of the degree of turbulence. Usually n will be between 1.0 and 0.5.

A plot of Δp^2 $\left(= \bar{p}_R^2 - p_{wf}^2 \right)$ versus q_{sc} on logarithmic coordinates is a straight line of slope $\frac{1}{n}$ as shown in Figure 3-1. Such a plot is used to obtain the deliverability potential of the well against any sandface pressure, including the AOF, which is the

deliverability against a zero sandface pressure. C and n may be considered to be constant for a limited range of flow rates and it is expected that this form of the deliverability relationship will be used only for the range of flow rates used during the test. Extrapolation beyond the tested flow rates can lead to erroneous results (Govier, 1961).
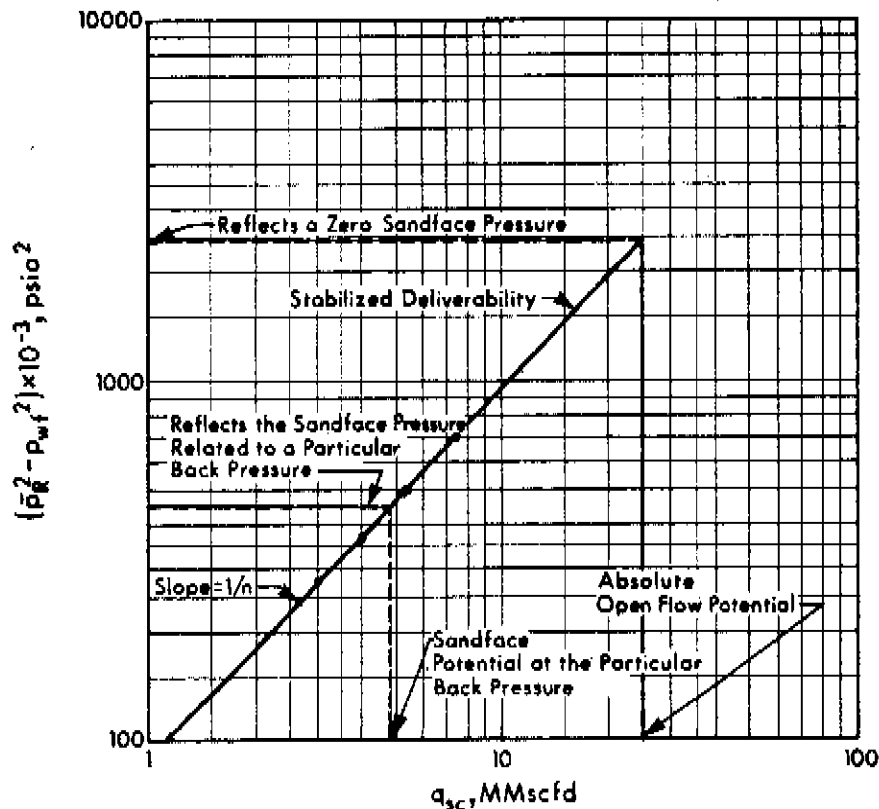
FIGURE 3-1. DELIVERABILITY TEST PLOT-SIMPLIFIED FLOW ANALYSIS

To obtain a greater understanding of the factors that affect C and n, the empirically derived equation, Equation (3-1) is compared to the more rigorous analysis in the Notes to this chapter. The relationships of interest are given by Equations (3N-3), (3N-4), (3N-7) and (3N-8). These equations show that, for a flow rate representative of the range of flow rates tested, C and n depend on gas properties such as viscosity, temperature and compressibility

factor, and reservoir properties such as permeability, net pay thickness, external boundary radius, wellbore radius and well damage. As long as these factors do not change appreciably, the same stabilized deliverability plot should apply throughout the life of the well. In practice, the viscosity, the compressibility factor of the gas and the condition of the well may change during the producing life of the well, and it is advisable to check the values of C and n occasionally.

2.2 LIT Flow Analysis

Pressure-Squared Approach

The utility of Equation (3-1), is limited by its approximate nature. The theory of flow developed in Chapter 2 and in the Notes to this chapter confirms that the straight line plot of Figure 3-1 is really only an approximation applicable to the limited range of flow rates tested. The true relationship if plotted on logarithmic coordinates is a curve with an initial slope of $\frac{1}{n} = 1.0$ at very low values of q_{sc}, and an ultimate slope of $\frac{1}{n} = 2.0$ at very high values of q_{sc}.

Outside North America, there has been in general use a quadratic form of the flow equation often called the Forchheimer or the Houpeurt equation or sometimes called the turbulent flow equation. It is actually the laminar-inertial-turbulent (LIT) flow equation of Chapter 2, developed further in the Notes to this chapter, and is given by Equation (3N-2) as

$$\Delta p^2 \equiv \bar{p}_R^2 - p_{wf}^2 = a' q_{sc} + b' q_{sc}^2 \qquad (3-2)$$

where

$\quad a' q_{sc} = $ pressure-squared drop due to laminar flow and wellbore effects

$\quad b' q_{sc}^2 = $ pressure-squared drop due to intertial-turbulent flow effects.

Equation (3-2) applies for all values of q_{sc}. It is shown in

the Notes to this chapter that Equation (3-1) is only an approximation of Equation (3-2) for limited ranges of q_{sc}.

In the derivation of Equation (3-2), an idealized situation was assumed for the well and for the reservoir. It is important to know the extent and the applicability of the assumptions made when test results are being interpreted. Sometimes anomalous results may be explainable in terms of deviations from the idealized situations. Accordingly, the assumptions which are clearly defined in Chapter 2, Section 5.1 are summarized below:

1. Isothermal conditions prevail throughout the reservoir.
2. Gravitational effects are negligible.
3. The flowing fluid is single phase.
4. The medium is homogeneous and isotropic, and the porosity is constant.
5. Permeability is independent of pressure.
6. Fluid viscosity and compressibility factor are constant. Compressibility and pressure gradients are small.
7. The radial-cylindrical flow model is applicable.

Pressure Approach

Since this approach is seldom used for the analysis of deliverability tests, relevant equations have not been derived in the Notes as was done for the pressure-squared approach. However, it can be shown, by procedures similar to those for the pressure-squared approach, that

$$\Delta p \equiv \bar{p}_R - p_{wf} = a'' \, q_{sc} + b'' \, q_{sc}^2 \qquad (3-3)$$

where

$a'' q_{sc}$ = pressure drop due to laminar flow and well effects

$b'' q_{sc}^2$ = pressure drop due to inertial-turbulent flow effects

The application of Equation (3-3) is also restricted by the assumptions listed for the pressure-squared approach.

Pseudo-Pressure Approach

Assumption (6) mentioned above can be a cause of serious errors, particularly in the flow of gas from tight reservoirs where the pressure gradient is seldom small. It is shown in Chapter 2 that if the pseudo-pressure approach is used, instead of the pressure-squared or pressure approaches, the need for assumption (6) is eliminated and the resulting equation is more rigorous than either Equation (3-2) or Equation (3-3) for all ranges of pressure. The rigorous LIT flow equation is developed in the Notes to this chapter and is given by Equation (3N-9) as

$$\Delta\psi \equiv \bar{\psi}_R - \psi_{wf} = a\, q_{sc} + b\, q_{sc}^2 \tag{3-4}$$

where

$\bar{\psi}_R$ = pseudo-pressure corresponding to $\bar{p}_R$

ψ_{wf} = pseudo-pressure corresponding to p_{wf}

$a\, q_{sc}$ = pseudo-pressure drop due to laminar flow and well conditions

$b\, q_{sc}^2$ = pseudo-pressure drop due to inertial-turbulent flow effects.

Since the pseudo-pressure analysis is more rigorous than either the pressure or the pressure-squared analyses, the LIT approach incorporating the pseudo-pressure, henceforth referred to as the LIT(ψ) approach, is used in this manual.

The pseudo-pressure concept is treated in greater detail in Chapter 2 but its application is reviewed here. A curve of ψ versus p is constructed for a particular gas at reservoir temperature (see Example 2-1). This curve is then used for converting p to ψ, and vice versa, and instead of using p or p^2 as the working variable, ψ is used. Once the $\psi - p$ curve has been constructed, this approach becomes just as easy as the p^2 approach.

When ψ_{wf} reflects the stabilized pressure due to a constant flow rate q_{sc}, a no longer increases with duration of flow but stays constant at a stabilized value. A plot of $\Delta\psi$ versus q_{sc} on arithmetic

coordinates would give a curve, concave upwards, passing through the origin. This curve has an initial slope of 1, corresponding to laminar flow, whereas at the higher flow rates the slope increases to 2, reflecting turbulent flow. Consequently, for large extrapolations, a considerable difference would be observed in the AOF values obtained from this curve and from the straight line plot of the Simplified analysis.

In order to obtain a plot that is consistent with Figure 3-1, the arithmetic coordinate plot is discarded in favour of a logarithmic plot of Equation (3-4). A straight line may be obtained by plotting $(\Delta\psi - bq_{sc}^2)$ versus q_{sc} as shown in Figure 3-2. This particular method is chosen since the ordinate then represents the pseudo-pressure drop due to laminar flow effects, a concept which is consistent with the Simplified analysis.
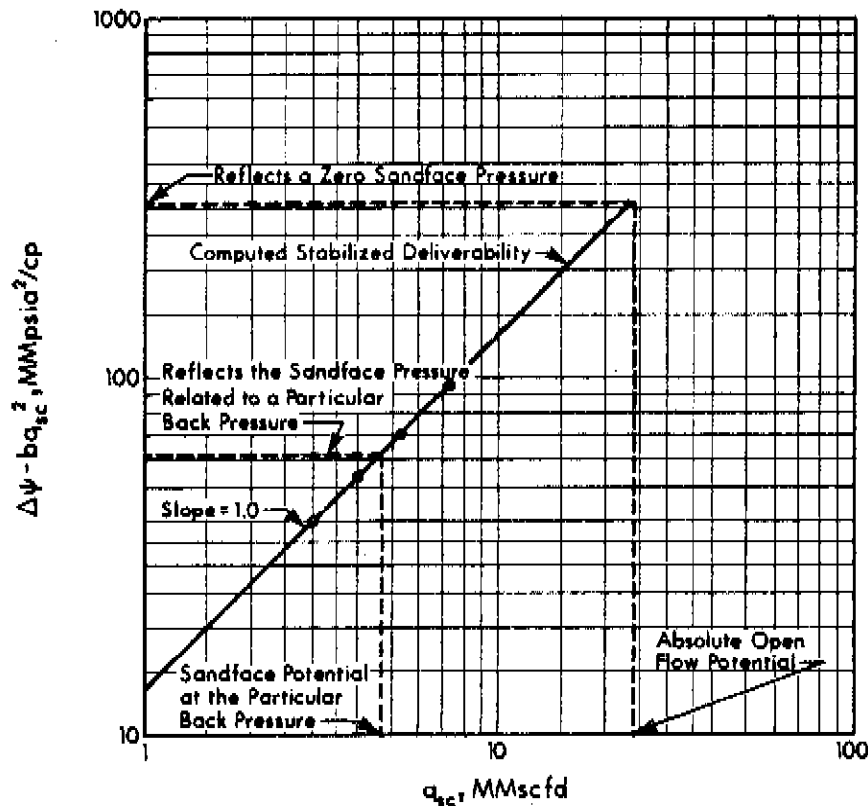
FIGURE 3-2. DELIVERABILITY TEST PLOT-LIT(ψ) FLOW ANALYSIS

The deliverability potential of a well against any sandface pressure may be obtained by solving the quadratic Equation (3-4) for the particular value of $\Delta\psi$

$$q_{sc} = \frac{-a + \sqrt{(a^2 + 4\ b\ \Delta\psi)}}{2\ b} \tag{3-5}$$

a and b in the LIT(ψ) flow analysis depend on the same gas and reservoir properties as do C and n in the Simplified analysis except for viscosity and compressibility factor. These two variables have been taken into account in the conversion of p to ψ, and consequently, will not affect the deliverability relationship constants a and b. It follows, therefore, that the stabilized deliverability Equation (3-4), or its graphical representation, is more likely to be applicable throughout the life of a reservoir than Equations (3-1), (3-2) or (3-3).

3 DETERMINATION OF STABILIZED FLOW CONSTANTS

Deliverability tests have to be conducted on wells to determine, among other things, the values of the stabilized flow constants. Several techniques are available to evaluate C and n, of the Simplified analysis, and a and b, of the LIT(ψ) flow analysis, from deliverability data.

3.1 Simplified Analysis

A logarithmic coordinate plot of Δp^2 versus q_{sc} should yield a straight line over the range of flow rates tested. The slope of this stabilized deliverability line gives $\frac{1}{n}$ from which n can be calculated. The coefficient C in Equation (3-1) is then obtained from

$$C = \frac{q_{sc}}{\left(\bar{P}_R^2 - P_{wf}^2\right)^n} \tag{3-6}$$

3.2 LIT(ψ) Flow Analysis

Least Squares Method

A plot of $(\Delta\psi - bq_{sc}^2)$ versus q_{sc}, on logarithmic coordinates, should give the stabilized deliverability line. a and b may be obtained from the equations given below (Kulczycki, 1955) which are derived by the curve fitting method of least squares

$$a = \frac{\sum \frac{\Delta\psi}{q_{sc}} \sum q_{sc}^2 - \sum q \sum \Delta\psi}{N \sum q_{sc}^2 - \sum q_{sc} \sum q_{sc}} \qquad (3-7)$$

$$b = \frac{N \sum \Delta\psi - \sum q_{sc} \sum \frac{\Delta\psi}{q_{sc}}}{N \sum q_{sc}^2 - \sum q_{sc} \sum q_{sc}} \qquad (3-8)$$

where

N = number of data points

Graphical Method

This method utilizes the "general curve," developed by Willis (1965), shown in Figure 3-3. Before discussion on the use of the general curve method, the details of its development should be clearly understood.

Equation (3-4), with $a = b = 1$ can be written as

$$\Delta\psi = q_{sc} + q_{sc}^2 \qquad (3-9)$$

The straight lines in Figure 3-3, which is a logarithmic coordinate plot of $\Delta\psi$ versus q, are represented by the equations

$$\Delta\psi = q_{sc} \qquad (3-10)$$

and

$$\Delta\psi = q_{sc}^2 \qquad (3-11)$$

If the plots of Equations (3-10) and (3-11) are added for the same value of q_{sc}, the resulting plot is the general curve.

To distinguish Figure 3-3 from a data plot, the latter will be referred to as the deliverability plot.

To determine a and b, actual data are plotted on logarithmic coordinates of the same size as Figure 3-3. This stabilized deliverability data plot is laid upon the general curve plot, and keeping the axes of the two plots parallel, a position is found where the general curve best fits the points on the data plot. The stabilized deliverability curve is now a trace of the general curve. The value of a is read directly as $\Delta\psi$ for the point on the deliverability plot where the line given by Equation (3-10) intersects the line $q_{sc} = 1$ of the deliverability plot. The value of b is read directly as $\Delta\psi$ for the point on the deliverability plot where the line given by Equation (3-11) intersects the line $q_{sc} = 1$ of the deliverability plot.

If the point at which "a" is to be read does not intersect the $q_{sc} = 1$ line of the deliverability plot, "a" may instead be read where q_{sc} equals 10 or 100 and must then be divided by 10 or 100, respectively, to get the correct value. Similarly, b may be read where q_{sc} equals 10 or 100 and must then be divided by 10^2 or 100^2, respectively.

The advantage of this method is the speed with which deliverability data can be analyzed. However, it should be used only when reliable data are available.

The above procedure may be applied to data from a conventional test to yield a stabilized deliverability curve. With isochronal data, however, it will yield a transient deliverability curve. To obtain the stabilized deliverability curve, it should be remembered that the value of b is independent of duration of flow and must be the same for the stabilized and the transient deliverability relationships. Accordingly, the general curve is positioned so that it passes through the stabilized flow point and maintains the value of b obtained from the transient deliverability curve.

The application of this graphical method to calculate a and b is illustrated by Example 3-4 in Section 4.3.
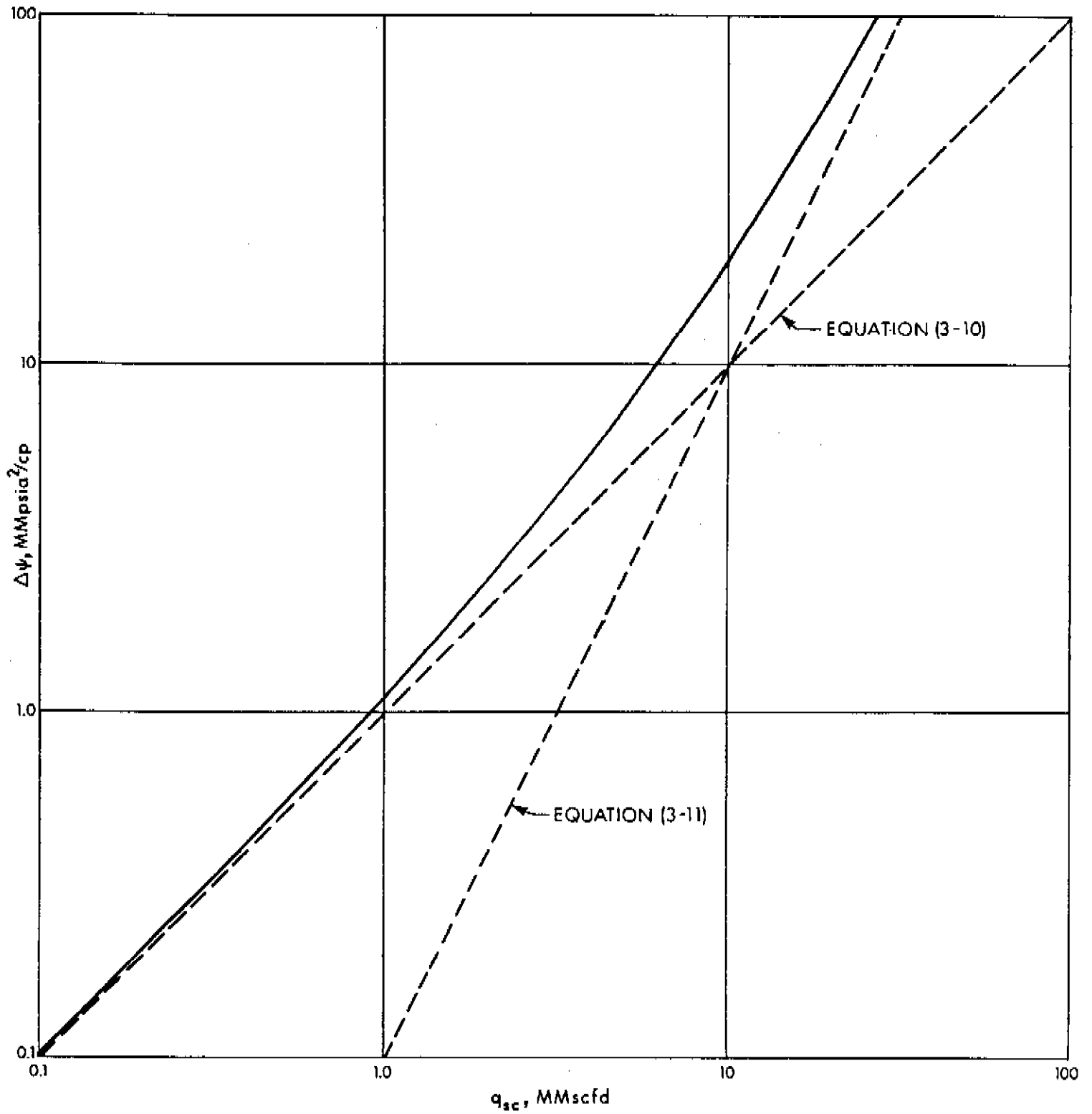
FIGURE 3-3. GENERAL CURVE FOR THE ANALYSIS OF DELIVERABILITY DATA

From R. B. Willis (1965)

The general curve of Figure 3-3 may also be used with the LIT(p^2) approach. The method is the same as described above except Equation (3-2) is now fit instead of Equation (3-4).

4 TESTS INVOLVING STABILIZED FLOW

In the preceding analyses, C or a are constant only when stabilization has been reached. Before stabilization is achieved, the flow is said to be transient. Tests to determine the stabilized deliverability of a well may combine both transient and stabilized conditions. Various tests that may be used directly to obtain the deliverability or the AOF of a well are described in this section along with examples of their interpretation by both the Simplified and the LIT(ψ) flow analyses. General guidelines for the field conduct and reporting of these tests are discussed in a later chapter. All the tests treated in this section have at least one, and sometimes all, of the flow rates run until pressure stabilization is achieved. This is very important as, otherwise, the deliverability obtained will not reflect stabilized conditions and will thus be incorrect. Tests in which no one flow rate is extended to stabilized conditions will be discussed in Section 5.

4.1 Conventional Test

As mentioned in Section 1, Pierce and Rawlins (1929) were the first to propose and set out a method for testing gas wells by gauging the ability of the well to flow against various back pressures. This type of flow test has usually been designated the "conventional" deliverability test. To perform a conventional test, the stabilized shut-in reservoir pressure, $\bar{p}_R$, is determined. A flow rate, q_{sc}, is then selected and the well is flowed to stabilization. The stabilized flowing pressure, p_{wf}, is recorded. The flow rate is changed three or four times and every time the well is flowed to pressure stabilization. The flow-rate and pressure histories for such a test are depicted in

Figure 3-4. Interpretation of the pressures and flow rates as shown below will give the desired deliverability relationship.
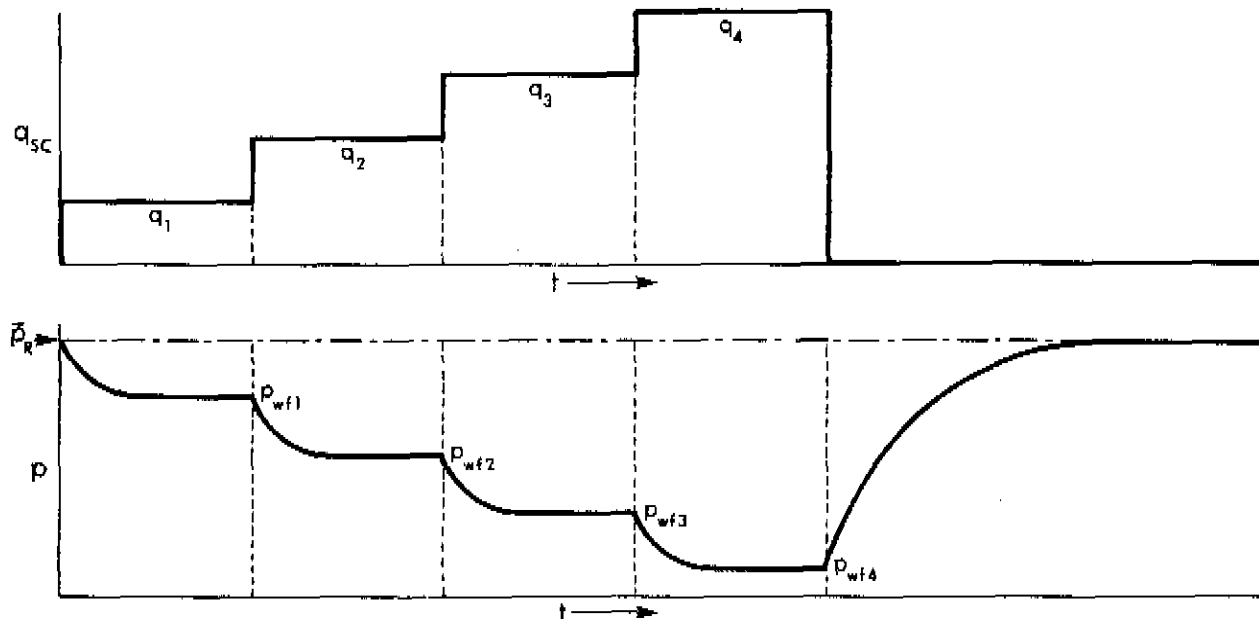
FIGURE 3-4. CONVENTIONAL TEST — FLOW RATE AND PRESSURE DIAGRAMS

Simplified Analysis

A graph of Δp^2 $(= \bar{p}_R^2 - p_{wf}^2)$ versus q_{sc}, on logarithmic coordinates, is constructed as shown in Figure 3-1. This gives a straight line of slope $\frac{1}{n}$ or reciprocal slope, n, known as the "back pressure line" or the deliverability relationship. From this straight line and Equation (3-1) the AOF or the deliverability of the well against any sandface back pressure may be obtained.

LIT(ψ) Flow Analysis

The values of p_{wf} are converted to ψ_{wf} using the applicable $\psi - p$ curve, similar to Figure 2-4. The values of a and b are calculated by the methods of Section 3 and the deliverability relationship is expressed in form of Equation (3-4). The deliverability q_{sc} for any known $\Delta\psi$ may then be obtained from Equation (3-5).

It is recommended that even though the deliverability

relationship is derived by computation, the equation obtained should be plotted on logarithmic coordinates along with the data points. Data which contain significant errors will then show up easily. Erroneous data points must be discarded and the deliverability relationship then recalculated.

A sample deliverability calculation for a conventional test by both the Simplified and the LIT(ψ) flow analyses is shown in Example 3-1 (for gas composition see Example A-1; for the ψ - p curve see Figure 2-4).

Although in many instances, both the Simplified and LIT(ψ) flow analyses will give the same result, extrapolation by the Simplified analysis beyond the range of flow rates tested can cause significant errors. Such a situation is well illustrated by the calculations for a conventional test (Example 3-1). The LIT(ψ) flow analysis gives an AOF of 37.8 MMscfd while the Simplified analysis yields an AOF of 44.0 MMscfd.

This method of testing and the interpretation of the data is relatively simple, and the method has been considered the basic acceptable standard for testing gas wells for many years.

In a reservoir of very high permeability, the time required to obtain stabilized flow rates and flowing pressures, as well as a stabilized shut-in formation pressure is usually not excessive. In this type of reservoir a properly stabilized conventional deliverability test may be conducted in a reasonable period of time. On the other hand, in low permeability reservoirs the time required to even approximate stabilized flow conditions may be very long. In this situation, it is not practical to conduct a completely stabilized test, and since the results of an unstabilized test can be very misleading, other methods of testing should be used to predict well behaviour.

4.2   Isochronal Test

The conventional deliverability test carried out under stabilized conditions, qualifies as an acceptable approach to attaining the relationship which is essential to the proper interpretation of tests, because it extends each flow rate over a period of time

sufficient to permit the radius of investigation to reach the outer edge of the reservoir or the point of interference between neighbouring wells. This ensures that the effective drainage radius is constant. The effective drainage radius concept is discussed in Section 7.1. If each flow rate of a multi-point test extends for a fixed period of time insufficient for stabilization, the effective drainage radius, r_d, which is a function of the duration of flow, is the same for each point. The isochronal flow test which was proposed by Cullender (1955), is based on the principle that the effective drainage radius in a given reservoir is a function only of dimensionless time, and is independent of the flow rate. He suggested that a series of flow tests at different rates for equal periods of time would result in a straight line on logarithmic coordinates and demonstrated that such a performance curve would have a value of the exponent n essentially the same as that established under stabilized flow conditions. LIT(ψ) flow theory confirms that b too is independent of the duration of flow (Section 3N.3) and may, therefore, be determined from short flow tests. For different flow rates, C and a stay constant provided the duration of each flow is constant. Whereas n or b may be obtained from short (transient) isochronal flow tests, C or a can only be derived from stabilized conditions.

The isochronal flow data may thus be used in conjunction with only one stabilized flow point to replace a fully stabilized conventional deliverability test. Briefly, the isochronal test consists of alternately closing in the well until a stabilized, or very nearly stabilized pressure, $\bar{p}_R$, is reached and flowing the well at different rates for a set period of time t, the flowing sandface pressure, p_{wf}, at time t being recorded. One flow test is conducted for a time period long enough to attain stabilized conditions and is usually referred to as the extended flow period. The flow rate and pressure sequence are depicted in Figure 3-7.

A brief discussion of the theoretical validity of isochronal tests is given in Section 3N.5 of the Notes to this chapter.

EXAMPLE 3-1 ILLUSTRATING DELIVERABILITY CALCULATIONS FOR A CONVENTIONAL TEST. SEE FIGURES 3-5 AND 3-6 FOR PLOTS OF Δp^2 VERSUS q_{sc} AND $(\Delta\psi - bq_{sc}^2)$ VERSUS q_{sc}, RESPECTIVELY. (NOTE: q IMPLIES q_{sc})

SIMPLIFIED ANALYSIS

	DURATION hours	SANDFACE PRESSURE psia	CALC.	MEAS.	$p^2 \times 10^{-3}$ psia^2	$\Delta p^2 \times 10^{-3}$ psia^2	FLOW RATE(q) MMscfd
INITIAL SHUT-IN		201		x	40.4		
FLOW 1	3	196		x	38.4	2.0	2.73
SHUT-IN							
FLOW 2	2	195		x	38.0	2.4	3.97
SHUT-IN							
FLOW 3	2	193		x	37.2	3.2	4.44
SHUT-IN							
FLOW 4	4	190		x	36.1	4.3	5.50
EXTENDED FLOW							
FINAL SHUT-IN							

RESULTS

$q = C\left(\bar{p}_R^2 - p_{wf}^2\right)^n$

slope $n = \underline{0.93}$

$\bar{p}_R = \underline{201}$ psia

$C = \dfrac{q}{\left(\bar{p}_R^2 - p_{wf}^2\right)^n}$

$= \underline{0.00229}$

AOF (MMscfd)

$= \underline{44.0}$

LIT (ψ) ANALYSIS

	DURATION hours	SANDFACE PRESSURE psia	ψ MM psia^2/cp	$\Delta\psi$ MM psia^2/cp	FLOW RATE (q) MMscfd	$\Delta\psi/q$	q^2	$\Delta\psi - bq^2$
INITIAL SHUT-IN		201	3.56					
FLOW 1	3	196	3.38	0.18	2.73	0.0659	7.5	0.174
SHUT-IN								
FLOW 2	2	195	3.35	–	–	–	–	–
SHUT-IN								
FLOW 3	2	193	3.28	0.28	4.44	0.0631	19.7	0.263
SHUT-IN								
FLOW 4	4	190	3.18	0.38	5.50	0.0691	30.3	0.355
TOTAL = Σ				0.84	12.67	0.1981	57.5	
EXTENDED FLOW								
FINAL SHUT-IN								

RESULTS

DISCARDED POINT __Flow 2__

$N = \underline{3}$ $\bar{\psi}_R = \underline{3.56}$ MMpsia^2/cp

$a, \underset{}{\alpha} = \dfrac{\Sigma\frac{\Delta\psi}{q}\,\Sigma q^2 - \Sigma q\,\Sigma\Delta\psi}{N\,\Sigma q^2 - \Sigma q\,\Sigma q} = \underline{0.0625}$

$b = \dfrac{N\,\Sigma\Delta\psi - \Sigma q\,\Sigma\frac{\Delta\psi}{q}}{N\,\Sigma q^2 - \Sigma q\,\Sigma q} = \underline{0.00084}$

(EXTENDED FLOW) $\Delta\psi = \underline{\quad}$ $q = \underline{\quad}$ $b = \underline{\quad}$

$a = \dfrac{\Delta\psi - bq^2}{q} = \underline{\quad}$

TRANSIENT FLOW: $\bar{\psi}_R - \psi_{wf} = a_t q + bq^2$

i.e. $\underline{\quad} - \psi_{wf} = \underline{\quad} q + \underline{\quad} q^2$

STABILIZED FLOW: $\bar{\psi}_R - \psi_{wf} = aq + bq^2$

i.e. $\underline{3.56} - \psi_{wf} = \underline{0.0625}\,q + \underline{0.00084}\,q^2$

DELIVERABILITY:

$q = \dfrac{1}{2b}\left[-a + \sqrt{a^2 + 4b\left(\bar{\psi}_R - \psi_{wf}\right)}\,\right]$

FOR $\psi_{wf} = 0$, $q = AOF = \underline{37.8}$ MMscfd
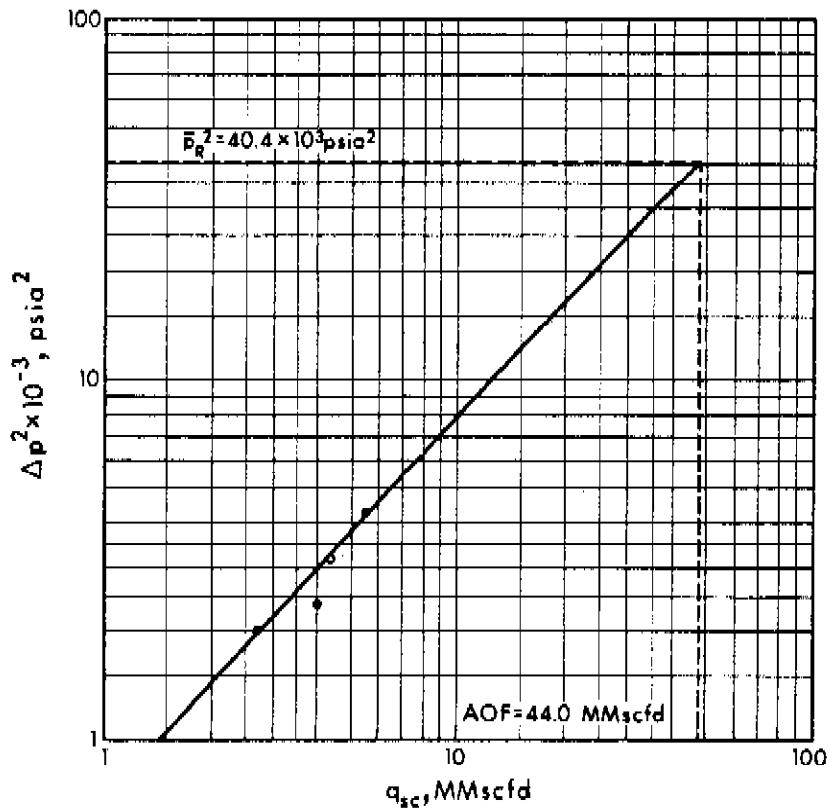
FIGURE 3-5. PLOT OF Δp^2 VERSUS q_{sc} – CONVENTIONAL TEST
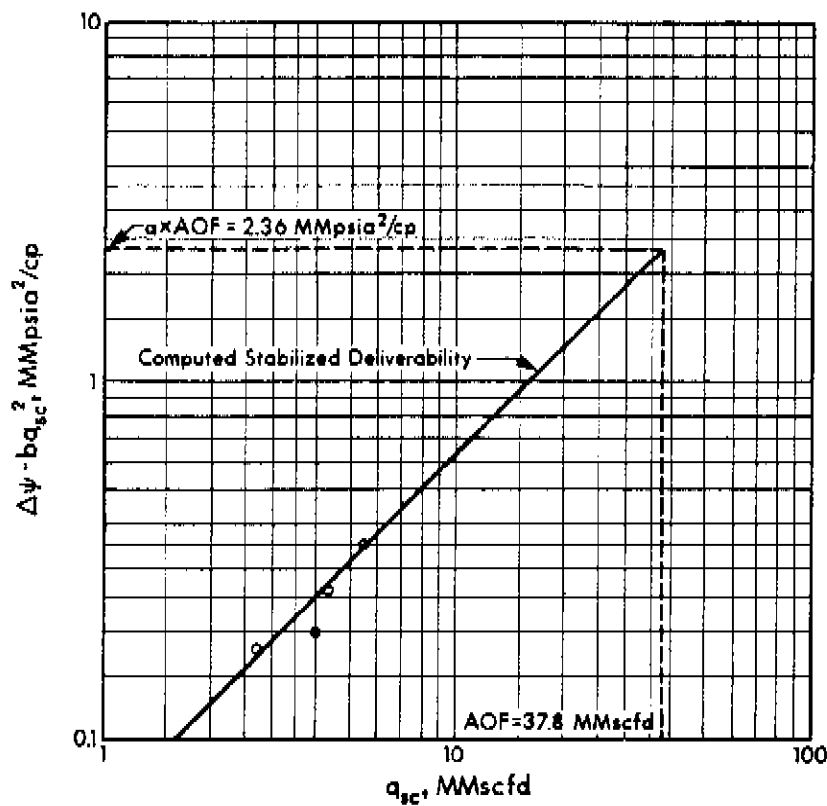
FIGURE 3-6. PLOT OF $(\Delta\psi - bq_{sc}^2)$ VERSUS q_{sc} – CONVENTIONAL TEST
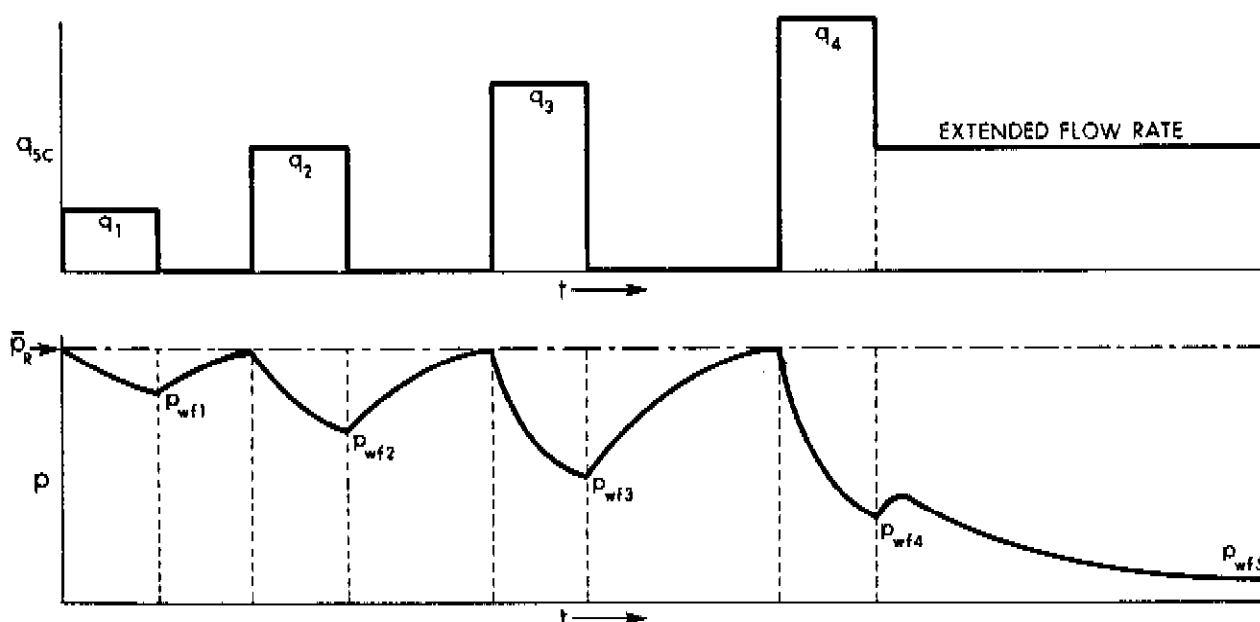
FIGURE 3-7. ISOCHRONAL TEST—FLOW RATE AND PRESSURE DIAGRAMS

Simplified Analysis

The best straight line is drawn through the isochronal points plotted on logarithmic coordinates. This is the transient deliverability line. A straight line parallel to the transient deliverability line drawn through the stabilized point is the stabilized deliverability line from which the AOF or flow against any sandface back pressure can be read.

LIT(ψ) Flow Analysis

From the isochronal flow rates and the corresponding pseudo-pressures a_t and b can be obtained from Equations (3-7) and (3-8); a_t refers to the value of a at the isochronal time t. A logarithmic plot of $(\Delta\psi - bq_{sc}^2)$ versus q_{sc} is made and the isochronal data are also plotted. This plot is used as before to identify erroneous data which must be rejected and a_t and b recalculated, if necessary.

The data obtained from the extended flow rate, $\Delta\psi$ and q_{sc} are used with the value of b already determined in Equation (3-4) to obtain the stabilized value of a. This is given by

$$a = \frac{\Delta\psi - b \ q_{sc}^2}{q_{sc}} \tag{3-12}$$

a and b are now known and the stabilized deliverability relationship may be evaluated from Equation (3-4) and plotted on the deliverability plot.

A sample calculation of stabilized deliverability from an isochronal test is shown in Example 3-2 (for gas composition see Example A-1; for the ψ - p curve see Figure 2-4). The values of AOF calculated by the two methods are not too different since only a small extrapolation is required. However, the LIT(ψ) flow analysis does give a more correct value and should be used instead of the Simplified analysis.

4.3 Modified Isochronal Test

In very tight reservoirs, it is not always practical to attain a completely stabilized reservoir pressure before the initial flow period, nor is it always practical during the test to shut-in the reservoir until the original pressure is attained. As a result, the true isochronal test proves impractical as a means of testing many wells.

Katz et al. (1959, p. 448) suggested that a modified isochronal test conducted with a shut-in period equal to the flow period may give satisfactory results provided the associated unstabilized shut-in pressure is used instead of $\bar{p}_R$ in calculating the difference of pseudo-pressure or pressure-squared for the next flow rate. This method has been used for testing many wells, and indeed has given results which appear quite satisfactory. As in the isochronal test, two lines are obtained, one for the isochronal data and one through the stabilized point. This latter line is the desired stabilized deliverability curve. This method, referred to as the modified isochronal test, does not yield a true isochronal curve but closely approximates the true curve. The pressure and flow rate sequence of the modified isochronal flow test are depicted in Figure 3-10.

EXAMPLE 3-2 ILLUSTRATING DELIVERABILITY CALCULATIONS FOR AN ISOCHRONAL TEST. SEE FIGURES 3-8 AND 3-9 FOR PLOTS OF Δp^2 VERSUS q_{sc} AND $(\Delta\psi - bq_{sc}^2)$ VERSUS q_{sc}. RESPECTIVELY. (NOTE: q IMPLIES q_{sc})

SIMPLIFIED ANALYSIS

	DURATION hours	SANDFACE PRESSURE psia	CALC.	MEAS.	$p^2 \times 10^{-3}$ psia^2	$\Delta p^2 \times 10^{-3}$ psia^2	FLOW RATE(q) MMscfd
INITIAL SHUT-IN	48	1952		x	3810		
FLOW 1	12	1761		x	3101	709	2.6
SHUT-IN	15	1952		x	3810		
FLOW 2	12	1657		x	2746	1064	3.3
SHUT-IN	17	1952		x	3810		
FLOW 3	12	1510		x	2280	1530	5.0
SHUT-IN	18	1952		x	3810		
FLOW 4	12	1320		x	1742	2068	6.3
EXTENDED FLOW	72	1151		x	1325	2485	6.0
FINAL SHUT-IN	100	1952		x	3810		

RESULTS

$q = C\left(\bar{P}_R^2 - P_{wf}^2\right)^n$

slope n = 0.87

$\bar{P}_R$ = 1952 psia

$C = \dfrac{q}{\left(\bar{P}_R^2 - P_{wf}^2\right)^n}$

= 0.000017

AOF (MMscfd)

= 9.0

LIT (ψ) ANALYSIS

	DURATION hours	SANDFACE PRESSURE psia	ψ MM psia^2/cp	$\Delta\psi$ MM psia^2/cp	FLOW RATE(q) MMscfd	$\Delta\psi/q$	q^2	$\Delta\psi - bq^2$
INITIAL SHUT-IN	48	1952	316					
FLOW 1	12	1761	261	55	2.6	21.15	6.8	42.36
SHUT-IN	15	1952	316					
FLOW 2	12	1657	233	–	–	–	–	–
SHUT-IN	17	1952	316					
FLOW 3	12	1510	195	121	5.0	24.20	25.0	74.25
SHUT-IN	18	1952	316					
FLOW 4	12	1320	151	165	6.3	26.19	37.7	90.78
TOTAL = Σ				341	13.9	71.54	69.5	
EXTENDED FLOW	72	1151	15	201	6.0			133.68
FINAL SHUT-IN	100	1952	316					

DISCARDED POINT ___Flow 2___

N = ___3___ $\bar{\psi}_R$ = ___316___ MMpsia^2/cp

$\bar{x}, a_T = \dfrac{\Sigma\frac{\Delta\psi}{q}\Sigma q^2 - \Sigma q\,\Sigma\Delta\psi}{N\,\Sigma q^2 - \Sigma q\,\Sigma q}$ = 15.182

$b = \dfrac{N\,\Sigma\Delta\psi - \Sigma q\,\Sigma\frac{\Delta\psi}{q}}{N\,\Sigma q^2 - \Sigma q\,\Sigma q}$ = 1.870

(EXTENDED FLOW) $\Delta\psi$ = 201   q = 6.0   b = 1.870

$a = \dfrac{\Delta\psi - bq^2}{q}$ = 22.28

RESULTS

TRANSIENT FLOW: $\bar{\psi}_R - \psi_{wf} = a_t q + bq^2$

i.e. 316 $- \psi_{wf} =$ 15.182 q + 1.870 q^2

STABILIZED FLOW: $\bar{\psi}_R - \psi_{wf} = aq + bq^2$

i.e. 316 $- \psi_{wf} =$ 22.28 q + 1.870 q^2

DELIVERABILITY:

$q = \dfrac{1}{2b}\left[-a + \sqrt{a^2 + 4b\left(\bar{\psi}_R - \psi_{wf}\right)}\right]$

FOR ψ_{wf} = 0, q = AOF = ___8.3___ MMscfd
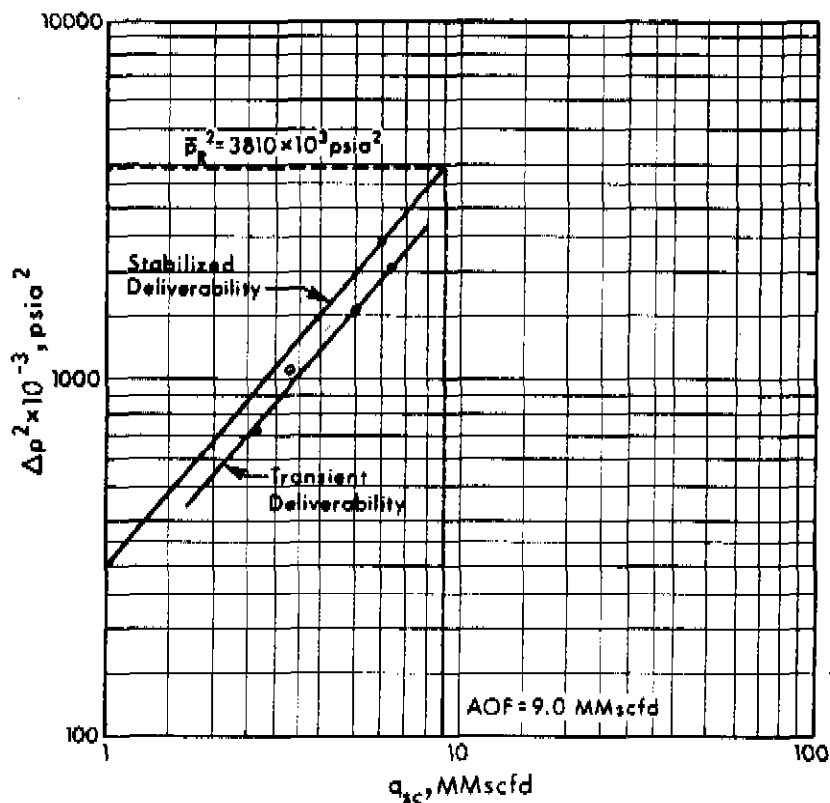
FIGURE 3-8. PLOT OF Δp^2 VERSUS q_{sc} - ISOCHRONAL TEST
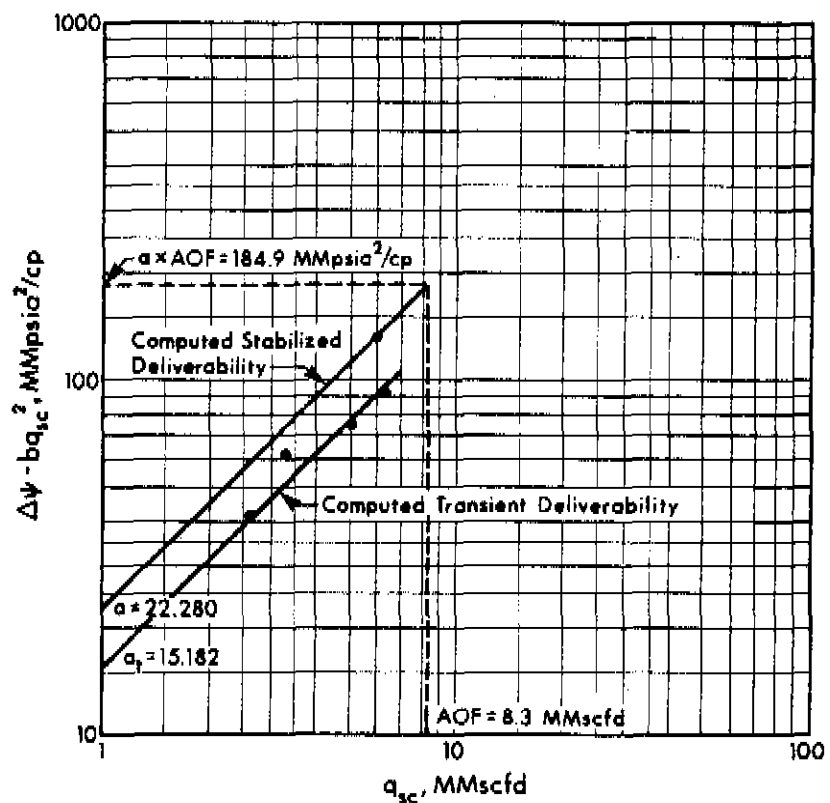
FIGURE 3-9. PLOT OF $(\Delta\psi - bq_{sc}^2)$ VERSUS q_{sc} - ISOCHRONAL TEST

A brief discussion of the theoretical validity of modified isochronal tests is given in Section 3N.5 of the Notes to this chapter.
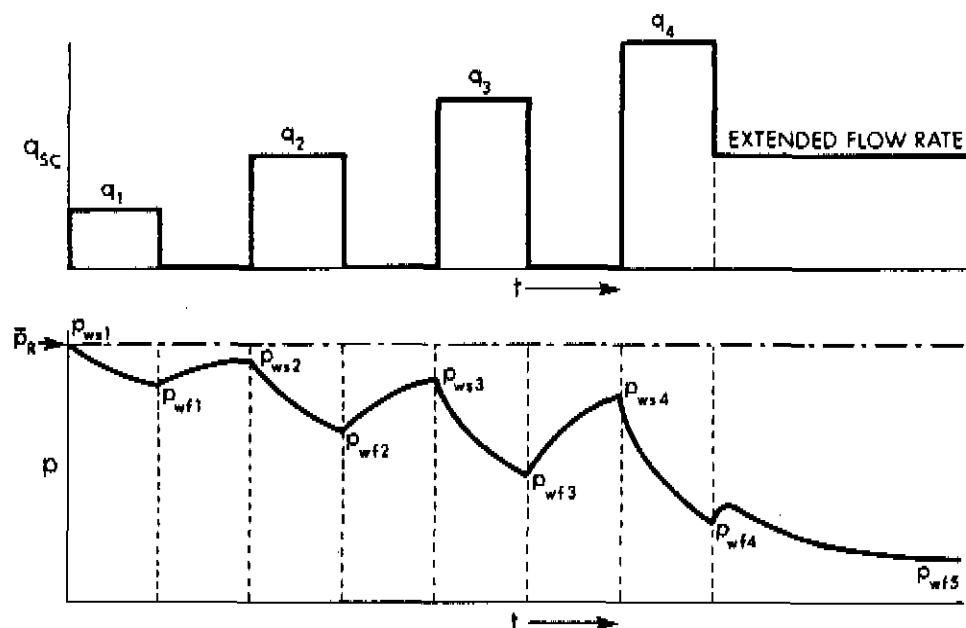
FIGURE 3-10. MODIFIED ISOCHRONAL TEST—FLOW RATE
AND PRESSURE DIAGRAMS

Analysis

The method of analysis of the modified isochronal test data is the same as that of the preceding isochronal method except that instead of $\bar{p}_R$, the preceding shut-in pressure is used in obtaining Δp^2 or $\Delta \psi$. The shut-in pressure to be used for the stabilized point is $\bar{p}_R$, the true stabilized shut-in pressure.

A sample calculation of stabilized deliverability from a modified isochronal test is shown in Example 3-3 (for gas composition see Example A-1; for the $\psi - p$ curve see Figure 2-4). The values for AOF obtained by the different methods are very nearly the same because of the small extrapolation. The test of Example 3-3 may also be analyzed by the graphical method of Section 3.2 as shown in the following example, Example 3-4.

EXAMPLE 3-3 ILLUSTRATING DELIVERABILITY CALCULATIONS FOR A MODIFIED ISOCHRONAL TEST. SEE FIGURES 3-11 AND 3-12 FOR PLOTS OF Δp^2 VERSUS q_{sc} AND $(\Delta\psi - bq_{sc})$ VERSUS q_{sc}, RESPECTIVELY. (NOTE: q IMPLIES q_{sc})

SIMPLIFIED ANALYSIS

	DURATION hours	SANDFACE PRESSURE psia	CALC.	MEAS.	$p^2 \times 10^{-3}$ psia²	$\Delta p^2 \times 10^{-3}$ psia²	FLOW RATE(q) MMscfd
INITIAL SHUT-IN	20	1948		x	3795		
FLOW 1	12	1784		x	3183	612	4.50
SHUT-IN	12	1927		x	3713		
FLOW 2	12	1680		x	2822	891	5.60
SHUT-IN	12	1911		x	3652		
FLOW 3	12	1546		x	2390	1262	6.85
SHUT-IN	12	1887		x	3561		
FLOW 4	12	1355		x	1836	1725	8.25
EXTENDED FLOW	81	1233		x	1520	2275	8.00
FINAL SHUT-IN	120	1948		x	3795		

RESULTS

$$q = C\left(\bar{p}_R^2 - p_{wf}^2\right)^n$$

slope n = __0.60__

$\bar{p}_R$ = __1948__ psia

$$C = \frac{q}{\left(\bar{p}_R^2 - p_{wf}^2\right)^n}$$

= __0.00124__

AOF (MMscfd)

= __11.0__

LIT (ψ) ANALYSIS

	DURATION hours	SANDFACE PRESSURE psia	ψ MM psia²/cp	$\Delta\psi$ MM psia²/cp	FLOW RATE(q) MMscfd	$\Delta\psi/q$	q^2	$\Delta\psi \cdot bq^2$
INITIAL SHUT-IN	20	1948	315					
FLOW 1	12	1784	267	48	4.50	10.67	20.3	14.77
SHUT-IN	12	1927	308					
FLOW 2	12	1680	239	69	5.60	12.32	31.4	17.54
SHUT-IN	12	1911	304					
FLOW 3	12	1546	204	100	6.85	14.60	46.9	23.00
SHUT-IN	12	1887	297					
FLOW 4	12	1355	158	139	8.25	16.85	68.1	27.31
TOTAL = Σ				356	25.20	54.44	166.7	
EXTENDED FLOW	81	1233	132	183	8.00			77.98
FINAL SHUT-IN	120	1948	315					

RESULTS

DISCARDED POINT __-__

N = __4__ $\bar{\psi}_R$ = __315__ MMpsia²/cp

$a_t = \dfrac{\Sigma\frac{\Delta\psi}{q}\,\Sigma q^2 - \Sigma q\,\Sigma\Delta\psi}{N\,\Sigma q^2 - \Sigma q\,\Sigma q}$ = __3.273__

$b = \dfrac{N\,\Sigma\Delta\psi - \Sigma q\,\Sigma\frac{\Delta\psi}{q}}{N\,\Sigma q^2 - \Sigma q\,\Sigma q}$ = __1.641__

(EXTENDED FLOW) $\Delta\psi$ = __183__   q = __8.00__   b = __1.641__

$a = \dfrac{\Delta\psi - bq^2}{q}$ = __9.747__

TRANSIENT FLOW: $\bar{\psi}_R - \psi_{wf} = a_t q + bq^2$

i.e. __315__ − ψ_{wf} = __3.273__ q + __1.641__ q^2

STABILIZED FLOW: $\bar{\psi}_R - \psi_{wf} = aq + bq^2$

i.e. __315__ − ψ_{wf} = __9.747__ q + __1.641__ q^2

DELIVERABILITY:

$$q = \frac{1}{2b}\left[-a + \sqrt{a^2 + 4b\left(\bar{\psi}_R - \psi_{wf}\right)}\right]$$

FOR $\psi_{wf} \doteq 0$, q ≐ AOF = __11.2__ MMscfd
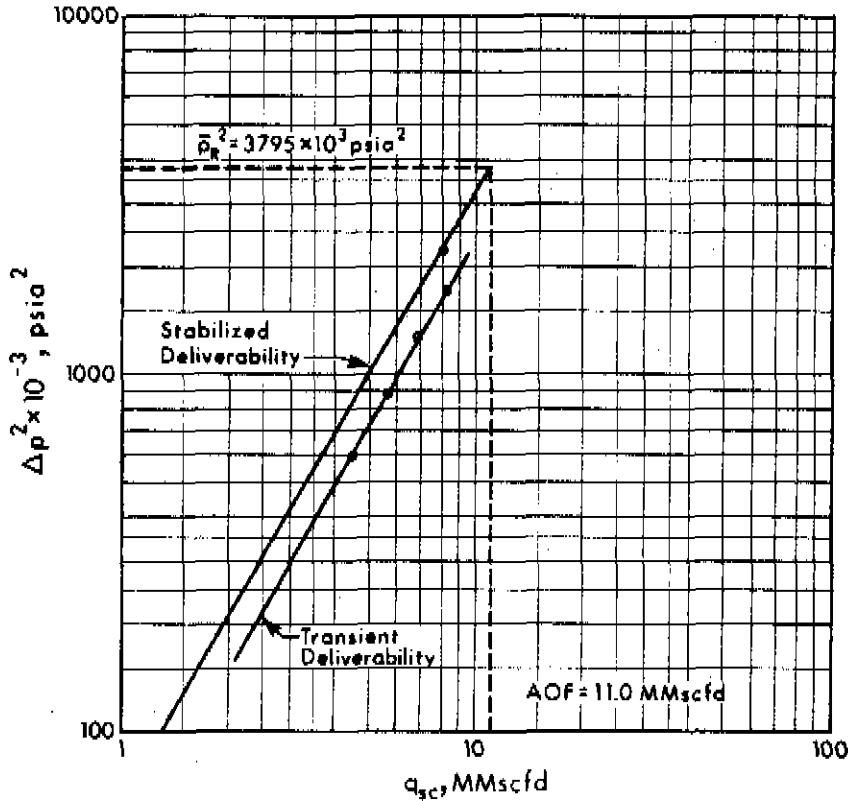
FIGURE 3-11. PLOT OF Δp^2 VERSUS q_{sc} - MODIFIED ISOCHRONAL TEST
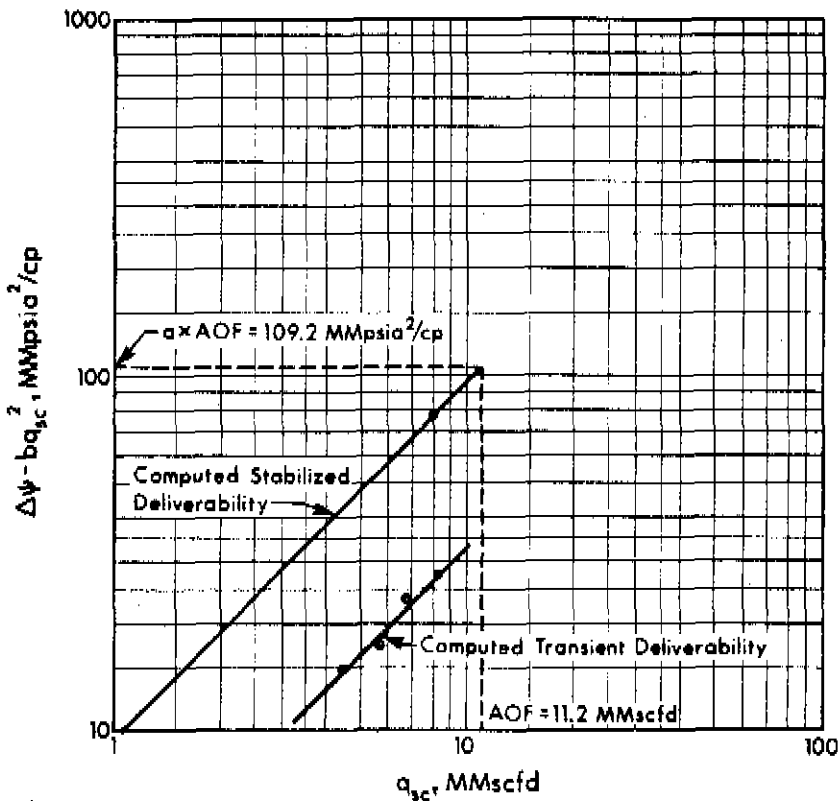
FIGURE 3-12. PLOT OF $(\Delta\psi - bq_{sc}^2)$ VERSUS q_{sc} - MODIFIED ISOCHRONAL TEST

EXAMPLE 3-4

Introduction   This example illustrates the application of the graphical
method of Section 3-2 to the analysis of modified isochronal test data.

Problem   Calculate the values of a, b and AOF for the modified
isochronal test data of Example 3-3.

Solution   Plot $\Delta\psi$ versus q_{sc} (transient, modified isochronal data) on
3×3 logarithmic coordinates of the same size as the general curve of
Figure 3-3.   This deliverability data plot is shown in Figure 3-13.
        The transient deliverability curve is drawn from the best
match of the deliverability data plot and the general curve.   The values
of a_t and b are obtained from the intersections of the straight lines,
represented by Equations (3-10) and (3-11), with the $q_{sc} = 1$ line of
the deliverability data plot.   This gives

$$a_t = 3.3$$

$$b = 1.6$$

        Plot the stabilized flow point and maintaining the value of
b = 1.6 draw the stabilized deliverability curve.   The intersection of
the straight line, represented by Equation (3-10), with the $q_{sc} = 1$ line
of the deliverability data plot gives

$$a = 9.75$$

and the resulting deliverability curve shows an

$$AOF = 11.7 \text{ MMscfd}$$

Discussion   Figure 3-3 may be used to obtain good approximations for
a, b, and AOF, but it is recommended that the calculation methods of
Examples 3-1, 3-2 and 3-3 using the LIT(ψ) flow analysis be used for
better results.
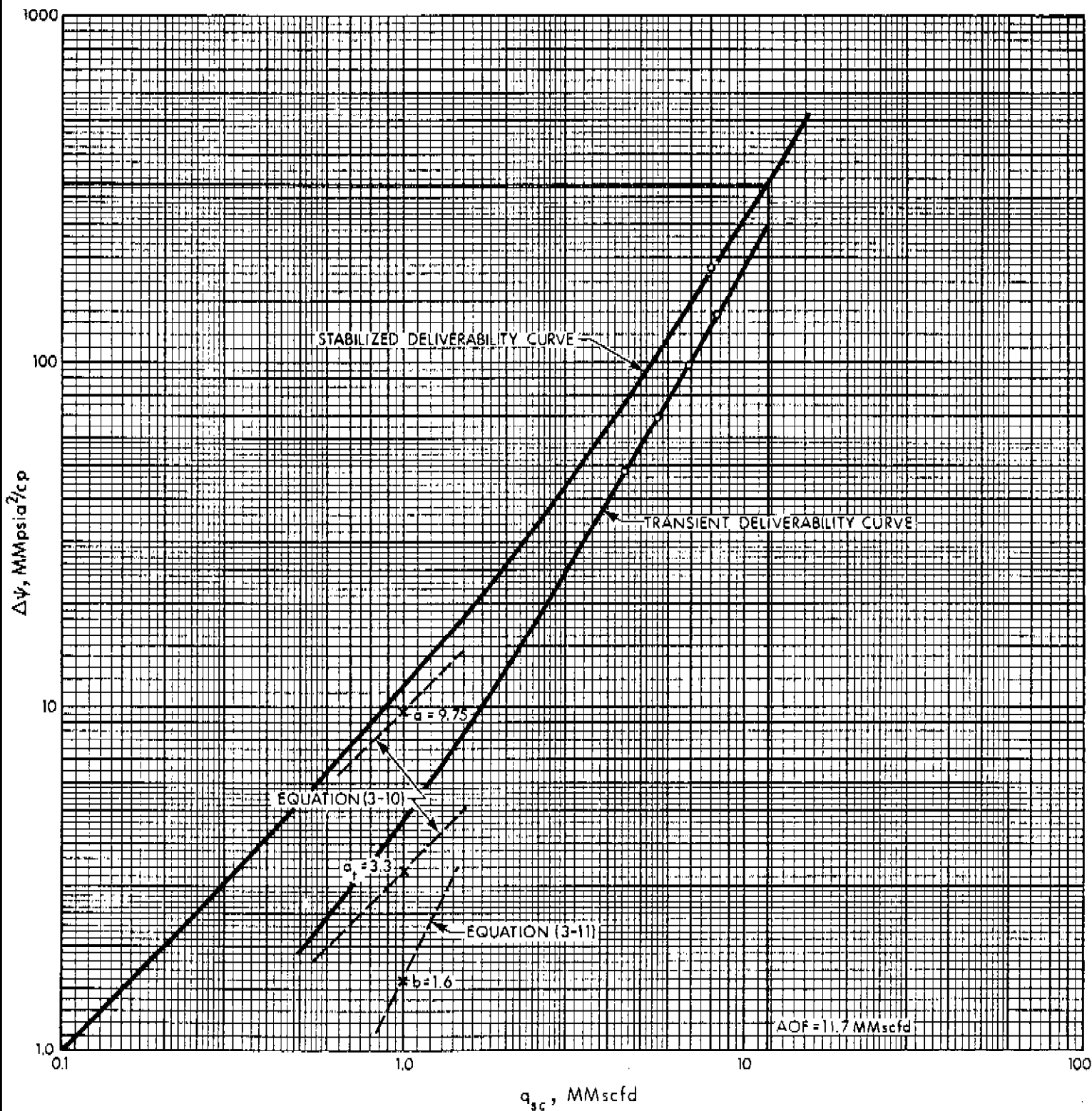
FIGURE 3-13. DELIVERABILITY DATA PLOT FOR EXAMPLE 3-4.

4.4 Single-Point Test

If from previous tests conducted on the well, the reciprocal slope n or the inertial-turbulent (IT) flow effect constant, b, is known, only one stabilized flow point is required to give the deliverability relationship. This is done by selecting one flow rate and flowing the well at that rate to stabilized conditions. Often this test is conducted as part of a pressure survey in a reservoir on production. The gas in this test is usually flowed into a pipeline and not wasted. Care is taken to ensure that the well is producing at a constant rate and has stabilized. This rate and the flowing pressure are recorded. The well is then shut-in long enough that the stabilized shut-in pressure $\bar{p}_R$ can be determined.

Knowing the static pressure $\bar{p}_R$, the stabilized flowing sandface pressure, p_{wf}, and the rate q_{sc}, either the Simplified or the LIT(ψ) analysis may be used to obtain the stabilized deliverability of the well. For the Simplified analysis the stabilized point is plotted on the usual logarithmic coordinates and through it a straight line of inverse slope, n, is drawn. In the LIT(ψ) flow analysis, the stabilized data, $\Delta\psi$ and q_{sc}, are inserted with the previously known value of b into Equation (3-12) to yield a value for a. The stabilized deliverability is then given by Equation (3-4).

A sample calculation of stabilized deliverability from a single-point test is shown in Example 3-5. n and b are known from previous tests; n = 0.60, b = 1.641 (for gas composition see Example A-1; for the ψ - p curve see Figure 2-4).

5 TESTS NOT INVOLVING STABILIZED FLOW

In the previous sections, tests which would yield the deliverability of a well, directly, were described. Each of those tests included at least one flow rate being run to pressure stabilization. In the case of tight reservoirs, stabilization could take months or even years. This is obviously a great inconvenience and alternative methods

must be used to determine the stabilized deliverability without having to conduct stabilized flow tests. The LIT(ψ) flow analysis of transient flow tests, along with a knowledge of the well's drainage volume, may be used to obtain a stabilized deliverability relationship by calculation. Subsequently, when the well has been placed on production, it is desirable to monitor an extended flow rate and using the single-point test analysis confirm the accuracy of the calculated deliverability.

It has been stated before that b is the same for transient or stabilized conditions. In Sections 4.2 and 4.3 it was shown that b could be obtained from isochronal and modified isochronal flow data, and that the same value is applicable to stabilized flow. From Equation (3N-10) of the Notes to this chapter the stabilized value for a is given by

$$a = 3.263 \times 10^6 \frac{T}{k\,h} \left[\log \frac{0.472\, r_e}{r_w} + \frac{s}{2.303} \right] \qquad (3\text{-}13)$$

where

k = effective permeability to gas, md

h = net pay thickness, ft

T = temperature of the reservoir, $^\circ$R

r_e = external radius of the drainage area, ft

r_w = well radius, ft

s = skin factor, dimensionless

Usually r_e, r_w, h, and T are known and only k and s need to be determined before the stabilized value of a can be calculated. In Chapters 4 and 5 it is shown how k and s may be obtained by the analysis of the transient drawdown or build-up data. For the present purpose it is only necessary to note that reliable values of k and s may be obtained from transient tests alone.

Thus to obtain the stabilized deliverability relationship, it is sufficient to conduct the isochronal part of the tests described in Sections 4.2 and 4.3. The extended flow points are not required. The isochronal data are used to obtain the value of b from Equation (3-8).

EXAMPLE 3-5 ILLUSTRATING DELIVERABILITY CALCULATIONS FOR A SINGLE POINT TEST. SEE FIGURES 3-14 AND 3-15 FOR PLOTS OF Δp^2 VERSUS q_{sc} AND $(\Delta \psi - bq_{sc}^2)$ VERSUS q_{sc}, RESPECTIVELY. (NOTE: q IMPLIES q_{sc})

SIMPLIFIED ANALYSIS

	DURATION hours	SANDFACE PRESSURE psia	CALC.	MEAS.	$p^2 \times 10^{-3}$ psia^2	$\Delta p^2 \times 10^{-3}$ psia^2	FLOW RATE(q) MMscfd
INITIAL SHUT-IN							
FLOW 1							
SHUT-IN							
FLOW 2							
SHUT-IN							
FLOW 3							
SHUT-IN							
FLOW 4							
EXTENDED FLOW	275	1155		x	1334	2391	7.20
FINAL SHUT-IN		1930		x	3725		

RESULTS

$q = C\left(\bar{p}_R^2 - p_{wf}^2\right)^n$

slope $n = \underline{\quad 0.60 \quad}$

$\bar{p}_R = \underline{\quad 1930 \quad}$ psia

$C = \dfrac{q}{\left(\bar{p}_R^2 - p_{wf}^2\right)^n}$

$= \underline{\quad 0.00108 \quad}$

AOF (MMscfd)

$= \underline{\quad 9.5 \quad}$

LIT (ψ) ANALYSIS

	DURATION hours	SANDFACE PRESSURE psia	ψ MM psia^2/cp	$\Delta \psi$ MM psia^2/cp	FLOW RATE(q) MMscfd	$\Delta\psi/q$	q^2	$\Delta\psi - bq^2$
INITIAL SHUT-IN								
FLOW 1								
SHUT-IN								
FLOW 2								
SHUT-IN								
FLOW 3								
SHUT-IN								
FLOW 4								
TOTAL = Σ								
EXTENDED FLOW	275	1155	116	183	7.2			97.93
FINAL SHUT-IN		1930	309					

RESULTS

DISCARDED POINT _____

$N = \underline{\qquad}$ $\bar{\psi}_R = \underline{\quad 309 \quad}$ MMpsia^2/cp

$a, a_t = \dfrac{\Sigma \frac{\Delta\psi}{q} \Sigma q^2 - \Sigma q \Sigma \Delta\psi}{N \Sigma q^2 - \Sigma q \Sigma q} = \underline{\qquad}$

$b = \dfrac{N \Sigma \Delta\psi - \Sigma q \Sigma \frac{\Delta\psi}{q}}{N \Sigma q^2 - \Sigma q \Sigma q} = \underline{\qquad}$

(EXTENDED FLOW) $\Delta\psi = \underline{\ 183\ }$ $q = \underline{\ 7.2\ }$ $b = \underline{\ 1.641\ }$

$a = \dfrac{\Delta\psi - bq^2}{q} = \underline{\ 13.601\ }$

TRANSIENT FLOW: $\bar{\psi}_R - \psi_{wf} = a_t q + bq^2$

i.e. $\underline{\qquad} - \psi_{wf} = \underline{\qquad} q + \underline{\qquad} q^2$

STABILIZED FLOW: $\bar{\psi}_R - \psi_{wf} = aq + bq^2$

i.e. $\underline{\ 309\ } - \psi_{wf} = \underline{\ 13.601\ } q + \underline{\ 1.641\ } q^2$

DELIVERABILITY:

$q = \dfrac{1}{2b}\left[-a + \sqrt{a^2 + 4b\left(\bar{\psi}_R - \psi_{wf}\right)}\right]$

FOR $\psi_{wf} = 0$, $q = AOF = \underline{\ 10.2\ }$ MMscfd
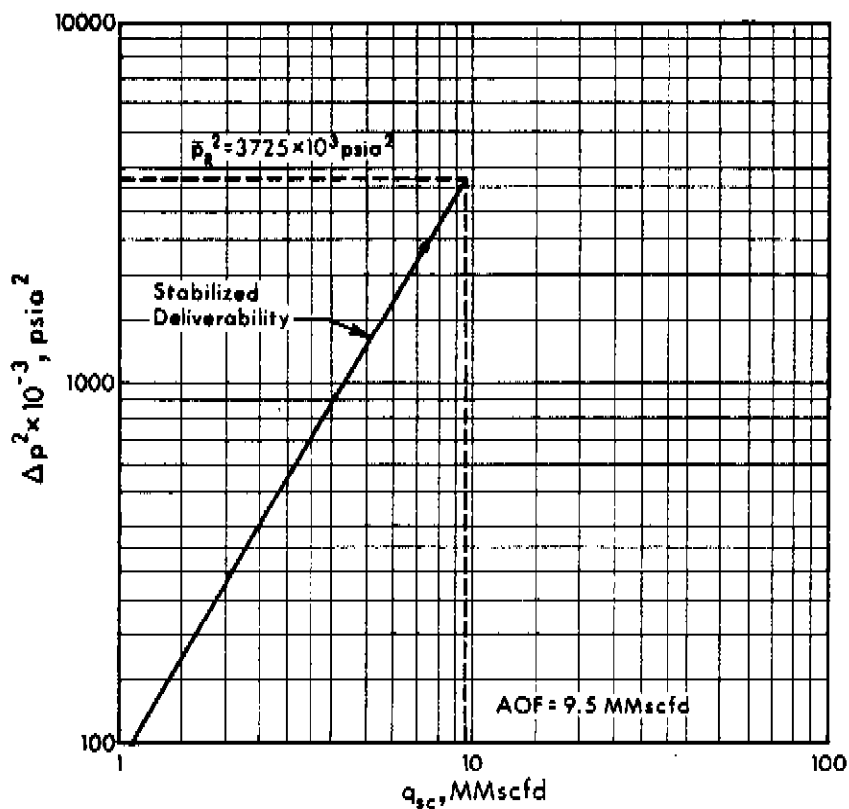
FIGURE 3-14. PLOT OF Δp^2 VERSUS q_{sc} - SINGLE POINT TEST
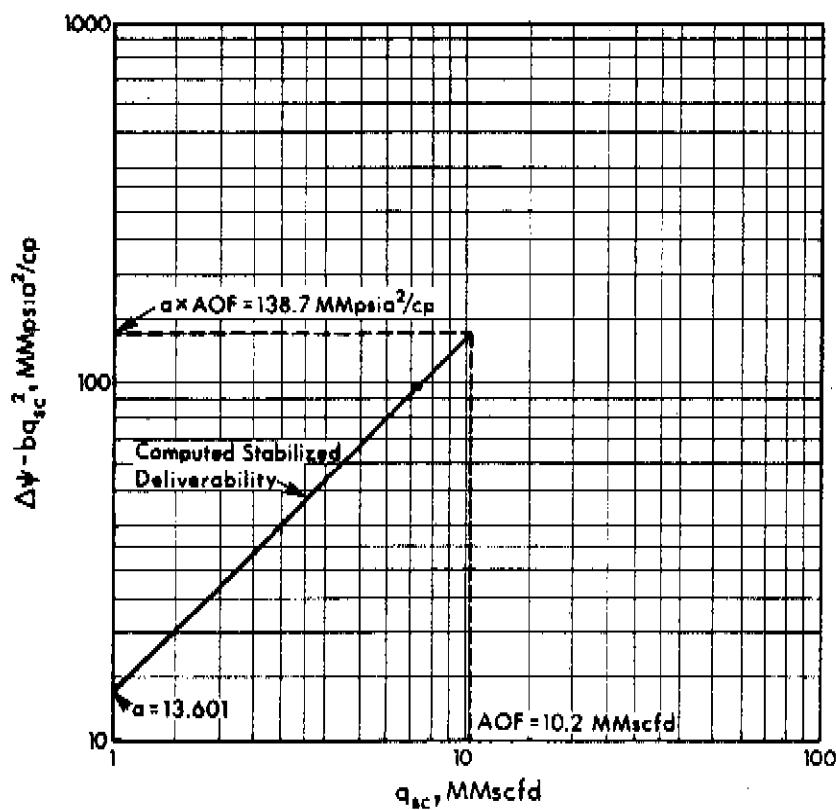
FIGURE 3-15. PLOT OF $(\Delta\psi - bq_{sc}^2)$ VERSUS q_{sc} — SINGLE POINT TEST

The value of a is calculated from Equation (3-13) having first determined k and s from the drawdown or build-up analyses.

6 WELLHEAD DELIVERABILITY

The deliverability relationships obtained by the tests described in the previous sections refer to sandface conditions, that is, all the pressures referred to are measured at the sandface. In practice it is sometimes more convenient to measure the pressures at the wellhead. These pressures may be converted to sandface conditions by the calculation procedure given in detail in Appendix B, and the deliverability relationship may then be obtained as before. However, in some instances, the wellhead pressures may be plotted versus flow rate in a manner similar to the sandface curves of Figures 3-1 or 3-2. The relationship thus obtained is known as the wellhead deliverability and is shown in Figure 3-16. On logarithmic coordinates the slope of the wellhead deliverability plot is not necessarily equal to that obtained using sandface pressures (Edgington and Cleland, 1967); moreover, unless corrections are made, variations of the flowing temperature in the wellbore may cause the plot to be a curve instead of a straight line (Wentink et al. 1971).

A wellhead deliverability plot is useful because it relates to a surface situation, for example, the gathering pipeline back pressure, which is more accessible than the reservoir. However, it has the disadvantage of not being unique for the well as it depends on the size of the pipe, tubing or annulus, in which the gas is flowing. Moreover, unlike the sandface relationship it does not apply throughout the life of the well since the pressure drop in the wellbore itself is a function not only of flow rate but also of pressure level.

Because the wellhead deliverability relationship is not constant throughout the life of a well, different curves are needed to represent the different average reservoir pressures, as shown in Figure 3-17. At any condition of depletion represented by $\bar{p}_R$, the sandface deliverability is valid and may be used to obtain the wellhead

deliverability by converting the sandface pressures to wellhead conditions using the method of Appendix B, in reverse.

7 IMPORTANT CONSIDERATIONS PERTAINING TO DELIVERABILITY TESTS

In all of the tests described so far, the time to stabilization is an important factor, and is discussed in detail below. Moreover, the flow rate is assumed to be constant throughout each flow period. This condition is not always easy to achieve in practice. The effect on test results of a non-constant flow rate is considered in this section. The choice of a sequence of increasing or decreasing flow rates is also discussed.

7.1 Time to Stabilization and Related Matters

Stabilization originated as a practical consideration and reflected the time when the pressure no longer changed significantly with time; that is, it had stabilized. With high permeability reservoirs this point was not too hard to observe. However, with tight formations, the pressure does not stabilize for a very long time, months and sometimes years. Moreover, except where there is a pressure maintenance mechanism acting on the pool, true steady-state is never achieved and the pressure never becomes constant.

Stabilization is more properly defined in terms of a radius of investigation. This is treated, in detail in Chapter 2, but will be reviewed here. When a disturbance is initiated at the well, it will have an immediate effect, however minimal, at all points in the reservoir. At a certain distance from the well, however, the effect of the disturbance will be so small as to be unmeasurable. This distance, at which the effect is barely detectable is called the radius of investigation, r_{inv}. As time increases, this radius moves outwards into the formation until it reaches the outer boundary of the reservoir or the no-flow boundary between adjacent flowing wells. From then on, it
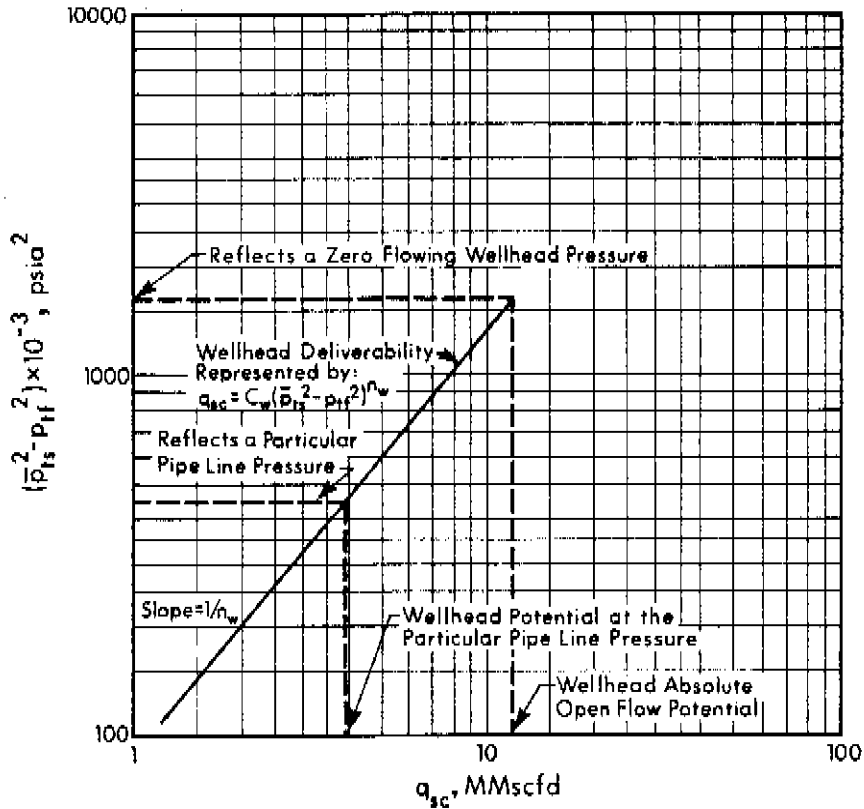
FIGURE 3-16. WELLHEAD DELIVERABILITY PLOT
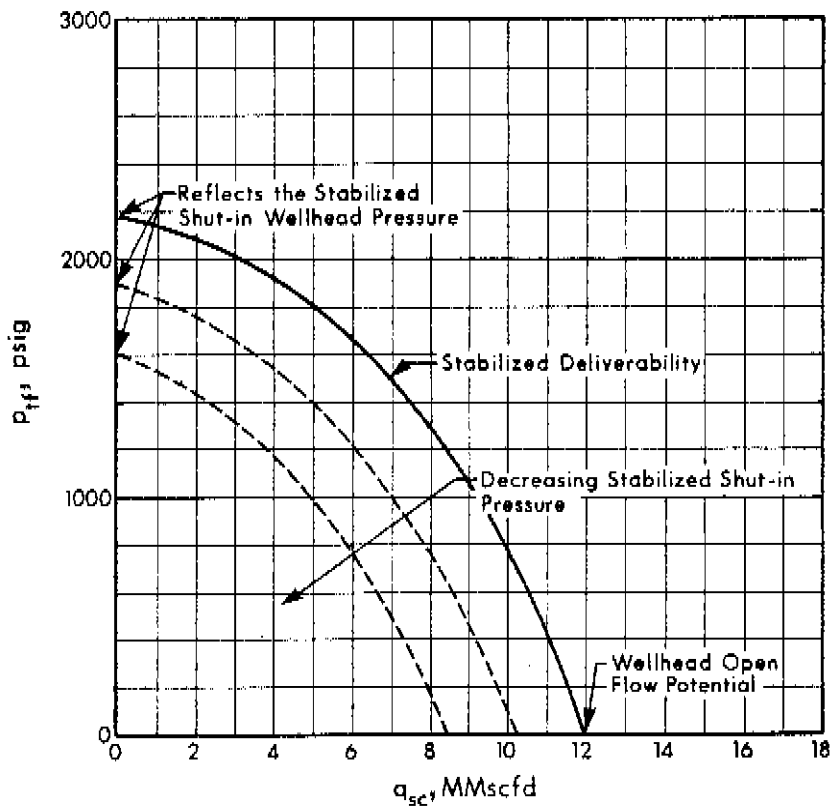
FIGURE 3-17. WELLHEAD DELIVERABILITY VERSUS FLOWING WELLHEAD
PRESSURE, AT VARIOUS STABILIZED SHUT-IN PRESSURES

stays constant, that is, $r_{inv} = r_e$, and stabilization is said to have been attained. This condition is also called pseudo-steady state. The pressure does not become constant but the rate of pressure decline does.

The time to stabilization can only be determined approximately and is given by Equation (3N-15) as

$$t_s \simeq 1000 \; \frac{\phi \, \bar{\mu} \, r_e^2}{k \, \bar{p}_R} \tag{3-14}$$

where

$\quad t_s \quad = \quad$ time to stabilization, hr

$\quad r_e \quad = \quad$ outer radius of the drainage area, ft

$\quad \bar{\mu} \quad = \quad$ gas viscosity at $\bar{p}_R$, cp

$\quad \phi \quad = \quad$ gas-filled porosity, fraction

$\quad k \quad = \quad$ effective permeability to gas, md

There exist various rule-of-thumb methods for determining when stabilization is reached. These are usually based on a rate of pressure decline. When the specified rate, for example, a 0.1 psi drop in 15 minutes, is reached, the well is said to be stabilized. Such over-simplified criteria can be misleading. It is shown in the Notes to this chapter that at stabilization, the rate of pressure decline at the well is given by Equation (3N-19) as

$$\frac{\partial p_{wf}}{\partial t} = -374 \; \frac{\bar{Z} \, T \, q_{sc}}{\phi \, h \, r_e^2} \tag{3-15}$$

This shows that the pressure decline in a given time varies from well to well, and even for a particular well, it varies with the flow rate. For these reasons, methods of defining stabilization which make use of a specified rate of pressure decline may not always be reliable.

The radius of investigation, r_{inv}, after t hours of flow is given by Equation (3N-21). This equation is portrayed graphically in Figure 3-18.

$$r_{inv} \simeq 0.032 \sqrt{\left(\frac{k \; \bar{p}_R \; t}{\phi \; \bar{\mu}}\right)} \qquad \text{for } r_{inv} < r_e \qquad (3\text{-}16)$$

As long as the radius of investigation is less than the exterior radius of the reservoir, stabilization has not been reached and the flow is said to be transient. Since gas well tests often involve interpretation of data obtained in the transient flow regime, a review of transient flow seems appropriate. For transient flow, Equations (3-1) and (3-4) still apply but neither C nor a is constant. Both C and a will change with time until stabilization is reached. From this time on, C and a will stay constant.

Effective Drainage Radius

A concept which relates transient and stabilized flow equations is that of effective drainage radius, r_d, which is discussed in detail in Chapter 2. It is defined as that radius which a hypothetical steady-state circular reservoir would have if the pressure at that radius were $\bar{p}_R$ and the drawdown at the well at the given flow rate were equal to the actual drawdown. Initially, the pressure drop at the well increases and so does r_d. Ultimately, when the radius of investigation reaches the exterior boundary, r_e, of a closed reservoir, the effective drainage radius is given by Equation (2-101)

$$r_d = 0.472 \; r_e \qquad (3\text{-}17)$$

The above equation is the source of the popular idea that the radius of drainage only moves half-way into the reservoir. It should be emphasized that at all times, drainage takes place from the entire reservoir and that r_d is only an equivalent radius which converts an unsteady-state flow equation to a steady-state one. Furthermore, the distinction between the concepts of effective drainage radius and radius of investigation should be understood as described in Chapter 2, Section 6.4.
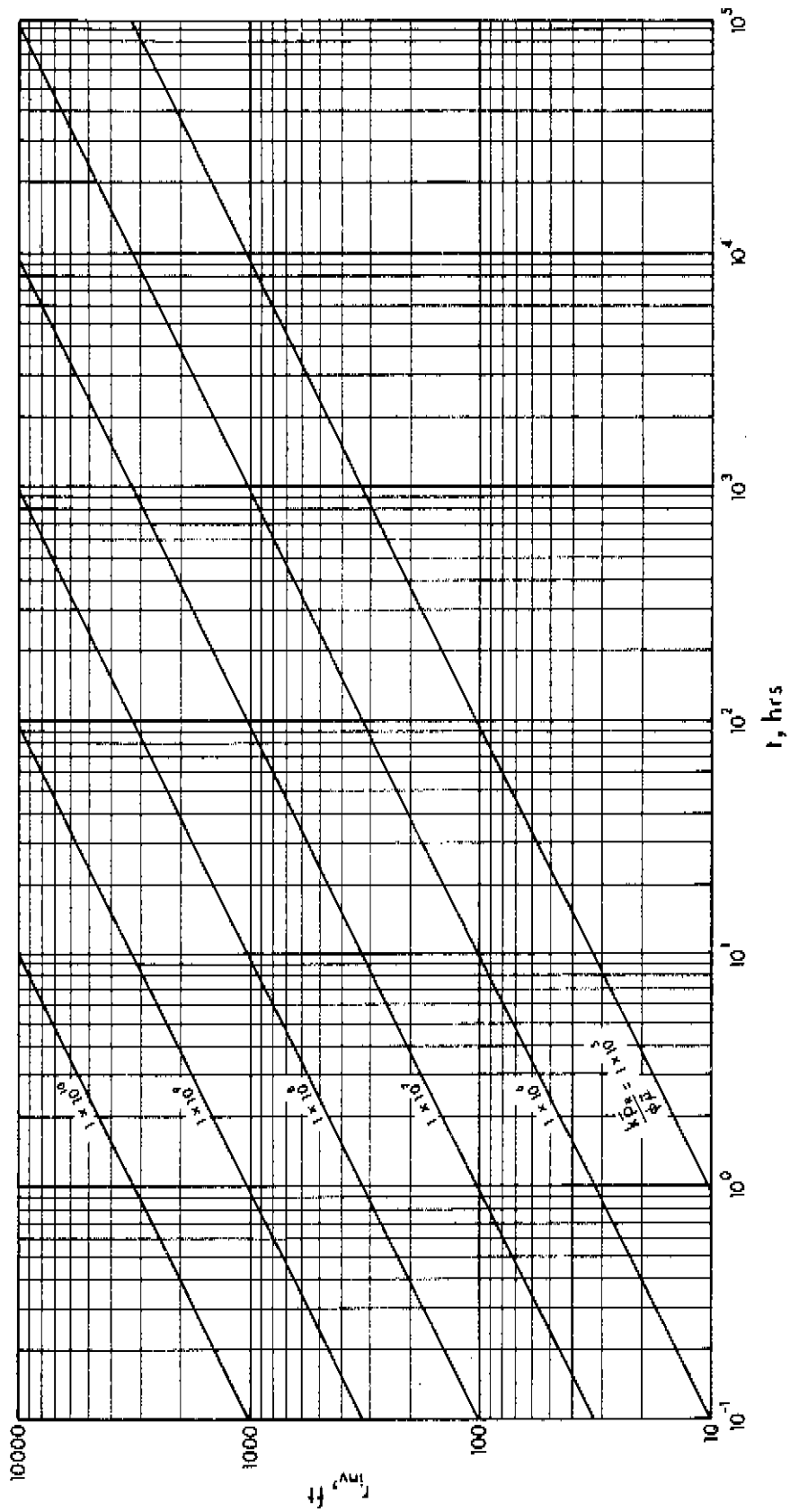
FIGURE 3-18. RADIUS OF INVESTIGATION

7.2   Sequence of Flow Rates

The usual practice in conducting deliverability tests is
to use, where possible, a sequence of increasing flow rates.   In a
conventional test, if there is a likelihood of hydrates forming, a
decreasing sequence is advisable as it results in higher wellbore
temperatures and a decreased tendency to form hydrates.   Where liquid
hold-up in the wellbore is a problem, a decreasing sequence may be
preferred.

If the conventional test or the isochronal test are properly
conducted, that is, stabilization of pressure is observed before a new
rate is selected, the rate sequence is immaterial.   Either an increasing
or a decreasing sequence will give the true deliverability relationship.
However, for the modified isochronal test, an increasing rate sequence
should be used, otherwise the test method loses accuracy, and may not
be acceptable.

The extended flow rate of the isochronal or modified
isochronal test may be run either at the beginning, if the well is
already on production, or at the end of the test.   If it is conducted
at the beginning, the well must then be shut in to essentially stabilized
conditions, prior to the commencement of the isochronal flow periods.
Often, the last isochronal rate is simply extended to stabilization, with
a pressure reading being taken at the appropriate (isochronal) time of
flow, and later at stabilization.   However, this need not necessarily
be so.   In fact, any suitable flow rate may be chosen with or without
a shut-in intervening between it and the last isochronal rate, as long
as the flow is extended to pressure stabilization.

7.3   Constancy of Flow Rate

In interpreting the theory applicable to the tests described
so far, the flow rate within each flow period is assumed to be constant.
In practice this situation is rarely achieved.   If the flow is being
measured through a critical flow prover, the upstream pressure declines

continuously with time, and hence the flow rate decreases correspondingly. If an orifice meter is being used to measure the gas flow, the usual practice is to set the choke, upstream of the orifice meter, at a fixed setting. This setting is not changed throughout the flow period. A declining wellhead pressure upstream of the choke coupled with a constant pressure downstream of the choke, resulting from the back pressure regulator, often results in a continuously declining flow rate. Moreover, the calculations of flow rates involve the gas flowing temperature. During short flow periods, the wellhead temperature is rarely constant, the variation being due to a gradual warming up of the well. All these factors make it difficult for an absolutely constant flow rate to be maintained.

Winestock and Colpitts (1965) developed a method of analysis to account for the variations in flow rate. Lee, Harrell and McCain (1972) confirmed, by numerical simulation, the validity of their approach. The results of their study related to drawdown testing are summarized in a later chapter, but some of the findings applicable to deliverability tests are given below.

Provided the changes in flow rate are not excessively rapid, instantaneous values of the flow rate and the corresponding flowing pressure should be used rather than values averaged over the entire flow period. In view of this, flow rates need not be kept absolutely constant, but may be allowed to vary smoothly and continuously with time, as is the case with flow provers or orifice meters. Since sudden changes in rate invalidate this approach, no change in orifice plates is permissible for whatever reason, not even in order to adhere to a prespecified schedule, once a flow period has commenced.

8 GUIDELINES FOR DESIGNING DELIVERABILITY TESTS

Once the decision has been made to run a deliverability test, all the information pertaining to the well and to the reservoir under investigation should be collected and utilized in specifying the test procedure. Such information may include logs, drill-stem tests,

previous deliverability tests conducted on that well, production
history, fluid composition and temperature, cores and geological
studies. In the absence of some of these details, data from neighbouring
wells completed in the same formation may be substituted. At all times,
the value of first-hand field experience must not be underestimated and
should certainly have a major influence on the design and conduct of
tests.

8.1 Choice of Test

A knowledge of the time required for stabilization is a very
important factor in deciding the type of test to be used for determining
the deliverability of a well. This may be known directly from previous
tests, such as drill-stem or deliverability tests, conducted on the well
or from the production characteristics of the well. If such information
is not available, it may be assumed that the well will behave in a
manner similar to neighbouring wells in the same pool, for which the
data are available.

When the approximate time to stabilization is not known, it
may be estimated from Equation (3-14). If the time to stabilization is
of the order of a few hours, a conventional test may be conducted.
Otherwise one of the isochronal tests is preferable. The isochronal
test is more accurate than the modified isochronal test and should be
used if the greater accuracy is warranted.

The choice of a test is discussed more fully in Chapter 1.
An important consideration is that if gas is to be flared, the duration
of the test should be minimized. This may be accomplished by testing
only new exploratory wells, using isochronal type tests rather than the
conventional deliverability test, and calculating the stabilized flow
point rather than flowing a well to stabilization. Where the well
being tested is tied into a pipeline, more flexibility is available in
choosing the type of test, but care must be taken to ensure sufficiently
long flow periods when stabilized flow points are to be obtained.

A single-point test is appropriate when the deliverability

relationship of the well is known from previous tests, and only updating of this relationship is desired. A convenient time to conduct such a test is prior to a shut-in for a pressure survey of the pool as the well is probably stabilized and all that is needed is a measurement of the flow rate and the flowing pressure.

8.2 Choice of Equipment

The various types of equipment used in gas well testing are mentioned in Chapter 6. Some of the factors affecting the choice of equipment are the expected flow rates and pressures, and the analysis of the gas and liquid effluent to be expected during the test. The possibility and location of hydrate formation must be investigated. This may be done by the methods outlined in Appendix A and will affect the choice of the heating equipment to be used during the test. Failure to prevent hydrate formation will result in anomalous flow data due to complete or partial plugging of sections of the equipment.

Production of liquid, be it water or condensate, causes fluctuations in the rate and pressure measurements. Long flow times, of at least six to eight hours, are needed before the liquid to gas ratio stabilizes. One or two separators at the surface must be included in the test equipment since the gas must be free of liquid before it can be measured with the standard orifice meters or critical flow provers. Calculations of sandface pressures from wellhead pressures become inaccurate when there is liquid in the wellbore and wherever practically possible the use of bottom hole pressure bombs becomes mandatory. Extremely sour gases may make the use of bottom hole equipment impossible because of problems with corrosion or sulphur deposition.

8.3 Choice of Flow Rates

In conducting a multi-point test, the minimum flow rate used should be at least equal to that required to lift the liquids, if any, from the well. It should also be sufficient to maintain a wellhead temperature above the hydrate point. Where these considerations do not

apply, the minimum and maximum flow rates are chosen, whenever practical, such that the pressure drops they cause at the well are approximately 5 per cent and 25 per cent, respectively, of the shut-in pressure. Alternatively, they may be taken to be about 10 per cent and 75 per cent, respectively, of the AOF. High drawdown rates that may cause well damage by sloughing of the formation or by unnecessarily coning water into the wellbore must be avoided. Care must also be taken to avoid retrograde condensation within the reservoir in the vicinity of the well or in the well itself. In the isochronal and modified isochronal tests, the extended flow rate is often taken to be approximately equal to the expected production rate. If flaring is taking place, flow should be at the minimum rate consistent with obtaining useful information.

Some idea of the flow rates at which a well is capable of flowing may be obtained from the drill-stem test or from the preliminary well clean-up flows. In the absence of any data whatsoever, the AOF may be estimated from Equation (3N-12) by assuming stabilized, purely laminar flow in the reservoir.

$$AOF \simeq \frac{k\,h\,\bar{\psi}_R}{3.263 \times 10^6\ T\left[\log\left(0.472\,\frac{r_e}{r_w}\right) + \frac{s}{2.303}\right]} \qquad (3\text{-}18)$$

s may be estimated from similar stimulation treatments performed on approximately similar wells in the formation, or from Table 7-1 in Chapter 7.

8.4 Duration of Flow Rates

In conducting tests which involve stabilized conditions, the conventional test, a single-point test and the extended rate of the isochronal and modified isochronal tests, the duration of flow must be at least equal to the approximate time to stabilization as calculated from Equation (3-14).

The duration of the isochronal periods is determined by two considerations, namely, (a) wellbore storage time and (b) the radius of

investigation.

    a. The wellbore storage time, t_{ws}, it the approximate time required for the wellbore storage effects to become negligible. This can be calculated from Equation (3N-24) which is developed in the Notes to this chapter:

$$t_{ws} = \frac{36177 \ \bar{\mu} \ V_{ws} \ c_{ws}}{k \ h} \tag{3-19}$$

where

        V_{ws} = volume of the wellbore tubing (and annulus, if there is no packer)

        c_{ws} = compressibility of the wellbore fluid evaluated at the mean wellbore pressure and temperature

Equation (3-19) is presented graphically in Figure 3-19 for the case of a three-inch internal diameter tubing string in a six-inch internal diameter casing, with and without an annulus packer.

    b. The radius of investigation has been discussed in Section 7.1. Rarely does wellbore damage or stimulation extend beyond 100 feet. In order to obtain data that are representative of the formation, the flow period must last longer than the time to investigate the first 100 feet. For wells with no damage or improvement an approximate time to investigate 100 feet is obtained from Equation (3-20) or from Figure 3-18. From Equation (3-14)

$$t_{100} \simeq 1000 \ \frac{\phi \ \bar{\mu}}{k \ \bar{p}_R} \ 100^2 = 1.0 \times 10^7 \ \frac{\phi \ \bar{\mu}}{k \ \bar{p}_R} \tag{3-20}$$

The greater of t_{ws} and t_{100} is the minimum duration of flow that will yield data representative of the bulk formation rather than the wellbore area. A duration equal to about four times this value is recommended for the isochronal periods.
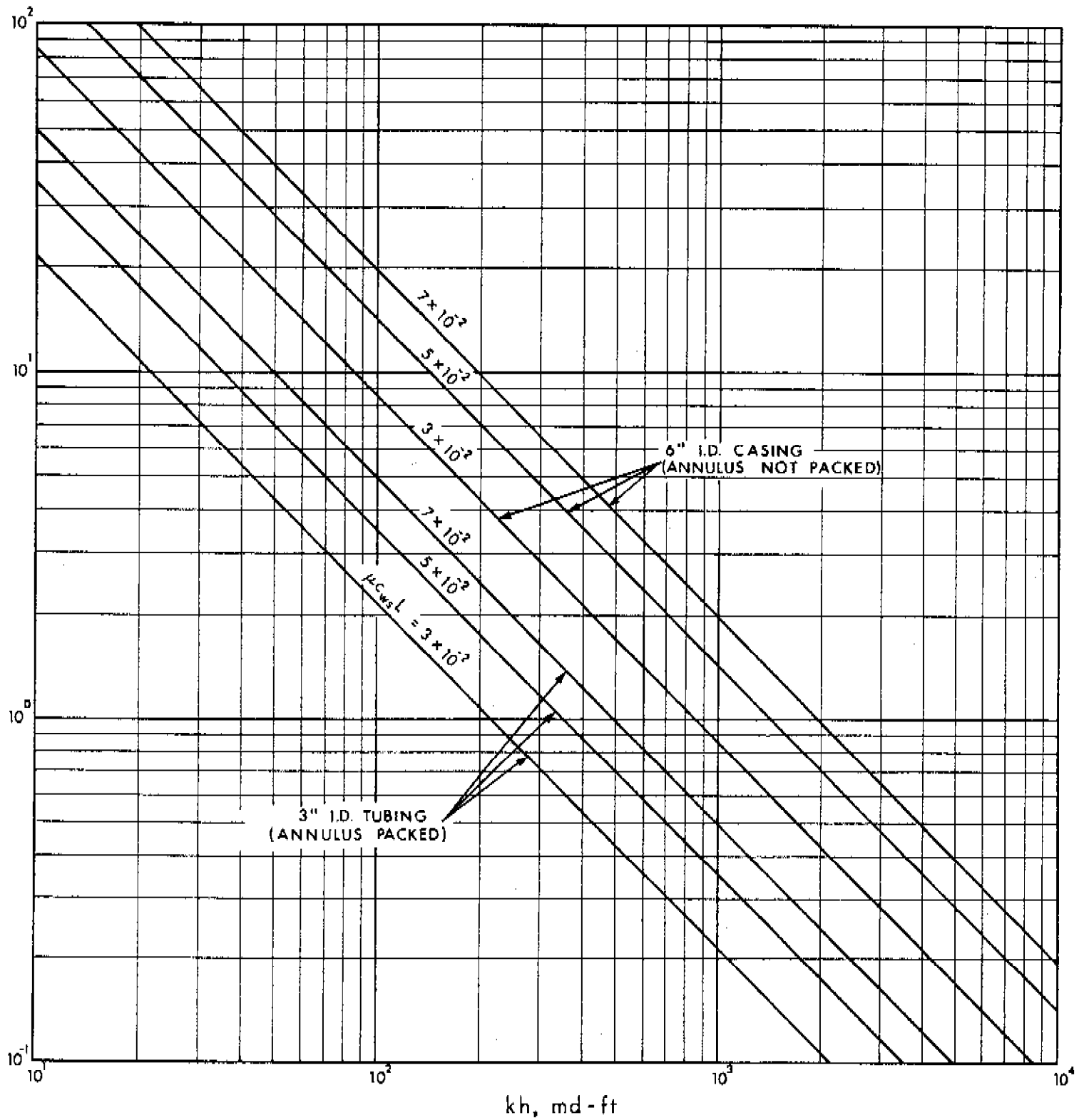
FIGURE 3-19. TIME REQUIRED FOR WELLBORE STORAGE EFFECTS
TO BECOME NEGLIGIBLE

EXAMPLE 3-6

Introduction   This example illustrates calculations that are essential to the design of a deliverability test.

Problem   A well was completed in a dry, sweet gas pool which is being developed with a one-section spacing between wells. It has been cored, logged and drill-stem tested, acidized and cleaned but no deliverability tests have, so far, been performed on it. Design a suitable deliverability test.

Solution

Choice of Test

Before the choice of a suitable test can be made, the approximate time to stabilization, t_s, must be known. This being the first well in the pool, and the drill-stem test flow rate not being stabilized, the time to stabilization is not known and should be estimated from Equation (3-14). This requires a knowledge of the following factors: r_e, $\bar{p}_R$, ϕ, k, $\bar{\mu}$,

a. r_e = 2640 ft, equivalent to a one-section spacing;

b. $\bar{p}_R$ = 2000 psia, obtained from the drill-stem test;

c. ϕ = 0.15, the gas filled porosity is obtained by multiplying the formation porosity by the gas saturation, both quantities being deducible from logs;

d. k = 120 md, the build-up period of the drill-stem test was analyzed by methods described in Chapter 5 to give an effective kh = 1200 md-ft. From logs, h = 10 ft;

e. $\bar{\mu}$ = 0.0158 cp, the gas composition is known and is the same as that of Example A-1. The reservoir temperature is 580°R.

From Equation (3-14)

$$t_s \simeq 1000 \frac{\phi \bar{\mu} r_e^2}{k \bar{P}_R}$$

$$= \frac{(1000)(0.15)(0.0158)(2640)^2}{(120)(2000)} = 69 \text{ hours}$$

This time to stabilization is considered to be too long to conduct the four rates of a conventional test. The isochronal procedures will be considered instead. The permeability and the build-up characteristics experienced during drill-stem testing suggest that if a modified isochronal test were to be used, the shut-in pressures between flows would build up sufficiently to make the modified isochronal test's validity comparable to that of an isochronal test. Therefore, a modified isochronal test is chosen to determine the deliverability relationship.

Flow Periods

The time necessary to investigate 100 feet into the reservoir is obtained from Equation (3-20)

$$t_{100} \simeq 1.0 \times 10^7 \frac{\phi \bar{\mu}}{k \bar{P}_R}$$

$$= \frac{(1.0 \times 10^7)(0.15)(0.0158)}{(120)(2000)} = 0.10 \text{ hours}$$

alternatively, from Figure 3-18 with

$$\frac{k \bar{P}_R}{\phi \bar{\mu}} = 1.01 \times 10^8, \qquad t_{100} \simeq 0.10 \text{ hours}$$

The time required for wellbore storage effects to become negligible is obtained from Equation (3-19) or Figure 3-19. Since there is a bottom hole packer, the wellbore volume is that of the tubing alone (diameter of tubing = 0.50 feet, length of tubing = 5000 feet). The average compressibility of the gas in the wellbore, knowing the gas composition and an assumed average pressure in the tubing of about 1800 psia, is 0.00060 psi^{-1}.

EXAMPLE 3-6

Introduction   This example illustrates calculations that are essential
to the design of a deliverability test.

Problem   A well was completed in a dry, sweet gas pool which is being
developed with a one-section spacing between wells. It has been cored,
logged and drill-stem tested, acidized and cleaned but no deliverability
tests have, so far, been performed on it. Design a suitable
deliverability test.

Solution

Choice of Test

      Before the choice of a suitable test can be made, the
approximate time to stabilization, t_s, must be known. This being the
first well in the pool, and the drill-stem test flow rate not being
stabilized, the time to stabilization is not known and should be
estimated from Equation (3-14). This requires a knowledge of the
following factors: r_e, $\bar{p}_R$, ϕ, k, $\bar{\mu}$,

    a. r_e = 2640 ft, equivalent to a one-section spacing;

    b. $\bar{p}_R$ = 2000 psia, obtained from the drill-stem test;

    c. ϕ = 0.15, the gas filled porosity is obtained by
               multiplying the formation porosity by the gas
               saturation, both quantities being deducible
               from logs;

    d. k = 120 md, the build-up period of the drill-stem
               test was analyzed by methods described in Chapter 5
               to give an effective kh = 1200 md-ft. From logs,
               h = 10 ft;

    e. $\bar{\mu}$ = 0.0158 cp, the gas composition is known and is the
               same as that of Example A-1. The reservoir
               temperature is 580°R.

From Equation (3-14)

$$t_s \simeq 1000 \, \frac{\phi \, \bar{\mu} \, r_e^2}{k \, \bar{p}_R}$$

$$= \frac{(1000)(0.15)(0.0158)(2640)^2}{(120)(2000)} = 69 \text{ hours}$$

This time to stabilization is considered to be too long to conduct the four rates of a conventional test. The isochronal procedures will be considered instead. The permeability and the build-up characteristics experienced during drill-stem testing suggest that if a modified isochronal test were to be used, the shut-in pressures between flows would build up sufficiently to make the modified isochronal test's validity comparable to that of an isochronal test. Therefore, a modified isochronal test is chosen to determine the deliverability relationship.

Flow Periods

The time necessary to investigate 100 feet into the reservoir is obtained from Equation (3-20)

$$t_{100} \simeq 1.0 \times 10^7 \, \frac{\phi \, \bar{\mu}}{k \, \bar{p}_R}$$

$$= \frac{(1.0 \times 10^7)(0.15)(0.0158)}{(120)(2000)} = 0.10 \text{ hours}$$

alternatively, from Figure 3-18 with

$$\frac{k \, \bar{p}_R}{\phi \, \bar{\mu}} = 1.01 \times 10^8, \qquad t_{100} \simeq 0.10 \text{ hours}$$

The time required for wellbore storage effects to become negligible is obtained from Equation (3-19) or Figure 3-19. Since there is a bottom hole packer, the wellbore volume is that of the tubing alone (diameter of tubing = 0.50 feet, length of tubing = 5000 feet). The average compressibility of the gas in the wellbore, knowing the gas composition and an assumed average pressure in the tubing of about 1800 psia, is 0.00060 psi^{-1}.

From Equation (3-19)

$$t_{ws} \simeq \frac{36177 \; \bar{\mu} \; V_{ws} \; c_{ws}}{k \; h}$$

$$= \frac{(36177)(0.0158)(\pi \cdot 0.25^2 \cdot 5000)(0.00060)}{(120)(10)} = 0.28 \text{ hours}$$

alternatively, from Figure 3-19 with

$$\bar{\mu} \; c_{ws} \; L_t = 4.7 \times 10^{-2}, \qquad t_{ws} \simeq 0.28 \text{ hours}$$

Since

$$t_{ws} > t_{100}$$

the duration of the isochronal periods

$$\simeq 4 \; t_{ws} = 1.12 \text{ hours} = 1.5 \text{ hours (say)}$$

the duration of the extended flow period

$$\simeq t_s = 69 \text{ hours} = 72 \text{ hours (say)}$$

Flow Rates

Because of a malfunction in the flow metering recorder, flow rates during well clean-up are not available. Accordingly an estimate of the AOF will be made from Equation (3-18). This requires a knowledge of the following factors:

a. r_w = 0.25 ft
b. T = 580°R, obtained during drill-stem testing
c. $\bar{\psi}_R$ = 330×10^6 psi^2/cp, from the $\psi - p$ curve of Figure 2-4
d. s = 0.0, no data available for this new pool

From Equation (3-18)

$$AOF \simeq \frac{k \; h \; \bar{\psi}_R}{3.263 \times 10^6 \; T \left[\log \left(0.472 \; \dfrac{r_e}{r_w} \right) + \dfrac{s}{2.303} \right]}$$

$$= \frac{(120)(10)(330 \times 10^6)}{(3.263 \times 10^6)(580)\left[\log \frac{(0.472)(2640)}{(0.25)}\right]} = 57 \text{ MMscfd}$$

10% of AOF $\simeq$ 6 MMscfd

75% of AOF $\simeq$ 45 MMscfd

A suitable range of approximate flow rates would be

first rate $=$ 6 MMscfd, for 1.5 hr

second rate $=$ 12 MMscfd, for 1.5 hr

third rate $=$ 24 MMscfd, for 1.5 hr

fourth rate $=$ 48 MMscfd, for 1.5 hr

An extended flow rate of about 25 MMscfd for 72 hours is recommended. Since there is no pipeline connected to the well, and since the extended flow rate would involve the flaring of some 75 MMscf of gas, it is recommended that this wastage be avoided by deferring this part of the test until a pipeline is connected. Meanwhile, the stabilized deliverability would be calculated from the isochronal test data, using the method described in Section 5.

Equipment

From a knowledge of the gas composition, the reservoir pressure and the reservoir temperature and by using the method outlined in Appendix A it can be seen that hydrates are not likely to form anywhere in the test equipment. No special heating equipment is necessary and the standard heater preceding and following the adjustable choke should be ample to handle unforeseen hydrate problems. Because of the pressures involved, all equipment should be rated for high-pressure operation. Because of the presence of small quantities of liquids, mostly water of condensation, a single separator will suffice prior to the orifice meter run. A bottom hole pressure gauge is desirable for measuring pressures.

9   CALCULATING AND PLOTTING TEST RESULTS

Earlier sections describe the various types of deliverability tests and their application. The calculation of the flow rates and the conversion of surface measured pressures to sub-surface pressures are discussed in Chapter 6 and Appendix B, respectively. Familiarity with these will be assumed. The methods for calculating and plotting test results are outlined in this section.

The calculations for determining the deliverability relationship may be carried out as shown in Examples 3-1 to 3-5. In these examples both the Simplified and the LIT(ψ) flow analyses were used for the purpose of illustration, but only one of these interpretations, preferably the more rigorous LIT(ψ) flow analysis, is needed. If approximate calculations need to be done in the field, the Simplified analysis may prove to be conventient.

The pressures used in the calculations are those at the sandface and may be obtained by direct measurement or by conversion of the wellhead pressures. In obtaining the differences in pressure-squared or pseudo-pressure, the pairs of pressures involved in the subtraction vary for the different tests. They are summarized in Figure 3-20 which shows the appropriate pressures connected by a vertical link. The conventional test will be used to explain the application of Figure 3-20.

The initial shut-in pressure and the pressure at the end of Flow 1 are converted to p^2, for the Simplified analysis, or to ψ, by using the appropriate $\psi - p$ curve, for the LIT(ψ) flow analysis. The difference in these two pressure-squared or pseudo-pressure terms, Δp^2 or $\Delta \psi$, correspond to the flow rate, q_1, of Flow 1. The same procedure is carried out for Flow 2, Flow 3 and Flow 4. For the other tests, Δp^2 or $\Delta \psi$ values are obtained from the pressures linked together in Figure 3-20. The points $(\Delta p^2, q_{sc})$ or $(\Delta \psi - b q_{sc}^2, q_{sc})$ are then plotted as detailed below.

	CONVENTIONAL	ISOCHRONAL	MODIFIED ISOCHRONAL	SINGLE POINT
INITIAL SHUT-IN			(1)	
FLOW 1				
SHUT-IN				
FLOW 2				
SHUT-IN				
FLOW 3				
SHUT-IN				
FLOW 4				
SHUT-IN				
EXTENDED FLOW				
STABILIZED SHUT-IN				

(1) In the modified isochronal test, the initial shut-in pressure may not be fully stabilized.

FIGURE 3-20. SANDFACE PRESSURES USED IN COMPUTING Δp^2 OR $\Delta \psi$ FOR DELIVERABILITY TEST ANALYSES

9.1 Simplified Analysis

The plot of Δp^2 versus q_{sc} should be made on logarithmic coordinates and a straight line should be drawn through a minimum of three points. If a straight line is not indicated by at least three points, and also if the LIT(ψ) flow analysis is not meaningful, consideration should be given to retesting the well. The reciprocal slope of the line is the exponent n. If the value of n is greater than 1.0 or less than 0.5, consideration should be given to retesting the well, unless experience with wells in that pool indicates that a different n value would not be obtained.

If a well has been retested, and the test is still unsatisfactory, the best fit line may be drawn through the points of the test which appear to be the most acceptable. If the resulting value of n is greater than 1.0, a line reflecting an n of 1.0 shall be drawn

through the highest flow rate point. If the value of n is less than 0.5, a line reflecting an n of 0.5 shall be drawn through the lowest flow rate point.

In the case of isochronal type tests the deliverability line should be positioned to reflect stabilized conditions. This is done by plotting the stabilized value of Δp^2 versus the appropriate flow rate. A line of reciprocal slope n is drawn through the point, as is illustrated in Figure 3-8.

9.2 LIT(ψ) Flow Analysis

The deliverability relationship represented by Equation (3-4) should be determined by calculating a and b from Equations (3-7) and (3-8). A plot of ($\Delta\psi - bq_{sc}^2$) versus q_{sc} on logarithmic coordinates should be made with the data points and the calculated deliverability relationship. Any data points showing an excessive deviation from the straight line plotted should be rejected, and the entire procedure of calculating a, a_t or b should be repeated with at least three data points. If the scatter of data points is excessive or if b is negative, consideration should be given to retesting the well, unless experience with wells in that pool indicates that a different line would not be obtained.

If the well has been retested, and the test is still unsatisfactory, a least squares fit of the data points that appear most acceptable should be made. If a_t or b still turn out to be negative, then a value of zero should be used in place of the negative number. These two conditions are equivalent to n = 1.0 (for b = 0) and n = 0.5 (for a = 0) in the Simplified analysis.

In any case, the relationship resulting from this second unsatisfactory test is only an estimated one, and consideration should be given to a retest within a one-year period. The retest should involve alterations in test procedure in an attempt to obtain a satisfactory relationship. This change may involve direct sandface pressure measurements if two-phase flow appears to be a possibility, or

it may involve another type of flow test.

In the case of isochronal type tests, the deliverability line should be positioned to reflect stabilized conditions. This is done by calculating a from Equation (3-12) if a stabilized flow was conducted, and plotting the resulting stabilized deliverability line as shown in Figure 3-9. In the absence of stabilized flow data a may be calculated from Equation (3-13).

NOTES TO CHAPTER 3

3N.1 LIT Flow Analysis

Pressure-Squared Relationship

Equation (3-1), the commonly used Rawlins and Schellhardt deliverability equation, was obtained empirically but may be related to a theoretically derived relationship, Equation (3-2), also called the LIT(p^2) flow equation.

Combining Equations (2-101) and (2-102), and substituting for various dimensionless variables from Tables 2-3 and 2-4 gives, for stabilized flow (pseudo-steady state)

$$\bar{p}_R^2 - p_{wf}^2 = \frac{1.417 \times 10^6 \, q_{sc} \, \mu \, Z \, T}{k \, h} \, \ln \left(0.472 \, \frac{r_e}{r_w} \right)$$

$$= \frac{3.263 \times 10^6 \, q_{sc} \, \mu \, Z \, T}{k \, h} \, \log \left(0.472 \, \frac{r_e}{r_w} \right) \qquad (3N-1)$$

The above equation assumes laminar flow in the reservoir. The skin factor, s, and inertial-turbulent flow effects, Dq_{sc}, discussed in Chapter 2, Section 9, may be introduced to give, from Equation (2-143)

$$\bar{p}_R^2 - p_{wf}^2 = \frac{3.263 \times 10^6 \ \mu \ Z \ T}{k \ h} \left[\log \left(\frac{0.472 \ r_e}{r_w} \right) + \frac{s}{2.303} \right] q_{sc}$$

$$+ \ \frac{1.417 \times 10^6 \ \mu \ Z \ T}{k \ h} \ D \ q_{sc}^2$$

$$= a' \ q_{sc} + b' \ q_{sc}^2 \tag{3N-2}$$

Therefore

$$a' = \frac{3.263 \times 10^6 \ \mu \ Z \ T}{k \ h} \left[\log \left(\frac{0.472 \ r_e}{r_w} \right) + \frac{s}{2.303} \right] \tag{3N-3}$$

$$b' = \frac{1.417 \times 10^6 \ \mu \ Z \ T}{k \ h} \ D \tag{3N-4}$$

The interrelationship of a' and b' to C and n of Equation (3-1) has been given in various forms by Houpeurt (1959), Carter, Miller and Riley (1963), Willis (1965) and Cornelson (1974). Tek, Grove and Poettman (1957) gave similar relationships, in graphical form, for various ranges of flow rates. One form of the interrelationship, as expressed by Cornelson (1974) assumes

a. Equation (3-1) is valid for $q_{min} \leq q_{sc} \leq q_{max}$. This defines the range of flow rates within which the $\bar{p}_R^2 - p_{wf}^2$ versus q_{sc} plot is a straight line on a log-log plot;

b. Equation (3-2) is valid for $0 \leq q_{sc} \leq AOF$;

c. The function $\bar{p}_R^2 - p_{wf}^2$ from Equations (3-1) and (3-2) is equal with the range q_{min} to q_{max};

d. The rate of change of the above functions is equal at the geometric mean of q_{min} and q_{max}, to give

$$a' = \left(\frac{1}{C} \right)^{\frac{1}{n}} \ q_{sc}^{\left(\frac{1}{n} - 1 \right)} \left(2 - \frac{1}{n} \right) \tag{3N-5}$$

$$b' = \left(\frac{1}{C}\right)^{\frac{1}{n}} q_{sc}^{\left(\frac{1}{n} - 2\right)} \left(\frac{1}{n} - 1\right) \qquad (3N-6)$$

and

$$C = \frac{q_{sc}}{\left(a' \ q_{sc} + b' \ q_{sc}^2\right) \dfrac{a' + b' \ q_{sc}}{a' + 2b' \ q_{sc}}} \qquad (3N-7)$$

$$n = \frac{a' + b' \ q_{sc}}{a' + 2b' \ q_{sc}} \qquad (3N-8)$$

In addition to the above interrelationship between Equations (3-1) and (3-2), it can be shown that Equation (3-1) is an approximation for Equation (3-2) for various ranges of flow rates. It is readily seen that:

for very low flow rates $a'q_{sc} \gg bq_{sc}^2$, $\Delta p^2 \simeq a'q_{sc}$ and n of Equation (3-1) = 1.0. Conversely, from Equation (3N-5) for $n = 1$, $a' = \left(\frac{1}{C}\right)$ and Equation (3-2) reduces to Equation (3-1);

for high flow rates $a'q_{sc} \ll bq_{sc}^2$, $\Delta p^2 \simeq b'q_{sc}^2$ and n of Equation (3-2) = 0.5. Conversely, from Equation (3N-6) for $n = 0.5$, $b' = \left(\frac{1}{C}\right)^2$ and Equation (3-2) reduces to Equation (3-1).

Hence n may vary from 1.0 for fully laminar flow to 0.5 for turbulent flow.

Pseudo-Pressure Relationship

Equation (3-4), the rigorous form of the LIT(ψ) flow equation, can be related to Equation (3-1) in a manner similar to that of the previous section. Equations (3N-5) to (3N-8) are applicable with a' and b' replaced by a and b.

An equivalent form of Equation (3N-2) in terms of pseudo-pressure is obtained by combining Equations (2-101) and (2-103) with

appropriate substitutions from Tables 2-3 and 2-4, and from Equation (2-143)

$$\bar{\psi}_R - \psi_{wf} = \frac{3.263 \times 10^6 \; T}{k \; h} \left[\log\left(\frac{0.472 \; r_e}{r_w}\right) + \frac{s}{2.303} \right] q_{sc}$$

$$+ \frac{1.417 \times 10^6 \; T}{k \; h} \; D \; q_{sc}^2$$

$$= a \; q_{sc} + b \; q_{sc}^2 \qquad\qquad (3N-9)$$

Therefore

$$a = \frac{3.263 \times 10^6 \; T}{k \; h} \left[\log\left(\frac{0.472 \; r_e}{r_w}\right) + \frac{s}{2.303} \right] \qquad (3N-10)$$

$$b = \frac{1.417 \times 10^6 \; T}{k \; h} \; D \qquad\qquad (3N-11)$$

The interrelationship of a and b to C and n of Equation (3-1) can be obtained from Equations (3N-5) to (3N-8) simply by replacing a' and b' by a and b.

An approximate idea of the absolute open flow potential of a well may be obtained from Equation (3N-9) by neglecting the Dq^2 term and estimating the skin factor, s, by the methods of Chapter 7, Table 7-1. Hence

$$AOF = q_{sc}\bigg|_{\psi_{wf}=0} \approx \frac{k \; h \; \bar{\psi}_R}{3.263 \times 10^6 \; T \left[\log\left(0.472 \; \frac{r_e}{r_w}\right) + \frac{s}{2.303} \right]} \qquad (3N-12)$$

3N.2 Time to Stabilization and Related Matters

Equations (3N-2) and (3N-9) apply to stabilized conditions only; that is, for $t > t_s$, the time to stabilization. Equation (2-104), with appropriate substitution for dimensionless quantities from

Table 2-3, can be written as

$$t_s \simeq \frac{1}{4} \frac{\phi \, \bar{\mu} \, \bar{c} \, r_e^2}{\lambda \, k} \tag{3N-13}$$

Substituting for λ from Table 2-4 gives

$$t_s \simeq 1000 \, \frac{\phi \, \bar{\mu} \, \bar{c} \, r_e^2}{k} \tag{3N-14}$$

Approximate compressibility as reciprocal pressure gives

$$t_s \simeq 1000 \, \frac{\phi \, \bar{\mu} \, r_e^2}{k \, \bar{p}_R} \tag{3N-15}$$

Stabilization is often, in practice, defined in terms of a specified rate of pressure decline. Such an approach is theoretically inconsistent as shown below.

At stabilization, the applicable flow equation (excluding skin and IT flow effects) in Equation (2-83) which can be written, with appropriate substitutions for dimensionless quantities in terms of pressure from Table 2-3 as

$$\bar{p}_R - p_{wf} = \frac{\gamma \, \bar{Z} \, T \, q_{sc} \, \bar{\mu}}{\bar{p} \, k \, h} \left[\frac{2 \, \lambda \, k \, t}{\phi \, \bar{\mu} \, \bar{c} \, r_e^2} + \ln \frac{r_e}{r_w} - \frac{3}{4} \right] \tag{3N-16}$$

The rate of pressure decline is obtained by differentiating Equation (3N-16) with respect to time

$$\frac{\partial p_{wf}}{\partial t} = - \frac{2 \, \gamma \, \lambda \, \bar{Z} \, T \, q_{sc}}{\bar{p} \, \phi \, h \, \bar{c} \, r_e^2} \tag{3N-17}$$

Substituting for γ and λ from Table 2-4 gives

$$\frac{\partial P_{wf}}{\partial t} = - \frac{2\ (7.085 \times 10^5)(2.637 \times 10^{-4})\ \bar{Z}\ T\ q_{sc}}{\bar{p}\ \phi\ h\ \bar{c}\ r_e^2}$$

$$= -\ 374\ \frac{\bar{Z}\ T\ q_{sc}}{\bar{p}\ \phi\ h\ \bar{c}\ r_e^2} \tag{3N-18}$$

Approximating compressibility as reciprocal pressure gives

$$\frac{\partial P_{wf}}{\partial t} = -\ 374\ \frac{\bar{Z}\ T\ q_{sc}}{\phi\ h\ r_e^2} \tag{3N-19}$$

Equation (3N-19) shows that at stabilization the rate of pressure decline depends upon the flow rate and reservoir characteristics such as T, ϕ, h and r_e. Any specified pressure decline rate that does not take all of these factors into account is obviously unacceptable as a definition of stabilization.

Before stabilization is achieved, the radius of investigation, r_{inv}, as defined by Equation (2-105), is a function of time and is given by

$$r_{inv} \simeq 2\left[\frac{\lambda}{\phi}\frac{k}{\bar{\mu}}\frac{t}{\bar{c}}\right]^{0.5} \tag{3N-20}$$

Substituting for λ from Table 2-4 and assuming compressibility may be approximated by the reciprocal pressure

$$r_{inv} \simeq 0.032\left[\frac{k\ \bar{P}_R\ t}{\phi\ \bar{\mu}}\right]^{0.5} \tag{3N-21}$$

3N.3 Transient Relationship

The deliverability relationships, represented by Equations (3N-1) and (3N-9), apply at stabilized conditions, that is, for $r_{inv} = r_e$. When $r_{inv} < r_e$, the flow conditions are said to be transient. For transient flow, combining Equations (2-72) and (2-143) with appropriate substitutions from Tables 2-3 and 2-4 gives

$$\bar{\psi}_R - \psi_{wf} = \frac{3.263 \times 10^6 \ T}{k \ h} \left[\frac{1}{2} \left(\log \frac{2.637 \times 10^{-4} \ k \ t}{\phi \ \mu_i \ c_i \ r_w^2} + \frac{0.809}{2.303} \right) \right.$$

$$\left. + \frac{s}{2.303} \right] q_{sc} + \frac{1.417 \times 10^6 \ T}{k \ h} \ D \ q_{sc}^2$$

$$= a_t \ q_{sc} + b \ q_{sc}^2 \qquad (3N-22)$$

Therefore

$$a_t = \frac{3.263 \times 10^6 \ T}{k \ h} \left[\frac{1}{2} \left(\log \frac{2.637 \times 10^{-4} \ k \ t}{\phi \ \mu_i \ c_i \ r_w^2} + \frac{0.809}{2.303} \right) + \frac{s}{2.303} \right]$$

$$= \frac{1.632 \times 10^6 \ T}{k \ h} \left[\log \left(\frac{k \ t}{\phi \ \mu_i \ c_i \ r_w^2} \right) - 3.23 + 0.869 \ s \right] \qquad (3N-23)$$

a_t is obviously a function of the duration of flow. For equal durations of flow, as in an isochronal test, t is a constant and therefore a_t is a constant. This forms the theoretical basis for isochronal tests. b is initially independent of time and has the same value for transient and stabilized flow as shown by Equations (3N-9) and (3N-22).

3N.4 Wellbore Storage Time

Equation (2-154) with appropriate substitutions for λ from Table 2-4 and η from Equation (2-150) becomes

$$t_{ws} = 36177 \ \frac{\bar{\mu} \ V_{ws} \ c_{ws}}{k \ h} \qquad (3N-24)$$

3N.5 Isochronal Type Tests

Aziz (1967b) established the theoretical validity of isochronal and modified isochronal tests using the Simplified flow equation,

Equation (3-1), radial unsteady-state laminar flow equations and several
simplifying assumptions. Noting that in the publication by Aziz (1967),
Modified Isochronal Testing and Another Modification of the Isochronal
Test should be reversed since the latter is actually the proper modified
isochronal test, the theoretical justification may be extended quite
simply to include the LIT(ψ) flow equation, Equation (3-4), skin and IT
flow effects. Such an analysis would, however, assume that the
principle of superposition may be applied to the unsteady-state LIT flow
equation.

CHAPTER 4   DRAWDOWN TESTS

1   INTRODUCTION

The deliverability tests described in Chapter 3 have a
historical and empirical origin. However, their validity and
applicability is confirmed in that chapter using the theory developed
in Chapter 2. These theoretical developments may also be used in
formulating various tests designed to determine important reservoir
characteristics. Among such tests are single-rate and multi-rate flow
tests, commonly called "drawdown tests."

There is a multitude of drawdown tests that may be analyzed
by essentially the same equations. In general, all that is needed for
the analysis is the flowing pressure-time data and the flow rate
history. Since there is no limit to the possible flow rate histories,
this chapter is confined to what are considered to be the more practical
tests, without attempting to limit the applicability of the analysis to
other situations.

Both single-rate and multi-rate drawdown tests are described
in this chapter. The multi-rate tests are those which do not include
any shut-in periods. Tests which include shut-in periods and the
analysis of pressure-time data from such periods are dealt with in the
next chapter.

Unlike the deliverability tests described in the previous
chapter, drawdown tests are extensions from oil well testing practice
and are based on a theoretical rather than an empirical background.
The simplest drawdown test consists of measuring the bottom hole
pressure continuously during a period of flow at a constant rate,
commencing from a stabilized reservoir pressure. The duration of the
flow period may be from a few hours to a few months, depending on the
nature of the reservoir and the objectives of the test. The purpose of
drawdown testing is to determine the reservoir characteristics that will
affect flow performance. Some of the important characteristics are the

permeability thickness, kh, the skin factor, s, and the IT flow
factor, D.

As in the previous chapter, the reservoir is idealized by
making the assumptions (1) to (5) in Chapter 3, Section 2.2. Under
these conditions, the behaviour of the flowing sandface pressure, p_{wf},
is depicted in Figure 4-1.
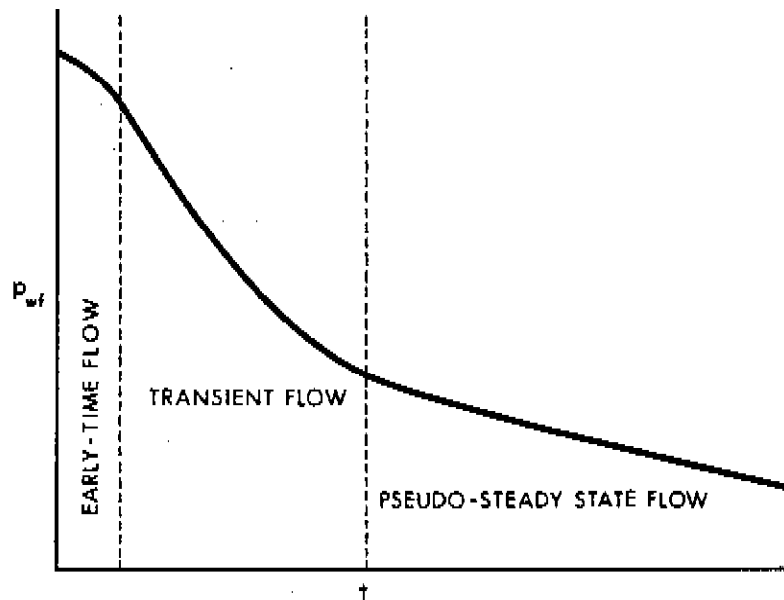
FIGURE 4-1. PRESSURE - TIME HISTORY FOR A
CONSTANT RATE DRAWDOWN

Initially, during early-time flow, wellbore storage and skin
effects dominate the flow. The portion of the curve called transient
flow represents that duration of flow during which flowing pressure-time
data plot as a straight line on semilogarithmic coordinates. During
this period, the reservoir is infinite-acting, and the boundary effects
have not been sensed. The last portion of the curve represents that
duration of flow where boundary effects dominate. This pseudo-steady
state flow causes depletion of the reservoir and the flowing pressure-
time data plot as a straight line on arithmetic coordinates.

Figure 4-1 represents the pressure decline for a well,
centrally located, in a circular reservoir with closed outer boundaries.
In many cases, the actual well/reservoir configuration may be different
from the assumed model. In such cases there will exist a transition

period between the transient flow and pseudo-steady state flow periods. This transient period is often called the late-transient period. It represents the partial effect of some of the boundaries and varies with each well/reservoir configuration. It should also be noted, for topical interest, that the late-transient period is practically non-existent for the case of a well in the centre of a square reservoir (Ramey and Cobb, 1971).

2 FUNDAMENTAL RELATIONSHIPS

The different flow regimes depicted in Figure 4-1 are governed by different relationships. It is therefore convenient to treat each one separately.

2.1 Early-Time Flow Regime

Early-time data are affected, in particular, by wellbore storage and linear flow through fractures. Usually, in the pressure analysis of flow tests, the early-time data are ignored and the analysis concentrates on transient flow and pseudo-steady state flow data. Consequently, it becomes necessary to define the length of the flow period influenced by early-time effects or, alternatively, to define the time of start of the transient flow period.

Several methods have been suggested either for correcting flow data to account for wellbore storage effects (Gladfelter, Tracy and Wilsey, 1955, Russell, 1966) or for analyzing the early-time data to determine the reservoir parameters (Ramey, 1970, McKinley, 1970, Earlougher and Kersch, 1974, Maer, 1974). Several studies, both analytical and numerical, of vertical fractures have been conducted by various authors (Prats, 1961, Prats, Hazebroek and Strickler, 1963, Scott, 1963, Russell and Truit, 1964, Prats and Levine, 1965, Millheim and Cichowicz, 1968, Kazemi, 1969, Raghavan, Cady and Ramey, 1972, Gringarten, Ramey and Raghavan, 1974, 1975, Gringarten and Ramey, 1974). The reader is referred to these publications for details concerning the

following sections and also to supplement the information given in Chapter 7 for the analysis of early-time data.

Wellbore Storage

As explained in Chapter 2, Section 9.3, when a well is opened at the surface for flow at a constant rate, the initial flow comes primarily from the wellbore itself, rather than from the formation. In fact, flow from the reservoir increases gradually from zero until the specified wellhead flow rate, q, is reached in a length of time, t_{ws}, given by Equation (2-154). This equation is developed into its final form in the Notes to Chapter 3 and is given by Equation (3N-24) as

$$t_{ws} = \frac{36177 \; \bar{\mu} \; V_{ws} \; c_{ws}}{k \; h} \tag{4-1}$$

Equation (4-1) applies to wells with zero skin effects. Ramey (1970), and Agarwal, Al-Hussainy and Ramey (1970) presented the combined effects of wellbore storage and skin in the form of the type curve of Figure 2-22. This type curve can be used quite effectively to define the time of start of transient flow and its use, in this context, is illustrated in Example 4-1. McKinley (1970) plotted only one family of type curves by assuming $k/(\phi\mu cr_w^2)$ equal to λ and a skin factor, s, equal to zero. Although this reduces the accuracy of a data match, it is easier to obtain a data match with McKinley's curves than it is with Ramey's type curves. Subsequently, McKinley (1974) showed how his figure could be used to obtain a rough estimate of the flow efficiency for a well with localized damage. Maer (1974) modified the McKinley type curves for gas flow usage.

Although early-time data are not analyzed in this chapter, it is of interest to note that in the presence of wellbore storage, a plot of Δp_D versus t_D on logarithmic coordinates will give a straight line of slope 1.0 for the initial data.

Vertical Hydraulic Fractures

A large number of gas wells are stimulated by hydraulic fracturing. Although the fractures may be quite complicated in terms of

their numbers, orientations, and depths of penetration, they are usually idealized by assuming them to be a single vertical fracture through the axis of the well. Agnew (1966) has shown that in deep wells the fractures are most likely to be vertical, but in shallow wells, less than 1500 feet, they may be either horizontal or vertical (Fraser and Pettitt, 1962). A hydraulic fracture is usually propped open and accordingly, its permeability is considered to be infinite.

In his study of the effects of a vertical fracture, Wattenbarger (1967, p. 87) confirmed that the net effect is equivalent to an effective wellbore radius equal to $x_f/2$, where x_f is the distance from the mid-point of the well to the tip of the fracture. In terms of a skin, this is equivalent to a negative skin factor, s, given by

$$s = \ln \frac{2 \, r_w}{x_f} \qquad (4-2)$$

When flow into the fracture first starts, it is linear, and the pressure behaviour is proportional to $\sqrt{t_D}$. This means that a plot of Δp_D versus t_D on logarithmic coordinates will give a straight line of slope 0.5 for early-time data. Such a plot would then deviate from this line of slope 0.5 and ultimately join the radial flow solution, characteristic of the transient region.

Gringarten, Ramey and Raghavan (1974) presented the effects of a vertical, hydraulic fracture in the form of the type curve of Figure 2-23. It is essentially a combination of the linear and radial flow equations. This curve can also be used to define the time of start of transient flow by noting from Figure 2-23 that transient flow starts at a time given by

$$t_D = \frac{2.637 \times 10^{-4} \, k \, t}{\phi \, \mu_i \, c_i \, x_f^2} \simeq 4 \qquad (4-3)$$

Vertical Natural Fractures

There are two important boundary conditions that may be imposed on the conductivity within a fracture. One is that of infinite conductivity which implies a zero pressure drop within the fracture itself. The hydraulic fracture discussed previously fits into this category. The other boundary condition is that of a uniform flux at all points in the fracture. This implies a small, but finite, pressure drop from the tip of the fracture to the well and corresponds to a high, but not infinite, fracture conductivity. The solution for a naturally fractured reservoir appears to match this solution better than the solution for an infinite conductivity reservoir.

Gringarten, Ramey and Raghavan (1974) obtained an analytical solution for this boundary condition and presented it in the form of the type curve of Figure 2-24. They showed that the solution for an infinite conductivity fracture is equal to the solution for a uniform flux fracture at a point equal to 0.732 x_f.

Horizontal Fractures

The existence of a horizontal fracture, either through natural causes or hydraulic fracturing, is possible, especially in the case of shallow wells. Gringarten and Ramey (1974) have presented a type curve to represent unsteady-state flow into a horizontally fractured well. However, as mentioned in Chapter 2, Section 10, this type curve is of little practical value in the analysis of gas well data.

Comparison of Flow Regimes
in Fractures

Gringarten and Ramey (1974) correlated their findings for flow in horizontal fractures in terms of a dimensionless formation thickness, h_D, defined as

$$h_D = \frac{h}{r_f} \sqrt{\frac{k_r}{k_z}} \qquad (4\text{-}4)$$

where

r_f =   radius of the fracture

k_r, k_z =   radial and vertical permeabilities, respectively

Figure 4-2 compares the behaviour of horizontal and vertical fractures. A horizontal fracture is characterized by a storage-type flow, with a slope of 1.0, which represents the depletion of the fracture volume. This is followed by linear flow, with a slope of 0.5, which indicates that linear flow (in the vertical direction) takes place into the fracture. A transition zone, characteristic of a horizontal fracture, is then followed by pseudo-radial flow. A vertical fracture is different in that linear flow (in a horizontal direction) takes place into the fracture and the transition from linear to pseudo-radial flow is very gradual. As shown in Figure 4-2, in the horizontal fracture case the transition zone involves a change in slope from 0.5 towards 1.0 for values of h_D less than 0.7. This has no counterpart in the vertical fracture case.
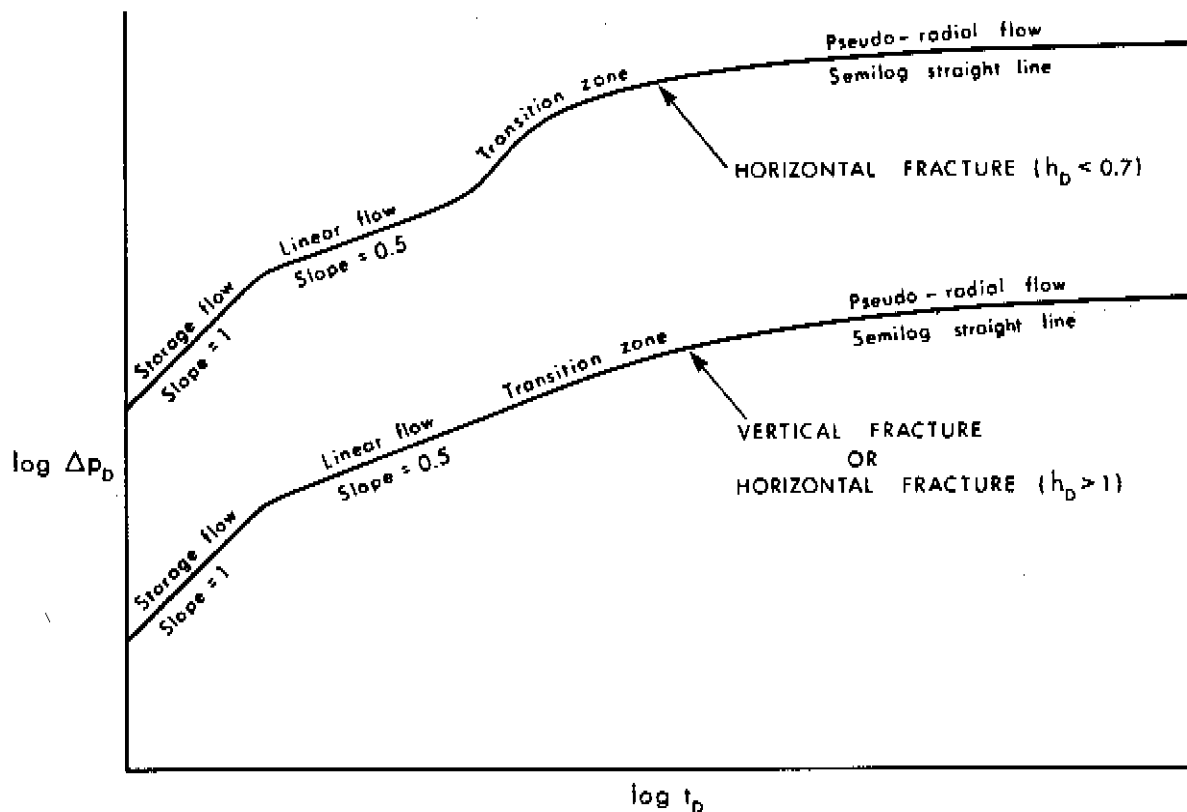
FIGURE 4-2. PRESSURE-TIME BEHAVIOUR IN INFINITE-ACTING RESERVOIRS WITH HORIZONTAL OR VERTICAL FRACTURES

In practice, h_D is often less than 0.7, but it is quite difficult to recognize the characteristic transition for horizontal fractures unless data are taken early enough during a flow test.

2.2 Transient Flow Regime

When the wellbore storage effects or the effects of fractures have diminished, the flow behaviour resembles that from a well in an infinite reservoir and is known as transient flow. In this flow regime the pressure is the same as that created by a line-source well with a constant skin.

Since a plot of Δp_D versus t_D on semilogarithmic coordinates will yield a straight line, the analysis of transient flow data is often referred to as a "semilog analysis."

The semilog analysis of drawdown data yields consistent values of reservoir parameters. Only the permeability thickness, kh, the skin factor, s, and the IT flow factor, D, may be determined from such an analysis. No indication of actual reserves may be obtained unless the end of the semilog straight line has been reached. This straight line continues as long as the reservoir is infinite-acting. If a fault is encountered in the reservoir, the slope of the line will double, and a new straight line will be established. The effects of a fault/barrier are discussed further in Section 4.1.

When the reservoir boundary begins to have a significant effect on well drawdown, the transient region ends. If the well is centrally located in a circular reservoir or in a square reservoir with no-flow outer boundaries (Ramey and Cobb, 1971), the pseudo-steady state or depletion phase directly follows the transient flow period. For other well/reservoir geometries there may be a late transient period which is discussed, for various drainage area shapes, in Section 6.3.

Effect of Multi-Layer Reservoirs

The flow models developed in Chapter 2 and subsequently used in other chapters assume single-layer reservoirs or homogeneous multi-layer reservoirs. In the latter case, computed values of kh represent

a net pay thickness. However, quite often the permeabilities of the
different layers of a multi-layer system may vary considerably.
Lefkovits, Hazebroek, Allen and Matthews (1961) investigated the behaviour
of heterogeneous, multi-layer systems with no cross flow during constant-
rate drawdown tests. They found the transient flow behaviour to be
similar to that of a single-layer system. However, between the transient
flow and pseudo-steady state flow periods there existed a long
transitional period, and the time to reach pseudo-steady state was about
50 times as long as that for a single-layer reservoir.

During the transient flow period, the flow rate from the more
permeable layers is larger than that from the less permeable layers.
Consequently, differential depletion takes place. However, as pseudo-
steady state is approached, the flow rate from each layer becomes
proportional to the ϕh product of that layer and differential depletion
ceases.

Heterogeneous, multi-layer reservoirs are not amenable to a
semilog analysis of transient flow data unless the layers are non-
communicating and each layer can be subjected to flow tests individually.

2.3 Pseudo-Steady State Flow Regime

If a constant-rate drawdown test is run for a sufficiently
long time, the boundary effects eventually dominate the pressure
behaviour at the well. The pressure starts declining at the same rate
at all points in the reservoir, hence the name pseudo-steady state. In
effect then, the total drainage area is being depleted at a constant
rate.

A plot of Δp_D versus t_D on arithmetic coordinates will yield
a straight line from which the reservoir pore volume occupied by gas and
the reservoir limits can be calculated. Accordingly, tests utilizing
this portion of the drawdown history are often known as reservoir
limits tests.

2.4   Type Curve Applications to Drawdown Testing

The analysis of data from the early-time, transient, and pseudo-steady state flow regimes is possible if each flow regime is considered separately.   If all these flow regimes are to be considered together, a simple analytical solution cannot be obtained.   However, the individual solutions, from early-time to pseudo-steady state can be combined and expressed graphically.   Such a graphical representation gives the type curves of Chapter 2, Section 10.   In the context of drawdown testing of gas wells, the most useful type curves are Figures 2-22, 2-23, and 2-24.

A type curve analysis essentially consists of matching the test data to the appropriate type curve.   When a match is obtained, the coordinates of the axes of the data plot and the type curve plot are said to correspond to each other, providing the scales of these axes also correspond.   Although a unique match is theoretically possible for any data plot, it is easy to appreciate that a very large set of type curves would be required to cover the multitude of well/reservoir conditions.   The use and merits of type curve analysis are discussed by Ramey (1970) and by several of the authors mentioned in the previous sections.

On account of some degree of ambiguity involved in obtaining a type curve match, its application to the analysis of transient flow data is not considered.   However, certain useful applications cannot be ignored.   The use of type curves for determining the time-of-start of the transient flow period is discussed in Section 4, and the type curve analysis of early-time data is discussed in Chapter 7.

3   TESTS UTILIZING EARLY-TIME DATA

In the context of drawdown testing, early-time data may be used to determine the time-of-start of transient flow.   A rigorous analysis of early-time data, however, becomes necessary only when it is not possible to conduct tests extending into the transient flow regime. The analysis of early-time data is described in Chapter 7.

4 TESTS UTILIZING TRANSIENT FLOW DATA

In Sections 2.1, 2.2, and 2.4 it has been indicated that early-time data may be used to determine when transient flow theory becomes applicable, without having wellbore storage or fracture effects masking the transient flow data. Data should be obtained, whenever possible, in the transient flow regime since reservoir parameters calculated by a transient flow analysis are far more reliable than those calculated by an early-time flow analysis.

Various drawdown tests, utilizing transient flow data, that may be used to determine well/reservoir parameters are discussed along with examples illustrating the analysis procedures. Whenever possible, these tests are related to the different types of deliverability tests described in Chapter 3.

4.1 Single-Rate Test

This test consists of flowing the well at a constant rate and continuously recording the flowing sandface pressure, p_{wf}, as a function of time of flow, t. Flow starts from stabilized shut-in conditions. In fact, this test is very similar to the single-point deliverability test described in Chapter 3, Section 4.4, except that the flowing sandface pressure is measured throughout, and not just at the end, of the test. Flow may be continued as long as desired, but the usable portion of the data in this analysis is that which falls on the semilog straight line. Sometimes, deviation from the semilog straight line may be due to the presence of a fault rather than boundary effects. In this case, if the drawdown test is continued, the first semilog straight line bends over and becomes another semilog straight line with twice the slope of the first line. To identify a straight line on a logarithmic data plot, data contributing to this line should extend for about a log cycle and never less than half a log cycle on the plot.

The data obtained from a single-rate test may be analyzed as described below to give values for kh and apparent skin factor, s'.

As shown by Equation (2-144), s' is composed of two parts, s due to the well completion, and Dq_{sc} due to IT flow effects. The value of s' is seen to be dependent on the flow rate used during the test. Thus if the single-rate test is repeated at a substantially different rate, starting again from stabilized shut-in conditions, a different value of s' will result. From the two values of s', s and D may be obtained separately. It is seen that, provided the duration of each flow period runs into the transient flow regime, the isochronal deliverability test, described in Chapter 3, Section 4.2, is in fact the equivalent of four single-rate tests and may be analyzed as such if the pressure is measured throughout the duration, and not just at the end, of the flow periods.

Analysis

During the transient flow regime, the flowing sandface pseudo-pressure in a bounded reservoir is given by Equation (4N-3) which is developed in the Notes to this chapter and is reproduced below

$$\psi_i - \psi_{wf} = 1.632 \times 10^6 \frac{q_{sc} T}{k\,h}\left[\log t + \log\left(\frac{k}{\phi\,\mu_i c_i r_w^2}\right) - 3.23 + 0.869\ s'\right]$$

$$(4\text{-}5)$$

A plot of $\Delta\psi$ ($= \psi_i - \psi_{wf}$) versus t on semilogarithmic coordinates should give a straight line of slope, m, from which

$$k\,h = \frac{1.632 \times 10^6\ q_{sc}\ T}{m} \qquad (4\text{-}6)$$

The apparent skin factor, s', can then be calculated using Equation (4N-5) given below

$$s' = 1.151\left[\frac{\Delta\psi_1}{m} - \log\left(\frac{k}{\phi\,\mu_i\,c_i\,r_w^2}\right) + 3.23\right] \qquad (4\text{-}7)$$

where

$\Delta\psi_1$ = the value of $\Delta\psi$ at $t = 1$. This value must be obtained from the straight line portion of the semilog plot (extrapolated, if necessary).

In using Equation (4-7) it is assumed that a value is available for ϕ and that k is obtainable from the kh calculated from Equation (4-6). Both ϕ and h are usually deducible from logs. In such cases, k/ϕ in the logarithmic term is conveniently replaced by $kh/(\phi h)$.

If two single-rate tests are conducted on the same well, using two different flow rates q_1 and q_2, Equation (2-144) may be written as

$$s_1' = s + D\, q_1 \qquad\qquad (4\text{-}8)$$

$$s_2' = s + D\, q_2 \qquad\qquad (4\text{-}9)$$

Solving these simultaneous equations will give the values of s and D. Whereas s may be positive (well damage) or negative (well improvement), D must always be positive. If D turns out to be a negative quantity, it is replaced by zero, and s becomes the average of s_1' and s_2'.

If more than two single-rate tests are conducted, as for the four rates of an isochronal deliverability test, the corresponding values of s' are obtained and s and D may then be evaluated from a least-squares analysis. Alternatively, a plot of s' versus q_{sc} may be fitted with a best straight line which will give a slope equal to D and an intercept on the $q_{sc} = 0$ axis equal to s.

The pressure drop due to skin effects may be obtained from

$$(\Delta\psi)_{skin} = 0.869\, m\, s \qquad\qquad (4\text{-}10)$$

Similarly, the pressure drop due to IT flow effects may be obtained from

$$(\Delta\psi)_{IT} = 0.869\, m\, D\, q_{sc} \qquad\qquad (4\text{-}11)$$

The total pressure drop directly attributed to skin and IT flow effects may then be obtained from

$$(\Delta\psi)_{s'} = 0.869\, m\, s' = 0.869\, m\, (s + D\, q_{sc}) \qquad\qquad (4\text{-}12)$$

The well flow efficiency, FE, is defined as the ratio of the drawdown at the well, without skin or IT flow effects, to the actual drawdown and may be calculated from

$$FE = \frac{(\psi_i - \psi_{wf}) - (\Delta\psi)_{s'}}{(\psi_i - \psi_{wf})} \qquad (4-13)$$

Sometimes it is convenient to express the drawdown in dimensionless terms. This is easily done as follows:

$$\Delta\psi_D = \frac{\psi_i - \psi_{wf}}{0.869\ m} \qquad (4-14)$$

The analysis of a single-rate test is illustrated by Example 4-1.

EXAMPLE 4-1

Introduction   The pressure-time data from a single-rate drawdown test are analyzed to give the reservoir parameters kh and s'. The use of type curves to establish the approximate time-of-start of transient flow is illustrated. The pressure-time data from a single-point or an isochronal deliverability test may also be analyzed by this method.

Problem   A well in a bounded reservoir was produced at a constant rate of 5.65 MMscfd. The pressure, p_i, throughout the reservoir prior to the test was 3732 psia. General data pertinent to the test are given below. The pressure-time data are also tabulated, and are given directly in the solution to this problem.

From a recombined gas analysis:

G = 0.68 P_c = 693 psia T_c = 376°R

H_2S = 1.28% CO_2 = 4.11% N_2 = 0.10%

μ_i = 0.0208 cp c_i = 0.00022 psia^{-1}

Well/reservoir data:

$$T = 673^O R \qquad h = 20 \text{ ft} \qquad r_e = 2640 \text{ ft}$$

$$\phi = 0.10 \qquad r_w = 0.29 \text{ ft}$$

Calculate the permeability, k, of the reservoir and the apparent skin factor, s'. Also calculate the flow efficiency of the well.

Solution   A $\psi - p$ curve, shown in Figure 4-3, is generated by the computer program, listed in Appendix D, which uses the numerical technique described in Example 2-1.
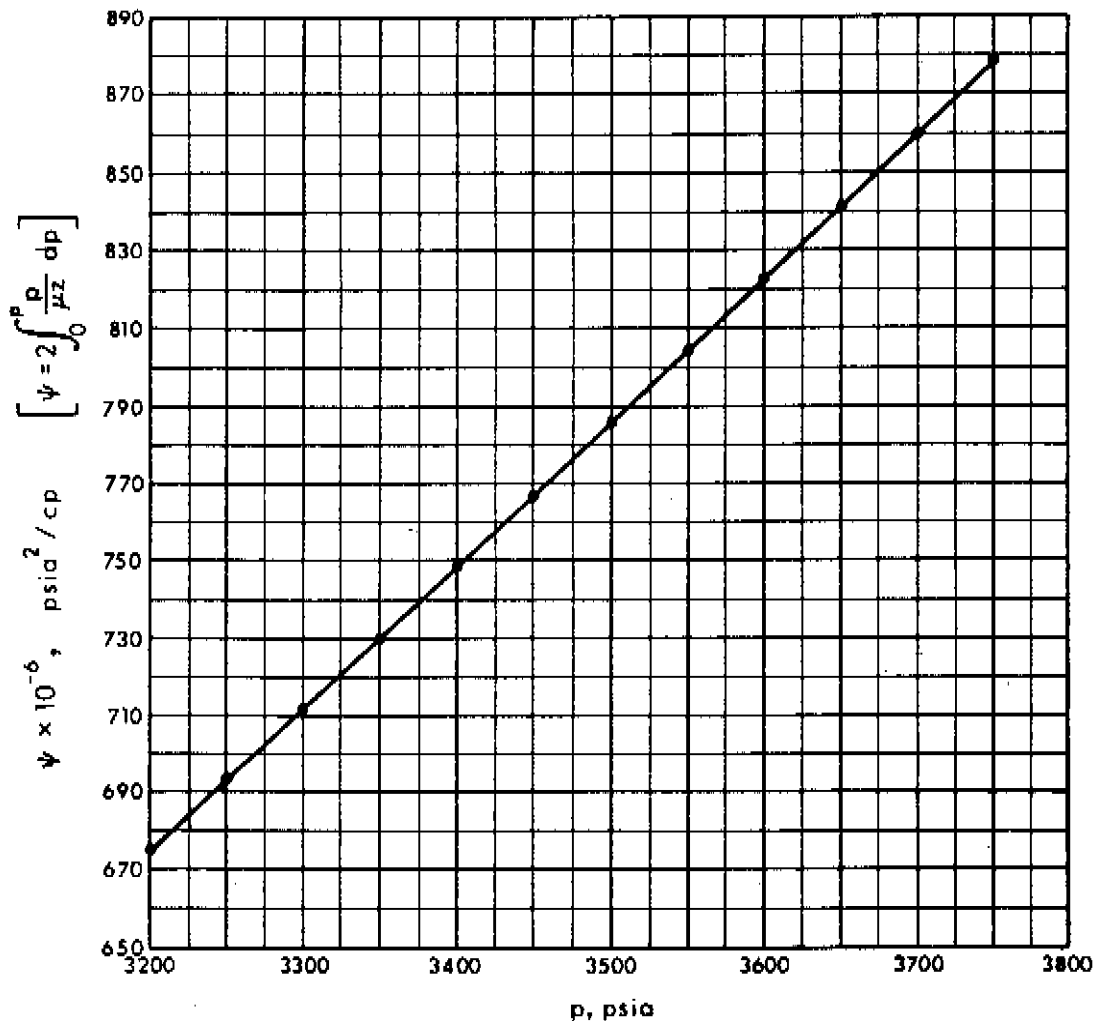
FIGURE 4-3. ψ-p CURVE FOR THE SINGLE-RATE DRAWDOWN
TEST OF EXAMPLE 4-1

$$p = 3732 \quad \leftrightarrow \quad \psi = 872.7 \times 10^6 \qquad \text{(Figure 4-3)}$$

$$\therefore \quad \psi_i = 872.7 \times 10^6 \ \text{psia}^2/\text{cp}$$

Using this value of ψ_i and Figure 4-3 the following tabulations may be made:

t (hr)	p_{wf} (psia)	ψ_{wf} (psia²/cp × 10⁻⁶)	$\Delta\psi = \psi_i - \psi_{wf}$ (psia²/cp × 10⁻⁶)
1.60	3729	871.55	1.15
2.13	3628	833.26	39.44
2.67	3546	802.44	70.26
3.20	3509	788.62	84.08
4.00	3496	783.77	88.93
5.07	3491	781.91	90.79
6.13	3481	778.19	94.51
8.00	3433	760.39	112.31
10.13	3413	753.01	119.69
15.20	3388	743.80	128.90
20.00	3366	735.71	136.99
30.13	3354	731.31	141.39
40.00	3342	726.92	145.78
60.27	3323	719.98	152.72
80.00	3315	717.06	155.64
100.27	3306	713.78	158.92
120.53	3295	709.77	162.93

Step 1: Plot $\Delta\psi$ versus t on 3×5 log-log graph paper (of the same size as the type curves of Chapter 2) as shown in Figure 4-4.

Step 2: A match of the above drawdown plot with the type curve $s = 0$, $C_{sD} = 0$ of Figure 2-22 indicates the time-of-start of the semilog straight line data is approximately 20 hours.

Step 3: Plot $\Delta\psi$ versus log t and draw the best straight line through the semilog straight line data, identified in Step 2, as shown in Figure 4-5, line A - A.
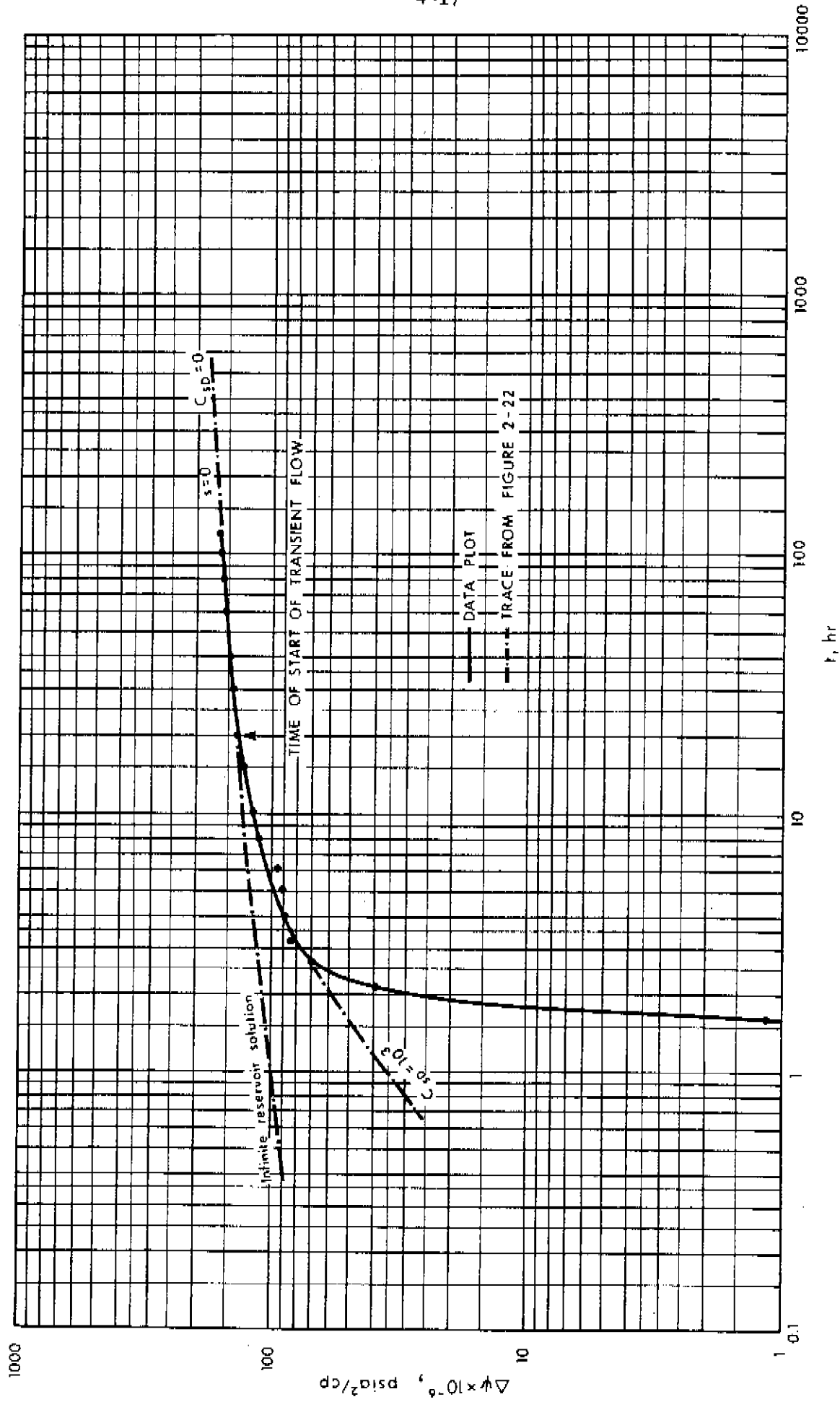
FIGURE 4-4. DATA PLOT FOR A TYPE CURVE MATCH (EXAMPLE 4-1)
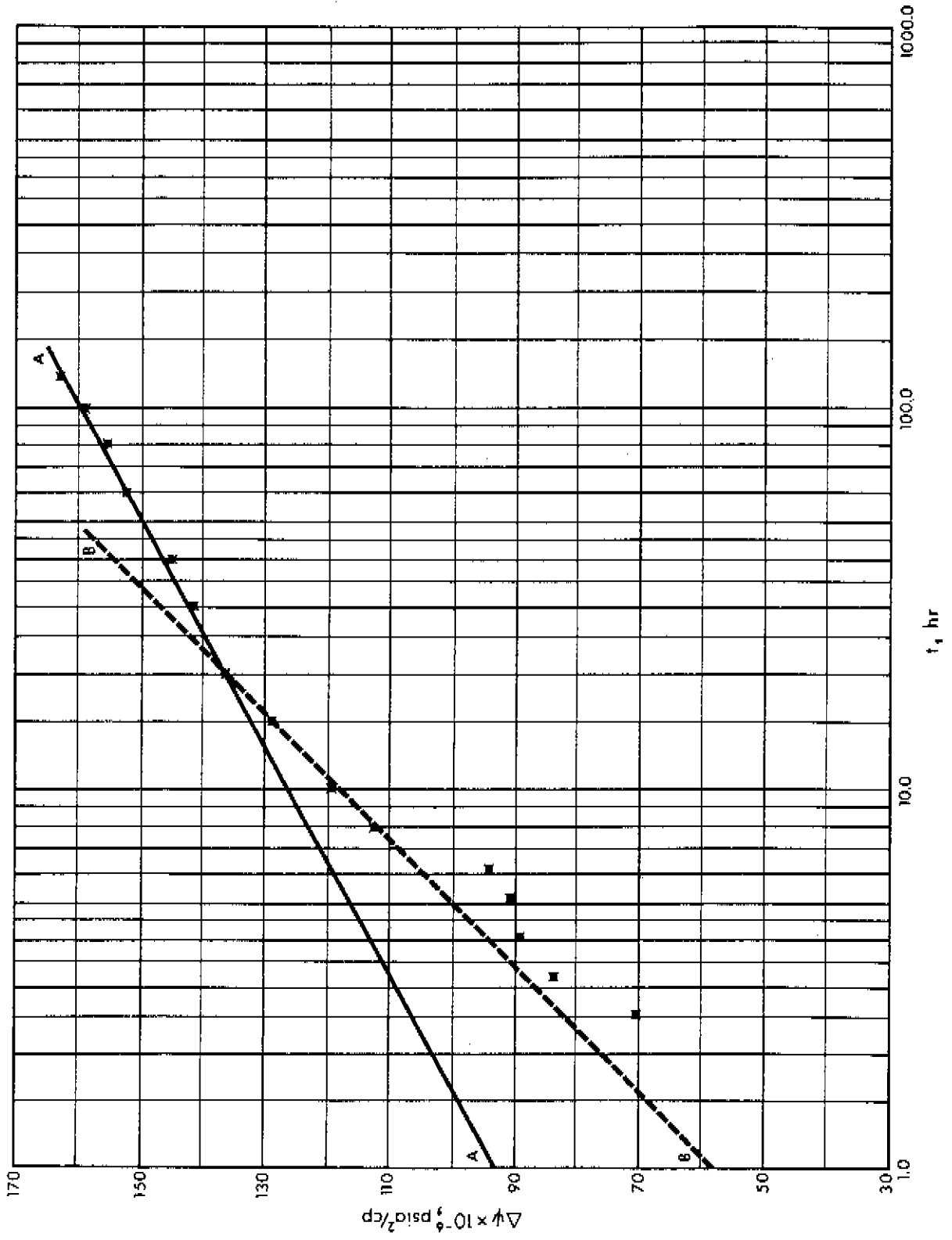
FIGURE 4-5. SEMILOG PLOT OF THE DRAWDOWN DATA OF EXAMPLE 4-1

From the straight line (A – A) of Figure 4–5

$$m = \frac{(159.5 - 126.5) \times 10^6}{\log 100 - \log 10} = 33 \times 10^6$$

$$\Delta\psi_1 = 93 \times 10^6$$

From Equation (4-6)

$$k\,h = \frac{1.632 \times 10^6 \; q_{sc} \; T}{m}$$

$$= \frac{(1.632 \times 10^6)(5.65)(673)}{(33 \times 10^6)} = 188 \text{ md ft}$$

$$k = \frac{188}{20} = 9.4 \text{ md}$$

From Equation (4-7)

$$s' = 1.151 \left[\frac{\Delta\psi_1}{m} - \log\left(\frac{k}{\phi \; \mu_i \; c_i \; r_w^2} \right) + 3.23 \right]$$

$$= 1.151 \left[\frac{93 \times 10^6}{33 \times 10^6} - \log \frac{9.4}{(0.10)(0.0208)(0.00022)(0.29)^2} + 3.23 \right]$$

$$= - 2.7$$

From Equation (4-12)

$$(\Delta\psi)_{s'} = 0.869 \; m \; s'$$

$$= 0.869 \; (33 \times 10^6)(-2.7) = - 77.4 \times 10^6$$

From Equation (4-13)

$$F E = \frac{(\psi_i - \psi_{wf}) - (\Delta\psi)_{s'}}{(\psi_i - \psi_{wf})}$$

$$= \frac{(162.93 \times 10^6) - (-77.4 \times 10^6)}{(162.93 \times 10^6)} = 1.5$$

Discussion   The use of a type curve match to identify the approximate
time-of-start of the semilog straight line results in a more reliable
value for kh. Without such a match, and in the absence of sufficient
data in the early-time and transient flow regimes, an erroneous straight
line B - B, shown in Figure 4-5, could result. This line would give a
permeability of 5.1 md compared to the calculated value of 9.4 md. The
apparent skin would be overestimated at a value of -3.9 compared to the
calculated value of -2.7.

As will be described in Chapter 5, type curves find similar
applications to build-up testing in that the time for wellbore loading
and other early-time effects can be identified. However, the application
is approximate since a desuperposition of build-up data is involved.

The separation of the skin and IT flow components of the
apparent skin factor simply involves the analysis of another single-rate
test by the methods described in this example with the only additional
step being the simultaneous solution of Equations (4-8) and (4-9).

4.2 Multi-Rate Tests

A multi-rate test simply consists of a sequence of different
constant flow rates without any intervening shut-in periods. It is
similar to the conventional deliverability test described in Chapter 3,
Section 4.1, except that each of the flow periods is not continued to
pressure stabilization. In fact, a multi-rate test is intended to
investigate the transient flow regime only so that kh, s and D may be
determined by a semilog analysis.

For reasons that are discussed later on in this section, the
analysis of multi-rate tests is not always reliable as far as the
calculation of kh, s and D is concerned. However, the application of
the principle of superposition in time, discussed in Chapter 2, Section
7.1, is of interest and is described below.

In a multi-rate test, flow starts from stabilized reservoir
conditions. A constant flow rate, q_1, is maintained for a period of
time, t_1. The flow rate is then changed to q_2 up to time t_2, after

which it is changed to q_3 up to time t_3, and so on. In general, the flow rate history may be summarized as

$$q_{sc} = q_1 \qquad \text{for} \qquad 0 < t < t_1$$

$$q_{sc} = q_2 \qquad \qquad t_1 < t < t_2$$

$$\vdots \qquad \qquad \qquad \vdots$$

$$q_{sc} = q_n \qquad \qquad t_{n-1} < t$$

Analysis

The pressure response obtained by changing the flow rate n times from q_1 to q_n may be obtained by applying the principle of superposition in time. The relevant equations from Chapter 2 are developed further in the Notes to this chapter. During the nth flow period of a multi-rate test, the pressure drawdown is given by Equation (4N-9) which is reproduced below:

$$\frac{\psi_i - \psi_{wf}}{q_n} = m' \sum_{j=1}^{n} \left[\frac{\Delta q_j}{q_n} \log (t - t_{j-1}) \right]$$

$$+ m' \left[\log \left(\frac{k}{\phi \, \mu_i \, c_i \, r_w^2} \right) - 3.23 + 0.869 \, s_n' \right] \qquad (4\text{-}15)$$

where

$$m' = \frac{1.632 \times 10^6 \ T}{k \ h}$$

$$\Delta q_j = q_j - q_{j-1}$$

$$t_0 = q_0 = 0$$

If the pressure-time data from the nth flow period are being analyzed, a plot of $(\psi_i - \psi_{wf})/q_n$ versus $\sum \Delta q_j / q_n \log (t - t_{j-1})$ on arithmetic coordinates should give a straight line of slope m', from which

$$k \ h = \frac{1.632 \times 10^6 \ T}{m'} \qquad (4\text{-}16)$$

The apparent skin factor, s_n', associated with the flow rate, q_n, may then be calculated from Equation (4N-11) given below

$$s_n' = 1.151 \left[\frac{\Delta\psi_0}{m'} - \log \left(\frac{k}{\phi \, \mu_i c_i \, r_w^2} \right) + 3.23 \right] \qquad (4\text{-}17)$$

where

$\Delta\psi_0$ = value of $(\psi_i - \psi_{wf})/q_n$ corresponding to a value of zero on the abscissa, obtained from the straight line (extrapolated, if necessary).

Data from each of the preceding flow periods may also be analyzed by the method described for the nth flow period. Such an analysis would yield values of s_1', s_2', ..., s_{n-1}' corresponding to the flow rates q_1, q_2, ..., q_{n-1}. The following equations

$$s_1' = s + D \, q_1$$

$$s_2' = s + D \, q_2$$

$$\vdots$$

$$s_n' = s + D \, q_n$$

$$(4\text{-}18)$$

may then be solved by the method of least squares to give

$$s = \frac{\sum s' \sum q^2 - \sum s' q \sum q}{N \sum q^2 - \sum q \sum q} \qquad (4\text{-}19)$$

$$D = \frac{N \sum s' q - \sum s' \sum q}{N \sum q^2 - \sum q \sum q} \qquad (4\text{-}20)$$

where

N = number of flow periods analyzed

As mentioned in Section 6.1 of this chapter, although data from different flow periods may be included on the same semilog plot, such an analysis is subject to the limitations mentioned therein.

Furthermore:

1. Winestock and Colpitts (1965) have shown that a multi-rate test can give misleading results. They identified a "reversal effect" in actual tests and also in gas-well simulator studies. Briefly, a well producing dry gas and no water was tested and later simulated. With the first change to a larger orifice plate, the flow rate increased as expected. However, with successive changes to still larger orifice plates, the flow rate decreased. No such reversal in the deliverability line occurred with an isochronal test run on the same well. Consequently, a semilog plot for cases where reversal effects cannot be clearly identified will give a value of kh which would be in error.

2. The analysis of a multi-rate test involves use of the principle of superposition which is rigorously applicable only to linear equations. When the term Dq is introduced, superposition of the resulting non-linear equation is questionable.

In view of these practical limitations, the use of multi-rate tests to determine kh should be utilized with due caution. A simplified form of a multi-rate test, called a two-rate test, is of considerable practical application and its conduct and analysis is given below.

Two-Rate Test

The two-rate test, developed by Russell (1963), is the simplest form of a multi-rate test. It consists of flowing the well at a constant rate, q_1, for a period of time, t, and then changing the flow rate to q_2. The first rate is usually the actual production rate of the well. Before the flow rate is changed, a bottom hole pressure gauge is lowered into the well to record the flowing sandface pressure. As will be seen in the analysis of this test, it is important to have a reliable value for the flowing sandface pressure immediately prior to the rate change. The flowing sandface pressure after the rate change is recorded continuously. Such data may be analyzed without using the pressure history before the rate change. If, however, this history happens to be available, it may be analyzed by the methods of the single-rate test analysis, described in Section 4.1, to obtain kh and s'. It should be noted that the duration, t, of the first flow, must be long enough to ensure that it is

in the transient flow regime, regardless of whether or not data from that flow rate are to be analyzed.

The two-rate test has several advantages over the single-rate test. If the pressure-time data for the first flow rate are available, along with the data from the second flow rate, a value for the IT flow factor, D, may be obtained directly. Consequently, the test time is shortened considerably for wells that have a long time to stabilization. Such wells would need a lengthy shut-in period prior to conducting a single-rate test in addition to the lengthy shut-in period between the two single-rate tests that would be necessary to determine the IT flow factor.

Furthermore, the time required for the start of the transient flow regime for the second flow rate is much shorter than would normally be required for a single-rate test or for a pressure build-up test. This is particularly so if a decreasing rate sequence is used. Russell (1963) explained that the attainment of a constant flow rate from the formation was achieved much quicker if the change was from a dynamic equilibrium to another dynamic equilibrium rather than from a static to a dynamic state, or vice versa. It is clear then, that when wellbore storage effects are significant, a two-rate test has a definite advantage. On some wells, a "hump" is observed on the pressure build-up curve when the well is shut-in. This hump is usually caused by phase redistribution in the wellbore (liquid fallout), explained by Stegmeier and Matthews (1958). Where these problems occur, a pressure build-up analysis may be impossible without the use of bottom hole shut-in and recording equipment. In these cases it has been observed that a two-rate test eliminates the problems caused by redistribution of the gas and liquid phases, and in fact it has become the standard test in some instances (Russell, 1963).

A two-rate test and its corresponding pressure response are depicted in Figure 4-6. The analysis of such a test will give kh, s, and D if p_i is available. If p_i is not available, the analysis will yield kh, s', and p_i.
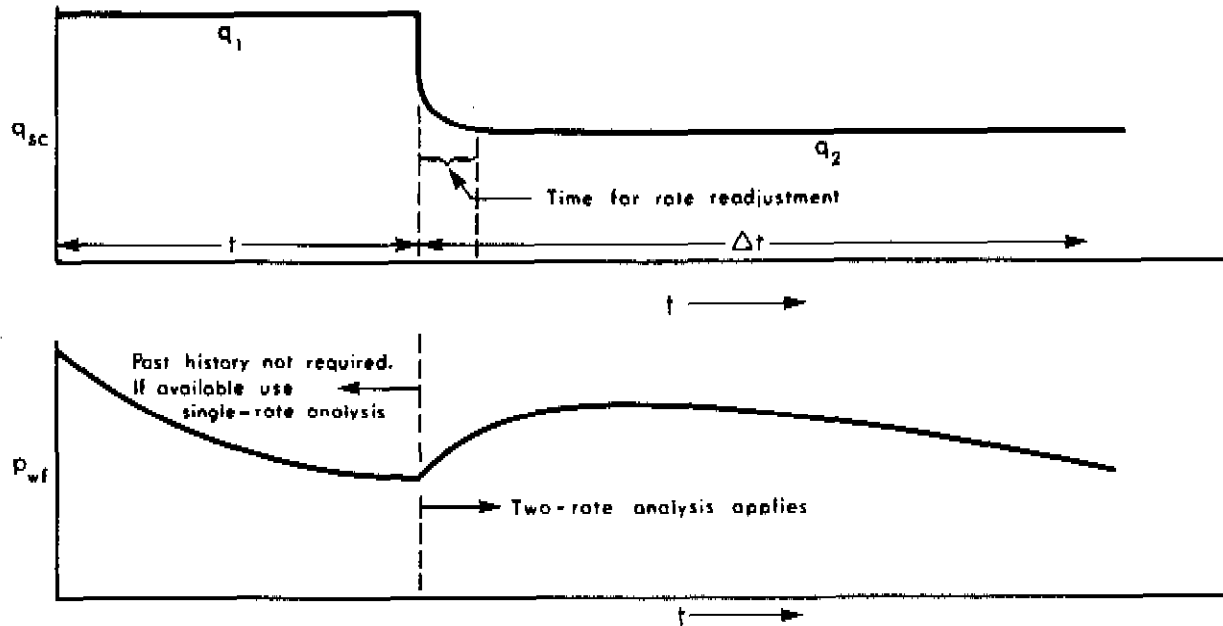
FIGURE 4-6. TWO-RATE TEST - FLOW RATE AND PRESSURE DIAGRAMS

Analysis

The pressure response obtained by changing the flow rate from q_1 to q_2 may be analyzed by applying the principle of superposition in time. The relevant equations from Chapter 2 are developed further in the Notes to this chapter. For the second flow period of a two-rate test, the pseudo-pressure drawdown is given by Equation (4N-13) which is reproduced below

$$\psi_i - \psi_{wf} = 1.632 \times 10^6 \frac{q_1 T}{k h} \left[\log \left(\frac{t + \Delta t}{\Delta t} \right) + \frac{q_2}{q_1} \log \Delta t \right]$$

$$+ 1.632 \times 10^6 \frac{q_2 T}{k h} \left[\log \left(\frac{k}{\phi \mu_i c_i r_w^2} \right) - 3.23 + 0.869 s_2' \right]$$

$$(4-21)$$

A plot of ψ_{wf} versus $\log \left(\frac{t + \Delta t}{\Delta t} \right) + \frac{q_2}{q_1} \log \Delta t$ on arithmetic

coordinates should give a straight line of slope, m, from which

$$k \, h = \frac{1.632 \times 10^6 \, q_1 \, T}{m} \qquad (4-22)$$

The apparent skin factor, s_2', associated with the flow rate, q_2, may then be calculated from Equation (4N-19) given below

$$q_1 \, s_1' - q_2 \, s_2' = \frac{(\psi_{wf1} - \psi_{wf0}) \, q_1}{0.87 \, m}$$

$$- \frac{(q_1 - q_2)}{0.87} \left[\log \left(\frac{k}{\phi \, \mu_i \, c_i \, r_w^2} \right) - 3.23 \right] \quad (4-23)$$

where

s_1' = apparent skin factor associated with the flow rate q_1

ψ_{wf1} = flowing sandface pseudo-pressure at $\Delta t = 1$, obtained from the straight line (extrapolated, if necessary)

ψ_{wf0} = flowing sandface pseudo-pressure at the time of changing the flow rate from q_1 to q_2

In order to utilize Equation (4-23) some additional information is necessary. Two alternative approaches may be considered.

Case 1. The initial reservoir pressure, p_i, and hence ψ_i is known. Since the single-rate analysis of Section 4.1 applies to the first flow period of a two-rate test, the apparent skin factor, s_1', related to the flow rate q_1 may be obtained from Equation (4-5) written as

$$s_1' = 1.151 \left[\frac{\psi_i - \psi_{wf0}}{m} - \log \left(\frac{k \, t}{\phi \, \mu_i \, c_i \, r_w^2} \right) + 3.23 \right] \qquad (4-24)$$

where

t = time of changing the flow rate from q_1 to q_2, that is, the time corresponding to the pseudo-pressure ψ_{wf0}

The value of s_1' calculated above may be substituted into the following form of Equation (4-23) to calculate the apparent skin factor, s_2', related to the flow rate q_2

$$s_2' = \frac{q_1}{q_2} s_1' - \frac{(\psi_{wf1} - \psi_{wf0}) \, q_1}{0.869 \, m \, q_2}$$

$$+ \frac{(q_1 - q_2)}{0.869 \, m \, q_2} \left[\log \left(\frac{k}{\phi \, \mu_i \, c_i \, r_w^2} \right) - 3.23 \right] \qquad (4-25)$$

The skin factor, s, and the IT flow factor, D, may then be calculated using the above values of s_1', s_2', and Equations (4-8) and (4-9).

Case 2. The initial reservoir pressure, p_i, and hence ψ_i is not known. In this case, the skin and IT flow effects cannot be separated. However, ψ_i may be estimated by assuming s_1' and s_2' to be equal to an average s', calculated from Equation (4-23) which may be written as

$$s' = 1.151 \left[\left(\frac{q_1}{q_1 - q_2} \right) \left(\frac{\psi_{wf1} - \psi_{wf0}}{m} \right) - \log \left(\frac{k}{\phi \, \mu_i \, c_i \, r_w^2} \right) + 3.23 \right]$$

$$(4-26)$$

and by substituting the calculated value of s' into the following equation, which is a form of Equation (4-24).

$$\psi_i = \psi_{wf0} + m \left[\log \left(\frac{k \, t}{\phi \, \mu_i \, c_i \, r_w^2} \right) - 3.23 + 0.869 \, s' \right] \qquad (4-27)$$

ψ_i may then be converted back to p_i.

EXAMPLE 4-2

Introduction   The pressure-time data from the second rate of a two-rate drawdown test are analyzed to give the reservoir parameters kh, s and D.

<u>Problem</u> A two-rate test was conducted on a well in a new reservoir. The initial reservoir pressure, p_i, was 4342 psia. The pressure-time data for the first flow rate, q_1 = 27.76 MMscfd, was not recorded. The flow rate was changed at t = 6 hours at which time the flowing sandface pressure, p_{wf_0}, was 3838 psi. The second flow rate, q_2 = 20.16 MMscfd, was continued for 37 hours during which time the flowing sandface pressure was monitored continuously. These pressure-time data are given in the tabulations for the solution to this problem. General data pertinent to the test are given below.

From a recombined gas analysis:

G = 0.60 P_c = 709 psia T_c = 362^0R

H_2S = 5.02% CO_2 = 1.46% N_2 = 0.25%

μ_i = 0.0220 cp c_i = 0.00017 $psia^{-1}$

Well/reservoir data:

T = 622^0R h = 32 ft r_e = 2640 ft

ϕ = 0.05 r_w = 0.40 ft

Calculate the permeability, k, of the reservoir, the skin factor, s, and the IT flow factor, D.

<u>Solution</u> A $\psi - p$ curve, shown in Figure 4-7, is generated by the computer program, listed in Appendix D, which uses the numerical technique described in Example 2-1.

p = 4342 $\leftrightarrow$ ψ = 1149.2×10^6 (Figure 4-7)

$\therefore \psi_i$ = 1149.2×10^6 $psia^2/cp$

p = 3838 $\leftrightarrow$ ψ = 948.2×10^6 (Figure 4-7)

$\therefore \psi_{wf_0}$ = 948.2×10^6 $psia^2/cp$
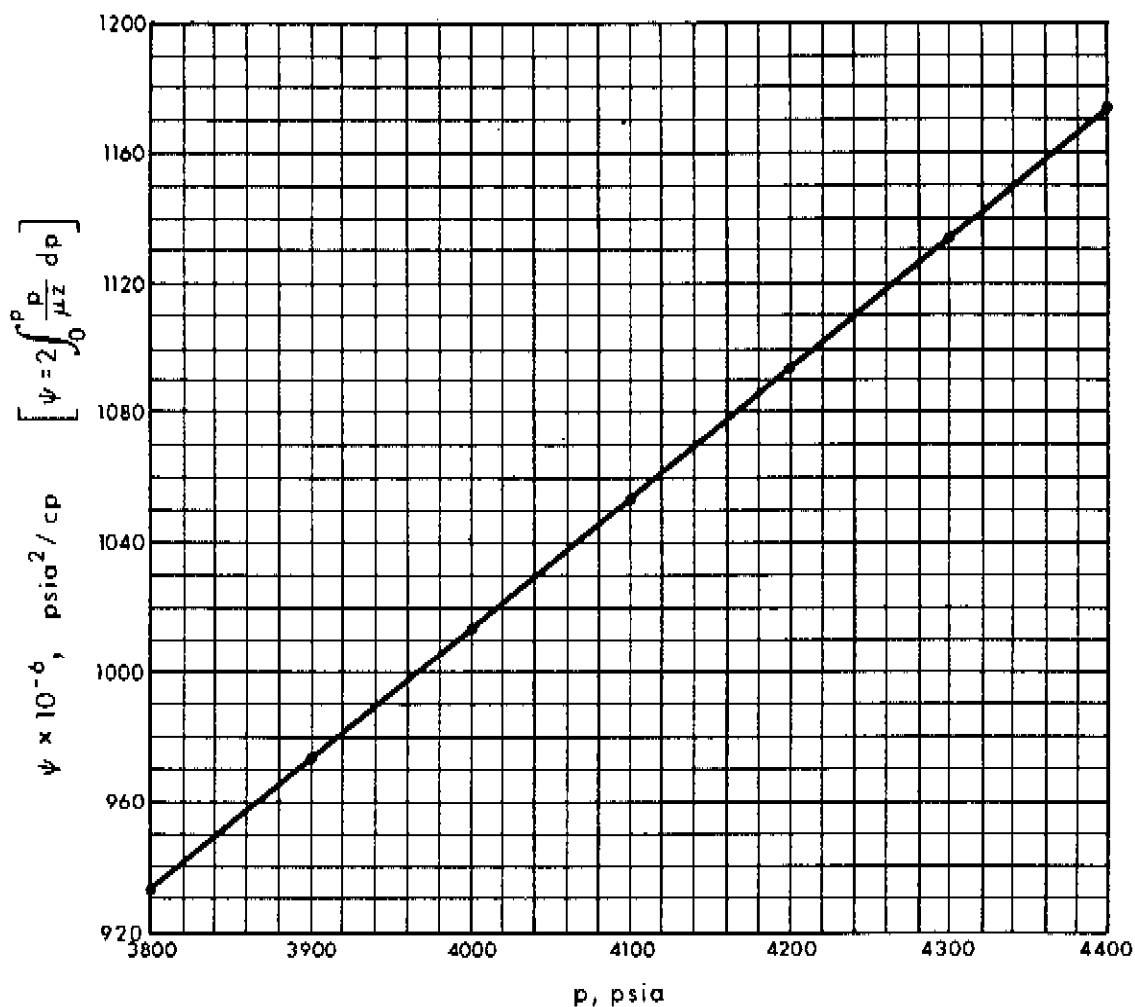
FIGURE 4-7. ψ-p CURVE FOR THE TWO-RATE
DRAWDOWN TEST OF EXAMPLE 4-2

Using the ψ-p curve of Figure 4-7, the following tabulations
may be made:

Δt (hr)	P_{wf} (psia)	$\log \dfrac{t + \Delta t}{\Delta t} + \dfrac{q_2}{q_1} \log \Delta t$	ψ_{wf} (psia^2/cp $\times 10^{-6}$)
1.0	3971	0.845	1000.7
3.0	3973	0.824	1001.5
5.0	3971	0.850	1000.7
7.0	3965	0.883	998.3

9.0	3960	0.915	996.3
11.0	3956	0.945	994.8
13.0	3951	0.974	992.8
15.0	3944	1.000	990.0
17.0	3941	1.025	988.8
19.0	3934	1.048	986.1
21.0	3931	1.070	984.9
23.0	3928	1.090	983.7
25.0	3925	1.109	982.5
27.0	3919	1.127	980.1
29.0	3913	1.144	977.8
31.0	3910	1.160	976.6
33.0	3907	1.175	975.4
35.0	3904	1.190	974.2
37.0	3901	1.204	973.0

Plot ψ_{wf} versus $\log \frac{t + \Delta t}{\Delta t} + \frac{q_2}{q_1} \log \Delta t$ and draw the best straight line as shown in Figure 4-8. From the straight line of Figure 4-8,

$$m = \frac{(1000 - 980) \times 10^6}{1.124 - 0.874} = 80.0 \times 10^6$$

$$\psi_{wf_1} = 1002.0 \times 10^6$$

From Equation (4-16)

$$k h = \frac{1.632 \times 10^6 \, q_1 \, T}{m}$$

$$= \frac{(1.632 \times 10^6)(27.76)(622)}{80.0 \times 10^6} = 352 \text{ md ft}$$

$$\therefore \quad k = \frac{352}{32} = 11.0 \text{ md}$$

Since p_i is known, it is possible to separate the skin and IT effects.
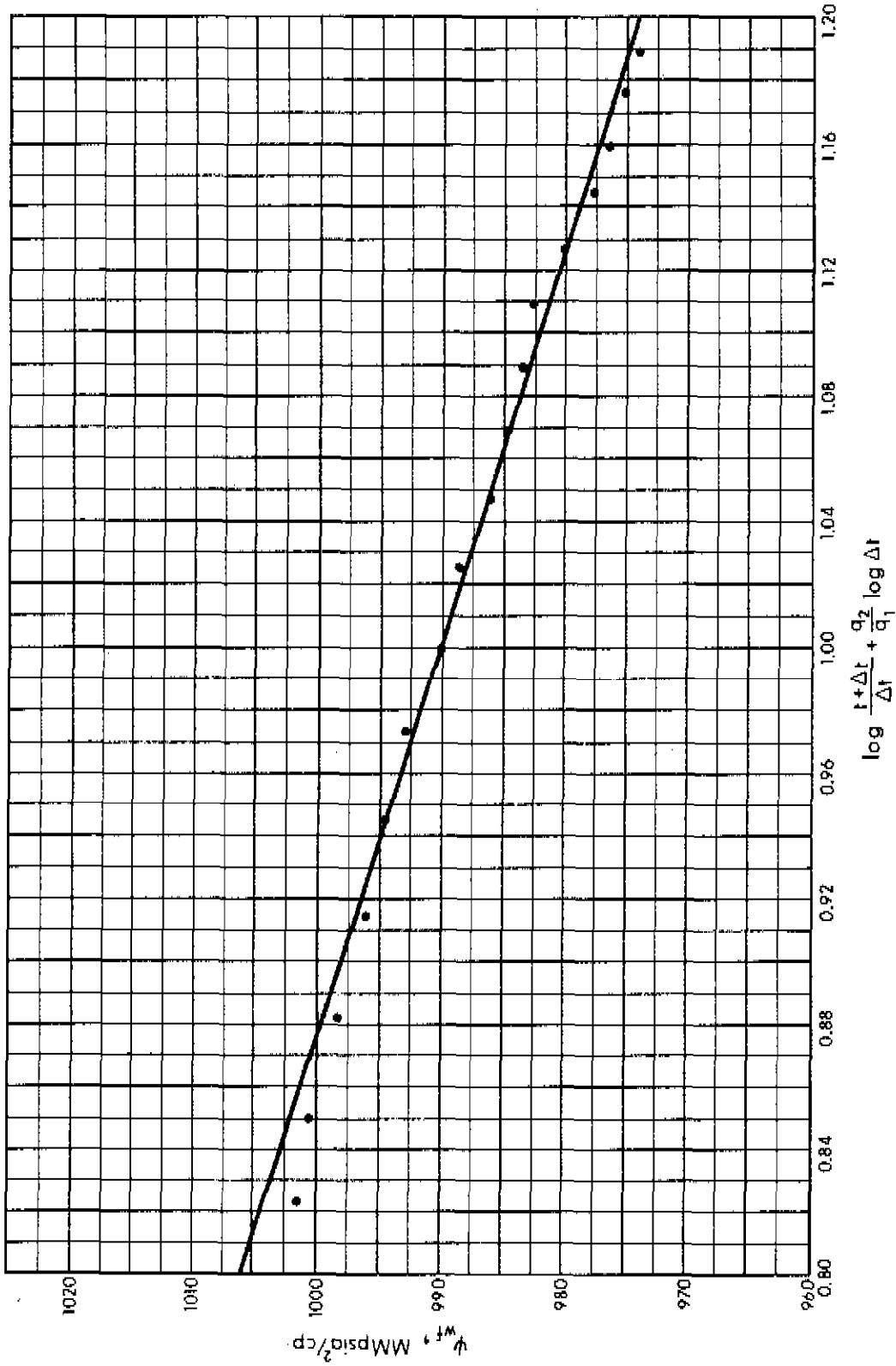
FIGURE 4-8. DATA PLOT FOR THE TWO-RATE TEST OF EXAMPLE 4-2

4-32

From Equation (4-18)

$$s_1' = 1.151 \left[\frac{\psi_i - \psi_{wf0}}{m} - \log\left(\frac{k\,t}{\phi\,\mu_i\,c_i\,r_w^2}\right) + 3.23 \right]$$

$$= 1.151 \left[\frac{(1149.2 - 948.2) \times 10^6}{80.0 \times 10^6} \right.$$

$$\left. - \log \frac{(11)(6)}{(0.05)(0.022)(0.00017)(0.4)^2} + 3.23 \right]$$

$$= -4.1$$

From Equation (4-19)

$$s_2' = \frac{q_1}{q_2} s_1' - \frac{(\psi_{wf1} - \psi_{wf0})\,q_1}{0.87\,m\,q_2} + \frac{(q_1 - q_2)}{0.87\,q_2} \left[\log\left(\frac{k}{\phi\,\mu_i\,c_i\,r_w^2}\right) - 3.23 \right]$$

$$= \frac{(27.76)(-4.1)}{20.16} - \frac{(1002.0 \times 10^6 - 948.2 \times 10^6)(27.76)}{(0.87)(80.0 \times 10^6)(20.16)}$$

$$+ \frac{(27.76 - 20.16)}{(0.87)(20.16)} \left[\log \frac{(11)}{(0.05)(0.022)(0.00017)(0.4)^2} - 3.23 \right]$$

$$= -4.4$$

From Equations (4-8) and (4-9)

$$s_1' = s + D\,q_1$$

$$s_2' = s + D\,q_2$$

$$\therefore\quad -4.1 = s + D\,(27.76)$$

$$-4.4 = s + D\,(20.16)$$

Solving the above pair of simultaneous equations gives

$$s = -5.2$$

$$D = 0.04$$

Discussion   In deriving Equation (4-17), which subsequently leads to Equation (4-19), it is assumed that (t/t+1) can be approximated by 1.0 thereby making the term log(t/t+1) equal to zero. In the above example, assuming this approximation cannot be made, the calculated values of s and D would be -5.5 and 0.05, respectively. This error is not considered significant in the estimation of skin and IT flow effects.

The time-of-start of transient flow, for the second flow period, is not easy to identify since it requires a rigorous desuper-position of data using type curves or any other analytical means. For this problem, an analysis of the pressure-time data of the first flow period indicated a time-of-start of approximately one hour. Since a decreasing rate sequence is used, the time-of-start of transient flow for the second flow period would be less than that for the first flow period. Consequently, all the tabulated data are included in the semilog plot.

If the drawdown were continued, pseudo-steady state would be indicated by a deviation from the semilog straight line. As a matter of interest, the approximate time to stabilization for this problem, calculated from Equation (3-14), is 160 hours.

5   TESTS UTILIZING PSEUDO-STEADY STATE DATA

The transient flow regime continues until boundary effects are felt. Flow is then pseudo-steady state for a well centrally located in a circular or square reservoir. The time to stabilization may be computed by the method described in Chapter 2, Section 6.4. For different well/reservoir configurations, the concept of shape factors introduced in Chapter 2, Section 7.4 may be used to define the start of pseudo-steady state flow.

Various tests utilizing pseudo-steady state flow data are described. In particular, a useful variation of a Reservoir Limits Test, called an Economic Limits Test, which utilizes transient flow data instead of pseudo-steady state flow data is discussed. Wherever possible, these tests are related to the different types of deliverability tests of Chapter 3.

5.1 Reservoir Limits Test

If a single-rate drawdown test is continued long enough, deviation from the semilog straight line will be observed. The constant-rate drawdown should be continued until it becomes evident that this deviation does not in fact become another semilog straight line, which would be indicative of a fault and not the reservoir boundaries. The reservoir boundary is reached when a plot of the bottom hole pressure versus time gives a straight line on arithmetic coordinates. The slope of the straight line is a function of the flow rate and the size of the reservoir.

Cornett (1961) described the application of reservoir limits testing and cited several case histories. He showed that in addition to defining reserves, such tests may give the direction of a fault by combining the results of tests conducted on several neighbouring wells. Jones (1962) showed that reservoir limits testing on one well may be used to determine the in-place gas in a small closed reservoir and the proved portion of the in-place gas within a large reservoir, the distance to an impermeable productive limit, the angle between two intersecting faults and interference effects. Similar testing on two or more wells would yield reservoir productivity, orientation of highest and lowest permeability in a homogeneous anisotropic reservoir, the position and strike of a fault and, the position and trend of a gas-water contact. Odeh (1969) presented graphs that describe the behaviour of a drawdown due to a radial discontinuity. Earlougher (1971) showed that the shape of a reservoir may be estimated by reservoir limits testing and the concept of shape factors. Earlougher (1972) explained that the use of an average rate, when a constant-rate test cannot be conducted, might give a reasonable indication of reserves.

The data from a reservoir limits test or from the first rate of a conventional deliverability test may be analyzed to give the in-place gas volume, V_p.

Analysis

During pseudo-steady state flow, the pressure at the well is given by Equation (4N-22) developed in the Notes to this chapter and reproduced below

$$\psi_i - \psi_{wf} = \frac{2348 \ q_{sc} \ T \ t}{\pi \ \phi \ \mu_i \ c_i \ r_e^2 \ h}$$

$$+ \ 3.263 \times 10^6 \ \frac{q_{sc} \ T}{k \ h} \left[\log \left(\frac{0.472 \ r_e}{r_w} \right) + \frac{s'}{2.303} \right]$$

$$(4\text{-}28)$$

A plot of $\Delta\psi$ ($= \psi_i - \psi_{wf}$) versus t on arithmetic coordinates should give a straight line of slope, m'', from which

$$V_p = \frac{2348 \ q_{sc} \ T}{\mu_i \ c_i \ m''} \qquad\qquad (4\text{-}29)$$

where

V_p = in-place gas volume of the reservoir, MMscf

$\therefore \ V_p \times 10^6 = \pi \ \phi \ h \ r_e^2$

Since ϕh is deducible from logs, r_e may be calculated.

5.2 Economic Limits Test

If a single-rate drawdown is continued and no deviation from the semilog straight line is observed, the reservoir limits cannot be defined. It is possible, however, to define a minimum in-place gas volume.

Reservoir Limits Tests can lead to flaring of large amounts of gas without defining the actual reservoir limits. This is especially true in low permeability reservoirs. In such situations, it is possible to design an Economic Limits Test to confirm the presence of the minimum in-place gas that would be necessary for economic exploitation of a reservoir.

Analysis

The radius of investigation, given by Equation (2-105), can be written with appropriate substitutions from Table 2-4 as

$$r_{inv} = 2 \left[\frac{2.637 \times 10^{-4} \; k \; t}{\phi \; \mu_i \; c_i} \right]^{0.5} \qquad (4-30)$$

Defining a minimum in-place gas volume, V_{pm} (in MMscf), as

$$V_{pm} \times 10^6 = \pi \; \phi \; h \; r_{inv}^2 \qquad (4-31)$$

Equation (4-30) may be substituted in Equation (4-31) to give

$$t = \frac{3.018 \times 10^8 \; \mu_i \; c_i \; V_{pm}}{k \; h} \qquad (4-32)$$

The permeability-thickness, kh, may be estimated by any suitable method that does not involve unnecessary flaring of gas. The other terms on the right-hand side of Equation (4-32) are either known or defined so that the duration of the flow period required to conduct an Economic Limits Test may be calculated. The value of kh may be confirmed by a transient analysis of the resulting transient data.

6 IMPORTANT CONSIDERATIONS PERTAINING TO DRAWDOWN TESTS

Although various drawdown tests have been conducted for a long time, they have not been used extensively to evaluate reservoir properties because there are several difficulties involved in the conduct and analysis of such tests. One of the difficulties in analyzing drawdown data is based on the variation of flow rate during the flow periods. The theory developed in Chapter 2 and subsequently applied in this chapter assumes constant flow rates during each flow period. For gas wells, this is a difficult requirement to satisfy, especially during the early life of a well when drawdown tests are usually conducted. A method to circumvent this problem and to analyze variable-rate data is

discussed. The duration of each flow period and the effects of drainage area shapes and well location are considered. The reliability of reservoir parameters obtained by a transient flow analysis is also discussed.

6.1   Constancy of Flow Rates

The factors restricting the conduct of constant-rate deliverability tests are summarized in Chapter 3, Section 7.3. The same difficulties arise in drawdown testing. Although the drawdown analysis procedures of Sections 4.1 and 4.2 are based on the requirement of constant flow rates, variations in flow rates may, in some instances, be accommodated by slight modification of these procedures.

If the rate variations are definable, and if difficulties like slugging can be avoided, variable rate drawdown data may be analyzed by the methods suggested by Winestock and Colpitts (1965) and Odeh and Jones (1965), described below.

The variations in rate may be accommodated, in some cases, by normalizing the drawdown. This is similar to the normalization technique described in Chapter 3, Section 7.3. For a flow test in which the rate variations are smooth, Winestock and Colpitts (1965) suggest a normalization technique which essentially modifies the equation for analyzing single-rate tests, Equation (4-5), to the form

$$\frac{\psi_i - \psi_{wf}}{q_{sc}} = 1.632 \times 10^6 \ \frac{T}{k\,h} \left[\log t + \log \left(\frac{k}{\phi\,\mu_i\,c_i\,r_w^2} \right) - 3.23 + 0.869\,s' \right]$$

$$(4\text{-}33)$$

A plot of $(\psi_i - \psi_{wf})/q_{sc}$ versus t on semilogarithmic coordinates should give a straight line from which good approximations of kh and s' may be made. Equation (4-33) is valid only if the range of flow rate variation is not too wide and does not extend into the turbulent region. This implies an assumption of a constant value for s'. If, however, wide flow variations are experienced, the variation of s' with q_{sc} must be

considered. Noting that $s' = s + Dq_{sc}$, Equation (4-5) may be written as

$$\frac{\psi_i - \psi_{wf}}{q_{sc}} = 1.632 \times 10^6 \frac{T}{k\,h} \left[\log t + 0.869\, D\, q_{sc} \right]$$

$$+ 1.632 \times 10^6 \frac{T}{k\,h} \left[\log \left(\frac{k}{\phi\, \mu_i\, c_i\, r_w^2} \right) - 3.23 + 0.869\, s \right]$$

$$(4\text{-}34)$$

A plot of $(\psi_i - \psi_{wf})/q_{sc}$ versus $(\log t + 0.869\, Dq_{sc})$ on arithmetic coordinates should give a straight line from which good approximations of kh and s' may be made. This method involves a graphical trial-and-error procedure in which values of D must be guessed until a straight line is obtained.

Odeh and Jones (1965) have proposed a method for analyzing variable rate data by treating the rate variations as step changes over small time intervals and then analyzing the data by multi-rate methods involving the principle of superposition.

Consider a drawdown time during which the flow rate declines smoothly. The time period may be divided into an equal number of intervals, n. The actual size of each interval depends on the rate of decline. For a sharply declining rate the intervals would have to be much smaller than for a slowly declining rate. The flow rates and drawdown may be averaged over each time interval. This procedure essentially yields a series of flow rates, the corresponding drawdown and time intervals, and may be analyzed by the multi-rate methods of Section 4.2. Equation (4-15) may be written as

$$\frac{\psi_i - \psi_{wf}}{q_n} = m' \sum_{j=1}^{n} \left[\frac{\Delta q_j}{q_n} \log (t - t_{j-1}) \right]$$

$$+ m' \left[\log \left(\frac{k}{\phi\, \mu_i\, c_i\, r_w^2} \right) - 3.23 + 0.869\, s' \right] \qquad (4\text{-}35)$$

where

$$s' = s_1' = s_2' = \ldots = s_n'$$

q_n = average flow rate over the time interval, $(t_n - t_{n-1})$

A plot of $(\psi_i - \psi_{wf})/q_n$ versus $\sum \Delta q_j / q_n \log (t - t_{j-1})$ on arithmetic coordinates should give a straight line from which good approximations of kh and s' may be obtained.

Equation (4-35) is valid only when the range over which the flow rate varies is not too wide and does not extend into the turbulent region. This implies an assumption of a constant apparent skin factor. If, however, wide flow variations extending into the turbulent flow region are experienced, the variations in s' must be considered. In such a case, noting that $s' = s + Dq_{sc}$, Equation (4-15) may be written as

$$\frac{\psi_i - \psi_{wf}}{q_n} = m'\left[\sum_{j=1}^{n}\left(\frac{\Delta q_j}{q_n} \log (t - t_{j-1})\right) + 0.869\, D\, q_n\right]$$

$$+ m'\left[\log\left(\frac{k}{\phi\, \mu_i\, c_i\, r_w^2}\right) - 3.23 + 0.869\, s\right] \qquad (4-36)$$

A plot of $(\psi_i - \psi_{wf})/q_n$ versus $\sum\left[\Delta q_j/q_n \log (t - t_{j-1})\right] + 0.869\, Dq_n$ on arithmetic coordinates should give a straight line from which good approximations of kh and s may be calculated. This method of analysis involves a graphical trial-and-error procedure in which values for D have to be guessed until a straight line is obtained.

6.2 Duration of Each Flow Regime

The time-of-start of the transient flow regime is usually delayed by wellbore storage or linear flow effects. The duration of these effects may be estimated from Equation (4-1) or from the type curve matching technique illustrated by Example 4-1.

The semilog straight line or transient flow data will continue until the effects of either a sealing fault or a boundary become manifest. The distance to that fault or boundary may be estimated from

the radius of investigation defined by Equation (3-16). Alternatively, if the distance to a boundary is known, the same equation may be used to estimate the end of the semilog straight line.

If, following the first straight line, a second semilog straight line results from continued drawdown, this would indicate the presence of one or more intersecting faults rather than a reservoir boundary. The ratio of the slopes of the two straight lines may be interpreted as describing the angle between those intersecting faults. For a well located on the bisector of the angle, θ, between intersecting boundaries, Van Poollen (1965) and Prasad (1973) have shown that the ratio of the slopes of the late-time and early-time semilog straight lines is $360/\theta$.

In a square or circular reservoir, with a centrally located well, deviation from the semilog straight line heralds the pseudo-steady state. The time to stabilization is defined by Equation (3-14). From this time on, pseudo-steady state persists till the drawdown is terminated.

6.3 Effect of Drainage Area Shape and Well Location

The shape of the drainage area and the relative location of the well will affect the end of the transient flow and may introduce a late-transitional period between the transient and pseudo-steady state flow regimes. In such an instance, transient flow will end when the radius of investigation becomes equal to the distance to the nearest boundary. Pseudo-steady state will start at a time given by the value of t_{DA} (defined in Chapter 2, Section 7.4, Table 2-6) corresponding to the particular well/reservoir geometry.

The transient flow equation is the same for non-circular as for circular reservoirs since the shape has no bearing on the development of flow equations for an infinite reservoir. However, the pseudo-steady state flow equation is different since it must accommodate the shape of the reservoir and the location of the well. A shape factor, C_A, introduced in Chapter 2, Section 7.4, modifies the flow equation to the

form given by Equation (4N-26) reproduced below.

$$\psi_i - \psi_{wf} = \frac{747\, q_{sc}\, T\, t}{\phi\, \mu_i\, c_i\, A\, h} + 1.632 \times 10^6\, \frac{q_{sc}\, T}{k\, h} \left[\log\left(\frac{2.246\, A}{r_w^2\, C_A}\right) + 0.869\, s' \right]$$

$$(4\text{-}37)$$

As explained in Chapter 2, Section 7-4, the late-transitional period, between the end of transient flow and the start of pseudo-steady state, may only be represented by Equation (2-125).

6.4 Reliability of Reservoir Parameters Estimated from Drawdown Tests

The general flow equation of Chapter 2, Section 5.6, in terms of pseudo-pressure, involves the product μc. The flow equation is linearized by assuming μc to be constant at initial conditions. The analytical solution of the linearized flow equation has been adapted, in this chapter, to the analysis of drawdown tests. The effects of linearization of the flow equation have been investigated by Wattenbarger (1967) along with considerations of the following factors: skin, wellbore storage, IT flow, and vertical fractures. His conclusions are summarized below:

1. The use of the pseudo-pressure approach in the analysis of transient flow drawdown tests gives good results. kh and s determined by this analysis are sufficiently accurate in the absence of IT flow effects.

2. When IT flow effects are significant, the kh calculated from a drawdown test could be as much as 35 per cent lower than the actual value. This discrepancy is claimed to be on account of assuming the IT flow factor, D, to be constant, whereas it is actually a function of viscosity, which is itself a function of pressure. The dependence of D on μ has been discussed in Chapter 2, Section 9.2.

3. The effect of a vertical fracture at the well is that of an apparent negative skin factor, which does not invalidate the value of kh obtained from the semilog straight line.

Notwithstanding the possible error in kh when IT flow effects are significant, drawdown tests, when properly conducted, will give acceptable values for kh, s and D.

7 DELIVERABILITY

The most common reason for conducting drawdown tests, in addition to the calculation of well/reservoir parameters, is the determination of long-term deliverability.

If flow tests are extended into the pseudo-steady state region, the calculation of deliverability is relatively simple. The stabilized flow constants, a and b, in Equation (3-4) reproduced below

$$\bar{\psi}_R - \psi_{wf} = a \ q_{sc} + b \ q_{sc}^2 \tag{4-38}$$

can be calculated by solving the simultaneous equations resulting from two tests conducted at different flow rates.

It is not always feasible to conduct the above-mentioned tests, especially in cases where the time to stabilization is relatively large. In such situations, it is possible to calculate a and b from transient flow data. The single-rate and multi-rate tests described in Section 4.1 and 4.2 yield values for kh, s and D. In the Notes to Chapter 3, Equations (3N-10) and (3N-11) relate a and b to various well/ reservoir parameters as shown below.

$$a = \frac{3.263 \times 10^6 \ T}{k \ h} \left[\log \left(\frac{0.472 \ r_e}{r_w} \right) + \frac{s}{2.303} \right] \tag{4-39}$$

$$b = \frac{1.417 \times 10^6 \ T}{k \ h} \ D \tag{4-40}$$

Hence a and b can be evaluated and substituted in Equation (4-35) to give the stabilized deliverability equation.

In order to determine Equation (4-38) in terms of Equations (4-39) and (4-40), it is necessary to conduct two single-rate tests at

different flow rates or a two-rate test. If, for any reason, it is not possible to conduct these tests and evaluate s and D separately, a simplification may be made. An alternate form of the deliverability equation is given below:

$$\bar{\psi}_R - \psi_{wf} = \frac{3.263 \times 10^6 \ T \ q_{sc}}{k \ h} \left[\log \left(\frac{0.472 \ r_e}{r_w} \right) + \frac{s'}{2.303} \right] \quad (4-41)$$

Equation (4-41) may be evaluated using the results of a single-rate test. However, this equation is then valid only for predicting the deliverability at flow rates near that used in the single-rate test.

Although s', determined from a single-rate test, is theoretically a constant only for the flow rate used, in practice it is, sometimes, reasonably constant over a significant range of flow rates. This is particularly so in the case of low deliverability wells. In such cases, a single-rate test used in conjunction with Equation (4-41) may provide a reasonable prediction of deliverability.

One point, worthy of note, is that for wells drilled into a formation of known kh, a test is still required in order to determine the apparent skin factor, s', before the stabilized deliverability equation can be obtained. s' may change from well to well, and varies with the method of drilling and with the effectiveness of well completion.

8 GUIDELINES FOR DESIGNING DRAWDOWN TESTS

Drawdown tests generally require the reservoir pressure to be stabilized prior to flowing the well. Hence, wells that have not been produced, or wells that have been shut-in long enough to permit pressure stabilization are suitable for drawdown testing and analysis. In the isochronal deliverability tests discussed in Chapter 3 a series of shut-in periods is required to attain pressure stabilization, while, in the conventional deliverability tests, each flow period must be continued to pressure stabilization. In either case, the time required

for stabilization may be very large and will limit the application of such tests. A drawdown test, properly conducted and analyzed is a viable alternative. Where economic considerations require a minimum loss of production time, a drawdown test may prove to be particularly attractive, since such a test minimizes the loss of production associated with a shut-in.

Drawdown tests may also be conducted to supplement information obtained from other tests such as build-up or deliverability tests.

When it is difficult to achieve stable flow rates because of slugging of the well, a drawdown test is not recommended.

8.1 Choice of Test

The choice of test need not be limited to the tests described in previous sections. If adequate pressure and flow rate data are acquired during the course of regular production of the well, a proper interpretation of these data according to the principles described previously constitutes a satisfactory test. Notwithstanding this, the various tests described in this chapter are applicable in different situations.

Tests utilizing early-time data, dominated by wellbore storage, should never be designed as such. Their interpretation is only recommended, if, after testing, it is found that they are the only data amenable to analysis.

Tests utilizing transient flow data are recommended when an accurate knowledge of reservoir characteristics and skin effects is desired. A single-rate test is acceptable when IT flow effects are negligible, otherwise two single-rate tests should be conducted to evaluate the skin and IT flow components of the apparent skin factor. In some situations, a long shut-in period is necessary between the two single-rate tests. When this is not practical, a two-rate test may be more appropriate. A two-rate test, with a declining rate sequence, is particularly suitable when wellbore storage effects are to be minimized or phase redistribution in the wellbore (upon shut-in) is to be eliminated. Variable-rate transient flow tests are rarely designed as

such. Usually they result a posteriori. Single-rate tests in which the flow rate cannot be maintained at a constant value lend themselves to a variable-rate analysis.

Where information on reservoir limits is desired, a single-rate reservoir limits test is unavoidable. However, because of the long duration of flow involved, only small-size reservoirs are amenable to such testing. Multi-rate tests are rarely conducted for this purpose, but a conventional deliverability test, when conducted with a continuous recording of the flowing well pressure may be analyzed to yield the same information. Economic Limits Tests should be used whenever possible to minimize flaring and wastage of gas.

When a well has been vertically fractured during stimulation, early-time data might provide a good match on the type curve of Figure 2-23. In such an instance the interpretation of early-time data (linear flow and not wellbore storage controlled) has been found to be reliable and where transient flow tests are economically prohibitive, tests may be designed with a view to utilizing early-time data. However, it is advisable to confirm the results, whenever possible, by an appropriate transient flow analysis.

8.2 Choice of Equipment

The same considerations apply for drawdown tests as those described for deliverability tests in Chapter 3, Section 8.2. In particular, bottom hole pressure bombs are recommended for use whenever possible. If possible, retrieval of the bomb to rewind the clock while a drawdown test is in progress should be avoided. For tests of long duration (longer than 1 week) a surface-recording bottom hole pressure bomb is a definite asset. When conducting a two-rate test in which the first flow rate is the production rate itself and only the second rate is being analyzed, the pressure bomb should be lowered into the well, preferably without stopping the first flow rate. This is quite easily achieved if a well has no tubing and flow is through the casing.

8.3   Choice of Flow Rates

The same considerations as discussed in Chapter 3, Section 8.3 apply to drawdown tests. Because of the long duration of many drawdown tests, it is often difficult to maintain a constant flow rate. In such a case, either a multi-rate analysis is called for, or if the change in rate has been smooth, the considerations of Section 6.1 apply.

8.4   Duration of Flow Rates

The criterion for the minimum length of flow of a drawdown test is that there should be sufficient data to permit interpretation using the semilog analysis. One log cycle of data in this region is usually sufficient. The time required to achieve transient flow may often be known from experience with similar well testing situations. Where it is not available from experience, the duration of the flow period may be estimated from the time required for wellbore storage effects to disappear. The flow must last for at least five, but preferably ten, times this wellbore storage time. The time required for wellbore storage effects to become negligible may be estimated from Equation (3-19). If all the parameters in this equation are not known, reasonable estimates may be used which will maximize the calculated value of the wellbore storage time. The minimum duration of flow applies to the single-rate test, the two single-rate tests, and the first rate of all multi-rate tests. In the second and subsequent rates of multi-rate tests the effect of wellbore storage is reduced and a shorter time of flow will suffice.

In the case of reservoir limits tests, the time required for a limit to become discernible is given by Equation (3-14) which defines the time to stabilization for a circular reservoir. A flow duration of about three times the time to stabilization would seem to be reasonable for confirming the straight line on arithmetic coordinates, from the slope of which the reserves are obtained. If in Equation (3-14) r_e is taken to represent the distance to a fault, the time calculated by that

equation would be that required for the effects of the fault to be felt at the well and a flow duration of at least five times this value should clearly permit the delineation of the second semilog straight line caused by the fault. The slope of this second line will be double the slope of the first.

If the reservoir is non-circular, then a reservoir limits test should be run for a time equal to at least three times that given by the value of t_{DA} in Table 2-7 for the appropriate shape.

For a vertically fractured well, with a large time-of-start of semilog data, the analysis of early-time (linear flow) data by type curve matching is permissible. In this instance the minimum time of flow should be greater than the duration of the purely linear (half-slope) period. This is because data from the half-slope section alone will not give a unique type curve match. The time of departure from the straight line of slope one half has been given by Wattenbarger (1967) as

$$t \simeq 0.04 \frac{\phi \, \mu_1 \, c_1 \, x_f^2}{k} \qquad (4\text{-}42)$$

Approximately ten to twenty times this value of t should be sufficient to match the data plot and type curves and possibly differentiate between a horizontal and a vertical fracture in shallow gas wells.

9 CALCULATING AND PLOTTING TEST RESULTS

Earlier sections describe the various types of drawdown tests and their application. The calculation of flow rates is discussed in Chapter 6. Although it is preferable to measure bottom hole pressures directly, in many instances it is only possible to monitor wellhead pressures. These surface measured pressures may be converted to their corresponding sub-surface values as shown in Appendix B. The methods for calculating and plotting test results are outlined in this section.

9.1 Semilog Analysis

The identification of the time-of-start of the semilog straight line by type curve matching has been illustrated by Example 4-1. This procedure is applicable to single-rate tests and to the first rate of a two-rate test. In two-rate tests, a decreasing rate sequence is usually used in which case the time-of-start of semilog data for the second rate is less than that for the first rate. A more exact identification of semilog data for the second rate requires rigorous desuperposition and matching techniques which have not been covered in this chapter.

Single-Rate Tests

After semilog data have been identified and the possibility of a semilog analysis has been confirmed, a plot of $\Delta\psi$ (= $\psi_i - \psi_{wf}$) versus log t is made. The best straight line is drawn through the semilog data, either visually or by a least-squares analysis. The slope of the line is measured and is termed m, while the intercept of the straight line (extrapolated, if necessary) at t = 1 is termed $\Delta\psi_1$.

Values for h and ϕ are usually known from a geological evaluation/well logs. r_w is known while μ_i and c_i may be estimated by the methods described in Appendix A. Using Equations (4-6) and (4-7), it is then possible to calculate the permeability, k, and the apparent skin factor, s'. Since it is usually unrealistic to expect s' to be constant over a wide range of flow rates, it must be separated into its constituents, s and Dq_{sc}. This is done by conducting another single-rate test, at a different flow rate, and solving Equations (4-8) and (4-9) for the values of s and D. In either case, that is whether or not IT effects may be assumed to be negligible, the stabilized deliverability equation can be obtained by the method outlined in Section 7.

Two-Rate Tests

The first rate of a two-rate test may be analyzed exactly as described above for a single-rate test. The start of semilog straight line for the second rate may be evident from the semilog plot of the

data, using the time-of-start previously identified for the first rate as a guideline.

A plot of ψ_{wf} versus $\log \left(\dfrac{t + \Delta t}{\Delta t}\right) + \dfrac{q_2}{q_1} \log \Delta t$ is made. The best straight line is drawn through the semilog data, either visually or by a least-squares analysis. The slope of the line is measured and is termed m, while the intercept of the straight line (extrapolated, if necessary) at $\Delta t = 1$ is termed ψ_{wf_1}. ψ_{wf_0} represents the pseudo-pressure at the time of the rate change.

Using Equations (4-22) and (4-23) along with the value of s_1' calculated from the analysis of the first rate, k and s_2' may be calculated. Equations (4-8) and (4-9) may then be solved for the values of s and D. If, however, IT effects can be assumed to be negligible, s' becomes the average of s_1' and s_2'. In either case, the stabilized deliverability equation can be obtained by the method outlined in Section 7.

Variable Rate Tests

The methods of analysis of tests in which it is not possible to maintain constant flow rates are included in Section 6.1.

When IT flow effects can be neglected, a plot of $\Delta\psi/q_{sc}$ (instead of $\Delta\psi$ for the constant rate case) versus $\log t$ is made. In this context, q_{sc} implies instantaneous rates if the method of Winestock and Colpitts (1965), represented by Equation (4-33), is being used. The more rigorous technique of Odeh and Jones (1965), represented by Equation (4-35), defines q_{sc} as the average rate over small time intervals that simulate step changes in the flow rate. In either case the slope of the semilog straight line is termed m', defined by Equation (4-15), from which k may be calculated. s' may then be evaluated from Equation (4-17).

When IT flow effects cannot be neglected, the calculation procedure becomes slightly more complex, involving graphical trial-and-error solutions. Either one of the equations, Equation (4-34) or Equation (4-36) is applicable depending on the magnitude and range of the rate variations.

9.2 Pseudo-Steady State Analysis

Reservoir Limits Test

A deviation from the semilog straight line of the transient flow regime usually indicates the effect of boundaries. Flow is continued until it is evident that the deviation is due to boundaries rather than faults/barriers. In the latter case a second semilog straight line would be obtained.

When the pseudo-steady state data have been identified, a plot of $\Delta\psi$ $(= \psi_i - \psi_{wf})$ versus t is made. The slope of the line is termed m''. Equation (4-29) may then be used to calculate the reservoir gas volume, V_p, or the reservoir limits, r_e.

Economic Limits Test

Although this test has been included under the heading of pseudo-steady state analysis, it is really a transient flow test in which the radius of investigation has not reached the reservoir boundaries. The minimum in-place gas volume required for economic exploitation is defined. The time required to conduct the test may then be estimated. This results in a minimization of flared gas, and a confirmation of in-place gas volumes and permeability-thickness.

NOTES TO CHAPTER 4

4N.1 Single-Rate Test

Analysis

In the transient flow regime, the flow behaviour resembles that from a well in an infinite reservoir with a constant skin.

Equations (2-143) and (2-144) may be combined to give

$$\Delta P_D \Big|_{well} \text{ (including skin and IT flow effects)} = P_t + s' \quad (4N-1)$$

For transient flow P_t is given by Equation (2-75) which may be substituted in Equation (4N-1) to give

$$\Delta p_D \bigg|_{well} = \frac{1}{2} (\ln t_D + 0.809) + s' \qquad (4N-2)$$

Equation (4N-2), with appropriate substitutions for the dimensionless terms from Table 2-3 and Table 2-4, may be rearranged as

$$\psi_i - \psi_{wf} = \frac{1.417 \times 10^6}{2} \frac{q_{sc} T}{k h} \left[\ln \left(\frac{2.637 \times 10^{-4} k t}{\phi \mu_i c_i r_w^2} \right) + 0.809 + 2 s' \right]$$

or

$$\psi_i - \psi_{wf} = 1.632 \times 10^6 \frac{q_{sc} T}{k h} \left[\log t + \log \left(\frac{k}{\phi \mu_i c_i r_w^2} \right) - 3.23 + 0.869 s' \right]$$

$$(4N-3)$$

A plot of $\Delta \psi$ ($= \psi_i - \psi_{wf}$) versus t on semilogarithmic coordinates will give a straight line of slope, m.

$$\therefore \quad k h = \frac{1.632 \times 10^6 q_{sc} T}{m} \qquad (4N-4)$$

Defining $\Delta \psi_1$ = value of $\Delta \psi$ at $t = 1$, obtained from the straight line (extrapolated, if necessary), and substituting these values in Equation (4N-3) gives

$$s' = 1.151 \left[\frac{\Delta \psi_1}{m} - \log \left(\frac{k}{\phi \mu_i c_i r_w^2} \right) + 3.23 \right] \qquad (4N-5)$$

4N.2 Multi-Rate Test

Analysis

For a multi-rate test, a well is flowed at a rate q_1 for time t_1. The flow rate is then changed to q_2 and flowed up to time t_2, that is, over the interval $(t_2 - t_1)$. This procedure may be repeated any number of times, say n.

During the first flow period, the pseudo-pressure drawdown at the well is given by Equation (4N-3) which may be written as

$$\psi_i - \psi_{wf} = 1.632 \times 10^6 \frac{q_1 T}{k\,h} \left[\log t + \log\left(\frac{k}{\phi\,\mu_i c_i r_w^2}\right) - 3.23 + 0.869\, s_1' \right]$$

$$\tag{4N-6}$$

During the second flow period, the pseudo-pressure drawdown at the well is given by the sum of the continuing effect of the first rate and the superposed effect of the change in rate. The principle of super-position in time, described in Chapter 2, Section 7.1, is applied to give, at any time during the second flow period,

$$\psi_i - \psi_{wf} = 1.632 \times 10^6 \frac{q_1 T}{k\,h} \left[\log t + \log\left(\frac{k}{\phi\,\mu_i\,c_i\,r_w^2}\right) - 3.23 \right]$$

$$+ 1.632 \times 10^6 \frac{(q_2 - q_1) T}{k\,h} \left[\log(t - t_1) + \log\left(\frac{k}{\phi\,\mu_i c_i r_w^2}\right) - 3.23 \right]$$

$$+ 1.632 \times 10^6 \frac{q_2 T}{k\,h} \left[0.869\, s_2' \right]$$

$$= 1.632 \times 10^6 \frac{q_1 T}{k\,h} \left[\log\left(\frac{t}{t - t_1}\right) + \frac{q_2}{q_1} \log(t - t_1) \right]$$

$$+ 1.632 \times 10^6 \frac{q_2 T}{k\,h} \left[\log\left(\frac{k}{\phi\,\mu_i c_i r_w^2}\right) - 3.23 + 0.869\, s_2' \right]$$

$$\tag{4N-7}$$

During the nth flow period, the pseudo-pressure drawdown at the well is obtained by a procedure similar to that given above for the second period. This includes a superposition of all the flow rates, up to and including the nth rate to give

$$\psi_i - \psi_{wf} = 1.632 \times 10^6 \frac{q_1 T}{k\,h} \left[\log t + \log\left(\frac{k}{\phi\,\mu_i\,c_i\,r_w^2}\right) - 3.23 \right]$$

$$+ 1.632 \times 10^6 \frac{(q_2 - q_1) T}{k\,h} \left[\log(t - t_1) + \log\left(\frac{k}{\phi\,\mu_i c_i r_w^2}\right) - 3.23 \right]$$

$$+ 1.632 \times 10^6 \frac{(q_3 - q_2) T}{k\,h} \left[\log(t - t_2) + \log \left(\frac{k}{\phi\, \mu_i c_i r_w^2} \right) - 3.23 \right]$$

$$\vdots$$

$$+ 1.632 \times 10^6 \frac{(q_n - q_{n-1}) T}{k\,h} \left[\log(t - t_{n-1}) + \log \left(\frac{k}{\phi\, \mu_i c_i r_w^2} \right) - 3.23 \right]$$

$$+ 1.632 \times 10^6 \frac{q_n T}{k\,h} \left[0.869\, s_n' \right] \tag{4N-8}$$

Equation (4N-8) may be written as:

$$\frac{\psi_i - \psi_{wf}}{q_n} = m' \sum_{j=1}^{n} \left[\frac{\Delta q_j}{q_n} \log\,(t - t_{j-1}) \right]$$

$$+ m' \left[\log \left(\frac{k}{\phi\, \mu_i\, c_i\, r_w^2} \right) - 3.23 + 0.869\, s_n' \right] \tag{4N-9}$$

where

$$m' = \frac{1.632 \times 10^6\, T}{k\,h}$$

$$\Delta q_j = q_j - q_{j-1}$$

$$t_0 = q_0 = 1$$

A plot of $(\psi_i - \psi_{wf})/q_n$ versus $\displaystyle\sum_{j=1}^{n} \frac{\Delta q_j}{q_n} \log\,(t - t_{j-1})$ on arithmetic coordinates will give a straight line of slope, m'.

$$\therefore\ k\,h = \frac{1.632 \times 10^6\, T}{m'} \tag{4N-10}$$

Defining

$\Delta \psi_0$ = value of $(\psi_i - \psi_{wf})/q_n$ corresponding to a value of zero on the abscissa, obtained from the straight line (extrapolated, if necessary).

Equation (4N-9) may be written as

$$s_n' = 1.151\left[\frac{\Delta\psi_0}{m'} - \log\left(\frac{k}{\phi\,\mu_i\,c_i\,r_w^2}\right) + 3.23\right] \qquad (4N-11)$$

4N.3 Two-Rate Test

Analysis

For a two-rate test, a well is flowed at a rate q_1 for time, t. The rate is then changed to q_2 and flowed for time Δt. The flow sequence is illustrated by Figure 4-6.

Prior to the rate change, that is, during the first flow period, the pseudo-pressure drawdown at the well is given by Equation (4N-3) which may be written as

$$\psi_i - \psi_{wf} = 1.632\times10^6\,\frac{q_1\,T}{k\,h}\left[\log t + \log\left(\frac{k}{\phi\,\mu_i c_i r_w^2}\right) - 3.23 + 0.869\,s_1'\right]$$

$$(4N-12)$$

During the second flow period, the pseudo-pressure drawdown at the well is given by the sum of the drawdown due to the continuing effect of the first rate and the drawdown due to the superposed effect of the change in rate. The principle of superposition in time, described in Section 7.1 of Chapter 2, may be applied to give, at any time during the second flow period,

$$\psi_i - \psi_{wf} = 1.632\times10^6\,\frac{q_1\,T}{k\,h}\left[\log(t+\Delta t) + \log\left(\frac{k}{\phi\,\mu_i c_i r_w^2}\right) - 3.23\right]$$

$$+ 1.632\times10^6\,\frac{(q_2-q_1)T}{k\,h}\left[\log\Delta t + \log\left(\frac{k}{\phi\,\mu_i c_i r_w^2}\right) - 3.23\right]$$

$$+ 1.632\times10^6\,\frac{q_2\,T}{k\,h}\left[0.869\,s_2'\right]$$

or,

$$\psi_i - \psi_{wf} = 1.632 \times 10^6 \frac{q_1 T}{k\,h} \left[\log\left(\frac{t+\Delta t}{\Delta t}\right) + \frac{q_2}{q_1} \log \Delta t \right]$$

$$+ 1.632 \times 10^6 \frac{q_2 T}{k\,h} \left[\log\left(\frac{k}{\phi\,\mu_i c_i r_w^2}\right) - 3.23 + 0.869\ s_2' \right]$$

$$(4N-13)$$

A plot of ψ_{wf} versus $\log\left(\dfrac{t+\Delta t}{\Delta t}\right) + \dfrac{q_2}{q_1} \log \Delta t$ on arithmetic coordinates will give a straight line of slope m

$$\therefore \quad k\,h = \frac{1.632 \times 10^6\ q_1\ T}{m} \qquad\qquad (4N-14)$$

Defining

$\psi_{wf\,0}$ = flowing sandface pseudo-pressure just prior to changing the flow rate

and

$\psi_{wf\,1}$ = flowing sandface pseudo-pressure at $\Delta t = 1$, obtained from the straight line (extrapolated, if necessary)

Equation (4N-12) may be written as

$$\psi_i - \psi_{wf\,0} = 1.632 \times 10^6 \frac{q_1 T}{k\,h} \left[\log t + \log\left(\frac{k}{\phi\,\mu_i c_i r_w^2}\right) - 3.23 + 0.869\ s_1' \right]$$

$$(4N-15)$$

and, Equation (4N-13) may be written as

$$\psi_i - \psi_{wf\,1} = 1.632 \times 10^6 \frac{q_1 T}{k\,h} \left[\log\ (t+1) + \frac{q_2}{q_1} \log 1 \right]$$

$$+ 1.632 \times 10^6 \frac{q_2 T}{k\,h} \left[\log\left(\frac{k}{\phi\,\mu_i c_i r_w^2}\right) - 3.23 + 0.869\ s_2' \right]$$

$$(4N-16)$$

Subtracting Equation (4N-16) from Equation (4N-15) gives

$$\psi_{wf_1} - \psi_{wf_0} = 1.632 \times 10^6 \frac{q_1 T}{k h} \left[\log \left(\frac{t}{t+1} \right) \right]$$

$$+ 1.632 \times 10^6 \frac{(q_1 - q_2) T}{k h} \left[\log \left(\frac{k}{\phi \mu_i c_i r_w^2} \right) - 3.23 \right]$$

$$+ 1.632 \times 10^6 \frac{T}{k h} \left[0.869 \, q_1 s_1' - 0.869 \, q_2 s_2' \right]$$

$$(4N-17)$$

Substituting Equation (4N-14) in Equation (4N-17) gives

$$\psi_{wf_1} - \psi_{wf_0} = m \log \left(\frac{t}{t+1} \right) + \frac{m(q_1 - q_2)}{q_1} \left[\log \left(\frac{k}{\phi \mu_i c_i r_w^2} \right) - 3.23 \right]$$

$$+ \frac{0.869 \, m}{q_1} (q_1 s_1' - q_2 s_2') \qquad (4N-18)$$

In Equation (4N-18), the first term on the right-hand side reduces to zero if $t \gg 1$ thereby making $\frac{t+1}{t} \approx 1.0$. Using this assumption, Equation (4N-18) may be rewritten as

$$q_1 s_1' - q_2 s_2' = \frac{(\psi_{wf_1} - \psi_{wf_0}) \, q_1}{0.869 \, m}$$

$$- \frac{(q_1 - q_2)}{0.869} \left[\log \left(\frac{k}{\phi \mu_i c_i r_w^2} \right) - 3.23 \right] \qquad (4N-19)$$

4N.4 Reservoir Limits Test

For pseudo-steady state flow, P_t is given by Equation (2-83) which may be substituted in Equation (4N-1) to give

$$\Delta p_D \Big|_{well} = \frac{2 \, t_D}{r_{eD}^2} + \ln r_{eD} - \frac{3}{4} + s' \qquad (4N-20)$$

Equation (4N-20), with appropriate substitutions for the dimensionless terms from Table 2-3 and Table 2-4, may be written as

$$\psi_i - \psi_{wf} = \frac{2348 \, q_{sc} \, T \, t}{\pi \, \phi \, \mu_i \, c_i \, r_e^2 \, h} + 1.417 \times 10^6 \, \frac{q_{sc} \, T}{k \, h} \left[\ln\left(\frac{r_e}{r_w}\right) - \frac{3}{4} + s' \right]$$

(4N-21)

Note that π is introduced into the first term on the right-hand side of Equation (4N-21) so that $\pi \phi r_e h$ represents the gas filled pore volume, V_p, of the reservoir. Equation (4N-21) may also be written as

$$\psi_i - \psi_{wf} = \frac{2348 \, q_{sc} \, T \, t}{\pi \, \phi \, \mu_i \, c_i \, r_e^2 \, h}$$

$$+ 3.263 \times 10^6 \, \frac{q_{sc} \, T}{k \, h} \left[\log\left(\frac{0.472 \, r_e}{r_w}\right) + \frac{s'}{2.303} \right]$$

(4N-22)

A plot of $\Delta\psi$ ($= \psi_i - \psi_{wf}$) versus t on arithmetic coordinates will give a straight line of slope m''.

$$\therefore \quad V_p = \pi \, \phi \, r_e^2 \, h = \frac{2348 \, q_{sc} \, T}{\mu_i \, c_i \, m''}$$

(4N-23)

4N.5 Effect of Reservoir/Well Geometry

For pseudo-steady state flow, P_t is given by Equation (2-133) which may be substituted in Equation (4N-1) to give

$$\Delta p_D \Big|_{well} = \frac{1}{2} \ln\left(\frac{4 \, A}{1.781 \, r_w^2 \, C_A}\right) + 2 \, \pi \, t_{DA} + s'$$

(4N-24)

Equation (4N-24), with appropriate substitution for t_{DA} from Equation (2-123) and for the dimensionless terms from Table 2-3 and Table 2-4 may be written as

$$\psi_i - \psi_{wf} = 1.632 \times 10^6 \, \frac{q_{sc} \, T}{k \, h} \left[\frac{4.58 \times 10^{-4} \, k \, t}{\phi \, \mu_i \, c_i \, A} \right]$$

$$+ \, 1.632 \times 10^6 \, \frac{q_{sc} \, T}{k \, h} \left[\log\left(\frac{2.246 \, A}{r_w^2 \, C_A} \right) + 0.869 \, s' \right]$$

$$(4N-25)$$

Equation (4N-25) may be simplified further to give

$$\psi_i - \psi_{wf} = \frac{747 \, q_{sc} \, T \, t}{\phi \, \mu_i \, c_i \, A \, h}$$

$$+ \, 1.632 \times 10^6 \, \frac{q_{sc} \, T}{k \, h} \left[\log\left(\frac{2.246 \, A}{r_w^2 \, C_A} \right) + 0.869 \, s' \right]$$

$$(4N-26)$$

CHAPTER 5   BUILD-UP TESTS

1   INTRODUCTION

Operationally, pressure build-up tests are the simplest of all gas well tests. The field conduct of such tests essentially involves a shut-in of the well being tested and subsequently monitoring the build-up of the bottom hole/wellhead pressure. Because of the absence of operational problems which are frequently associated with drawdown tests, like maintaining constant flow rates or preventing hydration in flow lines, a build-up test, properly conducted and interpreted, will usually give the most dependable results.

Build-up tests are often conducted as part of an annual pressure survey of a pool. The average pressure, resulting from a build-up analysis, reflects the remaining reserves. In high permeability reservoirs the pressure will build up to a stabilized value quickly, but in tight formations the pressure may continue to build up for months before stabilization is attained. Loss of production during a long shut-in may be intolerable economically. However, prohibitively long shut-in periods may be avoided when a proper analysis of the transient pressure-time data is possible. Such an analysis yields values of permeability, k, apparent skin factor, s', and the average reservoir pressure $\bar{p}_R$.

1.1   History

There are a few publications that form the core of pressure build-up analyses. These have resulted in three conventional methods of analysis, namely, the Horner plot, the Miller-Dyes-Hutchinson plot (often abbreviated as the MDH plot) and the Muskat plot.

Theis (1935), and later Horner (1951), showed that a plot of the shut-in pressure, p_{ws}, versus $\log (t + \Delta t/\Delta t)$ would result in a straight line for an infinite-acting reservoir. In the context of

build-up tests, t refers to the drawdown period prior to a build-up and Δt refers to the shut-in or build-up time. Matthews, Brons and Hazebroek (1954), abbreviated as MBH, extended the application of the Horner plot to finite reservoirs.

Miller, Dyes and Hutchinson (1950), and subsequently Perrine (1956), showed that if a well has been produced to pseudo-steady state flow conditions and then shut in, a plot of the shut-in pressure, p_{ws}, versus log Δt will give a straight line.

Muskat (1936), Larson (1963) and Russell (1966) stated that a plot of log $(\bar{p}_R - p_{ws})$ versus Δt would, under certain circumstances, give a straight line.

Up until recently, the validity and ranges of application of these three different plots had not been clearly established and a certain degree of confusion still exists in the petroleum industry. There is a general belief that the Horner plot is good for new wells in new reservoirs, whereas the MDH plot is valid for old wells in old reservoirs. This is definitely a misconception. In an excellent review of the various methods of analysis, Ramey and Cobb (1971) studied the build-up behaviour of a well in the centre of a closed, square drainage area over a large range of flowing and shut-in time periods. They defined the ranges of validity of each of the above methods and concluded that the Horner plot was generally more useful than the Muskat or MDH plots. Cobb and Smith (1974) extended this approach to reservoirs of other shapes. Consequently, the Horner plot and its extension by Matthews, Brons and Hazebroek, henceforth referred to as the Horner-MBH plot, is adopted in this manual as the standard build-up analysis procedure. For topical interest, however, the other methods and their extensions are also discussed.

In addition to the above-mentioned publications, there have been several other studies related to the various aspects of build-up testing and analysis. Some of these are incorporated in the following sections.

2 FUNDAMENTAL RELATIONSHIPS

In the conduct and analysis of build-up tests, it is very important to bear in mind that a build-up is always preceded by a drawdown, and also that the build-up data are directly affected by this drawdown. Ideally, the drawdown starts from a stabilized reservoir condition represented by the stabilized reservoir pressure, p_i. At a time, t, the well is shut-in and the build-up is continued for a time, Δt.

As in Chapters 3 and 4, the reservoir is idealized by making the assumptions (1) to (5) in Chapter 3, Section 2.2. Under these conditions, the behaviour of the static sandface pressure, p_{ws}, is depicted in Figure 5.1
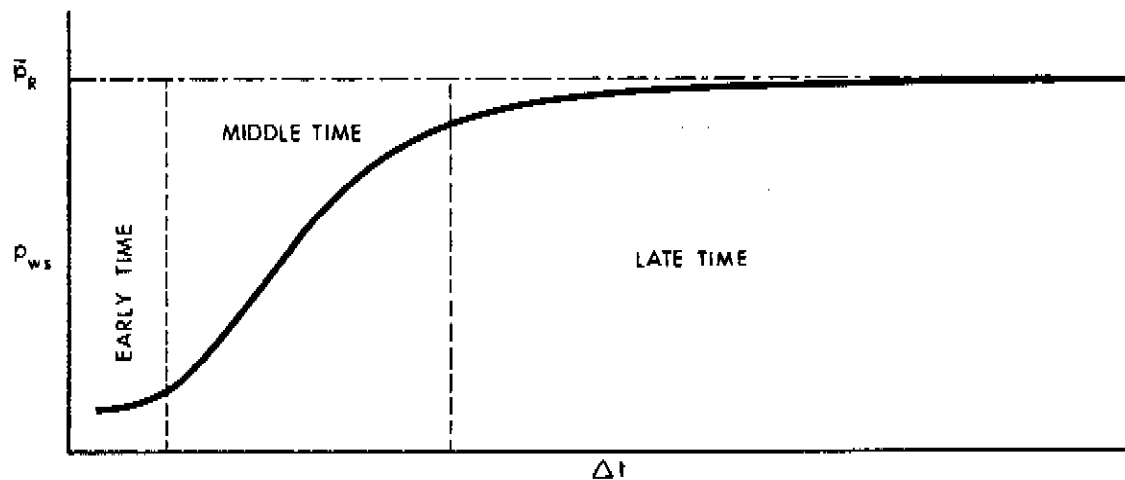
FIGURE 5-1. BEHAVIOUR OF THE STATIC SANDFACE PRESSURE UPON SHUT-IN OF A WELL

The early-time portion reflects the wellbore storage (after flow) and apparent skin effects. Wellbore storage results from closing the well at the surface instead of at the sandface. Production continues from the formation into the wellbore for some time after the flow at the surface has been stopped. In low-permeability gas-condensate reservoirs,

wellbore storage should be avoided and it is usually imperative to use a bottom hole shut-in tool (Dykstra, 1961). Skin effects result from wellbore damage, the nature of completion of the well and from IT flow.

The data that fall in the middle-time region constitute the most useful part of a build-up test. The previously mentioned plots, Horner-MBH, and the MDH, utilize these data to obtain a straight line plot on semilogarithmic coordinate graph paper. The permeability thickness, kh, is deduced from these semilog straight lines. Early-time data must be excluded from such plots. Wattenbarger and Ramey (1968) investigated the effects of turbulence, well damage, and wellbore storage and in every case found that the proper straight line was obtained following early-time deviations.

Late-time data are usually marked by a deviation from the semilog straight line of the middle-time region. This deviation reflects the effects of boundaries. If the shut-in period is sufficiently long, the final pressure attained, called the stabilized shut-in pressure, is in fact the average pressure of the reservoir volume being drained.

Conceptually, a build-up is treated as the result of two superposed effects. The principle of superposition in time is described in Chapter 2, Section 7.1. The application of this principle to the analysis of build-up tests is quite simple. The drawdown at a rate, q, prior to the build-up, is assumed to continue for all time, $t + \Delta t$, but at the time of shut-in, t, a drawdown at a rate, -q, is initiated. The net effect of a negative rate, or injection, is to simulate a flow rate of zero, which is the shut-in condition. Hence, at any shut-in time, Δt, the pressure behaviour at the well will be the sum of two effects, that due to a flow rate q for a time $(t + \Delta t)$, and that due to a flow rate -q for a time Δt. This treatment is identical to that for a two-rate drawdown test, Chapter 4, Section 4.2, with the second rate, q_2, taken equal to zero.

2.1 Type Curves and Desuperposition

The type curves given in Chapter 2, Section 10 and the related limitations discussed in Chapter 4, Section 2.4 are also applicable to the analysis of build-up tests. Even though type curve matching techniques are not discussed fully in this chapter, the implications of this powerful, yet simple analytical tool, must not be ignored. As shown in Example 4-1, type curve matching provides a simple method for determining the time-of-start of transient flow during drawdown tests. A similar approach may be used to determine the time-of-start of semilog straight line data in build-up tests with one additional step. Since a build-up is always preceded by a drawdown, the build-up data must be "desuperposed" before attempting a type curve match. Towards this end, the method of desuperposition is described. It may be noted that desuperposition can also be performed on the second rate of a two-rate test, as has been indicated in the discussion of Example 4-2.

Desuperposition

Consider the flow sequence of a build-up test. It is exactly the same as that for a two-rate test (Chapter 4, Section 4.2) with $q_1 = q_{sc}$ and $q_2 = 0$.

The "measured" pressure drawdown during the flow period preceding the build-up is plotted on a data plot for type curve matching (see Example 4-1). At this time it will be assumed that an appropriate type curve is available and also that a successful match can be made. The data plot can then be extrapolated, by tracing the type curve, beyond time, t, to predict the "future" behaviour if rate q_1 were continued. If the actual test data obtained during the shut-in period are plotted on the same data plot, they represent the following super-posed effects, namely, the continued effect of the flow rate, q_{sc}, and the added effect of the change in rate $(0 - q_{sc})$. By subtracting (desuperposing) the effect of rate q_{sc} from the above total effects, the effect of a single rate of magnitude $(0 - q_{sc})$ is obtained. This desuperposed effect may be considered to be a single-rate drawdown and

may be analyzed as such. It must be remembered that these desuperposed single-rate data are for an effective flow rate $(0 - q_{sc})$, and that $\Delta t = 0$ when the rate is changed. This procedure is illustrated by Figure 5-2 and Example 5-1.
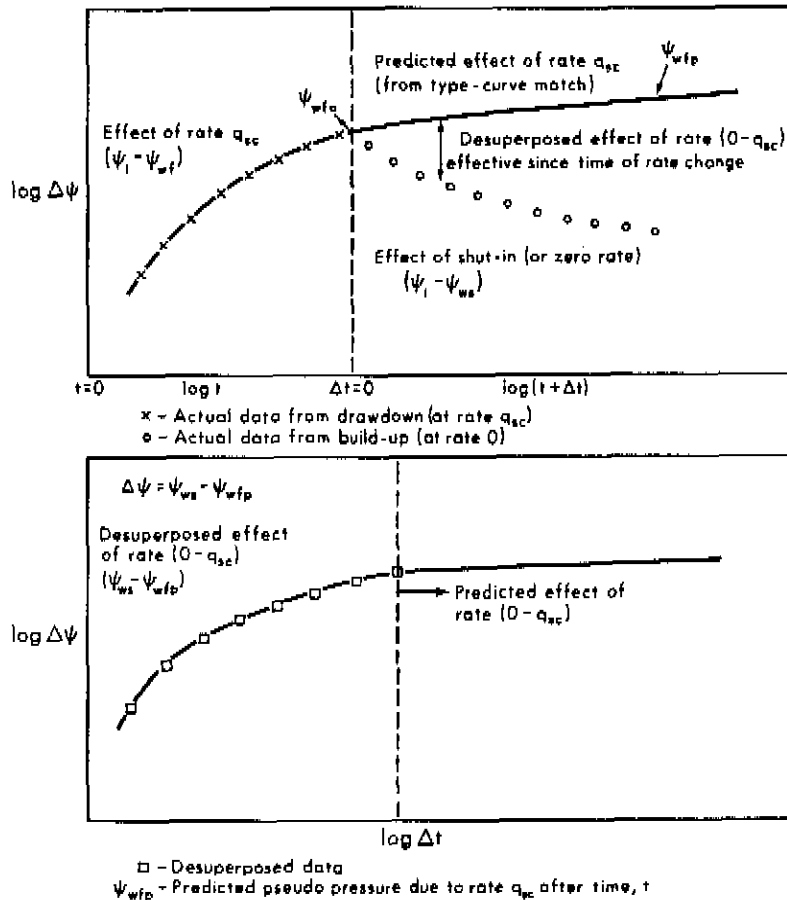
FIGURE 5-2. DATA PLOT FOR ACTUAL AND DESUPERPOSED EFFECTS
OF A DRAWDOWN FOLLOWED BY A BUILD-UP

An examination of Figure 5-2 reveals two important considerations that frequently limit the use and application of type curve matching for determining the time-of-start of the build-up semilog straight line.

1. In drawing Figure 5-2 it is assumed that a unique match is available, in effect implying that values can be obtained for ψ_{wfp}. This is not usually the case, and hence rigorous desuperposition is often not

possible through type curve matching. However, a simplification that is
of practical use has been suggested by Raghavan, Cady and Ramey (1972)
based on a publication by Agarwal, Al-Hussainy and Ramey (1970). They
have shown that under certain conditions, early-time data obtained during
a build-up may be desuperposed by assuming ψ_{wfp} to be constant at a value
ψ_{wf_0} (equivalent to the flowing pressure just prior to shut-in). However,
this analysis may extend for a shut-in time no greater than ten per cent
of the initial flow period. Needless to say, such an application is of
much interest in the analysis of early-time data (Chapter 7) but its use
in this chapter which involves the analysis of middle-time data is
questionable. In the context of transient pressure analysis, however,
it is very useful in determining the approximate time-of-start of
semilog data.

2. Because of the log-log nature of the type curves, equal
time intervals are much more crowded at later times than at earlier
times. For example, a nine-hour interval spans a much larger portion of
the abscissa for a time period of one to ten hours as compared to say,
sixty-one to seventy hours. This means that in order that the type
curves can be used effectively, the build-up periods should be
considerably longer than the initial flow period. This may be so
inconvenient, for example considering the lost production time, as to
render impractical the use of the described desuperposition procedure.

3 TESTS UTILIZING EARLY-TIME DATA

A rigorous analysis of early-time data may yield adequate
approximations of kh as will be shown in Chapter 7. Such an analysis
may be necessary only when middle-time data are not available. As
mentioned in the previous section, a desuperposition of build-up data
can give the equivalent of a drawdown plot and may be analyzed as such.
Consequently, the discussions related to the early-time flow regime in
Chapter 4, Section 2.1 generally apply to build-up tests as they do to
drawdown tests.

4 TESTS UTILIZING MIDDLE-TIME AND LATE-TIME DATA

In Chapter 4, Sections 2.1, 2.2 and 2.4 it has been shown that early-time data may be used to determine the time-of-start of transient flow data. A similar analysis applies to the early-time portion of a build-up. Data should be obtained, whenever possible, in the transient flow regime since reservoir parameters calculated by an analysis of middle-time data are much more reliable than those calculated from early-time data.

Data obtained from a properly conducted build-up test that follows either a single-rate or a two-rate drawdown test, and in some cases also a variable-rate drawdown, may be analyzed to yield reliable values of kh, s' and $\bar{p}_R$. The pressure build-up behaviour during the middle-time period is analogous to the transient flow period during a drawdown test. In other words, the reservoir is infinite-acting and boundaries do not affect the pressure-time data.

The analysis of middle-time data also yields a semilog straight line which should not be confused with the semilog straight line for a drawdown test. As will be seen below, this straight line, when extrapolated, yields values of an apparent reservoir pseudo-pressure, ψ^*, corresponding to p^*, which is subsequently used to calculate the average reservoir pseudo-pressure, $\bar{\psi}_R$, corresponding to the average reservoir pressure, $\bar{p}_R$.

4.1 Behaviour of Infinite-Acting Reservoirs

When the early-time effects become negligible, the pressure-time behaviour is that of a well producing at a zero flow rate from an infinite reservoir. As mentioned previously, a build-up is always preceded by a drawdown. Consider the simplest case of a single-rate drawdown conducted prior to the build-up.

During the drawdown period, the flowing sandface pressure is given by Equation (4-5) reproduced below.

$$\psi_i - \psi_{wf} = 1.632 \times 10^6 \frac{q_{sc} T}{k\ h} \left[\log t + \log \left(\frac{k}{\phi\ \mu_i\ c_i\ r_w^2} \right) - 3.23 + 0.869\ s' \right]$$

$$(5-1)$$

If the well is shut-in at time t, and allowed to build up for a time Δt, the effect of the shut-in may be obtained by the superposition of two effects. During the shut-in period, the static sandface pressure is given by the sum of the continuing effect of the drawdown rate, q_{sc}, and the superposed effect of the change in rate $(0 - q_{sc})$, and is represented by

$$\psi_i - \psi_{ws} = 1.632 \times 10^6 \frac{q_{sc} T}{k\ h} \left[\log(t + \Delta t) + \log \left(\frac{k}{\phi\ \mu_i\ c_i\ r_w^2} \right) - 3.23 \right]$$

$$+ 1.632 \times 10^6 \frac{(0 - q_{sc})T}{k\ h} \left[\log \Delta t + \log \left(\frac{k}{\phi\ \mu_i\ c_i\ r_w^2} \right) - 3.23 \right]$$

$$(5-2)$$

Note that the apparent skin, s', should not be superposed in time since it is a function only of the existing flow rate. However, if turbulence effects are negligible, $s' = s$ and even though it is incorrect to introduce a skin term in Equation (5-2), such a term, if introduced in Equation (5-2), will not affect the slope of the semilog plot.

The first term on the right-hand side of Equation (5-2) represents the effect due to the drawdown at a rate q_{sc} for a time $(t + \Delta t)$. The second term is the effect of the change in rate from q_{sc} to 0 for a time Δt. Combining these terms and simplifying Equation (5-2) gives

$$\psi_i - \psi_{ws} = 1.632 \times 10^6 \frac{q_{sc} T}{k\ h} \log \left(\frac{t + \Delta t}{\Delta t} \right) \qquad (5-3)$$

This relationship represents the commonly used Horner plot. It is obvious from this equation that a plot of ψ_{ws} versus $(t + \Delta t)/\Delta t$ on

semilogarithmic coordinates will give a straight line of slope, m, from which

$$k \, h \; = \; \frac{1.632 \times 10^6 \, q_{sc} \, T}{m} \tag{5-4}$$

A build-up plot for an infinite reservoir is shown in Figure 5-3(a). A commonly used alternative plot is shown in Figure 5-3(b) in which the time axis increases from the left to the right. In this manual Figure 5-3(a) is adopted as the standard build-up plot. It must be noted that in all semilog plots, representing drawdown or build-up tests, only the magnitude and not the sign of the slope is considered.

Defining ψ_{wf_0} as the pseudo-pressure just before shut-in, Equation (5-1) may be written as

$$\psi_i - \psi_{wf_0} = 1.632 \times 10^6 \, \frac{q_{sc} \, T}{k \, h} \left[\log t + \log \left(\frac{k}{\phi \, \mu_i \, c_i \, r_w^2} \right) - 3.23 + 0.869 \, s' \right]$$

$$\tag{5-5}$$

Subtracting Equation (5-3) from Equation (5-5) gives

$$\psi_{ws} - \psi_{wf_0} = m \left[\log \frac{t \; \Delta t}{t + \Delta t} + \log \left(\frac{k}{\phi \, \mu_i \, c_i \, r_w^2} \right) - 3.23 + 0.869 \, s' \right]$$

$$\tag{5-6}$$

Defining ψ_{ws_1} as the pseudo-pressure at $\Delta t = 1$, and assuming $\frac{t}{t+1} \simeq 1$, Equation (5-6) may be simplified to give

$$s' = 1.151 \left[\frac{\psi_{ws_1} - \psi_{wf_0}}{m} - \log \left(\frac{k}{\phi \, \mu_i \, c_i \, r_w^2} \right) + 3.23 \right] \tag{5-7}$$

Noting that ψ_{ws_1} should be obtained from the straight-line portion (extrapolated, if necessary) of the Horner plot, Equation (5-7) may be used to calculate s'. There is no way of separating s' into its components s and Dq_{sc} from a single build-up test. However, if another
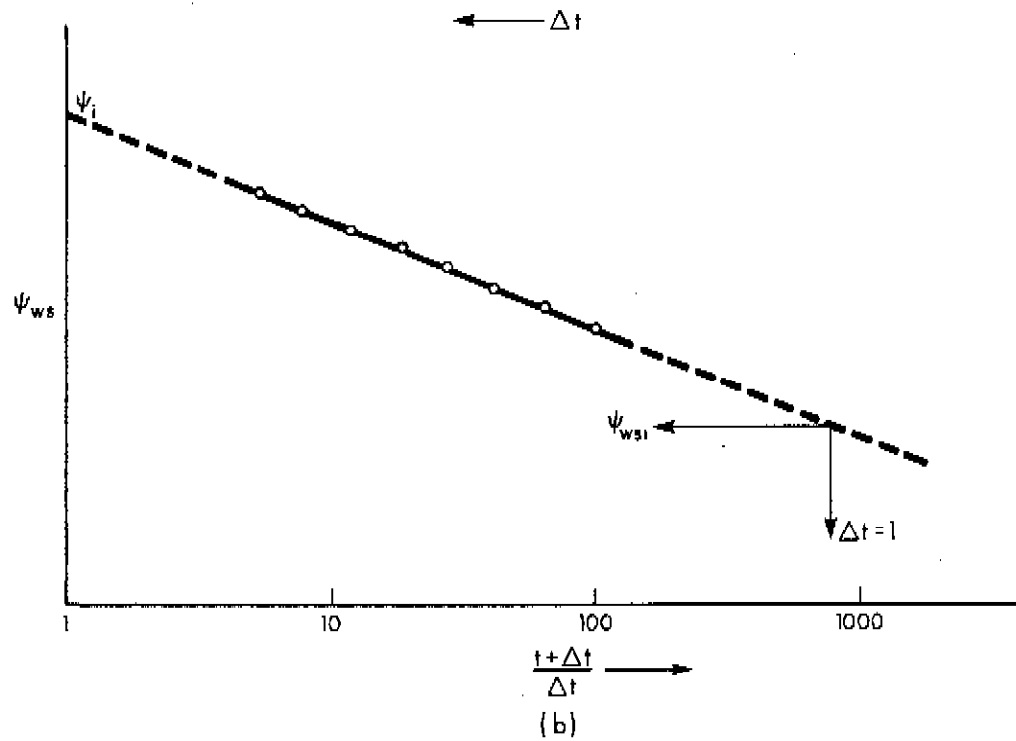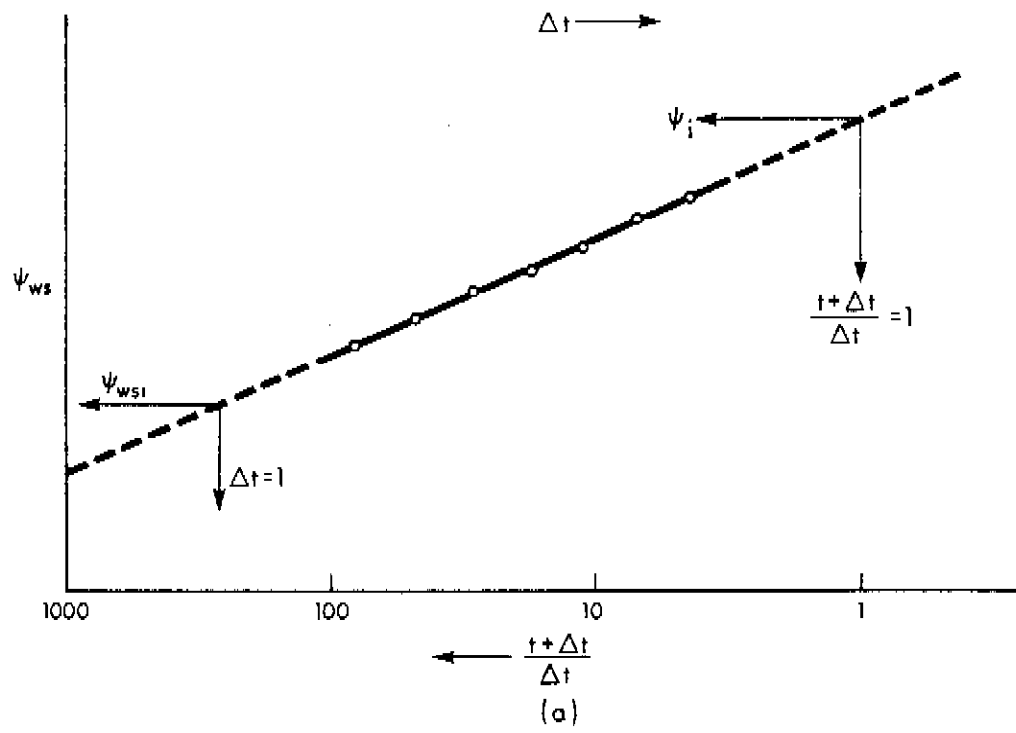
FIGURE 5-3. BUILD-UP SEMILOG PLOTS — INFINITE RESERVOIR

build-up is conducted following a substantially different single-rate drawdown, a different value of s' is obtained. The two different values of s' may be used with Equations (4-8) and (4-9) to calculate s and D separately.

The use of a Horner plot to calculate kh and s' is illustrated in Example 5-1.

EXAMPLE 5-1

Introduction   The pressure-time data from a build-up test following a single-rate drawdown are analyzed to give the reservoir parameters kh and s'. As shown in a later section, a build-up test may also be conducted and analyzed following a two-rate drawdown test.

The method of desuperposition described in Section 2.1 is also illustrated.

Problem   The single-rate drawdown test of Example 4-1 was followed by a build-up test. The pressure, p_1, throughout the reservoir prior to the test was 3732 psia. The well in a bounded reservoir was produced at a constant rate of 5.65 MMscfd for 120.53 hours. The well was shut-in for 49.87 hours during which time the pressure build-up was monitored continuously. The pressure just prior to shut-in was 3295 psia. General data pertinent to the test are given below. The pressure-time data are also tabulated, and are given directly in the solution to this problem. From a recombined gas analysis:

$$G = 0.68 \qquad P_c = 693 \text{ psia} \qquad T_c = 376^{O}R$$

$$H_2S = 1.28\% \qquad CO_2 = 4.11\% \qquad N_2 = 0.10\%$$

$$\mu_i = 0.0208 \text{ cp} \qquad c_i = 0.00022 \text{ psia}^{-1}$$

Well/reservoir data:

$$T = 673^{O}R \qquad h = 20 \text{ ft} \qquad r_e = 2640 \text{ ft}$$

$$\phi = 0.10 \qquad r_w = 0.29 \text{ ft}$$

Calculate the permeability, k, of the reservoir and the apparent skin factor, s'.

<u>Solution</u> The $\psi - p$ curve, shown in Figure 4-3, is applicable to this problem.

$$p \quad = \quad 3732 \quad \leftrightarrow \quad \psi = 872.70 \times 10^6 \qquad \text{(Figure 4-3)}$$

$$\therefore \quad \psi_i \quad = \quad 872.70 \times 10^6 \text{ psia}^2/\text{cp}$$

$$p \quad = \quad 3295 \quad \leftrightarrow \quad \psi = 709.77 \times 10^6 \qquad \text{(Figure 4-3)}$$

$$\psi_{wf_0} \quad = \quad 709.77 \times 10^6 \text{ psia}^2/\text{cp}$$

$$t \quad = \quad 120.53 \text{ hr.}$$

Using the above values of t and ψ_{wf_0}, the following tabulations may be made:

Δt (hr)	$\dfrac{t + \Delta t}{\Delta t}$	P_{ws} (psia)	ψ_{ws} (psia^2/cp$\times 10^{-6}$)	$\Delta \psi = \psi_{ws} - \psi_{wf_0}$ (psia^2/cp$\times 10^{-6}$)
.53	228.42	3296	710.14	0.37
1.33	91.62	3296	710.14	0.37
1.60	76.33	3385	742.69	32.92
2.13	57.59	3521	793.09	83.32
2.67	46.14	3547	802.81	93.04
3.20	38.67	3562	808.43	98.66
3.73	33.31	3573	812.56	102.79
4.27	29.23	3582	815.94	106.17
4.80	26.11	3591	819.32	109.55
5.33	23.61	3599	822.33	112.56
5.87	21.53	3605	824.59	114.82
6.40	19.83	3609	826.10	116.33
6.93	18.39	3614	827.98	118.21
7.47	17.14	3619	829.86	120.09
8.00	16.07	3623	831.37	121.60

9.07	14.29	3630	834.01	124.24
9.87	13.21	3634	835.52	125.75
10.93	12.03	3640	837.79	128.02
12.00	11.04	3644	839.30	129.53
13.60	9.86	3650	841.57	131.80
14.67	9.22	3654	843.08	133.31
16.53	8.29	3660	845.35	135.58
18.67	7.46	3664	846.87	137.10
21.33	6.65	3668	848.38	138.61
24.53	5.91	3672	849.90	140.13
29.33	5.11	3676	851.41	141.64
35.73	4.37	3684	854.45	144.68
45.87	3.63	3688	855.97	146.20
49.87	3.42	3691	857.10	147.33

The last column in the above tabulations is useful only in some instances. As indicated in Section 2.1, an approximate desuperposition of build-up data may be done for a build-up time extending up to ten per cent of the drawdown time. However, an examination of the log-log plot of the drawdown data (Figure 4-4) shows a very small increase in the predicted drawdown over the interval 120 hours to 170 hours. Hence the approximation $\psi_{wfp} = \psi_{wf_0}$ is extended over the entire build-up interval. The purpose of this desuperposition is to define, by type curve matching, the time-of-start of middle-time data. Once the build-up data have been desuperposed, the method used is similar to that for drawdown tests (Example 4-1).

Step 1: Plot $\Delta\psi$ versus Δt on 3×5 log-log graph paper (of the same size as the type curves of Chapter 2) as shown in Figure 5-4.

Step 2: A match of the above desuperposed build-up data plot with the type curve $s = 0$, $C_{sD} = 0$ of Figure 2-22 indicates the time-of-start of the middle-time (or Horner semilog straight line) data is approximately 15.0 hours.

Step 3: Plot ψ_{ws} versus $\log (t + \Delta t)/\Delta t$ and draw the best straight line through the semilog straight line data, identified in Step 2, as shown in Figure 5-5.

From the straight line of Figure 5-5

$$m = \frac{(873.0 - 842.5) \times 10^6}{\log 10 - \log 1} = 30.5 \times 10^6$$

$$\psi_{ws1} = 809.0 \times 10^6$$

From Equation (5-4)

$$k\,h = \frac{1.632 \times 10^6\, q_{sc}\, T}{m}$$

$$= \frac{(1.632 \times 10^6)(5.65)(673)}{30.5 \times 10^6} = 203.5\ \text{md·ft}$$

$$k = \frac{203.5}{20} = 10.2\ \text{md}$$

From Equation (5-7)

$$s' = 1.151 \left[\frac{\psi_{ws1} - \psi_{wf0}}{m} - \log\left(\frac{k}{\phi\,\mu_1\,c_1\,r_w^2}\right) + 3.23 \right]$$

$$= 1.151 \left[\frac{(809.0 - 709.77) \times 10^6}{30.5 \times 10^6} \right.$$

$$\left. - \log \frac{10.2}{(0.10)(0.0208)(0.00022)(0.29)^2} + 3.23 \right]$$

$$= -2.2$$

Discussion   The values of k and s' calculated from the build-up analysis agree very well with those from the drawdown analysis of Example 4-1. For this test, both the drawdown (Example 4-1) and the build-up were in the transient flow regime, that is, the reservoir was infinite-acting. This is a reasonable supposition for a well in a new reservoir, or where the combined drawdown and build-up time (t + Δt) is less than the time to stabilization.   (t + Δt) for this test was only 170.40 hours (120.53 + 49.87) while the time to stabilization, estimated from
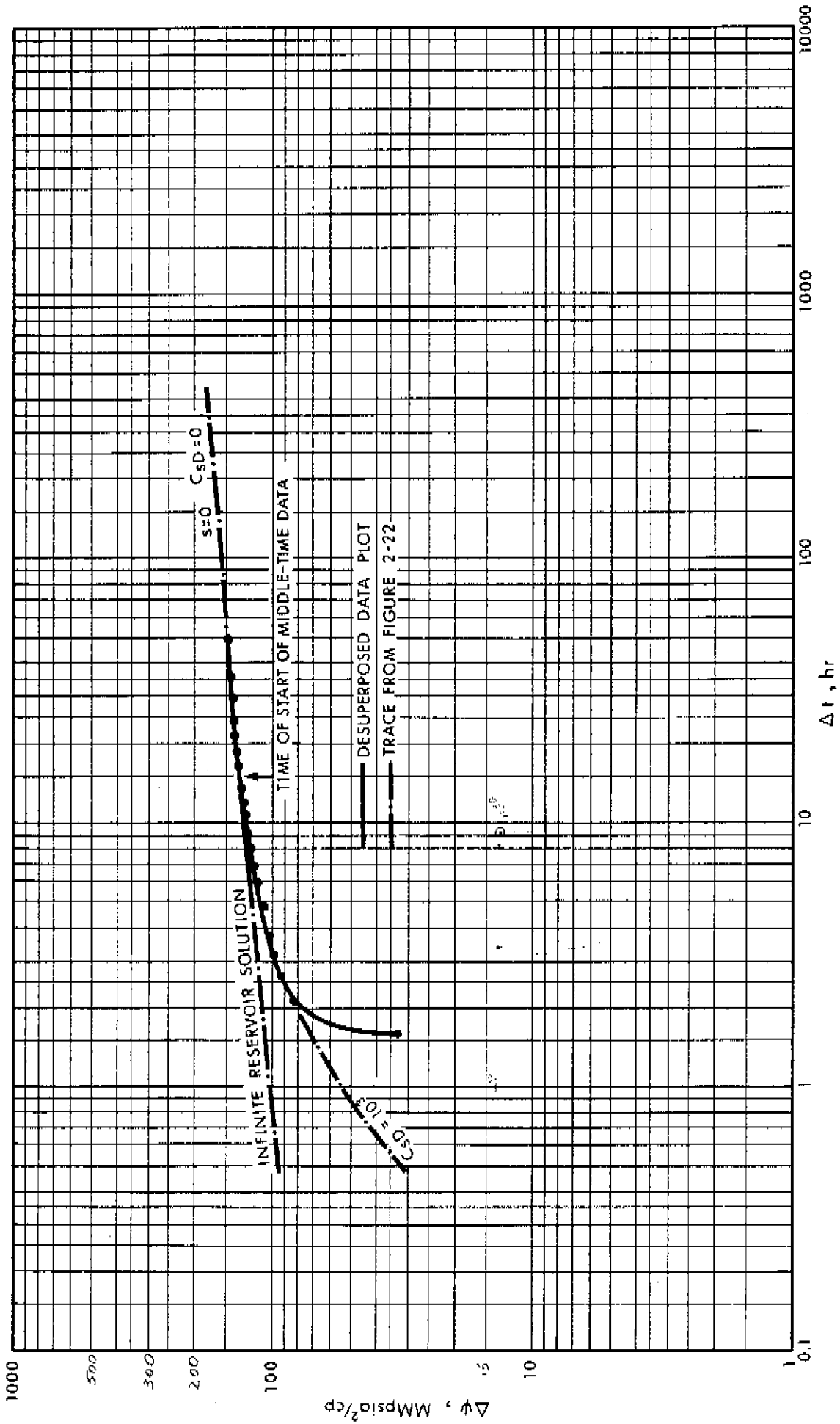
FIGURE 5-4 TYPE CURVE MATCH FOR THE DESUPERPOSED BUILD-UP DATA OF EXAMPLE 5-1
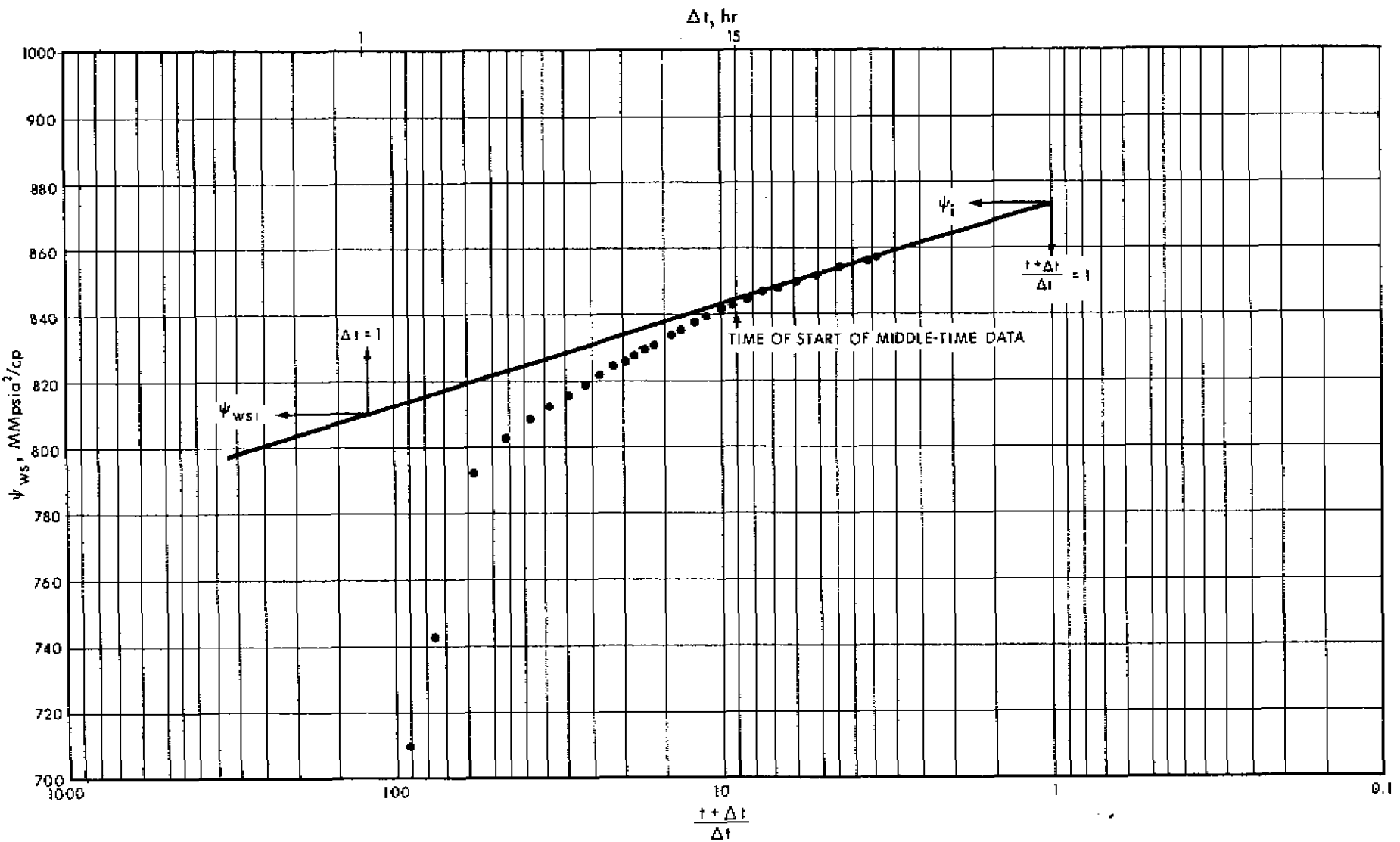
FIGURE 5-5. HORNER BUILD-UP PLOT FOR EXAMPLE 5-1

Equation (3-14), is approximately 380.0 hours.

As shown in later sections of this chapter, the semilog straight line analysis applies only to data in the transient or middle-time region. Consequently, the duration of the drawdown prior to the build-up has a significant effect on the build-up analysis.

Extrapolation of the Horner Plot

For an infinite-acting reservoir, in which the depletion due to the drawdown is assumed to be negligible, extrapolation of the semilog straight line yields the initial pseudo-pressure, ψ_i. This follows simply from Equation (5-3). At large shut-in times, $(t + \Delta t)/\Delta t \simeq 1$, which on substitution in Equation (5-3) gives $\psi_{ws} = \psi_i$. This is illustrated by Example 5-1. The Horner plot (Figure 5-5), when extrapolated to $\frac{t + \Delta t}{\Delta t} \approx 1$, yields a value of $\psi_i = 873.0 \times 10^6$ psia^2/cp which corresponds to an initial pressure $p_i = 3733$ psia. In gas well testing, the reservoir pressure can sometimes be allowed to build up to its final value. However, in many instances the time required for a complete build-up may be too large, in which case an extrapolation becomes necessary.

For finite reservoirs, an extrapolation of the semilog straight line to $(t + \Delta t)/\Delta t = 1$ yields a value of ψ^*, defined in Chapter 2, Section 7.4. In such cases the average reservoir pressures may be calculated using the value of ψ^* obtained from a Horner plot and the methods described below.

4.2   Finite Reservoir Behaviour

When boundary effects become significant, Equation (5-3) no longer applies. As shown in Chapter 2, Section 7-4, flow from a finite reservoir may be represented by Equation (2-125), in the absence of skin and IT flow effects.

Equation (2-125) may be written in terms of pseudo-pressure with appropriate substitutions for dimensionless quantities, and including an apparent skin factor, s', as

$$\psi_i - \psi_{wf} = 1.632 \times 10^6 \frac{q_{sc} T}{k h} \left[\log t + \log \left(\frac{k}{\phi \mu_i c_i r_w^2} \right) - 3.23 \right.$$

$$\left. + \frac{4 \pi t_{DA}}{2.303} - \frac{F}{2.303} + 0.869 s' \right] \qquad (5-8)$$

Superposition of a build-up on the drawdown then gives

$$\psi_i - \psi_{ws} = 1.632 \times 10^6 \frac{q_{sc} T}{k h} \left[\log \left(\frac{t + \Delta t}{\Delta t} \right) + \frac{4 \pi t_{DA}}{2.303} \right.$$

$$\left. - \frac{1}{2.303} \left(F \big|_{t + \Delta t} - F \big|_{\Delta t} \right) \right] \qquad (5-9)$$

for $\Delta t \ll t$ $\quad F \big|_{\Delta t} \simeq 0 \quad\quad F \big|_{t + \Delta t} \simeq F \big|_t$

Equation (5-9), for $\Delta t \ll t$, then becomes

$$\psi_i - \psi_{ws} = 1.632 \times 10^6 \frac{q_{sc} T}{k h} \left[\log \frac{t + \Delta t}{\Delta t} + \frac{4 \pi t_{DA}}{2.303} - \frac{F \big|_t}{2.303} \right]$$

$$(5-10)$$

Equation (5-10), which applies for small values of Δt, shows that a plot of ψ_{ws} versus $\log (t+\Delta t/\Delta t)$ gives, initially, a straight line of slope m. However, unlike the infinite reservoir case, the extrapolation to $(t + \Delta t)/\Delta t = 1$ does not result in a value for ψ_i. The extrapolated value is called ψ^*.

A typical build-up plot for a finite reservoir is illustrated by Figure 5-6.

Average Reservoir Pressure from
 MBH Curves

The average reservoir pressure for a bounded reservoir may be calculated as shown below using the values of m and ψ^*, obtained from the Horner plot, and the MBH curves.

From Equation (5-10) for $(t + \Delta t)/\Delta t \simeq 1.0$
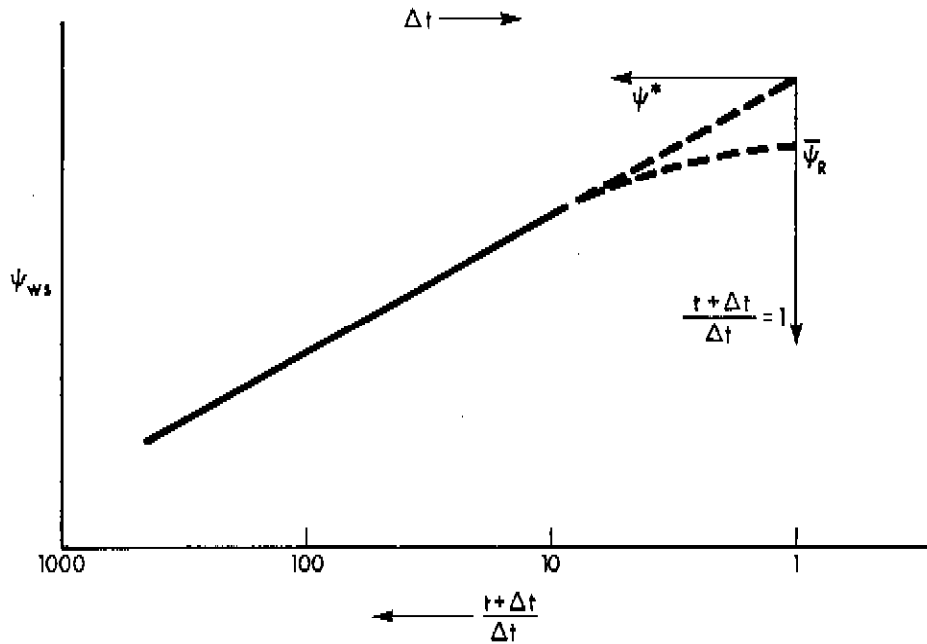
FIGURE 5-6. BUILD-UP SEMILOG PLOT ———— FINITE RESERVOIR

$$\psi_i - \psi^* = 1.632 \times 10^6 \; \frac{q_{sc} \; T}{k \; h} \left[\frac{4 \; \pi \; t_{DA}}{2.303} - \frac{F}{2.303} \right] \tag{5-11}$$

where

$$t_{DA} = \frac{2.637 \times 10^{-4} \; k \; t}{\phi \; \mu_i \; c_i \; A} \tag{5-12}$$

Equation (5-11) is the defining equation for ψ^* and is equivalent to Equation (2-127).

The material balance, Equation (2-94), may be written in terms of ψ with appropriate substitutions for dimensionless quantities as

$$\psi_i - \bar{\psi}_R = 1.632 \times 10^6 \; \frac{q_{sc} \; T}{k \; h} \left(\frac{4 \; \pi \; t_{DA}}{2.303} \right) \tag{5-13}$$

Subtracting Equation (5-11) from Equation (5-13) gives

$$\psi^* - \bar{\psi}_R = m \frac{F}{2.303} \qquad (5\text{-}14)$$

or

$$\bar{\psi}_R = \psi^* - \frac{m}{2.303} F \qquad (5\text{-}15)$$

Equation (5-15), which is equivalent to Equation (2-129), may be used to calculate the average reservoir pressure for a finite reservoir.

m is obtained as illustrated by Example 5-1 while ψ^* is the value of ψ_{ws} corresponding to $(t+\Delta t)/\Delta t \simeq 1$ from the extrapolated semilog straight line.

F, which is the MBH dimensionless pressure function, may be obtained from Figures C-1(a) to (g) corresponding to the appropriate well/reservoir configuration and reservoir shape. In using these figures, values of t_{DA} may be calculated from Equation (5-12). If the MBH figures do not provide a particular configuration, F may be calculated for the limiting cases either from Equation (2-130) or from Equation (2-131), whichever is appropriate.

The procedure described above is applicable if t_{DA} can be calculated from a knowledge of k, ϕ, μ_i, c_i, and A. If, however, all of these parameters are not known, an alternate method described by Odeh and Al-Hussainy (1971) may be used to calculate $\bar{\psi}_R$.

The method described by Odeh and Al-Hussainy (1971) requires a knowledge of ψ_i. Details of the method may be obtained from their paper, but a brief description is given below.

Equation (5-13) may be written as

$$t_{DA} = \frac{2.303}{4\pi m} (\psi_i - \bar{\psi}_R) \qquad (5\text{-}16)$$

Substituting Equation (5-16) in Equation (5-11) and rearranging gives

$$\frac{\psi_i - \psi^*}{m} = \frac{\psi_i - \bar{\psi}_R}{m} - \frac{F}{2.303} \qquad (5\text{-}17)$$

Equation (5-17) may also be obtained by rearranging Equation (5-15).

A graphical solution is then necessary. A number of values are assumed for $(\psi_i - \bar{\psi}_R)/m$. Corresponding values of t_{DA} are calculated from Equation (5-16). The appropriate MBH curve, Figures C-1(a) to C-1(g), is chosen and values for F are obtained for the calculated values of t_{DA}. Equation (5-17) is then used to calculate $(\psi_i - \psi^*)/m$. A plot is made of $(\psi_i - \bar{\psi}_R)/m$ versus $(\psi_i - \psi^*)/m$. Odeh and Al-Hussainy (1971) have prepared such plots corresponding to a few of the MBH dimensionless pressure functions. Since ψ_i is known and ψ^* and m can be obtained from the Horner plot, $(\psi_i - \bar{\psi}_R)/m$ is easily obtained from the above plot. Hence $\bar{\psi}_R$ can be calculated.

The methods described above, that is, the Horner-MBH plot and the extension by Odeh and Al-Hussainy, involve an extrapolation of the Horner straight line to $(t + \Delta t)/\Delta t = 1$ and the use of an apparent pseudo-pressure, ψ^*. Ramey and Cobb (1971) have described a method for directly calculating $\bar{\psi}_R$ from a Horner plot. This method involves the simultaneous solution of Equation (5-10) and Equation (5-13) for the value of $(t + \Delta t)/\Delta t$ at which $\psi_{ws} = \bar{\psi}_R$. The solution yields

$$\left(\frac{t + \Delta t}{\Delta t} \right)_{\psi_{ws} = \bar{\psi}_R} = e^F \tag{5-18}$$

F may be calculated from either Equation (2-130) or from Equation (2-131), whichever is appropriate. Thus $\bar{\psi}_R$ may be read directly from the extrapolation of the Horner straight line to a value of $(t + \Delta t)/\Delta t$ determined from Equation (5-18).

5 ALTERNATIVE METHODS OF ANALYSIS

Several alternative methods for analyzing pressure build-up data are available. A few of the most commonly used alternatives have been cited in Section 1.1, and are reviewed in greater detail in this section.

5.1 Miller, Dyes and Hutchinson (MDH) Method

When the drawdown period, prior to the build-up, is long enough to extend into the pseudo-steady state flow regime, the analysis suggested by Miller, Dyes and Hutchinson (1950) and Perrine (1956) may be used. They recommended a plot of p_{ws} versus log Δt which would result in a straight line following the deviation due to early-time data. Using the pseudo-pressure approach, the slope of this straight line is m, the same as that of the Horner plot. This is confirmed by an examination of Equation (5-3) which can be written for large producing times, that is, for $t \gg \Delta t$ as

$$\psi_i - \psi_{ws} = 1.632 \times 10^6 \frac{q_{sc} T}{k h} \left[\log t - \log \Delta t \right] \qquad (5-19)$$

Hence a plot of ψ_{ws} versus Δt on semilogarithmic coordinates should give a straight line of slope m, from which kh may be calculated. The apparent skin factor, s', may be obtained from Equation (5-7).

The average reservor pseudo-pressure, $\bar{\psi}_R$, is obtained from Figure 5-7. The curves shown on Figure 5-7 were derived theoretically for the geometries shown, assuming pseudo-steady state flow prior to shut-in (Miller, Dyes and Hutchinson, 1950, Perrine, 1956, Pitzer, 1964). Ramey (1967) and Earlougher and Ramey (1968) have presented similar curves for reservoirs of various other shapes.

The value of Δt_{De} is calculated at any chosen shut-in time, Δt, from

$$\Delta t_{De} = \frac{2.637 \times 10^{-4} k \Delta t}{\phi \mu_i c_i r_e^2} \qquad (5-20)$$

where

$$r_e^2 = \frac{A}{\pi} \text{ for non-circular geometries}$$

The corresponding value of Δp_D is obtained from Figure 5-7 or an appropriate curve. The average reservoir pressure is then calculated from

$$\Delta t_{D_e} = \frac{2.637 \times 10^{-4} \, k \Delta t}{\phi \mu_i c_i r_e^2}$$

$$\Delta p_D = \frac{1.151(\overline{\psi}_R - \psi_{wf})}{m}$$
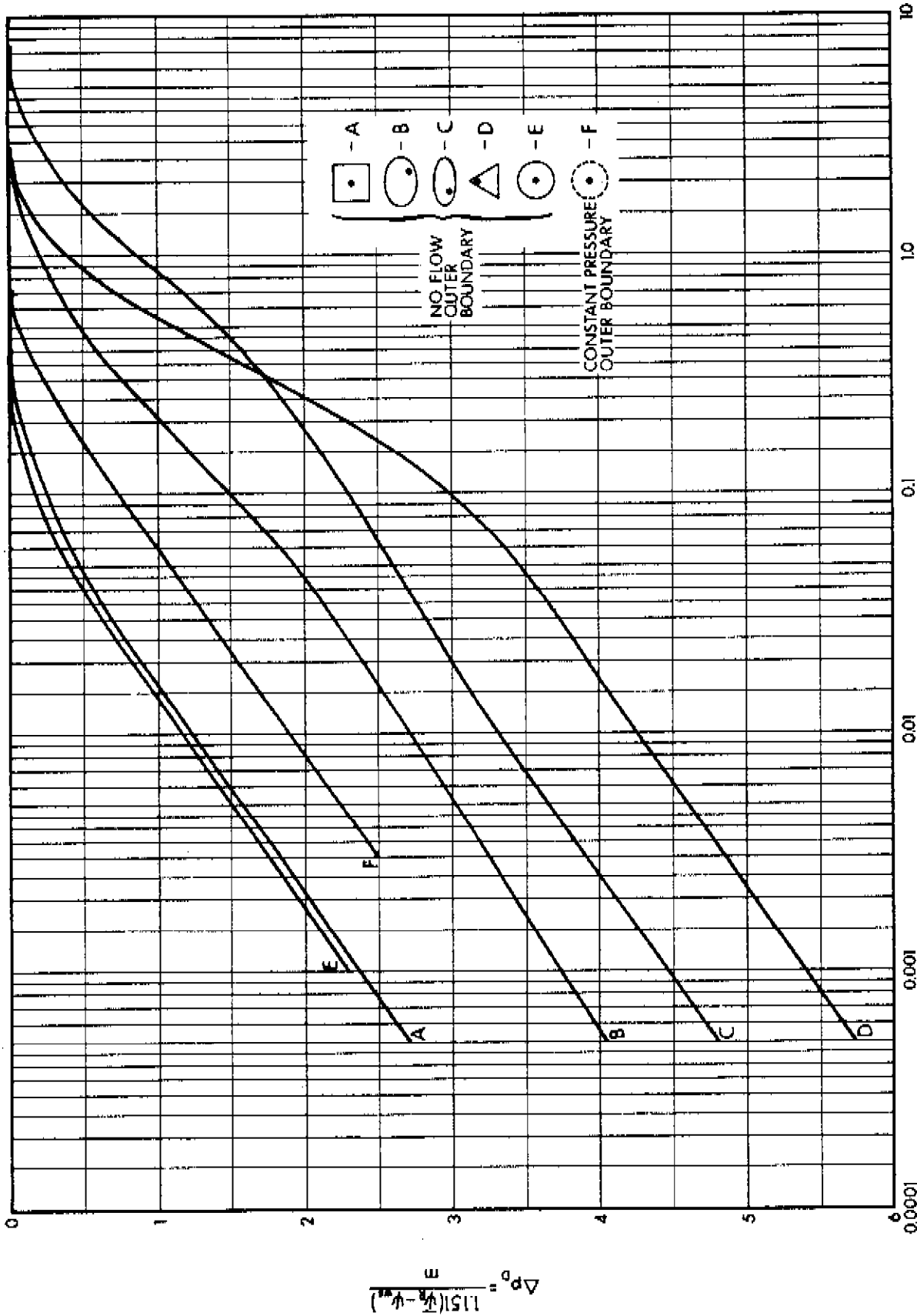
FIGURE 5-7. MDH DIMENSIONLESS PRESSURES

A,B,C,D — From Pitzer (1964)
E,F — From Perrine (1956). Reproduced by Permission from API Drilling and Production Practice (1956)

$$\bar{\psi}_R = \psi_{ws} + \frac{m}{1.151} \Delta p_D \qquad\qquad (5\text{-}21)$$

where

m   =   slope of the MDH semilog straight line

ψ_{ws} =   value of the pseudo-pressure corresponding to the chosen shut-in time, Δt, from the straight line

The curves of Figure 5-7 are valid only if pseudo-steady state flow conditions prevailed prior to shut-in. Where such a condition does not exist, the curves presented by Ramey and Cobb (1971) and by Cobb and Smith (1974) may be used. In such cases, although a semilog straight line is still obtained for the build-up data, this straight line lasts for a shorter duration than when pseudo-steady state flow conditions are achieved prior to shut-in.

5.2 Extended Muskat Method

This method is based on that of Muskat (1937) as developed by Larson (1963) and Russell (1966) and essentially gives a straight line for data that occur in the late-time region. It assumes that the well has been produced to pseudo-steady state flow conditions before shut-in. Under such conditions, it has been suggested that a plot of log $(\bar{p}_R - p_{ws})$ versus Δt will result in a straight line. Since $\bar{p}_R$ is not known, a graphical trial-and-error procedure becomes necessary. The correct value of $\bar{p}_R$ is that which results in a straight line data plot. The slope of this straight line is a function of $\phi\mu cA/k$ and may be used to estimate either ϕ or A. It is this fact that makes it worthy of consideration. However, Ramey and Cobb (1971) have shown that only a very small portion of the data is straightened out by this method. For example, for a well in the middle of a square, the data must lie in the range of $0.05 < t_{DA} < 0.09$.

Ramey and Cobb (1971) also showed that the production period does not necessarily have to extend into the pseudo-steady state flow regime. However, the time required to reach the proper straight line

does increase as production time decreases below the time required to reach pseudo-steady state flow conditions.

Since the Muskat plot straightens build-up data over such a restricted pressure range and also since the time required to acquire the necessary data is usually much longer than that required for either a Horner or MDH plot, practical considerations often limit the application of this method.

5.3 Desuperposition--Slider Method

Desuperposition, which is discussed in Section 2.1 and is illustrated by Example 5-1 may be used to analyze middle-time build-up data. As indicated in Section 2.1, the continued effect of drawdown during the shut-in period must be known. It may be predicted by type curve matching or by the use of appropriate equations. The approach proposed by Slider (1966, 1971) is illustrated by Figure 5-8.
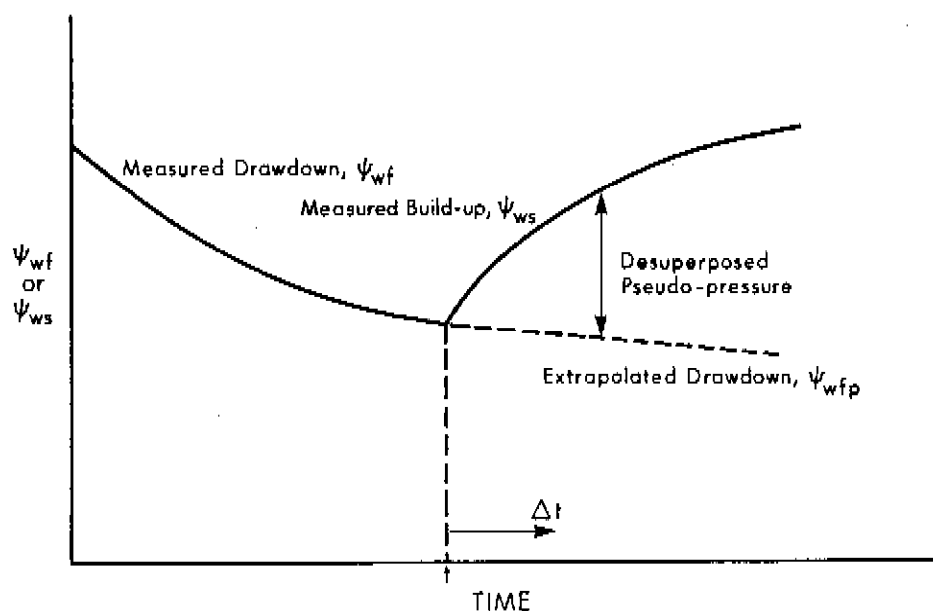
FIGURE 5-8. DESUPERPOSITION FOR THE SLIDER PLOT

The drawdown behaviour must be such that it can be extrapolated as shown by the dotted line. This may be done either by type curve matching (Section 2.1) or by the use of appropriate equations. Equation (4-5) applies prior to pseudo-steady state ($t < t_s$) while Equation (4-28) applies thereafter. The desuperposed pseudo-pressure ($\psi_{ws} - \psi_{wfp}$) at any shut-in time Δt is obtained by subtracting the extrapolated drawdown, ψ_{wfp}, from the measured build-up pseudo-pressure, ψ_{ws}. This desuperposed pressure, if plotted against log Δt should give a straight line of slope m, equal to the slope from the Horner plot. Eventually, when $\Delta t = t_s$, deviation from the straight line will be observed, indicating the influence of a boundary. Slider (1966, 1971) proposed the use of this method after flow has reached a pseudo-steady state since the extrapolation of drawdown is easily obtained as a straight line of constant slope on arithmetic coordinates. Slider also showed that this procedure gives a straight line of a longer duration than that obtained by any other method.

The practical limitations of this method, however, restrict its application in many cases.

6 IMPORTANT CONSIDERATIONS PERTAINING TO BUILD-UP TESTS

The theoretical relationships and the analysis procedures discussed in the previous sections refer to an ideal situation of a well in an homogeneous formation that is shut in after having produced at a constant rate. In practice, these idealized conditions are quite often not met and consequently the build-up behaviour, infinite or finite, is affected. Various factors that limit or affect the analysis procedures are discussed below.

6.1 Effect of the Duration of Drawdown Prior to Build-Up

The MDH and Horner methods are similar in that they require a semilogarithmic plot of the test data. In both cases, a portion of the

plotted data should result in a straight line of slope m, which is inversely proportional to the formation permeability. At the time these methods were proposed, the MDH method required pseudo-steady state flow conditions prior to build-up, whereas the Horner method assumed infinite reservoirs so that drawdown and build-up data would be transient flow and middle-time, respectively. Although the obviously smaller time requirements for the latter method suggest its use in preference to the former method, Ramey and Cobb (1971) have shown that the MDH method does not necessarily require pseudo-steady state flow prior to build-up and is often applicable in cases where the production time is not known.

In the analysis of build-up tests, it is possible to define the time-of-start of the semilog straight line by application of desuperposition methods and type curves as described in Section 2.1 and illustrated by Example 5-1. For the MDH or Horner plot, the straight line starts immediately after the early-time data. However, unlike drawdown tests where the end of transient flow can be defined through the concept of a radius of investigation or observed deviations from the straight line plot, the end of the build-up semilog straight line is not so easily identified. This is because the point of deviation from the Horner or MDH straight lines is a function, not only of reservoir boundaries, but also of the duration of the flow period prior to build-up. So far no simple correlations have been developed that account for both these factors.

Miller, Dyes and Hutchinson (1950) have shown that for a well located in the centre of a closed circular reservoir, produced to pseudo-steady state prior to shut-in, the semilog straight line ends at a Δt_{DA} of 0.024 where

$$\Delta t_{DA} = \frac{2.64 \times 10^{-4} \ k \ \Delta t}{\phi \ \mu \ c \ A} \tag{5-22}$$

Matthews and Russell (1967) have suggested that the straight line exists for a Δt_{DA} of 0.032. Ramey and Cobb (1971) compared the time required to reach the end of the semilog straight line for the MDH and Horner plots. A very significant finding was the dependence of time-of-end of

the semilog straight line on the duration of drawdown prior to build-up. Although the restriction of pseudo-steady state flow prior to build-up for an MDH plot is not necessary, the length of the proper semilog straight line becomes very short as the producing time shortens. For the same drawdown period, the Horner plot straightens out build-up data over much longer shut-in times than does an MDH plot.

A comprehensive analysis of the problem of defining the time-of-end of the semilog straight line and its dependence on duration of flow has been conducted by Cobb and Smith (1974). In investigating these methods of analysis for a wide variety of well locations in square and rectangular reservoirs for a wide range of producing times, they confirm the dependence of the time-of-end of the semilog straight line on duration of flow and also confirm that the Horner plot yields a straight line over a longer shut-in time period than the MDH plot. They also presented a larger number of graphical correlations to predict the maximum shut-in time for a Horner or MDH analysis.

$$\Delta p_{DHOR} = \frac{kh(\psi_i - \psi_{ws})}{1.417 \times 10^6 \, Tq_{sc}}$$

$$\Delta p_{DMDH} = \frac{kh(\bar{\psi}_R - \psi_{ws})}{1.417 \times 10^6 \, Tq_{sc}}$$

$$t_{DA} = \frac{2.637 \times 10^{-4} \, kt}{\phi \mu_i c_i A}$$
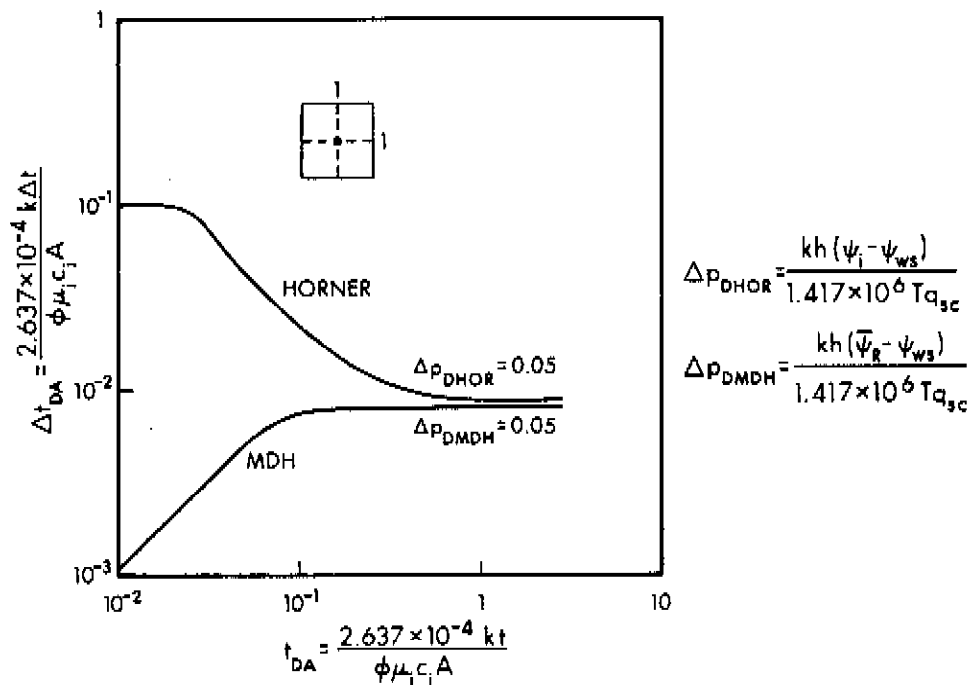
FIGURE 5-9. COMPARISON OF TIMES REQUIRED TO REACH
THE END OF HORNER AND MDH STRAIGHT LINES
From Cobb and Smith (1974)

Figure 5-9, adapted from Cobb and Smith (1974), compares the time-of-end of the semilog straight line for a well in the centre of a square reservoir. The curves represent the shut-in time where deviation from the semilog straight line is less than ten per cent. The distinct advantage of using a Horner plot for the analysis of build-up data following short-time flow tests is obvious from the figure. Even for longer flow durations the Horner plot permits a longer semilog straight line. For other criteria of accuracy or for other well/reservoir configurations and geometries, the information may be found in Cobb and Smith (1974).

Excessive Duration of Drawdown

When the duration of drawdown extends into the pseudo-steady state region, the value of t used in a Horner plot can have a significant effect on the calculated results. Pinson (1972) has discussed the case of build-up tests on oil wells where the production time prior to shut-in was greater than that required to reach pseudo-steady state. He suggests that any value of t greater than t_s, the time to stabilization, may be used in the Horner plot providing that the same value of t is used with the MBH curves to convert p^* to $\bar{p}_R$. Kazemi (1974) has extended this concept to gas flow. However, he has pointed out that the MBH curves were derived principally for liquid flow, and that they are applicable to gas flow only up to a certain value of t_{DA}, depending on the reservoir geometry and flow rate. This is clearly illustrated by Figure 5-10, from Al-Hussainy (1967, p. 63), for a well in the centre of a circular reservoir.

A substantial error may be caused in the straight line plot when $t \gg t_s$. Accordingly, for a gas well producing at pseudo-steady state flow conditions prior to shut-in, it is preferable to use a time, t, approximately equal to but larger than t_s, in constructing the Horner plot and in obtaining values of F from the MBH curves. It should be noted, when calculating t_{DA}, that μ and c, which are usually evaluated at initial conditions (for gas flow using the ψ treatment), should be evaluated at the average reservoir pressure prevailing at a time t_s

hours before shut-in. This may involve an iterative procedure and a material balance calculation. Since a good first estimate is usually available from the pressure build-up, the number of iterations will be small, usually two or three in most cases.
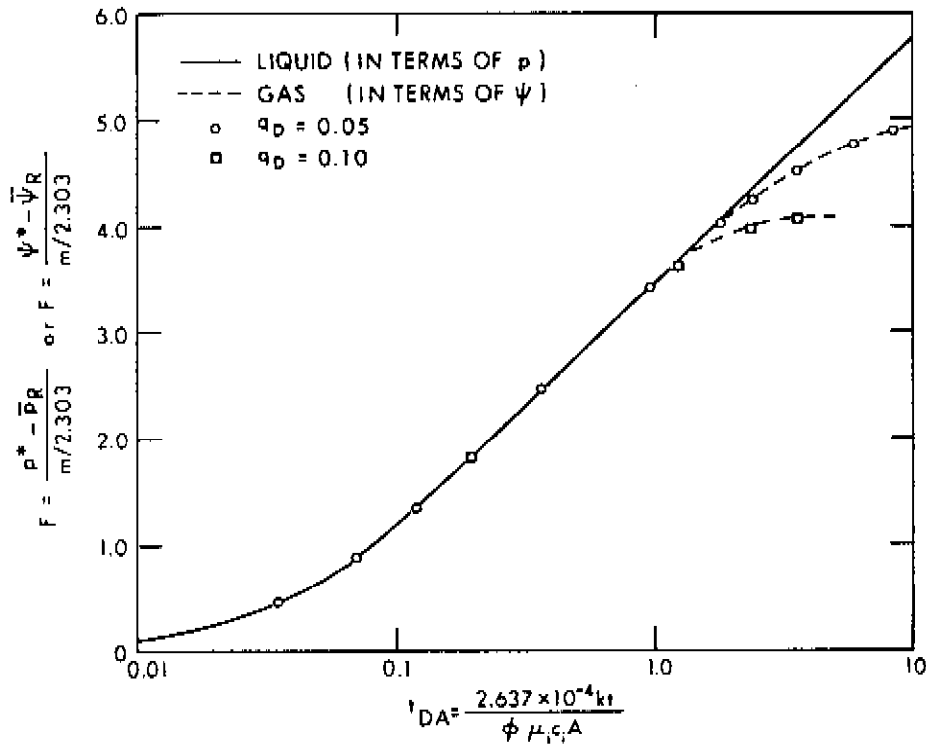
FIGURE 5-10. MBH DIMENSIONLESS PRESSURE FUNCTION FOR ONE
WELL IN THE CENTER OF A CIRCLE
From Al-Hussainy (1967, p. 63)

6.2 Build-Up Following a Two-Rate Drawdown Test

The two-rate drawdown test, described in Chapter 4, Section 4.2, is often conducted to permit separation of the apparent skin factor, s', into its components s and Dq_{sc}. Such a test may also be analyzed to calculate the value of kh. The analysis of a build-up that follows a two-rate drawdown can yield values of kh that provide a check on the results of a drawdown analysis.

The flow rate and time sequences used to develop the multirate drawdown analysis still apply but with slight modification. A well

is flowed at a rate q_1 up to time t_1, at a rate q_2 up to time t and then shut-in. The shut-in time is represented, as before, by Δt. Using this notation, Equation (4-15) may be modified to represent the build-up period as

$$
\begin{aligned}
\psi_1 - \psi_{ws} &= \frac{1.632 \times 10^6 \, q_1 \, T}{k \, h} \left[\log(t + \Delta t) + \log\left(\frac{k}{\phi \, \mu_i \, c_i \, r_w^2}\right) - 3.23 \right] \\
&+ \frac{1.632 \times 10^6 \, (q_2 - q_1) T}{k \, h} \left[\log(t + \Delta t - t_1) + \log\left(\frac{k}{\phi \mu_i c_i r_w^2}\right) - 3.23 \right] \\
&+ \frac{1.632 \times 10^6 \, (0 - q_2) T}{k \, h} \left[\log \Delta t + \log\left(\frac{k}{\phi \mu_i c_i r_w^2}\right) - 3.23 \right]
\end{aligned}
$$

$$(5\text{-}23)$$

The first term on the right-hand side of Equation (5-23) represents the effect due to the drawdown at rate q_1 for time $(t + \Delta t)$. The second term is the effect of the change in drawdown rate $(q_2 - q_1)$ for time $(t + \Delta t - t_1)$. The third term is the effect of the change in rate $(0 - q_2)$ for time Δt. Combining these terms and simplifying Equation (5-23) gives

$$
\psi_1 - \psi_{ws} = \frac{1.632 \times 10^6 q_1 \, T}{k \, h} \left[\log\left(\frac{t + \Delta t}{t + \Delta t - t_1}\right) + \frac{q_2}{q_1} \log\left(\frac{t + \Delta t - t_1}{\Delta t}\right) \right]
$$

$$(5\text{-}24)$$

Hence a plot of ψ_{ws} versus $\log\left(\frac{t + \Delta t}{t + \Delta t - t_1}\right) + \frac{q_2}{q_1} \log\left(\frac{t + \Delta t - t_1}{\Delta t}\right)$ on arithmetic coordinates should give a straight line of slope, m, from which

$$
k \, h = \frac{1.632 \times 10^6 \, q_1 \, T}{m}
$$

$$(5\text{-}25)$$

The restrictions mentioned before for the analysis of two-rate

tests and for the identification of the proper straight line on a Horner plot also apply to the above analysis. For a bounded reservoir, the intercept of the straight line on the ordinate of the plot should yield ψ^* which may then be used as described in Section 4.2 to calculate $\bar{\psi}_R$.

6.3 Build-Up Following a Variable-Rate Drawdown

The various factors restricting the conduct of constant-rate deliverability tests are summarized in Chapter 3, Section 7.3 The effects of variable rates on the analysis of drawdown tests are discussed in Chapter 4, Section 6.1. The methods for accommodating rate variations in the drawdown preceding a build-up are essentially the same as for the analysis of variable-rate drawdown tests.

In particular the methods of Odeh and Jones (1965) may be adapted as follows for analyzing a build-up following a variable-rate drawdown. Supposing that the rate variations can be represented by step changes and also that the drawdown can be averaged over each of the time intervals, the flow sequence becomes: a flow rate q_1 up to time t_1, a flow rate q_2 up to time t_2, and so on, to a flow rate q_n up to time t_n. The total drawdown time is again represented by t, that is, $t = t_n$. The shut-in following rate q_n extends over the time period Δt. Using these notations, Equation (4-35) may be extended to include the shut-in period to give

$$\frac{\psi_1 - \psi_{ws}}{q_n} = m' \sum_{j=1}^{n+1} \left[\frac{\Delta q_j}{q_n} \log (t + \Delta t - t_{j-1}) \right]$$

(5-26)

where

$$m' = \frac{1.632 \times 10^6 \ T}{k \ h}$$

$$\Delta q_j = q_j - q_{j-1}$$

$$q_{n+1} = 0$$

$$t_0 = q_0 = 0$$

$$t = t_n$$

A plot of $(\psi_i - \psi_{ws})/q_n$ versus $\sum_{j=1}^{n+1} \left[\dfrac{\Delta q_j}{q_n} \log (t + \Delta t - t_{j-1}) \right]$ on arithmetic coordinates should give a straight line from which kh may be obtained.

Defining ψ_{wf0} as the pseudo-pressure just before shut-in, Equation (4-35) may be written as

$$\frac{\psi_i - \psi_{wf0}}{q_n} = m' \sum_{j=1}^{n} \frac{\Delta q_j}{q_n} \log (t - t_{j-1})$$

$$+ m' \left[\log \left(\frac{k}{\phi \, \mu_i \, c_i \, r_w^2} \right) - 3.23 + 0.869 \, s' \right] \quad (5-27)$$

Subtracting Equation (5-26) from Equation (5-27) gives

$$\frac{\psi_{ws} - \psi_{wf0}}{q_n} = m' \sum_{j=1}^{n} \frac{\Delta q_j}{q_n} \log \left(\frac{t + \Delta t - t_{j-1}}{t - t_{j-1}} \right)$$

$$+ m' \frac{(0 - q_n)}{q_n} \log \Delta t$$

$$+ m' \left[\log \left(\frac{k}{\phi \, \mu_i \, c_i \, r_w^2} \right) - 3.23 + 0.869 \, s' \right] \quad (5-28)$$

Defining ψ_{ws1} as the pseudo-pressure at $\Delta t = 1$, and assuming $\dfrac{(t + 1 - t_{j-1})}{(t - t_{j-1})} \simeq 1$ for all $j = 1, \ldots, n$, Equation (5-28) may be simplified to give

$$s' = 1.151 \left[\frac{\psi_{ws1} - \psi_{wf0}}{m' \, q_n} - \log \left(\frac{k}{\phi \, \mu_i \, c_i \, r_w^2} \right) + 3.23 \right] \quad (5-29)$$

Equation (5-29) is valid when IT flow effects are negligible or when the assumption $s' = s'_1 = s'_2 = \ldots = s'_n$ can be made. When IT flow effects cannot be neglected, the above equations may be modified to include $s' = s + Dq_{sc}$. A graphical trial-and-error procedure (Chapter 4, Section 6.1) is then necessary to calculate kh, s and D.

The above procedures are fairly involved and quite often the added accuracy is not justified. In some cases, good approximations can be obtained by much simpler procedures outlined below.

Simplified Approaches

Horner (1951) stated, without any substantiation, that as a "good working approximation" a corrected time of flow, t_c, should be used in place of the actual flow time, t, when the flowing rate has been variable. The corrected time of flow is defined as

$$t_c = \frac{\text{cumulative production}}{\text{last flow rate}} \qquad (5-30)$$

Equation (5-3) still represents the flow behaviour with t replaced by t_c and q_{sc} replaced by the last flow rate. The latter replacement also applies for calculating kh from Equation (5-4). Generally, this is a reasonable approximation which leads to a correct extrapolation to ψ^* but may give inaccurate values of kh. Odeh and Nabor (1966) showed that this simplification could sometimes lead to a complete misinterpretation of the build-up data.

Nisle (1956) showed that in the event of a short-term shut-in (of duration δ_1), if the subsequent production (of duration δ_2) is at least ten times as long as the shut-in, that is, $\delta_2 \geq 10\,\delta_1$, the effect of the shut-in on subsequent build-up data would be less than ten per cent and could be ignored. However, if deemed necessary, the temporary shut-in may be completely accounted for by plotting ψ_{ws} versus $\log\left[(t+\Delta t)/\Delta t\right]\left[(\delta_2+\Delta t)/(\delta_1+\delta_2+\Delta t)\right]$ only for cases where the flow rate before and after the temporary shut-in is the same.

Brauer (1965) applied the principle of superposition to show that any rate variations that had occurred a reasonably long time before the final shut-in (say, not later than 0.1 t) would have little effect on the build-up pressures. In these instances the actual flow time and the last flow rate are used in the analysis.

Odeh and Selig (1963) developed equations for a modified rate q^* to be used with a modified time t^* in the Horner plot. The q^*, t^*

method was obtained from the superposition of the variable rate effects. However, it should be used only when the shut-in time is at least one-and-a-half times the production period, as in a drill-stem test or a pressure build-up following a short-term flow test. When the flow rates have varied stepwise, t^* and q^* are given by

$$t^* = 2\left[t - \frac{1}{2 Q_T} \sum_{j=1}^{n} q_j \ (t_j^2 - t_{j-1}^2) \right] \tag{5-31}$$

$$q^* = \frac{Q_T}{t^*}$$

where

Q_T = cumulative production during time t

t_0 = 0

6.4 Radius of Investigation

Several correlations have been published for calculating the radius of investigation from build-up tests (Gray, 1965, Odeh and Nabor, 1966, Matthews and Russell, 1967, p. 94, Gibson and Campbell, 1970). Most of the correlations give conflicting results. In general, these were derived for infinite-acting reservoirs and can thus be very misleading.

Odeh and Nabor (1966) observed that the time of departure from a semilog straight line was approximately four times larger for a drawdown than for a build-up. Consequently, they postulated the presence of a transitional (late transient) zone between the transient and pseudo-steady state periods. They also gave an equation for calculating the radius of investigation for drawdown tests and another one for build-up tests.

At best, any equation for radius of investigation from a build-up test is very approximate. Furthermore, no simple equation has been found to be valid in all cases. In a reservoir that is known to be infinite-acting, the radius of investigation is simply obtained by

replacing t in Equation (3-16) by $(t + \Delta t)$. However, this calculation is valid only for $r_{inv} < r_e$ or $(t + \Delta t) < t_s$ and it is usually difficult to deduce the time for which a reservoir is infinite-acting from the straight line of a build-up plot. The fact that the build-up plot is straight does not imply that the reservoir is still infinite-acting. This was demonstrated conclusively by Ramey and Cobb (1971). They showed that even a finite reservoir which had been produced for a very long period $(t > t_s)$, exhibited a straight line of the correct slope on a Horner plot. Therefore, for a finite reservor, the published radius of investigation equations are not valid for build-up data.

A rigorous determination of the radius of investigation from build-up data involves desuperposition of the data and an analysis of the desuperposed data by drawdown techniques. The desuperposition procedure, sometimes called the Slider plot (Section 5.3) is also discussed in Section 2.1 and Example 5-1. If the drawdown preceding the build-up extended into the pseudo-steady state, the desuperposed data plot (log $\Delta\psi$ versus log Δt) will give a straight line until $\Delta t = t_s$ at which point deviation will start. This value of t_s is the upper limit of applicability of Equation (3-16) which may be used to determine the radius of investigation during the build-up test by replacing t by Δt. If, however, the drawdown does not extend into pseudo-steady state flow conditions, the desuperposed data plot will give a straight line until $t + \Delta t = t_s$ at which point deviation will start. In such a case the radius of investigation will be the same as for an infinite-acting reservoir. The above procedures are, of course, subject to the restrictions that apply to desuperposition methods.

In conclusion, it is emphasized that the fact that a Horner plot is straight does not indicate that boundary effects have not yet been felt. As a corollary, the point of deviation from the Horner straight line is a function not only of reservoir boundaries, but also of the duration of flow prior to build-up. So far no simple correlation has been developed to account for both of these factors.

6.5 Effects of Reservoir Heterogeneities
and Other Factors

The pressure build-up analysis methods presented in the previous sections are based on the ideal reservoir model of Chapter 2. Several deviations that may include reservoir heterogeneities, phase redistribution, wellbore storage, interference effects, and so forth, will affect the data collected during build-up tests. Some of these deviations may be recognized from a Horner plot. A few of the important deviations from the idealized reservoir model are shown in Figure 5-11 which is referred to, as necessary, in the following sections.

Well Near a Barrier/Sealing Fault

Horner (1951) has shown that the effect of a fault/barrier in an otherwise infinite-acting reservoir is to cause the build-up plot to start off as a straight line with the proper slope, gradually bend over, and eventually become another straight line with twice the slope of the first. This is illustrated by Figure 5-11(g). The first straight line gives the proper value of kh. The second straight line gives the proper extrapolation to ψ_i. The distance between the well and the fault may be obtained by simultaneous solution of the equations representing the two straight lines. If Δt_i represents the time at which the two lines intersect and if $(d/2)$ represents the distance to the fault, then, for long producing times,

$$- Ei \left(- \frac{\phi\, \mu\, c\, (d/2)^2}{2.637 \times 10^{-4}\, k\, t} \right) = 2.303\, \log \left(\frac{t + \Delta t_i}{\Delta t_i} \right) \qquad (5-32)$$

Equation (5-27) may be solved for d using the plot of the Ei function (Figure 2-6) or from Tables of Mathematical Functions (Jahnke and Emde, 1945). Gray (1965) has shown that this equation is valid only for large producing times and can give substantially erroneous values for short flow periods, as in drill-stem tests. He has also presented several approximations and graphical procedures for calculating the distance to a fault. In some cases, the Ei function of Equation (5-32)
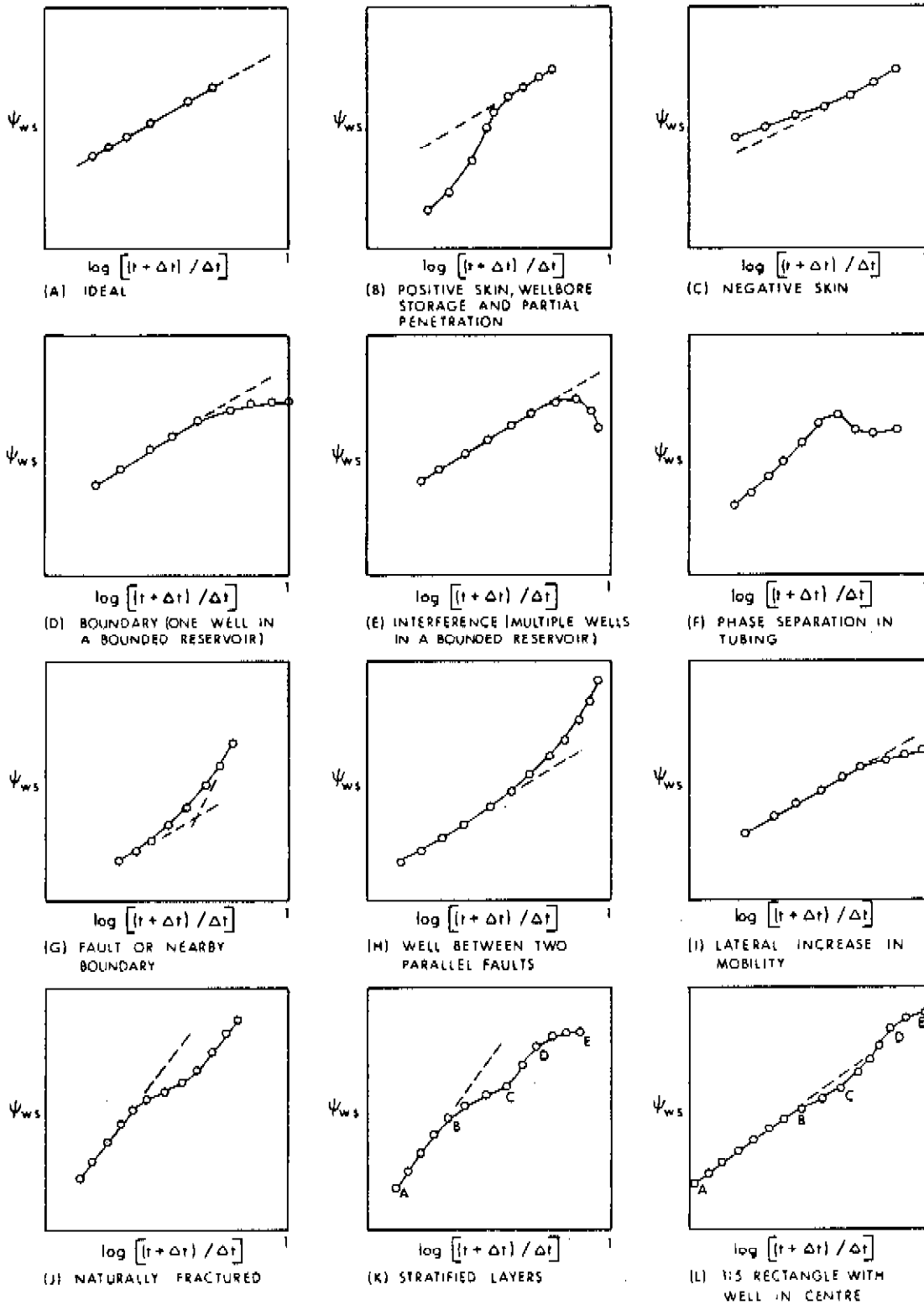
FIGURE 5-11. EXAMPLE BUILDUP CURVES

A to G, I — From Matthews and Russell (1967, p.123)

may be approximated by a logarithmic expression. Gray (1965) has found that the expression given by Davis and Hawkins (1963) for drawdown tests seems to apply reasonably well to build-up tests. The approximation takes the final form

$$\frac{d}{2} = \left(\frac{1.48 \times 10^{-4} \ k \ \Delta t_i}{\phi \ \mu \ c} \right)^{0.5} \tag{5-33}$$

Gibson and Campbell (1970) have reviewed the various methods of calculating the distance to a barrier, both constant pressure and no-flow, from build-up tests. They quote the work of Ishteiwy and Van Poollen (1967) which consists of determining the value of $(t + \Delta t)/\Delta t$ at the point of deviation from the first straight line to obtain the following approximation

$$\frac{d}{2} = \left[\frac{9.33 \times 10^{-4} \ k \ t}{\phi \ \mu \ c \left(\dfrac{t+\Delta t}{\Delta t} \right)_{deviation}} \right]^{0.5} \tag{5-34}$$

The equations given above, along with any others in the literature yield only order of magnitude answers. The build-up behaviour of a well between two barriers is shown in Figure 5-11(h).

Multi-Layer Reservoirs

As mentioned in Chapter 4, Section 2.2, the drawdown calculation procedures developed for single-layer reservoirs also apply to multi-layer, homogeneous reservoirs. The same is true for a build-up analysis of such reservoirs.

Some reservoirs, however, consist of layers of widely different permeabilities, with varying degrees of cross flow. The analysis of the behaviour of these systems is not possible by the methods developed in previous sections. A simplified model in which it is assumed that no cross flow takes place between layers, often called a commingled system, involves communication between the layers only at the wellbore. The behaviour of commingled systems has been studied extensively by several authors (Lefkovits, Hazebroek, Allen and Matthews,

1961, Kazemi, 1970, Cobb, Ramey and Miller, 1972, Raghavan, Topaloglu, Cobb and Ramey, 1973, Earlougher, Kersch and Kunzman, 1974).

In general, the build-up behaviour of commingled systems (stratified layers) is as shown in Figure 5-11(k). The straight line AB that follows early-time data gives the proper value of $\overline{kh}$ where

$$\overline{k\,h} = \sum_{i=1}^{n} k_i \, h_i \qquad (5\text{-}35)$$

The flattening portion BC represents the fact that the more permeable layers, which deplete to a larger extent than the less permeable layers during drawdown, have attained the average pressure of those layers.

Since the less permeable layers are depleted less than the more permeable ones, their average pressures are higher. The portion CD represents a repressurization of the more permeable layers until DE is reached. This last portion indicates that all layers are now at the same average reservoir pressure and that the build-up is complete.

Although multi-layer systems usually exhibit the build-up curve of Figure 5-11(k), they could also have a completely different shape, to the extent that they may not be distinguishable from single-layer systems. Note for example, the similarity of Figures 5-11(k) and 5-11(l), the latter applying to a single-layer system. One way of differentiating between multi-layer and single-layer systems is by inspection of the final rise CD. For multi-layer systems the magnitude of the final rise depends on both the producing rate and the duration of the flow period prior to build-up. If either of these is changed, the magnitude of CD is altered. The authors mentioned above have correlated the final rise with permeability ratios and with pay thickness ratios, or MBH-type pressure functions, for various multi-layer systems. Their correlations may be used to determine $\overline{p}_R$.

Since the time for wellbore storage effects to become negligible is controlled by wellbore conditions, it is the same as for single-layer systems. The semilog straight line, which gives $\overline{kh}$, ends at about the same shut-in time as it would if the layer with the

smallest value of ϕ/k acted alone.

Naturally Fractured Reservoirs

As a method of analysis for naturally fractured reservoirs, Pollard (1959) has suggested the plotting of log $(\bar{p}_R - p_{ws})$ versus Δt. By graphical differencing, the pressure drop due to skin and that due to flow through the fractures may be identified individually. The volume of the fractures may also be estimated. Pirson and Pirson (1961) have extended the Pollard analysis using an electrical analogue to determine not only the skin factor and the fracture pore volume but also the matrix pore volume and the radius of drainage of the well.

Warren and Root (1963) have idealized a naturally fractured reservoir by assuming the reservoir to consist of a primary porosity system, the matrix, and a secondary porosity system, the fracture. They introduced two factors, namely, ω, which is a measure of the capacity (ϕc) of each system and λ which reflects the degree of interporosity flow. A typical build-up curve consists of two parallel straight lines as shown in Figure 5-11(j).

Dyes and Johnston (1953) and Odeh (1965) have concluded in apparent contradiction to the findings of Warren and Root (1963) that build-up in fractured reservoirs is similar to and indistinguishable from that in a homogeneous reservoir. This inconsistency was resolved by Kazemi (1969) who has found that a naturally fractured reservoir behaves as has been suggested by Warren and Root (1963). A two-parallel slope system is evident on drawdown or build-up plots. Kazemi (1969) has also shown that the finding of Odeh (1965), indicating that the behaviour is essentially that of a homogeneous system, is compatible with the Warren and Root model for small block dimensions (3 feet) and a matrix permeability greater than 0.01 md. However, these conditions often do not exist. He also concluded that the Pollard pressure build-up plot has only an apparent validity in evaluating pore volumes and that at large times a fractured reservoir behaves like an equivalent homogeneous one.

Crawford, Hagedorn and Pierce (1973) have confirmed the

applicability of the model proposed by Warren and Root (1963) for a naturally fractured reservoir. They obtained a multi-slope (parallel sections) behaviour as required by the model, in both drawdown and build-up analyses, from which the effective permeability and initial pressure of the formation could be obtained. The results of Odeh (1965) are consistent with the Warren and Root model, but his conclusions apply to the particular situation that he considered and may not be generalized.

Adams, Ramey and Burgess (1968) have observed that the pressure build-up in fractured carbonate reservoirs does not conform to that proposed by Warren and Root (1963) nor to that of Odeh (1965). They obtained two, and sometimes three, straight lines of different slopes which indicates an increasing permeability. Accordingly, they hypothesized a model of two concentric regions, the inner one reflecting the true permeability of the matrix and the outer one representing the effects of the fractures. Their results indicate that the first straight line should yield the proper matrix permeability and the second line should be extrapolated to give the stabilized shut-in pressure.

Non-Circular and Non-Symmetrical Reservoirs

A typical build-up plot in a non-circular reservoir is shown in Figure 5-11(1). The build-up behaviour and the determination of average drainage area pressure by the Horner-MBH method are affected by the shape of the drainage area. Often the well/reservoir configuration may be assumed to be circular or square with the well in the centre, and the methods of analysis described previously may be applied. However, this is not always so, and it is then important to determine the appropriate drainage pattern. When two wells are producing from the same pool, there will exist between them a no-flow boundary. This was investigated by Matthews, Brons and Hazebroek (1954) and by Matthews and Lefkovits (1955) in a sequel to the MBH publication. They constructed a flow model using permanganate crystals to delineate the flow lines. They showed that approximate drainage boundaries may be drawn and that these could be approximated by rectangles, squares, triangles, or their

combinations. Starting with the well producing at the highest rate, the line joining it and a neighbouring well may be divided in the ratio $q_H/q_L \simeq d_H/d_L$, where subscripts H and L refer to the high and low flow rates and d is the distance to the no-flow boundary that will exist between the wells. This is repeated for surrounding wells. If the volume thus obtained is less than q_H/q_{total}, the drainage area must be adjusted to "finger" between the wells with the lowest rate or in the direction of a sparsely drilled section of the reservoir. Examples of models used to represent asymmetric drainage areas are shown in Figure 5-12. The MBH pressure functions for the model reservoirs are given in Figures C-1(a) to C-1(g).

Interference Effects

If the shut-in well is in a reservoir from which other wells continue to produce, at long shut-in times the continued production at other wells will influence the build-up behaviour. This is illustrated by Figure 5-11(e). Theoretically, the analysis of data acquired from one of many wells in a bounded reservoir requires a superposition of the effects of each of the producing wells at the shut-in well. This forms the basis for analyzing so-called interference tests. The utility of interference tests in testing gas wells is very limited on account of the difficulty in measurement of the pressure response that is masked or delayed by the compressibility of the gas. The application of interference tests in oil wells is described by Matthews and Russell (1967).

6.6 Reliability of Build-Up Test Analysis

As mentioned in Chapter 4, Section 6.4, a linearized form of the general flow equation of Chapter 2, Section 5.6 has been adapted to the analysis of drawdown tests. In this chapter, the same linearized flow equation has been adapted to the analysis of build-up tests. Wattenbarger (1967) has investigated the effects of this linearization. His conclusions are summarized below:

1. The permeability thickness, kh, can be determined accurately from
    the Horner build-up plot using the pseudo-pressure approach, for
    reasonable flow rates. For high flow rates, $q_D \geq 0.1$, the
    calculated value may be low. For the cases simulated, this error
    was always less than ten per cent.

2. Wellbore storage, skin and IT flow effects are all early-time
    effects in build-up testing and do not affect the ultimate slope of
    the straight-line portion, if a straight line exists. In cases
    where outer boundary effects are significant, it is possible that
    the proper straight line portion will not exist.

3. The existence of turbulence can lead to serious errors in the
    calculation of kh in some drawdown tests. However, for build-up
    tests it has been observed that turbulence has little or no effect
    on the determination of kh. Therefore, when turbulence is
    significant, more confidence can be placed in the kh determined from
    a build-up test than from a drawdown test.

Notwithstanding the small error in kh when IT flow effects are
significant, build-up tests, when properly conducted, will usually give
accurate values for kh, s and D.

7 DELIVERABILITY

Even though a build-up test does not involve the production of
gas, the results may be used to calculate the stabilized deliverability
potential of a well. This may be accomplished by the procedures
described in Chapter 4, Section 7. The parameters kh and s' obtained
from a build-up analysis may be used in Equation (4-41) to estimate the
deliverability. The limitations of Equation (4-41) include its application
to low flow rates or to flow rates near that used in the drawdown
preceding the build-up.

If a deliverability equation is required for application over
a wide range of flow rates, it becomes necessary to conduct two build-up
tests following substantially different flow rates. This permits
calculation of s'_1 and s'_2 from which s and D may be calculated.
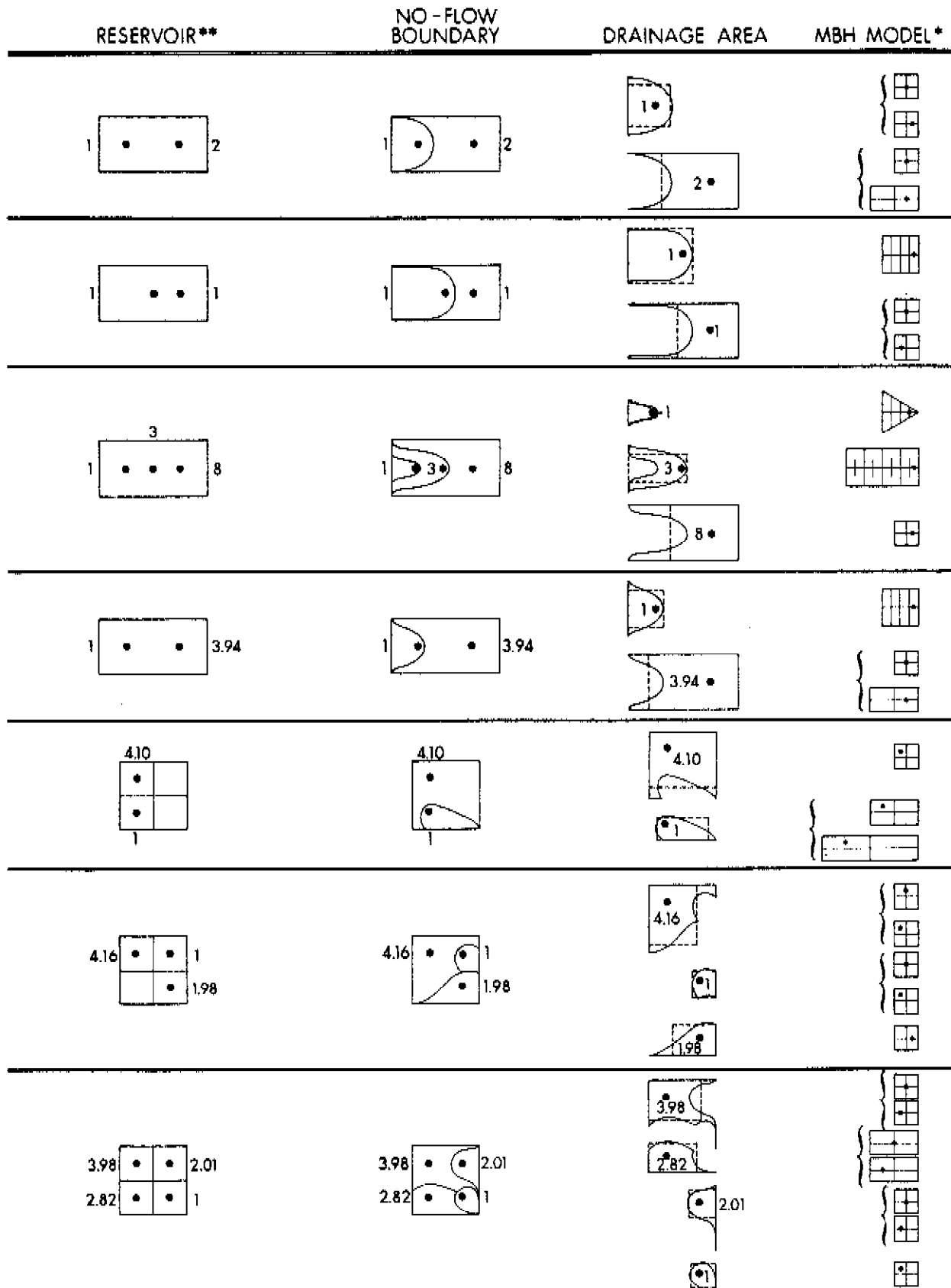
FIGURE 5-12. NON-SYMMETRICAL DRAINAGE AREAS
From Matthews and Lefkovits (1955)

*The brace, {, about two models means that an average of the values for these two models is used.

**Numbers indicate ratios of flowrates.

FIGURE 5-12. NON-SYMMETRICAL DRAINAGE AREAS

From Matthews and Lefkovits (1955)

*The brace, {, about two models means that an average of the values for these two models is used.

**Numbers indicate ratios of flowrates.

Equations (4-39) and (4-40) may then be used to calculate the stabilized flow constants a and b. The quadratic form of the deliverability equation, Equation (3-4), is then applicable to all flow rates.

8 GUIDE-LINES FOR DESIGNING BUILD-UP TESTS

Since a build-up test involves a drawdown period followed by a shut-in period, it usually serves a multiple purpose. In addition to confirming the results obtained from drawdown tests or possibly from the drawdown period of the build-up test, the proper conduct and analysis of a build-up test provides accurate values of the permeability thickness, kh, the apparent skin factor, s', and the average reservoir pressure, $\bar{p}_R$. Furthermore, these parameters may be used to predict the stabilized deliverability relationship and thereby confirm the result of deliverability tests. The calculation of $\bar{p}_R$ is an important function of build-up analyses and is essential to the material balance calculations of reserves.

Relevant experience is perhaps the most valuable asset in gas well testing and whenever possible it must be utilized in the design of build-up tests. In the absence of such knowledge, the guide-lines discussed below may be used to supplement the related information contained in Chapter 3, Section 8 and in Chapter 4, Section 8.

8.1 Choice of Analysis Method

With due regard to the relevance and accuracy of the various methods discussed in previous sections, it is necessary to appreciate the practicality and economics of the tests that can be conducted in an effort to acquire good data. Each situation warrants special attention and may or may not be conducive to the more accurate analysis procedures.

In cases where only transient data are acquired, the Horner-MDH method is eminently suited to calculation of kh, s' and $\bar{p}_R$. However, it is also possible that only late-time data may be acquired, in which case the extended Muskat method may be usable.

8.2 Choice of Equipment

The same general considerations apply for build-up tests as those described for deliverability tests in Chapter 3, Section 8.2 and for drawdown tests in Chapter 4, Section 8.2. In particular, bottom hole shut-in and pressure measurement equipment is recommended for use whenever possible. This avoids the problems associated with wellbore storage and phase redistribution in the wellbore.

8.3 Choice of Flow Rate and Duration of
Flow Rate Prior to Shut-In

The flow rate is chosen so that a significant drawdown is observable at the well. The duration of flow should preferably be long enough so that a semilog analysis of the drawdown data is possible, but an excessive duration of the drawdown period should be avoided for reasons given in Section 6.1 of this chapter. Furthermore, the duration of drawdown should be planned to minimize or eliminate flaring of gas. The values of kh and s' obtained from a drawdown analysis may then be compared with those obtained from the build-up data analysis and any inconsistencies investigated.

In general it is recommended that the duration of the flow period be at least five times the duration of early-time effects. This should then result in approximately half a log cycle of straight line on the semilog plot.

8.4 Duration of Shut-In

The well should be shut-in for as long as possible but at least for a period greater than five times the duration of early-time effects.

9 CALCULATING AND PLOTTING TEST RESULTS

Althouth various types of analysis methods have been described in previous sections, the following procedures apply only to the

Horner-MBH method of analyzing a pressure build-up preceded by a single-rate drawdown. The other methods of analysis and also the other testing sequences, like build-up periods following two-rate or variable-rate tests, simply involve slight modifications of these procedures.

The identification of the time-of-start of the semilog straight line by desuperposition and type curve matching has been described in Section 2 and illustrated by Example 5-1. If type curve matching techniques cannot be applied, a reasonable approximation of the duration of early-time effects may be made from equations that apply to drawdown tests, for example, Equation (3-19).

The top end of the semilog straight line may be estimated from Figure 5-9. If the drainage area/well configuration is very different from a square with a centrally located well, an appropriate figure may be obtained from Cobb and Smith (1974).

A plot of ψ_{ws} versus $(t + \Delta t)/\Delta t$ on semilogarithmic coordinates may be made and the best straight line may be drawn between the approximate limits defined above. The slope of the line is measured and is termed m, the intercept of the straight line (extrapolated, if necessary) at $\Delta t = 1$ is termed ψ_{ws1}. Using Equations (5-4) and (5-7) along with h and ϕ from geological evaluation/well logs, the known value of r_w and μ_i, c_i calculated by the methods described in Appendix A, the permeability, k, and the apparent skin factor, s', may be calculated. If s' is to be separated into its constituents, s and Dq_{sc}, a second build-up test may be conducted following a substantially different flow rate. Equations (4-8) and (4-9) may then be solved for the values of s and D.

The straight line of the Horner plot is extrapolated to $(t + \Delta t)/\Delta t = 1$ to give ψ^*. The appropriate value of t is used in Equation (5-12) to calculate t_{DA}. The appropriate MBH curve is selected from Figures C-1(a) to C-1(g) and a value is obtained for F. Alternatively, F may be calculated from Equations (2-130) or (2-131). Since m, F and ψ^* are known, $\bar{\psi}_R$ can be calculated from Equation (5-15) and then converted to $\bar{p}_R$.

10 DRILL-STEM TEST PRESSURE BUILD-UP ANALYSIS

The operational considerations in obtaining reliable DST
pressure data, the practical considerations in DST interpretation and
relevant references to DST pressure analysis have been presented in an
excellent review by Matthews and Russell (1967, pp. 84-91). The most
common test procedure in use is the double shut-in method involving the
following sequence of events: initial flow and initial shut-in periods,
and the final flow and final shut-in periods. These are illustrated by
the schematic DST pressure record of Figure 5-13.

A – Initial Mud   D – Initial Build-up   G – Final Mud
B – Packer Squeeze   E – Final Flow
C – Initial Flow   F – Final Build-up
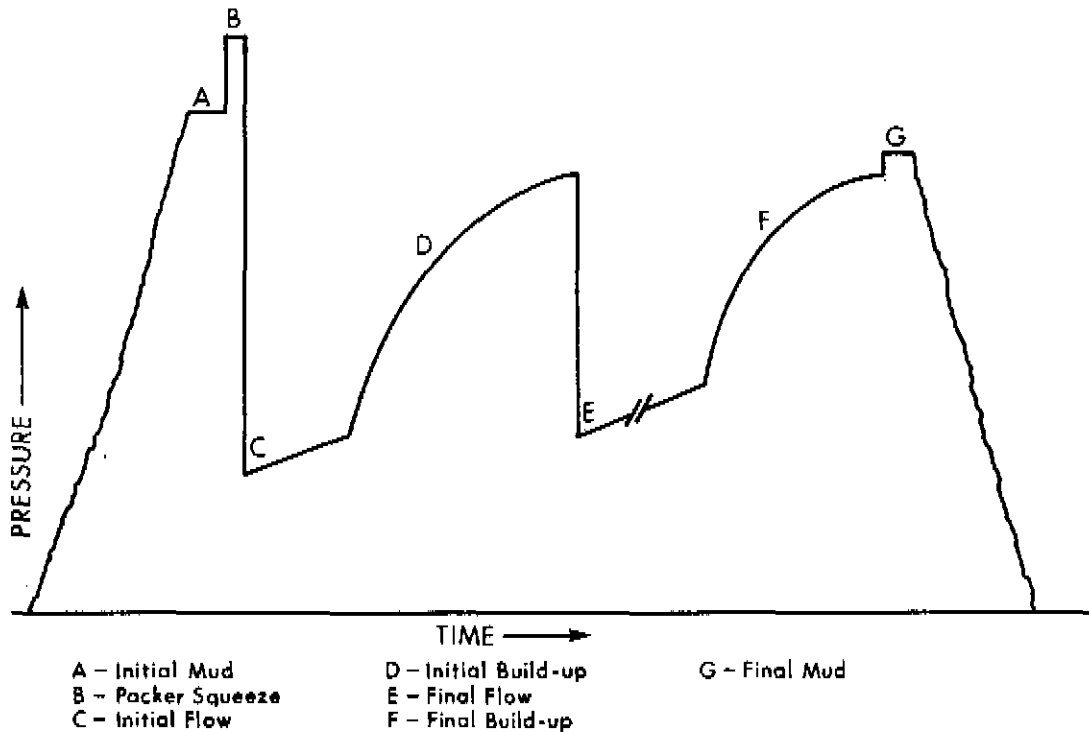
FIGURE 5-13. A TYPICAL SCHEMATIC DST PRESSURE RECORD

The pressure build-up analysis theory developed in this
chapter may be applied to the analysis of DST pressure build-up data.
In tests where the build-up is preceded by a flowing DST, the

requirement of a constant producing rate is often satisfied. Under such conditions the Horner-MBH method may be applied to the build-up data to obtain approximations of kh and s' using Equations (5-4) and (5-7). Since a drill-stem test is usually conducted on a new well, assuming negligible depletion, an extrapolation of the Horner plot yields the initial reservoir pressure.

However, in some cases and especially during a DST in which production is into the drill pipe, the flow rate usually decreases throughout the flow period. Furthermore, this rate of decline is usually constant. Under such conditions, the averaging procedure suggested by Dolan, Einarsen and Hill (1957) is acceptable. They have shown that as long as the difference in the initial and final production rates in the flow period prior to the build-up is not extreme, an average production rate can be used in the pressure build-up analysis. The average rate is simply obtained by dividing the fluid recovery by the length of the flow period.

Odeh and Selig (1963), however, do not recommend use of the Horner plot for analyzing a build-up preceded by a variable-rate drawdown. As described in Section 6.3, the method of Odeh and Selig requires that the duration of the build-up period be at least one-and-a-half times the duration of the preceding drawdown. This condition is satisfied by drill-stem testing procedures. Equation (5-31) was suggested for use with build-up data following short flow tests in which the flow-rate decline with time is known. In drill-stem testing, however, the rate of flow as a function of time is usually not known. Since the pressure as a function of time is usually known, an alternative equation of the following form is used to calculate t^*.

$$t^* = 2 \left[t - \frac{1}{2} \frac{\sum\limits_{j=1}^{n} (p_j - p_{j-1})(t_j + t_{j-1})}{\sum\limits_{j=1}^{n} (p_j - p_{j-1})} \right] \qquad (5-36)$$

where

p_0 = pressure at the start of the initial flow period, at t_0

p_n = pressure at the end of the final flow period, at t_n

t = duration of the initial flow, initial shut-in and final flow periods

Additional information that may be estimated from drill-stem tests includes the radius of investigation, changes in permeability, reservoir heterogeneities within the radius investigated by the test, and so forth. More comprehensive studies on drill-stem testing are available in the literature referenced by Matthews and Russell (1967, p. 91).

CHAPTER 6   GENERAL GUIDELINES RELATED TO THE FIELD
             CONDUCT AND REPORTING OF TESTS

1 INTRODUCTION

Previous chapters, related notes, and the appendices describe
the various types of deliverability, drawdown and build-up tests for the
estimation of reservoir/well behaviour and also recommend procedures
for the application of these tests. This chapter is intended as an
appropriate guideline regarding the field application of these testing
procedures.

General guidelines for the selection of testing equipment, for
the measurement of wellhead flow rates, for the measurement of wellhead
or bottom hole pressures, and for the sampling and analysis of produced
fluids are included in Sections 2 and 3. Some useful information related
to the field conduct and reporting of results from deliverability,
drawdown and build-up tests is included in Section 4.

For guidance in the selection of appropriate tests, the
magnitude of flow rates, the duration of flow and shut-in periods, and
related criteria for the selected test, reference may be made to the
chapter which relates to the type of test being undertaken.

2 GAS WELL TESTING FACILITIES

The two important factors which govern the selection of
testing equipment are the nature of the produced fluids and the type of
test being conducted. This section describes the essential features of
various wellhead testing facilities that are necessitated by the
presence of condensate, water, or acid gases in the natural gas being
produced. Variations in these configurations or alternative methods
that may be warranted by the specific requirement of different types of
tests are described in Sections 3 and 4, whenever necessary.

2.1   Sweet Dry Gas

The simplest configuration of wellhead testing facilities is required for a well producing a sweet dry gas. The testing equipment essentially consists of a flow rate measurement device, a shut-in and flowing pressure measurement device, a thermometer, gas sampling equipment and the necessary fittings for connecting the equipment to the wellhead.

When the produced gas is being vented to the atmosphere, a commonly used flow rate measurement device is a critical flow prover which is attached to the top of the wellhead. Unless there are regulations to the contrary, the gas vented from the flow prover is not burned. A horizontal positioning of the flow prover should be avoided since high flow rates will set up a considerable torque which may cause the prover fittings or the wellhead to unwind.

If the well being tested is to be produced into a gas gathering system, the flow rate measurement is usually made with an orifice meter using a permanent or removable meter run.

In some instances, the production well that is to be tested does not have a permanently installed flow measurement device. To avoid interruption of flow or the disruption of stabilized flow in a well that has been producing for some time, a simple procedure illustrated by Figure 6-1 may be employed. As shown in this figure, if valve A is closed gradually while valve B is being opened, maintaining a constant pressure in the flow string, the flow rate being measured by the flow prover will be the same as the production rate.

The desirability of constant flow rates during tests has been stressed in Chapters 3, 4, 5 and 7, and is also the basis for most of the theoretical considerations of Chapter 2. Figure 6-2 illustrates the wellhead rigging that may provide constant flow rates. Flow downstream from the flow prover is usually vented to the atmosphere. If, however, the produced gas must be flared, care must be taken to ensure critical flow conditions are maintained in the flow prover.
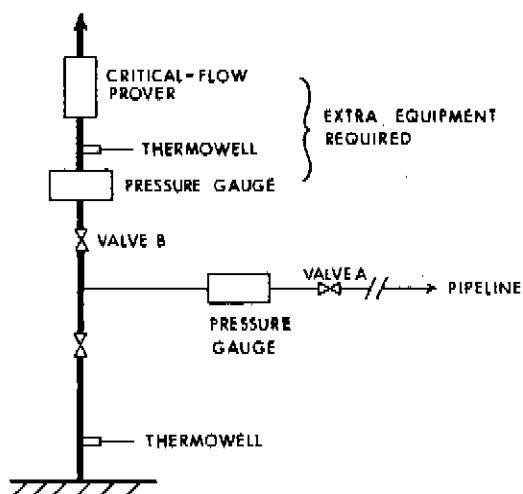
FIGURE 6-1. SCHEMATIC FLOW DIAGRAM FOR MEASURING FLOW RATES OF PRODUCTION WELLS NOT EQUIPPED WITH FLOW RATE MEASUREMENT EQUIPMENT
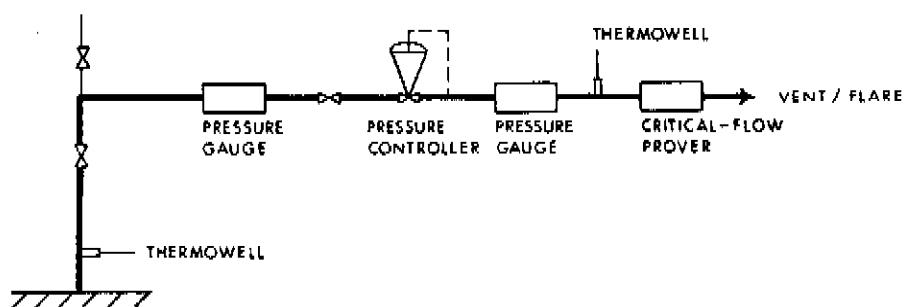
FIGURE 6-2. SCHEMATIC FLOW DIAGRAM OF WELLHEAD RIGGING FOR CONSTANT-RATE TESTS

2.2 Sweet Wet Gas

The term "wet" is used to describe a natural gas containing heavier hydrocarbons which appear as a condensate in the produced gas. The phenomenon of retrograde condensation is described in Appendix A, Section 8. In some instances, water may also be produced but it is not included in the definition of a wet gas.

The presence of condensate in produced gas creates requirements for more complex testing facilities than those required for sweet dry gas wells. A typical facility includes flow rate measurement devices, pressure measurement devices, thermometers, gas and condensate sampling equipment, line heaters and separation facilities. Several stages of separation and a combination of measurements may be required for highly productive wells, but the most commonly used configurations involve either a single separator or two separators in series. These are illustrated by Figures 6-3 and 6-4, which are intended only as a guide in the selection of test equipment and for the understanding of the recombination calculation procedures described in Appendix A, Section 8, and do not represent the complete wellhead and separation facilities.

The requirement for line heaters is necessitated by the possibility of hydrate formation within the flow lines and testing equipment. Alternatively, glycol or alcohol may be injected into the gas stream. In some cases a hot oil circulation string may be used to avoid hydrate problems within the wellbore. The conditions that are conducive to hydrate formation and methods for their elimination are discussed in Appendix A, Section 8.

2.3 Sour Gas

For testing sour gas wells more elaborate facilities are required than for sweet gas wells. In addition to the equipment mentioned in Section 2.1 or Section 2.2, depending on whether the gas is dry or wet, a gas meter and a flow line to an appropriate flare stack is required. In addition, liquid seals may also be necessary to protect the gas meter and dead-weight tester from H_2S gas.

3 MEASUREMENT AND SAMPLING

The accurate measurement of gas and liquid production rates and also of static and flowing pressures is essential to the proper conduct and analysis of well tests. Correct sampling procedures are also necessary in order to obtain representative samples of the produced fluids and an accurate estimate of the constituents of the reservoir gas. This section should be used as a guide in selecting flow and pressure measurement devices although equally reliable alternatives may be used at the discretion of the tester.

3.1 Gas Flow Rate Measurement

All flow measurement devices should be installed in accordance with recommended specifications since biased measurement errors can cause anomalous test results. Some of the more common biased errors are caused by insufficient pipe upstream and downstream of the meter, insufficient liquid retention time in the separators, inadequate liquid dumping cycles, incorrect meter coefficients or calibration factors, meter vibration and other metering problems.

The most commonly used gas flow measurement devices are orifice meters and critical flow provers. Turbine and displacement meters are not so commonly used, but it is expected that with the advent of portable units their utility will increase.

Orifice Meters

When a well is being tested directly into a gas gathering system, the gas flow measurement is normally carried out with an orifice meter. However, a portable testing unit including an orifice-type meter is used in many instances even though gas is being flared.

Some limitations in the use of orifice meters are described in the American Gas Association Committee Report No. 3 (1955), in particular the limitations of accuracy when the flow is turbulent, and when there are disturbances in the gas flow. When gas is measured with orifice meters,
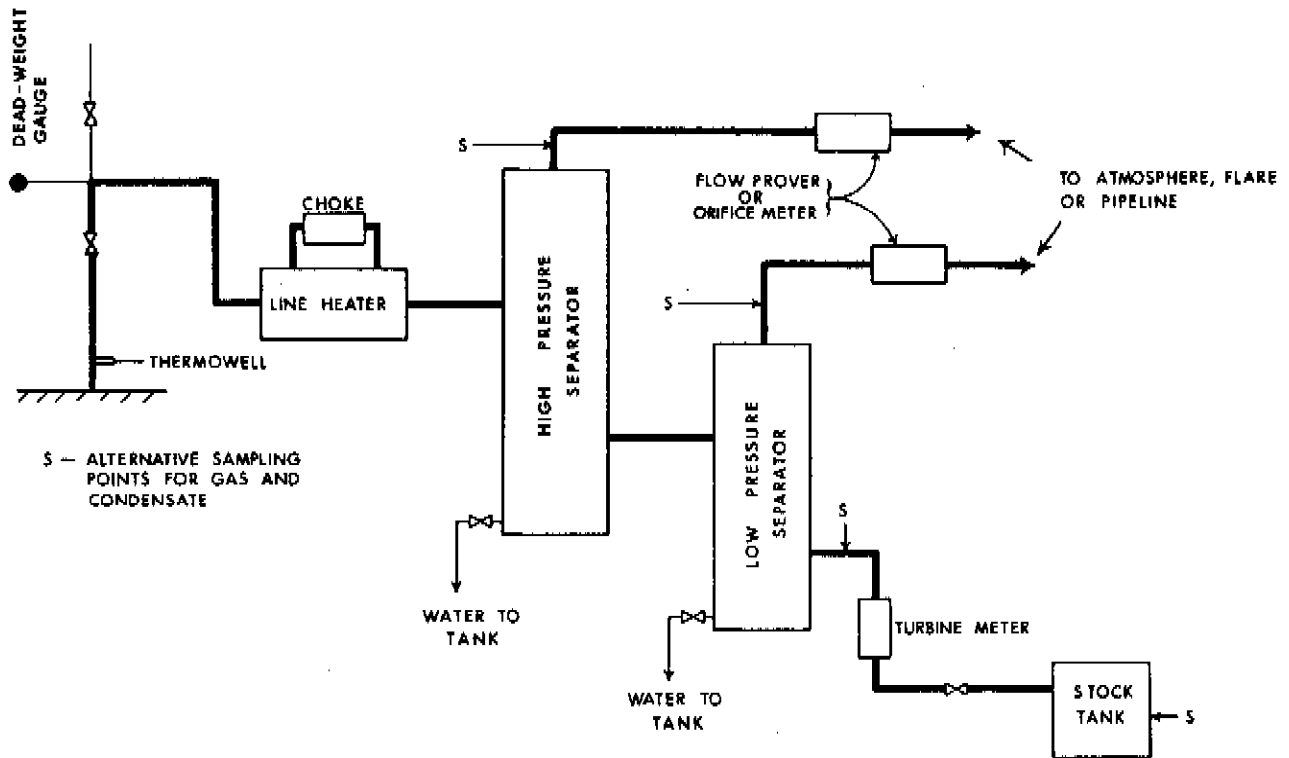
FIGURE 6-3. SCHEMATIC FLOW DIAGRAM OF SURFACE
WELL - TESTING FACILITIES FOR WET GAS (TWO SEPARATORS)
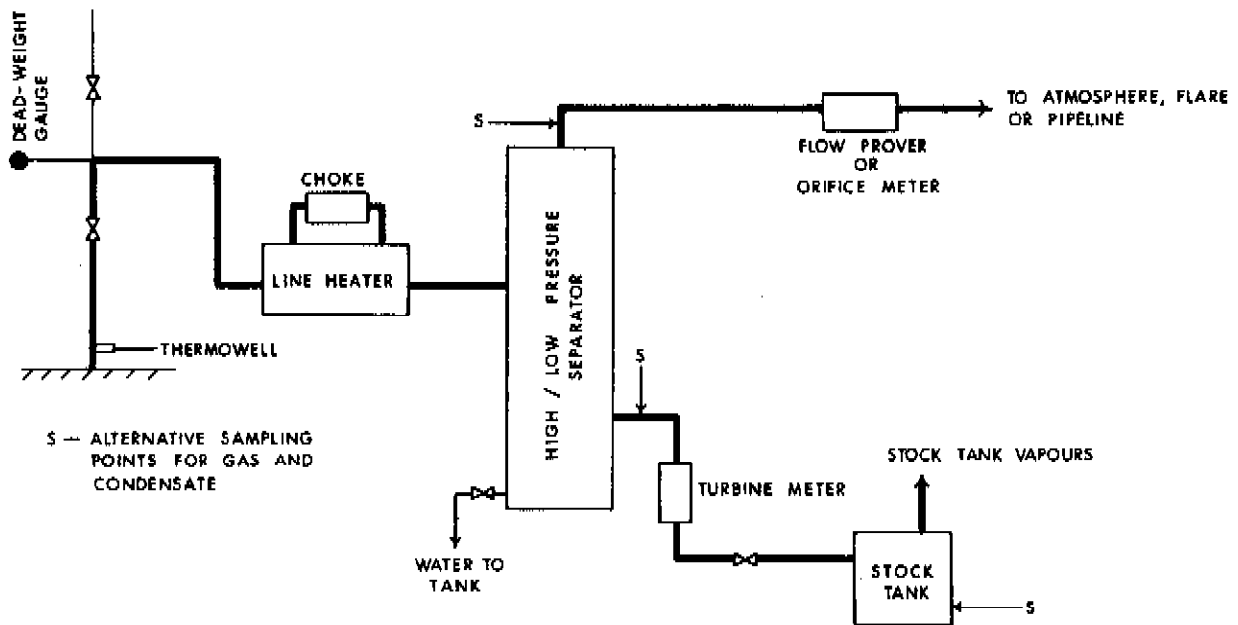
FIGURE 6-4. SCHEMATIC FLOW DIAGRAM OF SURFACE
WELL - TESTING FACILITIES FOR WET GAS (SINGLE SEPARATOR)

measurements are made under conditions of non-critical flow, and the calculations are based on the differential pressure (usually in inches of water) across the orifice and the upstream or downstream pressure. Accordingly, any disturbance in the gas stream that may affect the differential pressure across the orifice also affects the accuracy of the gas flow rate measurement. The same logic applies to the non-critical flow of gas through an orifice where the flow is vented to the atmosphere.

A number of publications are available which outline methods for calculating gas flow rates from basic orifice meter data. Some of these are the American Gas Association Committee Report No. 3 (1955) and the back pressure testing manuals of the Kansas State Corporation Commission (1959) and the Interstate Oil Compact Commission (1962). The methods and coefficients published in these manuals differ slightly and in most cases have been based on the work done by the American Gas Association (AGA). The Board accepts the AGA report entitled "Orifice Metering of Natural Gas" (Reprinted 1972) as the standard reference for the installation and use of orifice meters. The equation for calculating the gas flow rate is given below and is also given on Form EG-34 included in Appendix E of this manual.

$$q_{sc} = 24 \times 10^{-6} \ c' \ \sqrt{h_w \ P_f} \qquad (6-1)$$

where

q_{sc} = flow rate, MMscfd

c' = orifice flow constant

h_w = differential pressure, inches of water at $60^\circ F$

P_f = absolute static pressure, psia

The above-mentioned orifice flow constant can be calculated, and subsequently used in Equation (6-1), by the methods described in the AGA publication referred above.

If there is no liquid knock out vessel upstream of the orifice, the meter run should be installed in a vertical position. If such an orientation presents a pipe fitting problem and there is no alternative

but to use a horizontal run, liquid drain lines should be connected to the orifice changer and bled-off frequently to ensure against liquid accumulation in the primary device.

Critical-Flow Provers

The measurement of gas flow rates with critical-flow provers is based upon the fundamentals of gas flow through orifices under critical conditions or conditions where the gas velocity has reached a maximum and remains constant. These conditions are normally assumed to occur, and the use of a critical-flow prover is considered valid, when the ratio of the downstream pressure to the upstream pressure is less than approximately 0.5.

Critical-flow provers are well adapted for measuring gas flow rates, especially where the gas is vented to the atmosphere. Since the downstream pressure is atmospheric while the upstream pressure is usually much higher, the criterion for critical flow is satisfied. Furthermore, under conditions of critical flow, measurement difficulties due to turbulence are eliminated. This is a distinct advantage over orifice meters which are sensitive to turbulence. However, there is often a large pressure drop across the orifice of a flow prover which may cause the formation of ice or hydrates, resulting in incorrect measurements.

The U.S. Bureau of Mines, Monograph 7 (1936), first published the method and provided appropriate coefficients for the use of critical-flow provers. However, the formula proposed in Monograph 7 was based on ideal gas behaviour. It is now recognized that deviations from such behaviour exist and should be accommodated in the formula. The Railroad Commission of Texas (1950) and others have published appropriate modifications to the formula through use of a gas super-compressibility factor. The gas flow rate may be calculated from the following equation

$$q_{sc} = 10^{-3} \ C \ P \ F_{tf} \ F_g \ F_{pv} \tag{6-2}$$

where

$$q_{sc} = \text{flow rate, MMscfd}$$

C   =   coefficient of the orifice (Table 6-1)

P   =   flowing pressure upstream of the prover, psia

F_{tf} = flowing temperature factor

F_g = specific gravity factor

F_{pv} = super-compressibility factor

The coefficients for use in Equation (6-2) are given in Table 6-1. The above equation is also shown on Form EG-34 in Appendix E.

Size of Orifice (inches)	2-Inch Pipe C	Size of Orifice (inches)	4-Inch Pipe C
1/16	0.0846	1/4	1.384
3/32	0.1863	3/8	3.110
1/8	0.3499	1/2	5.564
3/16	0.8035	5/8	8.668
7/32	1.1090	3/4	12.422
1/4	1.4360	7/8	16.893
5/16	2.2080	1	22.007
3/8	3.1420	1 1/8	27.721
7/16	4.5030	1 1/4	34.229
1/2	5.6530	1 3/8	41.210
5/8	8.5500	1 1/2	49.106
3/4	12.4900	1 3/4	67.082
7/8	17.1800	2	88.628
1	22.5800	2 1/4	113.617
1 1/8	28.9200	2 1/2	142.490
1 1/4	36.5100	2 3/4	176.420
1 3/8	44.8600	3	216.790
1 1/2	55.6400		

TABLE 6-1 ORIFICE COEFFICIENTS FOR 2" AND 4" FLOW PROVERS
From Railroad Commission of Texas (1950)

3.2 Condensate Flow/Accumulation Rate Measurement

When the condensate flow rate is being measured, turbine or displacement meters are usually used. The meter should be installed with sufficient straight pipe and should be located upstream of a snap-acting valve. This valve should be regulated so that there is sufficient retention time to ensure equilibrium of the gas and condensate in the separator. The dumping cycle must also be of a sufficient time duration so that slippage errors are minimized. Gas breakout in the meter must be kept to a minimum since it causes turbine and displacement meters to spin, registering volumes that are too high. the condensate must be metered at approximately the same temperature and pressure conditions as the separator in order to obtain correct recombined gas volumes.

In many instances, condensate is gauged in a stock tank. This method should be used only in instances where the input to the stock tank is from a low-pressure separator or when the flashed vapours are being collected. In the former case, care should be taken to ensure that the amount of flashed vapours is small enough to be neglected in recombination calculations. Furthermore, flash calculations or actual laboratory measurements of a shrinkage factor should be conducted to permit conversion of stock tank liquids to their equivalent separator liquid volumes.

3.3 Water Flow/Accumulation Rate

Water flow rates may be measured with turbine or displacement meters, or gauged in a storage tank. If meters are being used, a snap-acting water dump valve should be used to ensure that there is a sufficient flow to motivate the meter. Since water, if present in gas, often presents a problem in the operation of gas wells and gas gathering systems, it is important to monitor any water production during a test. A knowledge of water production during tests is also important to the analysis and application of test results. Provision has been made on Form EG-32 in Appendix E to report this production.

3.4 Measurement of Pressure

The accurate measurement of static pressures and the pressures corresponding to flow rates measured during the flow periods of various tests is of great importance in gas well testing. Since interpretation of deliverability, drawdown and build-up test results must be based on the theory of flow in the reservoir, it follows that the important pressure in interpreting the tests is the reservoir sandface pressure. Ideally, this pressure is measured directly through use of an accurate, carefully calibrated bottom hole pressure gauge. There are many types of such gauges available today, all of which, when used properly, are quite adequate for accurate measurement of sandface pressures. A detailed discussion of the general working principles and use of common gauges is available in the Board's "Guide for the Planning, Conducting and Reporting of Subsurface Pressure Tests" (1974).

In some instances, due to mechanical difficulties, sour gases, or other reasons, it is not practical to use a bottom hole gauge. In such situations, wellhead pressures are measured and subsequently converted to reservoir sandface pressures by the method described in Appendix B. The highest possible accuracy in wellhead pressure measurement is important, and for best results these pressures should be taken with a dead-weight gauge. A discussion of the operation of a dead-weight gauge is contained in the AGA Gas Measurement Manual (1963).

Details of the Cullender and Smith method for converting wellhead pressures to sandface pressures are given in Appendix B along with a discussion of the possible sources of error. For shallow wells, the accuracy of this method is acceptable, so bottom hole gauge measurements may not be necessary. However, experience indicates that calculations of sandface pressures at high flow rates (greater than about 10 MMscfd) are often subject to excessive errors. The reason for this may be the difficulty in accurately estimating friction effects at very high flow velocities. For relatively deep, high capacity wells, flowing at high rates, the sandface pressure drawdown is normally small whereas the losses due to friction are very high. Consequently, a small

error in determining the weight of gas in the flow string and the friction loss can render the calculated pressure loss meaningless. For these reasons, in cases where wells will be tested at high flow rates, serious consideration should be given to directly measuring the sandface pressures wherever physically possible.

In some instances, flowing bottom hole pressures may be calculated from static annulus pressure measurements. The calculation procedures are described in Appendix B.

Although many methods are available for calculation of sandface pressures when there are two phases present in the wellbore, as mentioned in Appendix B, it is recommended that wherever an appreciable amount of liquid is suspected in the wellbore, the bottom hole pressure be measured directly.

Furthermore, it is recommended that wellhead pressure measurements be recorded at all times, regardless of whether or not a bottom hole pressure gauge is being used. Such data, in addition to providing a check on bottom hole measurements, may be used to calculate wellhead deliverabilities.

For sour gases, the dead-weight tester should be protected with a liquid seal. However, in such cases care must be taken to ensure that no gas is trapped in the liquid system.

When subsurface pressure measurements are being made, the bottom hole pressure gauge should preferably be calibrated with a dead-weight tester, before and after each run. Also, any dead-weight testers that are being used for pressure measurements or for calibrating other gauges should be calibrated against a master dead-weight tester (for example, the Board's dead-weight tester located in Edmonton is the Primary Standard for Alberta) at least once a year.

3.5 Sampling and Analysis of Produced Fluids

All gas and condensate streams produced at the wellhead should be accurately metered, sampled and analyzed in order that an accurate recombination may be obtained. Sampling procedures for

obtaining representative samples are usually available in gas well testing handbooks published by the oil industry or testing companies. It is usually preferable to obtain liquid samples at separator conditions since this eliminates the calculation and analysis procedures associated with converting stock tank volumes to equivalent separator volumes. All sampling points and sampling conditions should be noted on a line diagram of wellhead facilities. This enables an accurate compilation and analysis of data.

4 FIELD CONDUCT AND REPORTING OF TEST RESULTS

4.1 Deliverability Tests

Field Conduct

In describing the field conduct of deliverability tests, considerable use has been made of the recommended form of rules of procedure included in the Interstate Oil Compact Commission (1972) test manual.

The well to be tested should be produced prior to the initial shut-in period for a time sufficient to clear the wellbore of any liquids that may have accumulated. If the well cannot be cleared of liquids while producing into a pipeline, or if the well is not connected to a pipeline, it should be blown down through appropriate separation facilities and the gas should be flared or vented to the atmosphere until it is obvious that the wellbore is cleared of liquids. Particulars of blowing the well should be recorded in detail on Form EG-29 in Appendix E. The well should then be shut-in for a period long enough to ensure stabilized pressure conditions.

The lowest flow rate should exceed that which is just sufficient to keep the wellbore clear of a liquid column. Although in some instances this may not be feasible if a sufficient spread of points is to be obtained, an appreciable quantity of liquids should not be permitted to accumulate in the wellbore. Care must be taken at all times to prevent damage by unnecessarily coning water into the wellbore at higher flow rates.

If the flow rate changes gradually during a flow period, the test may still be analyzed by the methods of Chapter 3. However, the flowing pressure and the corresponding flow rate at the end of each flow period should be used. If it is not possible to achieve a stable flow rate due to liquid slugging, deliverability testing is not recommended.

In the case of deep wells with high flow rates, and particularly where two-phase flow is suspected, wherever possible the flowing and shut-in sandface pressures should be directly measured with a bottom hole pressure gauge. In every case the wellhead pressures and corresponding flow rates should be measured at least twice, but preferably continually, during each flow and shut-in period. One of these measurements should be made at the end of each flow period. When the stabilized deliverability is to be obtained by calculations rather than from an extended flow rate (see Chapter 4, Section 7; Chapter 5, Section 7; and Chapter 7, Section 4), the pressure should be recorded more frequently to permit an analysis of the transient pressure-time data.

If bottom hole pressures are to be calculated from top hole measurements, the gas temperature at the wellhead should be recorded with each wellhead pressure reading. In addition, the specific gravity of the produced gas, as well as liquids if separation takes place, should be accurately determined and recorded. This may be done by direct measurement using proper techniques, or alternatively by careful sampling, analysis, and the necessary computations. The determination of specific gravity need only be carried out during one flow period. The measurement, and subsequent calculation, of flow rates should follow the guidelines given in Section 3 of this chapter.

In all cases where the separation of gas and liquids takes place, the separator liquid producing rate should be accurately measured and recorded with the gas flow data on Form EG-29 in Appendix E. The measurement of the produced liquids should be such that it permits the accurate determination of the producing gas-liquid ratio for each flow rate. Diagrams of surface separation facilities and the locations of sampling points should be included in the test report. These may be modelled after Figures 6-3 and 6-4.

Reporting the Test Results

A complete report of a test should, wherever possible, include the following:

a. Field notes. These will include a report of the sequence of events, a record of wellhead pressures, time, temperatures, orifice sizes, and so forth. A schematic diagram of the testing equipment which also indicates the location of the pressure, temperature, and flow rate measurement points is valuable. Any problems encountered, for example, hydrate formation or sulphur deposition, and any relevant details, such as the presence of a water spray, should also be reported. Forms EG-29, EG-29A and EG-29B in Appendix E, may be used to record the field data.

b. A summary sheet, Form EG-32 in Appendix E, with details of the salient characteristics of the test, and the important conclusions.

c. Flow rate calculations. Each of the effluent streams is measured and the total "recombined gas" flow rate is calculated. If the water production rate exceeds that which would be expected due to condensation, it should be reported. Gas flow rates may be calculated using Form EG-34 in Appendix E. If these calculations are performed by computers, details need not be shown.

d. A fluid analysis report. A "recombined gas" analysis with physical and chemical properties at reservoir conditions is desirable. Form EG-35 in Appendix E may be used in calculating the amount, gravity and pseudo-critical properties of the recombined well effluent. If these calculations are performed by computers, details need not be shown.

e. A $p - \psi$ conversion table or graph. A computer output or a hand calculated relationship of p to ψ should be submitted with any analysis which utilizes the ψ approach.

f. A bottom hole pressure survey, including a wellbore pressure gradient determination. When bottom hole pressure gauges are not used, the conversion of wellhead pressures to bottom hole conditions should be clearly indicated and presented.

g. A stabilized bottom hole deliverability relationship. This is

expressed in the form of a quadratic equation and may be determined by the methods of Chapter 3. From this the wellhead deliverability at various reservoir sandface pressures may be obtained and displayed graphically.

h. Nomenclature. Any uncommon symbols should be clearly defined.

Standard forms for reporting the above data and calculations may be readily designed, or the recommended Energy Resources Conservation Board forms in Appendix E may be used.

4.2 Drawdown Tests

Field Conduct

The field conduct of drawdown tests is very similar to that of deliverability tests described in Section 4.1. The reader is referred to that section for details, many of which are directly applicable to drawdown tests.

As described in Section 4.1, the well should be flowed to clear the wellbore of any liquids. After the well has been shut-in and the pressure allowed to stabilize, the well is produced at the selected flow rate for the required time (for the selection of flow rate and duration see Chapter 4). Gradual changes in the flow rate are permissible and variable-rate data may be analyzed by the methods described in Chapter 4, Section 6.1. However, if it is not possible to achieve a stable flow rate due to liquid slugging, drawdown testing is not recommended.

Both flow rates and flowing pressures are recorded throughout the test. The following schedule is recommended for noting the flowing pressures.

Period	Frequency of Measurement
0 to 20 minutes	every 5 minutes
20 minutes to 1 hour	every 10 minutes
1 hour to 2 hours	every 30 minutes

2 hours to 24 hours	every hour
24 hours to 72 hours	every 6 hours
beyond 72 hours	every 24 hours

In multi-rate drawdown tests, specifically a two-rate test, the rate should be changed as quickly as possible. If a shut-in is necessary, it should be kept to an absolute minimum.

When two single-rate tests are being conducted, the well is shut-in after the first test and the pressure is allowed to stabilize before the second test is started. The pressure build-up between the two tests may be monitored as described in Section 4.3 and analyzed by the methods of Chapter 5 to provide supplementary information.

Reporting the Test Results

In addition to the items listed in Section 4.1, a complete report of a drawdown test should include a detailed analysis of the pressure-time data by the methods described in Chapter 4 or by any other comparable techniques.

4.3 Build-Up Tests

Field Conduct

In many ways, the field conduct of build-up tests is similar to that of the deliverability tests described in Section 4.1 of this chapter. The reader is referred to that section for details.

Normally the well is shut-in and the pressure is allowed to build up completely. If a bottom hole pressure gauge is to be used, it is usually lowered in the hole at this time. The test is started by flowing the well at a constant rate and taking pressure and flow rate measurements. Samples of the well effluent should also be taken. Flow should be extended into the transient period, as described in Chapter 5, before the well is shut in. An excessively long drawdown should be avoided. The well is then shut in for the final build-up period. Wellhead and bottom hole pressures are recorded throughout this shut-in period. These readings must begin as soon as possible after shut-in so

that early-time as well as middle-time data are obtained. A recommended schedule for recording the pressures is given in Section 4.2 of this chapter. When sufficient data have been obtained to clearly identify the semilog straight line portion on the build-up plot or when the pressure is completely built up, the test is complete as far as data acquisition is concerned and the equipment may be withdrawn from the well.

For low permeability reservoirs, and in some other situations, the time required to obtain a complete build-up may be excessively long. In such cases the two shut-in periods required by the normal testing procedure described above may not be economically feasible. A suggested alternative is to shut in a well that has been producing for some time and acquire build-up data during this shut-in. The bottom hole pressure gauge should preferably be lowered into the wellbore without interrupting the flow. If that is not possible and the well has to be shut in before the gauge is lowered, flow must be resumed at the same rate as that prior to shut-in and extended for at least ten times the duration of the temporary shut-in. The flowing pressure is then measured and the build-up test conducted as described previously.

Reporting the Test Results

In addition to the items listed in Section 4.1 of this chapter a complete report of a build-up test should contain analyses of the pressure time data by the methods described in Chapter 5 or by any other comparable techniques.

CHAPTER 7   THE ESTIMATION OF RESERVOIR PARAMETERS
AND FLOW BEHAVIOUR FROM LIMITED DATA

1   INTRODUCTION

The drawdown and build-up tests discussed in Chapters 4 and 5, respectively, result in a knowledge of various reservoir parameters and flow characteristics of gas wells. However, these detailed tests are not always successful and in some cases may be uneconomical to conduct. In the former case it becomes necessary to salvage the maximum possible information from the limited data available while in the latter case it is often necessary to conduct short-flow tests. In either case, some useful information may be obtained through the use of limited or short-time data and some judiciously estimated parameters.

This chapter discusses a few methods of utilizing limited data to estimate the reservoir parameters kh, s and $\bar{p}_R$, and the stabilized deliverability equation for a well. Since these methods involve a substantial number of approximations, the added accuracy of the pseudo-pressure approach is not warranted. Accordingly, any of the three approaches, p, p^2 or ψ is used, as and when convenient.

2   BASIC THEORY

The stabilized deliverability equation or the LIT flow equation, in terms of pressure-squared has been derived in the Notes to Chapter 3 and is given by Equation (3N-2) reproduced below:

$$\bar{p}_R^2 - p_{wf}^2 = a'q_{sc} + b'q_{sc}^2 \qquad (7\text{-}1)$$

The parameters a' and b' are defined by Equations (3N-3) and (3N-4), respectively, reproduced below:

$$a' = \frac{3.263 \times 10^6 \; \mu \; Z \; T}{k \; h} \; \log\left(\frac{0.472 \; r_e}{r_w}\right) + \frac{s}{2.303} \qquad (7\text{-}2)$$

$$b' = \frac{1.417 \times 10^6 \; \mu \; Z \; T}{k \; h} \; D \qquad (7\text{-}3)$$

where

μ = gas viscosity, cp

Z = compressibility factor of the gas

T = reservoir temperature, $^{\circ}R$

k = reservoir permeability, md

h = net pay thickness, ft

r_e = external radius of the reservoir, ft

r_w = wellbore radius, ft

s = skin factor, dimensionless

D = IT flow factor, $MMscfd^{-1}$

Equations (7-1), (7-2) and (7-3) form the basis for most calculations in Section 4 of this chapter. However, the reservoir characteristics and gas properties reflected in Equations (7-2) and (7-3) may have to be evaluated in order to obtain the stabilized deliverability relationship represented by Equation (7-1). Accordingly, the next section covers the methods for estimating kh, s, D and T which are used in subsequent sections to develop the LIT flow equation.

3 ESTIMATION OF RESERVOIR PARAMETERS

The reservoir parameters, kh and s, may be estimated from limited data or short-flow tests. The skin factor, s, may also be approximated from well completion details. The IT flow factor, D, may be calculated through estimates or laboratory measurements of the turbulence factor, β. The temperature, T, of the reservoir may be estimated from established temperature gradients for the region in cases where direct measurements are not available.

3.1 Estimation of Permeability-Thickness and Skin Factors from Type Curves

The permeability-thickness, kh, and the skin factor, s, are usually calculated by the analysis of drawdown or build-up test data as described in Chapters 4 and 5, respectively. In some instances, however, the available data are not amenable to a transient analysis in which case it becomes necessary to analyze limited data or short-flow test data. Type curve matching techniques are suited to this purpose, but should only be used as a last resort (Earlougher and Kersch, 1974).

Several type curves (Chapter 2, Section 10) have been published for the analysis of early-time and transient flow data. The general principles related to their application are discussed in Chapter 4, Section 2, and in Chapter 5, Section 2.

Two of the type curves given in Chapter 2, Section 10, namely, Figures 2-23 and 2-24 are particularly useful for the analysis of early-time data. The use of these type curves along with one due to Earlougher and Kersch (1974) is described in this section.

Unfractured Wells

In unfractured wells, the early-time data are controlled by wellbore storage and skin effects (Ramey, 1970, Earlougher and Kersch, 1974). Figure 7-1, developed by Earlougher and Kersch (1974), is particularly useful for analyzing wellbore storage controlled early-time data. The application of this type curve, to estimate kh and s, after it has been ascertained that an analysis of early-time data is desirable, as described by Earlougher and Kersch (1974) is given below:

Step 1: Plot the observed test data as $\Delta p/t$ versus t (where Δp is the pressure change during the test, and t is the time since the beginning of the test) on transparent logarithmic graph paper of the same size as Figure 7-1. This plot is referred to as the data plot.

Step 2: Estimate the wellbore storage coefficient expected from well

completion details using Equation (2-149) reproduced below:

$$C_s = V_{ws} c_{ws} \qquad \text{(7-4)}$$

Step 3: Calculate the location of the horizontal asymptote on the data plot

$$\left(\frac{\Delta p}{t}\right)_{1.0} = \frac{(q_{sc} \times 10^6)\ B}{24\ C_s} \qquad \text{(7-5)}$$

where

$$B = \frac{P_{sc}}{p}\frac{T}{T_{sc}} Z$$

The quantity on the left-hand side of Equation (7-5) is the value of $(\Delta p/t)$ observed on the data plot when

$$\left(\frac{\Delta p}{t}\ \frac{24\ C_s}{(q_{sc} \times 10^6)\ B}\right)_{\text{Figure 7-1}} = 1.0$$

Step 4: Place the data plot over Figure 7-1 so that the asymptote calculated in Equation (7-5) overlies the value of 1.0 on the ordinate of Figure 7-1.

Step 5: Slide the data plot horizontally until the best match is obtained with any one of the curves on Figure 7-1. In order to get a good match, it may be necessary to add a small amount of vertical movement to the data plot. In any case, it is important that the grids of the data plot and Figure 7-1 be kept parallel to each other.

Step 6: Sketch the matched curve onto the data plot and keep the data plot transfixed on the type curve (Figure 7-1). From Figure 7-1 read the value of

$$\left(C_{sD}\ e^{2s}\right)_M$$
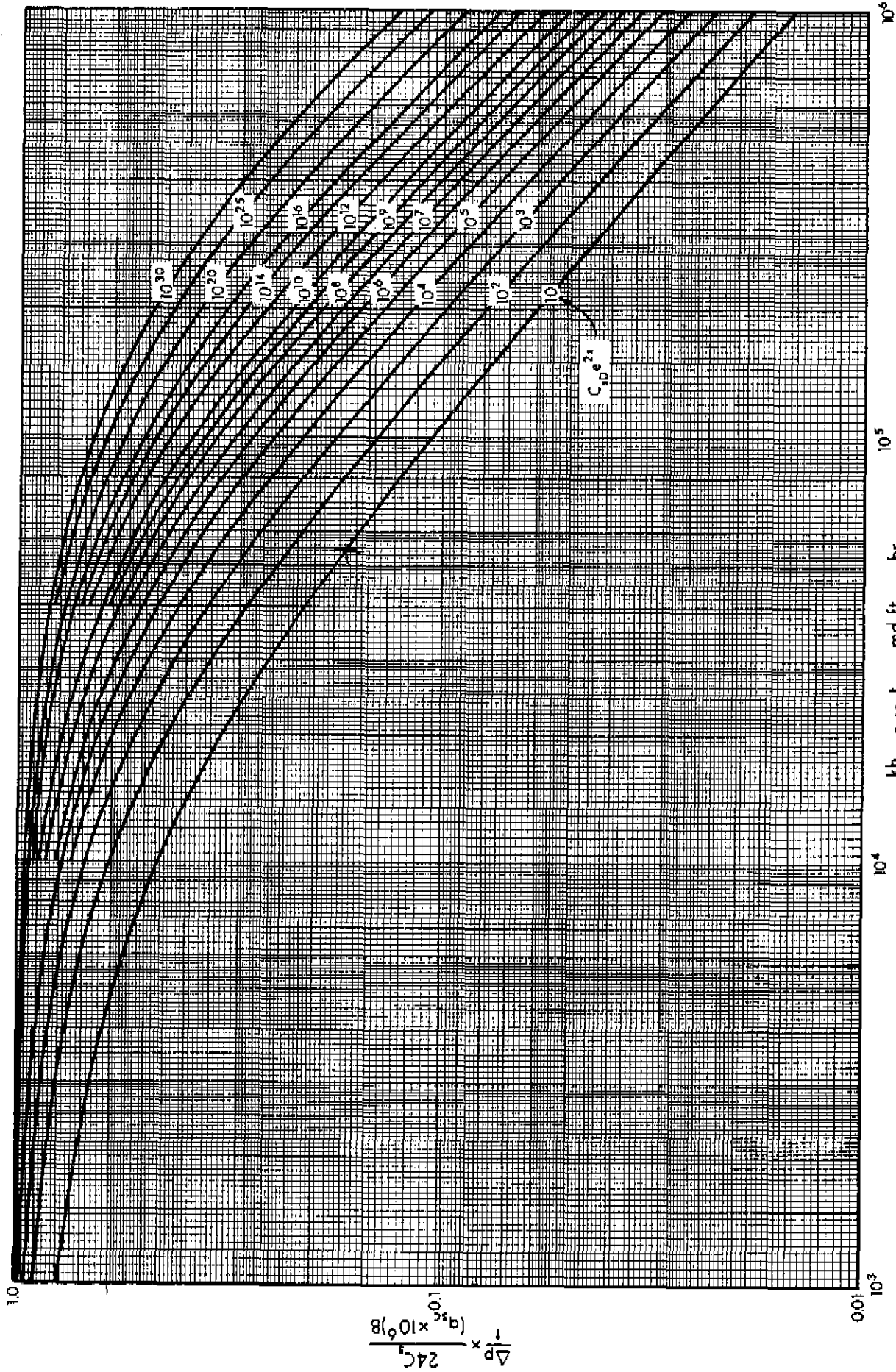
FIGURE 7-1. TYPE CURVE FOR MATCHING SHORT-FLOW TEST DATA

From Earlougher and Kersch (1974)

Pick any convenient match point and read the following values

$(\Delta p/t)_M$ and $(t)_M$ from the data plot

$$\left(\frac{\Delta p}{t} \ \frac{24 \ C_s}{(q_{sc} \times 10^6) \ B}\right)_M \quad \text{and} \quad \left(\frac{k \ h}{\mu} \ 5.61 \ \frac{t}{C_s}\right)_M$$

from Figure 7-1

where subscript M refers to a match point or match curve.

Step 7: If any vertical movement was necessary during the matching process, recalculate the wellbore storage coefficient

$$C_s = \frac{(q_{sc} \times 10^6) \ B \left(\dfrac{\Delta p}{t} \ \dfrac{24 \ C_s}{(q_{sc} \times 10^6) \ B}\right)_M}{24 \left(\dfrac{\Delta p}{t}\right)_M} \tag{7-6}$$

where q_{sc} and B are observed for the test, and the other quantities are obtained from Step 6. This value of C_s should be relatively close to that calculated from well completion data in Step 2. If it is not, it is important to search for a reason, such as washed out sections of the hole, voids connecting with the wellbore, and so forth.

Step 8: Estimate formation transmissibility from

$$\frac{k \ h}{\mu} = \frac{C_s \left(\dfrac{k \ h}{\mu} \ 5.61 \ \dfrac{t}{C_s}\right)_M}{5.61 \ (t)_M} \tag{7-7}$$

where C_s is from Equation (7-6). μ may be estimated by the method described in Appendix A and hence the permeability-thickness, kh, may be estimated.

Step 9: Estimate the skin factor from the value of $C_{sD}e^{2s}$ obtained in Step 6. C_{sD} is defined by Equation (2-150).

$$s = \frac{1}{2} \ln \left[\frac{\phi \, h \, c \, r_w^2}{0.159 \, C_s} \left(C_{sD} \, e^{2s} \right)_M \right] \qquad (7-8)$$

where C_s is from Equation (7-6).

The values of kh and s, obtained by this type curve matching technique, are not exact and should be compared with values obtained from alternative sources to improve their reliability. In the absence of any other information, they serve merely as an indication of the magnitude of these parameters and should be treated as such. The uncertainty in the estimated values occurs because of the similar shape of the curves in Figure 7-1 and the possibility of matching more than one curve to the same data plot. However, this curve-matching method will give a much more accurate value of kh, if C_s and s are known from different sources.

EXAMPLE 7-1

Introduction   The use of the type curve (Figure 7-1) presented by Earlougher and Kersch (1974) to analyze wellbore storage controlled early-time data is illustrated. Although Figure 2-22 may be utilized in a similar fashion, it is considerably more difficult to obtain a match with these curves unless data extending into the transient flow region are also available.

Problem   A short-flow test was conducted on a well which was produced at a constant rate of 1.10 MMscfd. The pressure, p_i, in the reservoir prior to the test was 3730 psia. General data pertinent to the test are given below. The early pressure-time data are also tabulated and are given directly in the solution to this problem.

From a recombined gas analysis

$$\bar{\mu} = 0.021 \text{ cp} \qquad \bar{c} = 0.00024 \text{ psia}^{-1}$$

$$c_{ws} = 0.00028 \text{ psia}^{-1}$$

Well/reservoir data:

$T = 670^\circ R$ $h = 20$ ft $\phi = 0.10$

$L = 7200$ ft $r_w = 0.50$ ft $B = 4.5 \times 10^{-3}$

Estimate the permeability, k, of the reservoir and the skin factor, s.

Solution   The following tabulations may be made from the available short-flow test data

t, hr	P_{wf}, psia	$\frac{\Delta p}{t} = \left(\frac{P_i - P_{wf}}{t}\right)$
0	3730	
0.20	3707	115.0
0.30	3696	113.0
0.40	3685	112.5
0.50	3677	106.0
0.60	3668	103.0
0.70	3660	100.0
0.80	3652	97.5
0.90	3643	96.7
1.00	3636	94.0
2.00	3574	78.0
3.00	3526	68.0
4.00	3494	59.0
5.00	3475	51.0
6.00	3459	45.2
7.00	3443	41.0
8.00	3434	37.0
9.00	3424	34.0
10.00	3415	31.5

Step 1:   Plot $\Delta p/t$ versus t on log-log graph paper (of the same size as the type curve of Figure 7-1) as shown in Figure 7-2.

Step 2:   From Equation (7-4)

$$C_s = V_{ws} \, c_{ws}$$

$$= \pi(0.50)^2 \,(7200)\,(0.00028) = 1.583 \text{ ft}^3/\text{psia}$$

Step 3: From Equation (7-5)

$$\left(\frac{\Delta p}{t}\right)_{1.0} = \frac{(q_{sc} \times 10^6)\; B}{24\; C_s}$$

$$= \frac{(1.10 \times 10^6)(4.5 \times 10^{-3})}{(24)(1.583)} \cong 130$$

Step 4: A match of the data plot (Figure 7-2) with the type curve $C_{sD}e^{2S} = 10^2$ of Figure 7-1 is possible by keeping the asymptote calculated in Step 3 over the value of 1.0 on the ordinate of Figure 7-1 and sliding the data plot horizontally.

From a convenient match point

$$\left(\frac{\Delta p}{t}\right)_M = 100 \qquad\qquad (t)_M = 1.0$$

$$\left(\frac{\Delta p}{t}\; \frac{24\; C_s}{(q_{sc} \times 10^6)\; B}\right)_M = 0.78 \qquad\qquad \left(\frac{k\,h}{\mu}\; 5.61\; \frac{t}{C_s}\right)_M = 5000$$

Since no vertical movement was necessary, the value of C_s calculated in Step 2 need not be adjusted.

From Equation (7-7)

$$\frac{k\,h}{\mu} = \frac{C_s\left(\dfrac{k\,h}{\mu}\; 5.61\; \dfrac{t}{C_s}\right)_M}{5.61\;(t)_M}$$

$$= \frac{(1.583)(5000)}{(5.61)(1.0)} = 1411$$
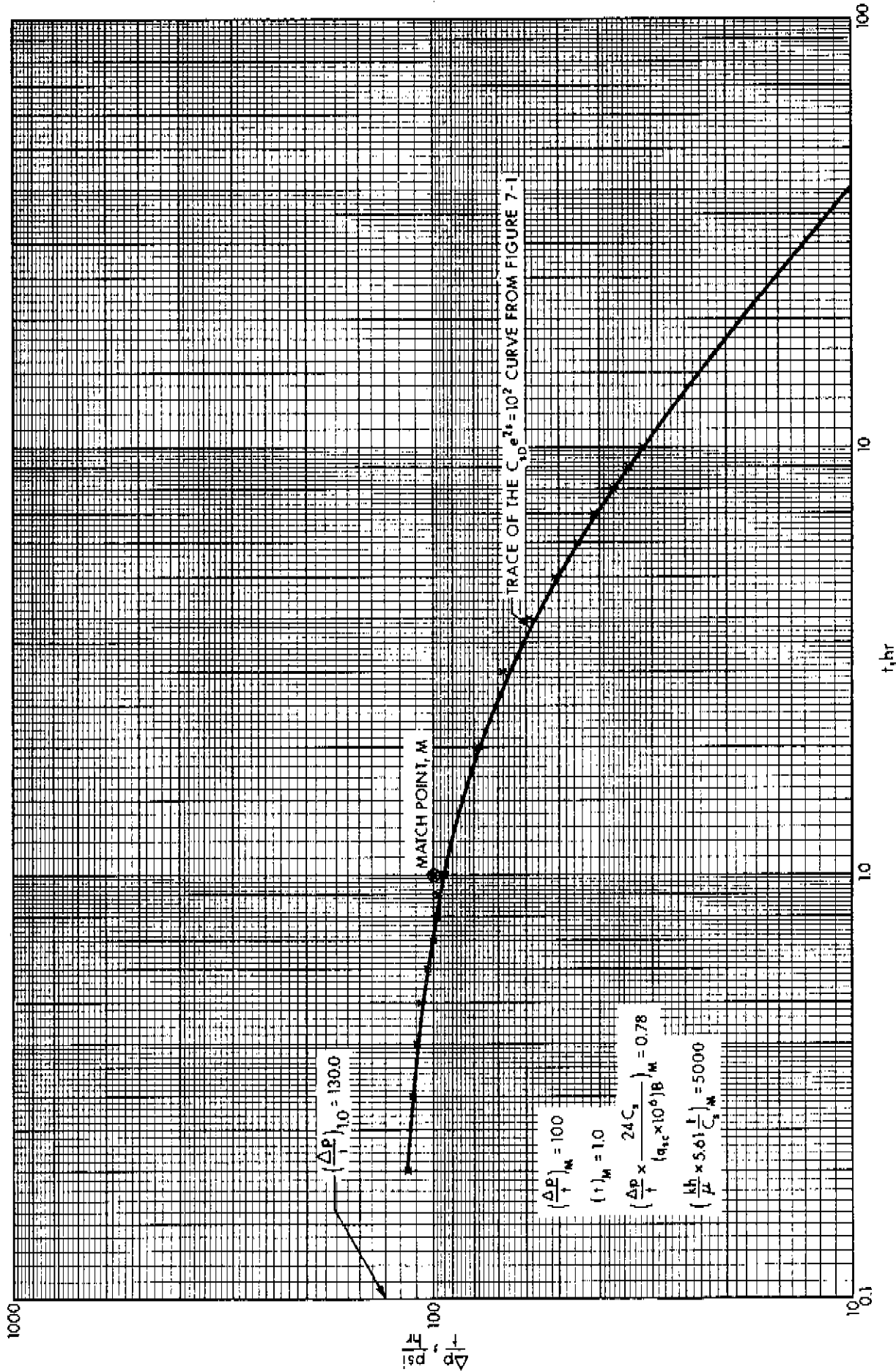
FIGURE 7-2. DATA PLOT AND TYPE-CURVE MATCH FOR THE SHORT-FLOW TEST OF EXAMPLE 7-1

$$\therefore \quad k = \frac{(1411)(0.021)}{(20)} = 1.5 \text{ md}$$

From Equation (7-8)

$$s = \frac{1}{2} \ln \left[\frac{\phi \, h \, c \, r_w^2}{0.159 \, C_s} \left(C_{sD} \, e^{2s} \right)_M \right]$$

$$= \frac{1}{2} \ln \left[\frac{(0.10)(20)(0.00024)(0.50)^2}{(0.159)(1.583)} (100) \right]$$

$$= -1.5$$

Discussion   This example should not be considered as being completely representative of the application of type curves. Data from different tests will not necessarily provide a match and even if they do, the results should always be confirmed by some alternative method. On the other hand, it is easy to see how any one set of data may give a match with more than one of the type curves. For example, if it were not possible to calculate $(\Delta p/t)_{1.0}$, the data of Figure 7-2 could also be matched quite easily to the $C_{sD} e^{2s} = 10^{10}$ type curve of Figure 7-1 in which case the calculated values of k and s would be 5.5 md and 7.7, respectively.

In conclusion, caution must be excercised in using this type curve analysis method and back-up information should be used whenever possible to confirm the results.

Fractured Wells

In fractured wells, linear flow through fractures, rather than wellbore storage, controls early-time data. Figures (2-23) and (2-24) may be used for the analysis of such data to yield values of kh and s.

Although the ordinate and abscissa of Figures (2-23) and (2-24) are given in terms of ψ, they may be modified quite easily for use with either the p or p^2 treatment methods by using appropriate definitions of Δp_d and t_D from Tables 2-3 and 2-4.

After the desirability of an early-time data analysis has been

established, the following procedure may be used to estimate the permeability-thickness, kh, the fracture half-length, x_f, and the skin factor, s.

Step 1: Plot the observed test data as $\Delta\psi$ ($= \psi_i - \psi_{wf}$) versus t on transparent logarithmic graph paper of the same size as Figure 2-23 or Figure 2-24.

Step 2: Slide the data plot over either Figure 2-23 or Figure 2-24, both horizontally and vertically, keeping the axes of the plot parallel until the best match is obtained. The most likely curve is that for $x_e/x_f = \infty$, except where the fracture length and the duration of the test are unusually large.

Step 3: Sketch the matched curve onto the data plot, and keep the data plot transfixed on the type curve (Figure 2-23 or Figure 2-24). Pick any convenient match point and read the following values:

$$(\Delta\psi)_M \qquad \text{and} \qquad (t)_M \qquad \text{from the data plot}$$

$$\left(\frac{k\,h\,\Delta\psi}{1.417 \times 10^6\ T\ q_{sc}}\right)_M \qquad \text{and} \qquad \left(\frac{2.637 \times 10^{-4}\ k\ t}{\phi\ \mu_i\ c_i\ x_f^2}\right)_M$$

$$\text{from Figure 2-23 or Figure 2-24}$$

where subscript M refers to a match point.

Step 4: Estimate the permeability-thickness from

$$k\,h = \frac{1.417 \times 10^6\ T\ q_{sc} \left(\dfrac{k\,h\,\Delta\psi}{1.417 \times 10^6\ T\ q_{sc}}\right)_M}{(\Delta\psi)_M} \tag{7-9}$$

Step 5: Estimate the fracture half-length from

$$x_f = \sqrt{\frac{2.637 \times 10^{-4}\ k\ (t)_M}{\phi\ \mu_i\ c_i \left(\dfrac{2.637 \times 10^{-4}\ k\ t}{\phi\ \mu_i\ c_i\ x_f^2}\right)_M}} \tag{7-10}$$

Step 6:   Estimate the skin factor from Equation (4-2) written as

$$s = - \ln \frac{x_f}{2 \, r_w} \tag{7-11}$$

The application of Figures 2-23 and 2-24 is similar to that of Figure 7-1.

Variable Flow Rates

The type curve analysis methods described above assume that a constant flow rate is maintained during the short-flow test. However, the requirement of constant flow rates is often difficult to satisfy in actual practice (Chapter 3, Section 7.3; Chapter 4, Section 6.1; Chapter 5, Section 6.2). This is particularly so in the case of most drill-stem tests or short-flow tests in low permeability reservoirs. It should be understood that a short-flow test does not necessarily imply a test of short duration. Flow tests that do not extend sufficiently into transient flow may also be labelled short-flow tests even though a fairly large period of flow time is involved, as in the case of low permeability reservoirs.

Variable-rate tests may also be analyzed by type curve analysis techniques. However, the rate variations should be smooth in order that the normalization method described in Chapter 4, Section 6.1 may be extended for use with type curves. The normalization of data is possible with all the type curves presented since q_{sc} occurs in the denominator of the ordinate.

For unfractured wells, Figure 7-1 may be used but the data plot should include $\Delta p/(t \, q_{sc} \times 10^6)$ instead of $\Delta p/t$. Equations (7-4) to (7-8) may be modified accordingly.

For fractured wells, Figures 2-23 and 2-24 may be used but the data plot should include $(\psi_i - \psi_{wf})/q_{sc}$ instead of $(\psi_i - \psi_{wf})$. Equations (7-9) and (7-10) may be modified to accommodate this change.

3.2 Estimation of Skin Factors from
Well Completion Data

Various types of stimulation treatment are often performed to improve the skin factor for a well. This is particularly so in low permeability wells where acidizing or fracturing techniques may be applied. Table 7-1 lists the probable skin factors that may result under different well completion conditions.

Type of Stimulation	Skin Factor, s
Natural Completion	0
Light Acid	- 0.5
Medium Acid or Light Fracture	- 1.0
Heavy Acid or Medium Fracture	- 2.0
Heavy Fracture	- 3.0
Heavy Fracture in Low Permeability	- 4.0
Very Large Fracture in Low Permeability	- 5.0

TABLE 7-1. PROBABLE SKIN FACTORS UNDER VARIOUS
WELL COMPLETION CONDITIONS
from Riley (1970)

The classification of acidizing or fracturing as light, medium or heavy is purely qualitative. In general, light fracturing involves up to 1000 gallons of fracturing fluid per foot of net pay, whereas more than 4000 gal/ft is usually considered fairly heavy. Light acidizing involves up to 300 gal/ft, whereas heavy acidizing usually exceeds 600 gal/ft. The effect of either acidizing or fracturing is much greater for tight sands than for fairly permeable sands. This too is a qualitative classification requiring some engineering judgement. Generally, formations of permeability less than 5 md are considered tight, while those of permeability less than 1 md are considered very tight. A formation permeability more than 25 md is considered to be high.

Simple rules, like the ones described above, have not been developed for estimating positive skin factors. A positive skin factor usually represents a damaged wellbore and modern completion techniques generally avoid this situation.

3.3 Estimation of Inertial-Turbulent Flow Factors

Before any calculations of b', as defined by Equation (7-3), can be made it is necessary to estimate the value of the IT flow factor, D. Swift and Kiel (1962) presented the following equation relating D to the turbulence factor, β.

$$D = \frac{2.715 \times 10^{-12} \beta \, k \, M \, p_{sc}}{h \, \mu \, r_w \, T_{sc}} \qquad (7\text{-}12)$$

where

D	=	IT flow factor, $(\text{MMscfd})^{-1}$
β	=	turbulence factor, ft^{-1}
k	=	reservoir permeability, md
M	=	molecular weight of reservoir gas, $\text{lb}_m/\text{lb mole}$
p_{sc}, T_{sc}	=	pressure and temperature at standard conditions, 14.65 psia and 520°R
h	=	net pay thickness, ft
μ	=	gas viscosity, cp
r_w	=	wellbore radius, ft

Equation (7-12) may also be derived from Equations (2-142) and (2-145) with some simplifying assumptions. Assuming μ to be invariant with pressure and $\frac{1}{r_w} \gg \frac{1}{r_d}$, Equation (2-145) may be integrated and substituted in Equation (2-142) to obtain D as given above.

In Equation (7-12) all parameters are readily available except for β. Cornell and Katz (1953) summarized the characteristics of several consolidated samples of sandstones, dolomites and limestones including values for β and the permeability, k. Janicek and Katz (1955) correlated β versus k with the porosity, ϕ, as a parameter. Katz and

Cornell (1955) reviewed these data and proposed the simple relationship of β to k given below.

$$\beta = \frac{4.11 \times 10^{10}}{k^{4/3}} \tag{7-13}$$

This relationship applies only to sandstones, dolomites and limestones. Substituting Equation (7-13) in Equation (7-12), replacing M by 28.966 G (G = gas gravity) and substituting values for p_{sc} and T_{sc} (14.65 psia, 60°F) gives

$$D = \frac{9.106 \times 10^{-2} \, G}{k^{1/3} \, \mu \, r_w \, h} \tag{7-14}$$

A reasonable approximation of D may be made from Equation (7-14). If different relationships are available for β or if actual laboratory measurements can be made, Equation (7-12) may be used.

3.4 Estimation of Reservoir Temperature

Reservoir or formation temperatures should be measured wherever possible. If no such measurements exist, the temperature may be estimated on the basis of measurements in similar reservoirs in the immediate proximity. When neither of the above methods is applicable, due to a lack of the necessary information, the temperature gradients of the type shown in Figure 7-3 for Alberta may be used. A commonly used gradient of 0.021°F/ft usually serves as a reasonable approximation.

The surface temperature should be measured in order to calculate the temperature gradient in the wellbore. If surface temperature measurements are not available, a mean surface temperature may be obtained from Figure 7-4 which shows the annual mean surface temperatures in the Province of Alberta. The use of a constant mean surface temperature for any area is usually satisfactory, since the ground temperature at a depth of 50 feet can be expected to be at or near the mean annual surface temperature of the area.
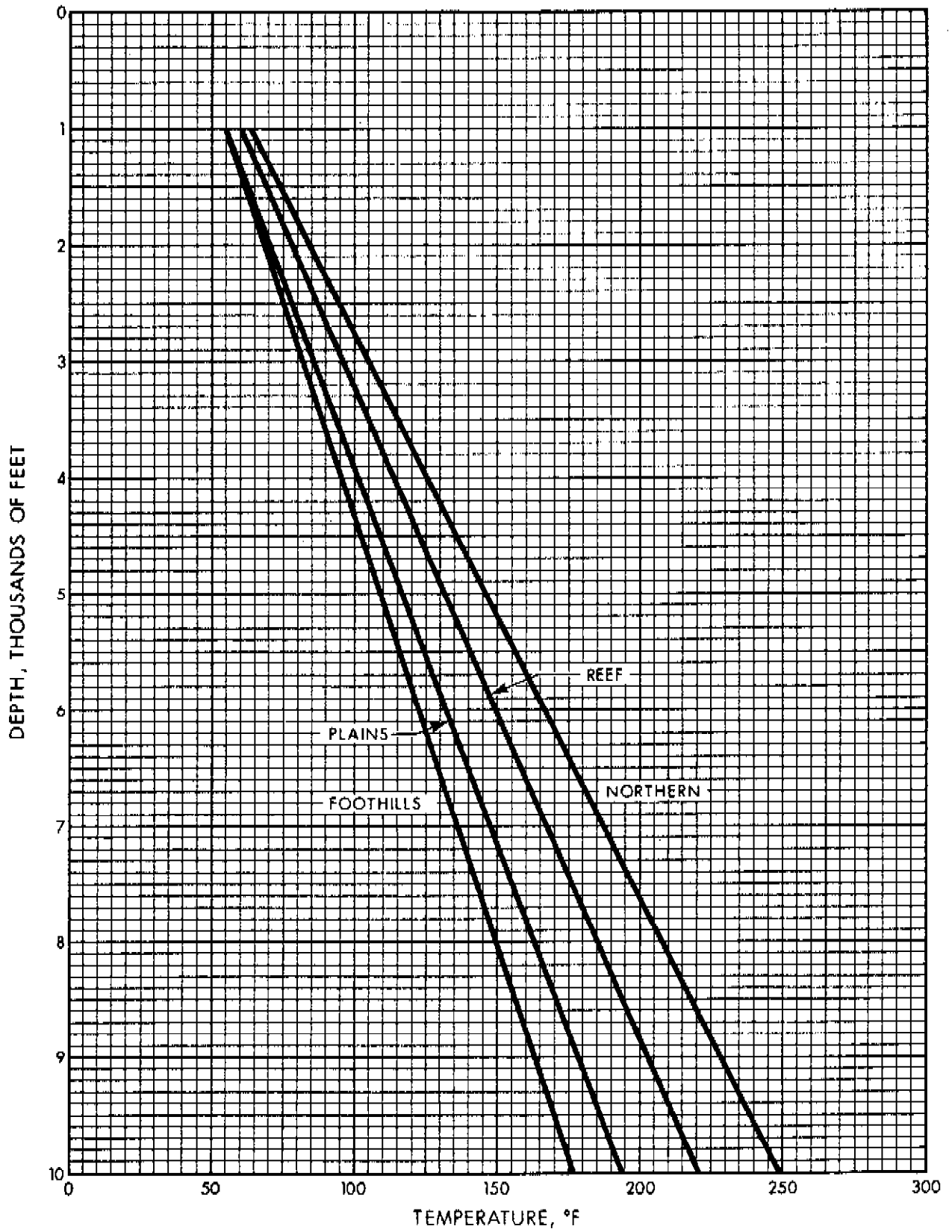
FIGURE 7-3. TEMPERATURE GRADIENTS – PROVINCE OF ALBERTA
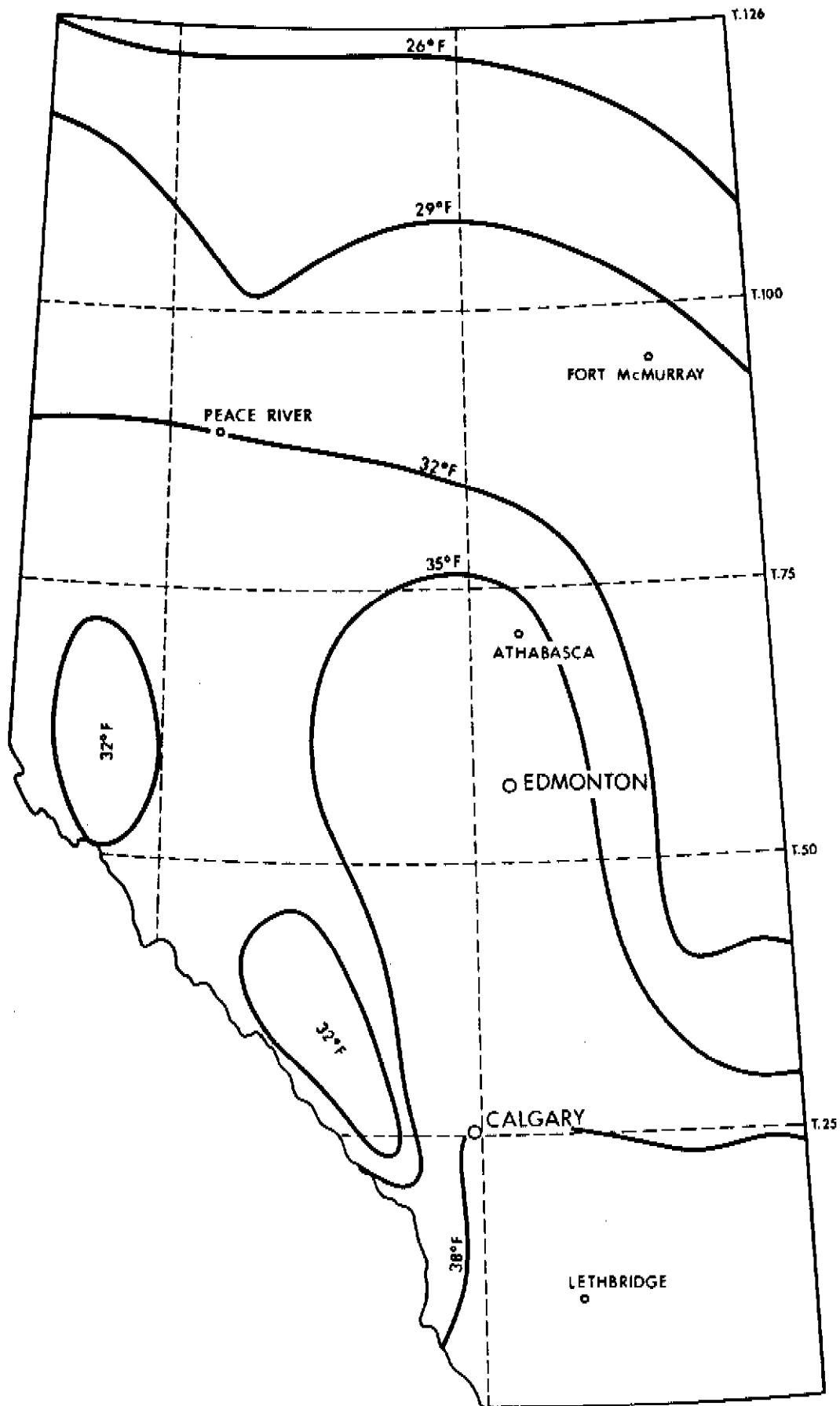
FIGURE 7-4. MEAN ANNUAL SURFACE TEMPERATURES
PROVINCE OF ALBERTA
From Beach (1952)

4 ESTIMATION OF FLOW BEHAVIOUR

In order to estimate the flow behaviour of a well, as represented by Equation (7-1), the following approximate methods may be used where the methods of Chapter 3 cannot be applied.

4.1 LIT Flow Equation (Stabilized) from Estimated Gas and Reservoir Properties

a' and b', as represented by Equation (7-2) and Equation (7-3), respectively, may be calculated if the following parameters are known or estimated: μ, Z, T, k, h, r_e, r_w, s, β, G.

μ, Z and G may be estimated by methods given in Appendix A. T may be obtained from Section 3.4; k, h from Section 3.1; s from Section 3.1 or 3.2; r_e, r_w from field data; β from Equation (7-13) or any other suitable correlation.

For convenience, Equation (7-3) may be expressed in terms of β rather than D by substituting for D from Equation (7-12) to give

$$b' = \frac{3.14 \times 10^{-6}\ \beta\ G\ Z\ T}{h^2\ r_w} \qquad (7\text{-}15)$$

The use of Equations (7-2) and (7-15) to calculate the parameters a' and b' and hence obtain the LIT flow equation is illustrated by Example 7-2.

EXAMPLE 7-2

Introduction The stabilized deliverability relationship is normally obtained by conducting the deliverability tests and associated analyses described in Chapter 3. An approximation may also be obtained by the methods described in this and following sections.

Problem Given the following gas and well/reservoir properties, establish the stabilized deliverability potential of the well.

$\bar{\mu}$ = 0.02 cp (at estimated average reservoir conditions, App. A, Sec. 7)

$\bar{Z}$ = 0.81 (at estimated average reservoir conditions, App. A, Sec. 5)

G = 0.78 (for recombined gas, App. A, Sec. 8)

T = 630°R (from field data and Sec. 3.4)

k = 14 md (from a type curve analysis, Sec. 3.1)

h = 45 ft (from well logs)

r_w = 0.3 ft (from field data)

r_e = 2600 ft (from well spacing for the area)

s = − 2 (from Table 7-1)

Solution

From Equation (7-13)

$$\beta = \frac{4.11 \times 10^{10}}{k^{4/3}}$$

$$= \frac{4.11 \times 10^{10}}{(14)^{4/3}} = 1.22 \times 10^{9} \ ft^{-1}$$

From Equation (7-2)

$$a' = \frac{3.263 \times 10^{6} \ \mu \ Z \ T}{k \ h} \left[\log \left(0.472 \ \frac{r_e}{r_w} \right) + \frac{s}{2.303} \right]$$

$$= \frac{(3.263 \times 10^{6})(0.02)(0.81)(630)}{(14)(45)} \left[\log \frac{(0.472)(2640)}{(0.3)} - \frac{2}{2.303} \right]$$

$$= 145366 \ \frac{psia^2}{MMscfd}$$

From Equation (7-15)

$$b' = \frac{3.14 \times 10^{-6} \ \beta \ G \ Z \ T}{h^2 \ r_w}$$

$$= \frac{(3.14 \times 10^{-6})(1.22 \times 10^{9})(0.78)(0.81)(630)}{(45)^2 \ (0.3)} = 2510 \ \frac{psia^2}{MMscfd^2}$$

From Equation (7-1)

$$\bar{p}_R^2 - p_{wf}^2 = a \, q_{sc} + b \, q_{sc}^2$$

$$\therefore \quad \bar{p}_R^2 - p_{wf}^2 = 145366 \, q_{sc} + 2510 \, q_{sc}^2$$

The above equation may be plotted on logarithmic coordinates to give a stabilized deliverability line of the type shown in Figure 3-2.

4.2 LIT Flow Equation (Stabilized Flow) from a Single Stabilized Flow Test

If a single stabilized flow test is conducted on a well, for example the single-point deliverability test of Chapter 3, Section 4.4, it may be used to replace the least reliable information, in this case the skin factor, s. Hence the procedure simply involves the calculation of b' as shown in Section 4.1. The single-point test yields values for $\bar{p}_R$, p_{wf} and q_{sc}. These values may be substituted in Equation (7-1) to obtain a'. The calculation procedure is illustrated by Example 7-3.

EXAMPLE 7-3

Introduction   In conducting the necessary test, flow must commence from a stabilized pressure, $\bar{p}_R$, and must subsequently continue to stabilized conditions. This may limit application of the test, especially in low permeability reservoirs.

Problem   Given the data of the previous example, except for the skin factor, s, estimate the stabilized deliverability equation for a well that gives a stabilized flowing pressure, p_{wf}, of 2835 psia at a flow rate of 6.0 MMscfd. The average reservoir pressure, $\bar{p}_R$, at the time of the test is 3000 psia.

Solution

From Example 7-2

$$b' = 2510 \ \frac{psia^2}{MMscfd^2}$$

From Equation (7-1)

$$\bar{p}_R^2 - p_{wf}^2 = a'q_{sc} + b'q_{sc}^2$$

$$(3000)^2 - (2835)^2 = a'(6.0) + (2510)(6.0)^2$$

$$a' = 145402 \ \frac{psia^2}{MMscfd}$$

The stabilized deliverability is given by

$$\bar{p}_R^2 - p_{wf}^2 = 145402 \ q_{sc} + 2510 \ q_{sc}^2$$

The above equation may be plotted on logarithmic coordinates to give a stabilized deliverability line of the type shown in Figure 3-2.

4.3 LIT Flow Equation (Stabilized Flow) from a Single Unstabilized Flow Test

It is often desirable, especially for low permeability reservoirs, to predict the stabilized productivity without actually conducting the stabilized flow test of Section 4.2. This may be accomplished through use of a parameter called the stabilization factor (abbreviated SF) defined by McMahon (1961) as the ratio of the stabilized deliverability to the actual deliverability at the time of test.

Obviously, SF is a function of the duration of the test, the reservoir and gas characteristics and the well spacing. Riley (1970) developed the set of curves shown in Figures 7-5(a,b,c,d) assuming a 640 acre spacing, a zero skin factor, $\ln(r_e/r_w) = 9$, and various test times of interest.

The use of these figures is quite simple. The test duration (4, 8, 24 or 72 hours) and a shut-in pressure are taken from the
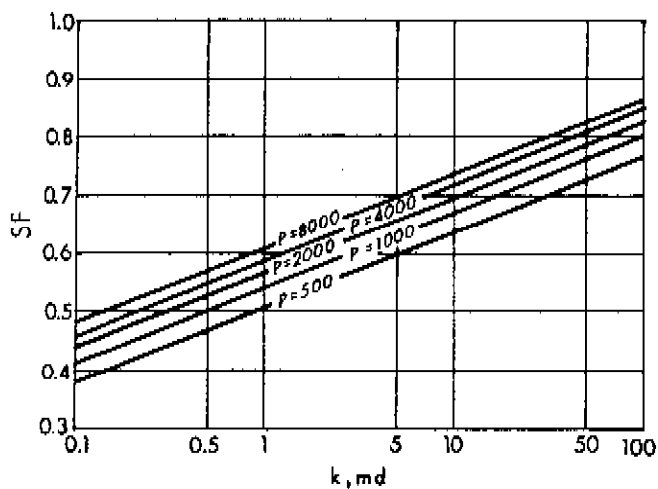
FIGURE 7-5(a). STABILIZATION FACTORS FOR GAS WELLS
TEST DURATION, 4 HOURS
From Riley (1970)
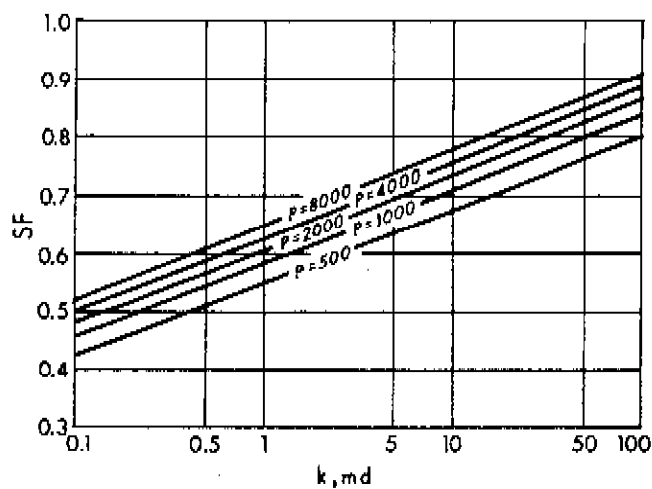
FIGURE 7-5(b). STABILIZATION FACTORS FOR GAS WELLS
TEST DURATION, 8 HOURS
From Riley (1970)
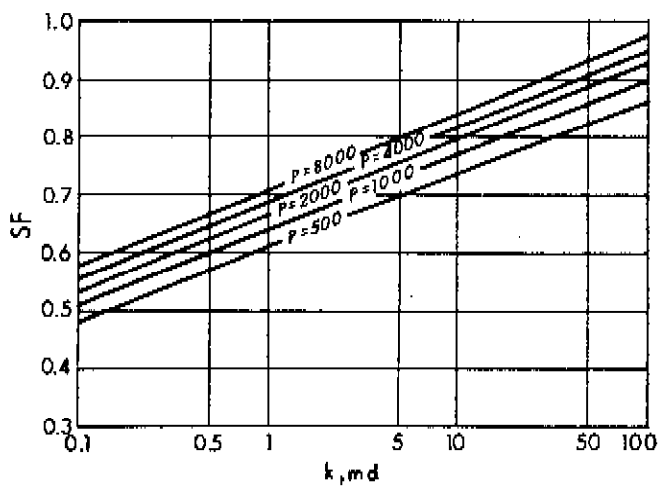
FIGURE 7-5(c). STABILIZATION FACTORS FOR GAS WELLS
TEST DURATION, 24 HOURS
From Riley (1970)
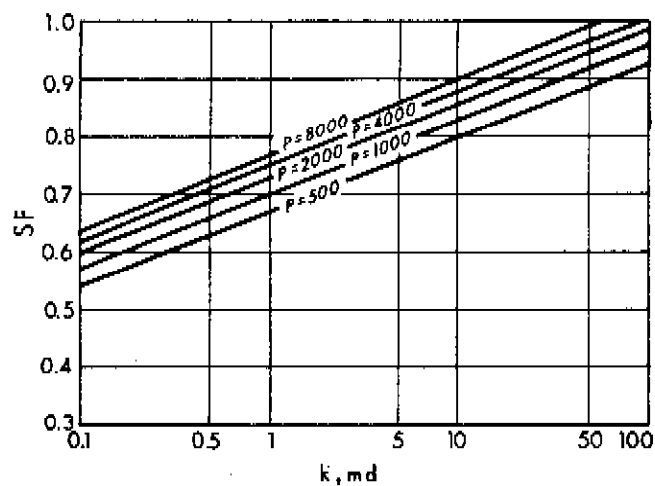
FIGURE 7-5(d). STABILIZATION FACTORS FOR GAS WELLS
TEST DURATION, 72 HOURS
From Riley (1970)

available short-term test. The only other term then needed is permeability, which may be estimated by the methods of Section 3.1, from core data or any other reliable source. Selecting the proper time graph, SF is obtained corresponding to the permeability and shut-in pressure. This factor, when applied to the short-term flow rate, gives a reasonable approximation of the stabilized flow rate at the back pressure obtained in the flow test.

Simple adjustments may be made to the value of SF for cases where the well spacing is different from 640 acres or where the skin factor is not zero.

$$SF \text{ (corrected)} = \frac{SF \text{ (from graph)} \times 9 + s}{\ln (r_e/r_w) + s} \qquad (7\text{-}16)$$

Values for s may be estimated as shown in Section 3.2.

The method described above is based on equations which neglect turbulence effects. It has been shown in the Notes to Chapter 3 that for fully laminar flow Equation (7-1) reduces to

$$\bar{p}_R^2 - p_{wf}^2 = a'q_{sc} \qquad (7\text{-}17)$$

When turbulence exists, this approximation should be used to predict the deliverability only for flow rates in the vicinity of the flow rate used to develop this equation.

Using the value of SF, calculated above, to obtain a stabilized q_{sc} corresponding to the Δp^2 (= $\bar{p}_R^2 - p_{wf}^2$), a' may be calculated as illustrated by Example 7-4.

EXAMPLE 7-4

Introduction   In well testing situations where turbulence effects can be neglected, it is possible to estimate the stabilized deliverability equation without actually conducting a stabilized flow test.

Problem   A short-flow test (four hours), conducted on the well of

of Examples 7-2 and 7-3 gave a flowing sandface pressure, p_{wf}, of 2905 psia at a flow rate of 6.0 MMscfd. Calculate the stabilized deliverability relationship assuming negligible turbulence effects.

Solution

From Example 7-3

$$\bar{P}_R = 3000 \text{ psia}$$

From Example 7-2

$$k = 14 \text{ md}$$

From Figure 7-5(a), for a permeability of 14 md and at a pressure of 3000 psia,

$$SF = 0.72$$

From Example 7-3 it is seen that the well spacing is the same as that for the curves of Figure 7-1, whereas the skin equals -2.

From Equation (7-13)

$$SF \text{ (corrected)} = \frac{SF \text{ (graph)} \times 9 + s}{\ln (r_e/r_w) + s}$$

$$= \frac{(0.72)(9) - 2}{9 - 2} = 0.64$$

∴ Equivalent stabilized flow rate $= 0.64 \times 6$

$$= 3.84 \text{ MMscfd}$$

From Equation (7-14)

$$\bar{P}_R^2 - P_{wf}^2 = a'q$$

$$3000^2 - 2905^2 = a'(3.84)$$

$$a' = 146087 \frac{\text{psia}^2}{\text{MMscfd}}$$

Hence the stabilized deliverability is given by

$$\bar{p}_R^2 - p_{wf}^2 = 146087 \, q_{sc}$$

5 PREDICTION OF AVERAGE RESERVOIR PRESSURE

The detailed method for predicting average reservoir pressures, discussed in Chapter 5, Section 4.2, may only be applied to middle-time data acquired during build-up tests. The prediction of average reservoir pressures from short-flow tests and from deliverability tests is described in the following sections.

5.1 Average Reservoir Pressure from the Stabilized Deliverability Equation

The stabilized deliverability equation, or the LIT flow equation, may be obtained from limited data or short-flow tests by the methods described in the previous sections or by the methods of Chapter 3. The average reservoir pressure, at any time of interest during the life of a well may then be calculated quite easily. The test simply involves the measurement of the stabilized flow rate and the associated bottom hole pressure. The calculation procedure is illustrated by Example 7-5.

EXAMPLE 7-5

Introduction The stabilized deliverability equation for a well theoretically changes with any variations in the parameters appearing in Equations (3-2) and (3-3). In many instances, however, the variation of these parameters with declining pressure or production life is small enough to be neglected, and the LIT flow equation may be considered to be valid over a lengthy period of time.

Problem Assuming that the stabilized deliverability equation developed

in Example 7-3 represents accurately the present production period for the well, calculate the average reservoir pressure if the flowing bottom hole pressure, p_{wf}, is 2475 psia corresponding to a stabilized flow rate of 10 MMscfd.

Solution

From Example 7-3

$$\bar{p}_R^2 - p_{wf}^2 = 145402 \ q_{sc} + 2510 \ q_{sc}^2$$

$$\bar{p}_R^2 - (2475)^2 = 145402 \ (10) + 2510 \ (10)^2$$

$$\bar{p}_R = \sqrt{7830645}$$

$$\approx 2800 \text{ psia}$$

5.2 Average Reservoir Pressure Not Knowing the Stabilized Deliverability Equation

When the stabilized deliverability equation is not known or when there is reason to believe that a previously obtained deliverability equation no longer applies to a partially depleted reservoir, the average reservoir pressure at any time during the producing life of the well may be obtained as follows.

If the value of b' is known, say from an isochronal deliverability test (Chapter 3, Section 4.2), a procedure similar to a two-rate test may be used. When a well is producing at a stabilized rate, measure q_1 and the corresponding flowing bottom hole pressure, p_{wf_1}. Then Euqation (7-1) may be written as

$$\bar{p}_R^2 - p_{wf_1}^2 = a'q_1 + b'q_1^2 \tag{7-18}$$

Immediately change the flow rate to q_2 and when the pressure has stabilized determine the flowing bottom hole pressure, p_{wf_2}. Again,

from Equation (7-1)

$$\bar{p}_R^2 - p_{wf_2}^2 = a'q_2 + b'q_2^2 \qquad (7\text{-}19)$$

Eliminating a' from Equations (7-18) and (7-19) gives

$$\bar{p}_R^2 = \frac{q_2\, p_{wf_1}^2 - q_1\, p_{wf_2}^2}{q_2 - q_1} - b'q_1q_2 \qquad (7\text{-}20)$$

Bennett and Forgerson (1974) suggest a similar procedure when Equation (3-1) is used as the stabilized deliverability equation. In this case n is calculated from an isochronal deliverability test (Chapter 3, Section 4.2), and using exactly the same testing procedure as described above the following relationship may be derived

$$\bar{p}_R^2 = \frac{q_2^{1/n}\, p_{wf_1} - q_1^{1/n}\, p_{wf_2}^2}{q_2^{1/n} - q_1^{1/n}} \qquad (7\text{-}21)$$

When the value of b' or n is not known, the above analysis is simply extended to include a third flow rate. This yields a set of three simultaneous equations in three unknowns which may be solved to obtain $\bar{p}_R$.

EXAMPLE 7-6

Introduction   The flow constant, b', may be estimated by methods discussed in previous sections of this chapter or by the analysis of the deliverability tests of Chapter 3, Section 4. The average reservoir pressure at any time during the producing life of the well may then be estimated from a simple test.

Problem   A well that had been producing for some time gave a stabilized flow rate of 4.0 MMscfd and a corresponding bottom hole flowing pressure of 1320 psia. When the rate was changed to 6.0 MMscfd and the pressure permitted to stabilize a flowing bottom hole pressure of 860.0 psia was

obtained.

A previously conducted isochronal test on the same well gave a value for b' equal to 13400 psia^2/MMscfd. Assuming that this value of b' may still be considered valid for the well, calculate the average reservoir pressure at the time of the test.

Solution

$$q_1 = 4.0 \text{ MMscfd} \qquad\qquad p_{wf_1} = 1320 \text{ psia}$$

$$q_2 = 6.0 \text{ MMscfd} \qquad\qquad p_{wf_2} = 860 \text{ psia}$$

From Equation (7-20)

$$\bar{p}_R^2 = \frac{q_2 \, p_{wf_1}^2 - q_1 \, p_{wf_2}^2}{q_2 - q_1} - b' q_1 q_2$$

$$= \frac{(6)(1320)^2 - (4)(860)^2}{(6 - 4)} - (13400)(4)(6)$$

$$= 3426400$$

$$\bar{p}_R = 1851 \text{ psia}$$

Discussion   A similar procedure may be used if the simplified approach represented by Equation (3-1) is being used. However, the limitations of Equation (3-1), described in Chapter 3, Section 2, should be kept in mind when using the simplified method.

APPENDIX A

PROPERTIES OF NATURAL GASES

This appendix reviews those physical properties of natural
gases that are of importance in the evaluation of gas well performance.
It presents a summary of prediction methods, associated formulae, graphs
and tables related to these properties.

The properties of a natural gas may be determined either
directly by laboratory tests or by prediction from the known chemical
composition of the gas. In the latter case the calculations are based
on the physical properties of individual components of the gas and upon
physical laws, often referred to as mixing rules, relating the properties
of the components to those of the mixture.

1. Properties of Constituent Components

The relevant physical properties of typical constituent
components of natural gases are listed in Table A-1. The data include
molecular weight, critical pressure, critical temperature, condensate
vaporizing volume ratio and gross heating value of each component.

The molecular weight of a substance is the sum of the atomic
weights of the atoms in each molecule of the substance, the weight of
an atom of oxygen being taken as 16.

The critical temperature of a pure substance may be defined
as the maximum temperature at which liquid and vapour phases can coexist
in equilibrium. The vapour pressure at this temperature is called the
critical pressure.

The condensate vaporizing volume ratio is the ratio of the
volume of gas at standard conditions of temperature and pressure ($60^{\circ}F$
and 14.65 psia) to the volume that it would occupy in the liquid state
at the same temperature and pressure.

The gross heating value of a gas in the total heat liberated
when a unit volume of the gas is burned under specified conditions.
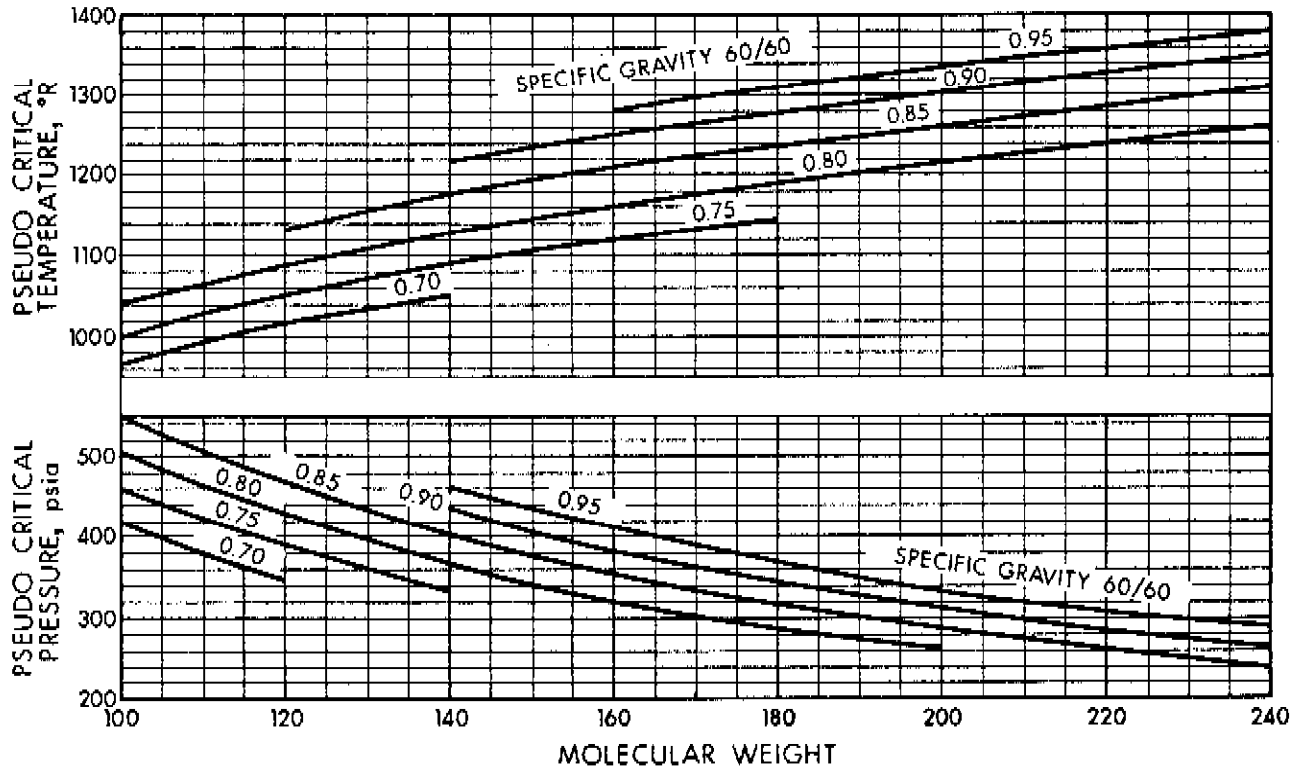
FIGURE A-1. CORRELATION CHARTS FOR ESTIMATION OF THE PSEUDOCRITICAL TEMPERATURE AND PRESSURE OF HEPTANES PLUS FRACTIONS FROM MOLECULAR WEIGHT AND SPECIFIC GRAVITY

From Katz (1942)

2. The Gas Law

The ideal gas law provides a relationship between the pressure, the temperature and the specific volume of an ideal gas. This relationship is modified by use of a compressibility factor, Z, to account for deviations, from ideality, in the behaviour of real gases. Commonly referred to as the Gas Law, the relationship for real gases is:

$$pv = \frac{Z\,R\,T}{M} \qquad (A-1)$$

where

p = pressure under which the gas exists

v = specific volume of the gas

Z = compressibility factor for the real gas

Component	M	P_{ci}	T_{ci}	V_i	Gross Heating Value
	lb_m/lb mole	psia	°R	scf gas/Imp.gal. at 14.65 psia and 60°F	Btu/ft³ at 14.65 psia and 60°F (dry)
N_2	28.013	493.0	227.27	-	-
CO_2	44.010	1071.0	547.57	71.61	-
H_2S	34.076	1306.0	672.37	88.34	635.0
[1]He	4.003	33.2	9.80	-	-
CH_4	16.042	667.8	343.04	71.26	1006.5
C_2H_6	30.070	707.8	549.76	45.17	1763.3
C_3H_8	44.097	616.3	665.68	43.87	2509.5
iC_4H_{10}	58.124	529.1	734.65	36.92	3242.5
nC_4H_{10}	58.124	550.7	765.32	38.31	3251.9
iC_5H_{12}	72.151	490.4	828.77	32.99	3987.8
nC_5H_{12}	72.151	488.6	845.37	33.33	3996.9
C_6H_{14}	86.178	436.9	913.37	29.36	4741.2
[2]$C_7H_{16}^+$	114.232	360.6	1023.89	23.58	6230.1

[1]Data for He from Reid and Sherwood (1966).

[2]Physical properties of octane are used for the C_7^+ fraction. Alternatively, the pseudo-critical temperature and pseudo-critical pressure may be obtained from Figure A-1 which gives these properties as a function of molecular weight and specific gravity of the C_7^+ fraction.

TABLE A-1. PHYSICAL PROPERTIES OF TYPICAL COMPONENTS OF NATURAL GASES

From GPSA Engineering Data Book (1974)

T = absolute temperature

M = molecular weight of the gas

R = gas constant, 10.7 when p is in psia, v is in ft^3/lb_m, T is in ^OR and M is in lb_m/lb mole

Equation (A-1) may be rearranged to a more convenient form:

$$\rho = \frac{1}{v} = \frac{2.707\ G\ p}{Z\ T} \qquad (A-2)$$

where

ρ = density of the gas

G = specific gravity of the gas (air = 1) = $M/28.964$

3. Theorem of Corresponding States

This theorem states that the deviation of a real gas from the ideal gas law is the same for different gases at corresponding conditions as related to some basic property such as the critical temperature or critical pressure. These corresponding conditions are found at the same fraction of the absolute critical temperature and pressure, which are defined as follows:

$$\text{Reduced temperature,}\ T_{ri} = T/T_{ci} \qquad (A-3)$$

$$\text{Reduced pressure,}\ P_{ri} = p/p_{ci} \qquad (A-4)$$

where

T_{ci} = critical temperature of any pure component i

P_{ci} = critical pressure of any pure component i

4. Properties of Natural Gases

Kay (1936) formulated mixing rules which are used, unless otherwise specified, to determine the physical properties of a natural gas from the properties of its consitutent components. These pseudo-properties of a natural gas are determined as follows:

Pseudo-critical temperature, $T_c = \sum_i x_i T_{ci}$ (A-5)

Pseudo-critical pressure, $P_c = \sum_i x_i P_{ci}$ (A-6)

Pseudo-reduced temperature, $T_r = T/T_c$ (A-7)

Pseudo-reduced pressure, $P_r = p/P_c$ (A-8)

where

x_i = mole fraction of component i

The calculation procedure for determining pseudo properties of a sweet natural gas from its composition is illustrated by Example A-1.

EXAMPLE A-1

Problem   Compute the pseudo-critical properties of a sweet natural gas of known composition: N_2, 1.38%; CH_4, 93.0%; C_2H_6, 3.29%; C_3H_8, 1.36%; iC_4H_{10}, 0.23%; nC_4H_{10}, 0.37%; iC_5H_{12}, 0.12%; nC_5H_{12}, 0.10%; C_6H_{14}, 0.08% and $C_7H_{16}^+$, 0.05%.

Solution   The tabulations below illustrate the calculation procedure:

Component	Mole Fraction x_i	Mol. Weight M_i	$x_i M_i$	Critical Temp. °R T_{ci}	$x_i T_{ci}$	Critical Pres.psia P_{ci}	$x_i P_{ci}$
N_2	0.0138	28.013	0.3866	227.29	3.14	493.0	6.80
CH_4	0.9302	16.042	14.9223	343.06	319.11	667.8	621.19
C_2H_6	0.0329	30.070	0.9893	549.78	18.09	707.8	23.29
C_3H_8	0.0136	44.097	0.5997	665.70	9.05	616.3	8.38
iC_4H_{10}	0.0023	58.124	0.1337	734.67	1.69	529.1	1.22
nC_4H_{10}	0.0037	58.124	0.2151	765.34	2.83	550.7	2.04
iC_5H_{12}	0.0012	72.151	0.0866	828.79	0.99	490.4	0.59
nC_5H_{12}	0.0010	72.151	0.0722	845.39	0.85	488.6	0.49
C_6H_{14}	0.0008	86.178	0.0689	913.39	0.73	436.9	0.35
$C_7H_{16}^+$	0.0005	114.232	0.0571	1023.91	0.51	360.6	0.18

$$M = \sum x_i M_i = 17.5315 \qquad \sum x_i T_{ci} = 356.99 \qquad \sum x_i P_{ci} = 664.53$$

$$G = M/28.964 = 0.605$$

$$T_c = 356.99^{\circ}R$$

$$P_c = 664.53 \text{ psia}$$

In cases where the composition of a natural gas is not available, the pseudo-critical pressure and pseudo-critical temperature may be approximated from Figure A-2 and the gas gravity. The specific gravity of the gas in Example A-1 is 0.605. From Figure A-2, the pseudo-critical temperature is $358^{\circ}R$ compared with $356.99^{\circ}R$ calculated; the pseudo-critical pressure is 671 psia compared with 664.53 psia calculated.

Thomas, Hankinson and Phillips (1970) took data from Figure A-2 and more recent data from other sources to obtain the following correlations:

$$T_c = 170.491 + 307.344 \, G \qquad\qquad (A-9)$$

$$P_c = 709.604 - 58.718 \, G \qquad\qquad (A-10)$$

The allowable concentrations of sour gases and other non-hydrocarbons for the above equations are 3% H_2S, 5% N_2, or a total impurity content of 7%. Consequently, these equations should be applicable to the natural gas of Example A-1. For a gas gravity of 0.61, Equations (A-9) and (A-10) give a pseudo-critical temperature of $356.43^{\circ}R$ and a pseudo-critical pressure of 674.08 psia. For sour natural gases, Kay's mixing rules are used along with the relevant physical properties of the sour gas constituent components to determine the pseudo-critical properties. The calculation procedure for determining the pseudo properties of a sour natural gas from its composition is illustrated by Example A-2.

EXAMPLE A-2

Problem   Compute the pseudo-critical properties of a sour natural gas of known composition: N_2, 2.36%; CO_2, 1.64%; H_2S, 18.41%; CH_4, 77.00%; C_2H_6, 0.42%; C_3H_8, 0.05%; iC_4H_{10}, 0.03%; nC_4H_{10}, 0.03%; iC_5H_{12}, 0.01%;

nC_5H_{12}, 0.01%; C_6H_{14}, 0.01%; $C_7H_{16}^+$, 0.03%.

<u>Solution</u> The tabulations below illustrate the calculation procedure:

Component	Mole Fraction x_i	Mol. Weight M_i	x_iM_i	Critical Temp. °R T_{ci}	x_iT_{ci}	Critical Pres.psia p_{ci}	x_iP_{ci}
N_2	0.0236	28.013	0.6611	227.29	5.36	493.0	11.63
CO_2	0.0164	44.010	0.7218	547.57	8.98	1071.0	17.56
H_2S	0.1841	34.076	6.2734	672.37	123.78	1306.0	240.43
CH_4	0.7700	16.042	12.3523	343.06	264.16	667.8	514.21
C_2H_6	0.0042	30.070	0.1263	549.78	2.31	707.8	2.97
C_3H_8	0.0005	44.097	0.0220	665.70	0.33	616.3	0.31
iC_4H_{10}	0.0003	58.124	0.0174	734.67	0.22	529.1	0.16
nC_4H_{10}	0.0003	58.124	0.0174	765.34	0.23	550.7	0.17
iC_5H_{12}	0.0001	72.151	0.0072	828.79	0.08	490.4	0.05
nC_5H_{12}	0.0001	72.151	0.0072	845.39	0.08	488.6	0.05
C_6H_{14}	0.0001	86.178	0.0086	913.39	0.09	436.9	0.04
$C_7H_{16}^+$	0.0003	114.232	0.0343	1023.91	0.31	360.6	0.11

$$\sum x_iM_i = 20.2490 \qquad \sum x_iT_{ci} = 405.93 \qquad \sum x_iP_{ci} = 787.69$$

$$G = M/28.964 = 0.699$$
$$T_c = 405.93°R$$
$$P_c = 787.69 \text{ psia}$$

In cases where the composition of a natural gas is not available, the pseudo-critical temperature and the pseudo-critical pressure may be approximated from Figure A-2 and the gas gravity. The specific gravity of the gas in Example A-2 is 0.700. From Figure A-2, using the inserts to correct for the presence of H_2S, CO_2 and N_2, the pseudo-critical temperature is 409°R compared with 405.93 calculated; the pseudo-critical pressure is 785 psia compared with 787.69 psia calculated.
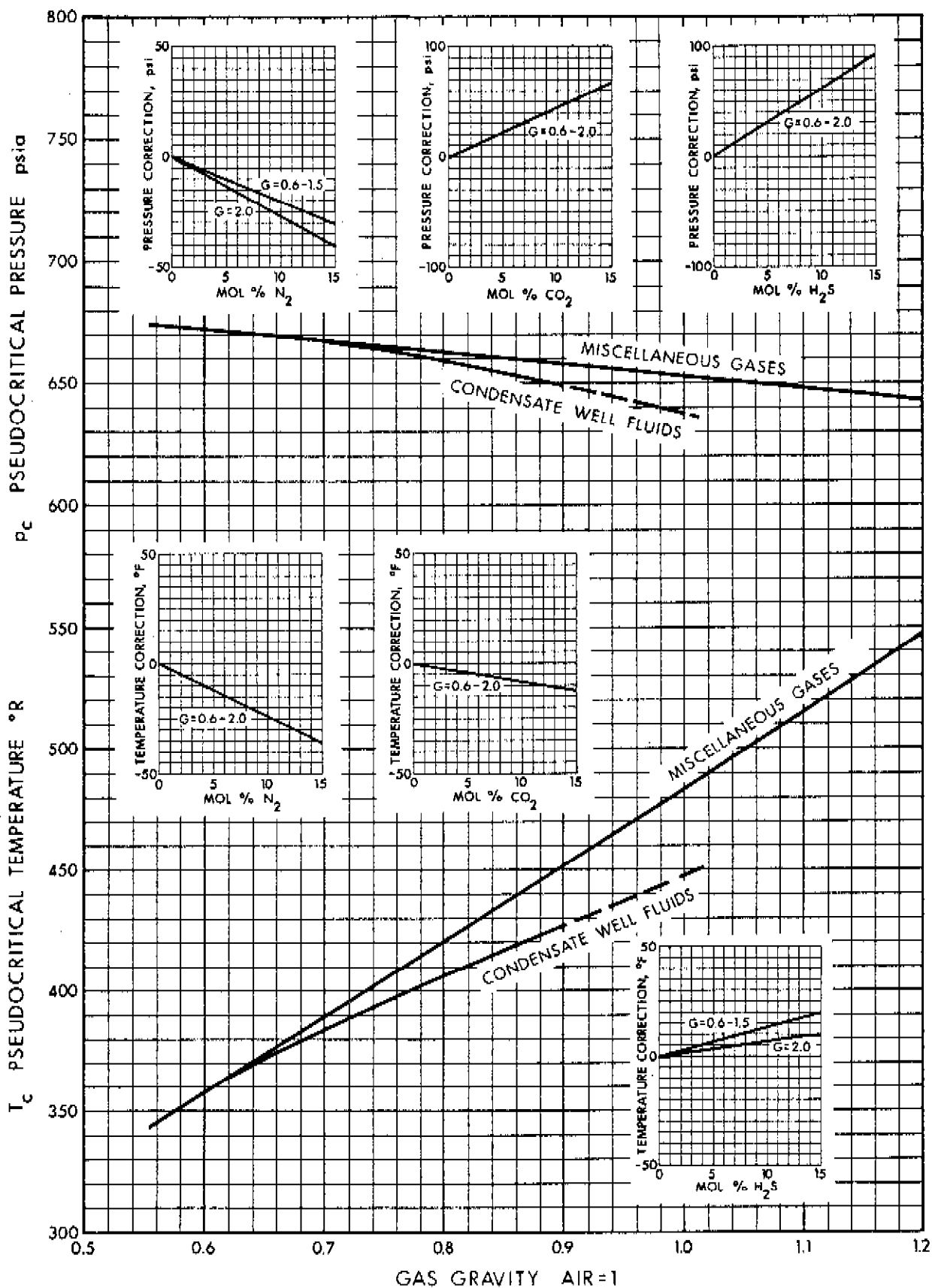
FIGURE A-2. PSEUDO CRITICAL PROPERTIES OF MISCELLANEOUS NATURAL GASES

From Brown, Katz, Oberfell and Alden (1948)

Inserts from Carr, Kobayashi and Burrows (1954)

5. Compressibility Factors for Natural Gases

The compressibility factor, Z, validates Equation (A-1) for real gases and defines the deviations of a real gas from ideal gas behaviour.

Standing and Katz (1942) presented a compressibility factor chart, Figure A-3, which represents compressibility factors of sweet natural gases as a function of pseudo-reduced temperature and pseudo-reduced pressure. This chart is generally reliable for sweet natural gases with minor amounts of non-hydrocarbons. It is one of the most widely accepted correlations in the oil and gas industry.

Henceforth referred to as the Standing-Katz Z factor chart, its use to predict compressibility factors is illustrated by Example A-3.

EXAMPLE A-3

Problem   Compute the compressibility factor for a sweet natural gas at a temperature of $200^{\circ}F$ and under a pressure of 2000 psia. A natural gas having the composition of Example A-1 may be used.

Solution

From Example A-1

$$T_c = 356.99^{\circ}R$$

$$p_c = 664.53 \text{ psia}$$

pseudo-reduced properties

$$T_r = T/T_c = (200 + 460)/356.99 = 1.85$$

$$p_r = p/p_c = 2000/664.53 = 3.01$$

From Figure A-3, at $T_r = 1.85$ and $p_r = 3.01$

$$Z = 0.907$$

For sour natural gases, the Standing-Katz Z factor chart may be used with appropriate adjustment of the pseudo-critical pressure and temperature. Wichert and Aziz (1972) have developed a graph, Figure A-4, which gives a pseudo-critical temperature adjustment factor, ε_3, to be used in the equations given below.

$$T'_c = T_c - \varepsilon_3 \tag{A-11}$$

$$p'_c = \frac{p_c T'_c}{T_c + B (1-B) \varepsilon_3} \tag{A-12}$$

where

T'_c = adjusted pseudo-critical temperature

p'_c = adjusted pseudo-critical pressure

B = mole fraction in H_2S in the sour gas stream

Equations (A-11) and (A-12) give the adjusted pseudo-critical temperature and adjusted pseudo-critical pressure, from which the reduced temperature and reduced pressure are calculated for use in Figure A-3 to predict sour gas compressibility factors. The calculation procedure is illustrated by Example A-4.

EXAMPLE A-4

Problem   Compute the compressibility factor for a sour natural gas at temperature of 200°F and under a pressure of 2000 psia. A natural gas having the composition of Example A-2 may be used.

Solution

From Example A-2

$$T_c = 405.93°R$$

$$p_c = 787.69 \text{ psia}$$

From Figure A-4, for 18.41% H_2S and 1.64% CO_2,

$$\varepsilon_3 = 25.5°F$$
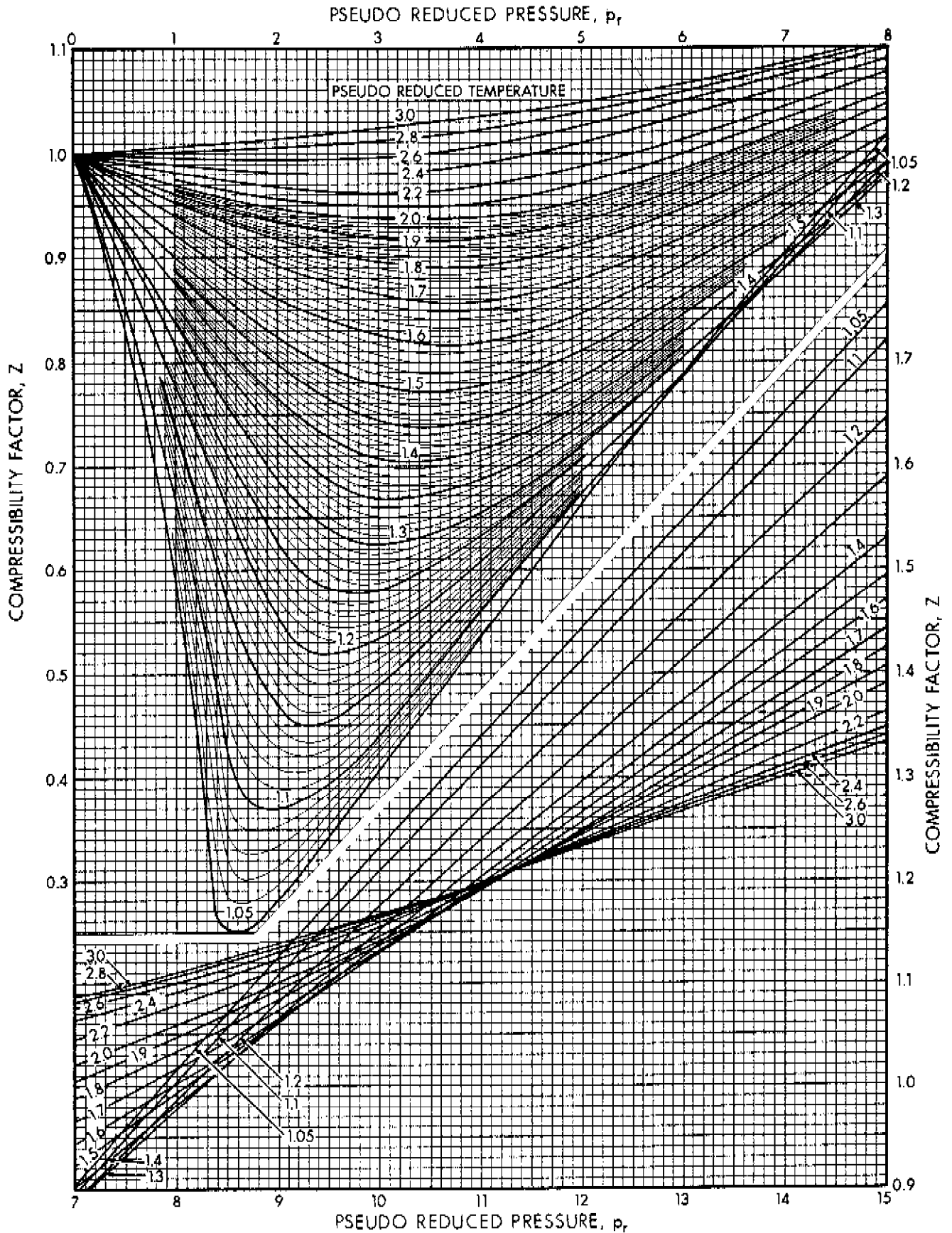
FIGURE A-3. THE COMPRESSIBILITY FACTOR FOR NATURAL GASES
From Standing and Katz (1942)
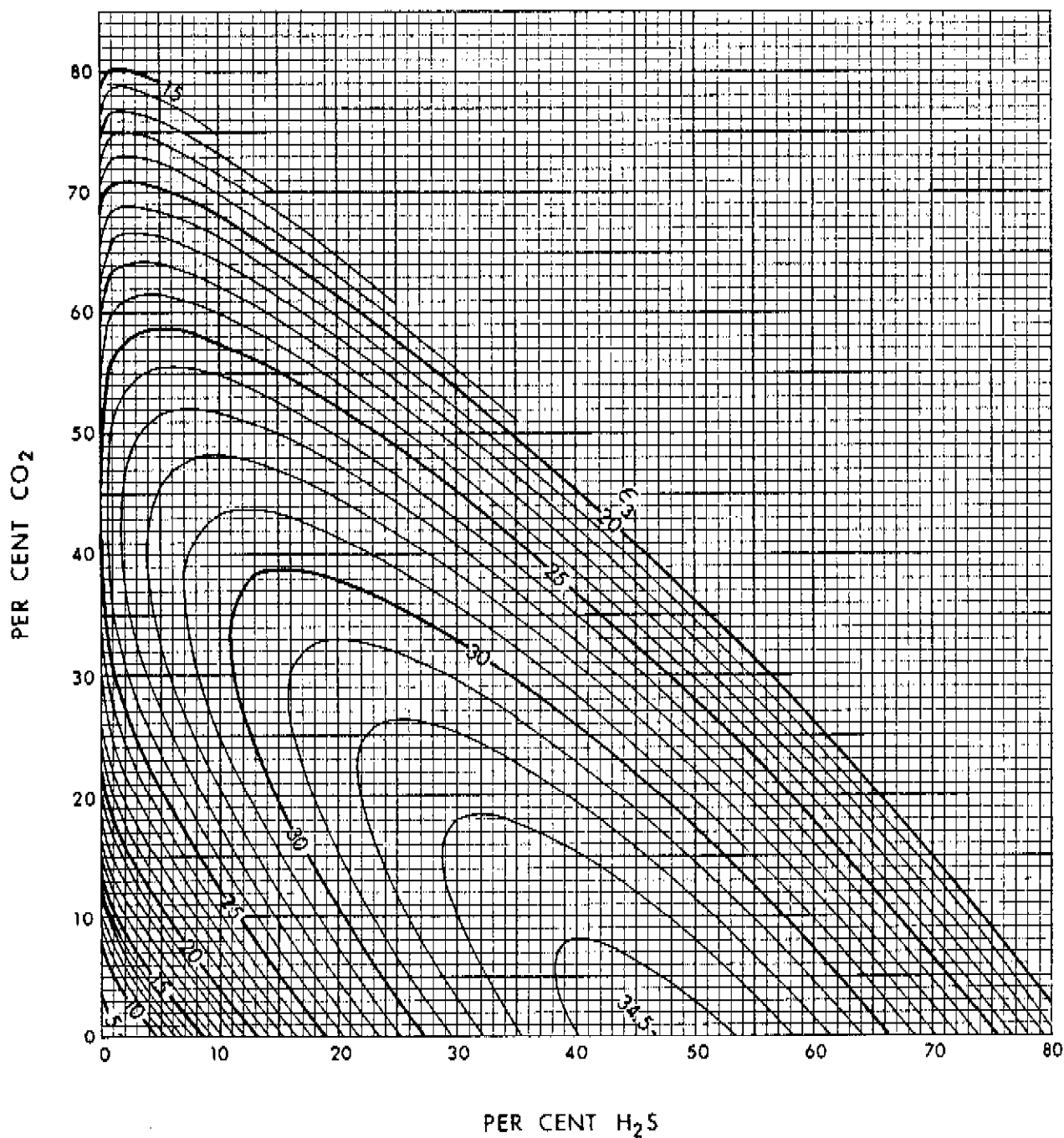
FIGURE A-4. PSEUDO-CRITICAL TEMPERATURE ADJUSTMENT FACTOR, ϵ_3, °F

From Wichert and Aziz (1972)

From Equation (A-11)

$$T_c' = 405.93 - 25.5 = 380.43\,^{\circ}R$$

From Equation (A-12)

$$p_c' = \frac{(787.69)(380.43)}{405.93 + 0.1841\ (1 - 0.1841)(25.5)} = 731.31$$

reduced properties

$$T_r = T/T_c' = (200 + 460)/380.43 = 1.73$$

$$p_r = p/p_c' = 2000/731.31 = 2.73$$

From Figure A-3, at $T_r = 1.73$ and $p_r = 2.73$

$$Z = 0.880$$

Although the Standing-Katz Z factor charts are easy to use in manual computations, digital computer programming involving compressibility factors requires tedious programming and the storage of tabulated compressibility factor data. This difficulty can be avoided by use of the BWR equation of state fitted by Dranchuk, Purvis and Robinson (1974) to adequately represent Figure A-3:

$$Z = 1 + \left(A_1 + A_2/T_r + A_3/T_r^3\right)\rho_r + \left(A_4 + A_5/T_r\right)\rho_r^2 + A_5 A_6 \rho_r^5/T_r$$

$$+ A_7 \rho_r^2/T_r^3 \left(1 + A_8 \rho_r^2\right) \exp\left(-A_8 \rho_r^2\right) \tag{A-13}$$

where

$$\rho_r = 0.27\ p_r/(Z\ T_r) \tag{A-14}$$

$A_1 = 0.31506237$	$A_2 = -1.04670990$	$A_3 = -0.57832729$
$A_4 = 0.53530771$	$A_5 = -0.61232032$	$A_6 = -0.10488813$
$A_7 = 0.68157001$	$A_8 = 0.68446549$	

Equatons (A-13) and (A-14) are incorporated in a FORTRAN subroutine

ZANDC given in Appendix D. The Dranchuk et al. (1974) expression for Z is essentially a good representation of the Standing-Katz Z factor charts and it is capable of generating the Z, p_r, T_r surface with a standard deviation of 0.00445 in Z.

For computer applications involving sour gases, subroutine ZANDC uses the adjustment procedures of Wichert and Aziz (1972), represented by Equation (A-15) given below. Figure A-4 may be represented by the equation

$$\varepsilon_3 = 120 \ (A^{0.9} - A^{1.6}) + 15 \ (B^{0.5} - B^{4.0}) \tag{A-15}$$

where

A = sum of the mole fractions of H_2S and CO_2

B = mole fraction of H_2S

6. Compressibility of Natural Gases

The isothermal compressibility, c, of a substance is defined as:

$$c = -\frac{1}{V} \left[\frac{\partial V}{\partial p} \right]_T \tag{A-16}$$

A commonly used approximation of Equation (A-16), for finite pressure and volume changes is given by

$$c = -\frac{V_1 - V_2}{V_1 (p_1 - p_2)} \tag{A-17}$$

Substituting Equation (A-1), the basic gas equation, in Equation (A-16) gives

$$c = \frac{1}{p} - \frac{1}{Z} \left[\frac{\partial Z}{\partial p} \right]_T \tag{A-18}$$

Since Z is usually expressed as a function of pseudo-reduced pressure, it is convenient to define a pseudo-reduced compressibility, thus

$$c_r = cp_c = \frac{1}{p_r} - \frac{1}{Z}\left[\frac{\partial Z}{\partial p_r}\right]_{T_r} \tag{A-19}$$

Using Equations (A-13) and (A-14) along with Equation (A-19), Mattar, Brar and Aziz (1975) have obtained an analytical expression for c_r given by

$$c_r = \frac{1}{p_r} - \frac{0.27}{Z^2\,T_r}\left[\frac{(\partial Z/\partial\rho_r)_{T_r}}{1 + \rho_r/Z\,(\partial Z/\partial\rho_r)_{T_r}}\right] \tag{A-20}$$

where

$$\left[\frac{\partial Z}{\partial\rho_r}\right]_{T_r} = (A_1 + A_2/T_r + A_3/T_r^3) + 2(A_4 + A_5/T_r)\rho_r$$

$$+ 5\,A_5A_6\rho_r^4/T_r + \frac{2\,A_7\rho_r}{T_r^3}\,(1 + A_8\rho_r^2 - A_8^2\rho_r^4)\exp\,(-A_8\rho_r^2) \tag{A-21}$$

Equations (A-20) and (A-21) were used to develop Figures A-5 and A-6 in which $c_r T_r$ is plotted as a function of p_r and T_r.

For manual calculations of compressibility, Figure A-5 or Figure A-6, along with the definition of pseudo-reduced compressibility from Equation (A-19) may be used. Example A-5 illustrates the calculation procedure.

EXAMPLE A-5

Problem   Calculate the compressibility of the natural gas of Example A-1 at a temperature and pressure of 39.8°F and 664.5 psia, respectively.

Solution

From Example A-1

$$T_c = 356.99°R$$

$$P_c \doteq 664.53 \text{ psia}$$

pseudo-reduced properties

$$T_r = (39.8 + 460)/356.99 = 1.4$$

$$P_r = 664.5/664.53 = 1.0$$

From Figure A-5, at $T_r = 1.4$ and $p_r = 1.0$

$$c_r T_r = 1.6$$

$$c_r = 1.6/T_r = 1.6/1.4 = 1.14$$

From Equation A-19

$$c = c_r/p_c = 1.14/664.53$$

$$= 0.001715 \text{ psia}^{-1}$$

For sour natural gases, the same procedure as above applies using values of reduced temperature and reduced pressure that have been adjusted by the method of Wichert and Aziz (1972).

For computer calculations, Equations (A-14), (A-20) and (A-21) have been incorporated in the FORTRAN subroutine ZANDC given in Appendix D. In summary, this subroutine calculates the compressibility factor, Z, and the compressibility, c, and also makes the necessary adjustments for sour gases.

7. Viscosity of Natural Gases

The viscosity of a Newtonian fluid is defined as the ratio of the shear force per unit area to the local velocity gradient. For most engineering work, viscosities are expressed in terms of poises, centipoises or micropoises. A poise denotes a viscosity of 1 dyne-sec/cm^2 or 1 g.mass/(sec)(cm) and can be expressed in other units as below:
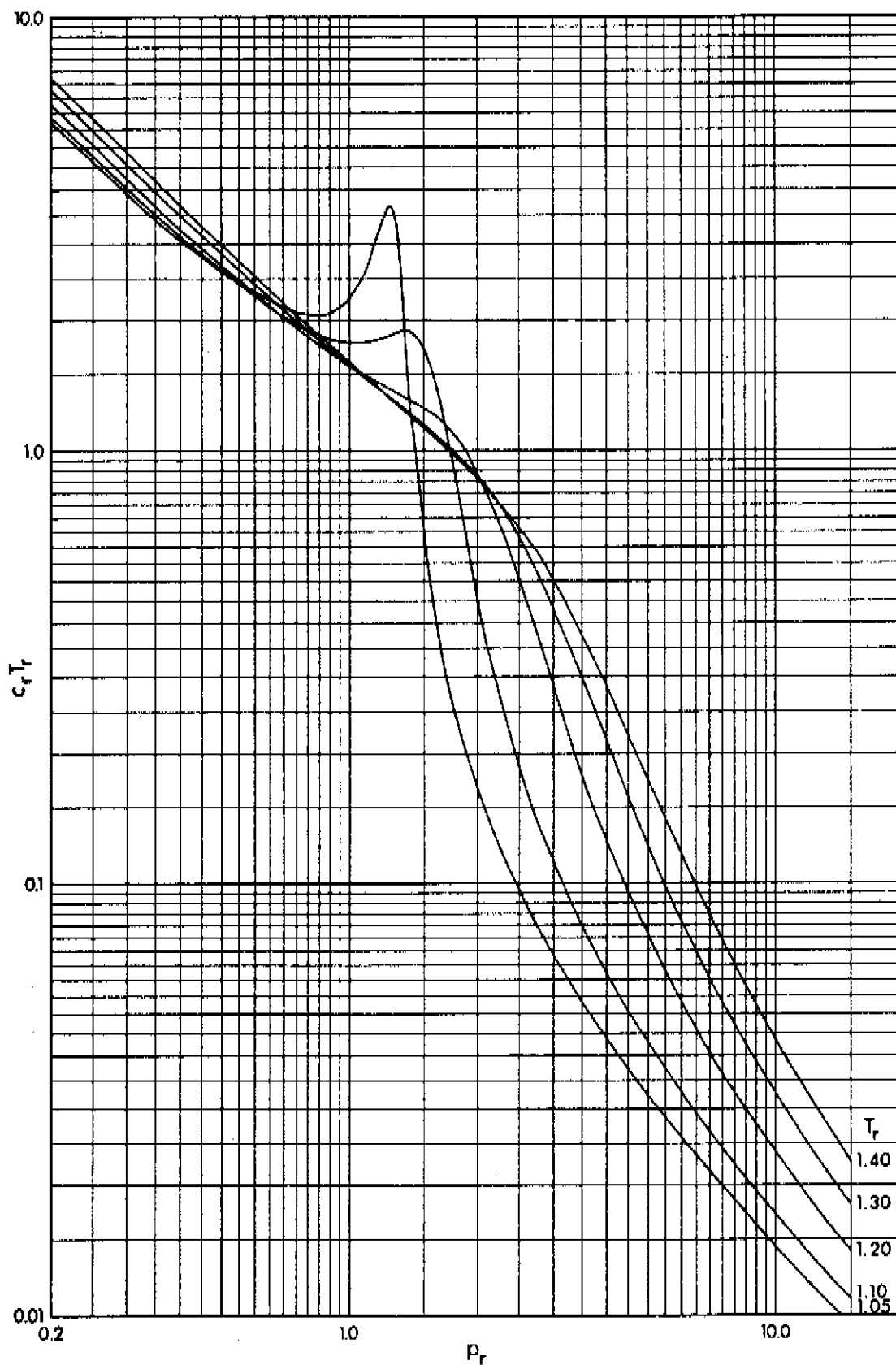
FIGURE A-5. VARIATION OF $c_r T_r$ WITH REDUCED TEMPERATURE AND PRESSURE
$(1.05 \leq T_r \leq 1.4 ; 0.2 \leq p_r \leq 15.0)$

From Mattar, Brar and Aziz (1975)
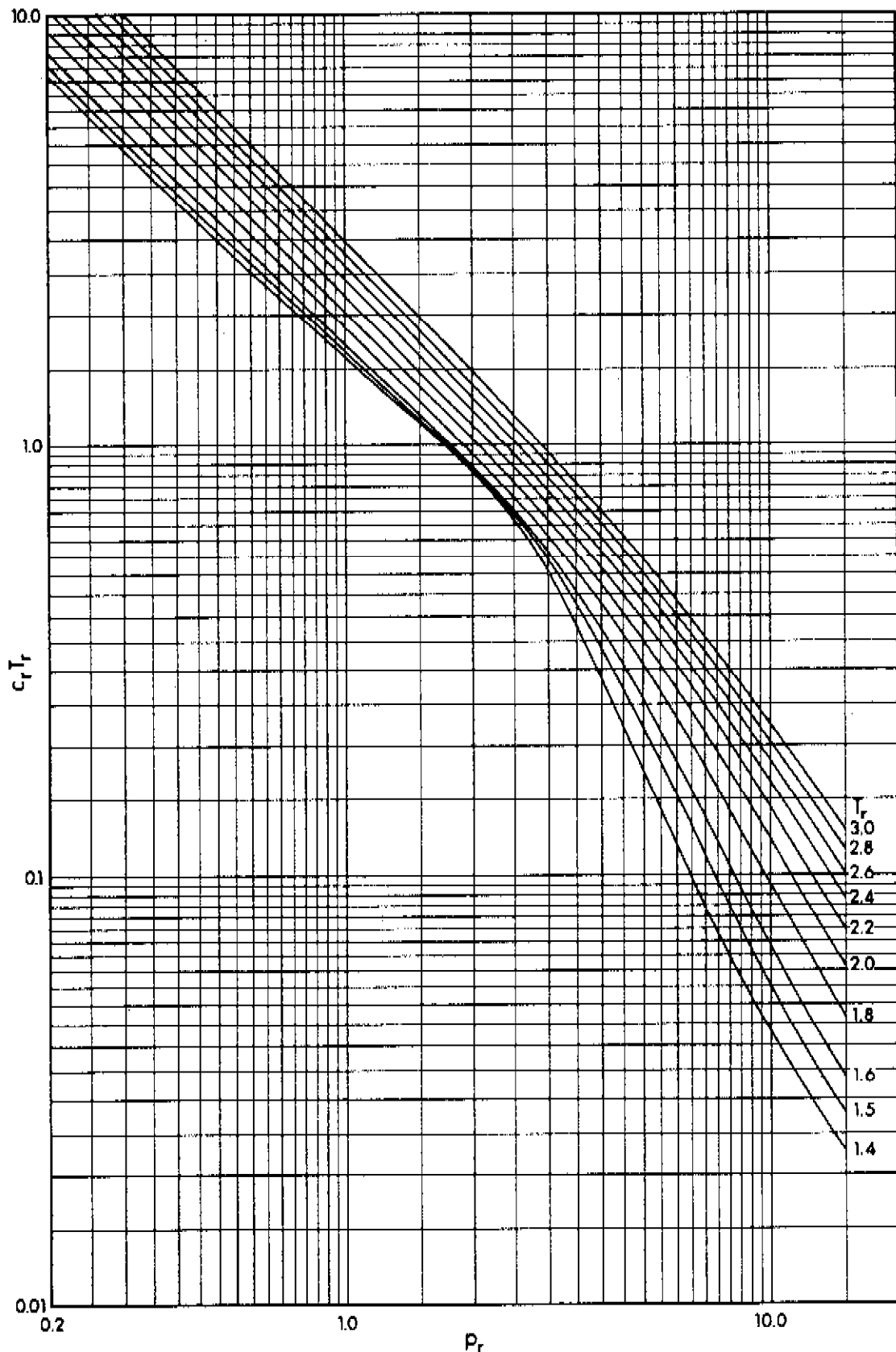
FIGURE A-6. VARIATION OF $c_r T_r$ WITH REDUCED TEMPERATURE AND PRESSURE
$(1.4 \leqslant T_r \leqslant 3.0 \; ; \; 0.2 \leqslant p_r \leqslant 15.0)$
From Mattar, Brar and Aziz (1975)

$$1 \text{ poise} = 1.00 \times 10^2 \text{ centipoises}$$
$$= 1.00 \times 10^6 \text{ micropoises}$$
$$= 6.72 \times 10^{-2} \text{ lb}_m/(\text{ft})(\text{sec})$$
$$= 2.09 \times 10^{-3} \text{ lb}_f\text{-sec/ft}^2$$

The viscosity of a pure gas depends upon temperature and pressure, but for gas mixtures it is also a function of the composition of the mixture.

For natural gases, the widely used correlations of Carr, Kobayashi and Burrows (1954) take the simple forms

$$\mu_1 = \phi\{M,T\} \qquad\qquad\qquad (A-22)$$

$$\mu/\mu_1 = \phi\{p_r, T_r\} \qquad\qquad\qquad (A-23)$$

where

μ_1 = low pressure or dilute-gas viscosity

μ = gas viscosity at high pressure

The correlation represented by Equation (A-23) is compatible with the correlations for compressibility factors since both are based on the concept of corresponding states.

Figures A-7, A-8 and A-9 give the Carr et al. (1954) correlations. Figure A-7 is a plot of dilute-gas viscosity as a function of molecular weight and temperature. The inserts are corrections for the presence of nitrogen, carbon-dioxide or hydrogen sulphide. Figures A-8 and A-9 give the viscosity ratio as a function of pseudo-reduced temperature and pseudo-reduced pressure. Example A-6 illustrates the use of these figures for prediction of natural gas viscosities.

EXAMPLE A-6

Problem   Calculate the viscosity of the natural gas of Example A-2 at a temperature and pressure of 100°F and 2000 psia, respectively.

Solution

From Example A-2

$$M = 20.25 \qquad G = 0.70$$

$$T_c = 405.93°R \qquad P_c = 787.69 \text{ psia}$$

From Figure A-7, for a molecular weight of 20.25 and a temperature of $100°F$

$$\mu_1 = 0.0107 \text{ cp}$$

From the inserts on Figure A-7

correction for 2.36 mole per cent N_2 = 0.00019 cp

correction for 1.64 mole per cent CO_2 = 0.00010 cp

correction for 18.41 mole per cent H_2S = 0.00041 cp
(extrapolated value)

$$\therefore \text{ corrected } \mu_1 = 0.0107 + (0.00019 + 0.00010 + 0.00041)$$

$$= 0.0114 \text{ cp}$$

$$T_r = (100 + 460)/405.93 = 1.38$$

$$P_r = 2000/787.69 = 2.54$$

From Figure A-8 or Figure A-9, for T_r = 1.38 and P_r = 2.54

$$\mu/\mu_1 = 1.52$$

$$\therefore \mu = 1.52 \times 0.0144 = 0.0173 \text{ cp}$$

The viscosity correlations of Carr et al. (1954) are incorporated in a FORTRAN subroutine VISCY given in Appendix D. This subroutine requires the storage of tabulated data and tedious interpolation methods. Several other correlations are available for the prediction of μ_1 and μ for pure gas and multicomponent gas mixtures.
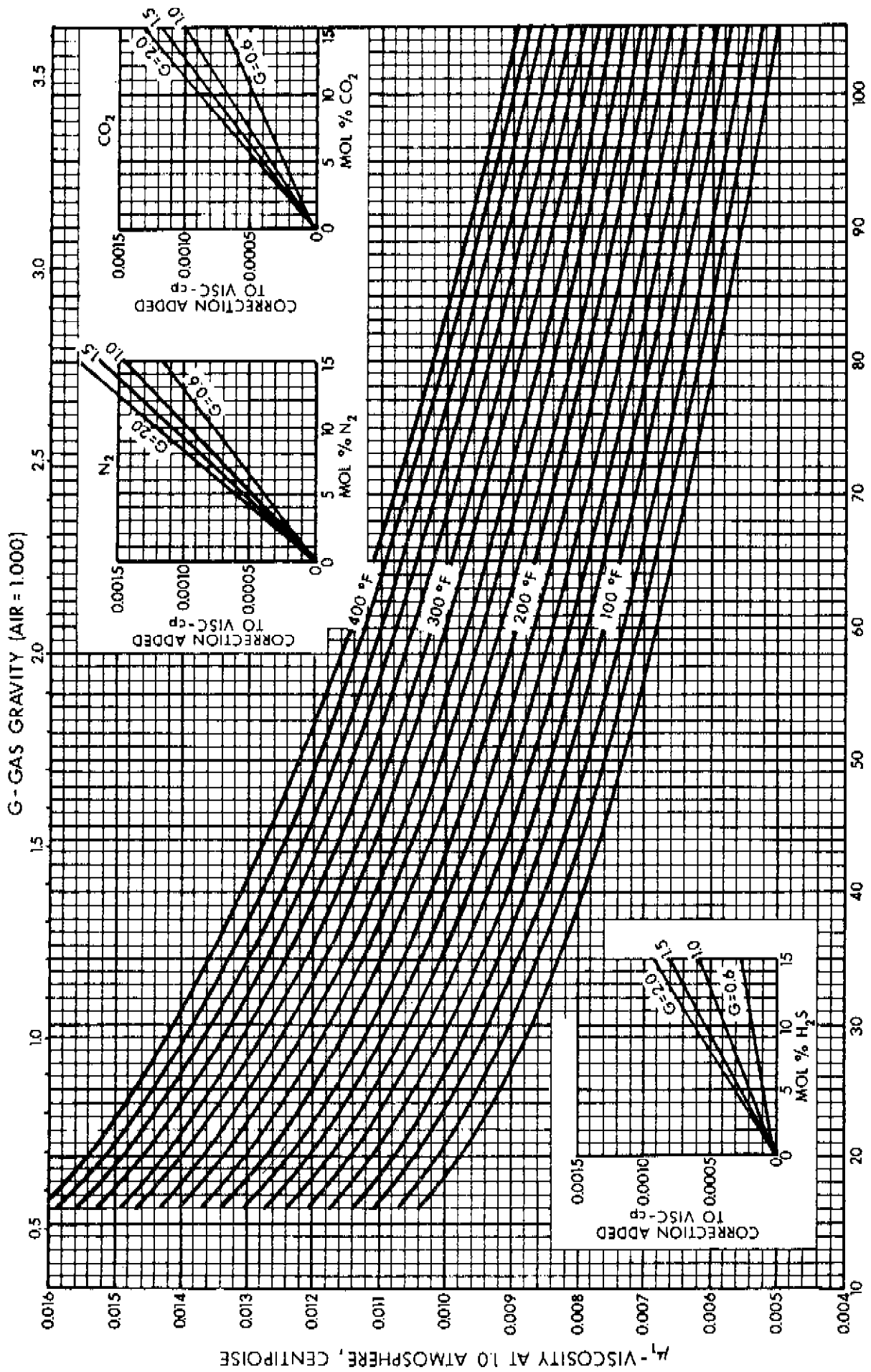
FIGURE A-7. VISCOSITY OF PARAFFIN HYDROCARBON GASES AT 1.0 ATMOSPHERE

From Carr, Kobayashi and Burrows (1954)
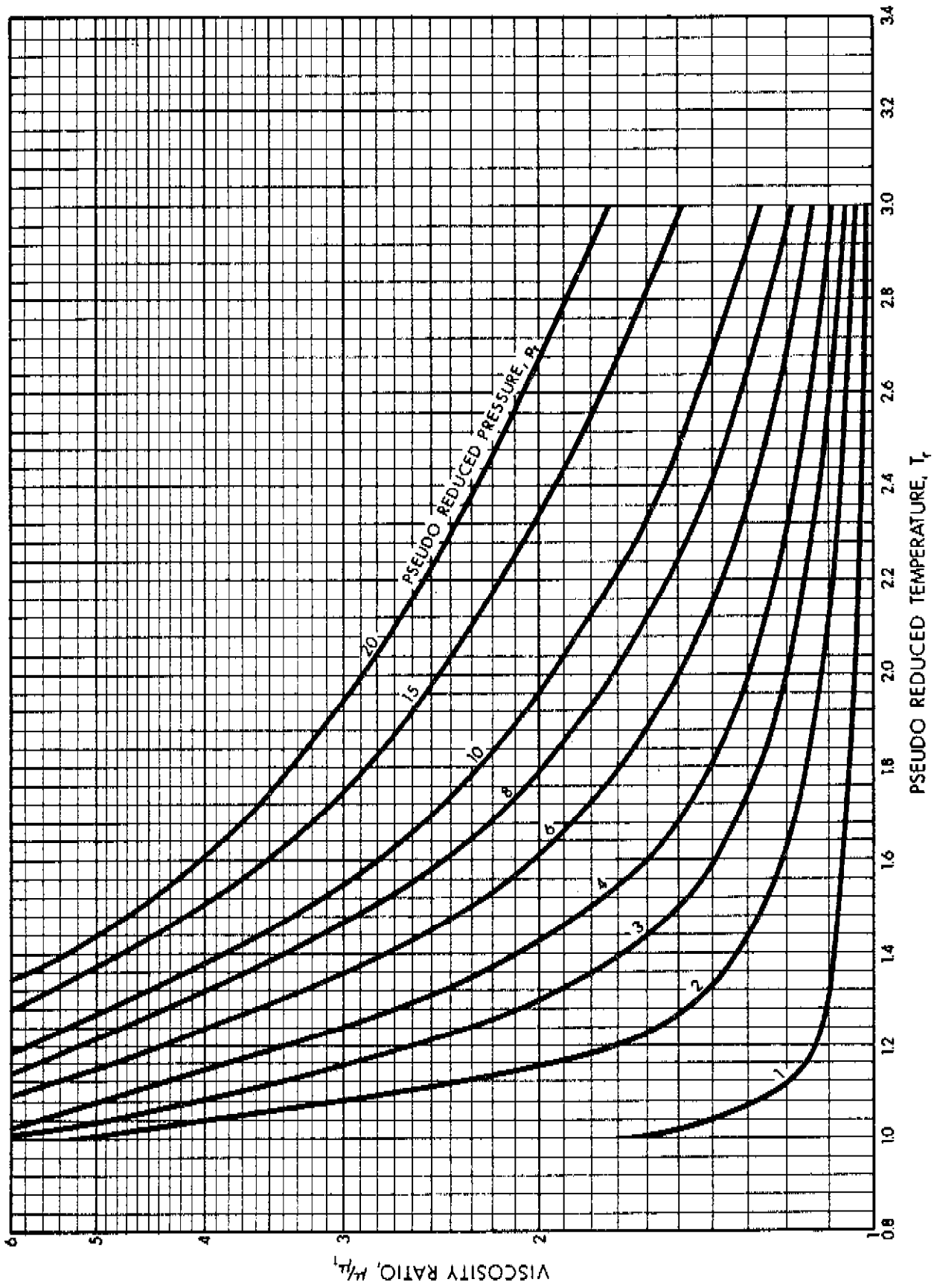
FIGURE A-8. VISCOSITY RATIO VERSUS PSEUDO REDUCED TEMPERATURE

From Carr, Kobayashi and Burrows (1954)
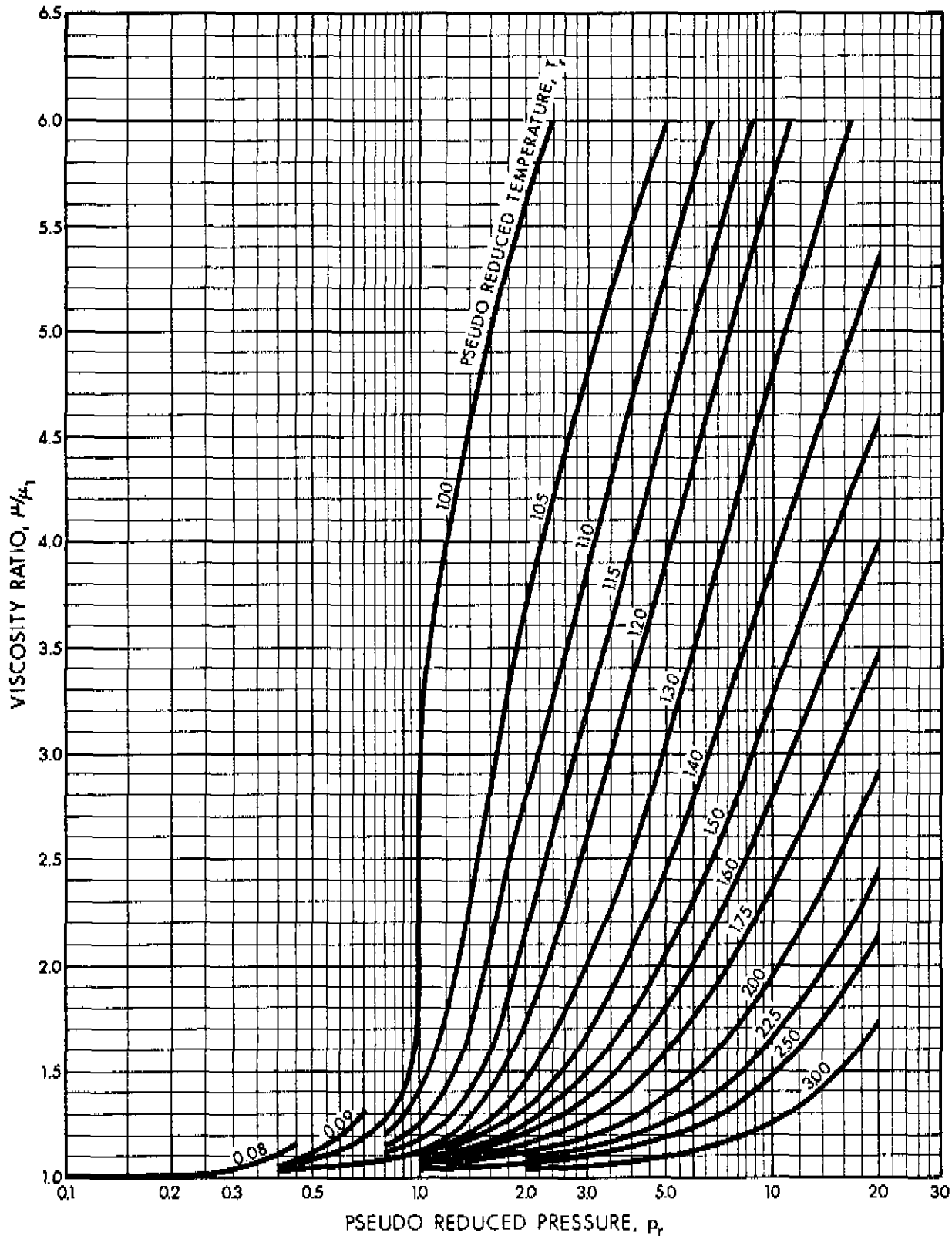
FIGURE A-9. VISCOSITY RATIO VERSUS PSEUDO REDUCED PRESSURE

From Carr, Kobayashi and Burrows (1954)

Some of these have been extended to predict viscosities of natural gases but none account for the presence of hydrogen sulphide, carbon dioxide, and nitrogen.

For example, Lee, Gonzalez and Eakin (1966) developed a semi-empirical expression of the form

$$\mu = K \exp (X \rho^Y) , \qquad \mu \text{ in } \mu p \qquad (A-24)$$
$$\rho \text{ in g/cc}$$

where

$$K = \frac{(9.4 + 0.02 \, M) \, T^{1.5}}{209 + 19 \, M + T} , \qquad T \text{ in } {}^oR$$

$$X = 3.5 + \frac{986}{T} + 0.01 \, M$$

$$Y = 2.4 - 0.2 \, X$$

Although the above correlation is readily adaptable to digital computer programming, it may not be applied to sour gases. As mentioned previously, the method of Carr et al. (1954) has been computerized even though it does involve some tedious programming. The advantages of using subroutine VISCY include an accurate reproduction of Figures A-7, A-8, and A-9, which are normally used for manual calculations, and its application to sour gases.

8. Condensate Wells, Retrograde Condensation and Recombination Calculations

Many gas wells produce an effluent which is single-phase (gas) in the reservoir and in the wellbore but is two-phase (gas and condensate) at wellhead separation conditions.

Condensation is caused by unusual phase changes which occur in the critical region of the gas mixture. This abnormal phenomenon, which does not occur for pure substances, is called "retrograde condensation." In simple terms, it is the phenomenon of liquid formation by isothermal expansion of a single-phase fluid. The term

retrograde condensation may also be applied to isobaric phenomena when the phase change occurring is opposite to that which would occur if the same change in conditions was applied to a pure substance.

The separation of reservoir gases into two phases at wellhead conditions creates requirements for monitoring flow rates, compositions and related properties of the gas and liquid streams. These measurements are essential to molal recombination calculations in which these separate gas and liquid streams are reconstituted to give the recombined composition of the reservoir gases.

Specific Gravity of Reservoir Gases from High Pressure Separator Streams

The specific gravity of reservoir gases may be calculated, assuming additive volumes, from the equation:

$$G = \frac{G_s + \dfrac{4608\ G_c}{R_c}}{1 + V_c/R_c} \tag{A-25}$$

where

G = specific gravity of the reservoir gas (air = 1)

G_s = specific gravity of the high pressure (hp) separator gas (air = 1)

G_c = specific gravity of the high pressure (hp) separator condensate (water = 1)

R_c = gas-condensate ratio, scf separator gas per barrel separator condensate (14.65 psi and 60°F)

V_c = condensate vaporizing volume ratio, scf per barrel separator condensate (14.65 psi and 60°F)

In using Equation (A-25) the following information is required:

1. Flow rates of the high-pressure separator gas and condensate streams—obtained from field measurements.

2. Specific gravity of the high-pressure separator gas and condensate—obtained from laboratory measurements.

3. Condensate vaporizing volume ratio—obtained from Figure A-10.
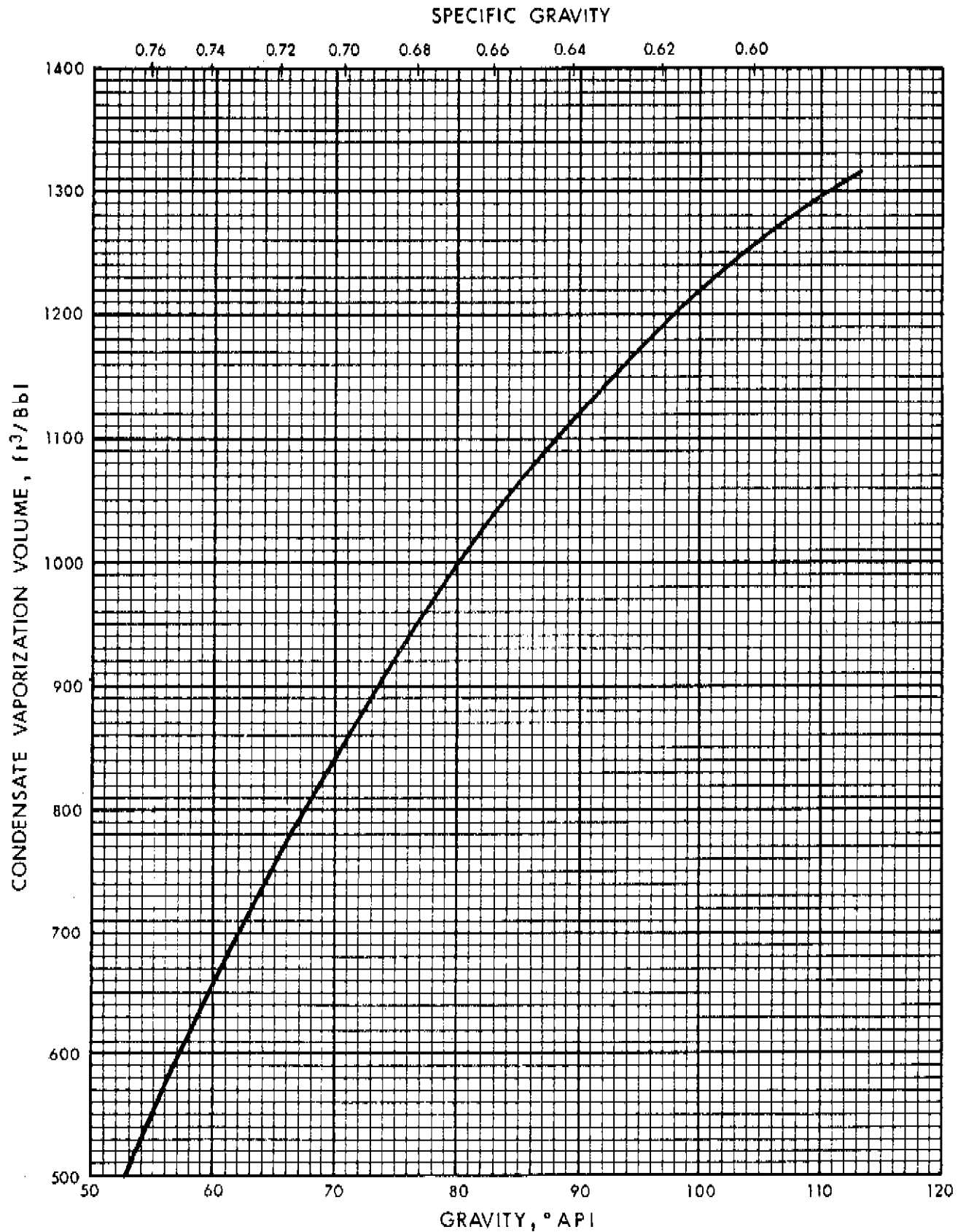
FIGURE A-10. RELATIONSHIP BETWEEN CONDENSATE VAPORIZATION
VOLUME RATIO AND API GRAVITY

The condensate vaporizing volume ratio, V_c, is dependent on the composition of the condensate which in turn is reflected by its specific gravity. Figure A-10 presents the relationship between V_c and the API gravity for pure paraffinic hydrocarbons. (For convenience in converting API gravities to liquid specific gravities, an abridged conversion table is presented in Table A-2.)

The procedure for calculating the specific gravity of reservoir gases from the specific gravities of the high-pressure separator streams is illustrated by Example A-7.

EXAMPLE A-7

Problem   Calculate the specific gravity of a reservoir gas given the following information:

Specific gravity of hp separator gas, G_s = 0.65

Gravity of hp separator condensate = 56°API

Gas-condensate ratio, R_c = 20,000 ft^3/bbl

Solution

From Table A-2, specific gravity of condensate

$$G_c = 0.75$$

From Figure A-10, for an API gravity of 56°

$$V_c = 575 \ scf/bbl$$

From Equation A-25

$$G = \frac{0.65 + \frac{(4608)(0.75)}{(20,000)}}{1 + (575)(20,000)} = 0.80$$

In using Figure A-10, the following must be clearly understood. This graph is applicable only for converting high-pressure separator condensate to an equivalent gas volume. In cases where measurements are

made on stock tank condensate, instead of the high-pressure separator condensate, the following section provides the procedure for calculating the specific gravity of a reservoir gas.

Specific Gravity of Reservoir Gas from HP Gas and Stock Tank Condensate

The specific gravity of reservoir gases may be calculated, assuming additive volumes, from the equation

$$G = \frac{G_s + \dfrac{4608\ G_{cs}}{R_{cs}}}{1 + V_{cs}/R_{cs}} \qquad (A\text{-}26)$$

where

G = specific gravity of the reservoir gas (air = 1)

G_s = specific gravity of the high-pressure (hp) separator gas (air = 1)

G_{cs} = specific gravity of the stock tank condensate (water = 1)

R_{cs} = gas-stock tank condensate ratio, scf separator gas per barrel stock tank condensate (14.65 psi and 60°F)

V_{cs} = stock tank condensate vaporizing volume ratio, scf per barrel stock tank condensate (14.65 psi and 60°F)

In using Equation (A-26) the following information is required:

1. Flow rate of the high-pressure separator gas stream and the accumulation rate of the stock tank condensate—obtained from field measurements.

2. Operating pressure of the high-pressure separator—obtained from field measurements.

3. Specific gravities of the high-pressure separator gas and stock tank condensate—obtained from laboratory measurements.

4. Stock tank condensate vaporizing volume ratio—obtained from Figure A-11.

°API	Specific Gravity	°API	Specific Gravity	°API	Specific Gravity
0	1.076	34	.8550	68	.7093
1	1.068	35	.8498	69	.7057
2	1.060	36	.8448	70	.7022
3	1.052	37	.8398	71	.6988
4	1.044	38	.8348	72	.6953
5	1.037	39	.8299	73	.6919
6	1.029	40	.8251	74	.6886
7	1.022	41	.8203	75	.6852
8	1.014	42	.8155	76	.6819
9	1.007	43	.8109	77	.6787
10	1.000	44	.8063	78	.6754
11	.9930	45	.8017	79	.6722
12	.9861	46	.7972	80	.6690
13	.9792	47	.7927	81	.6659
14	.9725	48	.7883	82	.6628
15	.9659	49	.7839	83	.6597
16	.9593	50	.7796	84	.6566
17	.9529	51	.7753	85	.6536
18	.9465	52	.7711	86	.6506
19	.9402	53	.7669	87	.6476
20	.9340	54	.7628	88	.6446
21	.9279	55	.7587	89	.6417
22	.9218	56	.7547	90	.6388
23	.9159	57	.7507	91	.6360
24	.9100	58	.7467	92	.6331
25	.9042	59	.7428	93	.6303
26	.8984	60	.7389	94	.6275
27	.8927	61	.7351	95	.6247
28	.8871	62	.7313	96	.6220
29	.8816	63	.7275	97	.6193
30	.8762	64	.7238	98	.6166
31	.8708	65	.7201	99	.6139
32	.8654	66	.7165	100	.6112
33	.8602	67	.7128		

$$\text{Specific Gravity} = \frac{141.5}{131.5 + °API}$$

TABLE A-2. CONVERSION OF API GRAVITY TO LIQUID SPECIFIC GRAVITY AT 60°F
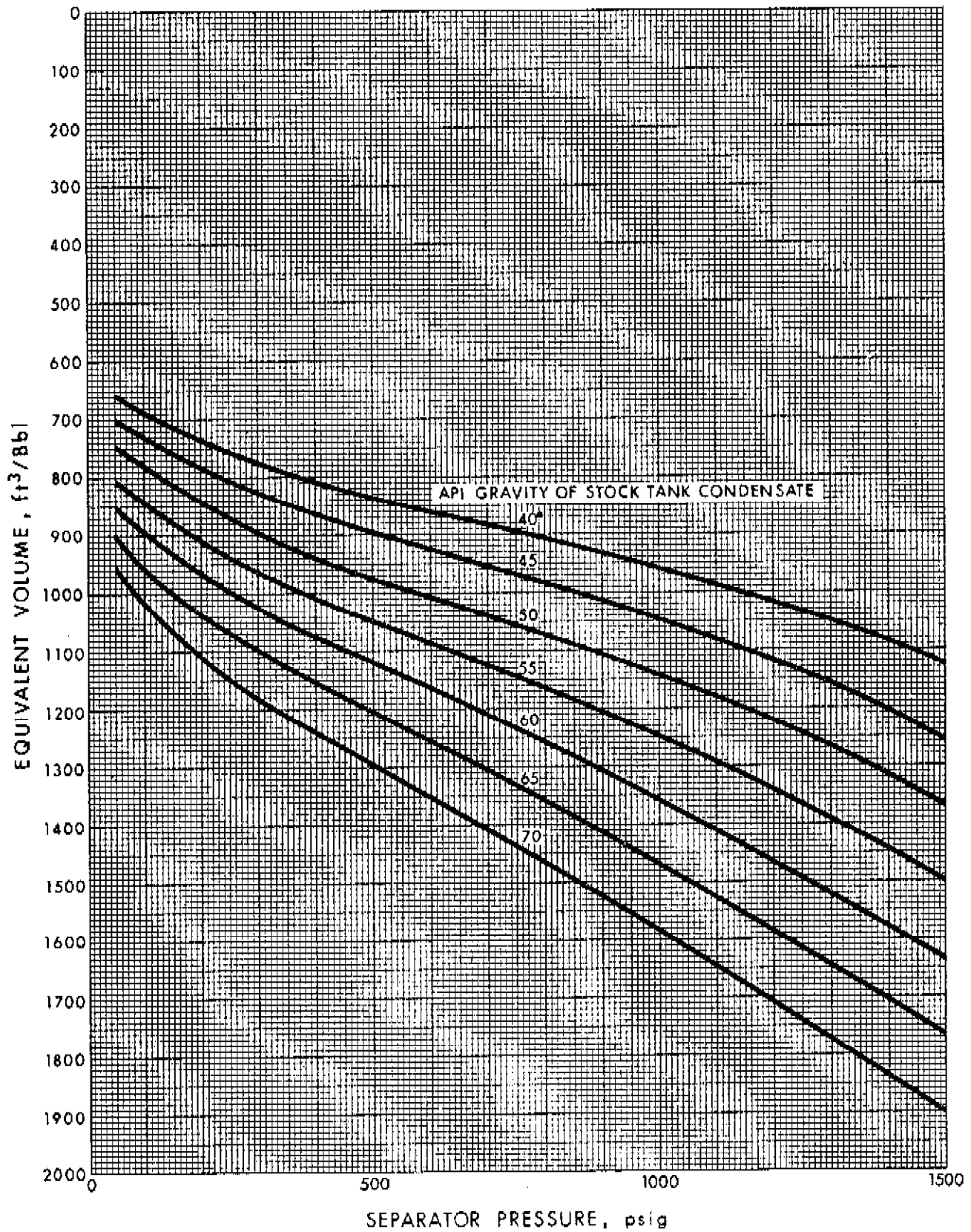
FIGURE A-11. EQUIVALENT GAS VOLUME OF STOCK TANK CONDENSATE

From Leshikar (1961)

The stock tank condensate vaporizing volume ratio, V_{cs}, is dependent on its specific gravity and the separator pressure. Figure A-11 presents V_{cs} as a function of API gravity and separator pressure. The value of V_{cs} obtained from this figure includes the gas vented from low-pressure separators, if any, and also includes the gas flashed on reduction of pressure into the stock tanks.

The procedure for calculating the specific gravity of a reservoir gas from the specific gravities of the high-pressure separator gas and stock tank condensate is illustrated by Example A-8.

EXAMPLE A-8

Problem Calculate the specific gravity of a reservoir gas given the following information:

Specific gravity of hp separator gas, G_s = 0.65

Gravity of stock tank condensate = 50°API

Gas-stock tank condensate ratio, R_c = 21,000

High-pressure separator pressure = 900 psig

Solution

From Table A-2, specific gravity of stock tank condensate

$$G_{cs} = 0.78$$

From Figure A-11, for an API gravity of 50° and a separator pressure of 900 psig

$$V_{cs} = 1110 \ scf/bbl$$

From Equation (A-26)

$$G = \frac{0.65 + \dfrac{(4608)(0.78)}{(21,000)}}{1 + (1110.)(21,000)} = 0.78$$

The specific gravity of a reservoir gas obtained by either of the two methods discussed above is reasonably accurate and may be used to obtain the pseudo-critical temperature and pseudo-critical pressure from Figure A-2. This procedure may be applied only when detailed information regarding the compositions of the various separator streams is not available. It is desirable, however, to know the composition of the reservoir gases in which case the more rigorous procedures outlined below may be used to calculate reservoir gas composition, specific gravity, and pseudo-critical properties.

Recombination Calculations

This section illustrates a typical calculation procedure, and describes alternative procedures necessitated by different wellhead separator configurations, to determine recombined reservoir gas properties. The composition of the total well fluid is calculated from the analyses of the produced gas(es) and liquid by recombining them in the ratio in which they are produced. Physical properties like pseudo-critical temperature and pseudo-critical pressure are then calculated using the methods illustrated by Examples A-1 or A-2.

A typical recombination calculation, illustrated by Example A-9, assumes the following:

1. The wellhead separator configuration, as given in Figure 6-3, consists of a high-pressure (hp) separator, a low-pressure (lp) separator, and a stock tank.

2. The stock tank gas volume is small and may be neglected.

EXAMPLE A-9

Problem   The effluent from a gas well was separated at the wellhead using the separator configuration of Figure 6-3. The flow rates and composition of the high-pressure gas, the low-pressure gas, and the stock tank liquid are given in Table A-3.

Calculate the total (recombined) gas produced, its composition, gravity, pseudo-critical temperature and pressure.

MOLAL RECOMBINATION CALCULATIONS

WELL _____ LOCATION _____ FIELD _____ POOL _____ DATE SAMPLED _____

<u>SEPARATOR CONDITIONS</u>   HP SEP. __920__ psig, __100__ °F   LP SEP. __25__ psig, __120__ °F

<u>SEPARATOR PRODUCTS</u>   HP GAS __7500.0__ Mscfd   LP GAS __500.0__ Mscfd

LIQUID: STOCK TANK __15.0__ Bbl/d   HP __-__ Bbl/d   LP __-__ Bbl/d

<u>LIQUID FLOW RATE CALCULATIONS</u>*   (STOCK TANK ☑,   HP ☐,   or   LP ☐ LIQUID)

MOLECULAR WEIGHT OF LIQUID, M_L = __124.0__ ,   SPECIFIC GRAVITY OF LIQUID, SG_L = __0.80__

LIQUID FLOW RATE (moles/d)   =   FLOW RATE(Bbl/d) × $\frac{SG_L}{M_L}$ × 350.51   = __33.92__

LIQUID FLOW RATE (Mscfd)   =   FLOW RATE (moles/d) × 0.38068   = __12.91__

COMP. i	M_i lb$_m$/lb·mole	T_{ci} °R	p_{ci} psia	LIQUID		HP GAS		LP GAS		TOTAL	RECOMBINED GAS PROPERTIES			
				MOLE FRACTION	Mscfd	MOLE FRACTION	Mscfd	MOLE FRACTION	Mscfd	Mscfd	x_i	$x_i M_i$	$x_i T_{ci}$	$x_i p_{ci}$
N_2	28.013	227.27	493.0	-	-	0.0087	65.25	0.0029	1.45	66.70	0.0083	0.233	1.89	4.1
CO_2	44.010	547.57	1071.0	-	-	0.0383	287.25	0.0283	14.15	301.40	0.0376	1.655	20.59	40.3
H_2S	34.076	672.37	1306.0	0.0027	0.03	0.1882	1411.50	0.3575	178.75	1590.28	0.1985	6.764	133.47	259.2
C_1	16.042	343.04	667.8	-	-	0.6404	4803.00	0.2510	125.50	4928.50	0.6150	9.866	210.97	410.7
C_2	30.070	549.76	707.8	0.0009	0.01	0.0752	564.00	0.1006	50.30	614.31	0.0767	2.306	42.17	54.3
C_3	44.097	665.68	616.3	0.0052	0.07	0.0265	198.75	0.0881	44.05	242.87	0.0303	1.336	20.17	18.7
iC_4	58.124	734.65	529.1	0.0069	0.09	0.0058	43.50	0.0347	17.35	60.94	0.0076	0.442	5.58	4.0
nC_4	58.124	765.32	550.7	0.0211	0.27	0.0098	73.50	0.0703	35.15	108.92	0.0136	0.790	10.41	7.5
iC_5	72.151	828.77	490.4	0.0246	0.32	0.0026	19.50	0.0264	13.20	33.02	0.0041	0.296	3.40	2.0
nC_5	72.151	845.37	488.6	0.0280	0.36	0.0025	18.75	0.0259	12.95	32.06	0.0040	0.289	3.38	2.0
C_6	86.178	913.37	436.9	0.1021	1.32	0.0015	11.25	0.0114	5.70	18.27	0.0023	0.198	2.10	1.0
**C_7^+	114.232	1023.89	360.6	0.8085	10.44	0.0005	3.75	0.0029	1.45	15.64	0.0020	0.228	2.05	0.7
Σ				1.0000	12.91	1.0000	7500.00	1.0000	500.00	8012.91	1.0000	24.402	456.17	804.4

RECOMBINED GAS PROPERTIES: FLOW RATE = __8.0129__ MMscfd,   G = __24.402__ /28.966 = __0.84__ , T_c = __456.17__ °R, p_c = __804.4__ psia

* THE LIQUID FLOW RATE(Bbl/d) AND SPECIFIC GRAVITY ARE TO BE MEASURED AT THE SAME CONDITIONS

BASE CONDITIONS = 14.65 psia and 60 °F

** PHYSICAL PROPERTIES OF OCTANES ARE USED FOR THE C_7^+ FRACTION

TABLE A-3. ILLUSTRATING EXAMPLE A-9

Solution

In Table A-3,

Columns (1), (2) and (3) contain the physical properties of constituent components which are obtained from Table A-1.

Columns (4), (6) and (8) contain the composition of the stock tank liquid, hp gas and lp gas, respectively.

$\sum$ (5), $\sum$ (9) and $\sum$ (11) are the stock tank liquid, hp gas and lp gas flow rates, respectively.

The entries in the remaining columns are calculated as follows:

$$(5) = \sum (5)/(4)$$

$$(7) = \sum (7)/(6)$$

$$(9) = \sum (9)/(8)$$

$$(10) = (5) + (7) + (9)$$

$$(11) = (10)/\sum (10)$$

$$(12) = (1) \times (11)$$

$$(13) = (2) \times (11)$$

$$(14) = (3) \times (11)$$

From Table A-3,

$$\text{Total gas} = 8.01 \text{ MMscfd}$$
$$G = 0.84$$
$$T_c = 456.17 \,^\circ R$$
$$P_c = 804.4 \text{ psia}$$

The calculation procedure illustrated by Table A-3 in Example A-9 is also applicable to other wellhead separator configurations, with little or no modification. A frequently used configuration, as given by Figure 6-4, consists of a high-pressure separator and a stock tank.

In such a case the stock tank gas volume may not be ignored. The stock tank liquid accumulation rate must be converted to an equivalent high-pressure liquid flow rate through use of a shrinkage factor.

$$\text{Equivalent high-pressure} \atop \text{liquid (bpd)} = \frac{\text{Stock tank liquid (bpd)}}{\text{Shrinkage factor}} \qquad \text{(A-27)}$$

The shrinkage factor is obtained by laboratory techniques or by flash calculations, and its application in recombination calculations is illustrated by Example A-10.

EXAMPLE A-10

Problem   The effluent from a gas well was separated at the wellhead using the separator configuration of Figure 6-4. The flow rate and composition of the high-pressure gas, the composition of the high-pressure liquid and the accumulation rate of the stock tank liquid are given in Table A-4.

Calculate the total gas produced, its composition, specific gravity, pseudo-critical temperature and pseudo-critical pressure.

Solution   The calculation procedure for this example is the same as that for Example A-9, except for the following changes:

$$\text{Shrinkage factor} \atop \text{(flash calculations)} = 0.7829 \frac{\text{bbl stock tank liquid}}{\text{bbl high-pressure liquid}}$$

From Equation (A-27)

$$\text{Equivalent hp liquid} = \frac{\text{Stock tank liquid}}{\text{Shrinkage factor}} = \frac{58.58}{0.7829} = 74.82$$

In Table A-4,
Column (4) contains the composition of the high-pressure liquid.
$\sum$ (5) is the calculated equivalent hp liquid.
Columns (8) and (9) remain blank.

MOLAL RECOMBINATION CALCULATIONS

WELL _____ LOCATION _____ FIELD _____ POOL _____ DATE SAMPLED ____

SEPARATOR CONDITIONS   HP SEP. __1035__ psig, __101__ °F   LP SEP. __-__ psig, __-__ °F

SEPARATOR PRODUCTS   HP GAS __5005.0__ Mscfd   LP GAS __-__ Mscfd

LIQUID: STOCK TANK __58.58__ Bbl/d   HP __74.82__ Bbl/d   LP __-__ Bbl/d

LIQUID FLOW RATE CALCULATIONS*   (STOCK TANK ☐,   HP ☑,   or   LP ☐ LIQUID)

MOLECULAR WEIGHT OF LIQUID, M_L = __133.0__, SPECIFIC GRAVITY OF LIQUID, SG_L = __0.79__

LIQUID FLOW RATE (moles/d) = FLOW RATE(Bbl/d) × $\frac{SG_L}{M_L}$ × 350.51 = __155.77__

LIQUID FLOW RATE (Mscfd) = FLOW RATE (moles/d) × 0.38068 = __59.30__

COMP. i	M_i lb_m/lbmole	T_{ci} °R	p_{ci} psia	LIQUID MOLE FRACTION	LIQUID Mscfd	HP GAS MOLE FRACTION	HP GAS Mscfd	LP GAS MOLE FRACTION	LP GAS Mscfd	TOTAL Mscfd	x_i	x_iM_i	x_iT_{ci}	x_iP_{ci}
N_2	28.013	227.27	493.0	0.0050	0.30	0.0050	25.02	-	-	25.32	0.0050	0.140	1.14	2.5
CO_2	44.010	547.57	1071.0	0.0354	2.10	0.0650	325.32	-	-	327.42	0.0647	2.847	35.43	69.3
H_2S	34.076	672.37	1306.0	0.0941	5.58	0.0570	285.28	-	-	290.86	0.0574	1.956	38.59	75.0
C_1	16.042	343.04	667.8	0.2015	11.95	0.8144	4076.07	-	-	4088.02	0.8072	12.949	276.90	539.0
C_2	30.070	549.76	707.8	0.0366	2.17	0.0372	186.19	-	-	188.36	0.0372	1.119	20.45	26.3
C_3	44.097	665.68	616.3	0.0215	1.27	0.0091	45.55	-	-	46.82	0.0092	0.406	6.12	5.7
iC_4	58.124	734.65	529.1	0.0149	0.88	0.0030	15.01	-	-	15.89	0.0031	0.180	2.28	1.6
nC_4	58.124	765.32	550.7	0.0180	1.07	0.0031	15.52	-	-	16.59	0.0033	0.192	2.53	1.8
iC_5	72.151	828.77	490.4	0.0183	1.09	0.0015	7.51	-	-	8.60	0.0017	0.123	1.41	0.8
nC_5	72.151	845.37	488.6	0.0183	1.09	0.0010	5.01	-	-	6.10	0.0012	0.087	1.01	0.6
C_6	86.178	913.37	436.9	0.0576	3.42	0.0021	10.51	-	-	13.93	0.0028	0.241	2.56	1.2
**C_7^+	114.232	1023.89	360.6	0.4788	28.38	0.0016	8.01	-	-	36.39	0.0072	0.823	7.37	2.6
Σ				1.0000	59.30	1.0000	5005.00	1.0000	-	5064.30	1.0000	21.063	395.79	726.4

RECOMBINED GAS PROPERTIES: FLOW RATE = __5.005__ MMscfd,   G = __21.063__ /28.966 = __0.73__, T_c = __395.79__ °R, P_c = __726.4__ psia

* THE LIQUID FLOW RATE(Bbl/d) AND SPECIFIC GRAVITY ARE TO BE MEASURED AT THE SAME CONDITIONS

** PHYSICAL PROPERTIES OF OCTANES ARE USED FOR THE C_7^+ FRACTION

BASE CONDITIONS = 14.65 psia and 60 °F

TABLE A-4. ILLUSTRATING EXAMPLE A-10

From Table A-4,

$$\text{Total gas} = 5.005 \text{ Mscfd}$$

$$G = 0.73$$

$$T_c = 395.79\,^\circ R$$

$$P_c = 726.40 \text{ psia}$$

In some instances, the flow rate of the high-pressure liquid may be measured directly. The above calculations still apply but there is no need for flash calculations and the subsequent definition of a shrinkage factor.

9. Gas Hydrate Formation

Gas hydrates are crystalline compounds formed, by the chemical combination of natural gas and water, under pressure at temperatures considerably above the freezing point of water. In the presence of free water, hydrates will form when the temperature of the gas is below a certain temperature, called the "hydrate temperature." Hydrate formation is often confused with condensation and the distinction between the two must be clearly understood. Condensation of water from a natural gas under pressure occurs when the temperature is at or below the dew point at that pressure. Free water obtained under such conditions is essential to formation of hydrates which will occur at or below the hydrate temperature at the same pressure. Hence the hydrate temperature would be below, and perhaps the same as, but never above the dew point temperature.

While conducting tests, it becomes necessary to define, and thereby avoid, conditions that promote the formation of hydrates. This is essential to the proper field conduct of tests since hydrates may choke the flow string, surface lines, and well testing equipment. Hydrate formation in the flow string would result in a lower value for measured wellhead pressures. In a flow rate measuring device, hydrate

formation would result in lower flow rates. Excessive hydrate formation may also completely block flow lines and surface equipment.

In summary, conditions promoting hydrate formation are;
Primary conditions:

      a.   Gas must be at or below its water dew point with "free" water present,

      b.   Low temperature,

      c.   High pressure.

Secondary conditions:

      a.   High velocities,

      b.   Pressure pulsations,

      c.   Any type of agitation,

      d.   Presence of H_2S and of CO_2,

      e.   Introduction of a small hydrate crystal.

A rigorous technique for the prediction of conditions for hydrate formation involves the use of vapour-liquid equilibrium constants (Katz et al., 1959, p. 210). The calculations are analogous to dew point calculations for multi-component mixtures.

A practical technique for predicting hydrate formation conditions is illustrated in Examples A-11 and A-12 (GPSA Engineering Data Book, 1974).

For the purpose of gas well testing it is convenient to divide hydrate formation into two categories: (1) hydrate formation due to a decrease in temperature, with no sudden pressure drop, such as in the flow string or surface lines and (2) hydrate formation where a sudden expansion occurs such as in flow provers, orifices, back-pressure regulators or chokes. Both categories are reviewed with emphasis on the prediction of occurrence of hydrates prior to testing.

1. <u>Hydrate formation in the flow string and surface lines</u>. As mentioned above, free water is essential to hydrate formation. Free water is almost certain to be present during well testing since gas reservoirs are essentially water saturated and a decrease in temperature results in a lower solubility of water in gas. The hydrate temperature depends on the pressure and composition, reflected by its gravity, of

the gas. Figure A-12 gives approximate values of the hydrate temperature
as a function of pressure and specific gravity. Hydrates will form
whenever temperature and pressure plot to the left of the hydrate
formation line for the gas in question.

The application of Figure A-12 is illustrated by Example A-11.

EXAMPLE A-11

Problem

a. A gas of specific gravity 0.8 is at a pressure of 1000 psia. To
    what extent can the temperature be lowered without hydrate formation,
    assuming presence of free water?

b. A gas of specific gravity 0.8 is at a temperature of $50^\circ F$. What is
    the pressure above which hydrates could be expected to form,
    assuming presence of free water?

Solution

a. From Figure A-12, at a specific gravity of 0.8 and a pressure of
    1000 psia, hydrate temperature = $66^\circ F$.
    Hydrates may form at or below $66^\circ F$.

b. From Figure A-12, at a specific gravity of 0.8 and a temperature
    of $50^\circ F$, pressure = 275 psia.
    Hydrates may form at or above 275 psia.

Figure A-12 is applicable only to sweet natural gases. For
sour gases, it may be used, keeping in mind that the presence of H_2S
and CO_2 will increase the hydrate temperature and reduce the pressure
above which hydrates will form. In simple words, the presence of H_2S
or CO_2 enhances the possibility of hydrate formation.

2. Hydrate formation in flow provers, orifices and back-
pressure regulators. Sudden expansion in one of these devices is
accompanied by a temperature drop which may cause hydrate formation.
Figures A-13 to A-17 may be used to approximate the conditions for
hydrate formation. The limitations of Figure A-12, discussed above,
also apply to Figures A-13 to A-17. Figures A-13 to A-17 may be used

for gases with intermediate specific gravity by linear interpolation.
The use of these figures is illustrated by Example A-12.

EXAMPLE A-12

Problem

a. How much may a 0.8 gravity gas at 1000 psia and 100°F be expanded
without hydrate formation, assuming presence of free water?

b. How much may a 0.8 gravity gas at 800 psia and 100°F be expanded
without hydrate formation, assuming presence of free water?

c. A 0.8 gravity gas is to be expanded from 1000 psia to 440 psia.
What is the minimum initial temperature that will permit
expansion without danger of hydrates?

Solution

a. In Figure A-15, intersection of the 1000 psia initial pressure line
and the 100°F initial temperature line gives a final pressure of
440 psia. Hence the gas may be expanded to 440 psia without a
possibility of hydrate formation.

b. In Figure A-14, the 100°F initial temperature curve does not
intersect the 800 psia initial pressure line. Hence the gases may
be expanded to atmospheric pressure without hydrate formation.

c. In Figure A-15, intersection of the 1000 psia initial pressure line
and the 440 psia final pressure line gives an initial temperature of
100°F. Hence 100°F is the minimum initial temperature to avoid
hydrate formation.

FIGURE A-13. PERMISSIBLE EXPANSION OF A 0.6-GRAVITY
NATURAL GAS WITHOUT HYDRATE FORMATION

From GPSA Engineering Data Book (1974)
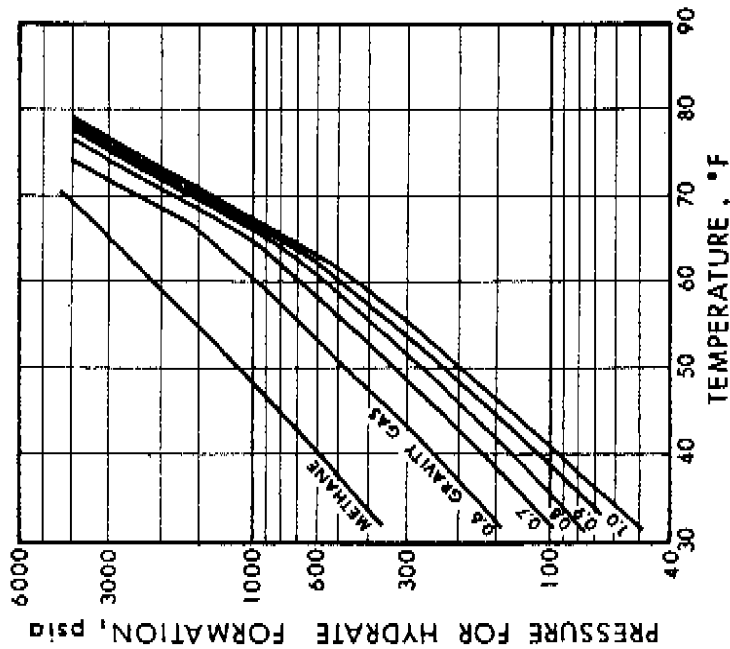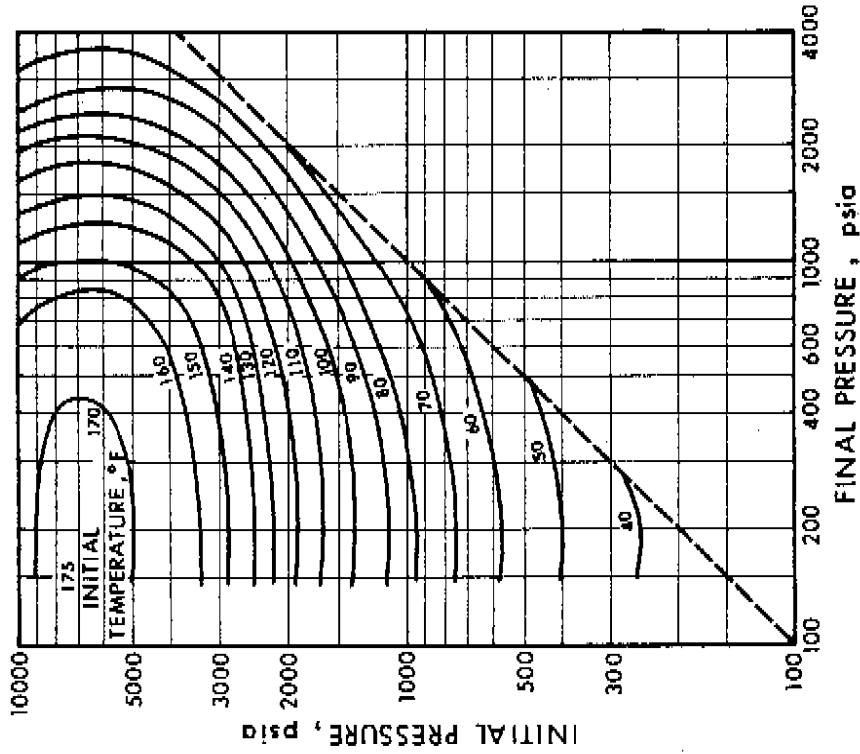
FIGURE A-12 PRESSURE-TEMPERATURE CURVES
FOR PREDICTING HYDRATE FORMATION

FIGURE A-15. PERMISSIBLE EXPANSION OF A
0.8-GRAVITY NATURAL GAS
WITHOUT HYDRATE FORMATION

FIGURE A-14. PERMISSIBLE EXPANSION OF A
0.7-GRAVITY NATURAL GAS
WITHOUT HYDRATE FORMATION

From GPSA Engineering Data Book (1974)

FIGURE A-17. PERMISSIBLE EXPANSION OF A 1.0-GRAVITY
NATURAL GAS WITHOUT HYDRATE FORMATION

From GPSA Engineering Data Book (1974)

FIGURE A-16. PERMISSIBLE EXPANSION OF A 0.9-GRAVITY
NATURAL GAS WITHOUT HYDRATE FORMATION

APPENDIX B

CALCULATION OF BOTTOM HOLE PRESSURES IN GAS WELLS

In order to estimate the productivity or absolute open flow potential of gas wells it is necessary to determine the bottom hole pressures, static and flowing, either by actual measurement with a bottom hole pressure gauge or by calculation from wellhead pressure measurements. Recognizing that it is often impractical to measure static and flowing bottom hole pressures, estimations have to be made from wellhead data.

Calculations of bottom hole pressures, for a single-phase (gas) in the wellbore, involves knowledge of the wellhead pressures, the properties of natural gases, the depths of wells, flow rates, formation and wellhead temperatures, and the size of flow lines. This appendix introduces the theory and basic equations relating these quantities. Various methods utilizing these basic equations, and the simplifying assumptions made in order to develop practical forms of these equations, are mentioned. The recommended standard procedure is considered in considerable detail and is illustrated by appropriate examples.

Also included in this appendix is a simple method for the estimation of bottom hole pressures for gas-condensate wells. Several alternative methods are described in the literature for the calculation of bottom hole pressures in wells where gas and liquid exist simultaneously in the wellbore, but they are not covered in detail in this appendix.

For convenience, the appendix is essentially divided into three sections: (1) Single-phase (gas) in the wellbore--calculation of static pressure; (2) single-phase (gas) in the wellbore--calculation of flowing pressure; and, (3) two-phase (gas and liquid) in the wellbore. A brief discussion of annular flow and the calculation of flowing wellhead pressures from static pressure measurements is also included.

Various methods for the calculation of bottom hole pressures, static or flowing, stem from the basic mechanical energy balance

equation (or the first law of thermodynamics). This energy balance, for steady-state flow, may be written as

$$\frac{144}{\rho} dp + \frac{u}{2 \alpha g_c} du + \frac{g}{g_c} dz + \frac{2 f u^2}{g_c D} dL + W_s = 0 \qquad (B-1)$$

where

ρ	=	density of the fluid, lb_m/ft^3
p	=	pressure, psia
u	=	average velocity of the fluid, ft/sec
α	=	correction factor to compensate for the variation of velocity over the tube cross section. It varies from 0.5 for laminar flow to 1.0 for fully developed turbulent flow.
z	=	distance in the vertical downward direction, ft
f	=	Fanning friction factor
D	=	inside diameter of the pipe, ft
L	=	length of the flow string, ft. For a vertical flow string, $L = z$
$\dfrac{u}{2 \alpha g_c} du$	=	pressure drop due to kinetic energy effects
$\dfrac{2 f u^2}{g_c D} dL$	=	pressure drop due to friction effects
W_s	=	mechanical work done on or by the gas. This term is taken to be zero in the following sections

1. Estimation of Static Bottom Hole Pressure--Single-Phase Gas

The static bottom hole pressure in a gas well is the sum of the static wellhead pressure and the pressure due to the weight of the gas column (hydrostatic head) in the well bore. For a static gas, the kinetic energy and friction effects are zero so that Equation (B-1) reduces to

$$dp = - \frac{\rho}{144} dz \qquad (B-2)$$

The density of the gas, as expressed by the Gas Law in Equation (A-2) is substituted in Equation (B-2) to give

$$\frac{dp}{p} = - \frac{G \, dz}{53.34 \, T \, Z} \qquad (B-3)$$

The only assumption involved in the derivation of Equation (B-3) is a single-phase gas described by the gas law. This equation is the basis for all methods for calculating bottom hole static pressures from wellhead static pressure measurements. These methods differ only in the assumptions made to simplify integration of a differential equation containing T and Z, both of which vary with depth. The variation of G with pressure is usually ignored.

Aziz (1963) conducted a detailed comparison of various methods to calculate static bottom hole pressures. Among the methods studied are:

1. The Average Temperature and Compressibility Method
2. The Average Density Method
3. Poettman's Method
4. The Cullender and Smith Method

Aziz (1963, 1967a) has indicated that the Cullender and Smith (1956) method is the most generally applicable method. It does not make any of the simplifying assumptions made by the other methods, it is applicable to shallow and deep wells, it can be used for sour gases and with slight modifications it is easily adapted to digital computer programming. Consequently, the Cullender and Smith method is adopted as the standard method for the calculation of static bottom hole pressures from wellhead observations, and is presented in detail with an appropriate example. However, it must be recognized that the other methods are reasonably accurate under certain conditions. Specifically, for shallow gas wells with relatively small temperature gradients, any of the above methods may be used.

The Average Temperature and Compressibility method described below, although not as accurate as the Cullender and Smith method, is described because of its simplicity and frequent use to approximate static bottom hole pressures.

The Average Temperature and Compressibility Method

Equation (B-3) may be integrated to give

$$\frac{G \ z}{53.34 \ \bar{T} \ \bar{Z}} = \ln \frac{P_{ws}}{P_{ts}} \tag{B-4}$$

or

$$P_{ws} = P_{ts} \ e^{S/2} \tag{B-4a}$$

where

P_{ws} = static bottom hole pressure

P_{ts} = static wellhead pressure

S = $2Gz/(53.34 \ \bar{T} \ \bar{Z})$

$\bar{T}$ = arithmetic mean of bottom hole and wellhead temperatures

$\bar{Z}$ = compressibility factor at the arithmetic mean temperature and arithmetic mean pressure.

The calculation procedure involves use of Equations (B-4) or (B-4a) which may be applied as a one-step calculation from the wellhead to the sandface or as a multi-step (usually two) calculation. The average value of compressibility, for each step, may be obtained by estimation or iteration.

The Cullender and Smith Method

This method avoids the use of simplifying assumptions for temperature and compressibility factor that have to be made to derive Equation (B-4). Equation (B-3) may be written as

$$\frac{G\,z}{53.34} = \int_{P_{ts}}^{P_{ws}} \frac{T\,Z}{p}\,dp \qquad (B-5)$$

The right-hand side of Equation (B-5) may be integrated numerically by determining the value of (TZ/p) for each of any number of increments in p between p_{ts} and p_{ws}.

In general, for limits in pressure of p_0 and p_n, the right-hand side of Equation (B-5) may be written as

$$\int_{P_0}^{P_n} \frac{T\,Z}{p}\,dp \simeq \frac{1}{2}\left[(p_1 - p_0)(I_1 + I_0) + (p_2 - p_1)(I_2 + I_1) + \cdots \right.$$

$$\left. + (p_n - p_{n-1})(I_n + I_{n-1})\right] \qquad (B-6)$$

where

$$I_n = (TZ/p)_n \qquad (B-7)$$

For digital computer programming, Equation (B-6) may be used with any number of increments in p to obtain an accurate value of p_{ws}.

In the case of a two-step calculation where only the intermediate value of pressure, that at the mid-depth, p_{ms}, is considered, Equation (B-6) may be expressed as

$$\int_{P_{ts}}^{P_{ws}} \frac{T\,Z}{p}\,dp \approx \frac{(p_{ms} - p_{ts})(I_{ms} + I_{ts})}{2} + \frac{(p_{ws} - p_{ms})(I_{ws} + I_{ms})}{2} \qquad (B-8)$$

Substituting Equation (B-8) in Equation (B-5) gives

$$0.0375\,G\,z = (p_{ms} - p_{ts})(I_{ms} + I_{ts}) + (p_{ws} - p_{ms})(I_{ws} + I_{ms}) \qquad (B-9)$$

Equation (B-9) may be separated into two expressions, one for each half of the flow string:

for the upper half,

$$0.0375 \ G \ \frac{z}{2} = (P_{ms} - p_{ts})(I_{ms} + I_{ts}) \tag{B-10}$$

for the lower half,

$$0.0375 \ G \ \frac{z}{2} = (p_{ws} - p_{ms})(I_{ws} + I_{ms}) \tag{B-11}$$

While this method may be used with any number of steps, Cullender and Smith (1956) have demonstrated that the equivalent of four-step accuracy may be obtained with a two-step calculation and parabolic interpolation (Simpson's rule). This procedure results in

$$0.0375 \ G \ z = \frac{P_{ws} - P_{ts}}{3} (I_{ts} + 4 \ I_{ms} + I_{ws}) \tag{B-12}$$

In order to solve Equations (B-9), (B-10), and (B-11), a linear temperature profile is assumed in the flow string. Lesem et al. (1957) have presented a method for calculating the temperature-depth relationship, but sufficient accuracy will normally be attained by assuming the relationship to be linear. The gas gravity may vary slightly with depth but will be assumed constant since knowledge of this variation is seldom available.

The following procedure is recommended for the solution of Equation (B-12):

1. Calculate the left-hand side of Equation (B-10) for the upper half of the flow string.

2. Calculate I_{ts} from Equation (B-7) and wellhead conditions.

3. Assume $I_{ms} = I_{ts}$ for the conditions at the average well depth or at the mid-point of the flow string.

4. Calculate p_{ms} from Equation (B-10).

5. Using the value of p_{ms} calculated in step 4 and the arithmetic average temperature, T_{ms}, determine the value of I_{ms} from Equation (B-7).

6. Recalculate p_{ms} from Equation (B-10) and if this

recalculated value is not within one psi of the p_{ms} calculated in step 4, repeat steps 5 and 6 until the above criterion is satisfied.

7. Assume $I_{ws} = I_{ms}$ for the conditions at the bottom of the flow string.

8. Repeat steps 4 to 6, using Equation (B-11) for the lower half of the flow string and obtain a value of the bottom hole pressure, p_{ws}.

9. Apply Simpson's rule as expressed by Equation (B-12) to obtain a more accurate value of the static bottom hole pressure.

The following example illustrates the use of the Cullender and Smith method to calculate static bottom hole pressures from wellhead measurements.

EXAMPLE B-1

Problem   Calculate the static bottom hole pressure by the method of Cullender and Smith from the following well data:

Gas gravity,	G	= 0.75
Well depth,	z	= 10,000 ft
Wellhead temperature,	T_{ts}	= 495°R
Formation temperature,	T_{ws}	= 705°R
Shut-in wellhead pressure,	P_{ts}	= 2500 psia
Pseudo-critical temperature,	T_c	= 408°R
Pseudo-critical pressure,	P_c	= 667 psia

Solution

$$T_{ms} = (T_{ts} + T_{ws})/2 = (495 + 705) = 600°R$$

Wellhead, $T_r = T_{ts}/T_c = 495/408 = 1.213$

Midpoint, $\quad T_r = T_{ms}/T_c = 600/408 = 1.471$

Bottom, $\quad T_r = T_{ws}/T_c = 705/408 = 1.728$

Wellhead, $\quad P_r = P_{ts}/P_c = 2500/667 = 3.748$

Left-hand side of Equations (B-10) and (B-11)

$$0.0375 \; G \; \frac{Z}{2} = (0.0375)(0.75)(10,000)/2 = 140.625$$

Calculate I_{ts}:

From Figure A-3, at a reduced temperature and pressure of 1.213 and 3.748, respectively

$$Z_{ts} = 0.593$$

$$I_{ts} = \frac{T_{ts} \; Z_{ts}}{P_{ts}} = \frac{(495)(0.593)}{(2500)} = 0.1174$$

Step 1   (the upper half of the flow string)

First trial

Assume

$$I_{ms} = I_{ts} = 0.1174$$

Solving Equation (B-10) for P_{ms}

$$140.625 = (P_{ms} - 2500)(0.1174 + 0.1174)$$

$$P_{ms} = 3099 \text{ psia}$$

Second trial

$$P_r = P_{ms}/P_c = 3099/667 = 4.646$$

$$Z_{ms} = 0.780 \quad \text{at} \quad T_r = 1.471, \quad P_r = 4.646 \quad \text{(Figure A-3)}$$

$$I_{ms} = \frac{T_{ms} \; Z_{ms}}{P_{ms}} = \frac{(600)(0.780)}{(3099)} = 0.1510$$

Solving Equation (B-10) for p_{ms}

$$140.625 = (p_{ms} - 2500)(0.1510 + 0.1174)$$

$$p_{ms} = 3024 \text{ psia}$$

Third trial

$$P_r = p_{ms}/p_c = 3024/667 = 4.534$$

$$Z_{ms} = 0.775 \quad \text{at} \quad T_r = 1.471, \quad p_r = 4.534 \qquad \text{(Figure A-3)}$$

$$I_{ms} = \frac{T_{ms} Z_{ms}}{P_{ms}} = \frac{(600)(0.775)}{(3024)} = 0.1538$$

Solving Equation (B-10) for p_{ms}

$$140.625 = (p_{ms} - 2500)(0.1538 + 0.1174)$$

$$p_{ms} = 3019 \text{ psia}$$

Fourth trial

$$P_r = p_{ms}/p_c = 3019/667 = 4.526$$

$$Z_{ms} = 0.775 \quad \text{at} \quad T_r = 1.471, \quad p_r = 4.526 \qquad \text{(Figure A-3)}$$

$$I_{ms} = \frac{T_{ms} Z_{ms}}{P_{ms}} = \frac{(600)(0.775)}{(3019)} = 0.1540$$

Solving Equation (B-10) for p_{ms}

$$140.625 = (p_{ms} - 2500)(0.1540 + 0.1174)$$

$$p_{ms} = 3018 \text{ psia}$$

Step 2   (the lower half of the flow string)

First trial

Assume

$$I_{ws} = I_{ms} = 0.1540$$

Solving Equation (B-11) for p_{ws}

$$140.625 = (p_{ws} - 3018)(0.1540 + 0.1540)$$

$$p_{ws} = 3475 \text{ psia}$$

Second trial

$$p_r = p_{ws}/p_c = 3475/667 = 5.210$$

$$Z_{ws} = 0.894 \quad \text{at} \quad T_r = 1.728, \quad p_r = 5.210 \qquad \text{(Figure A-3)}$$

$$I_{ws} = \frac{T_{ws} \, Z_{ws}}{p_{ws}} = \frac{(705)(0.894)}{3475} = 0.1814$$

Solving Equation (B-11) for p_{ws}

$$140.625 = (p_{ws} - 3018)(0.1814 + 0.1540)$$

$$p_{ws} = 3437 \text{ psia}$$

Third trial

$$p_r = p_{ws}/p_c = 3437/667 = 5.153$$

$$Z_{ws} = 0.892 \quad \text{at} \quad T_r = 1.728, \quad p_r = 5.153 \qquad \text{(Figure A-3)}$$

$$I_{ws} = \frac{T_{ws} \, Z_{ws}}{p_{ws}} = \frac{(705)(0.892)}{3437} = 0.1830$$

Solving Equation (B-11) for p_{ws}

$$140.625 = (p_{ws} - 3018)(0.1830 + 0.1540)$$

$$p_{ws} = 3435 \text{ psia}$$

Parabolic interpolation

From Equation (B-12)

$$(140.625 \times 2) = \frac{p_{ws} - p_{ts}}{3}(0.1174 + 4(0.1540) + 0.1830)$$

$$p_{ws} - p_{ts} = 921$$

$$p_{ws} = 2500 + 921 = 3421 \text{ psia}$$

For comparative purposes, a one-step calculation for the above example yielded a bottom hole static pressure of 3436 psia. This illustrates that a one-step calculation will not yield satisfactory results for deep, relatively high-pressure wells. On the other hand, a series of calculations for shallow gas wells (less than 5000 feet deep), as in Example B-1, indicates that the calculated pressures will not differ appreciably from those obtained by a one-step calculation.

The above method is also applicable to sour gas wells if appropriate corrections are included in the determination of compressibility factors as shown in Appendix A.

The solution of Example B-1 is also presented in a tabular form in Table B-1. Presentation of calculations in such a form is intended to simplify data reduction and may be used as a basis for preparing standard reporting forms.

A computer program called BHOLE is included in Appendix D. The program utilizes a third-order numerical integration scheme (Aziz, 1967a) instead of Simpson's rule.

2. Estimation of Flowing Bottom Hole Pressure--
Single-Phase Gas

The flowing bottom hole pressure in a gas well is the sum of the flowing wellhead pressure, the pressure due to the weight of the gas column in the wellbore, the kinetic energy change and the energy losses due to friction.

For a flowing gas Equation (B-1) reduces to

$$\frac{144}{\rho} \, dp + \frac{g}{g_c} \, dz + \frac{u}{2 \, \alpha \, g_c} \, du + \frac{2 \, f \, u^2}{g_c \, D} \, dL = 0 \tag{B-13}$$

The energy losses due to friction, as expressed in Equation (B-13), constitute the well-known Fanning equation

$$dp_f = \frac{2 \, f \, u^2}{g_c \, D} \, dL \tag{B-14}$$

The kinetic energy term, $u \, du/(2 \alpha g_c)$, has been shown to be negligible (Young, 1967, Dranchuk and McFarland, 1974) as compared to the total pressure drop in the well bore. Aziz (1963) has recommended that the change in kinetic energy may be neglected in all practical cases of gas flow calculations. Neglecting the kinetic energy term in Equation (B-13) gives

$$\frac{53.34 \, T \, Z}{G} \, \frac{dp}{p} + dz + \frac{2 \, f \, u^2}{g_c \, D} \, dL = 0 \tag{B-15}$$

Since the actual cross-sectional average lineal velocity of the gas at any point in the wellbore is given by

$$u = \frac{0.4152 \, T \, Z \, Q}{p \, D} \tag{B-16}$$

where

Q = production in MMscfd (14.65 psia, 60°F)

u = lineal velocity, ft/sec

Well Data: z = 10,000 ft $\qquad$ T_c = 408°R $\qquad$ p_c = 667 psia $\qquad$ G = 0.75

$\qquad$ T_{ts} = 495°R $\qquad$ T_{ws} = 705°R $\qquad$ p_{ts} = 2500 psia

Calculate: T_{ms} = 600°R $\qquad$ T_{ts}/T_c = 1.213 $\qquad$ T_{ms}/T_c = 1.471 $\qquad$ T_{ws}/T_c = 1.728

$\qquad$ Z_{ts} = 0.593 $\qquad$ p_{ts}/p_c = 3.748 $\qquad$ I_{ts} = 0.1174 $\qquad$ $0.0375\,G\,\dfrac{z}{2}$ = 140.625

Trial No	z	Assume p_n	p_r	T_n	T_r	z_n	I_n $\dfrac{T_n z_n}{p_n}$	M $I_0 + I_n$	N $0.0375\,\dfrac{Gz}{2}$	N/M Δp	Calc. p_n	
1	5000	2500	⎰assume	assume	$I_n = I_{ts}$		0.1174	0.2348	140.625	599	3099	⎱ I_{ts}
2	5000	3099	4.646	600	1.471	0.780	0.1510	0.2684	140.625	524	3024	
3	5000	3024	4.534	600	1.471	0.775	0.1538	0.2712	140.625	519	3019	
4	5000	3019	4.526	600	1.471	0.775	0.1540	0.2714	140.625	518	3018	⎱ I_{ms}
1	10,000	3018	⎰assume	assume	$I_n = I_{ms}$		0.1540	0.3080	140.625	457	3475	
2	10,000	3475	5.210	705	1.728	0.894	0.1814	0.3554	140.625	419	3437	
3	10,000	3437	5.153	705	1.728	0.892	0.1830	0.3370	140.625	417	3435	⎱ I_{ws}

Applying Simpson's rule: $\qquad$ $(140.625 \times 2) = \dfrac{p_{ws} - 2500}{3}\,(.1174 + 4(.1540) + .1830)$
Equation (B-12)

$\qquad\qquad\qquad\qquad$ p_{ws} = 2500 + 921 = 3421 psia

TABLE B-1. CULLENDER AND SMITH METHOD FOR CALCULATION OF STATIC BOTTOM-HOLE PRESSURES

Substitution of Equation (B-16) in Equation (B-15) gives

$$\frac{53.34 \; T \; Z}{G} \frac{dp}{p} + dz + 0.0107 \frac{f}{D^5} \left(\frac{T \; Z}{p}\right)^2 Q^2 \; dL = 0 \qquad (B-17)$$

The only assumptions involved in the derivation of Equation (B-17) are: single-phase gas described by the Gas Law and negligible change in kinetic energy. This equation is the basis of all methods for calculating bottom hole flowing pressures from wellhead observations.

Before considering the various methods for calculating flowing bottom hole pressure, a brief discussion of friction factors and a related parameter called relative roughness is necessary.

The Friction Factor

Regardless of the method used to solve Equation (B-17), knowledge of the parameter, f, is necessary. This friction factor is defined by Equations (B-13) and (B-14) and is the factor which validates these equations.

Much experimental work has been carried out, particularly in horizontal pipes, to determine the variables which influence f and in an effort to develop prediction methods. In recent years this work has been augmented by theoretical studies.

For rough, long tubes, as is the case in gas wells, it has been shown that the friction factor can be described by:

$$f = f \{Re, \; \delta/d\} \qquad (B-18)$$

where

Re $=$ Reynolds number, $Du\rho/\mu$

$\delta/d =$ relative roughness which is defined as the ratio of the absolute roughness, δ (the distance from the peaks to the valleys in pipe wall irregularities), to the internal pipe diameter, d.

for steady-state flow, the Reynolds number can be represented by

$$Re = \frac{20011 \; G \; Q}{\mu \; d} \qquad (B-19)$$

where Q is in MMscfd, μ is in cp, and d is in inches.

Of the numerous correlations published in the literature, the best equations available for the prediction of friction factors are those based on work by Von Karman (1931) and Nikuradse (1940). The Colebrook (1939) equation

$$\frac{1}{\sqrt{f}} = 4.0 \log \frac{d}{\delta} + 2.28 - 4.0 \log \left(1 + \frac{4.67 \ d/\delta}{Re \ \sqrt{f}} \right) \tag{B-20}$$

is such a relationship. For values of $(d/\delta)/(Re \ \sqrt{f})$ less than 0.01 (high flow rates) the Reynolds number is found to have no further effect on the friction factor, and Equation (B-20) reduces to

$$\frac{1}{\sqrt{f}} = 4.0 \log \frac{d}{\delta} + 2.28 \tag{B-21}$$

Equations (B-20) or (B-21) may be used to predict friction factors. The graphical presentation shown in Figure B-1, which gives Fanning friction factors as a function of Reynolds numbers and relative roughness may be used. Reynolds numbers are calculated quite easily, however, the relative roughness is not so easily determined.

Relative Roughness

For clean new pipe the relative roughness is determined by the method of manufacture and usually reflects an absolute roughness, δ, of 0.00055 to 0.0019 (Cullender and Binckley, 1950, Smith et al. 1954, Smith et al. 1956). For new pipe or tubing used in gas wells the absolute roughness has been found to be in the order of 0.00060 or 0.00065.

Figure B-2 is a plot of relative roughness, δ/d, versus the pipe diameter, d. It includes curves for well tubing, commercial steel and very dirty pipe along with experimental data points reported by Smith et al. (1954) and Smith et al. (1956).

Figure B-2 is recommended for quick estimations of relative roughness. If there is any doubt regarding pipe conditions, the line corresponding to an absolute roughness of 0.00060 inches is recommended.

REYNOLDS NUMBER, Re
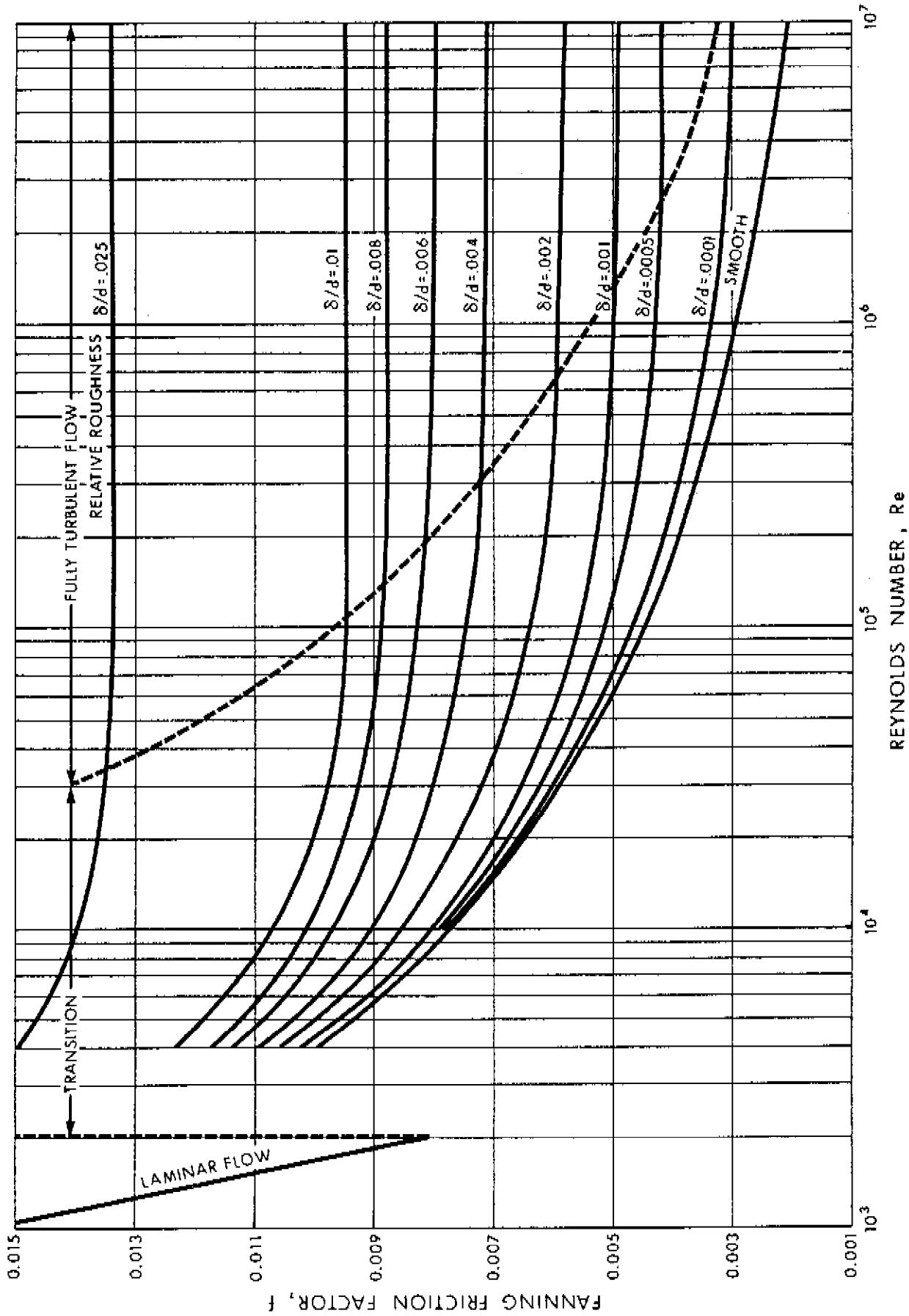
FIGURE B-1. FRICTION FACTOR FOR FLUID FLOW IN PIPES

From Knudsen and Katz (1958)
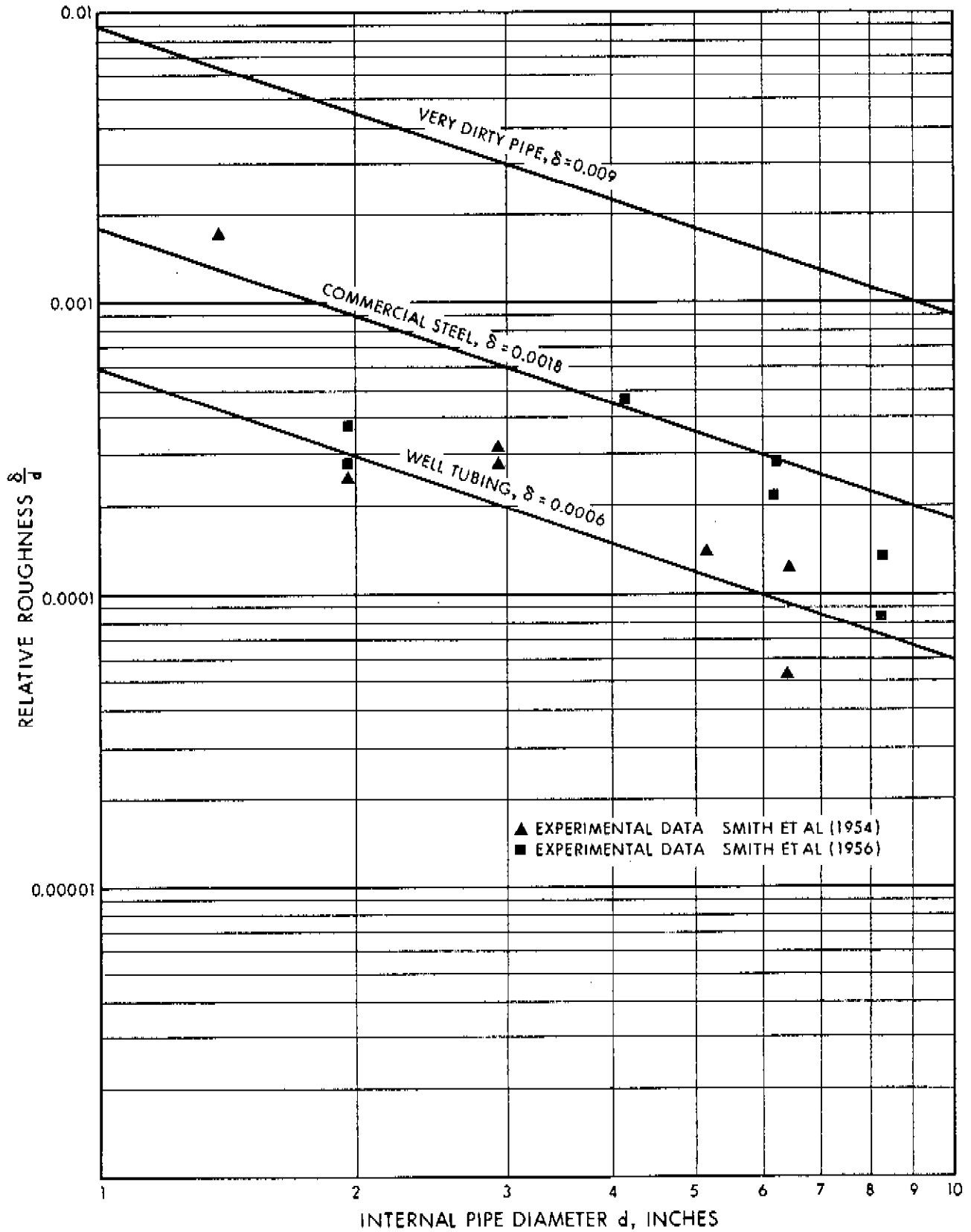
FIGURE B-2. RELATIVE ROUGHNESS OF PIPES

Aziz (1963) has conducted a detailed comparison of various methods to calculate flowing bottom hole pressures. Among the methods studied are:

1. The Average Temperature and Compressibility Method
2. The Average Density Method
3. The Sukkar and Cornell Method
4. The Cullender and Smith Method

These methods are based on Equation (B-17) and differ only in the assumptions made to simplify integration of a differential equation containing T, Z, and f, all of which may vary with depth. The variation of f with depth stems from its dependence on Reynolds numbers. Reynolds numbers are a function of μ, which varies with pressure. Unless otherwise mentioned, friction factors are assumed to be constant over the length of the well tubing.

Aziz (1963, 1967a) has shown that the Cullender and Smith method (1956) is the most generally applicable method. It does not make any of the simplifying assumptions made by the other methods, it is applicable to shallow and deep wells, it can be used for sour gases and with slight modifications it is easily adapted to computer programming. Consequently, the Cullender and Smith method is adopted for a standard method for estimation of flowing bottom hole pressures from wellhead observations, and is presented in detail with an appropriate example. However, it must be recognized that the other methods are reasonably accurate under certain conditions. Specifically, for shallow gas wells with relatively small temperature gradiens, any of the above methods may be used.

The Average Temperature and Compressibility method described below, although not as accurate as the Cullender and Smith method, is described because of its simplicity and frequent use to approximate flowing bottom hole pressures.

The Average Temperature and
  Compressibility Method

Assuming a vertical flow string, so that L = z, Equation (B-17) may be written as

$$Q = 0.1000 \left[\frac{\left(P_{wf}^2 - e^S \, P_{tf}^2 \right) \, d^5 \, S}{G \, \bar{T} \, \bar{Z} \, \bar{f} \, z \, (e^S - 1)} \right]^{0.5} \quad (B-22)$$

or

$$P_{wf}^2 = P_{tf}^2 \, e^S + \frac{100 \, G \, \bar{T} \, \bar{Z} \, \bar{f} \, z \, (e^S - 1) \, Q^2}{d^5 \, S} \quad (B-22a)$$

where

P_{wf}	=	flowing bottom hole pressure
P_{tf}	=	flowing wellhead pressure
S	=	$2Gz/(53.34 \, \bar{T}\bar{Z})$
$\bar{T}$	=	arithmetic mean of bottom hole and wellhead temperatures
$\bar{Z}$	=	compressibility at the arithmetic mean temperature and arithmetic mean pressure
$\bar{f}$	=	friction factor at the arithmetic mean temperature and arithmetic mean pressure

The calculation procedure involves use of Equation (B-22) or (B-22a) which may be applied as a one-step calculation from the wellhead to the sandface or as a multi-step (usually two) calculation. The average value of compressibility, for each step, may be obtained by estimation or iteration.

The Cullender and Smith Method

This method avoids the use of simplifying assumptions for temperature and compressibility factor that have to be made to derive Equation (B-22). Assuming a vertical flow string, so that $L = z$, Equation (B-17) may be written as

$$\frac{1000 \, G \, z}{53.34} = \int_{P_{tf}}^{P_{wf}} \frac{\left(\frac{p}{T \, Z} \right) \, dp}{F^2 + 0.001 \left(\frac{p}{T \, Z} \right)^2} \quad (B-23)$$

where

$$F^2 = \frac{2.6665 \, f \, Q^2}{d^5} \quad (B-24)$$

Equation (B-24) may be simplified by using the Nikuradse friction factor equation for fully turbulent flow, based on an absolute roughness of 0.00060, to give

$$F_r Q = F = \frac{0.10797\ Q}{d^{2.612}} \quad , \qquad d < 4.277\ \text{in} \qquad (B-25)$$

and

$$F_r Q = F = \frac{0.10337\ Q}{d^{2.582}} \quad , \qquad d > 4.277\ \text{in} \qquad (B-26)$$

Values of F_r for various tubing and casing sizes are presented in Table B-2. The right-hand side of Equation (B-23) may be integrated numerically by the procedure illustrated for calculation of static bottom hole pressures. For a two-step calculation, Equation (B-23) may be expressed as

$$\frac{1000\ G\ z}{53.34} = \int_{P_{tf}}^{P_{wf}} \frac{\left(\frac{p}{T\ Z}\right) dp}{F^2 + 0.001 \left(\frac{p}{T\ Z}\right)^2}$$

$$= \frac{(p_{mf} - p_{tf})(I_{mf} + I_{tf})}{2} + \frac{(p_{wf} - p_{mf})(I_{wf} + I_{mf})}{2}$$

or

$$37.5\ G\ z = (p_{mf} - p_{tf})(I_{mf} + I_{tf}) + (p_{wf} - p_{mf})(I_{wf} + I_{mf}) \qquad (B-27)$$

where

$$I_n = \frac{\left(\frac{p}{T\ Z}\right)_n}{F^2 + 0.001 \left(\frac{p}{T\ Z}\right)_n^2} \qquad (B-28)$$

Equation (B-27) may be separated into two expressions, one for each half of the flow string:

for the upper half,

$$37.5 \, G \, \frac{z}{2} = (p_{mf} - p_{tf})(I_{mf} + I_{tf}) \qquad \text{(B-29)}$$

for the lower half,

$$37.5 \, G \, \frac{z}{2} = (p_{wf} - p_{mf})(I_{wf} + I_{mf}) \qquad \text{(B-30)}$$

Again, Simpson's rule gives:

$$37.5 \, G \, z = \frac{p_{wf} - p_{tf}}{3} (I_{tf} + 4 \, I_{mf} + I_{wf}) \qquad \text{(B-31)}$$

The following procedure is recommended for the solution of Equation (B-31):

1. Calculate the left-hand side of Equation (B-29) for the upper half of the flow string.

2. Calculate F^2 from Equation (B-25) or (B-26), or from Table B-2.

3. Calculate I_{tf} from Equation (B-28) and wellhead conditions.

4. Assume $I_{mf} = I_{tf}$ for the conditions at the average well depth or at the mid-point of the flow string.

5. Calculate p_{mf} from Equation (B-29).

6. Using the value of p_{mf} calculated in step 5 and the arithmetic average temperature, T_{mf}, determine the value of I_{mf} from Equation (B-28).

7. Recalculate p_{mf} from Equation (B-29) and if this recalculated value is not within 1 psi of the p_{mf} calculated in step 5, repeat steps 6 and 7 until the above criterion is satisfied.

8. Assume $I_{wf} = I_{mf}$ for the conditions at the bottom of the flow string.

9. Repeat steps 5 to 7, using Equation (B-30) for the lower half of the flow string and obtain a value of the bottom hole pressure, p_{wf}.

(use only for internal diameters less than 4.277 inches)

$$F_r = \frac{0.10797}{d^{2.612}}$$

Nominal Size Inches	Outer Diameter Inches	Pounds per Foot	Internal Diameter Inches	F_r
1	1.315	1.80	1.049	0.095288
1-1/4	1.660	2.40	1.380	0.046552
1-1/2	1.990	2.75	1.610	0.031122
2	2.375	4.70	1.995	0.017777
2-1/2	2.875	6.50	2.441	0.010495
3	3.500	9.30	2.992	0.006167
3-1/2	4.000	11.00	3.476	0.004169
4	4.500	12.70	3.958	0.002970
4-1/2	4.750	16.25	4.082	0.002740
	4.750	18.00	4.000	0.002889
4-3/4	5.000	18.00	4.276	0.002427
	5.000	21.00	4.154	0.002617

(use only for internal diameters greater than 4.277 inches)

$$F_r = \frac{0.10337}{d^{2.582}}$$

Nominal Size Inches	Outer Diameter Inches	Pounds per Foot	Internal Diameter Inches	F_r
4-3/4	5.000	13.00	4.494	0.0021345
	5.000	15.00	4.408	0.0022437
5-3/16	5.500	14.00	5.012	0.0016105
	5.500	15.00	4.976	0.0016408
	5.500	17.00	4.892	0.0017145
	5.500	20.00	4.778	0.0018221
	5.500	23.00	4.670	0.0019329
	5.500	25.00	4.580	0.0020325
5-5/8	6.000	15.00	5.524	0.0012528
	6.000	17.00	5.450	0.0012972
	6.000	20.00	5.352	0.0013595
	6.000	23.00	5.240	0.0014358
	6.000	26.00	5.140	0.0015090
6-1/4	6.625	20.00	6.049	0.0009910
	6.625	22.00	5.989	0.0010169
	6.625	24.00	5.921	0.0010473
	6.625	26.00	5.855	0.0010781
	6.625	28.00	5.791	0.0011091
	6.625	31.80	5.675	0.0011686
	6.625	34.00	5.595	0.0012122

TABLE B-2. VALUES OF F_r FOR VARIOUS TUBING AND CASING SIZES

Nominal Size Inches	Outer Diameter Inches	Pounds per Foot	Internal Diameter Inches	F_r
6-5/8	7.000	20.00	6.456	0.0008876
	7.000	22.00	6.398	0.0008574
	7.000	24.00	6.336	0.0008792
	7.000	26.00	6.276	0.0009011
	7.000	28.00	6.214	0.0009245
	7.000	30.00	6.154	0.0009479
	7.000	40.00	5.836	0.0010871
7-1/4	7.625	26.40	6.969	0.0006875
	7.625	29.70	6.875	0.0007121
	7.625	33.70	6.765	0.0007424
	7.625	38.70	6.625	0.0007836
	7.625	45.00	6.445	0.0008413
	8.000	26.00	7.386	0.0005917
7-5/8	8.125	28.00	7.485	0.0005717
	8.125	32.00	7.385	0.0005919
	8.125	35.50	7.285	0.0006132
	8.125	39.50	7.185	0.0006354
8-1/4	8.625	17.50	8.249	0.0004448
	8.625	20.00	8.191	0.0004530
	8.625	24.00	8.097	0.0004667
	8.625	28.00	8.003	0.0004810
	8.625	32.00	7.907	0.0004962
	8.625	36.00	7.825	0.0005098
	8.625	38.00	7.775	0.0005183
	8.625	43.00	7.651	0.0005403
8-5/8	9.000	34.00	8.290	0.0004392
	9.000	38.00	8.196	0.0004523
	9.000	40.00	8.150	0.0004589
	9.000	45.00	8.032	0.0004765
9	9.625	36.00	8.921	0.0003634
	9.625	40.00	8.835	0.0003726
	9.625	43.50	8.755	0.0003814
	9.625	47.00	8.681	0.0003899
	9.625	53.50	8.535	0.0004074
	9.625	58.00	8.435	0.0004200
9-5/8	10.000	33.00	9.384	0.0004167
	10.000	55.50	8.908	0.0003648
	10.000	61.20	8.790	0.0003775
10	10.750	32.75	10.192	0.0002576
	10.750	35.75	10.136	0.0002613
	10.750	40.00	10.050	0.0002671
	10.750	45.50	9.950	0.0002741
	10.750	48.00	9.902	0.0002776
	10.750	54.00	9.784	0.0002863

TABLE B-2 cont. VALUES OF F_r FOR VARIOUS TUBING AND CASING SIZES

From   Cullender and Smith (1956)

10. Apply Simpson's rule as expressed by Equation (B-31), to obtain a more accurate value of the flowing bottom hole pressure.

The following example illustrates the use of the Cullender and Smith method to calculate flowing bottom hole pressure from wellhead measurements.

EXAMPLE B-2

Problem   Calculate the flowing bottom hole pressure by the method of Cullender and Smith from the following well data:

Gas gravity,	G	$=$ 0.75
Well depth,	z	$=$ 10,000 ft
Wellhead temperature,	T_{tf}	$=$ 570°R
Formation temperature,	T_{wf}	$=$ 705°R
Flowing wellhead pressure,	P_{tf}	$=$ 2000 psia
Flow rate,	Q	$=$ 4.915 MMscfd
Tubing inside diameter,	d	$=$ 2.441 in
Pseudo-critical temperature,	T_c	$=$ 408°R
Pseudo-critical pressure,	P_c	$=$ 667 psia

Solution

$$T_{mf} = (T_{tf} + T_{wf})/2 = (570 + 705)/2 = 638°R$$

Wellhead, $\quad T_r = T_{tf}/T_c = 570/408 = 1.397$

Midpoint, $\quad T_r = T_{mf}/T_c = 638/408 = 1.564$

Bottom, $\quad T_r = T_{wf}/T_c = 705/408 = 1.728$

Wellhead, $\quad P_r = P_{tf}/P_c = 2000/667 = 2.999$

From Equation (B-25)

$$F = \frac{(0.10797)(4.915)}{(2.441)^{2.612}} = 0.05158$$

$$F^2 = 0.00266$$

Left-hand side of Equations (B-29) and (B-30)

$$37.5 \; G \frac{z}{2} = (37.5)(0.75)(10,000)/2 = 140625.$$

Calculate I_{tf}:

From Figure A-3, at a reduced temperature and pressure of 1.397 and 2.999, respectively

$$Z_{tf} = 0.705, \; p_{tf}/T_{tf}Z_{tf} = (2000)/(570)(0.705) = 4.977$$

$$I_{tf} = \frac{(p_{tf}/T_{tf} \; Z_{tf})}{F^2 + \dfrac{(p_{tf}/T_{tf} \; Z_{tf})^2}{1000}} = \frac{(4.977)}{(0.00266) + \dfrac{(4.977)^2}{1000}} = 181.44$$

Step 1 (the upper half of the flow string)

First trial

Assume

$$I_{mf} = I_{tf} = 181.44$$

Solving Equation (B-29) for p_{mf}

$$140625. = (p_{mf} - 2000)(181.44 + 181.44)$$

$$p_{mf} = 2388 \; psia$$

Second trial

$$p_r = p_{mf}/p_c = 2388/667 = 3.580$$

$$Z_{mf} = 0.800 \quad at \quad T_r = 1.564, \quad p_r = 3.580 \quad (Figure \; A-3)$$

$$(p_{mf}/T_{mf} \; Z_{mf}) = (2388)/(638)(0.800) = 4.679$$

$$I_{mf} = 4.679/(.00266 + (4.679)^2/1000) = 190.57$$

Solving Equation (B-29) for p_{mf}

$$140625 = (p_{mf} - 2000)(190.57 + 181.44)$$

$$P_{mf} = 2378 \text{ psia}$$

Third trial

$$P_r = P_{mf}/P_c = 2378/667 = 3.565$$

$$Z_{mf} = 0.800 \quad \text{at} \quad T_r = 1.564, \quad P_r = 3.565 \qquad \text{(Figure A-3)}$$

$$(p_{mf}/T_{mf} \; Z_{mf}) = (2378)/(638)(0.800) = 4.659$$

$$I_{mf} = 4.659/(.00266 + (4.659)^2/1000) = 191.21$$

Solving Equation (B-29) for p_{mf}

$$140625 = (p_{mf} - 2000)(191.21 + 181.44)$$

$$P_{mf} = 2377 \text{ psia}$$

Step 2   (the lower half of the flow string)
First trial
Assume

$$I_{wf} = I_{mf} = 191.21$$

Solving Equation (B-30) for p_{wf}

$$140625 = (p_{wf} - 2377)(191.21 + 191.21)$$

$$P_{wf} = 2745 \text{ psia}$$

Second trial

$$P_r = P_{wf}/P_c = 2745/667 = 4.115$$

$$Z_{wf} = 0.869 \quad \text{at} \quad T_r = 1.728, \quad p_r = 4.115 \qquad \text{(Figure A-3)}$$

$$(p_{wf}/T_{wf} \ Z_{wf}) = (2745)/(705)(0.869) = 4.481$$

$$I_{wf} = 4.481/(0.00266 + 4.481)^2/1000) = 197.06$$

Solving Equation (B-20) for p_{wf}

$$140625 = (p_{wf} - 2377)(197.06 + 191.21)$$

$$p_{wf} = 2739 \ \text{psia}$$

Third trial

$$P_r = P_{wf}/P_c = 2739/667 = 4.106$$

$$Z_{wf} = 0.869 \quad \text{at} \quad T_r = 1.728, \quad p_r = 4.106 \qquad \text{(Figure A-3)}$$

$$(p_{wf}/T_{wf} \ Z_{wf}) = (2739)/(705)(0.869) = 4.471$$

$$I_{wf} = 4.471/(0.00266 + (4.471)^2/1000) = 197.40$$

Solving Equation (B-30) for p_{wf}

$$140625 = (p_{wf} - 2377)(197.40 + 191.21)$$

$$p_{wf} = 2739 \ \text{psia}$$

Parabolic Interpolation

From Equation (B-31)

$$(140625. \times 2) = \frac{p_{wf} - p_{tf}}{3} (181.44 + 4(191.21) + 197.40)$$

$$P_{wf} - P_{tf} = 738$$

$$P_{wf} = 2000 + 738 = 2738 \text{ psia}$$

The above method is also applicable to sour gas wells if appropriate corrections are included in the determination of compressibility factors as shown in Appendix A.

The solution of Example B-2 is also presented in a tabular form in Table B-3. Presentation of calculations in such a form is intended to simplify data reduction and may be used as a basis for preparing standard reporting forms.

As mentioned previously, the Cullender and Smith method is easily adapted to digital computer calculations. This has been discussed in detail by Aziz (1967a), and a computer program called BHOLE is included in Appendix D. In this computerized version of the Cullender and Smith method a third-order numerical integration scheme, rather than Simpson's rule is used. Friction factors are calculated by the Colebrook equation. The trial-and-error procedure necessary in the calculation scheme is handled by the Newton-Raphson iteration method. This procedure converges very rapidly and good accuracy can be obtained in three or four iterations even when no estimate of the bottom hole pressure is available. The program can calculate static and flowing bottom hole pressures from static and flowing wellhead measurements, respectively, for single-phase systems.

Annular Flow

In most cases where the well is flowing in the annulus between the casing and the tubing, it is possible to measure the corresponding shut-in tubing pressure, p_{ts}. The static bottom hole pressure may then be calculated as shown in Section 1 of this appendix.

However, it is sometimes necessary to calculate the flowing bottom hole pressure of an annular column from the flowing wellhead pressure. Rigorous equations for determination of friction factors for annular flow are not available. It is therefore necessary to use the

equations for flow in a circular pipe, incorporating an effective diameter for the annular space.

A commonly used hydraulic radius formula may be written as

$$D_{eff} = \frac{4 \text{ cross-sectional area of flow}}{\text{wetted perimeter}}$$

which, for the annulus, reduces to:

$$D_{eff} = D_2 - D_1 \tag{B-32}$$

where

D_2 = inside diameter of the casing

D_1 = inside diameter of the tubing

Various equations, developed earlier in the appendix may now be written as follows to represent annular flow.

Equation (B-14) representing the energy loss due to friction becomes:

$$dp_f = \frac{2 f u^2}{g_c (D_2 - D_1)} dL \tag{B-33}$$

Equation (B-15) for actual lineal velocity becomes:

$$u = \frac{0.4152 \, T \, Z \, Q}{p(D_2^2 - D_1^2)} \tag{B-34}$$

Reynolds number is now defined by

$$Re = \frac{20011 \, G \, Q}{\mu(d_1 + d_2)}$$

Equation (B-17), the basic flow equation, becomes:

$$\frac{53.34 \, T \, Z}{G} \frac{dp}{p} + dz + 0.0107 \frac{f}{D_2 - D_1} \left(\frac{T \, Z}{p}\right)^2 \left(\frac{Q}{D_2^2 - D_1^2}\right)^2 dL = 0$$

$$\tag{B-35}$$

Equations (B-25) and (B-26) become:

Well Data: $z = 10{,}000$ ft $T_c = 408°R$ $Q = 4.915$ MMscfd $T_{wf} = 705°R$

$G = 0.75$ $p_c = 667$ psia $T'_{tf} = 570°R$ $p_{wf} = 2000$ psia $d = 2.441$ in

Calculate: $T_{mf} = 638°R$ $T_{tf}/T_c = 1.397$ $T_{mf}/T_c = 1.564$ $T_{wf}/T_c = 1.728$

$Z_{tf} = 0.705$ $p_{tf}/p_c = 2.999$ $I_{tf} = 181.44$

$F^2 = 0.00266$ $(F_r q)^2 =$ $37.5\ G \frac{z}{2} = 140{,}625$

Trial No	z	Assume p_n	p_r	T_n	T_r	Z_n	A $\frac{p_n}{T_n Z_n}$	B $\frac{A^2}{1000}$	I_n $\frac{A}{F^2+B}$	M $I_0 + I_n$	N $37.5\frac{Gz}{2}$	N/M Δp	Calc. p_n
1	5000	2000	assume $I_n = I_{tf}$						181.44	362.88	140,625	388	2388
2	5000	2388	3.580	638	1.564	0.800	4.679	0.02189	190.57	372.01	140,625	378	2378
3	5000	2378	3.565	638	1.564	0.800	4.659	0.02171	191.21	372.65	140,625	377	2377
1	10,000	2377	assume $I_n = I_{mf}$						191.21	382.42	140,625	368	2745
2	10,000	2745	4.115	705	1.728	0.869	4.481	0.02008	197.06	388.27	140,625	362	2739
3	10,000	2739	4.106	705	1.728	0.869	4.471	0.01999	197.40	388.61	140,625	362	2739

Applying Simpson's rule: Equation (B-31)

$$(140625 \times 2) = \frac{p_{wf} - 2000}{3} = (181.44 + 4(191.21) + 197.40)$$

$$p_{wf} = 2000 + 738 = 2738 \text{ psia}$$

TABLE B-3. CULLENDER AND SMITH METHOD FOR CALCULATION OF FLOWING BOTTOM-HOLE PRESSURES

$$F_r Q = F = \frac{0.10797\ Q}{(d_2 - d_1)^{1.612}\ (d_2 - d_1)} \ , \quad d < 4.277 \text{ in} \qquad \text{(B-36)}$$

$$F_r Q = F = \frac{0.10377\ Q}{(d_2 - d_1)^{1.582}\ (d_2 - d_1)} \ , \quad d > 4.277 \text{ in} \qquad \text{(B-37)}$$

The values of F, as defined by Equations (B-36) or (B-37) may be used, instead of Equations (B-25) or (B-26), for the Cullender and Smith method for calculating flowing bottom hole pressures when flow is in the annulus.

Flowing Tubing Pressures from Static
 Casing Pressure Measurements

In the previous sections it is assumed that the wellhead flowing pressures are measured directly. Although this is the normal practice, quite often the static casing pressures are monitored when flow is through the tubing and there is no packer between the tubing and casing. Such static casing pressure measurements may be used, if necessary, to calculate the flowing tubing pressures.

For the situation defined above, the following equations define the flowing bottom hole pressure. Since flow is in the tubing,

$$P_{wf} = P_{tf} + \Delta p_{HH} + \Delta p_f \qquad \text{(B-38)}$$

where

Δp_{HH} = hydrostatic head of the fluid in the tubing
Δp_f = pressure drop due to friction

Since the fluid in the casing is static,

$$P_{wf} = P_{cs} + \Delta p'_{HH} \qquad \text{(B-39)}$$

where

P_{cs} = static wellhead casing pressure
$\Delta p'_{HH}$ = hydrostatic head of the fluid in the casing

Subtracting Equation (B-39) from Equation (B-38) gives

$$P_{tf} = P_{cs} + (\Delta p'_{HH} - \Delta p_{HH}) - \Delta p_f \qquad \text{(B-40)}$$

The first term on the right-hand side of Equation (B-40) is measured while the remaining terms may be calculated by the methods described in previous sections. Equation (B-39) is useful when liquids are being produced along with gas through the tubing. If there is no accumulation of liquids in the wellbore, p_{wf} calculated from Equation (B-39) is likely to be more accurate than p_{wf} calculated by Equation (B-38). This is because the term Δp_f in Equation (B-38) represents the friction pressure drop of a two-phase system and is consequently inaccurate.

3. Static and Flowing Bottom Hole Pressures— Two Phases (Gas and Liquid)

The preceding sections have dealt with the calculation of bottom hole pressures from wellhead measurements, for the case where only one phase (gas) is present in the wellbore. With the trend towards the discovery of deep, high pressure, retrograde-type, condensate reservoirs, the case where two phases, gas and liquid, exist in the wellbore becomes increasingly important. Also, where wells are producing significant amounts of free water from the formation, consideration should be given to the effect of this liquid phase on the calculation of bottom hole pressures.

In the static case, if two phases exist in the wellbore, the liquid phase will exist as a "liquid leg" at the bottom of the flow string. In this situation the bottom hole pressure must be measured directly with a bottom hole pressure gauge, or calculated from a knowledge of the level of the liquid in the wellbore and the gradient within the liquid phase. In the latter case, the pressure is calculated from the wellhead down to the interface by the normal means for a gas well, and then the bottom hole pressure is calculated from a knowledge of the liquid gradient. Since the level of the liquid and its gradient are seldom known, the normal means of determining the static bottom hole pressure in the two-phase case is by direct measurement.

For the two-phase flowing case, in addition to the possibility

of direct measurement, there are a number of methods available for calculating the flowing bottom hole pressure from wellhead measurements, as described by Govier and Aziz (1972), Aziz, Govier and Fogarasi (1972), and Govier and Fogarasi (1975). A complete discussion of the subject is beyond the scope of this manual.

In the special case of gas-condensate systems the conditions in the wellbore are usually such that the flowing bottom hole pressure can be calculated, with reasonable accuracy using single-phase methods. This approach has been discussed by Govier and Fogarasi (1975). Example B-3 illustrates the application of the Cullender and Smith method to gas-condensate wells, assuming the existence of a pseudo single-phase gas of gravity equal to the recombined gas gravity, and a flow rate equal to that of the recombined stream.

EXAMPLE B-3

Problem   Calculate the flowing bottom hole pressure by the method of Cullender and Smith from the following well data:

Recombined gas gravity,	G	= 0.83
Well depth,	z	= 6020 ft
Wellhead temperature,	T_{tf}	= 566°R
Formation temperature,	T_{wf}	= 628°R
Flowing wellhead pressure,	P_{tf}	= 1157 psia
Recombined flow rate,	Q	= 10.98 MMscfd
Tubing inside diameter,	d	= 2.441 in
Pseudo-critical temperature,	T_c	= 421°R
Pseudo-critical pressure,	P_c	= 672 psia
Absolute roughness,	δ	= 0.0024 in

Solution   Since δ = 0.0024 in, Equation (B-25) may not be used to calculate F. Instead, either Equation (B-20) or (B-21) may be used to

calculate the friction factor, f, which may then be substituted in Equation (B-24) to calculate F.

Using a value of $\mu = 0.0155$ cp (estimated at wellhead conditions), from Equation (B-19)

$$Re = \frac{20011 \ G \ Q}{\mu \ d}$$

$$= \frac{(20011)(0.83)(10.98)}{(0.0155)(2.441)} = 4.8 \times 10^6$$

From such a high Reynolds number, Equation (B-21) is valid and may be used to give

$$\frac{1}{\sqrt{f}} = 4.0 \ \log \frac{d}{\delta} + 2.28$$

$$= 4.0 \ \log (2.441/0.0024) + 2.28$$

$$\therefore \ f = 0.00488$$

From Equation (B-24)

$$F^2 = \frac{2.6665 \ f \ Q^2}{d^5}$$

$$= \frac{(2.6665)(0.00488)(10.98)^2}{(2.441)^5} = 0.01810$$

Using the value of F^2 calculated above and the procedures illustrated by Example B-2, the flowing bottom hole pressure is calculated as

$$P_{wf} = 1977 \ \text{psia}$$

This calculated value compares well with the actual measured value of 1939 psia. The more rigorous methods, based on an annular-mist flow model (Govier and Fogarasi, 1975), will give approximately similar results. The computer program, BHOLE, given in Appendix D, may be applied to gas condensate wells with appropriate entries for gas flow rates and specific gravities.

APPENDIX C

FIGURES AND TABLES

This appendix contains the supplementary figures and tables mentioned in Chapter 2, Section 7.4.

$$t_{DA} = \frac{2.637 \times 10^{-4} kt}{\phi \mu c A}$$

$$F = 2 \frac{\psi - \psi_i}{\psi_i q_D} = 4\pi t_{DA} + \sum_{N=1}^{\infty} E_i \left(-\frac{d_N^2}{4 A t_{DA}} \right)$$
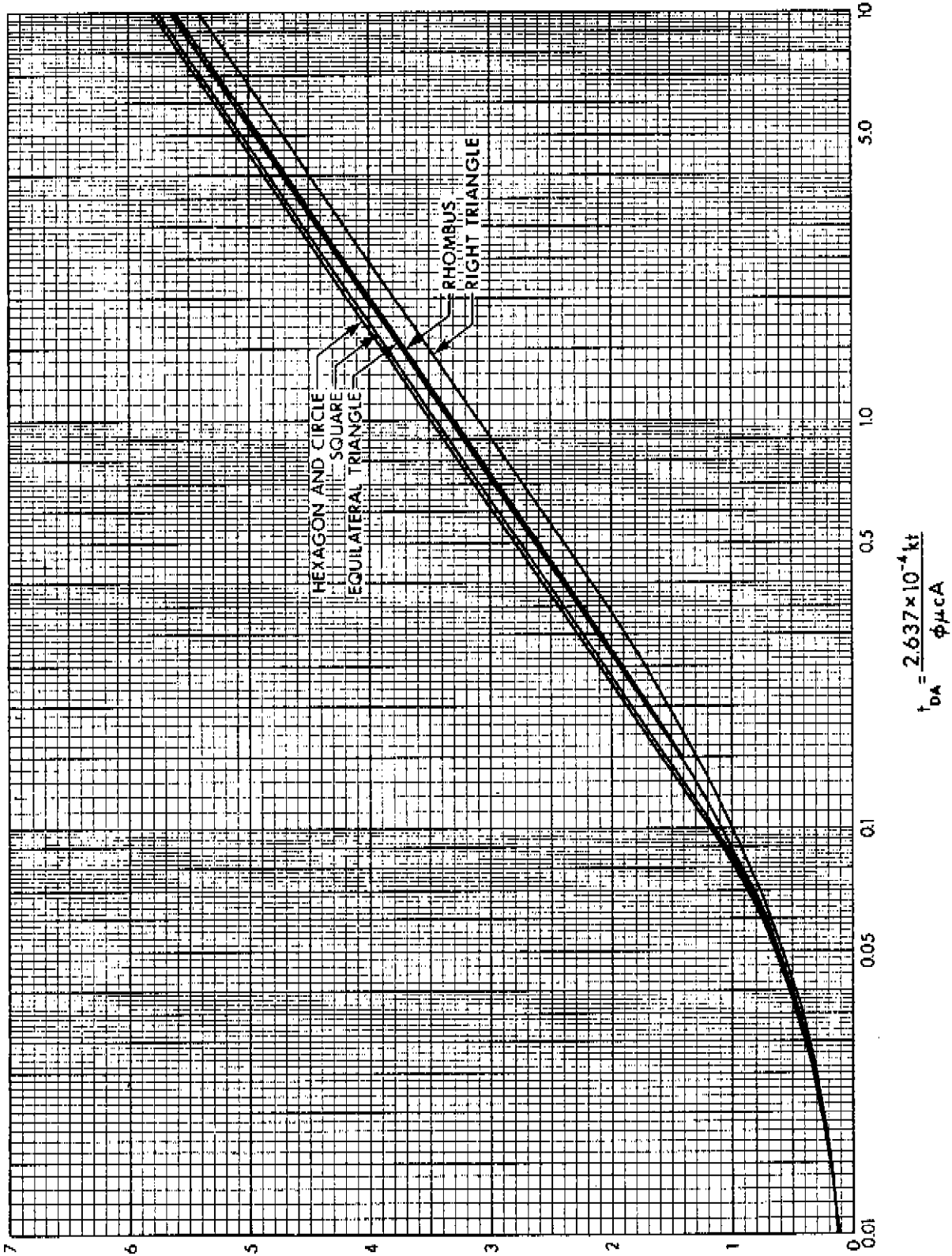
FIGURE C-1(a). PRESSURE FUNCTION FOR ONE WELL IN CENTER OF EQUILATERAL FIGURES

Redrawn from Matthews, Brons and Hazebroek (1954)

$$t_{oA} = \frac{2.637 \times 10^{-4} \, kt}{\phi \mu c A}$$

$$F = 2 \frac{\psi - \psi_R}{\psi_i \, q_D} = 4 \pi \, t_{DA} + \sum_{N=1}^{\infty} Ei\left(-\frac{d_N^2}{4A \, t_{DA}}\right)$$
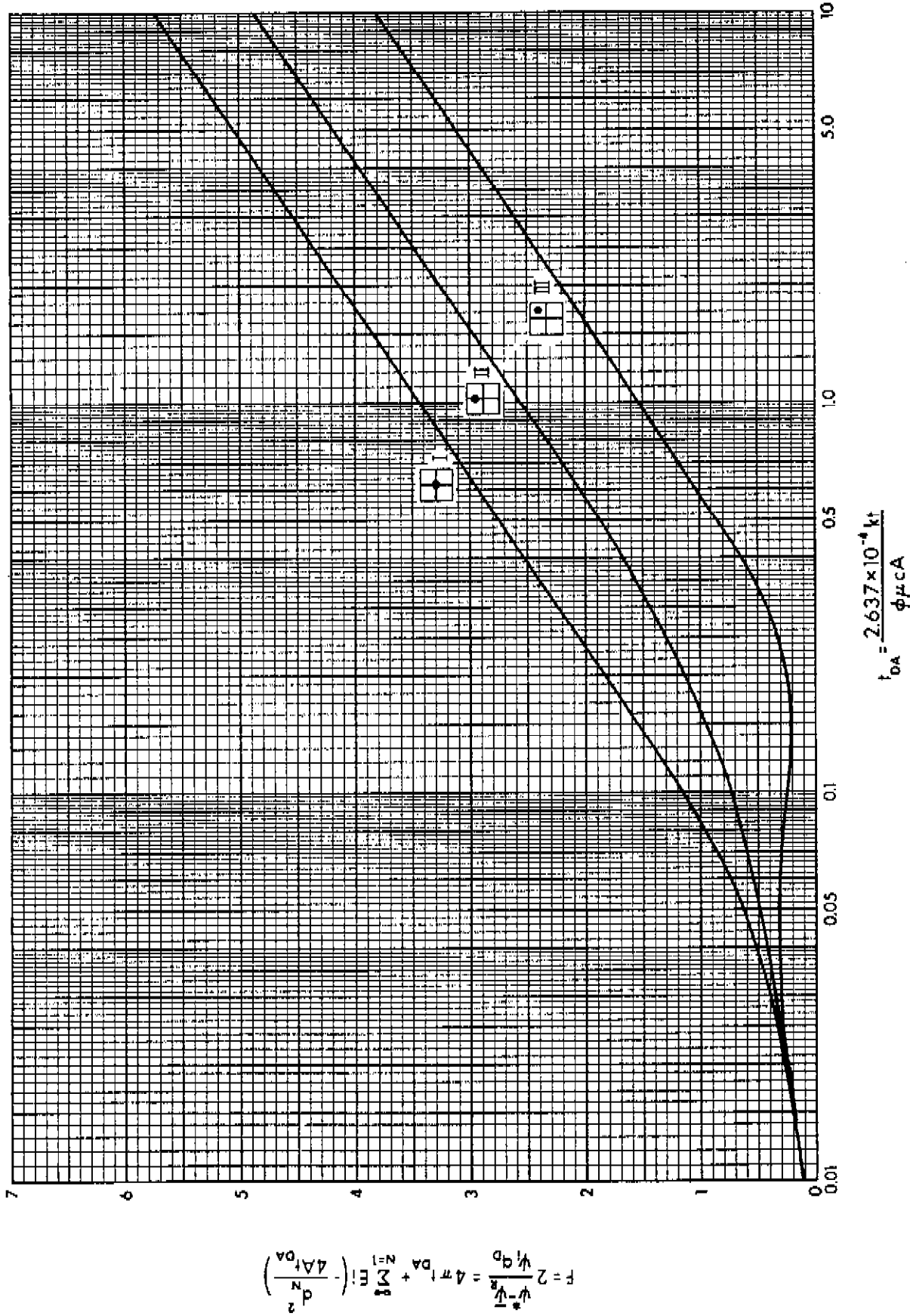
FIGURE C-1(b). PRESSURE FUNCTION FOR DIFFERENT WELL LOCATIONS IN A SQUARE BOUNDARY

Redrawn from Matthews, Brons and Hazebroek (1954)
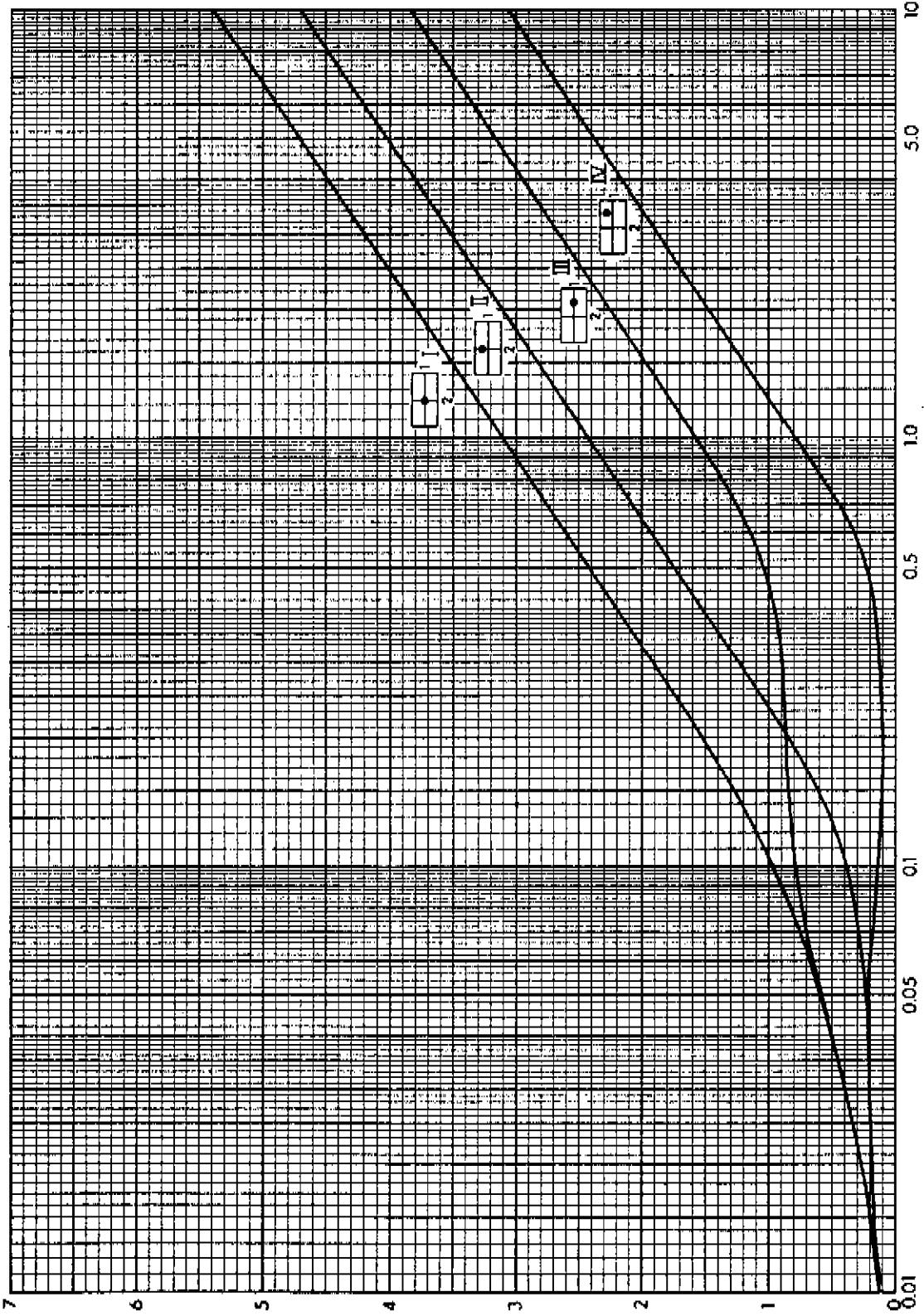
FIGURE C-1(c). PRESSURE FUNCTION FOR DIFFERENT WELL LOCATIONS IN A 2:1 RECTANGULAR BOUNDARY
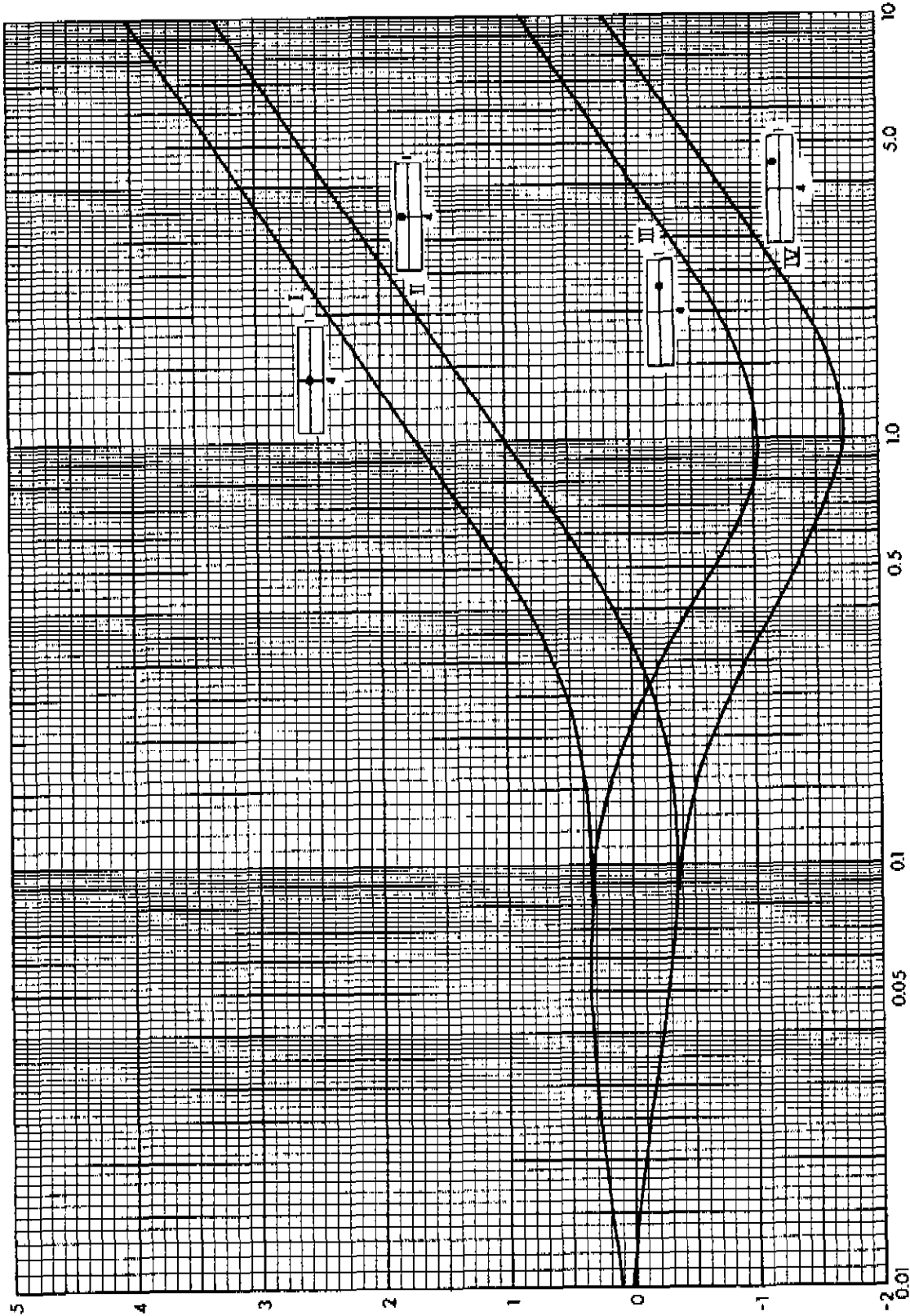
Redrawn from Matthews, Brons and Hazebroek (1954)

FIGURE C-1(d). PRESSURE FUNCTION FOR DIFFERENT WELL LOCATIONS IN A 4:1 RECTANGULAR BOUNDARY

Redrawn from Matthews, Brons and Hazebroek (1954)
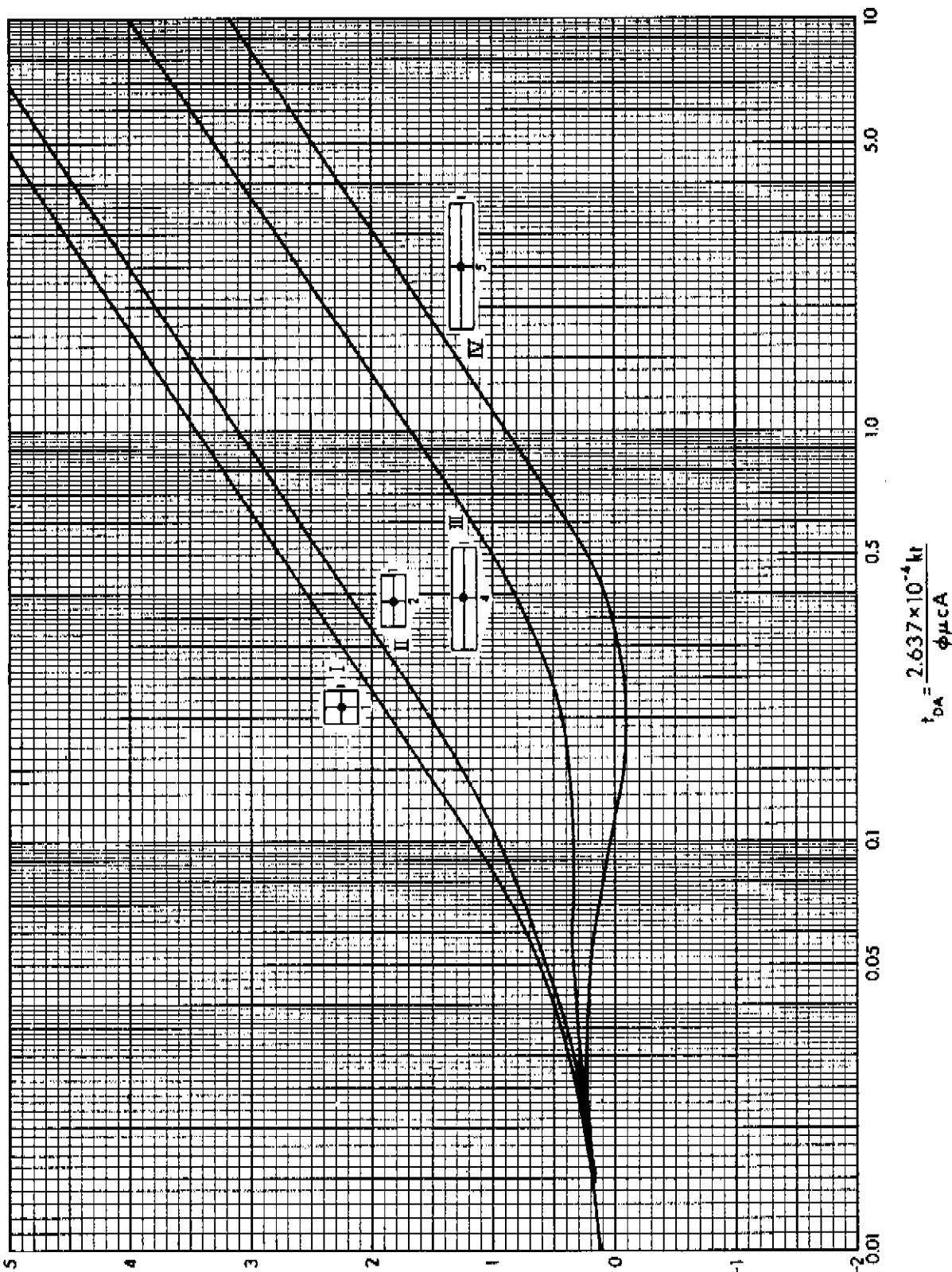
FIGURE C-1 (e). PRESSURE FUNCTION FOR RECTANGLES OF VARIOUS SHAPES

Redrawn from Matthews, Brons and Hazebroek (1954)
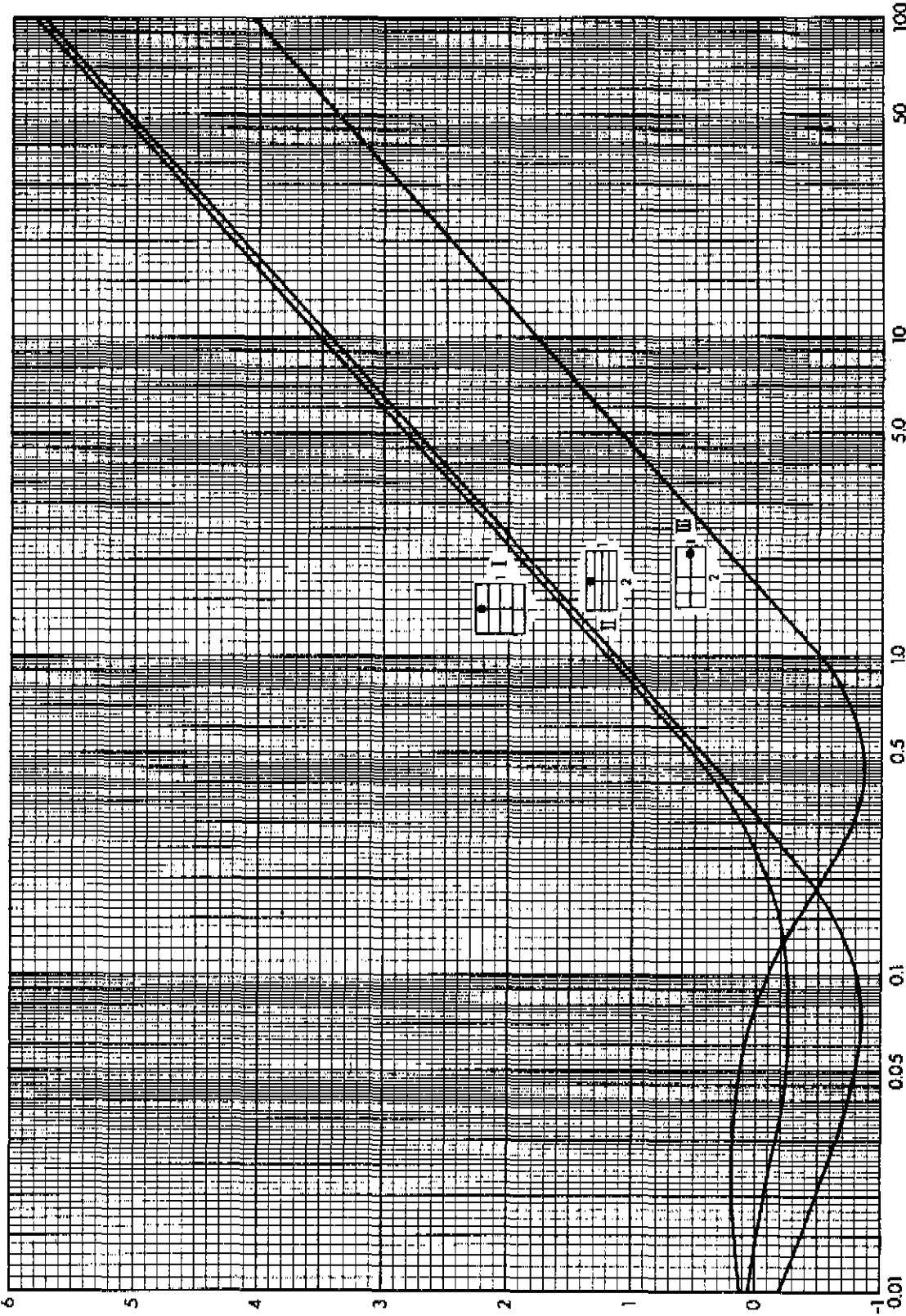
FIGURE C-1(f). PRESSURE FUNCTION IN A SQUARE AND IN 2:1 RECTANGLES

Redrawn from Matthews, Brons and Hazebroek (1954)

$$t_{DA} = \frac{2.637 \times 10^{-4} \, kt}{\phi \mu c A}$$

$$F = 2 \, \frac{\psi^* - \bar{\psi}}{\psi \, q_o} = 4 \pi t_{DA} + \sum_{N=1}^{\infty} E_i \left(- \frac{d_N^2}{4 A t_{DA}}\right)$$

$$I_{DA} = \frac{2.637 \times 10^{-4} kt}{\phi \mu c A}$$

$$F = 2\frac{\psi^* - \overline{\psi}}{\psi_i q_0} = 4\pi I_{DA} + \sum_{N=1}^{\infty} Ei\left(-\frac{d_N^2}{4A I_{DA}}\right)$$
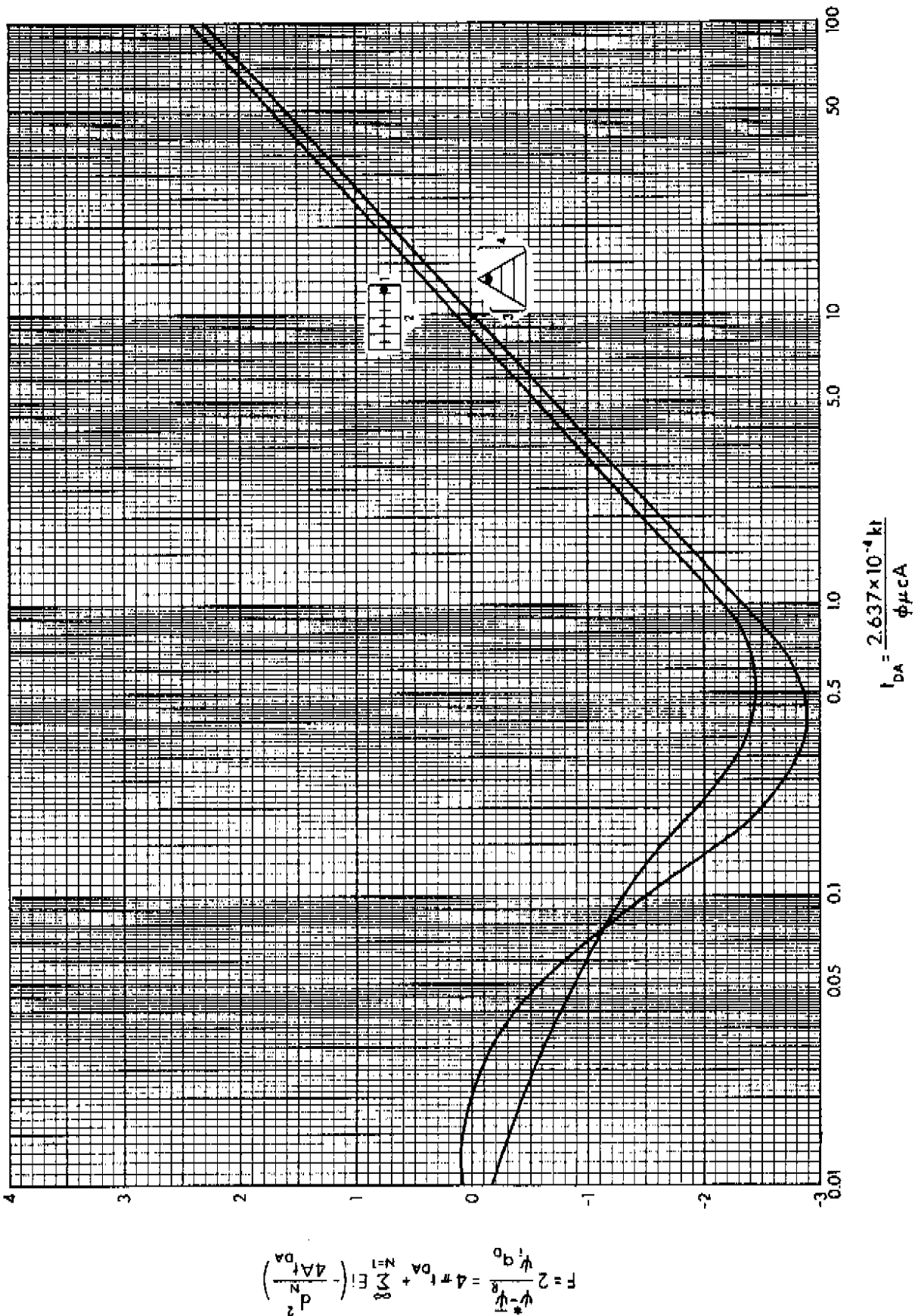
FIGURE C-1(g). PRESSURE FUNCTION IN A 2:1 RECTANGLE AND AN EQUILATERAL TRIANGLE

Redrawn from Matthews, Brons and Hazebroek (1954)

DIMENSIONLESS PRESSURE DROP, Δp_D

DIMENSIONLESS TIME

OBSERVATION POINTS

t_{DA}	WELL POINT X=0.5005 Y=0.5000	X=0.6250 Y=0.5000	X=0.6250 Y=0.6250	X=0.7500 Y=0.5000	X=0.7500 Y=0.7500	X=0.8750 Y=0.5000	X=0.8750 Y=0.7500	X=0.8750 Y=0.8750	X=1.0000 Y=0.5000	X=1.0000 Y=0.7500	X=1.0000 Y=1.0000
A/B**2=		64.0000	32.0000	16.0000	8.0000	7.1111	4.9231	3.5556	4.0000	3.2000	2.0000
0.0020	4.89814	0.02609	0.00212	0.00002	0.00000	0.00000	0.00000	0.00000	0.00000	0.00000	0.00000
0.0030	5.10087	0.06750	0.01987	0.00045	0.00000	0.00000	0.00000	0.00000	0.00000	0.00000	0.00000
0.0040	5.24471	0.11411	0.02609	0.00212	0.00002	0.00001	0.00000	0.00000	0.00000	0.00000	0.00000
0.0050	5.35628	0.16068	0.04559	0.00557	0.00045	0.00021	0.00001	0.00000	0.00000	0.00000	0.00000
0.0060	5.44744	0.20534	0.06750	0.01087	0.00108	0.00056	0.00004	0.00001	0.00001	0.00000	0.00000
0.0070	5.52452	0.24751	0.09060	0.01781	0.00212	0.00118	0.00012	0.00002	0.00003	0.00001	0.00000
0.0080	5.59128	0.28712	0.11411	0.02609	0.00361	0.00212	0.00027	0.00005	0.00012	0.00002	0.00000
0.0090	5.65018	0.32428	0.13756	0.03544	0.00564	0.00342	0.00052	0.00012	0.00042	0.00005	0.00000
0.0100	5.70286	0.35918	0.16068	0.04559	0.01781	0.00502	0.00211	0.00038	0.00114	0.00081	0.00000
0.0200	6.04943	0.62106	0.35918	0.16068	0.10324	0.03502	0.01211	0.00359	0.01114	0.00424	0.00054
0.0300	6.25221	0.79389	0.50653	0.26848	0.15497	0.08256	0.04044	0.01769	0.04361	0.02188	0.00618
0.0400	6.39655	0.92321	0.62242	0.36278	0.19497	0.14854	0.08756	0.04373	0.09128	0.05324	0.02227
0.0500	6.5099	1.0279	0.7192	0.4470	0.2276	0.2125	0.1807	0.0800	0.1469	0.0947	0.0498
0.0600	6.6050	1.1178	0.8041	0.5242	0.2904	0.2772	0.2366	0.1241	0.2065	0.1431	0.0872
0.0700	6.6888	1.1983	0.8815	0.5968	0.3532	0.3418	0.2948	0.1740	0.2678	0.1962	0.1321
0.0800	6.7654	1.2728	0.9539	0.6661	0.4160	0.4061	0.3546	0.2279	0.3299	0.2525	0.1826
0.0900	6.8374	1.3434	1.0231	0.7334	0.4788	0.4700	0.4153	0.2846	0.3925	0.3109	0.2369
0.1000	6.9063	1.4114	1.0902	0.7992	0.5417	0.5336	0.4763	0.3433	0.4551	0.3708	0.2939
0.2000	7.5468	2.0501	1.7271	1.4335	1.1700	1.1636	1.0393	0.9632	1.0834	0.9931	0.9103
0.3000	8.1753	2.6786	2.3556	2.0620	1.7983	1.7919	1.6676	1.5913	1.7117	1.6213	1.5384
0.4000	8.8036	3.3069	2.9839	2.6903	2.4266	2.4202	2.2959	2.2196	2.3400	2.2496	2.1667
0.5000	9.4318	3.9352	3.6122	3.3186	3.0549	3.0486	2.9242	2.8479	2.9683	2.8779	2.7950
0.6000	10.0603	4.5636	4.2406	3.9469	3.6833	3.6769	3.5525	3.4763	3.5966	3.5062	3.4233
0.7000	10.6886	5.1919	4.8689	4.5752	4.3116	4.3052	4.1808	4.1046	4.2249	4.1346	4.0517
0.8000	11.3169	5.8202	5.4972	5.2036	4.9399	4.9335	4.8092	4.7329	4.8533	4.7629	4.6800
0.9000	11.9452	6.4485	6.1255	5.8319	5.5682	5.5618	5.4375	5.3612	5.4816	5.3912	5.3083
1.0000	12.5735	7.0768	6.7538	6.4602	6.1965	6.1901	6.0658	5.9895	6.1099	6.0195	5.9366
2.0000	18.8567	13.3600	13.0370	12.7434	12.4733	12.3490	12.2727	12.2633	12.3931	12.3027	12.2198
3.0000	25.1399	19.6432	19.3202	19.0265	18.7565	18.6321	18.5558	18.5464	18.6762	18.5858	18.5029
4.0000	31.4210	25.9263	25.6033	25.3097	25.0397	24.9153	24.8390	24.8296	24.9594	24.8690	24.7861
5.0000	37.7062	32.2095	31.8865	31.5929	31.3228	31.1985	31.1222	31.1128	31.2426	31.1522	31.0693
6.0000	43.9894	38.4926	38.1697	37.8760	37.6060	37.4816	37.4054	37.3960	37.5257	37.4353	37.3524
7.0000	50.2726	44.7758	44.4528	44.1592	43.8892	43.7648	43.6885	43.6791	43.8089	43.7185	43.6356
8.0000	56.5557	51.0590	50.7360	50.4424	50.1723	50.0480	49.9717	49.9623	50.0920	50.0017	49.9188
9.0000	62.8389	57.3421	57.0192	56.7255	56.4555	56.3311	56.2549	56.2455	56.3752	56.2849	56.2019
10.0000	69.1220	63.6253	63.3023	63.0087	62.7386	62.6143	62.5380	62.5287	62.6584	62.5680	62.4851
12.0000	81.6883	76.1916	75.8686	75.5750	75.3050	75.1806	75.1043	75.0949	75.2247	75.1363	75.0515
15.0000	100.5379	93.0411	92.7182	94.4245	94.1545	94.0301	93.9538	93.9448	94.0742	93.9838	93.9009
20.0000	131.9537	126.4570	126.1340	125.8403	125.5703	125.4459	125.3696	125.3602	125.4908	125.3997	125.3168
30.0000	194.7853	189.2886	188.9656	188.6720	188.4019	188.2776	188.2013	188.1919	188.3217	188.2313	188.1484
$\ln C_A$ / C_A	3.4305 / 30.8925	14.4240 / 1.8376E6	15.0699 / 3.5058E6	15.6572 / 6.3073E6	16.1973 / 1.0825E7	16.4460 / 1.3880E7	16.5985 / 1.6167E7	16.6167 / 1.6167E7	16.3579 / 1.2710E7	16.5386 / 1.5227E7	16.7044 / 1.7973E7
t_{DA}(pss)	0.10	0.10	0.10	0.10	0.04	0.10	0.10	0.10	0.07	0.10	0.10

x_D

y_D

TABLE C-1(a). Δp_D VERSUS t_{DA} FOR A CLOSED SQUARE WITH WELL AT x_D = 0.5, y_D = 0.5, $\dfrac{\sqrt{A}}{r_w}$ = 2000

From Earlougher and Ramey (1973)

DIMENSIONLESS PRESSURE DROP, Δp_D

DIMENSIONLESS TIME

OBSERVATION POINTS

t_{DA}	WELL POINT X=0.5005 Y=0.7500	X=0.5000 Y=0.0000	X=0.5000 Y=0.2500	X=0.5000 Y=0.5000	X=0.5000 Y=1.0000	X=0.7500 Y=0.2500	X=0.7500 Y=0.5000	X=0.7500 Y=0.7500	X=1.0000 Y=0.0000	X=1.0000 Y=0.5000	X=1.0000 Y=1.0000
A/R**2~	1.7778	4.0000	16.0000	16.0000	16.0000	3.2000	8.0000	16.0000	1.2508	3.2000	3.2000
0.0020	4.89814	0.00000	0.00000	0.00002	0.00005	0.00000	0.00000	0.00002	0.00000	0.00000	0.00000
0.0030	5.10087	0.00000	0.00000	0.00045	0.00090	0.00000	0.00000	0.00045	0.00000	0.00000	0.00000
0.0040	5.24471	0.00000	0.00000	0.00212	0.00423	0.00000	0.00000	0.00212	0.00000	0.00000	0.00000
0.0050	5.35628	0.00000	0.00000	0.00557	0.01114	0.00000	0.00014	0.00557	0.00000	0.00000	0.00000
0.0060	5.44745	0.00000	0.00000	0.01087	0.02173	0.00000	0.00045	0.01087	0.00000	0.00000	0.00000
0.0070	5.52453	0.00000	0.00001	0.01781	0.03561	0.00000	0.00108	0.01781	0.00000	0.00000	0.00000
0.0080	5.59131	0.00000	0.00002	0.02609	0.05219	0.00000	0.00212	0.02610	0.00000	0.00000	0.00001
0.0090	5.65024	0.00000	0.00006	0.03544	0.07089	0.00001	0.00361	0.03545	0.00000	0.00001	0.00004
0.0100	5.70299	0.00011	0.00014	0.04559	0.09119	0.00002	0.00557	0.04562	0.00000	0.00005	0.00009
0.0200	6.05500	0.00166	0.00557	0.16073	0.32135	0.00212	0.04564	0.16285	0.00000	0.00424	0.00847
0.0300	6.27399	0.00685	0.02183	0.26848	0.53530	0.01096	0.10324	0.27949	0.00000	0.02188	0.04346
0.0400	6.44192	0.0167	0.04591	0.36278	0.71870	0.02688	0.16497	0.38922	0.00210	0.05324	0.10438
0.0500	6.5822	0.0313	0.0746	0.4470	0.8772	0.0482	0.2276	0.4935	0.0070	0.0947	0.1824
0.0600	6.7031	0.0501	0.1064	0.5242	1.0172	0.0740	0.2904	0.5933	0.0162	0.1431	0.2700
0.0700	6.8161	0.0727	0.1405	0.5968	1.1435	0.1036	0.3532	0.6894	0.0300	0.1962	0.3624
0.0800	6.9187	0.0989	0.1766	0.6661	1.2596	0.1363	0.4160	0.7823	0.0484	0.2525	0.4566
0.0900	7.0150	0.1283	0.2148	0.7334	1.3679	0.1720	0.4788	0.8724	0.0712	0.3109	0.5507
0.1000	7.1066	0.1566	0.2548	0.7992	1.4701	0.2102	0.5417	0.9598	0.0979	0.3708	0.6437
0.2000	7.8916	0.5496	0.7385	1.4335	2.3175	0.6896	1.1700	1.7370	0.5123	0.9931	1.4739
0.3000	8.5756	1.0995	1.3114	2.0620	3.0244	1.2625	1.7983	2.4208	1.0621	1.6213	2.1805
0.4000	9.2246	1.6986	1.9190	2.6903	3.6820	1.8791	2.4266	3.0698	1.6611	2.2496	2.8381
0.5000	9.8606	2.3160	2.5397	3.3186	4.3212	2.4907	3.0549	3.7058	2.2785	2.8779	3.4773
0.6000	10.4918	2.9403	3.1651	3.9469	4.9536	3.1162	3.6833	4.3370	2.9028	3.5062	4.1097
0.7000	11.1212	3.5671	3.7924	4.5752	5.5834	3.7434	4.3116	4.9664	3.5296	4.1346	4.7395
0.8000	11.7499	4.1948	4.4203	5.2036	6.2123	4.3713	4.9399	5.5951	4.1574	4.7629	5.3684
0.9000	12.3783	4.8229	5.0484	5.8319	6.8408	4.9995	5.5682	6.2235	4.7855	5.3912	5.9969
1.0000	13.0067	5.4512	5.6767	6.4602	7.4692	5.6278	6.1965	6.8519	5.4137	6.0195	6.6253
2.0000	19.2899	11.7343	11.9598	12.7433	13.7524	11.9109	12.4797	13.1351	11.6968	12.3027	12.9085
3.0000	25.5731	18.0175	18.2430	19.0265	20.0356	18.1941	18.7629	19.4183	17.9800	18.5858	19.1917
4.0000	31.8563	24.3006	24.5262	25.3097	26.3187	24.4772	25.0460	25.7015	24.2632	24.8696	25.4749
5.0000	38.1394	30.5838	30.8093	31.5928	32.6019	30.7604	31.3292	31.9846	30.5463	31.1522	31.7580
6.0000	44.4226	36.8669	37.0925	37.8760	38.8851	37.0436	37.6124	38.2678	36.8295	37.4355	38.0412
7.0000	50.7058	43.1501	43.3757	44.1592	45.1682	43.3267	43.8955	44.5510	43.1126	43.7185	44.3244
8.0000	56.9889	49.4333	49.6588	50.4423	51.4514	49.6099	50.1787	50.8341	49.3958	50.0017	50.6075
9.0000	63.2721	55.7164	55.9420	56.7255	57.7346	55.8931	56.4619	57.1173	55.6790	56.2848	56.8907
10.0000	69.5553	61.9995	62.2251	63.0087	64.0178	62.1762	62.7450	63.4005	61.9621	62.5680	63.1739
12.0000	82.1216	74.5659	74.7914	75.5750	76.5841	74.7425	75.1113	75.9668	74.5284	75.1343	75.7402
15.0000	104.9711	93.4154	93.6409	94.4245	95.4335	93.5920	94.1608	94.8163	93.3779	93.9838	94.5896
20.0000	132.3869	124.8312	125.0567	125.8494	126.8494	125.0078	125.5766	126.2321	124.7937	125.3996	126.0055
30.0000	195.2185	187.6627	187.8883	188.6719	189.6810	187.8394	188.4082	189.0632	187.6252	188.2312	188.8371
$t_D c_A$	2.5641	17.6755	17.2244	15.6573	13.6391	17.3222	16.1846	14.8737	17.7564	16.5386	15.3269
c_A	12.9887	4.7466E7	3.0231E7	6.3072E6	8.3825E5	3.3338E7	1.0688E7	2.6811E6	5.1157E7	1.5228E7	4.5340E6
t_{DA} (PSS)	0.40	0.40	0.10	0.10	0.40	0.40	0.03	0.40	0.40	0.10	0.40

TABLE C-1(b). Δp_D VERSUS t_{DA} FOR A CLOSED SQUARE

WITH WELL AT $x_D = 0.5$, $y_D = 0.75$, $\dfrac{\sqrt{A}}{r_w} = 2000$

From Earlougher and Ramey (1973)

DIMENSIONLESS PRESSURE DROP, Δp_D

DIMENSIONLESS TIME t_{DA}	WELL POINT	OBSERVATION POINTS									
	X=-0.7505 Y=-0.7500	X=0.0000 Y=0.0000	X=-0.2500 Y=-0.2500	X=0.5000 Y=-0.0000	X=-0.5000 Y=-0.2500	X=-0.5000 Y=-0.5000	X=-0.7500 Y=-0.2500	X=-0.7500 Y=-0.5000	X=-1.0000 Y=-0.0000	X=-1.0000 Y=-0.5000	X=-1.0000 Y=-1.0000
	A/π**2~	0.8889	2.0000	1.6000	3.2000	8.0000	4.0000	16.0000	1.6000	8.0000	8.0000
0.0020	4.89814	0.00000	0.00000	0.00000	0.00000	0.00000	0.00000	0.00000	0.00000	0.00000	0.00000
0.0030	5.10087	0.00000	0.00000	0.00000	0.00000	0.00000	0.00000	0.00000	0.00000	0.00000	0.00000
0.0040	5.26471	0.00000	0.00000	0.00000	0.00000	0.00000	0.00000	0.00002	0.00000	0.00000	0.00009
0.0050	5.35628	0.00000	0.00000	0.00000	0.00000	0.00014	0.00000	0.00045	0.00000	0.00000	0.00054
0.0060	5.44745	0.00000	0.00000	0.00000	0.00000	0.00045	0.00000	0.00557	0.00000	0.00000	0.00180
0.0070	5.52453	0.00000	0.00000	0.00000	0.00000	0.00108	0.00000	0.01781	0.00000	0.00000	0.00433
0.0080	5.59133	0.00000	0.00000	0.00000	0.00000	0.00212	0.00002	0.02610	0.00000	0.00009	0.00847
0.0090	5.65030	0.00000	0.00000	0.00000	0.00000	0.00361	0.00006	0.03545	0.00000	0.00721	0.01443
0.0100	5.70313	0.00000	0.00000	0.00000	0.00000	0.00557	0.00570	0.04562	0.00000	0.01114	0.02227
0.0200	6.06073	0.00002	0.00014	0.00003	0.0130	0.04564	0.02337	0.16285	0.00009	0.09124	0.18238
0.0300	6.29704	0.00022	0.00155	0.00091	0.0237	0.10324	0.05168	0.27940	0.00180	0.20557	0.40934
0.0400	6.49299	0.0011	0.0130	0.00435	0.0482	0.16497	0.0871	0.38922	0.00848	0.32559	0.64271
0.0500	6.6668	0.0034	0.0237	0.0117	0.0740	0.2276	0.1281	0.4935	0.0223	0.4434	0.8645
0.0600	6.8256	0.0076	0.0376	0.0236	0.1036	0.2904	0.1733	0.5933	0.0438	0.5572	1.0705
0.0700	6.9728	0.0144	0.0547	0.0399	0.1363	0.3532	0.2217	0.6894	0.0721	0.6665	1.2608
0.0800	7.1102	0.0239	0.0749	0.0604	0.1720	0.4160	0.2728	0.7823	0.1065	0.7716	1.4367
0.0900	7.2393	0.0365	0.0981	0.0849	0.2102	0.4788	0.3260	0.8724	0.1458	0.8728	1.5997
0.1000	7.3611	0.0508	0.1302	0.1129	0.2625	0.5417	0.3260	0.9598	0.1894	0.9704	1.7514
0.2000	8.3255	0.3199	0.6568	0.5308	0.6896	1.1700	0.9162	1.7370	0.7416	1.8092	2.8768
0.3000	9.0702	0.8020	0.9895	1.0806	1.2625	1.7983	1.5392	2.4208	1.3593	2.5160	3.6726
0.4000	9.7406	1.3732	1.5772	1.6797	1.8761	2.4266	2.1668	3.0698	1.9862	3.1735	4.3609
0.5000	10.3844	1.9800	2.1902	2.2971	2.4907	3.0549	2.7950	3.7058	2.6143	3.8128	5.0112
0.6000	11.0185	2.6002	2.8128	2.9214	3.1162	3.6833	3.4233	4.3370	3.2426	4.4451	5.6477
0.7000	11.6490	3.2255	3.4389	3.5482	3.7434	4.3116	4.0517	4.9664	3.8709	5.0750	6.2790
0.8000	12.2781	3.8527	4.0665	4.1759	4.3713	4.9399	4.6800	5.5951	4.4992	5.7038	6.9085
0.9000	12.9067	4.4806	4.6945	4.8041	4.9995	5.5682	5.3083	6.2235	5.1275	6.3324	7.5372
1.0000	13.5351	5.1088	5.3227	5.4323	5.6278	6.1965	5.9366	6.8519	5.7558	6.9608	8.1657
2.0000	19.8186	11.3918	11.6058	11.7154	11.9109	12.4797	12.2198	13.1351	12.0390	13.2440	14.4490
3.0000	26.1016	17.6750	17.8889	17.9986	18.1941	18.7629	18.5029	19.4183	18.3222	19.5271	20.7321
4.0000	32.3847	23.9581	24.1721	24.2817	24.4772	25.0460	24.7861	25.7014	24.6053	25.8103	27.0152
5.0000	38.6679	30.2413	30.4553	30.5649	30.7604	31.3292	31.0692	31.9846	30.8885	32.0935	33.2985
6.0000	44.9511	36.5244	36.7384	36.8480	37.0636	37.6124	37.3524	38.2678	37.1716	38.3766	39.5817
7.0000	51.2342	42.8076	43.0216	43.1312	43.3267	43.8955	43.6356	44.5510	43.4548	44.6598	45.8648
8.0000	57.5173	49.0908	49.3048	49.4144	49.6099	50.1787	49.9187	50.8341	49.7380	50.9429	52.1479
9.0000	63.8006	55.3740	55.5879	55.6975	55.8931	56.4619	56.2019	57.1173	56.0211	57.2261	58.4311
10.000	70.0837	61.6571	61.8711	61.9807	62.1762	62.7450	62.4850	63.4004	62.3043	63.5093	64.7143
12.000	82.6500	74.2234	74.4374	74.5470	74.7425	75.3113	75.0514	75.9668	74.8706	76.0756	77.2806
15.000	101.4995	93.0729	93.2869	93.3965	93.5920	94.1608	93.9008	94.8162	93.7201	94.9231	96.1301
20.000	132.9153	124.4887	124.7027	124.8133	125.0078	125.5766	125.3166	126.2320	125.1358	126.3409	127.5459
30.000	195.7470	187.3202	187.5343	187.6438	187.8394	188.4082	188.1483	189.0637	187.9674	189.1726	190.3776
ln c_A	1.5072	18.3604	17.9324	17.7132	17.3222	16.1846	16.7045	14.8737	17.0660	14.6560	12.2460
c_A	4.5141	9.4149E7	6.1369E7	4.9289E7	3.3338E7	1.0688E7	1.3976E7	2.8812E6	2.5804E7	2.3176E6	2.0814E5
t_DA (PSS)	0.50	0.50	0.50	0.40	0.40	0.03	0.20	0.40	0.20	0.40	0.50

TABLE C-1(c). Δp_D VERSUS t_{DA} FOR A CLOSED SQUARE

WITH WELL AT $x_D = 0.75$, $y_D = 0.75$, $\dfrac{\sqrt{A}}{r_w} = 2000$

From Earlougher and Ramey (1973)

DIMENSIONLESS PRESSURE DROP, Δp_D

DIMENSIONLESS TIME

t_{DA}	WELL POINT X=-0.5004 Y=0.5000	OBSERVATION POINTS X=-0.5000 Y=0.7500	X=-0.5000 Y=0.8750	X=0.5000 Y=1.0000	X=0.7500 Y=0.2500	X=0.7500 Y=0.5000	X=0.7500 Y=1.0000	X=0.8750 Y=0.5000	X=1.0000 Y=0.5000	X=1.0000 Y=0.7500	X=1.0000 Y=1.0000
A/R**2=	32.0000	14.2222	8.0000	8.0000	6.4000	8.0000	4.0000	3.5556	2.0000	1.8824	1.6000
0.0020	4.89814	0.00212	0.00000	0.00000	0.00000	0.00000	0.00000	0.00000	0.00000	0.00000	0.00000
0.0030	5.10087	0.01087	0.00000	0.00000	0.00000	0.00000	0.00000	0.00000	0.00000	0.00000	0.00000
0.0040	5.24471	0.02609	0.00000	0.00005	0.00000	0.00002	0.00000	0.00000	0.00000	0.00000	0.00000
0.0050	5.33628	0.04559	0.00118	0.00027	0.00002	0.00010	0.00002	0.00000	0.00000	0.00000	0.00000
0.0060	5.44744	0.06751	0.00342	0.00090	0.00010	0.00045	0.00010	0.00000	0.00000	0.00000	0.00000
0.0070	5.52452	0.09060	0.00715	0.00216	0.00029	0.00108	0.00091	0.00001	0.00000	0.00000	0.00000
0.0080	5.59128	0.11411	0.01234	0.00423	0.00066	0.00212	0.00205	0.00002	0.00000	0.00000	0.00000
0.0090	5.65018	0.13758	0.01883	0.00721	0.00125	0.00361	0.00405	0.00006	0.00000	0.00000	0.00000
0.0100	5.70286	0.16073	0.02644	0.01114	0.00212	0.00557	0.00695	0.00027	0.00027	0.00018	0.00009
0.0200	6.04970	0.36260	0.03502	0.09119	0.02662	0.04564	0.04360	0.00343	0.00314	0.00246	0.00180
0.0300	6.25525	0.52176	0.14843	0.20468	0.07156	0.10324	0.09128	0.01563	0.01168	0.01007	0.00847
0.0400	6.40714	0.65608	0.27522	0.32147	0.12626	0.16497	0.12147	0.03637	0.0272	0.0248	0.0223
0.0500	6.5325	0.7744	0.39713	0.4328	0.1854	0.2276	0.1469	0.0641	0.0498	0.0468	0.0438
0.0600	6.6424	0.8814	0.5105	0.5370	0.2466	0.2904	0.2065	0.0978	0.0788	0.0755	0.0721
0.0700	6.7421	0.9799	0.6155	0.6342	0.3086	0.3532	0.2678	0.1364	0.1136	0.1100	0.1065
0.0800	6.8344	1.0717	0.7112	0.7256	0.3711	0.4160	0.3299	0.1792	0.1531	0.1495	0.1459
0.0900	6.9211	1.1582	0.8046	0.8118	0.4338	0.4788	0.3925	0.2255	0.1968	0.1931	0.1894
0.1000	7.0034	1.2405	0.8910	0.8939	0.4965	0.5417	0.4551	0.2748	0.2490	0.2453	0.2416
0.2000	7.7080	1.9450	1.6776	1.5984	1.1248	1.1700	1.0834	0.8493	0.7490	0.7453	0.7416
0.3000	8.3469	2.5839	2.3165	2.2373	1.7531	1.7983	1.7117	1.4701	1.3668	1.3630	1.3593
0.4000	8.9767	3.2137	2.9462	2.8671	2.3814	2.4266	2.3400	2.0974	1.9937	1.9899	1.9862
0.5000	9.6052	3.8422	3.5748	3.4956	3.0098	3.0549	2.9683	2.7256	2.6218	2.6180	2.6143
0.6000	10.2336	4.4705	4.2031	4.1239	3.6381	3.6833	3.5966	3.3539	3.2509	3.2463	3.2426
0.7000	10.8619	5.0988	4.8314	4.7522	4.2664	4.3116	4.2249	3.9822	3.8784	3.8746	3.8709
0.8000	11.4902	5.7271	5.4597	5.3806	4.8947	4.9399	4.8533	4.6105	4.5067	4.5029	4.4992
0.9000	12.1185	6.3555	6.0881	6.0089	5.5230	5.5682	5.4816	5.2388	5.1350	5.1312	5.1275
1.0000	12.7468	6.9838	6.7164	6.6372	6.1513	6.1965	6.1099	5.8671	5.7633	5.7595	5.7558
2.0000	19.0306	13.2670	12.9996	12.9204	12.4345	12.4797	12.3931	12.1503	12.0465	12.0427	12.0390
3.0000	25.3132	19.5501	19.2827	19.2036	18.7177	18.7629	18.6762	18.4335	18.3296	18.3259	18.3222
4.0000	31.5963	25.8333	25.5659	25.4867	25.0008	25.0460	24.9594	24.7167	24.6128	24.6091	24.6054
5.0000	37.8795	32.1165	31.8490	31.7699	31.2840	31.3292	31.2426	30.9998	30.8960	30.8922	30.8885
6.0000	44.1626	38.3996	38.1322	38.0530	37.5672	37.6123	37.5257	37.2830	37.1791	37.1754	37.1717
7.0000	50.4458	44.6828	44.4154	44.3362	43.8503	43.8955	43.8089	43.5662	43.4623	43.4586	43.4549
8.0000	56.7290	50.9660	50.6986	50.6194	50.1335	50.1787	50.0920	49.8493	49.7455	49.7417	49.7380
9.0000	63.0122	57.2492	56.9817	56.9026	56.4167	56.4619	56.3752	56.1325	56.0286	56.0249	56.0211
10.0000	69.2953	63.5323	63.2649	63.1857	62.6998	62.7450	62.6584	62.4156	62.3118	62.3081	62.3043
12.0000	81.8616	76.0986	75.8312	75.7520	75.2662	75.3113	75.2247	74.9820	74.8781	74.8744	74.8706
15.0000	100.7111	94.9481	94.6807	94.6015	94.1157	94.1608	94.0742	93.8314	93.7276	93.7239	93.7202
20.0000	132.1269	126.3639	126.0965	126.0173	125.5315	125.5766	125.4900	125.2472	125.1434	125.1397	125.1360
30.0000	194.9585	189.1955	188.9281	188.8490	188.3631	188.4082	188.3217	188.0789	187.9750	187.9713	187.9676
$\ln \frac{C_A}{C_A}$	3.0840 / 21.8448	15.1448 / 3.77836E6	15.3031 / 4.42658E6	16.1846 / 1.0687E7	16.2749 / 1.169887E7	16.3578 / 1.270987E7	16.8433 / 2.0652E7	17.0510 / 2.54196E7	17.0585 / 2.5609E7	17.0659 / 2.58016E7
t_{DA}(PSS)	0.20	0.20	0.20	0.20	0.03	0.06	0.07	0.20	0.20	0.20	0.20

TABLE C-1(d). Δp_D VERSUS t_{DA} FOR A CLOSED 2:1 RECTANGLE

WITH WELL AT $x_D = 0.5$, $y_D = 0.5$, $\frac{\sqrt{A}}{r_w} = 2000$

From Earlougher and Ramey (1973)

DIMENSIONLESS

DIMENSIONLESS PRESSURE DROP, Δp_D

t_{DA}	WELL POINT X=0.5004 Y=0.7500	X=-0.5000 Y=0.0000	X=-0.5000 Y=0.2500	X=-0.5000 Y=0.5000	X=0.5000 Y=0.5000	X=0.5000 Y=1.0000	X=0.7500 Y=0.2500	X=0.7500 Y=0.5000	X=0.7500 Y=0.7500	X=1.0000 Y=0.0000	X=1.0000 Y=0.5000	X=1.0000 Y=1.0000
A/R²=	3.5556	3.5556	8.0000	32.0000	32.0000	32.0000	4.0000	6.4000	8.0000	1.2800	1.8824	1.8824
0.0020	4.69814	0.00000	0.00000	0.00000	0.00212	0.00423	0.00000	0.00000	0.00000	0.00000	0.00000	0.00000
0.0030	5.10087	0.00000	0.00000	0.00000	0.01047	0.02173	0.00000	0.00000	0.00000	0.00000	0.00000	0.00000
0.0040	5.24473	0.00000	0.00002	0.00000	0.02609	0.05219	0.00000	0.00002	0.00002	0.00000	0.00000	0.00000
0.0050	5.35642	0.00000	0.00014	0.00000	0.04559	0.09119	0.00000	0.00014	0.00014	0.00000	0.00000	0.00000
0.0060	5.44789	0.00000	0.00045	0.00000	0.06751	0.13501	0.00001	0.00010	0.00045	0.00000	0.00000	0.00000
0.0070	5.52560	0.00002	0.00108	0.00001	0.09060	0.18119	0.00001	0.00029	0.00109	0.00000	0.00000	0.00000
0.0080	5.59340	0.00005	0.00212	0.00002	0.11411	0.22821	0.00002	0.00066	0.00214	0.00000	0.00000	0.00000
0.0090	5.65378	0.00011	0.00361	0.00006	0.13758	0.27512	0.00006	0.00125	0.00367	0.00000	0.00000	0.00000
0.0100	5.70843	0.00361	0.00570	0.00014	0.16073	0.32135	0.00014	0.00212	0.00570	0.00000	0.00000	0.00000
0.0200	6.09502	0.06684	0.04586	0.00570	0.36260	0.71835	0.03562	0.01662	0.05116	0.00001	0.00018	0.00035
0.0300	6.35450	0.03086	0.10543	0.03087	0.52176	1.01265	0.02270	0.07156	0.12414	0.00041	0.00246	0.00452
0.0400	6.55674	0.07004	0.17187	0.12626	0.65608	1.24212	0.04988	0.12626	0.20637	0.00271	0.01007	0.01743
0.0500	6.72240	0.1194	0.2413	0.1854	0.7744	1.4293	0.0846	0.1854	0.2899	0.0689	0.0248	0.0406
0.0600	6.8613	0.1751	0.3121	0.2466	0.8614	1.5878	0.1251	0.2466	0.3717	0.0205	0.0468	0.0731
0.0700	6.9931	0.2349	0.3832	0.3086	0.9799	1.8664	0.1700	0.3086	0.4510	0.0379	0.0755	0.1130
0.0800	7.1059	0.2971	0.4541	0.3711	1.0718	1.9558	0.2182	0.3711	0.5277	0.0614	0.1100	0.1587
0.0900	7.2086	0.3607	0.5244	0.4338	1.2404	2.0559	0.2692	0.4338	0.6021	0.0904	0.1931	0.2086
0.1000	7.3034	0.4250	0.5939	0.4965	1.2404	2.0559	0.3223	0.4965	0.6745	0.1246	0.1931	0.2616
0.2000	8.0521	1.0672	1.2543	1.3409	1.9450	2.8228	0.9125	1.1248	1.3409	0.6315	0.7453	0.8592
0.3000	8.6964	1.6984	1.8878	1.9745	2.5839	3.4693	1.5355	1.7531	1.9745	1.2419	1.3630	1.4842
0.4000	9.3269	2.3272	2.5169	2.6035	3.2137	4.1901	2.1631	2.3814	2.6035	1.8677	1.9899	2.1121
0.5000	9.9555	2.9555	3.1453	3.2319	3.8422	4.7288	2.7913	3.0098	3.2319	2.4957	2.6180	2.7404
0.6000	10.5839	3.5838	3.7736	3.8603	4.4705	5.3532	3.4196	3.6381	3.8603	3.1239	3.2463	3.3687
0.7000	11.2122	4.2122	4.4019	4.4886	5.0988	5.9855	4.0479	4.2664	4.4886	3.7522	3.8766	3.9970
0.8000	11.8405	4.8405	5.0303	5.1169	5.7271	6.6138	4.6762	4.8947	5.1169	4.3806	4.5029	4.6253
0.9000	12.4688	5.4688	5.6586	5.7452	6.3555	7.2421	5.3045	5.5230	5.7452	5.0089	5.1312	5.2536
1.0000	13.0971	6.0971	6.2869	6.3736	6.9838	7.8705	5.9329	6.1513	6.3736	5.6371	5.7595	5.8819
2.0000	19.3803	12.1803	12.5701	12.6567	13.2669	14.1336	12.2160	12.4345	12.6567	11.9203	12.0427	12.1651
3.0000	25.6635	18.6434	18.8532	18.9399	19.5501	20.4368	18.4992	18.7177	18.9399	18.2035	18.3359	18.4483
4.0000	31.9466	24.9466	25.1364	25.2230	25.8333	26.7199	24.7824	25.0008	25.2230	24.4867	24.6091	24.7314
5.0000	38.2298	31.2297	31.4195	31.5062	32.1164	33.0031	31.0655	31.2840	31.5062	30.7698	30.8922	31.0146
6.0000	44.5130	37.5129	37.7027	37.7894	38.3996	39.2863	37.3487	37.5672	37.7894	37.0530	37.1754	37.2978
7.0000	50.7961	43.7961	43.9859	44.0725	44.6828	45.5694	43.6319	43.8503	44.0725	43.3362	43.4586	43.5809
8.0000	57.0793	50.0793	50.2690	50.3557	50.9659	51.8526	49.9150	50.1335	50.3557	49.6193	49.7417	49.8641
9.0000	63.3625	56.3624	56.5522	56.6389	57.2491	58.1358	56.1981	56.4167	56.6389	55.9024	56.0248	56.1473
10.000	69.6456	62.6456	62.8353	62.9220	63.5323	64.4190	62.4813	62.6998	62.9220	62.1856	62.3080	62.4304
12.000	82.2119	75.2119	75.4017	75.4884	76.0986	76.9852	75.0476	75.2661	75.4884	74.7519	74.8744	74.9967
15.000	101.0614	94.0614	94.2512	94.3378	94.9481	95.8348	93.8971	94.1156	94.3378	93.6014	93.7238	93.8463
20.000	132.4772	125.4771	125.6669	125.7536	126.3639	127.2506	125.3129	125.5314	125.7536	125.0172	125.1396	125.2621
30.000	195.3088	188.3087	188.4986	188.5853	189.1955	190.0822	188.1445	188.3630	188.5853	187.8488	187.9712	188.0937
ln C_A	2.3833	16.3935	16.0039	15.8305	14.6101	12.8366	16.7120	16.2750	15.8305	17.3034	17.0585	16.8137
C_A	10.8410	1.3039E7	8.9209E6	7.5009E6	2.2133E6	3.7573E5	1.8111E7	1.1699E7	7.5009E6	3.2715E7	2.5610E7	2.0049E7
t_{DA}(PSS)	0.30	0.07	0.20	0.20	0.20	0.30	0.20	0.06	0.20	0.30	0.20	0.20

OBSERVATION POINTS

TABLE C-1(e). Δp_D VERSUS t_{DA} FOR A CLOSED 2:1 RECTANGLE WITH WELL AT $x_D = 0.5$, $y_D = 0.75$, $\frac{\sqrt{A}}{r_w} = 2000$

From Earlougher and Ramey (1973)

DIMENSIONLESS PRESSURE DROP, Δp_D

DIMENSIONLESS TIME

t_{DA}	WELL POINT X=0.7500 Y=0.5000	X=0.0000 Y=0.5000	X=0.0000 Y=1.0000	X=0.2500 Y=0.5000	X=0.2500 Y=1.0000	X=0.5000 Y=0.5000	X=0.5000 Y=1.0000	X=0.7500 Y=0.7500	X=0.7500 Y=1.0000	X=1.0000 Y=0.5000	X=1.0000 Y=1.0000
$A/R^2=$	0.8889	0.8000	2.0000	1.6000	8.0000	4.0000	8.0000	32.0000	8.0000	8.0000	8.0000
0.0020	4.89814	0.00000	0.00000	0.00000	0.00000	0.00000	0.00000	0.00212	0.00000	0.00000	0.00000
0.0030	5.10087	0.00000	0.00000	0.00000	0.00000	0.00000	0.00000	0.01087	0.00000	0.00000	0.00000
0.0040	5.24471	0.00000	0.00000	0.00000	0.00000	0.00002	0.00000	0.02609	0.00005	0.00005	0.00000
0.0050	5.35628	0.00000	0.00000	0.00000	0.00000	0.00014	0.00000	0.04559	0.00027	0.00027	0.00000
0.0060	5.44744	0.00000	0.00000	0.00000	0.00000	0.00045	0.00001	0.06751	0.00090	0.00096	0.00003
0.0070	5.52452	0.00000	0.00000	0.00000	0.00000	0.00108	0.00005	0.09060	0.00216	0.00216	0.00009
0.0080	5.59128	0.00000	0.00000	0.00000	0.00000	0.00212	0.00012	0.11411	0.00423	0.00423	0.00025
0.0090	5.65018	0.00000	0.00000	0.00000	0.00000	0.00361	0.00027	0.13758	0.00721	0.00721	0.00054
0.0100	5.70286	0.00000	0.00000	0.00000	0.00000	0.00557	0.00057	0.16073	0.01114	0.01114	0.00094
0.0200	6.04984	0.00000	0.00000	0.00014	0.00005	0.04564	0.03925	0.36269	0.09124	0.09128	0.02227
0.0300	6.25684	0.00001	0.00000	0.00157	0.00090	0.10324	0.09128	0.52299	0.20558	0.20647	0.08720
0.0400	6.41301	0.00012	0.00009	0.00584	0.00424	0.16497	0.15682	0.66111	0.32370	0.32982	0.18247
0.0500	6.5462	0.0006	0.0005	0.0136	0.0112	0.2276	0.1469	0.7868	0.4440	0.4545	0.2934
0.0600	6.6674	0.0020	0.0018	0.0249	0.0219	0.2904	0.2065	0.9048	0.5588	0.5788	0.4411
0.0700	6.7815	0.0046	0.0044	0.0395	0.0362	0.3532	0.2678	1.0175	0.6702	0.7018	0.5312
0.0800	6.8910	0.0090	0.0087	0.0571	0.0536	0.4160	0.3299	1.1264	0.7784	0.8231	0.6532
0.0900	6.9970	0.0153	0.0150	0.0774	0.0738	0.4788	0.3925	1.2321	0.8839	0.9424	0.7699
0.1000	7.1004	0.0238	0.0235	0.1001	0.0964	0.5417	0.4551	1.3353	0.9870	1.0596	0.8868
0.2000	8.0336	0.2262	0.2259	0.4241	0.4203	1.1700	1.0834	2.2681	1.9196	2.1138	1.9408
0.3000	8.8470	0.5931	0.5928	0.8675	0.8638	1.7983	1.7117	3.0813	2.7328	3.0035	2.8305
0.4000	9.5882	1.0619	1.0615	1.3830	1.3793	2.4266	2.3400	3.8224	3.4740	3.7914	3.6184
0.5000	10.2855	1.5928	1.5924	1.9424	1.9387	3.0549	2.9683	4.5196	4.1712	4.5173	4.3442
0.6000	10.9559	2.1616	2.1613	2.5287	2.5249	3.6833	3.5966	5.1900	4.8416	5.2049	5.0320
0.7000	11.6100	2.7536	2.7533	3.1314	3.1276	4.3116	4.2249	5.8440	5.4956	5.8695	5.6966
0.8000	12.2540	3.3597	3.3594	3.7440	3.7402	4.9399	4.8533	6.4880	6.1395	6.5200	6.3471
0.9000	12.8919	3.9745	3.9742	4.3627	4.3590	5.5682	5.4816	7.1259	6.7774	7.1619	6.9889
1.0000	13.5260	4.5946	4.5943	4.9852	4.9814	6.1965	6.1099	7.7600	7.4116	7.7985	7.6255
2.0000	19.8183	10.8649	10.8646	11.2593	11.2556	12.4797	12.3931	14.0523	13.7039	14.0945	13.9215
3.0000	26.1015	17.1477	17.1477	17.5424	17.5387	18.7629	18.6762	20.3355	19.9871	20.3777	20.2048
4.0000	32.3847	23.4311	23.4308	23.8255	23.8218	25.0460	24.9594	26.6187	26.2703	26.6609	26.4880
5.0000	38.6679	29.7143	29.7140	30.1087	30.1050	31.3292	31.2426	32.9019	32.5534	32.9441	32.7711
6.0000	44.9510	35.9975	35.9972	36.3918	36.3881	37.6123	37.5258	39.1850	38.8366	39.2272	39.0543
7.0000	51.2342	42.2807	42.2804	42.6751	42.6713	43.8955	43.8089	45.4681	45.1197	45.5104	45.3374
8.0000	57.5174	48.5638	48.5635	48.9582	48.9545	50.1787	50.0920	51.7513	51.4029	51.7936	51.6206
9.0000	63.8005	54.8470	54.8467	55.2414	55.2376	56.4619	56.3752	58.0345	57.6861	58.0767	57.9038
10.0000	70.0837	61.1301	61.1298	61.5245	61.5208	62.7450	62.6584	64.3177	63.9693	64.3599	64.1870
12.0000	82.6500	73.6964	73.6961	74.0908	74.0871	75.3113	75.2247	76.8840	76.5356	76.9263	76.7533
15.0000	101.4995	92.5460	92.5457	92.9404	92.9366	94.0742	93.9876	95.7335	95.3851	95.7757	95.6027
20.0000	132.9153	123.9617	123.9615	124.3561	124.3524	125.3766	125.2900	127.1493	126.8009	127.1915	127.0186
30.0000	195.7469	186.7934	186.7931	187.1877	187.1841	188.4082	188.3217	189.9809	189.6325	190.0231	189.8502
$\ln c_A$	1.5072	19.4144	19.4150	18.6256	18.6330	16.1846	16.3578	13.0392	13.7361	12.9548	13.3007
c_A	4.5140	2.7012E8	2.7023E8	1.2274E8	1.2365E8	1.0687E7	1.2709E7	4.6009E5	9.2362E5	4.2285E5	5.9760E5
t_{DA}(PSS)	0.80	0.90	0.90	0.80	0.80	0.03	0.07	0.80	0.80	0.90	0.90

OBSERVATION POINTS

y_D axis: 2, 1, 0 ; x_D axis: 0, 1

TABLE C-1(f). Δp_D VERSUS t_{DA} FOR A CLOSED 2:1 RECTANGLE

WITH WELL AT $x_D = 0.75$, $y_D = 0.5$, $\dfrac{\sqrt{A}}{r_w} = 2000$

From Earlougher and Ramey (1973)

DIMENSIONLESS PRESSURE DROP, Δp_D

OBSERVATION POINTS

DIMENSIONLESS TIME t_{DA}	WELL POINT X=0.7504 Y=0.7500	X=0.0000 Y=0.0000	X=0.0000 Y=0.5000	X=0.0000 Y=1.0000	X=0.2500 Y=0.0000	X=0.2500 Y=0.2500	X=0.2500 Y=0.5000	X=0.2500 Y=0.7500	X=0.2500 Y=1.0000	X=0.5000 Y=0.0000	X=0.5000 Y=0.2500
	1.8824	0.7111	0.8649	0.8649	1.2800	1.6000	1.8824	2.0000	1.8824	2.4615	4.0000
0.0020	4.89814	0.00000	0.00000	0.00000	0.00000	0.00000	0.00000	0.00000	0.00000	0.00000	0.00000
0.0030	5.10087	0.00000	0.00000	0.00000	0.00000	0.00000	0.00000	0.00000	0.00000	0.00000	0.00000
0.0040	5.24473	0.00000	0.00000	0.00000	0.00000	0.00000	0.00000	0.00000	0.00000	0.00000	0.00000
0.0050	5.36642	0.00000	0.00000	0.00000	0.00000	0.00000	0.00000	0.00000	0.00000	0.00000	0.00000
0.0060	5.44789	0.00000	0.00000	0.00000	0.00000	0.00000	0.00000	0.00000	0.00000	0.00000	0.00001
0.0070	5.52560	0.00000	0.00000	0.00000	0.00000	0.00000	0.00000	0.00000	0.00000	0.00000	0.00002
0.0080	5.59340	0.00000	0.00000	0.00000	0.00000	0.00000	0.00000	0.00000	0.00000	0.00000	0.00006
0.0090	5.65378	0.00000	0.00000	0.00000	0.00000	0.00000	0.00000	0.00000	0.00000	0.00000	0.00014
0.0100	5.70843	0.00000	0.00000	0.00000	0.00000	0.00000	0.00000	0.00000	0.00000	0.00000	0.00562
0.0200	6.09318	0.00000	0.00000	0.00000	0.00001	0.00002	0.00009	0.00017	0.00012	0.00105	0.02270
0.0300	6.35651	0.00000	0.00001	0.00001	0.00020	0.00048	0.00123	0.00226	0.00160	0.00810	0.04988
0.0400	6.56447	0.00001	0.00003	0.00001	0.00136	0.00239	0.00504	0.00872	0.00640	0.02421	0.0846
0.0500	6.7421	0.0002	0.0006	0.0009	0.0045	0.0067	0.0124	0.0180	0.0145	0.0490	0.1251
0.0600	6.9001	0.0009	0.0019	0.0028	0.0102	0.0141	0.0234	0.0328	0.0270	0.0809	0.1700
0.0700	7.0442	0.0025	0.0045	0.0065	0.0190	0.0245	0.0379	0.0512	0.0426	0.1186	0.2182
0.0800	7.1779	0.0055	0.0088	0.0122	0.0309	0.0380	0.0554	0.0727	0.0610	0.1609	0.2692
0.0900	7.3035	0.0101	0.0151	0.0202	0.0458	0.0545	0.0756	0.0967	0.0826	0.2070	0.3223
0.1000	7.4226	0.0168	0.0236	0.0305	0.0635	0.0737	0.0982	0.1228	0.1060	0.2561	0.9225
0.2000	8.4137	0.2045	0.2260	0.2475	0.3618	0.3795	0.4222	0.4650	0.4430	0.8306	1.5355
0.3000	9.2341	0.5673	0.5930	0.6186	0.8002	0.8193	0.8657	0.9120	0.8880	1.4514	2.1631
0.4000	9.9762	1.0353	1.0617	1.0881	1.3148	1.3342	1.3811	1.4281	1.4030	2.0887	2.7913
0.5000	10.6736	1.5661	1.5926	1.6191	1.8741	1.8935	1.9406	1.9876	1.9620	2.7069	3.4196
0.6000	11.3441	2.1349	2.1614	2.1879	2.4603	2.4798	2.5268	2.5739	2.5480	3.3352	4.0479
0.7000	11.9981	2.7269	2.7534	2.7799	3.0630	3.0824	3.1295	3.1765	3.1510	3.9635	4.6762
0.8000	12.6621	3.3331	3.3596	3.3861	3.6756	3.6951	3.7421	3.7892	3.7640	4.5918	5.3045
0.9000	13.2800	3.9479	3.9744	4.0009	4.2944	4.3138	4.3608	4.4079	4.3820	5.2201	5.9329
1.0000	13.9152	4.5679	4.5944	4.6209	4.9168	4.9363	4.9833	5.0304	5.0050	5.8484	5.9329
2.0000	20.2064	10.8382	10.8648	10.8912	11.1909	11.2104	11.2574	11.3045	11.2800	12.1316	12.2160
3.0000	26.4896	17.1213	17.1478	17.1743	17.4740	17.4934	17.5405	17.5876	17.5630	18.4147	18.4992
4.0000	32.7728	23.4044	23.4309	23.4574	23.7572	23.7766	23.8236	23.8707	23.8460	24.6979	24.7824
5.0000	39.0560	29.6876	29.7141	29.7406	30.0403	30.0598	30.1068	30.1539	30.1290	30.9810	31.0655
6.0000	45.3392	35.9708	35.9973	36.0238	36.3235	36.3429	36.3900	36.4370	36.4120	37.2642	37.3487
7.0000	51.6223	42.2540	42.2805	42.3070	42.6067	42.6261	42.6732	42.7202	42.6950	43.5474	43.6319
8.0000	57.9055	48.5371	48.5636	48.5901	48.8898	48.9093	48.9563	49.0034	48.9780	49.8305	49.9150
9.0000	64.1886	54.8202	54.8468	54.8734	55.1730	55.1924	55.2395	55.2866	55.2610	56.1137	56.1981
10.0000	70.4718	61.1034	61.1299	61.1565	61.4561	61.4755	61.5226	61.5697	61.5440	62.3968	62.4813
12.0000	83.0381	73.6697	73.6962	73.7228	74.0224	74.0419	74.0889	74.1360	74.1100	74.9632	75.0476
15.0000	101.8876	92.5192	92.5458	92.5723	92.8720	92.8914	92.9385	92.9855	92.9600	93.8126	93.8971
20.0000	133.3034	123.9350	123.9615	123.9881	124.2877	124.3072	124.3542	124.4013	124.3760	125.2284	125.3129
30.0000	196.1350	186.7666	186.7932	186.8197	187.1193	187.1388	187.1859	187.2329	187.2070	188.0600	188.1445
ln C_A	0.7309	19.4679	19.4148	19.3617	18.7624	18.7235	18.6293	18.5352	18.4963	16.8809	16.7120
C_A	2.0770	2.8496E8	2.7023E8	2.5625E8	1.4073E8	1.3537E8	1.2320E8	1.1213E8	1.0786E8	2.1443E7	1.8411E7
t_{DA}(PSS)	0.80	0.90	0.90	0.90	0.80	0.80	0.80	0.80	0.80	0.20	0.20

TABLE C-1(g). Δp_D VERSUS t_{DA} FOR A CLOSED 2:1 RECTANGLE WITH WELL AT $x_D=0.75$, $y_D=0.75$, $\dfrac{\sqrt{A}}{r_w}=2000$

From Earlougher and Ramey (1973)

DIMENSIONLESS PRESSURE DROP, Δp_D

DIMENSIONLESS TIME t_{DA}

OBSERVATION POINTS

t_{DA}	X=0.5000 Y=0.5000	X=0.5000 Y=0.7500	X=0.5000 Y=1.0000	X=0.7500 Y=0.0000	X=0.7500 Y=0.2500	X=0.7500 Y=0.5000	X=0.7500 Y=1.0000	X=1.0000 Y=0.0000	X=1.0000 Y=0.5000	X=1.0000 Y=1.0000
WELL POINT $A/r^{**}2=$	6.4000	8.0000	6.4000	3.5556	8.0000	32.0000	32.0000	2.4615	6.4000	6.4000
0.0020	0.00000	0.00000	0.00000	0.00000	0.00000	0.00212	0.00423	0.00000	0.00000	0.00000
0.0030	0.00000	0.00000	0.00000	0.00000	0.00000	0.01087	0.02173	0.00000	0.00000	0.00000
0.0040	0.00000	0.00000	0.00000	0.00000	0.00002	0.02609	0.05219	0.00000	0.00001	0.00001
0.0050	0.00002	0.00014	0.00005	0.00000	0.00014	0.04559	0.09119	0.00000	0.00005	0.00009
0.0060	0.00010	0.00045	0.00020	0.00000	0.00045	0.06751	0.13501	0.00000	0.00020	0.00040
0.0070	0.00029	0.00109	0.00058	0.00000	0.00108	0.09060	0.18119	0.00000	0.00058	0.00117
0.0080	0.00066	0.00214	0.00132	0.00002	0.00212	0.11411	0.22821	0.00000	0.00132	0.00264
0.0090	0.00125	0.00367	0.00253	0.00005	0.00361	0.13758	0.27512	0.00000	0.00251	0.00502
0.0100	0.00212	0.00570	0.00423	0.00011	0.00589	0.16073	0.32135	0.00000	0.00424	0.00847
0.0200	0.02662	0.05116	0.05219	0.00685	0.04589	0.36269	0.71853	0.00210	0.05324	0.10438
0.0300	0.07156	0.12414	0.13502	0.03106	0.10590	0.52299	1.01492	0.01620	0.14311	0.27002
0.0400	0.12626	0.20637	0.22830	0.07139	0.17426	0.66111	1.25084	0.04840	0.25241	0.55643
0.0500	0.1854	0.3717	0.3218	0.1238	0.2481	0.7868	1.4498	0.0977	0.3702	0.6428
0.0600	0.2466	0.4510	0.4122	0.1853	0.3261	0.9048	1.6243	0.1608	0.4912	0.8216
0.0700	0.3086	0.5237	0.4987	0.2538	0.4075	1.0175	1.7813	0.2346	0.6127	0.9909
0.0800	0.3711	0.6021	0.5813	0.3275	0.4915	1.1264	1.9253	0.3164	0.7334	1.1504
0.0900	0.4338	0.6745	0.6606	0.4053	0.5775	1.2321	2.0590	0.4039	0.8524	1.3010
0.1000	0.4965	0.7369	0.7369	0.4860	0.6648	1.3353	2.1846	0.4955	0.9695	1.4434
0.2000	1.1248	1.3409	1.4190	1.3368	1.5396	2.2681	3.1994	1.4566	2.0236	2.5906
0.3000	1.7531	1.9745	2.0548	2.1401	2.3458	3.0813	4.0224	2.3355	2.9133	3.4911
0.4000	2.3814	2.6035	2.6842	2.8860	3.0861	3.8224	4.7648	3.1220	3.7012	4.2803
0.5000	3.0098	3.2319	3.3127	3.5771	3.7832	4.5196	5.4622	3.8476	4.4269	5.0062
0.6000	3.6381	3.8603	3.9410	4.2474	4.4535	5.1900	6.1326	4.5354	5.1147	5.6940
0.7000	4.2664	4.4886	4.5693	4.9014	5.1075	5.8440	6.7866	5.2000	5.7793	6.3587
0.8000	4.8947	5.1169	5.1976	5.5434	5.7515	6.4880	7.4306	5.8505	6.4298	7.0092
0.9000	5.5230	5.7452	5.8259	6.1833	6.3894	7.1259	8.0685	6.4923	7.0717	7.6510
1.0000	6.1513	6.3736	6.4543	6.8174	7.0235	7.7600	8.7026	7.1289	7.7083	8.2876
2.0000	12.4345	12.6567	12.7374	13.1097	13.3158	14.0523	14.9949	13.4249	14.0042	14.5836
3.0000	18.7177	18.9399	19.0206	19.3329	19.5990	20.3355	21.2781	19.7082	20.2875	20.8668
4.0000	25.0008	25.2230	25.3037	25.6761	25.8822	26.6187	27.5613	25.9914	26.5707	27.1501
5.0000	31.2840	31.5062	31.5869	31.9592	32.1653	32.9018	33.8444	32.2745	32.8539	33.4332
6.0000	37.5672	37.7894	37.8701	38.2424	38.4485	39.1850	40.1276	38.5557	39.1370	39.7164
7.0000	43.8503	44.0725	44.1532	44.5255	44.7316	45.4681	46.4107	44.8408	45.4201	45.9995
8.0000	50.1335	50.3557	50.4364	50.8087	51.0148	51.7513	52.6939	51.1240	51.7033	52.2827
9.0000	56.4167	56.6389	56.7196	57.0919	57.2980	58.0345	58.9771	57.4071	57.9865	58.5659
10.0000	62.6998	62.9220	63.0028	63.3751	63.5812	64.3177	65.2603	63.6903	64.2697	64.8490
12.0000	75.2661	75.4884	75.5691	75.9414	76.1475	76.8840	77.8266	76.2566	76.8360	77.4154
15.0000	94.1156	94.3378	94.4186	94.7908	94.9969	95.7335	96.6761	95.1060	95.6855	96.2648
20.0000	125.5314	125.7536	125.8344	126.2066	126.4127	127.1492	128.0919	126.5219	127.1013	127.6807
30.0000	188.3630	188.5853	188.6660	189.0382	189.2443	189.9808	190.9235	189.3534	189.9329	190.5123
$\ln C_A$	16.2750	15.8305	15.6691	14.9245	14.5123	13.0393	11.1540	14.2940	13.1352	11.9765
C_A	1.1699E7	7.5009E6	6.3826E6	3.0312E6	2.0072E6	4.6013E5	6.9845E4	1.6136E6	5.0648E5	1.5898E5
t_{DA}(PSS)	0.06	0.20	0.20	0.80	0.80	0.80	0.80	0.65	0.90	0.90

TABLE C-1(g) cont. Δp_D VERSUS t_{DA} FOR A CLOSED 2:1 RECTANGLE WITH WELL AT $x_D = 0.75$, $y_D = 0.75$, $\dfrac{\sqrt{A}}{r_w} = 2000$

From Earlougher and Ramey (1973)

DIMENSIONLESS PRESSURE DROP, Δp_D

OBSERVATION POINTS

DIMENSIONLESS TIME t_{DA}	WELL POINT x=0.5004 y=0.8750	X=0.5000 Y=0.0000	X=0.5000 Y=0.5000	X=0.5000 Y=1.0000	X=0.7500 Y=0.0000	X=0.7500 Y=0.5000	X=0.7500 Y=0.7500	X=0.7500 Y=1.0000	X=1.0000 Y=0.0000	X=1.0000 Y=0.5000	X=1.0000 Y=1.0000
A/R**2=		2.6122	14.2222	128.0000	1.9692	5.1200	7.5294	7.5294	1.1327	1.7534	1.9692
0.0020	4.90026	0.00000	0.00001	0.22821	0.00000	0.00000	0.00000	0.00000	0.00000	0.00000	0.00000
0.0030	5.11174	0.00000	0.00021	0.41068	0.00000	0.00000	0.00000	0.00000	0.00000	0.00000	0.00000
0.0040	5.27681	0.00000	0.00118	0.57424	0.00000	0.00000	0.00003	0.00000	0.00000	0.00000	0.00000
0.0050	5.40188	0.00000	0.00342	0.71835	0.00000	0.00002	0.00017	0.00009	0.00000	0.00000	0.00000
0.0060	5.51495	0.00000	0.00715	0.84595	0.00000	0.00006	0.00062	0.00032	0.00000	0.00000	0.00000
0.0070	5.61511	0.00000	0.01234	0.95997	0.00000	0.00016	0.00155	0.00084	0.00000	0.00000	0.00000
0.0080	5.70539	0.00000	0.01883	1.06281	0.00000	0.00036	0.00315	0.00174	0.00000	0.00000	0.00000
0.0090	5.78773	0.00000	0.02644	1.15636	0.00000	0.00068	0.00552	0.00311	0.00000	0.00000	0.00000
0.0100	5.86353	0.00000	0.03502	1.24211	0.00000	0.00068	0.00871	0.00502	0.00000	0.00000	0.00000
0.0200	6.40860	0.00152	0.14843	1.84461	0.00025	0.01534	0.07908	0.05300	0.00000	0.00012	0.00048
0.0300	6.75849	0.01109	0.27522	2.21861	0.00311	0.05144	0.18395	0.13343	0.00017	0.00199	0.00571
0.0400	7.01706	0.03271	0.39713	2.49047	0.01205	0.10117	0.29436	0.22387	0.00147	0.00894	0.02094
0.0500	7.2223	0.0657	0.5105	2.7041	0.0286	0.1579	0.4010	0.3148	0.0057	0.0231	0.0473
0.0600	7.3927	0.1078	0.6155	2.8801	0.0527	0.2179	0.5015	0.4030	0.0144	0.0446	0.0834
0.0700	7.5385	0.1565	0.7132	3.0300	0.0835	0.2794	0.5959	0.4876	0.0287	0.0731	0.1270
0.0800	7.6663	0.2100	0.8046	3.1609	0.1199	0.3416	0.6850	0.5687	0.0488	0.1075	0.1762
0.0900	7.7806	0.2667	0.8910	3.2775	0.1610	0.4042	0.7694	0.6467	0.0747	0.1469	0.2294
0.1000	7.8844	0.3256	0.9731	3.3831	0.2060	0.4669	0.8500	0.7220	0.1060	0.1905	0.2854
0.2000	8.6642	0.9487	1.6776	4.1692	0.7640	1.0951	1.5487	1.4000	0.5990	0.7427	0.8969
0.3000	9.3124	1.5776	2.3165	4.8181	1.3825	1.7235	2.1868	2.0352	1.2072	1.3604	1.5242
0.4000	9.9434	2.2061	2.9462	5.4492	2.0095	2.3518	2.8164	2.6645	1.8327	1.9873	2.1524
0.5000	10.5721	2.8944	3.5748	6.0779	2.6376	2.9801	3.4449	3.2930	2.4607	2.6154	2.7806
0.6000	11.2005	3.4627	4.2031	6.7063	3.2659	3.6084	4.0733	3.9213	3.0889	3.2437	3.4090
0.7000	11.8288	4.0910	4.8314	7.3346	3.8942	4.2367	4.7016	4.5496	3.7172	3.8720	4.0373
0.8000	12.4571	4.7193	5.4597	7.9629	4.5225	4.8650	5.3299	5.1779	4.3456	4.5003	4.6656
0.9000	13.0854	5.3476	6.0881	8.5913	5.1508	5.4933	5.9582	5.8062	4.9738	5.1286	5.2939
1.0000	13.7138	5.9760	6.7164	9.2196	5.7792	6.1217	6.5866	6.4345	5.6021	5.7569	5.9222
2.0000	19.9969	12.2591	12.9995	15.5027	12.0623	12.4048	12.8697	12.7177	11.8853	12.0401	12.2054
3.0000	26.2801	18.5623	19.2827	21.7859	18.3455	18.6880	19.1529	19.0009	18.1685	18.3233	18.4886
4.0000	32.5632	24.8254	25.5658	28.0690	24.6287	24.9712	25.4360	25.2840	24.4517	24.6064	24.7717
5.0000	38.8464	31.1086	31.8490	34.3523	30.9118	31.2543	31.7192	31.5672	30.7348	30.8896	31.0549
6.0000	45.1296	37.3917	38.1322	40.6354	37.1950	37.5375	38.0024	37.8504	37.0180	37.1727	37.3381
7.0000	51.4127	43.6749	44.4154	46.9185	43.4781	43.8207	44.2855	44.1335	43.3012	43.4559	43.6212
8.0000	57.6959	49.9581	50.6985	53.2017	49.7613	50.1038	50.5687	50.4167	49.5842	49.7391	49.9044
9.0000	63.9791	56.2412	56.9817	59.4849	56.0444	56.3870	56.8519	56.6999	55.8674	56.0222	56.1875
10.0000	70.2622	62.5244	63.2648	65.7681	62.3276	62.6701	63.1350	62.9830	62.1506	62.3054	62.4707
12.0000	82.8285	75.0907	75.8312	78.3343	74.8939	75.2364	75.7014	75.5494	74.7169	74.8717	75.0370
15.0000	101.6781	93.9402	94.6807	97.1839	93.7434	94.0859	94.5509	94.3989	93.5664	93.7212	93.8866
20.0000	133.0938	125.3559	126.0964	128.5986	125.1592	125.5017	125.9667	125.8146	124.9822	125.1370	125.3023
30.0000	195.9254	188.1875	188.9288	191.4312	187.9908	188.3333	188.7983	188.6463	187.8137	187.9686	188.1339
ln C_A	1.1501	16.6258	15.1449	10.1384	17.0194	16.3344	15.7085	15.4045	17.3734	17.0638	16.7331
C_A	3.1585	1.6615E7	3.7787E6	2.5297E4	2.4628E7	1.2414E7	6.6392E6	4.8988E6	3.5089E7	2.5746E7	1.8497E7
t_{DA}(PSS)	0.30	0.10	0.20	0.30	0.20	0.07	0.20	0.20	0.30	0.20	0.20

TABLE C-1(h). Δp_D VERSUS t_{DA} FOR A CLOSED 2:1 RECTANGLE WITH WELL AT $x_D = 0.5$, $y_D = 0.875$, $\dfrac{\sqrt{A}}{r_w} = 2000$

From Earlougher and Ramey (1973)

DIMENSIONLESS PRESSURE DROP, Δp_D

DIMENSIONLESS TIME

OBSERVATION POINTS

t_{DA}	WELL POINT X=0.8754 Y=0.5000	X=0.0000 Y=0.5000	X=0.0000 Y=1.0000	X=0.2500 Y=0.5000	X=0.2500 Y=0.7500	X=0.5000 Y=0.5000	X=0.5000 Y=1.0000	X=0.7500 Y=0.5000	X=0.7500 Y=0.7500	X=1.0000 Y=0.5000	X=1.0000 Y=1.0000
$A/\beta^2=$		0.6531	0.6038	1.2800	1.2308	3.5556	2.4615	32.0000	16.0000	32.0000	6.4000
0.0020	4.89814	0.00000	0.00000	0.00000	0.00000	0.00000	0.00000	0.00212	0.00092	0.00423	0.00000
0.0030	5.10087	0.00000	0.00000	0.00000	0.00000	0.00000	0.00000	0.01087	0.00045	0.02173	0.00000
0.0040	5.24474	0.00000	0.00000	0.00000	0.00000	0.00000	0.00000	0.02609	0.00212	0.05219	0.00901
0.0050	5.35642	0.00000	0.00000	0.00000	0.00000	0.00000	0.00000	0.04559	0.00557	0.09119	0.00009
0.0060	5.44790	0.00000	0.00000	0.00000	0.00000	0.00000	0.00000	0.06750	0.01087	0.13501	0.00040
0.0070	5.52562	0.00000	0.00000	0.00000	0.00000	0.00000	0.00002	0.09060	0.01781	0.18119	0.00117
0.0080	5.59343	0.00000	0.00000	0.00000	0.00000	0.00001	0.00000	0.11411	0.02610	0.22821	0.00264
0.0090	5.65383	0.00000	0.00000	0.00000	0.00000	0.00002	0.00000	0.13258	0.03546	0.27512	0.00502
0.0100	5.70849	0.00000	0.00000	0.00000	0.00000	0.00006	0.00000	0.16073	0.04564	0.32135	0.00847
0.0200	6.09564	0.00000	0.00000	0.00000	0.00000	0.00343	0.00305	0.36277	0.16497	0.71870	0.10438
0.0300	6.35899	0.00000	0.00000	0.00010	0.00008	0.01563	0.01563	0.52412	0.29028	1.01718	0.27003
0.0400	6.57271	0.00001	0.00000	0.00070	0.00062	0.03637	0.02421	0.66345	0.41540	1.25954	0.45660
0.0500	6.7605	0.0001	0.0001	0.0024	0.0022	0.0641	0.0490	0.7968	0.5395	1.4700	0.6436
0.0600	6.9326	0.0003	0.0003	0.0109	0.0105	0.0918	0.0809	0.9226	0.6619	1.6696	0.8242
0.0700	7.0938	0.0009	0.0008	0.0182	0.0179	0.1364	0.1186	1.0445	0.7824	1.8371	0.9965
0.0800	7.2466	0.0020	0.0020	0.0279	0.0275	0.1792	0.1699	1.1635	0.9068	2.0030	1.1606
0.0900	7.3926	0.0040	0.0040	0.0399	0.0395	0.2255	0.2070	1.2798	1.0168	2.1603	1.3171
0.1000	7.5327	0.0072	0.0071	0.0399	0.0395	0.2748	0.2561	1.3936	1.1305	2.3103	1.4668
0.2000	8.7168	0.1286	0.1286	0.2735	0.2731	0.8493	0.8306	2.4168	2.1535	3.5533	2.7095
0.3000	9.6661	0.4229	0.4228	0.6604	0.6600	1.4701	1.4514	3.2856	3.0233	4.5307	3.6869
0.4000	10.4879	0.8437	0.8436	1.1412	1.1408	2.0974	2.0787	4.0623	3.7991	5.3685	4.5247
0.5000	11.2340	1.3449	1.3448	1.6795	1.6791	2.7256	2.7069	4.7806	4.5174	6.1243	5.2805
0.6000	11.9342	1.8955	1.8954	2.2529	2.2525	3.3539	3.3352	5.4639	5.2007	6.8304	5.9865
0.7000	12.6063	2.4764	2.4763	2.8477	2.8473	3.9822	3.9635	6.1258	5.8625	7.5061	6.6623
0.8000	13.2614	3.0757	3.0757	3.4555	3.4551	4.6105	4.5918	6.7746	6.5113	8.1634	7.3196
0.9000	13.9061	3.6863	3.6863	4.0713	4.0709	5.2388	5.2201	7.4154	7.1521	8.8094	7.9656
1.0000	14.5464	4.3039	4.3038	4.6920	4.6916	5.8671	5.8484	8.0513	7.7681	9.4485	8.6047
2.0000	20.8630	10.5703	10.5702	10.9633	10.9629	12.1503	12.1316	14.3464	14.0831	15.7484	14.9046
3.0000	27.1263	16.8534	16.8533	17.2264	17.2260	18.4335	18.4147	20.6296	20.3664	22.0317	21.1879
4.0000	33.4095	23.1364	23.1363	23.5295	23.5291	24.7167	24.6979	26.9128	26.6496	28.3149	27.4711
5.0000	39.6927	29.4196	29.4196	29.8127	29.8123	30.9998	30.9811	33.1960	32.9327	34.5981	33.7543
6.0000	45.9758	35.7027	35.7027	36.0959	36.0955	37.2830	37.2643	39.4791	39.2159	40.8813	40.0375
7.0000	52.2589	41.9860	41.9860	42.3791	42.3787	43.5662	43.5474	45.7622	45.4990	47.1643	46.3205
8.0000	58.5421	48.2691	48.2691	48.6622	48.6618	49.8493	49.8306	52.0454	51.7822	53.4476	52.6037
9.0000	64.8253	54.5523	54.5523	54.9454	54.9450	56.1325	56.1137	58.3286	58.0654	59.7107	58.8870
10.0000	71.1085	60.8355	60.8354	61.2285	61.2281	62.4156	62.3969	64.6118	64.3485	66.0139	65.1701
12.0000	83.6749	73.4018	73.4017	73.7948	73.7944	74.9820	74.9633	76.9149	76.9149	78.5803	77.7365
15.0000	102.5243	92.2513	92.2513	92.6444	92.6440	93.8314	93.8127	95.0276	95.7643	97.4297	96.5859
20.0000	133.9401	123.6671	123.6671	124.0601	124.0598	125.2472	125.2286	127.4434	127.1802	128.8455	128.0018
30.0000	196.7717	186.4987	186.4987	186.8914	186.8914	188.0789	188.0602	190.2750	190.0118	191.6771	190.8333
ln C_A	-0.5424	20.0037	20.0037	19.2173	19.2181	16.8433	16.8808	12.4510	12.9775	9.6468	11.3346
C_A	0.5813	4.869568E8	4.8699E8	2.2185E8	2.2203E8	2.0652E7	2.1440E7	2.5551E5	4.325E5	1.5472E4	8.364984E4
t_{DA}(PSS)	0.90	0.90	0.90	0.90	0.90	0.20	0.20	0.90	0.90	0.90	0.90

TABLE C-1(i). Δp_D VERSUS t_{DA} FOR A CLOSED 2:1 RECTANGLE

WITH WELL AT $x_D=0.875$, $y_D=0.5$, $\dfrac{\sqrt{A}}{r_w}=2000$

From Earlougher and Ramey (1973)

DIMENSIONLESS

DIMENSIONLESS PRESSURE DROP, Δp_D

t_{DA}	WELL POINT X=0.5000 Y=0.5000	X=0.5000 Y=0.7500	X=0.5000 Y=1.0000	X=0.6250 Y=0.5000	X=0.7500 Y=0.5000	X=0.7500 Y=0.7500	x=0.7500 Y=1.0000	X=1.0000 Y=0.5000	X=1.0000 Y=0.7500	X=1.0000 Y=1.0000
A/B**2=	64.0000	16.0000	16.0000	16.0000	4.0000	3.7647	3.2000	1.0000	0.9846	0.9412
0.0020	4.89814	0.02609	0.00005	0.00002	0.00000	0.00000	0.00000	0.00000	0.00000	0.00000
0.0030	5.10087	0.06751	0.00090	0.00045	0.00000	0.00000	0.00000	0.00000	0.00000	0.00000
0.0040	5.24471	0.11411	0.00423	0.00212	0.00000	0.00000	0.00000	0.00000	0.00000	0.00000
0.0050	5.35628	0.16073	0.01114	0.00557	0.00000	0.00000	0.00000	0.00000	0.00000	0.00000
0.0060	5.44745	0.20555	0.02173	0.01087	0.00000	0.00000	0.00000	0.00000	0.00000	0.00000
0.0070	5.52453	0.24897	0.03561	0.01781	0.00001	0.00000	0.00000	0.00000	0.00000	0.00000
0.0080	5.59133	0.28830	0.05219	0.02610	0.00004	0.00000	0.00000	0.00000	0.00000	0.00000
0.0090	5.65030	0.32640	0.07089	0.03546	0.00012	0.00004	0.00001	0.00000	0.00000	0.00000
0.0100	5.70313	0.36260	0.09119	0.04564	0.00014	0.00009	0.00003	0.00000	0.00000	0.00000
0.0200	6.06057	0.65608	0.32147	0.16491	0.02489	0.00504	0.00424	0.00000	0.00000	0.00000
0.0300	6.29579	0.88141	0.53693	0.28938	0.05678	0.02338	0.02188	0.00003	0.00003	0.00003
0.0400	6.48746	1.07139	0.72519	0.41154	0.05500	0.05500	0.05324	0.00036	0.00036	0.00036
0.0500	6.6551	1.2388	0.8923	0.5298	0.0984	0.0965	0.0947	0.0017	0.0017	0.0017
0.0600	6.8065	1.3901	1.0435	0.6436	0.1468	0.1450	0.1431	0.0049	0.0049	0.0049
0.0700	6.9457	1.5292	1.1826	0.7530	0.2000	0.1981	0.1962	0.0109	0.0109	0.0109
0.0800	7.0752	1.6587	1.3122	0.8581	0.2563	0.2544	0.2525	0.0202	0.0202	0.0201
0.0900	7.1968	1.7804	1.4338	0.9593	0.3147	0.3128	0.3109	0.0330	0.0330	0.0330
0.1000	7.3119	1.8954	1.5488	1.0569	0.3745	0.3727	0.3708	0.0496	0.0495	0.0495
0.2000	8.2439	2.8275	2.4809	1.8957	0.9968	0.9950	0.9931	0.3862	0.3862	0.3862
0.3000	8.9833	3.5668	3.2203	2.6025	1.6259	1.6232	1.6213	0.9037	0.9037	0.9037
0.4000	9.6530	4.2365	3.8899	3.2600	2.2533	2.2515	2.2496	1.4906	1.4906	1.4906
0.5000	10.2967	4.8803	4.5337	3.8992	2.8816	2.8798	2.8779	2.1036	2.1035	2.1035
0.6000	10.9308	5.5143	5.1678	4.5316	3.5100	3.5062	3.5062	2.7261	2.7261	2.7261
0.7000	11.5612	6.1448	5.7982	5.1614	4.1383	4.1364	4.1346	3.3523	3.3523	3.3523
0.8000	12.1903	6.7739	6.4273	5.7903	4.7666	4.7647	4.7629	3.9798	3.9798	3.9798
0.9000	12.8189	7.4025	7.0559	6.4188	5.3949	5.3931	5.3912	4.6078	4.6078	4.6078
1.0000	13.4474	8.0309	7.6843	7.0472	6.0232	6.0214	6.0195	5.2361	5.2360	5.2360
2.0000	19.7306	14.3142	13.9676	13.3305	12.3064	12.3045	12.3027	11.5191	11.5191	11.5191
3.0000	26.0238	20.5973	20.2508	19.6136	18.3896	18.5877	18.5858	17.8023	17.8023	17.8023
4.0000	32.2969	26.8805	26.5339	25.8968	24.8727	24.8709	24.8690	24.0855	24.0855	24.0835
5.0000	38.5801	33.1637	32.8171	32.1800	31.1559	31.1540	31.1522	30.3686	30.3686	30.3686
6.0000	44.8633	39.4468	39.1003	38.4631	37.4391	37.4372	37.4353	36.6518	36.6518	36.6518
7.0000	51.1464	45.7300	45.3834	44.7463	43.7222	43.7204	43.7185	42.9350	42.9350	42.9350
8.0000	57.4295	52.0131	51.6665	51.0294	50.0054	50.0035	50.0017	49.2182	49.2182	49.2181
9.0000	63.7127	58.2963	57.9497	57.3126	56.2885	56.2867	56.2848	55.5013	55.5013	55.5013
10.0000	69.9959	64.5795	64.2329	63.5958	62.5717	62.5698	62.5680	61.7844	61.7844	61.7844
12.0000	82.5622	77.1458	76.7992	76.1621	75.1380	75.1362	75.1343	74.3508	74.3508	74.3508
15.0000	101.4117	95.6887	95.5487	95.0116	93.9875	93.9856	93.9838	93.2003	93.2003	93.2003
20.0000	132.8275	127.4111	127.0646	126.4274	125.4033	125.4015	125.3996	124.6160	124.6161	124.6161
30.0000	195.6591	190.2627	189.8961	189.2590	188.2349	188.2331	188.2312	187.4476	187.4477	187.4477
ln C_A C_A	1.6828 5.3806	12.5157 2.7259E5	13.2088 5.451685	14.4831 1.949486	16.5312 1.5111E7	16.5349 1.5171E7	16.5386 1.5228E7	18.1057 7.2981E7	18.1057 7.2981E7	18.1057 7.2980E7
t_{DA}(PSS)	0.50	0.50	0.50	0.40	0.10	0.10	0.10	0.50	0.50	0.50

OBSERVATION POINTS

TABLE C-1(j). Δp_D VERSUS t_{DA} FOR A CLOSED 4:1 RECTANGLE

WITH WELL AT $x_D = 0.5$, $y_D = 0.5$, $\dfrac{\sqrt{A}}{r_w} = 2000$

From Earlougher and Ramey (1973)

DIMENSIONLESS

DIMENSIONLESS PRESSURE DROP, Δp_D

OBSERVATION POINTS

t_DA	WELL POINT X=0.7500 Y=0.5000	X=0.0000 Y=0.5000	X=0.0000 Y=0.7500	X=0.0000 Y=1.0000	X=0.1250 Y=0.5000	X=0.2500 Y=0.5000	X=0.2500 Y=0.7500	X=0.2500 Y=1.0000	X=0.3750 Y=0.5000	X=0.5000 Y=0.5000	X=0.5000 Y=0.7500
A/R**2 =		0.4444	0.4414	0.4324	0.6400	1.0000	0.9846	0.9412	1.7778	4.0000	3.7647
0.0020	4.89814	0.00000	0.00000	0.00000	0.00000	0.00000	0.00000	0.00000	0.00000	0.00000	0.00000
0.0030	5.10087	0.00000	0.00000	0.00000	0.00000	0.00000	0.00000	0.00000	0.00000	0.00000	0.00000
0.0040	5.24471	0.00000	0.00000	0.00000	0.00000	0.00000	0.00000	0.00000	0.00000	0.00000	0.00000
0.0050	5.35628	0.00000	0.00000	0.00000	0.00000	0.00000	0.00000	0.00000	0.00000	0.00000	0.00000
0.0060	5.44745	0.00000	0.00000	0.00000	0.00000	0.00000	0.00000	0.00000	0.00000	0.00000	0.00000
0.0070	5.52453	0.00000	0.00000	0.00000	0.00000	0.00000	0.00000	0.00000	0.00000	0.00000	0.00000
0.0080	5.59133	0.00000	0.00000	0.00000	0.00000	0.00000	0.00000	0.00000	0.00000	0.00000	0.00000
0.0090	5.65030	0.00000	0.00000	0.00000	0.00000	0.00000	0.00000	0.00000	0.00000	0.00006	0.00004
0.0100	5.70313	0.00000	0.00000	0.00000	0.00000	0.00000	0.00000	0.00000	0.00006	0.00014	0.00009
0.0200	6.06057	0.00000	0.00000	0.00000	0.00000	0.00000	0.00000	0.00000	0.00001	0.00584	0.00504
0.0300	6.29581	0.00000	0.00000	0.00000	0.00000	0.00002	0.00002	0.00002	0.00098	0.02489	0.02338
0.0400	6.48765	0.00000	0.00000	0.00000	0.00000	0.00018	0.00018	0.00018	0.00447	0.05678	0.05300
0.0500	6.6560	0.0000	0.0000	0.0000	0.0000	0.0008	0.0008	0.0008	0.0118	0.0984	0.0965
0.0600	6.8090	0.0000	0.0000	0.0000	0.0002	0.0025	0.0025	0.0025	0.0236	0.1468	0.1450
0.0700	6.9531	0.0001	0.0001	0.0001	0.0005	0.0054	0.0054	0.0054	0.0395	0.2090	0.1981
0.0800	7.0853	0.0002	0.0002	0.0002	0.0012	0.0101	0.0101	0.0101	0.0594	0.2563	0.2584
0.0900	7.2134	0.0005	0.0005	0.0005	0.0025	0.0165	0.0165	0.0163	0.0826	0.3147	0.3128
0.1000	7.3367	0.0012	0.0012	0.0012	0.0044	0.0248	0.0248	0.0248	0.1088	0.3745	0.3727
0.2000	8.4340	0.0472	0.0472	0.0472	0.0790	0.1965	0.1965	0.1965	0.4462	0.9968	0.9950
0.3000	9.4056	0.1989	0.1989	0.1989	0.2648	0.4820	0.4820	0.4820	0.9066	1.6250	1.6232
0.4000	10.3000	0.4520	0.4520	0.4520	0.5463	0.8444	0.8444	0.8444	1.3908	2.2533	2.2515
0.5000	11.1361	0.7869	0.7869	0.7869	0.9035	1.2652	1.2652	1.2652	1.9068	2.8816	2.8798
0.6000	11.9267	1.1859	1.1859	1.1859	1.3199	1.7313	1.7313	1.7313	2.4473	3.5100	3.5081
0.7000	12.6818	1.6351	1.6351	1.6351	1.7827	2.2330	2.2330	2.2330	3.0071	4.1383	4.1364
0.8000	13.4092	2.1234	2.1234	2.1234	2.2817	2.7623	2.7623	2.7623	3.5818	4.7666	4.7647
0.9000	14.1149	2.6423	2.6423	2.6423	2.8089	3.3132	3.3132	3.3132	4.1683	5.3949	5.3931
1.0000	14.8037	3.1852	3.1852	3.1852	3.3583	3.8811	3.8811	3.8811	4.7639	6.0232	6.0214
2.0000	21.2846	9.1888	9.1888	9.1888	9.3832	9.9666	9.9666	9.9666	10.9401	12.3064	12.3045
3.0000	27.5846	15.4483	15.4483	15.4483	15.6445	16.2330	16.2331	16.2331	17.2142	18.5896	18.5877
4.0000	33.8691	21.7295	21.7295	21.7295	21.9258	22.5148	22.5148	22.5148	23.4966	24.8727	24.8709
5.0000	40.1524	28.0125	28.0125	28.0125	28.2088	28.7978	28.7979	28.7979	29.7797	31.1559	31.1540
6.0000	46.4356	34.2956	34.2956	34.2956	34.4920	35.0810	35.0810	35.0810	36.0629	37.4391	37.4372
7.0000	52.7188	40.5787	40.5787	40.5787	40.7751	41.3642	41.3642	41.3642	42.3460	43.7222	43.7204
8.0000	59.0020	46.8619	46.8619	46.8619	47.0582	47.6472	47.6473	47.6473	48.6291	50.0054	50.0035
9.0000	65.2851	53.1450	53.1450	53.1451	53.3414	53.9304	53.9304	53.9304	54.9123	56.2885	56.2867
10.0000	71.5683	59.4282	59.4282	59.4282	59.6246	60.2136	60.2136	60.2136	61.1955	62.5717	62.5698
12.0000	84.1346	71.9946	71.9946	71.9946	72.1909	72.7799	72.7800	72.7800	73.7618	75.1380	75.1362
15.0000	102.9840	90.8441	90.8441	90.8441	91.0405	91.6295	91.6295	91.6295	92.6113	93.9875	93.9856
20.0000	134.3999	122.2598	122.2598	122.2598	122.4562	123.0452	123.0453	123.0453	124.0271	125.4033	125.4015
30.0000	197.2314	185.0915	185.0916	185.0916	185.2879	185.8769	185.8769	185.8769	186.8587	188.2349	188.2331
ln C_A	-1.4619	22.8182	22.8182	22.8181	22.4255	21.2473	21.2473	21.2473	19.2837	16.5312	16.5349
C_A	0.2318	8.1252E9	8.1246E9	8.1244E9	5.4860E9	1.6888E9	1.6888E9	1.6888E9	2.3702E8	1.5115E7	1.5171E7
C_DA (PSS)	2.00	2.00	2.00	2.00	2.00	2.00	2.00	2.00	1.00	0.10	0.10

TABLE C-1(k). Δp_D VERSUS t_DA FOR A CLOSED 4:1 RECTANGLE WITH WELL AT $x_D = 0.75$, $y_D = 0.5$, $\frac{\sqrt{A}}{r_w} = 2000$

From Earlougher and Ramey (1973)

DIMENSIONLESS PRESSURE DROP, Δp_D

OBSERVATION POINTS

DIMENSIONLESS TIME t_{DA}	WELL POINT X=0.5000 Y=1.0000	X=0.6250 Y=0.5000	X=0.6250 Y=0.7500	X=0.7500 Y=0.7500	X=0.7500 Y=1.0000	X=0.8750 Y=0.5000	X=0.8750 Y=0.7500	X=1.0000 Y=0.5000	X=1.0000 Y=0.7500	X=1.0000 Y=1.0000
A/r**2=	3.2000	16.0000	12.8000	64.0000	16.0000	16.0000	12.8000	4.0000	3.7647	3.2000
0.0020	0.00000	0.00002	0.00000	0.02609	0.00005	0.00002	0.00000	0.00000	0.00000	0.00000
0.0030	0.00000	0.00043	0.00010	0.06151	0.00090	0.00045	0.00010	0.00000	0.00000	0.00000
0.0040	0.00000	0.00212	0.00066	0.11411	0.00423	0.00212	0.00066	0.00000	0.00000	0.00000
0.0050	0.00000	0.00557	0.00212	0.16073	0.01114	0.00557	0.00212	0.00000	0.00000	0.00000
0.0060	0.00000	0.01087	0.00474	0.20555	0.02173	0.01087	0.00474	0.00000	0.00000	0.00000
0.0070	0.00000	0.01781	0.00838	0.24807	0.03561	0.01781	0.00858	0.00001	0.00000	0.00000
0.0080	0.00001	0.02610	0.01358	0.28830	0.05219	0.02610	0.01358	0.00005	0.00003	0.00001
0.0090	0.00002	0.03546	0.01964	0.32640	0.07089	0.03546	0.01964	0.00012	0.00008	0.00004
0.0100	0.00015	0.04564	0.02662	0.36260	0.09119	0.04564	0.02662	0.00027	0.00018	0.00009
0.0200	0.00424	0.16491	0.12620	0.65608	0.32147	0.16497	0.12626	0.01168	0.01007	0.00843
0.0300	0.02188	0.28938	0.24561	0.88143	0.53694	0.29036	0.24655	0.04978	0.04677	0.04376
0.0400	0.05324	0.41154	0.36670	1.07157	0.72537	0.41601	0.37110	0.11356	0.11061	0.10648
0.0500	0.0947	0.5298	0.4848	1.2396	0.8931	0.5416	0.4965	0.1968	0.1931	0.1894
0.0600	0.1431	0.6438	0.5987	1.3925	1.0460	0.6672	0.6220	0.2937	0.2899	0.2862
0.0700	0.1962	0.7535	0.7086	1.5347	1.1881	0.7925	0.7473	0.3999	0.3961	0.3924
0.0800	0.2525	0.8593	0.8142	1.6688	1.3222	0.9174	0.8722	0.5123	0.5085	0.5048
0.0900	0.3109	0.9617	0.9166	1.7969	1.4503	1.0418	0.9967	0.6288	0.6251	0.6213
0.1000	0.3708	1.0612	1.0161	1.9202	1.5736	1.1656	1.1204	0.7479	0.7442	0.7404
0.2000	0.9931	1.9604	1.9153	3.0172	2.6706	2.1476	2.3024	1.9464	1.9427	1.9390
0.3000	1.6213	2.7766	2.7315	3.9885	3.6419	3.4185	3.3733	3.0511	3.0474	3.0437
0.4000	2.2496	3.5491	3.5040	4.8827	4.5362	4.3936	4.3484	4.0546	4.0509	4.0472
0.5000	2.8779	4.2898	4.2447	5.7186	5.3721	5.2931	5.2479	4.9764	4.9726	4.9689
0.6000	3.5062	5.0058	4.9607	6.5091	6.1625	6.1333	6.0881	5.8340	5.8303	5.8265
0.7000	4.1346	5.7027	5.6576	7.2641	6.9175	6.9271	6.8819	6.6415	6.6378	6.6340
0.8000	4.7629	6.3846	6.3395	7.9914	7.6448	7.6848	7.6396	7.4098	7.4061	7.4023
0.9000	5.3912	7.0548	7.0097	8.6971	8.3505	8.4141	8.3690	8.1473	8.1438	8.1401
1.0000	6.0195	7.7158	7.6707	9.3858	9.0393	9.1214	9.0762	8.8613	8.8576	8.8538
2.0000	12.3027	14.1059	14.0608	15.8666	15.5201	15.6628	15.6176	15.4240	15.4202	15.4165
3.0000	18.5858	20.3982	20.3531	22.1666	21.8200	21.9679	21.9227	21.7308	21.7271	21.7234
4.0000	24.8690	26.6821	26.6370	28.4511	28.1046	28.2528	28.2077	28.0160	28.0122	28.0085
5.0000	31.1522	32.9653	32.9202	34.7344	34.3879	34.5362	34.4910	34.2993	34.2956	34.2918
6.0000	37.4353	39.2485	39.2034	41.0176	40.6710	40.8196	40.7742	40.5825	40.5787	40.5750
7.0000	43.7185	45.5317	45.4866	47.3008	46.9542	47.1025	47.0574	46.8657	46.8620	46.8583
8.0000	50.0017	51.8149	51.7698	53.5840	53.2374	53.3858	53.3406	53.1489	53.1452	53.1415
9.0000	56.2848	58.0980	58.0529	59.8671	59.5205	59.6689	59.6237	59.4321	59.4283	59.4246
10.0000	62.5680	64.3811	64.3361	66.1503	65.8037	65.9521	65.9069	65.7152	65.7115	65.7077
12.0000	75.1343	76.9475	76.9024	78.7166	78.3700	78.5184	78.4732	78.2815	78.2778	78.2740
15.0000	93.9838	95.7969	95.7518	97.5660	97.2194	97.3678	97.3226	97.1272	97.1234	97.1234
20.0000	125.3996	127.2128	127.1677	128.9819	128.6354	128.7837	128.7385	128.5868	128.5431	128.5394
30.0000	188.2312	190.0443	189.9992	191.8134	191.4669	191.6152	191.5700	191.3783	191.3746	191.3709
$\ln C_A$ / C_A	16.5386 / 1.52288E7	12.9123 / 4.0526E5	13.0025 / 4.4351E5	9.3741 / 1.1779E4	10.0672 / 2.3558E4	9.7705 / 1.7509E4	9.8608 / 1.9164E4	10.2442 / 2.8118E4	10.2516 / 2.8339E4	10.2591 / 2.8541E4
c_{DA}(PSS)	0.10	1.00	1.00	2.00	2.00	2.00	2.00	0.03	0.03	0.03

TABLE C-1(k)cont. Δp_D VERSUS t_{DA} FOR A CLOSED 4:1 RECTANGLE
WITH WELL AT $x_D=0.75$, $y_D=0.5$, $\dfrac{\sqrt{A}}{r_w}=2000$

From Earlougher and Ramey (1973)

(Schematic diagram of a 4:1 rectangle with axes x_D (horizontal) and y_D (vertical), with well and observation points marked; axis markers 0, 1, 4.)

DIMENSIONLESS PRESSURE DROP, Δp_D

DIMENSIONLESS TIME t_{DA}	WELL POINT X=0.5003 Y=0.7500	OBSERVATION POINTS X=0.5000 Y=0.0000	X=0.5000 Y=0.5000	X=0.5000 Y=1.0000	X=0.7500 Y=0.0000	X=0.7500 Y=0.5000	X=0.7500 Y=0.7500	X=0.7500 Y=1.0000	X=1.0000 Y=0.0000	X=1.0000 Y=0.5000	X=1.0000 Y=1.0000
$A/R^{**}2\to$		7.1111	64.0000	64.0000	2.5600	3.7647	4.6000	3.7647	0.8767	0.9846	0.9846
0.0020	4.89816	0.00000	0.02609	0.05219	0.00000	0.00000	0.00000	0.00000	0.00000	0.00000	0.00000
0.0030	5.10132	0.00000	0.06751	0.13501	0.00000	0.00000	0.00000	0.00000	0.00000	0.00000	0.00000
0.0040	5.24683	0.00002	0.11411	0.22821	0.00000	0.00000	0.00000	0.00000	0.00000	0.00000	0.00000
0.0050	5.36185	0.00011	0.16073	0.32135	0.00000	0.00000	0.00000	0.00000	0.00000	0.00000	0.00000
0.0060	5.45831	0.00042	0.20555	0.41068	0.00000	0.00000	0.00000	0.00000	0.00000	0.00000	0.00000
0.0070	5.54232	0.00112	0.24807	0.49503	0.00000	0.00001	0.00001	0.00001	0.00000	0.00000	0.00000
0.0080	5.61738	0.00235	0.28830	0.57424	0.00000	0.00003	0.00003	0.00003	0.00000	0.00000	0.00000
0.0090	5.68562	0.00424	0.32640	0.64856	0.00000	0.00007	0.00016	0.00007	0.00000	0.00000	0.00000
0.0100	5.74845	0.00684	0.36260	0.71835	0.00001	0.00016	0.00036	0.00016	0.00001	0.00000	0.00000
0.0200	6.21016	0.07004	0.65608	1.24212	0.00136	0.00769	0.00872	0.00769	0.00504	0.00002	0.00003
0.0300	6.52065	0.17510	0.88141	1.58773	0.01023	0.03274	0.03654	0.03274	0.02338	0.00017	0.00023
0.0400	6.75887	0.29685	1.07139	1.84593	0.03068	0.07226	0.07933	0.07226	0.05500	0.00049	0.00036
0.0500	6.9549	0.4238	1.2388	2.0538	0.0623	0.0965	0.1208	0.0965	0.1308	0.0013	0.0021
0.0600	7.1236	0.5504	1.3901	2.2297	0.1029	0.1450	0.1748	0.1450	0.1871	0.0040	0.0059
0.0700	7.2735	0.6743	1.5292	2.3841	0.1502	0.1981	0.2320	0.1981	0.2460	0.0093	0.0125
0.0800	7.4098	0.7943	1.6587	2.5232	0.2023	0.2544	0.2912	0.2544	0.3064	0.0179	0.0224
0.0900	7.5357	0.9099	1.7804	2.6509	0.2579	0.3128	0.3517	0.3128	0.3677	0.0301	0.0359
0.1000	7.6535	1.0211	1.8954	2.7698	0.3157	0.3727	0.4130	0.3727	0.4296	0.0461	0.0530
0.2000	8.5904	1.9462	2.8275	3.7088	0.9338	0.9950	1.0382	0.9950	1.0561	0.3810	0.3914
0.3000	9.3299	2.6855	3.5669	4.4482	1.5620	1.6232	1.6665	1.6232	1.6843	0.8984	0.9090
0.4000	9.9995	3.3551	4.2365	5.1179	2.1903	2.2515	2.2948	2.2515	2.3127	1.4854	1.4959
0.5000	10.6433	3.9989	4.8803	5.7617	2.8186	2.8798	2.9231	2.8798	2.9410	2.0983	2.1088
0.6000	11.2774	4.6329	5.5143	6.3957	3.4469	3.5081	3.5514	3.5081	3.5693	2.7208	2.7314
0.7000	11.9078	5.2634	6.1448	7.0262	4.0752	4.1364	4.1797	4.1364	4.1976	3.3470	3.3576
0.8000	12.5369	5.8925	6.7739	7.6553	4.7036	4.7647	4.8081	4.7647	4.8259	3.9745	3.9851
0.9000	13.1655	6.5211	7.4025	8.2838	5.3319	5.3931	5.4364	5.3931	5.4542	4.6026	4.6131
1.0000	13.7939	7.1495	8.0309	8.9123	5.9602	6.0214	6.0647	6.0214	6.0826	5.2360	5.2413
2.0000	20.0772	13.4328	14.3142	15.1956	12.2433	12.3045	12.3479	12.3045	12.3657	11.5191	11.5244
3.0000	26.3604	19.7159	20.5973	21.4787	18.5265	18.5877	18.6310	18.5877	18.6489	17.7970	17.8076
4.0000	32.6435	25.9991	26.8805	27.7619	24.8096	24.8709	24.9142	24.8709	24.9321	24.0855	24.0908
5.0000	38.9267	32.2823	33.1636	34.0451	31.0928	31.1540	31.1974	31.1540	31.2152	30.3686	30.3739
6.0000	45.2098	38.5654	39.4468	40.3282	37.3760	37.4372	37.4805	37.4372	37.4984	36.6518	36.6570
7.0000	51.4930	44.8486	45.7300	46.6114	43.6591	43.7203	43.7637	43.7203	43.7815	42.9296	42.9402
8.0000	57.7761	51.1316	52.0131	52.8945	49.9423	50.0035	50.0468	50.0035	50.0647	49.2181	49.2234
9.0000	64.0593	57.4149	58.2963	59.1777	56.2254	56.2867	56.3300	56.2867	56.3479	55.5012	55.5065
10.0000	70.3425	63.6980	64.5794	65.4609	62.5086	62.5698	62.6131	62.5698	62.6310	61.7844	61.7897
12.0000	82.9088	76.2644	77.1457	78.0271	75.0749	75.1362	75.1795	75.1362	75.1974	74.3507	74.3563
15.0000	101.7583	95.1138	95.9952	96.8766	93.9244	93.9856	94.0290	93.9856	94.0468	93.2002	93.2055
20.0000	133.1741	126.5296	127.4411	128.2925	125.3402	125.4014	125.4448	125.4014	125.4626	124.6160	124.6213
30.0000	196.0057	189.3612	190.2427	191.1241	188.1718	188.2330	188.2764	188.2330	188.2943	187.4476	187.4529
1+ C_A / C_A	0.9896 / 2.6902	14.2386 / 1.5890E6	12.5158 / 2.7260E5	10.7529 / 4.6765E4	16.6574 / 1.7148E7	16.5350 / 1.5172E7	16.4483 / 1.3912E7	16.5350 / 1.5172E7	16.4125 / 1.3424E7	18.1057 / 7.2982E7	18.0952 / 7.2215E7
t_{DA} (PSS)	0.50	0.01	0.50	0.50	0.10	0.10	0.10	0.10	0.09	0.50	0.50

TABLE C-1(I). Δp_D VERSUS t_{DA} FOR A CLOSED 4:1 RECTANGLE

WITH WELL AT $x_D = 0.5$, $y_D = 0.75$, $\dfrac{\sqrt{A}}{r_w} = 2000$

From Earlougher and Ramey (1973)

DIMENSIONLESS PRESSURE DROP, Δp_D

DIMENSIONLESS TIME t_{DA}

OBSERVATION POINTS

t_{DA}	WELL POINT X=0.7503 Y=0.7508	X=0.0000 Y=0.0000	X=0.0000 Y=0.5000	X=0.0000 Y=1.0000	X=0.2500 Y=0.2500	X=0.2500 Y=0.5000	X=0.2500 Y=0.7500	X=0.5000 Y=0.0000	X=0.5000 Y=0.2500	X=0.5000 Y=0.5000	X=0.5000 Y=0.7500
A/r_w^2=	0.4183	0.4414	0.4414	0.4414	0.9412	0.9646	1.0000	2.5600	3.2000	3.7647	4.0000
0.0020	4.89816	0.00000	0.00000	0.00000	0.00000	0.00000	0.00000	0.00000	0.00000	0.00000	0.00000
0.0030	5.10132	0.00000	0.00000	0.00000	0.00000	0.00000	0.00000	0.00000	0.00000	0.00000	0.00000
0.0040	5.24683	0.00000	0.00000	0.00000	0.00000	0.00000	0.00000	0.00000	0.00000	0.00000	0.00000
0.0050	5.36185	0.00000	0.00000	0.00000	0.00000	0.00000	0.00000	0.00000	0.00000	0.00000	0.00000
0.0060	5.45831	0.00000	0.00000	0.00000	0.00000	0.00000	0.00000	0.00000	0.00000	0.00000	0.00000
0.0070	5.54232	0.00000	0.00000	0.00000	0.00000	0.00000	0.00000	0.00000	0.00000	0.00000	0.00001
0.0080	5.61738	0.00000	0.00000	0.00000	0.00000	0.00000	0.00000	0.00000	0.00001	0.00001	0.00003
0.0090	5.68562	0.00000	0.00000	0.00000	0.00000	0.00000	0.00000	0.00004	0.00001	0.00009	0.00007
0.0100	5.74845	0.00000	0.00000	0.00000	0.00001	0.00000	0.00000	0.00016	0.00009	0.00009	0.00016
0.0200	6.21016	0.00000	0.00000	0.00000	0.00002	0.00009	0.00002	0.00239	0.00136	0.00504	0.00769
0.0300	6.52067	0.00000	0.00000	0.00000	0.00001	0.00002	0.00018	0.01403	0.01023	0.02338	0.03274
0.0400	6.75910	0.00000	0.00000	0.00000	0.00008	0.00008	0.00922	0.03776	0.03068	0.05500	0.07226
0.0500	6.9559	0.0000	0.0000	0.0000	0.0007	0.0008	0.0010	0.0623	0.0723	0.0965	0.1208
0.0600	7.1264	0.0000	0.0000	0.0000	0.0021	0.0025	0.0028	0.1029	0.1152	0.1450	0.1748
0.0700	7.2796	0.0001	0.0001	0.0001	0.0049	0.0054	0.0060	0.1502	0.1642	0.1981	0.2320
0.0800	7.4207	0.0002	0.0002	0.0002	0.0093	0.0101	0.0109	0.2023	0.2175	0.2544	0.2912
0.0900	7.5533	0.0005	0.0005	0.0006	0.0155	0.0165	0.0175	0.2579	0.2739	0.3128	0.3517
0.1000	7.6796	0.0011	0.0012	0.0012	0.0236	0.0248	0.0260	0.3157	0.3323	0.3727	0.4130
0.2000	8.7823	0.0470	0.0472	0.0474	0.1946	0.1965	0.1983	0.9338	0.9517	0.9950	1.0382
0.3000	9.7540	0.1987	0.1989	0.1991	0.4801	0.4820	0.4839	1.5620	1.5798	1.6232	1.6665
0.4000	10.6485	0.4518	0.4520	0.4523	0.8425	0.8444	0.8463	2.1903	2.2081	2.2515	2.2948
0.5000	11.4845	0.7867	0.7869	0.7871	1.2633	1.2652	1.2670	2.8186	2.8364	2.8798	2.9231
0.6000	12.2751	1.1857	1.1859	1.1862	1.7293	1.7313	1.7332	3.4469	3.4648	3.5081	3.5514
0.7000	13.0302	1.6351	1.6353	1.6353	2.2311	2.2330	2.2348	4.0752	4.0931	4.1364	4.1797
0.8000	13.7576	2.1234	2.1236	2.1236	2.7604	2.7623	2.7641	4.7036	4.7214	4.7647	4.8081
0.9000	14.4633	2.6423	2.6426	2.6426	3.3113	3.3132	3.3151	5.3319	5.3497	5.3931	5.4364
1.0000	15.1521	3.1849	3.1854	3.1854	3.8792	3.8811	3.8830	5.9602	5.9780	6.0214	6.0647
2.0000	21.6331	9.1886	9.1891	9.1891	9.9648	9.9666	9.9685	12.2433	12.2612	12.3045	12.3479
3.0000	27.9930	15.4481	15.4485	15.4465	16.2312	16.2331	16.2349	18.5265	18.5444	18.5877	18.6310
4.0000	34.2176	21.7293	21.7297	21.7297	22.5148	22.5168	22.5167	24.8096	24.8275	24.8709	24.9142
5.0000	40.5009	28.0122	28.0127	28.0127	28.7960	28.7978	28.7997	31.0928	31.1107	31.1540	31.1974
6.0000	46.7840	34.2954	34.2959	34.2959	35.0791	35.0810	35.0829	37.3760	37.3938	37.4372	37.4805
7.0000	53.0672	40.5787	40.5790	40.5790	41.3623	41.3642	41.3660	43.6591	43.6770	43.7203	43.7637
8.0000	59.3505	46.8616	46.8621	46.8621	47.6453	47.6472	47.6491	49.9423	49.9602	50.0035	50.0468
9.0000	65.6336	53.1447	53.1453	53.1453	53.9285	53.9304	53.9323	56.2254	56.2433	56.2867	56.3300
10.0000	71.9167	59.4282	59.4284	59.4284	60.2117	60.2136	60.2155	62.5086	62.5265	62.5698	62.6131
12.0000	84.6830	71.9943	71.9948	71.9948	72.7780	72.7799	72.7818	75.0749	75.0928	75.1362	75.1795
15.0000	103.3325	90.8439	90.8444	90.8444	91.6276	91.6295	91.6314	93.9244	93.9423	93.9856	94.0290
20.0000	134.7484	122.2595	122.2601	122.2601	123.0433	123.0452	123.0471	125.3402	125.3581	125.4014	125.4448
30.0000	197.5799	185.0912	185.0918	185.0918	185.8750	185.8769	185.8787	188.1718	188.1897	188.2330	188.2764
ln C_A	-2.1588	22.8187	22.8182	22.8177	21.2511	21.2473	21.2536	16.6574	16.6216	16.5350	16.4483
C_A	0.1153	8.1293E9	8.1232E9	8.1210E9	1.6953E9	1.6889E9	1.6825E9	1.7148E7	1.6545E7	1.5172E7	1.3912E7
t_{DA}(pss)	2.00	2.00	2.00	2.00	2.00	2.00	2.00	0.10	0.10	0.10	0.10

TABLE C-1(m). Δp_D VERSUS t_{DA} FOR A CLOSED 4:1 RECTANGLE WITH WELL AT x_D=0.75, y_D=0.75, $\dfrac{\sqrt{A}}{r_w}$ = 2000

From Earlougher and Ramey (1973)

DIMENSIONLESS PRESSURE DROP, Δp_D

OBSERVATION POINTS

t_{DA}	WELL POINT X=0.5000 Y=1.0000	X=0.6250 Y=0.5000	X=0.6250 Y=0.7500	X=0.7500 Y=0.2500	X=0.7500 Y=0.5000	X=0.8750 Y=0.5000	X=0.8750 Y=0.7500	X=1.0000 Y=0.0000	X=1.0000 Y=0.5000	X=1.0000 Y=1.0000
A/R**2=	3.7647	12.8000	16.0000	16.0000	64.0000	12.8000	16.0000	2.5600	3.7647	3.7647
0.0020	0.00000	0.00000	0.00002	0.00002	0.02609	0.00000	0.00002	0.00000	0.00000	0.00000
0.0030	0.00000	0.00010	0.00045	0.00045	0.06751	0.00014	0.00045	0.00000	0.00000	0.00000
0.0040	0.00000	0.00066	0.00214	0.00212	0.11411	0.00066	0.00214	0.00000	0.00000	0.00000
0.0050	0.00000	0.00212	0.00570	0.00557	0.16073	0.00212	0.00570	0.00000	0.00000	0.00000
0.0060	0.00000	0.00474	0.01132	0.01087	0.20555	0.00474	0.01132	0.00000	0.00000	0.00000
0.0070	0.00001	0.00858	0.01889	0.01782	0.24807	0.00838	0.01889	0.00000	0.00001	0.00001
0.0080	0.00003	0.01358	0.02821	0.02614	0.28830	0.01358	0.02821	0.00000	0.00003	0.00005
0.0090	0.00008	0.01964	0.03905	0.03557	0.32640	0.01964	0.03905	0.00000	0.00008	0.00015
0.0100	0.00017	0.02662	0.05116	0.04586	0.36260	0.02662	0.05116	0.00000	0.00018	0.00035
0.0200	0.00872	0.12621	0.20629	0.17187	0.65608	0.12626	0.20637	0.00271	0.01007	0.01743
0.0300	0.03654	0.24561	0.37043	0.31207	0.88143	0.24655	0.37172	0.02046	0.04677	0.07308
0.0400	0.07933	0.36670	0.52215	0.45392	1.07157	0.37110	0.52774	0.06137	0.11001	0.15865
0.0500	0.1308	0.4848	0.6604	0.5932	1.2396	0.4965	0.6765	0.1246	0.1931	0.2616
0.0600	0.1871	0.5987	0.7873	0.7286	1.3925	0.6220	0.8144	0.2058	0.2899	0.3741
0.0700	0.2460	0.7084	0.9055	0.8597	1.5347	0.7473	0.9494	0.3004	0.3961	0.4919
0.0800	0.3064	0.8142	1.0169	0.9868	1.6688	0.8722	1.0808	0.4045	0.5085	0.6126
0.0900	0.3677	0.9166	1.1229	1.1104	1.7969	0.9967	1.2096	0.5152	0.6251	0.7349
0.1000	0.4296	1.0161	1.2247	1.2306	1.9202	1.1204	1.3363	0.6304	0.7442	0.8560
0.2000	1.0561	1.9153	2.1285	2.3223	3.0172	2.3024	2.5241	1.8207	1.9427	2.0647
0.3000	1.6843	2.7315	2.9447	3.2935	3.9885	3.3733	3.5931	2.9253	3.0474	3.1695
0.4000	2.3127	3.5040	3.7172	4.1877	4.8827	4.3484	4.5703	3.9287	4.0509	4.1731
0.5000	2.9410	4.2467	4.4579	5.0236	5.7186	5.2479	5.4697	4.8505	4.9726	5.0948
0.6000	3.5693	4.9607	5.1739	5.8141	6.5491	6.0881	6.3099	5.7081	5.8303	5.9524
0.7000	4.1976	5.6576	5.8708	6.5691	7.2641	6.8819	7.1037	6.5156	6.6378	6.7599
0.8000	4.8259	6.3395	6.5527	7.2964	7.9914	7.6196	7.8614	7.2839	7.4061	7.5282
0.9000	5.4542	7.0097	7.2229	8.0021	8.6971	8.3689	8.5907	8.0216	8.1438	8.2659
1.0000	6.0826	7.6107	7.8839	8.6908	9.3858	9.0762	9.2980	8.7354	8.8576	8.9737
2.0000	12.3657	14.0608	14.2740	15.1716	15.8666	15.6176	15.8394	15.2981	15.4202	15.5424
3.0000	18.6489	20.3531	20.5663	21.4715	22.1666	21.9227	22.1445	21.6049	21.7271	21.8493
4.0000	24.9321	26.6370	26.8502	27.7561	28.4511	28.2077	28.4295	27.8900	28.0122	28.1344
5.0000	31.2152	32.9202	33.1334	34.0394	34.7344	34.4910	34.7128	34.1734	34.2956	34.4177
6.0000	37.4984	39.2034	39.4166	40.3225	41.0176	40.7742	40.9960	40.4566	40.5787	40.7009
7.0000	43.7815	45.4866	45.6998	46.6057	47.3008	47.0573	47.2792	46.7397	46.8619	46.9841
8.0000	50.0647	51.7697	51.9830	52.8890	53.5840	53.3406	53.5624	53.0230	53.1452	53.2673
9.0000	56.3479	58.0529	58.2661	59.1721	59.8671	59.6237	59.8455	59.3061	59.4283	59.5505
10.0000	62.6310	64.3360	64.5492	65.4552	66.1502	65.9069	66.1287	65.5893	65.7115	65.8336
12.0000	75.1974	76.9024	77.1156	78.0215	78.7166	78.4732	78.6950	78.1556	78.2277	78.3999
15.0000	94.0468	95.7518	95.9650	96.8709	97.5660	97.3226	97.5444	97.0049	97.1271	97.2493
20.0000	125.4626	127.1617	127.3809	128.2868	128.9818	128.7385	128.9603	128.4208	128.5430	128.6652
30.0000	188.2943	189.9992	190.2124	191.1184	191.8134	191.5700	191.7918	191.2524	191.3745	191.4967
½ ln C_A	16.4125	13.0025	12.5761	10.7642	9.3741	9.8609	9.4372	10.4960	10.2517	10.0073
C_A	1.3424E7	4.6353E5	2.8955E5	4.7297E4	1.1780E4	1.9165E4	1.2299E4	3.6172E4	2.8330E4	2.2189E4
t_{DA}(PSS)	0.09	1.00	1.00	2.00	2.00	2.00	2.00	0.04	0.03	2.00

TABLE C-1(m)cont. Δp_D VERSUS t_{DA} FOR A CLOSED 4:1 RECTANGLE
WITH WELL AT $x_D = 0.75$, $y_D = 0.75$, $\frac{\sqrt{A}}{r_w} = 2000$

From Earlougher and Ramey (1973)

DIMENSIONLESS PRESSURE DROP, Δp_D

t_{DA} (DIMENSIONLESS TIME)	WELL POINT X=0.5002 Y=0.5000	OBSERVATION POINTS X=0.5000 Y=0.7500	X=0.5000 Y=1.0000	X=0.6250 Y=0.5000	X=0.7500 Y=0.5000	X=0.7500 Y=0.7500	X=0.7500 Y=1.0000	X=0.8750 Y=0.5000	X=1.0000 Y=0.5000	X=1.0000 Y=0.7500	X=1.0000 Y=1.0000
$A/R^{**}2=$		80.0000	20.0000	12.8000	3.2000	3.0769	2.7586	1.4222	0.8000	0.7921	0.7692
0.0020	4.89814	0.04559	0.00027	0.00000	0.00000	0.00000	0.00000	0.00000	0.00000	0.00000	0.00000
0.0030	5.10087	0.10234	0.00309	0.00010	0.00000	0.00000	0.00000	0.00000	0.00000	0.00000	0.00000
0.0040	5.24471	0.16073	0.01114	0.00066	0.00000	0.00000	0.00000	0.00000	0.00000	0.00000	0.00000
0.0050	5.35629	0.21640	0.02492	0.00212	0.00000	0.00000	0.00000	0.00000	0.00000	0.00000	0.00000
0.0060	5.44747	0.26846	0.04360	0.00473	0.00000	0.00000	0.00000	0.00000	0.00000	0.00000	0.00000
0.0070	5.52462	0.31706	0.06604	0.00854	0.00000	0.00000	0.00000	0.00000	0.00000	0.00000	0.00000
0.0080	5.59156	0.36260	0.09119	0.01348	0.00000	0.00000	0.00000	0.00000	0.00000	0.00000	0.00000
0.0090	5.65078	0.40550	0.11819	0.01942	0.00001	0.00001	0.00000	0.00000	0.00000	0.00000	0.00000
0.0100	5.70400	0.44613	0.14641	0.02622	0.00002	0.00002	0.00001	0.00001	0.00000	0.00000	0.00000
0.0200	6.07435	0.77442	0.43281	0.12128	0.00234	0.00217	0.00200	0.00028	0.00000	0.00000	0.00000
0.0300	6.33067	1.02636	0.68037	0.23716	0.01360	0.01327	0.01295	0.00173	0.00000	0.00000	0.00000
0.0400	6.54356	1.23876	0.89225	0.35844	0.03631	0.03593	0.03556	0.00547	0.00007	0.00007	0.00007
0.0500	6.7308	1.4259	1.0793	0.4794	0.0691	0.0688	0.0684	0.0125	0.0004	0.0005	0.0005
0.0600	6.8999	1.5950	1.2485	0.5979	0.1099	0.1095	0.1091	0.0238	0.0016	0.0016	0.0016
0.0700	7.0555	1.7506	1.4040	0.7130	0.1566	0.1562	0.1558	0.0371	0.0042	0.0042	0.0042
0.0800	7.2003	1.8954	1.5488	0.8245	0.2076	0.2072	0.2068	0.0547	0.0087	0.0087	0.0087
0.0900	7.3363	2.0314	1.6848	0.9336	0.2618	0.2614	0.2610	0.0756	0.0156	0.0156	0.0156
0.1000	7.4649	2.1601	1.8135	1.0373	0.3184	0.3180	0.3176	0.0985	0.0252	0.0252	0.0252
0.2000	8.5041	3.1992	2.8527	1.9645	0.9305	0.9301	0.9297	0.4251	0.2750	0.2750	0.2750
0.3000	9.3122	4.0074	3.6608	2.6995	1.5581	1.5577	1.5573	0.9267	0.7249	0.7249	0.7249
0.4000	10.0219	4.7170	4.3705	3.3853	2.1864	2.1860	2.1856	1.4975	1.2719	1.2719	1.2719
0.5000	10.6872	5.3823	5.0357	4.0397	2.8147	2.8143	2.8140	2.0997	1.8633	1.8633	1.8633
0.6000	11.3323	6.0274	5.6808	4.6799	3.4430	3.4426	3.4423	2.7162	2.4748	2.4749	2.4748
0.7000	11.9682	6.6633	6.3168	5.3136	4.0713	4.0710	4.0706	3.3391	3.0955	3.0955	3.0955
0.8000	12.6000	7.2951	6.9485	5.9443	4.6997	4.6993	4.6989	3.9650	3.7204	3.7204	3.7204
0.9000	13.2299	7.9250	7.5784	6.5738	5.3280	5.3276	5.3272	4.5922	4.3472	4.3472	4.3472
1.0000	13.8589	8.5540	8.2074	7.2026	5.9563	5.9559	5.9555	5.2200	4.9748	4.9748	4.9748
2.0000	20.1426	14.8377	14.4911	13.4862	12.2395	12.2391	12.2387	11.5028	11.2574	11.2574	11.2574
3.0000	26.4258	21.1209	20.7744	19.7693	18.5226	18.5223	18.5219	17.7859	17.5405	17.5405	17.5405
4.0000	32.7089	27.4041	27.0575	26.0525	24.8058	24.8054	24.8050	24.0691	23.8237	23.8237	23.8237
5.0000	38.9921	33.6872	33.3407	32.3356	31.0890	31.0886	31.0882	30.3523	30.1068	30.1068	30.1069
6.0000	45.2753	39.9704	39.6238	38.6188	37.3721	37.3717	37.3714	36.6354	36.3900	36.3900	36.3900
7.0000	51.5585	46.2536	45.9071	44.9020	43.6553	43.6549	43.6545	42.9186	42.6731	42.6731	42.6731
8.0000	57.8416	52.5367	52.1901	51.1851	49.9384	49.9381	49.9377	49.2017	48.9563	48.9563	48.9563
9.0000	64.1248	58.8199	58.4733	57.4683	56.2216	56.2212	56.2208	55.4849	55.2395	55.2395	55.2395
10.0000	70.4079	65.1030	64.7564	63.7514	62.5048	62.5044	62.5040	61.7681	61.5227	61.5227	61.5227
12.0000	82.9743	77.6694	77.3228	76.3178	75.0711	75.0707	75.0703	74.3344	74.0890	74.0890	74.0890
15.0000	101.8237	96.5189	96.1723	95.1673	93.9206	93.9202	93.9198	93.1839	92.9385	92.9384	92.9385
20.0000	133.2395	127.9347	127.5881	126.5831	125.3364	125.3360	125.3356	124.5997	124.3543	124.3543	124.3543
30.0000	196.0711	190.7662	190.4197	189.4147	188.1680	188.1676	188.1673	187.4313	187.1858	187.1858	187.1858
$\ln C_A$	0.8589	11.4686	12.1617	14.1717	16.6658	16.6658	16.6665	18.1384	18.6292	18.6292	18.6292
C_A	2.3605	9.566584	1.913385	1.4279E6	1.727987	1.729287	1.730627	7.5404E7	1.231988	1.231818	1.231988
t_{DA} (PSS)	0.60	0.60	0.60	0.50	0.20	0.20	0.20	0.50	0.60	0.60	0.60

5

y_D

0 — 1

x_D
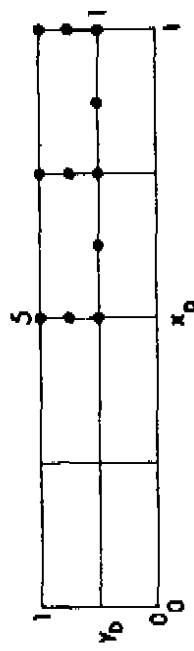
TABLE C-1(n). Δp_D VERSUS t_{DA} FOR A CLOSED 5:1 RECTANGLE WITH WELL AT $x_D=0.5$, $y_D=0.5$, $\dfrac{\sqrt{A}}{r_w}=2000$

From Earlougher and Ramey (1973)

APPENDIX D

COMPUTER PROGRAMS

This appendix contains listings of the following programs:

     BHOLE   –   for conversion of wellhead pressures to bottom
                          hole pressures;

     P-PSI   –   for conversion of pressures to pseudo-pressures;

and the following subroutines:

     FFCFLO   –   for use with BHOLE to calculate friction factors;

     VISCY   –   for use with BHOLE and P-PSI to calculate natural
                          gas viscosities;

     XLGR4   –   for use with VISCY to interpolate viscosity
                          tables;

     ZANDC   –   for use with BHOLE and P-PSI to calculate natural
                          gas compressibility factors. This subroutine also
                          calculates natural gas compressibilities.

The program and subroutines listings are self-explanatory and
complete decks are available from the Energy Resources Conservation
Board.

Examples D-1 to D-8 given in this appendix illustrate the
various options of the program BHOLE. Examples D-9 and D-10 illustrate
the computer calculations for the data from Examples B-1 and B-2 in
Appendix B.

Example D-11 illustrates the operation of program P-PSI using
data from Example 2-1 in Chapter 2. With slight modification, the
program can also list corresponding viscosity, compressibility factor
and compressibility values.

DESCRIPTION OF INPUT DATA FOR PROGRAM BHOLE

CARD NO.				DESCRIPTION	FORMAT
KODEA =					
1	2	3	4		
1	1	1	1	Title	17A4, A2
2	2	2	2	KODEA, KODEB	2I5
3	–	–	–	Specific gravity of the gas	F10.4
–	3	–	–	Specific gravity of the gas, mole fractions of hydrogen sulphide, carbon-dioxide and nitrogen	4F10.4
–	–	3	3	Complete gas composition	12F6.4
–	–	–	4	Pseudo-critical temperature, pseudo-critical pressure and molecular weight $C7^+$	3F10.2
4	4	4	5	Tubing diameter, well depth, tubing length and absolute roughness of tubing	4F10.4
5	5	5	6	Flow rate, wellhead temperature, bottom hole temperature, wellhead pressure, estimated bottom hole pressure	5F10.4

DESCRIPTION OF INPUT DATA FOR PROGRAM P-PSI

CARD NO.	DESCRIPTION	FORMAT
1	Title	17A4, A2
2	Maximum pressure, pressure increment, gas temperature and specific gravity	4F10.4
3	Pseudo-critical temperature, pseudo-critical pressure, mole per cent of H_2S, CO_2 and N_2	5F10.4

```
C   ************************************************************
C   * PROGRAM NAME    - BHOLE, BOTTOM HOLE PRESSURES IN GAS WELLS
C   *
C   * PURPOSE         - THIS PROGRAM CONVERTS STATIC AND FLOWING
C   *                   WELLHEAD PRESSURES TO CORRESPONDING BOTTOM
C   *                   HOLE PRESSURES
C   *
C   * METHOD          - BOTTOM HOLE PRESSURES ARE CALCULATED BY THE
C   *                   METHOD OF CULLENDER & SMITH (1956), AS
C   *                   MODIFIED BY AZIZ (1967A). THE MODIFICATION
C   *                   INVOLVES USAGE OF A ONE-STEP, THIRD-ORDER
C   *                   NUMERICAL INTEGRATION SCHEME INSTEAD OF
C   *                   SIMPSON'S RULE
C   *
C   * LANGUAGE        - FORTRAN IV
C   *
C   * SUBROUTINES USED - FFCPLD
C   *                  - VISCY
C   *                  - ZLRKG
C   *                  - ZANOC
C   *
C   * DATA INPUT, OUTPUT AND VARIABLES
C   *
C   * ABSRNS - ABSOLUTE ROUGHNESS OF THE PIPE. ASSUMED EQUAL TO
C   *          .00065 IF READ ZERO.
C   * A(I)   - PARAMETERS IN THE ONE-STEP, THIRD-ORDER NUMERICAL
C   *          INTEGRATION SCHEME OF AZIZ(1967A)
C   * CNCH2S - MOL PERCENT H2S IN NATURAL GAS
C   * CNCCO2 - MOL PERCENT CO2 IN NATURAL GAS
C   * CNCN2  - MOL PERCENT N2 IN NATURAL GAS
C   * DIAT   - TUBING INSIDE DIAMETER, INCHES. FOR PRODUCTION
C   *          THROUGH CASING REPLACE WITH EFFECTIVE DIAMETER
C   * LFM    - WELL DEPTH, FEET
C   * FRCI(I)- MOL FRACTION OF COMPONENT (I), READ IN FOLLOWING
C   *          ORDER - H2S, CO2, N2, C1, C2, C3, IC4, NC4, IC5,
C   *          NC5, C6, C7+
C   * KODEA  - 1 - SWEET GAS, READ SPECIFIC GRAVITY, SPG
C   *        - 2 - SOUR GAS, READ SPG AND MOLE PERCENT HYDROGEN
C   *              SULPHIDE, CNCH2S, CARBON DIOXIDE, CNCCO2, AND
C   *              NITROGEN, CNCN2
C   *        - 3 - SWEET OR SOUR GAS, READ COMPLETE COMPOSITION,
C   *              MOLE FRACTION H2S, CO2, N2 ... C7+, ASSUME PROPERTIES OF
C   *              C7+ EQUAL TO C6 PROPERTIES
C   *        - 4 - SAME AS KODEA=3, ALSO READ CRITICAL PRESSURE,
C   *              PRSCI(12), CRITICAL TEMPERATURE, TEMCI(12),
C   *              AND MOLECULAR WEIGHT, MWTI(12) OF C7+ FRACTION
C   * KODEB  - 1 - STATIC PRESSURE CALCULATION
C   *        - 2 - FLOWING PRESSURE CALCULATION
C   * LTH    - LENGTH OF FLOW STRING, FEET. FOR VERTICAL WELLS
C   *          READ ZERO, NEGATIVE FOR INJECTION WELLS.
C   * MWT    - MOLECULAR WEIGHT OF NATURAL GAS
C   * MWTI   - MOLECULAR WEIGHT OF COMPONENT I
C   * NCOMP  - NUMBER OF COMPONENTS IN NATURAL GAS (USUALLY THE
C   *          TWELVE LISTED ABOVE). READ FOR KODEA=3 & KODEA=4
C   * PRSCI  - CRITICAL PRESSURE OF COMPONENT I
C   * PRSPC  - PSEUDO-CRITICAL PRESSURE OF THE NATURAL GAS, PSIA
C   * PRST   - STATIC OR FLOWING WELLHEAD (TOP HOLE) PRESSURE,
C   *          PSIA, READ MEASURED VALUE.
C   * PRSN   - STATIC OR FLOWING BOTTOM HOLE PRESSURE,
C   *          PSIA, CALCULATED BY THIS PROGRAM.
C   * PRSME  - STATIC OR FLOWING BOTTOM HOLE PRESSURE,
C   *          PSIA, READ ESTIMATED VALUE. IF CANNOT ESTIMATE,
C   *          READ ZERO.
C   * RTEG   - GAS FLOW RATE AT STANDARD CONDITIONS (14.65 PSIA,
C   *          60 DEGREES F). READ ZERO FOR STATIC CASE.
C   * STEMCI - WHEN KODEA=4, THE ORIGINAL VALUE OF TEMCI(12) IS
C   *          STORED BEFORE THE NEW VALUE IS READ
C   * SPRSCI - WHEN KODEA=4, THE ORIGINAL VALUE OF PRSCI(12) IS
C   *          STORED BEFORE THE NEW VALUE IS READ
C   * SMWTI  - WHEN KODEA=4, THE ORIGINAL VALUE OF MWTI(12) IS
C   *          STORED BEFORE THE NEW VALUE IS READ
C   * SPG    - SPECIFIC GRAVITY OF THE NATURAL GAS, EITHER READ
C   *          OR CALCULATED BY THIS PROGRAM FROM GAS COMPOSITION
C   * TEMCI  - CRITICAL TEMPERATURE OF COMPONENT I
C   * TEMPC  - PSEUDO-CRITICAL TEMPERATURE OF THE NATURAL GAS,
C   *          DEGREES R
C   * TEMT   - STATIC OR FLOWING WELLHEAD (TOP HOLE) TEMPERATURE,
C   *          DEGREES F, READ MEASURED VALUE.
C   * TEMW   - STATIC OR FLOWING BOTTOM HOLE TEMPERATURE,
C   *          DEGREES F, READ MEASURED VALUE.
C   * Y, YY  - INTEGRANDS IN THE CULLENDER AND SMITH METHOD, SEE
C   *          ALSO AZIZ(1967A)
C   * ZED    - NATURAL GAS COMPRESSIBILITY FACTOR CALCULATED BY
C   *          SUBROUTINE ZANOC
C   ************************************************************

    REAL MWTI, MWT, LTH
C
    DIMENSION FRCI(12), TEMCI(12), PRSCI(12), MWTI(12), A(4),
   *          TITLE(18)
C
    COMMON CNCH2S, CNCCO2, CNCN2, PRSPC, TEMPC, SPG, DIAT, RTEG,
   *       ABSRNS, DPH, LTH
C
    DATA IW/6/, IR/5/, NCOMP/12/
C
    DATA TEMCI /
   * 672.3, 547.52, 227.27, 343.34, 549.58, 665.86,
   * 734.25, 765.32, 828.77, 845.37, 913.37, 1023.89/
C
    DATA PRSCI /
   * 1306.0, 1071.0, 493.0, 667.8, 707.8, 616.3,
   * 529.1, 550.7, 490.4, 488.6, 436.9, 360.6/
C
    DATA MWTI /
   * 34.076, 44.010, 28.013, 16.042, 30.070, 44.097,
   * 58.124, 58.124, 72.151, 72.151, 86.178, 114.232/
C
    DATA A /0.125, 0.375, 0.375, 0.125/
C
C   ************************************************************
C   * READ AND WRITE FORMAT STATEMENTS
C   ************************************************************
100 FORMAT (12A4, A2)
101 FORMAT (8I5)
102 FORMAT (8F10.4)
103 FORMAT (3F10.2)
105 FORMAT (1H ,////)
201 FORMAT (1H0,'INPUT DATA:'//1H ,25X,'WELL',13X,'PIPE',15X,
   *        'GAS FLOW',3X,'TEMPERATURE',4X,'PRESSURE, PSIA'//1H,
   *        'DEPTH',4X,'LENGTH',3X,'INSIDE',3X,'ABSOLUTE',5X,
   *        'RATE',4X,'TOP',3X,'BOTTOM',4X,'TOP',3X,'BOTTOM',/
   *        'FT.','DIAMETER',3X,'ROUGHNESS',3X,'MSCF/D',3X,
   *        'WELL',4X,'BOTTOM',4X,'WELL',4X,'HOLE'/1H ,23X,
   *        'INCHES',13X,'ION','HEAD',4X,'HOLE',4X,'HEAD (ASSUMED)'/)
202 FORMAT (1H ,F6.0,3X,F6.0,3X,F5.3,5X,F5.4,5X,F5.0,5X,F5.2)
203 FORMAT (1H ,'GAS COMPOSITION, MOLE FRACTION'//1H ,1X,'H2S',
   *        4X,'CO2',5X,'N2'/)
204 FORMAT (1H ,F5.4/)
205 FORMAT (1H ,2X,'C1',3X,'C2',5X,'C3',4X,'IC4',4X,'NC4',
   *        4X,'IC5',4X,'NC5',5X,'C6',4X,'C7+'/)
206 FORMAT (1H ,F5.4)
207 FORMAT (1H ,'PROPERTIES'/)
208 FORMAT (1H0,'PSEUDO-CRITICAL PRESSURE, PSIA',16X,'=',F7.2)
209 FORMAT (1H0,'PSEUDO-CRITICAL TEMPERATURE, DEGREES RANKINE','=')
210 FORMAT (1H0,'MOLECULAR WEIGHT',8X,'=',F6.2)
211 FORMAT (1H0,'GAS GRAVITY',3X,'=',F6.4//)
212 FORMAT (1H0,'CALCULATED GAS PROPERTIES:')
213 FORMAT (1H ,79(1H*))
214 FORMAT (1H ,'GAS GRAVITY =',F7.4)
215 FORMAT (1H ,'GAS GRAVITY =',F7.4)
216 FORMAT (1H ,'NO CONVERGENCE')
301 FORMAT (1H0,'STATIC BOTTOM HOLE PRESSURE =',F6.1,19X,
   *        'NUMBER OF ITERATIONS =',I2)
302 FORMAT (1H0,'FLOWING BOTTOM HOLE PRESSURE =',F6.1,19X,
   *        'NUMBER OF ITERATIONS =',I2)
303 FORMAT (1H1)
```

```
C   ************************************************************
C   * READ TITLE, KODEA, KODEB AND THE APPROPRIATE INPUTS AS
C   * REQUIRED BY THE VALUE OF KODEA TO CALCULATE THE PSEUDO-
C   * CRITICAL TEMPERATURE, PSEUDO-CRITICAL PRESSURE AND THE
C   * MOLECULAR WEIGHT OF THE NATURAL GAS
C   ************************************************************
400 READ (IR,100,END=415) TITLE
    WRITE (IW,303)
    WRITE (IW,201) TITLE
    READ (IR,101) KODEA, KODEB
    WRITE (IW,105)
    IF (KODEA.GE.3) GO TO 401
    READ (IR,103) SPG,(FRCI(I), I = 1, 3)
    CNCH2S = FRCI(1) * 100.
    CNCCO2 = FRCI(2) * 100.
    CNCN2  = FRCI(3) * 100.
    GO TO 403
401 READ (IR,101) (FRCI(I), I = 1, NCOMP)
    IF (KODEA.EQ.4) GO TO 402
    STEMCI = TEMCI(12)
    SPRSCI = PRSCI(12)
    SMWTI  = MWTI(12)
402 READ (IR,104) TEMCI(12), PRSCI(12), MWTI(12)
    CNCH2S = FRCI(1) * 100.
    CNCCO2 = FRCI(2) * 100.
    CNCN2  = FRCI(3) * 100.
    GO TO 404
C
C   ************************************************************
C   * CALCULATE THE PSEUDO-CRITICAL TEMPERATURE, PSEUDO-CRITICAL
C   * PRESSURE AND THE MOLECULAR WEIGHT OF THE NATURAL GAS
C   ************************************************************
403 MWT   = SPG * 28.964
    TEMPC = 170.491 + 307.344 * SPG
    PRSPC = 709.604 - 58.718 * SPG
    GO TO 406
404 PRT   = 0.0
    TEMPC = 0.0
    PRSPC = 0.0
    DO 405 I = 1, NCOMP
    MWT   = MWT  + MWTI(I) * FRCI(I)
    TEMPC = TEMPC + TEMCI(I) * FRCI(I)
405 PRSPC = PRSPC + PRSCI(I) * FRCI(I)
    SPG = MWT / 28.964
C
C   ************************************************************
C   * READ REMAINING INPUT DATA, WRITE CALCULATED GAS PROPERTIES
C   ************************************************************
406 READ (IR,103) DIAT, DPH, LTH, ABSRNS
    READ (IR,103) RTEG, TEMT, TEMW, PRST, PRSME
    IF (PRSME.EQ.0.) PRSME = PRST + 200.
    IF (ABSRNS.EQ.0.) ABSRNS = .00065
    IF (LTH .EQ.0.) LTH = DPH
    WRITE (IW,202) DPH, LTH, DIAT, ABSRNS, RTEG, TEMT, TEMW,
   *               PRST, PRSME
    IF (KODEA .GT.1) GO TO 407
    WRITE (IW,214) SPG
    GO TO 410
407 WRITE (IW,203)
    WRITE (IW,204) FRCI(1), FRCI(2), FRCI(3)
    IF (KODEA.EQ.1) GO TO 408
    WRITE (IW,215) SPG
    GO TO 410
408 WRITE (IW,205)
    WRITE (IW,206) (FRCI(I), I = 4, NCOMP)
    IF (KODEA.EQ.4) GO TO 409
    GO TO 410
409 WRITE (IW,207)
    WRITE (IW,208) PRSCI(12)
    WRITE (IW,209) TEMCI(12)
    WRITE (IW,210) MWTI(12)
    PRSCI(12) = SPRSCI
    TEMCI(12) = STEMCI
    MWTI(12)  = SMWTI
410 WRITE (IW,212)
    WRITE (IW,208) PRSPC
    WRITE (IW,210) TEMPC
    WRITE (IW,210) MWT
    IF (KODEA.GT.2) WRITE (IW,211) SPG
    WRITE (IW,213)
C
C   ************************************************************
C   * START OF BOTTOM HOLE PRESSURE CALCULATION
C   ************************************************************
    QE = 0.01875 * SPG * DPH
    IF (KODEB.EQ.2) QL = RTEG/1000.
    CALL ZANOC (TEMT, TEMPC, PRST, PRSPC, CNCH2S,
   *            CNCCO2, ZED, CMPG, IERR)
    PTZ   = (TEMT + 460.) * ZED / PRST
    ITER  = 0
    IF (KODEB .EQ. 2) CALL FFCPLD (TEMT, PRST, PTZ)
    YY    = A(1) * PTZ
    YEA   = PRST
    YT    = YY
    ITER  = YY
    YTEA  = YY
    PRSINC = (PRSN - PRST) / 3.
    TEMINC = (TEMW - TEMT) / 3.
C
C   ************************************************************
C   * INTEGRATION LOOP
C   ************************************************************
    DO 412 I = 2, 4
    PRS = PRS + PRSINC
    TEM = TEM + TEMINC
    CALL ZANOC (TEM, TEMPC, PRS, PRSPC, CNCH2S,
   *            CNCCO2, ZED, CMPG, IERR)
    PTZ = (TEM + 460.) * ZED / PRS
    IF (KODEB .EQ. 2) CALL FFCPLD (TEM, PRS, PTZ)
412 YY  = YY + A(I) * PTZ
C
C   ************************************************************
C   * NEWTON-RAPHSON ITERATION
C   ************************************************************
    YUN  = QE - (PRSN - PRST) * YY
    PRSN = PRSN - YUN
    FRER = ABS (PRSN - PRSN) / PRSN
    PRSN = PRSN
    IF (FRER.LT.0.001) GO TO 413
    IF (ITER .GT.20) GO TO 414
    PRS  = PRST
    TER  = TEMT
    YY   = YY
    GO TO 411
413 IF (KODEB .EQ. 1) WRITE (IW,301) PRSN, ITER
    IF (KODEB .EQ. 2) WRITE (IW,302) PRSN, ITER
    GO TO 400
414 IF (KODEB .EQ. 1) WRITE (IW,301) PRSN, ITER
    IF (KODEB .EQ. 2) WRITE (IW,302) PRSN, ITER
    GO TO 400
415 STOP
    END
```

```
*************************************************
*  PROGRAM NAME    - P-PSI, PSEUDO PRESSURE CALCULATIONS
*
*  PURPOSE         - THIS PROGRAM CONVERTS PRESSURE TO THEIR
*                    CORRESPONDING PSEUDO-PRESSURES
*
*  METHOD          - PSEUDO-PRESSURES, AS DEFINED BY AL-HUSSAINY
*                    (1965), ARE CALCULATED BY THE NUMERICAL
*                    INTEGRATION METHOD ILLUSTRATED BY EXAMPLE
*                    8-1.
*
*  LANGUAGE        - FORTRAN IV
*
*  SUBROUTINES USED
*                  - VISCY
*                  - XLGR4
*                  - ZANDC
*
*  DATA INPUT, OUTPUT AND VARIABLES
*
*  CNCH2S  - MOL PERCENT H2S IN THE NATURAL GAS
*  CNCCO2  - MOL PERCENT CO2 IN THE NATURAL GAS
*  CNCN2   - MOL PERCENT N2 IN THE NATURAL GAS
*  PRSDEL  - PRESSURE INCREMENT FOR NUMERICAL INTEGRATION
*  PRSMAX  - UPPER LIMIT OF PRESSURE, PSIA, UPTO WHICH THE
*            PSEUDO-PRESSURE CONVERSION IS REQUIRED
*  PRSPC   - PSEUDO-CRITICAL PRESSURE OF THE NATURAL GAS, PSIA
*  PRSSI   - DENOTES PSEUDO-PRESSURE, (PSIA)**2/CENTIPOISE
*  SPG     - SPECIFIC GRAVITY OF THE NATURAL GAS
*  TEMPC   - RESERVOIR TEMPERATURE OF THE NATURAL GAS,
*            DEGREES F
*  TEMPC   - PSEUDO-CRITICAL TEMPERATURE OF THE NATURAL GAS,
*            DEGREES R
*  VISG    - NATURAL GAS VISCOSITY, CENTIPOISE, CALCULATED BY
*            THE SUBROUTINE VISCY
*  ZED     - NATURAL GAS COMPRESSIBILITY FACTOR, CALCULATED BY
*            THE SUBROUTINE ZANDC
*************************************************
C
      DATA IR/1/, IW/3/
      DIMENSION TITLE(18)
*************************************************
*  READ AND WRITE FORMAT STATEMENTS
*************************************************
  100 FORMAT (17A4,A2)
  110 FORMAT (8F10.4)
  200 FORMAT (1H1)
  210 FORMAT (1H0,17A4,A2/)
  220 FORMAT (1H0,'RESERVOIR TEMPERATURE, DEGREES F    =',F10.2,/
     A       1H ,'GAS GRAVITY                          =',F10.2,/
     B       1H ,'PSEUDO-CRITICAL TEMP., DEGREES R     =',F10.2,/
     C       1H ,'PSEUDO-CRITICAL PRESSURE, PSIA       =',F10.2,/
     D       1H ,'MOLE PERCENT - HYDROGEN SULPHIDE     =',F10.2,/
     E       1H ,'MOLE PERCENT - CARBON DIOXIDE        =',F10.2,/
     F       1H ,'MOLE PERCENT - NITROGEN              =',F10.2,//)
  230 FORMAT (1H0,'PRESSURE',10X,'PSEUDO-PRESSURE'/1H ,1X,
     A        '(PSIA)',13X,'(PSIA)**2/CP'//)
  240 FORMAT (1H ,F7.1,18X,E13.7)
*************************************************
*  READ INPUT DATA
*************************************************
      READ  (IR, 100, END=400) TITLE
      WRITE (IW, 200)
      WRITE (IW, 210) TITLE
      READ  (IR, 110) PRSMAX, PRSDEL, TEM, SPG
      READ  (IR, 110) TEMPC, PRSPC, CNCH2S, CNCCO2, CNCN2
      WRITE (IW, 220) TEM, SPG, TEMPC, PRSPC, CNCH2S, CNCCO2, CNCH2
*************************************************
*  PSEUDO-PRESSURE CALCULATION BY NUMERICAL INTEGRATION
*************************************************
      PRS    = 0.0
      PRSSI  = 0.0
      GO TO 320
  310 PRS    = PRS + PRSDEL
      TEMPRD = (TEM + 460.)/TEMPC
      PRSPRD = PRS / PRSPC
      CALL ZANDC (VISG, TEMPC, PRS, PRSPC, CNCH2S,
     A            CNCCO2, CNCN2, VISG, ZED, IERR)
      CALL VISCY (TEMPRD, PRSPRD, SPG, TEM, CNCH2S,
     A            CNCCO2, CNCN2, VISGR, VISG, IERR)
      PRSSI  = 2. * PRS / (VISG * ZED)
      PRSSI  = (PRSSI + PRSSII)/2. * PRSDEL + PRSSI
      WRITE (IW, 240) PRS, PRSSI
      PRSSII = PRSSI
      IF (PRS .LT. PRSMAX) GO TO 310
  400 STOP
      END
```

```
*************************************************
*  PROGRAM NAME    - NATURAL GAS VISCOSITY DETERMINATION
*
*  PURPOSE         - THIS SUBROUTINE WILL DETERMINE THE VISCOSITY
*                    FOR NATURAL GAS INCORPORATING A CORRECTION
*                    FOR THE PRESENCE OF HYDROGEN SULPHIDE,
*                    CARBON DIOXIDE AND NITROGEN.
*
*  LANGUAGE        - FORTRAN IV
*
*  CALLING SEQUENCE
*                  - CALL VISCY (TEMPRD, PRSPRD, SPG, TEM,
*                    CNCH2S, CNCCO2, CNCN2, VISGR,
*                    VISG, IERR)
*
*  PARAMETERS
*
*  1. INPUT PARAMETERS
*
*  TEMPRD  = PSEUDO REDUCED TEMPERATURE AT WHICH THE NATURAL
*            GAS EXISTS
*  PRSPRD  = PSEUDO REDUCED PRESSURE AT WHICH THE NATURAL
*            GAS EXISTS
*  SPG     = SPECIFIC GRAVITY OF THE NATURAL GAS
*  TEM     = TEMPERATURE OF THE NATURAL GAS (DEGREES F)
*  CNCH2S  = MOL PERCENT HYDROGEN SULPHIDE IN NATURAL GAS
*  CNCCO2  = MOL PERCENT CARBON DIOXIDE IN NATURAL GAS
*  CNCN2   = MOL PERCENT NITROGEN IN NATURAL GAS
*
*  2. OUTPUT PARAMETERS
*
*  VISGR   = VISCOSITY RATIO
*  VISG    = VISCOSITY OF THE NATURAL GAS, CENTIPOISE
*  IERR    = ERROR FLAG INDICATING BOUNDS ERROR
*
*  VARIABLES
*
*  CORCO2  = CORRECTION FOR CO2
*  CORH2S  = CORRECTION FOR H2S
*  CORN2   = CORRECTION FOR N2
*  ICALL   = INDICATES THE POSITION IN THE PROGRAM FROM WHICH
*            THE CALL IS MADE
*  IHLTEM  = HIGHEST INDEX TO BE CHECKED IN THE TABLE OF
*            TEMPERATURE INDEXES, TEMTBL
*  IHIPRS  = HIGHEST INDEX TO BE CHECKED IN THE TABLE OF
*            PRESSURE INDEXES, PRSTBL
*  LOTEM   = LOWEST INDEX TO BE CHECKED IN THE TABLE OF
*            TEMPERATURE INDEXES, TEMTBL
*  LOPRS   = LOWEST INDEX TO BE CHECKED IN THE TABLE OF
*            PRESSURE INDEXES, PRSTBL
*  TEMTBL  = TABLE OF INDEXES TO THE APPROPRIATE TEMPERATURE
*            COLUMN IN THE VISCOSITY TABLE, VISTBL
*  PRSTBL  = TABLE OF INDEXES TO THE APPROPRIATE PRESSURE ROW
*            IN THE VISCOSITY TABLE, VISTBL
*  VISGA   = VISCOSITY AT 1 ATM PRESSURE (CORRECTED-H2S-CO2-N2)
*  VISGU   = VISCOSITY AT 1 ATM PRESSURE (UNCORRECTED)
*  VISI    = INTERPOLATED VISCOSITY RATIO
*  VISTBL  = TABLE OF VISCOSITY RATIOS
*  VISTB1  = EQUIVALENT TO APPROXIMATELY THE FIRST HALF OF
*            VISTBL
*            SET UP BECAUSE VISTBL COULD NOT BE INITIALIZED
*            WITH 1 DATA STATEMENT
*  VISTB2  = EQUIVALENT TO APPROXIMATELY THE LATTER HALF OF
*            VISTBL
*************************************************
      SUBROUTINE VISCY (TEMPRD, PRSPRD, SPG, TEM, CNCH2S, CNCCO2,
     A            CNCN2, VISGR, VISG, IERR)
      DIMENSION TEMTBL(11), PRSTBL(22), VISTBL(22,13), VISTB1(22,7),
     A          VISTB2(22,6)
```

```
      EQUIVALENCE (VISTB1(1,1), VISTBL(1,1)), (VISTB2(1,1), VISTBL(1,8))
      DATA TEMTBL /
     A 1.05,1.10,1.15,1.20,1.30,1.40,1.50,1.60,1.75,2.00,2.25,2.50,3.00 /
      DATA PRSTBL /
     A 0.1 , 0.2 , 0.3 , 0.4 , 0.5 , 0.6 , 0.7 , 0.8 , 0.9 , 1.0 , 1.2 ,
     B 1.4 , 1.6 , 1.8 , 2.0 , 3.0 , 4.0 , 6.0 , 8.0 ,10.0 ,15.0 ,20.0 /
      DATA VISTB1 /
      ...
      DATA VISTB2 /
      ...
```

```
*************************************************
*  INITIALIZE UPPER AND LOWER BOUNDS FOR THE TABLES OF
*  PSEUDO REDUCED TEMPERATURE AND PRESSURE INDEXES, OF
*                ERROR FLAG, IERR, TO 0
*************************************************
      LOPRS  = 1
      IHIPRS = 22
      LOTEM  = 1
      IHITEM = 11
      IERR   = 0
*************************************************
*  CHECK UPPER AND LOWER LIMITS OF THE PARAMETERS SPECIFIED
*  BY THE FOLLOWING RANGES (INCLUSIVE) -
*       1. TEMPRD  -  1.05  TO   3.00
*       2. PRSPRD  -  0.05  TO  20.00
*       3. SPG     -  0.55  TO   1.50
*       4. TEM     - 40.00  TO 400.00
*  IF ANY VALUE IS OUTSIDE THE RANGE, SET IERR = 1 & VISGR = 0
*                & RETURN TO THE MAINLINE
*************************************************
      IF (TEMPRD .LT. 1.05 .OR. TEMPRD .GT. 3.00) GO TO 340
      IF (PRSPRD .LT. 0.05 .OR. PRSPRD .GT. 20.00) GO TO 340
      IF (SPG    .LT. 0.55 .OR. SPG    .GT. 1.50) GO TO 340
      IF (TEM    .LT. 45.0 .OR. TEM    .GT. 400.0) GO TO 340
*************************************************
*  LOCATE TEMPRD IN THE TEMPERATURE INDEX
*************************************************
      DO 100 J = LOTEM, IHITEM
      IF (TEMTBL(J) .GE. TEMPRD) GO TO 120
  100 CONTINUE
      J = IHITEM + 1
*************************************************
*  CHECK PRSPRD AGAINST THE PRESSURE INDEX.
*    1. IF PRSPRD .LE. THE LOWEST INDEX VALUE, PERFORM THE
*       LAGRANGE INTERPOLATION USING RATIOS FOR PRSTBL(1).
*       CALCULATE THE VISCOSITY RATIO, VISGR.
*    2. IF PRSPRD .GE. THE HIGHEST INDEX VALUE, PERFORM THE
*       LAGRANGE INTERPOLATION USING RATIOS FOR
*       PRSTBL(IHIPRS). CALCULATE THE VISCOSITY RATIO, VISGR.
*       SET THE VISCOSITY RATIO TO THE INTERPOLATED VALUES.
*    3. OTHERWISE, LOCATE PRSPRD IN THE PRESSURE INDEX.
*       PERFORM THE LAGRANGE INTERPOLATION IN THE INDEX.
*       PERFORM THE LAGRANGE INTERPOLATION.
*       CALCULATE THE VISCOSITY RATIO USING A STRAIGHT LINE
*       INTERPOLATION.
*************************************************
  120 IF (PRSTBL(LOPRS - 1) .LT. PRSPRD) GO TO 160
      ICALL  = 1
      GO TO 320
  140 VISGR  = 1.00 + (PRSPRD * (VISI - 1.0))
      GO TO 300
  160 IF (PRSTBL(IHIPRS + 1) .GT. PRSPRD) GO TO 200
      ICALL  = 1
  180 VISGR  = VISI
      GO TO 300
  200 IF (PRSTBL(I) .LE. PRSPRD) GO TO 240
  220 CONTINUE
  240 I = IHIPRS + 1
      ICALL  = 320
  260 VISI   = YISI
      ICALL  = 320
  280 VISGR  = VISI + ((PRSPRD-PRSTBL(I-1))/(PRSTBL(I)-PRSTBL(I-1)))
     A         * (VISI-VISI)
*************************************************
*  CALCULATE PARTIAL VISCOSITY, VISGU.  MODIFY THE
*  VALUE BY APPLYING CORRECTIONS DEPENDENT UPON THE PERCENTAGE
*  CONTENT OF H2S, CO2 AND N2 TO OBTAIN THE PARTIAL VISCOSITY
*  AT 1 ATM PRESSURE.
*  CALCULATE THE OVERALL VISCOSITY, VISG
*************************************************
  300 VISGU  = 10.128988E-11 - 10.011803E-08/SPG + 10.369574E-02*SPG
     A         +SPG + 10.465174E-03/SPG*SPG*TEM
      CORH2S = 10.000048*CNCH2S*SPG - 0.000034*CNCH2S + 0.000003)
      CORCO2 = 10.000037*CNCCO2*SPG - 0.000024*CNCCO2 + 0.000004*SPG)
      CORN2  = 10.000170*CNCN2 *SPG + 0.000021*CNCN2 + 0.000010*SPG)
      VISGA  = VISGU + CORH2S + CORCO2 + CORN2
      GO TO 340
*************************************************
*  CALL TO LAGRANGE INTERPOLATION ROUTINE
*************************************************
  320 CALL XLGR4 (TEMPRD, TEMTBL(J-3), TEMTBL(J-1), TEMTBL(J),
     A            TEMTBL(J+1), VISI, VISTBL(I,J-3), VISTBL(I,J-1),
     B            VISTBL(I,J), VISTBL(I,J+1))
      GO TO (140, 180, 260, 280), ICALL
*************************************************
*  DATA ERROR PROCEDURE
*************************************************
  340 IERR   = 1
      VISGR  = 0.00
      VISG   = 0.00
*************************************************
*  RETURN PROCEDURE
*************************************************
  360 RETURN
      END
```

```
*****************************************
* PROGRAM NAME  - LAGRANGE INTERPOLATION
* PURPOSE       - THIS SUBROUTINE IS USED BY SUBROUTINE VISCY
*                 TO PROVIDE INTERPOLATED VISCOSITY RATIO
*                 VALUES CORRESPONDING TO GIVEN VALUES OF
*                 PSEUDO-CRITICAL TEMPERATURE AND PSEUDO-
*                 CRITICAL PRESSURE
* METHOD        - THIS SUBROUTINE EVALUATES THE GENERAL
*                 LAGRANGE EQUATION ( R.L. NEILSON, METHODS IN
*                 NUMERICAL ANALYSIS, THE MACMILLAN COMPANY,
*                 (1956) FOR A Y VALUE CORRESPONDING TO A
*                 GIVEN X VALUE LYING WITHIN THE RANGE OF
*                 FOUR GIVEN POINTS: (X1,Y1), (X2,Y2),
*                 (X3,Y3) AND (X4,Y4)
* LANGUAGE      - FORTRAN IV
* CALLING SEQUENCE
*               - CALL XLGR4 (X, X1, X2, X3, X4,
*                            Y, Y1, Y2, Y3, Y4)
*****************************************

      SUBROUTINE XLGR4 (X, X1, X2, X3, X4, Y, Y1, Y2, Y3, Y4)

      A1 = X1 - X2
      A2 = X1 - X3
      A3 = X1 - X4
      A4 = X2 - X3
      A5 = X2 - X4
      A6 = X3 - X4
      ...
      Y = B1 / A1 * B2 * B3 / A2 / A4 / A6 * Y1 +
     1    B1 / A1 * B3 / A4 / A5 * Y2 +
     1    B1 / A2 * B2 / A5 / A6 * Y3 +
     1    B1 / A3 * B2 / A5 / A6 * Y4

*****************************************
* RETURN PROCEDURE
*****************************************

      RETURN
      END
```

```
*****************************************
* PROGRAM NAME  - FRICTION FACTOR DETERMINATION
* PURPOSE       - THIS SUBROUTINE IS USED BY THE BOTTOM HOLE
*                 PRESSURE CALCULATION PROGRAM FOR COMPUTING
*                 THE VARIABLE PTZ FOR THE FLOWING PRESSURE
* LANGUAGE      - FORTRAN IV
* CALLING SEQUENCE
*               - CALL FFCFLO (TEM, PRS, PTZ)
* PARAMETERS    -
*   1. INPUT PARAMETERS
*   TEM  - TEMPERATURE OF THE GAS, DEGREES F
*   PRS  - PRESSURE OF THE GAS, PSIA
*   2. OUTPUT PARAMETER
*   PTZ  - PARAMETER IN THE BOTTOM HOLE PRESSURE
*          CALCULATION SCHEME
* VARIABLES
*   FFC  - FRICTION FACTOR CALCULATED BY THE COLEBROOK
*          EQUATION
*   REYO - REYNOLDS NUMBER
*   VISC - NATURAL GAS VISCOSITY CALCULATED BY
*          SUBROUTINE VISCY
*****************************************

      SUBROUTINE FFCFLO (TEM, PRS, PTZ)
      REAL LTH
      COMMON CNCH2S, CNCCO2, CNCH2, PRSPC, TEMPC, SPG, DIAT, PTEG,
     1       ABSRNS, DPH, LTH

*****************************************
* CALCULATE THE REYNOLDS NUMBER FOR THE FLOWING GAS
*****************************************

      PTZ = PRS / PTZ
      PASPAG = PRS / PRSPC
      TEMPRD = (TEM + 460.) / TEMPC
      CALL VISCY (TEMPRD, PASPAG, SPG, TEM, CNCH2S,
     1            CNCCO2, CNCH2, VISOR, VISG, IERR)
      REYO = 20011. * SPG * PTEG * VISC * DIAT
      IF (ABSRNS .LE. 0.1 * ABSRNS * 0.00006)
      KELENS = ABSRNS / DIAT

*****************************************
* FRICTION FACTOR FROM COLEBROOK EQUATION AND NEWTON-RAPHSON
* ITERATION TECHNIQUE
*****************************************

      ITER = 0
      ...
  100 ...
  200 ...
  300 ...

*****************************************
* RETURN PROCEDURE
*****************************************

      RETURN
      END
```

```
*****************************************
* PROGRAM NAME  - NATURAL GAS COMPRESSIBILITY FACTOR
*                 AND COMPRESSIBILITIES DETERMINATION
* PURPOSE       - THIS SUBROUTINE DETERMINES COMPRESSIBILITY
*                 FACTORS AND COMPRESSIBILITIES OF NATURAL
*                 GAS. CORRECTION FACTORS FOR THE PRESENCE OF
*                 HYDROGEN SULPHIDE AND CARBON DIOXIDE ARE
*                 INCORPORATED.
* CORRELATIONS  - COMPRESSIBILITY FACTORS ARE CALCULATED FROM
*                 AN 8-PARAMETER ANALOG EQUATION OF STATE
*                 DEVELOPED BY DRANCHUK, PURVIS & ROBINSON
*                 (1974), THAT EFFECTIVELY REPRODUCES THE
*                 STANDING-KATZ Z-FACTOR CHARTS.
*                 COMPRESSIBILITIES ARE CALCULATED BY THE
*                 METHOD OF MATTAR, BRAR & AZIZ (1975) WHICH
*                 USES A DIFFERENTIATED FORM OF THE ABOVE
*                 EQUATION OF STATE.
*                 CORRECTIONS FOR THE PRESENCE OF HYDROGEN
*                 SULPHIDE AND CARBON DIOXIDE ARE APPLIED BY
*                 THE METHOD OF WICHERT & AZIZ (1974).
* LANGUAGE      - FORTRAN IV
* CALLING SEQUENCE
*               - CALL ZANDC (TEM, TEMPC, PRS, PRSPC, CNCH2S,
*                            CNCCO2, ZED, CMPG, IERR)
* PARAMETERS    -
*   1. INPUT PARAMETERS
*   TEM    - TEMPERATURE OF THE NATURAL GAS, DEGREES F
*   TEMPC  - PSEUDO-CRITICAL TEMPERATURE OF THE NATURAL GAS,
*            DEGREES R
*   PRS    - PRESSURE AT WHICH THE NATURAL GAS EXISTS, PSIA
*   PRSPC  - PSEUDO-CRITICAL PRESSURE OF THE NATURAL GAS, PSIA
*   CNCH2S - MOLE PERCENT HYDROGEN SULPHIDE IN THE NATURAL GAS
*   CNCCO2 - MOLE PERCENT CARBON DIOXIDE IN THE NATURAL GAS
*   2. OUTPUT PARAMETERS
*   ZED    - COMPRESSIBILITY FACTOR OF THE NATURAL GAS
*   CMPG   - COMPRESSIBILITY OF THE NATURAL GAS
*   IERR   - ERROR FLAG INDICATING BOUNDS ERROR
* VARIABLES
*   A      - CONSTANTS IN THE DRANCHUK ETAL- CORRELATION
*   CMPRC  - PSEUDO-REDUCED COMPRESSIBILITY
*   DENRD  - REDUCED DENSITY
*   DZED   - PARTIAL DIFFERENTIAL OF ZED WITH RESPECT TO DENRD
*   EPS    - WICHERT AND AZIZ ADJUSTMENT FOR H2S AND CO2
*   FRCA   - MOLE FRACTION H2S AND CO2
*   FRCB   - MOLE FRACTION H2S
*   PRSPCA - ADJUSTED PSEUDO-CRITICAL PRESSURE
*   PRSPRD - PSEUDO-REDUCED PRESSURE
*   TEMPCA - ADJUSTED PSEUDO-CRITICAL TEMPERATURE
*   TEMPRD - PSEUDO-REDUCED TEMPERATURE
*****************************************

      SUBROUTINE ZANDC (TEM, TEMPC, PRS, PRSPC, CNCH2S,
     1                  CNCCO2, ZED, CMPG, IERR)
      DIMENSION A(8)
      DATA A /
     1  0.3150237, -1.0467099, -0.57832729, 0.53530771,
     1 -0.61232032, -0.10489813, 0.68157001, 0.68446549 /

*****************************************
* CALCULATE ADJUSTMENT FOR PRESENCE OF H2S & CO2
*****************************************

      FRCA = (CNCH2S + CNCCO2) / 100.
      FRCB = CNCH2S / 100.
      EPS = 120. * (FRCA ** 0.9 - FRCA ** 1.6) + 15. * (FRCB ** 0.5
     1      - FRCB ** 4.0)

*****************************************
* ADJUST PSEUDO CRITICAL TEMPERATE AND PRESSURE. CALCULATE
* PSEUDO REDUCED TEMPERATURE AND PRESSURE
*****************************************

      TEMPCA = TEMPC - EPS
      PRSPCA = PRSPC * TEMPCA / (TEMPC + FRCB * (1. - FRCB) * EPS)
      TEMPRD = (TEM + 460.) / TEMPCA
      PRSPRD = PRS / PRSPCA

*****************************************
* SET ERROR FLAG, IERR, TO 0
* CHECK UPPER AND LOWER LIMITS OF THE PARAMETERS SPECIFIED
* BY THE FOLLOWING RANGES (INCLUSIVE) -
*   1. TEMPRD - 1.05 TO 3.00
*   2. PRSPRD - 0.00 TO 15.00
*   3. FRCA   - 0.00 TO 0.80
* IF ANY VALUE IS OUTSIDE THE RANGE, SET IERR = 1.0, ZED = 0.0,
*                   AND CMPG = 0.0 AND RETURN TO THE MAINLINE
*****************************************

      IERR = 0.0
      IF (TEMPRD .LT. 1.05 .OR. TEMPRD .GT. 3.00) GO TO 140
      IF (PRSPRD .LT. 0.00 .OR. PRSPRD .GT. 15.00) GO TO 140
      IF (FRCA .LT. 0.00 .OR. FRCA .GT. 0.80) GO TO 140

*****************************************
* INITIALIZE REDUCED DENSITY AND CALCULATE COMPRESSIBILITY
* FACTOR AND COMPRESSIBILITY OF THE NATURAL GAS
*****************************************

      ITER = 0
      T1 = A(1) * TEMPRD + A(2) + A(3) / (TEMPRD * TEMPRD)
      T2 = A(4) * TEMPRD + A(5)
      T3 = A(6)
      T4 = A(7) / (TEMPRD * TEMPRD)
      T5 = A(8)
      DENRD = 1.0
  100 ...
  110 ...
  120 ...
  130 ...
      CMPG = CMPRD / PRSPC

*****************************************
* DATA ERROR PROCEDURE
*****************************************

  140 IERR = 1.0
      ZED = 0.0
      CMPG = 0.0

*****************************************
* RETURN PROCEDURE
*****************************************

  150 RETURN
      END
```

EXAMPLE D-1.   (KODEA=1,KCDEB=1)

INPUT DATA:

DEPTH FEET	WELL LENGTH	PIPE INSIDE DIAMETER INCHES	ABSOLUTE ROUGHNESS	GAS FLOW RATE MMSCFD	TEMPERATURE DEGREES F WELL HEAD	BOTTOM HOLE	PRESSURE, PSIA WELL HEAD	BOTTOM HOLE (ASSUMED)
10471.	10471.	2.441	.0018	0.0	146.	242.	2685.	2685.

GAS GRAVITY = 0.9800

CALCULATED GAS PROPERTIES:

PSEUDO-CRITICAL PRESSURE, PSIA   = 652.06

PSEUDO-CRITICAL TEMPERATURE, DEGREES RANKINE   = 471.69

MOLECULAR WEIGHT   = 28.38

****

STATIC BOTTOM HOLE PRESSURE = 3961.   NUMBER OF ITERATIONS = 4

EXAMPLE D-2.   (KODEA=1,KCDEB=2)

INPUT DATA:

DEPTH FEET	WELL LENGTH	PIPE INSIDE DIAMETER INCHES	ABSOLUTE ROUGHNESS	GAS FLOW RATE MMSCFD	TEMPERATURE DEGREES F WELL HEAD	BOTTOM HOLE	PRESSURE, PSIA WELL HEAD	BOTTOM HOLE (ASSUMED)
10471.	10471.	2.441	.0018	11.716	146.	242.	2685.	2885.

GAS GRAVITY = 0.9800

CALCULATED GAS PROPERTIES:

PSEUDO-CRITICAL PRESSURE, PSIA   = 652.06

PSEUDO-CRITICAL TEMPERATURE, DEGREES RANKINE   = 471.69

MOLECULAR WEIGHT   = 28.38

****

FLOWING BOTTOM HOLE PRESSURE = 4557.   NUMBER OF ITERATIONS = 3

EXAMPLE D-3.   (KODEA=2,KCDEB=1)

INPUT DATA:

WELL DEPTH FEET	LENGTH	PIPE INSIDE DIAMETER INCHES	ABSOLUTE ROUGHNESS	GAS FLOW RATE MMSCFD	TEMPERATURE DEGREES F WELL HEAD	BOTTOM HOLE	PRESSURE, PSIA WELL HEAD	BOTTOM HOLE (ASSUMED)
10471.	10471.	2.441	.0018	0.0	146.	242.	2685.	2885.

GAS COMPOSITION, MOLE FRACTION

H2S	CO2	N2
.1706	.0320	.0192

GAS GRAVITY = 0.9800

CALCULATED GAS PROPERTIES:

PSEUDO-CRITICAL PRESSURE, PSIA   = 652.06

PSEUDO-CRITICAL TEMPERATURE, DEGREES RANKINE = 471.69

MOLECULAR WEIGHT   = 28.38

****

STATIC BOTTOM HOLE PRESSURE = 3870.   NUMBER OF ITERATIONS = 4

EXAMPLE D-4.   (KODEA=2,KCDEB=2)

INPUT DATA:

WELL DEPTH FEET	LENGTH	PIPE INSIDE DIAMETER INCHES	ABSOLUTE ROUGHNESS	GAS FLOW RATE MMSCFD	TEMPERATURE DEGREES F WELL HEAD	BOTTOM HOLE	PRESSURE, PSIA WELL HEAD	BOTTOM HOLE (ASSUMED)
10471.	10471.	2.441	.0018	11.716	146.	242.	2685.	2885.

GAS COMPOSITION, MOLE FRACTION

H2S	CO2	N2
.1706	.0320	.0192

GAS GRAVITY = 0.9800

CALCULATED GAS PROPERTIES:

PSEUDO-CRITICAL PRESSURE, PSIA   = 652.06

PSEUDO-CRITICAL TEMPERATURE, DEGREES RANKINE = 471.69

MOLECULAR WEIGHT   = 28.38

****

FLOWING BOTTOM HOLE PRESSURE = 4510.   NUMBER OF ITERATIONS = 3

EXAMPLE D-5.   (KODEA=3,KCOEB=1)

INPUT DATA:

WELL		PIPE		GAS FLOW	TEMPERATURE		PRESSURE, PSIA	
DEPTH	LENGTH	INSIDE	ABSOLUTE	RATE	DEGREES F		WELL	BOTTOM
FEET		DIAMETER	ROUGHNESS	MMSCFD	WELL	BOTTOM	HEAD	HOLE
		INCHES			HEAD	HOLE		(ASSUMED)
10471.	10471.	2.441	.0018	0.0	146.	242.	2685.	2885.

GAS COMPOSITION, MOLE FRACTION

H2S	CO2	N2
.1706	.0320	.0192

C1	C2	C3	IC4	NC4	IC5	NC5	C6	C7+
.5903	.0727	.0297	.0079	.0144	.0059	.0062	.0120	.0391

CALCULATED GAS PROPERTIES:

PSEUDO-CRITICAL PRESSURE, PSIA   = 767.88

PSEUDO-CRITICAL TEMPERATURE, DEGREES RANKINE = 476.78

MOLECULAR WEIGHT   = 28.39

GAS GRAVITY   = 0.9803

****

STATIC BOTTOM HOLE PRESSURE = 3953.   NUMBER OF ITERATIONS = 4

EXAMPLE D-6.   (KODEA=3,KCOEB=2)

INPUT DATA:

WELL		PIPE		GAS FLOW	TEMPERATURE		PRESSURE, PSIA	
DEPTH	LENGTH	INSIDE	ABSOLUTE	RATE	DEGREES F		WELL	BOTTOM
FEET		DIAMETER	ROUGHNESS	MMSCFD	WELL	BOTTOM	HEAD	HOLE
		INCHES			HEAD	HOLE		(ASSUMED)
10471.	10471.	2.441	.0018	11.716	146.	242.	2685.	2885.

GAS COMPOSITION, MOLE FRACTION

H2S	CO2	N2
.1706	.0320	.0192

C1	C2	C3	IC4	NC4	IC5	NC5	C6	C7+
.5903	.0727	.0297	.0079	.0144	.0059	.0062	.0120	.0391

CALCULATED GAS PROPERTIES:

PSEUDO-CRITICAL PRESSURE, PSIA   = 767.88

PSEUDO-CRITICAL TEMPERATURE, DEGREES RANKINE = 476.78

MOLECULAR WEIGHT   = 28.39

GAS GRAVITY   = 0.9803

****

FLOWING BOTTOM HOLE PRESSURE = 4563.   NUMBER OF ITERATIONS = 3

EXAMPLE D-7.   (KODEA=4,KODEB=1)

INPUT DATA:

WELL DEPTH FEET	LENGTH	PIPE INSIDE DIAMETER INCHES	ABSOLUTE ROUGHNESS	GAS FLOW RATE MMSCFD	TEMPERATURE DEGREES F WELL HEAD	BOTTOM HOLE	PRESSURE, PSIA WELL HEAD	BOTTOM HOLE (ASSUMED)
10471.	10471.	2.441	.0018	0.0	146.	242.	2685.	2885.

GAS COMPOSITION, MOLE FRACTION

H2S	CO2	N2
.1706	.0320	.0192

C1	C2	C3	IC4	NC4	IC5	NC5	C6	C7+
.5903	.0727	.0297	.0079	.0144	.0059	.0062	.0120	.0391

PROPERTIES OF C7+

PSEUDO-CRITICAL PRESSURE, PSIA   = 360.22

PSEUDO-CRITICAL TEMPERATURE, DEGREES RANKINE   =1045.22

MOLECULAR WEIGHT   = 124.52

CALCULATED GAS PROPERTIES:

PSEUDO-CRITICAL PRESSURE, PSIA   = 767.86

PSEUDO-CRITICAL TEMPERATURE, DEGREES RANKINE   = 477.61

MOLECULAR WEIGHT   = 28.80

GAS GRAVITY   = 0.9942

****

STATIC BOTTOM HOLE PRESSURE = 3976.   NUMBER OF ITERATIONS = 4

EXAMPLE D-8.   (KODEA=4,KODEB=2)

INPUT DATA:

WELL DEPTH FEET	LENGTH	PIPE INSIDE DIAMETER INCHES	ABSOLUTE ROUGHNESS	GAS FLOW RATE MMSCFD	TEMPERATURE DEGREES F WELL HEAD	BOTTOM HOLE	PRESSURE, PSIA WELL HEAD	BOTTOM HOLE (ASSUMED)
10471.	10471.	2.441	.0018	11.716	146.	242.	2685.	2885.

GAS COMPOSITION, MOLE FRACTION

H2S	CO2	N2
.1706	.0320	.0192

C1	C2	C3	IC4	NC4	IC5	NC5	C6	C7+
.5903	.0727	.0297	.0079	.0144	.0059	.0062	.0120	.0391

PROPERTIES OF C7+

PSEUDO-CRITICAL PRESSURE, PSIA   = 360.22

PSEUDO-CRITICAL TEMPERATURE, DEGREES RANKINE   =1045.22

MOLECULAR WEIGHT   = 124.52

CALCULATED GAS PROPERTIES:

PSEUDO-CRITICAL PRESSURE, PSIA   = 767.86

PSEUDO-CRITICAL TEMPERATURE, DEGREES RANKINE   = 477.61

MOLECULAR WEIGHT   = 28.80

GAS GRAVITY   = 0.9942

****

FLOWING BOTTOM HOLE PRESSURE = 4594.   NUMBER OF ITERATIONS = 4

EXAMPLE D-9.   DATA FROM EXAMPLE B-1.

INPUT DATA:

WELL DEPTH FEET	LENGTH	PIPE INSIDE DIAMETER INCHES	PIPE ABSOLUTE ROUGHNESS	GAS FLOW RATE MMSCFD	TEMPERATURE DEGREES F WELL HEAD	TEMPERATURE DEGREES F BOTTOM HOLE	PRESSURE, PSIA WELL HEAD	PRESSURE, PSIA BOTTOM HOLE (ASSUMED)
10000.	10000.	2.441	.0006	0.0	35.	245.	2500.	2700.

GAS GRAVITY = 0.7500

CALCULATED GAS PROPERTIES:

PSEUDO-CRITICAL PRESSURE, PSIA   = 665.57

PSEUDO-CRITICAL TEMPERATURE, DEGREES RANKINE = 401.00

MOLECULAR WEIGHT   = 21.72

****

STATIC BOTTOM HOLE PRESSURE = 3388.   NUMBER OF ITERATIONS = 5

EXAMPLE D-10.   DATA FROM EXAMPLE B-2.

INPUT DATA:

WELL DEPTH FEET	LENGTH	PIPE INSIDE DIAMETER INCHES	PIPE ABSOLUTE ROUGHNESS	GAS FLOW RATE MMSCFD	TEMPERATURE DEGREES F WELL HEAD	TEMPERATURE DEGREES F BOTTOM HOLE	PRESSURE, PSIA WELL HEAD	PRESSURE, PSIA BOTTOM HOLE (ASSUMED)
10000.	10000.	2.441	.0006	4.915	110.	245.	2000.	2200.

GAS GRAVITY = 0.7500

CALCULATED GAS PROPERTIES:

PSEUDO-CRITICAL PRESSURE, PSIA   = 665.57

PSEUDO-CRITICAL TEMPERATURE, DEGREES RANKINE = 401.00

MOLECULAR WEIGHT   = 21.72

****

FLOWING BOTTOM HOLE PRESSURE = 2725.   NUMBER OF ITERATIONS = 4

EXAMPLE D-11.   DATA FROM EXAMPLE 2-1.

```
RESERVOIR TEMPERATURE, DEGREES F        =    120.00
GAS GRAVITY                             =    0.6100
PSEUDO-CRITICAL TEMP., DEGREES R        =    357.00
PSEUDO-CRITICAL PRESSURE, PSIA          =    664.00
MOLE PERCENT - HYDROGEN SULPHIDE        =    0.0
MOLE PERCENT - CARBON DIOXIDE           =    0.0
MOLE PERCENT - NITROGEN                 =    0.0
```

PRESSURE (PSIA)	PSEUDO-PRESSURE (PSIA **2/CP)
0.0	0.0
400.0	0.1416346E 08
800.0	0.5636334E 08
1200.0	0.1251145E 09
1600.0	0.2175370E 09
2000.0	0.3304471E 09

APPENDIX E

REGULATIONS AND REPORTING FORMS

1 INTRODUCTION

In many countries, authorities with jurisdiction over natural gas production have developed regulations or equivalent requirements respecting the testing of gas wells. The Province of Alberta regulates gas well testing and related matters through The Oil and Gas Conservation Act. The Oil and Gas Conservation Regulations under that Act contain the primary requirements of the Board respecting gas well testing and the reporting of test results. Interim Directives and Informational Letters issued by the Board inform operators of new, revised, or supplementary requirements.

2 TESTING REQUIREMENTS

2.1 Objectives

The Board's main objectives respecting the gathering and utilization of gas well test data are to obtain reliable deliverability, reservoir pressure, and fluid analysis data for all gas reservoirs in the province, having regard for the accuracy of measurement, the conservation of resources, the preservation of the environment, and the safety of persons involved in the actual testing operations.

The information obtained from gas well tests is used by the Board in calculating reserves, forecasting production, determining appropriate well spacing, calculating allowables for both conservation and equity reasons, and in other ways which assist in the proper exploitation of gas reservoirs from their discovery through to their abandonment.

2.2 Requirements

The method and frequency of testing gas wells depends on
several considerations. Usually, there is a need to understand the
pressure/production relationships of a large number of the wells in a
given reservoir, and to make reliable estimates of the maximum daily
rates and the total volumes of gas which they can be expected to
produce. In general, all gas wells must be deliverability tested early
in their producing lives, and thereafter as appropriate for the specific
needs of industry and government. Parts 10 and 11 of the Oil and Gas
Conservation Regulations deal with the initial and subsequent testing
of gas wells.

In connection with rules respecting the field conduct and
reporting of tests, Part 6 of the Regulations deals with the control of
fluids produced during testing, Parts 7 and 11 with the testing of sour
gas wells, and Part 8 with the burning of vented gas. Part 11 deals
with the submission of technical reports of fluid sample analyses,
deliverability tests, flowing and static pressure measurements, pressure
build-up and drawdown tests, reservoir limits tests and interference
tests. Requirements respecting the measurement of fluid volumes are
included in Part 14, and the reporting of test production is dealt with
in Part 12.

3 REPORTING FORMS

3.1 Data Considerations

The forms which are included in this appendix contain provision
for the reporting of information which is usually available from the more
common types of tests conducted on gas wells. Chapter 6 gives an outline
of the main items which should be included in a test report. In
particular, supplementary calculations and comments showing the operator's
interpretation of the test should be submitted. These may include
calculations of effective bulk formation permeability, k, radius of

investigation, r_{inv}, at a particular flow time, time to stabilization, t_s, corresponding to a particular external radius, r_e, apparent skin factor, s', flow efficiency of the well, FE, and the calculations of bottom hole pressures from wellhead data. If the stabilized deliverability of the well is being obtained by some method other than a deliverability test, the sources of all parameters used in the calculation should be clearly indicated.

3.2 Sample Reporting Forms

Samples of reporting forms which the Board recommends for use are included at the end of this section. For convenience a list is provided below. Copies may be obtained from the Printing and Supplies Section at the Board's main office at 603 - 6th Avenue S.W., Calgary, Alberta, T2P 0T4.

Number	Title
EG-29	Gas Well Deliverability Test - Field Notes
EG-29A	Gas Well Deliverability Test - Field Notes
EG-29B	Gas Well Deliverability Test - Field Notes
EG-32	Gas Well Deliverability Test Summary
EG-33	Gas Well Deliverability Test Calculations
EG-34	Gas Well Deliverability Test Calculations - Flow Rates
EG-35	Molal Recombination Calculations
O-12	Subsurface Pressure Measurements
O-12A	Subsurface Pressure Measurements

GAS WELL DELIVERABILITY TEST – FIELD NOTES PAGE 1 OF _____

WELL NAME _____ LOCATION _____ W __

FIELD OR AREA _____ POOL OR ZONE _____

PERF./OPEN HOLE INTERVAL _____ PRODUCING THROUGH: TUBING ☐ ANNULUS ☐

WELL BLOWN FOR _____ minutes   SPRAY: WATER/CONDENSATE CLEAR IN _____ minutes

DATE SHUT-IN _____ 19 ___   TIME _____   TOTAL SHUT-IN TIME _____ hours

SHUT-IN NO.1 (INITIAL)

DATE	TIME	CUMULATIVE SHUT-IN TIME hours	WELLHEAD PRESSURE psig		WELLHEAD TEMPERATURE °F
			TUBING	CASING	

REMARKS

FLOW NO.1 WELL OPENED AT _____ AM/PM _____ 19 _____

DATE	TIME	CUMULATIVE FLOW TIME hours	WELLHEAD PRESSURE psig		WELLHEAD TEMPERATURE °F	METER OR PROVER DATA		
			TUBING	CASING		STATIC PRESSURE psig	DIFFERENTIAL inches H$_2$O	TEMPERATURE °F

METER RUN OR PROVER SIZE _____ inches   ORIFICE SIZE _____ inches

SEPARATOR CONDITIONS: HP SEP. _____ psig, _____ °F   LP SEP _____ psig, _____ °F

CONDENSATE PRODUCTION RATE _____ Bbl per hour   TOTAL _____ Bbl

WATER PRODUCTION RATE _____ Bbl per hour   TOTAL _____ Bbl

FINAL FLOWING WELLHEAD PRESSURE: TUBING _____ CASING _____ psig

WELL SHUT-IN AT _____ AM/PM _____ 19 ___   TOTAL FLOW TIME _____ hours

NOTE: FLOWING WELLHEAD PRESSURES AND TEMPERATURES MUST BE OBTAINED UPSTREAM OF ANY CHOKING DEVICE

EG-29-10-75

GAS WELL DELIVERABILITY TEST – FIELD NOTES PAGE _____ OF _____

SHUT-IN NO. _____ (INTERMEDIATE)

DATE	TIME	CUMULATIVE SHUT-IN TIME hours	WELLHEAD PRESSURE psig		WELLHEAD TEMPERATURE °F
			TUBING	CASING	

REMARKS

FLOW NO. _____   WELL OPENED AT _____ AM / PM   _____ 19 _____

DATE	TIME	CUMULATIVE FLOW TIME hours	WELLHEAD PRESSURE psig		WELLHEAD TEMPERATURE °F	METER OR PROVER DATA		
			TUBING	CASING		STATIC PRESSURE psig	DIFFERENTIAL inches H₂O	TEMPERATURE °F

METER RUN OR PROVER SIZE _____ inches   ORIFICE SIZE _____ inches

SEPARATOR CONDITIONS: HP SEP. _____ psig, _____ °F   LP SEP. _____ psig, _____ °F

CONDENSATE PRODUCTION RATE _____ Bbl per hour   TOTAL _____ Bbl

WATER PRODUCTION RATE _____ Bbl per hour   TOTAL _____ Bbl

FINAL FLOWING WELLHEAD PRESSURE: TUBING _____ CASING _____ psig

WELL SHUT-IN AT _____ AM/PM _____ 19 ___ TOTAL FLOW TIME _____ hours

GAS WELL DELIVERABILITY TEST – FIELD NOTES   PAGE _____ OF _____

CONTINUATION OF FLOW NO. _____ TO STABILIZATION

METER RUN OR PROVER SIZE _____ inches   ORIFICE SIZE _____ inches

SEPARATOR CONDITIONS: HP SEP. _____ psig, _____°F   LP SEP. _____ psig, _____°F

CONDENSATE PRODUCTION RATE _____ Bbl per hour   TOTAL _____ Bbl

WATER PRODUCTION RATE _____ Bbl per hour   TOTAL _____ Bbl

FINAL FLOWING WELLHEAD PRESSURE: TUBING _____ CASING _____ psig

WELL SHUT-IN AT _____ AM/PM _____ 19 ____ TOTAL FLOW TIME _____ hours

FINAL SHUT-IN WELLHEAD PRESSURE: TUBING _____ CASING _____ psig

DURATION OF FINAL SHUT-IN _____ hours   TESTED BY (CO.) _____

GAS WELL DELIVERABILITY TEST SUMMARY

GENERAL DATA

WELL NAME _____ LOCATION _____ W___

FIELD OR AREA _____ ELEVATION (CF)_____ (KB)_____ ft

POOL OR ZONE _____ RESERVOIR TEMPERATURE _____ °F

PERF./OPEN HOLE INTERVAL _____ ft (KB)

CASING ID _____ in   TUBING ID _____ in   OD _____ in   PACKER _____ ft (KB)

RESERVOIR GAS PROPERTIES: G _____ P_c _____ T_c _____   MOL %: N_2 ____ CO_2 ____ H_2S ____

LICENSEE _____ OPERATOR (Co) _____

TYPE OF TEST _____ FINAL DATE OF TEST _____ 19 ___

PRODUCTION DATA

RATE NO.	DURATION hours	GAS PRODUCTION Mscfd	CONDENSATE PRODUCTION Bbl/d	COND./GAS RATIO Bbl/Mscf	GAS-EQUIVALENT OF CONDENSATE Mscfd	TOTAL PRODUCTION-RATE Mscfd	WATER PRODUCTION Bbl/d	WATER/GAS RATIO Bbl/MMscf
EXTENDED RATE								

GAS PRODUCED THROUGH: TUBING ☐   ANNULUS ☐   TO: PIPE LINE ☐   VENT ☐   FLARE ☐

FLARE STACK HEIGHT _____ ft   DIAMETER _____ in

TOTAL VOLUME OF GAS PRODUCED DURING CLEANUP AND TEST _____ Mscf

EQUIPMENT LIST

LINE HEATER ☐

L.P. SEPARATOR ☐

H.P. SEPARATOR ☐

CRITICAL FLOW PROVER ☐

ORIFICE METER ☐

LIQUID STORAGE TANK ☐

_____ ☐

_____ ☐

_____ ☐

REMARKS

_____

_____

_____

_____

_____

_____

_____

STABILIZED SHUT-IN RESERVOIR PRESSURE ($\bar{P}_R$) _____ psia

ABSOLUTE OPEN FLOW POTENTIAL _____ Mscfd

WELLHEAD OPEN FLOW POTENTIAL _____ Mscfd

GAS WELL DELIVERABILITY TEST CALCULATIONS

(BASE CONDITIONS = 14.65 psia and 60 °F)

WELL NAME _____   LOCATION _____ W___

POOL OR ZONE _____   FINAL DATE OF TEST _____ 19___

SIMPLIFIED ANALYSIS

	DURATION hours	SANDFACE PRESSURE psia	CALC.	MEAS.	$p^2 \times 10^{-3}$ psia^2	$\Delta p^2 \times 10^{-3}$ psia^2	FLOW RATE (q) MMscfd
INITIAL SHUT-IN							
FLOW 1							
SHUT-IN							
FLOW 2							
SHUT-IN							
FLOW 3							
SHUT-IN							
FLOW 4							
EXTENDED FLOW							
FINAL SHUT-IN							

RESULTS

$q = C\left(\bar{p}_R^2 - p_{wf}^2\right)^n$

slope n = _____

$\bar{p}_R$ = _____ psia

$C = \dfrac{q}{\left(\bar{p}_R^2 - p_{wf}^2\right)^n}$

= _____

AOF (MMscfd)

= _____

LIT (ψ) ANALYSIS   (SEE NOTE ON REVERSE)

	DURATION hours	SANDFACE PRESSURE psia	ψ MM psia^2/cp	$\Delta\psi$ MM psia^2/cp	FLOW RATE (q) MMscfd	$\Delta\psi/q$	q^2	$\Delta\psi - bq^2$
INITIAL SHUT-IN								
FLOW 1								
SHUT-IN								
FLOW 2								
SHUT-IN								
FLOW 3								
SHUT-IN								
FLOW 4								
TOTAL = Σ								
EXTENDED FLOW								
FINAL SHUT-IN								

DISCARDED POINT _____

N = _____ $\tilde{\psi}_R$ = _____ MMpsia^2/cp

$a, a_t = \dfrac{\Sigma\frac{\Delta\psi}{q}\,\Sigma q^2 - \Sigma q\,\Sigma\Delta\psi}{N\,\Sigma q^2 - \Sigma q\,\Sigma q}$ = _____

$b = \dfrac{N\,\Sigma\Delta\psi - \Sigma q\,\Sigma\frac{\Delta\psi}{q}}{N\,\Sigma q^2 - \Sigma q\,\Sigma q}$ = _____

(EXTENDED FLOW) $\Delta\psi$ = _____   q = _____   b = _____

$a = \dfrac{\Delta\psi - bq^2}{q}$ = _____

RESULTS

TRANSIENT FLOW: $\bar{\psi}_R - \psi_{wf} = a_t q + bq^2$

i.e. _____ $- \psi_{wf}$ = _____ q + _____ q^2

STABILIZED FLOW: $\bar{\psi}_R - \psi_{wf} = aq + bq^2$

i.e. _____ $- \psi_{wf}$ = _____ q + _____ q^2

DELIVERABILITY:

$q = \dfrac{1}{2b}\left[-a + \sqrt{a^2 + 4b\left(\bar{\psi}_R - \psi_{wf}\right)}\,\right]$

FOR $\psi_{wf} = 0$, q = AOF = _____ MMscfd

EG-33-10-75

GAS WELL DELIVERABILITY TEST CALCULATIONS - FLOW RATES

(BASE CONDITIONS = 14.65 psia and 60 °F)

CRITICAL FLOW PROVER $\qquad q = 10^{-3} \ C \ P \ F_{tf} \ F_g \ F_{pv}$

RATE NO.	PROVER SIZE inches	ORIFICE DIAMETER inches	BASIC ORIFICE COEFFICIENT (C) Mscfd / lb.	STATIC PRESSURE (P) psia	FLOW. TEMP. FACTOR F_{tf}	SPECIFIC GRAVITY FACTOR F_g	SUPERCOMP FACTOR F_{pv}	FLOW RATE q MMscfd
1								
2								
3								
4								
5								

ORIFICE METER $\qquad q = 24 \times 10^{-6} \ C' \sqrt{h_w \ P_f}$ $\qquad\qquad F_{pb} = 1.0055$

$$C' = F_b \ F_{pb} \ F_{tb} \ F_g \ F_{tf} \ F_r \ Y \ F_{pv} \ F_m \qquad\qquad F_{tb} = 1.0000$$

RATE NO.	STAGE	METER RUN OR LINE SIZE inches	ORIFICE DIAMETER inches	STATIC PRESSURE P_f psia	DIFFERENTIAL INCHES H2O h_w	BASIC ORIFICE FACTOR F_b	SPECIFIC GRAVITY FACTOR F_g	FLOW. TEMP. FACTOR F_{tf}
1	H							
1	L							
2	H							
2	L							
3	H							
3	L							
4	H							
4	L							
5	H							
5	L							

ORIFICE METER CALCULATIONS (CONTINUED)

RATE NO.	STAGE	REYNOLDS FACTOR F_r	EXPANSION FACTOR Y	SUPERCOMP FACTOR F_{pv}	MANOMETER FACTOR F_m	C' ft^3/hr	$\sqrt{h_w \ P_f}$	FLOW RATE q MMscfd	TOTAL GAS PRODUCTION RATE MMscfd
1	H								
1	L								
2	H								
2	L								
3	H								
3	L								
4	H								
4	L								
5	H								
5	L								

MOLAL RECOMBINATION CALCULATIONS

WELL _____ LOCATION _____ FIELD _____ POOL _____ DATE SAMPLED _____

SEPARATOR CONDITIONS   HP SEP. _____ psig, _____ °F   LP SEP. _____ psig, _____ °F

SEPARATOR PRODUCTS   HP GAS _____ Mscfd   LP GAS _____ Mscfd

LIQUID: STOCK TANK _____ Bbl/d   HP _____ Bbl/d   LP _____ Bbl/d

LIQUID FLOW RATE CALCULATIONS*   (STOCK TANK ☐,   HP ☐,   or   LP ☐ LIQUID)

MOLECULAR WEIGHT OF LIQUID, M_L = _____ , SPECIFIC GRAVITY OF LIQUID, SG_L = _____

LIQUID FLOW RATE (moles/d)   =   FLOW RATE(Bbl/d) × $\dfrac{SG_L}{M_L}$ × 350.51   = _____

LIQUID FLOW RATE (Mscfd)   =   FLOW RATE (moles/d) × 0.38068   = _____

COMP. i	M_i lb_m/lb mole	T_{ci} °R	P_{ci} psia	LIQUID MOLE FRACTION	LIQUID Mscfd	HP GAS MOLE FRACTION	HP GAS Mscfd	LP GAS MOLE FRACTION	LP GAS Mscfd	TOTAL Mscfd	RECOMBINED GAS PROPERTIES x_i	$x_i M_i$	$x_i T_{ci}$	$x_i P_{ci}$
N_2	28.013	227.27	493.0											
CO_2	44.010	547.57	1071.0											
H_2S	34.076	672.37	1306.0											
C_1	16.042	343.04	667.8											
C_2	30.070	549.76	707.8											
C_3	44.097	665.68	616.3											
iC_4	58.124	734.65	529.1											
nC_4	58.124	765.32	550.7											
iC_5	72.151	828.77	490.4											
nC_5	72.151	845.37	488.6											
C_6	86.178	913.37	436.9											
** C_7^+	114.232	1023.89	360.6											
Σ				1.0000		1.0000		1.0000			1.0000			

RECOMBINED GAS PROPERTIES: FLOW RATE = _____ MMscfd,   G = _____ /28.964 = _____, T_c = _____ °R, P_c = _____ psia

* THE LIQUID FLOW RATE(Bbl/d) AND SPECIFIC GRAVITY ARE TO BE MEASURED AT THE SAME CONDITIONS

BASE CONDITIONS = 14.65 psia and 60 °F

** PHYSICAL PROPERTIES OF OCTANES ARE USED FOR THE C_7^+ FRACTION

EG - 35 - 10 - 75

SUBSURFACE PRESSURE MEASUREMENTS

PAGE _____ OF _____

1. BASIC DATA

COMPANY _____ WELL NAME _____

ADDRESS _____ LOCATION _____

FIELD and POOL _____ STATUS: OIL _____ GAS _____ OTHER: SPECIFY _____

TYPE OF TEST _____ DATE OF TEST _____

PERF./OPEN HOLE INTERVAL (CF) _____ ft PRODUCING THROUGH: _____ TUBING _____ CASING

ELEVATION (CF) _____ (KB) _____ ft MID-POINT OF PRODUCING INTERVAL (CF) _____ ft

POOL DATUM _____ ft (SUBSEA) DATUM DEPTH OF WELL (FROM CF) _____ ft

ELEMENT SERIAL NO. _____ RANGE _____ psig CLOCK RANGE _____ hours S☐ D☐ # _____ IH. #

CALIBRATION EQUATION _____ DATE OF LATEST CALIBRATION _____

2. STATIC TEST

TUBING/CASING PRESSURE _____ GAUGE _____ DWG _____ psig SHUT-IN TIME _____ hrs

RUN DEPTH (FROM CF) _____ ft ON BOTTOM/OFF BOTTOM _____

TEMPERATURE AT RUN DEPTH _____ °F SURFACE TEMPERATURE _____ °F

GRADIENT AT RUN DEPTH _____ psi/ft PRESSURE AT MID-POINT OF PERFORATIONS _____ psig

PRESSURE AT RUN DEPTH _____ psig DATUM DEPTH PRESSURE _____ psig

3. ACOUSTIC WELL SOUNDER TEST

DEPTH OF TUBING _____ ft SHUT-IN TIME _____ hrs

AVERAGE TUBING JOINT LENGTH _____ ft CURRENT WATER CUT _____ %

NO. OF JOINTS TO LIQUID _____ CASING PRESSURE _____ psig

LENGTH OF GAS COLUMN _____ ft GAS COLUMN PRESSURE _____ psig

LENGTH OF LIQUID COLUMN _____ ft LIQUID COLUMN PRESSURE _____ psig

GAS GRAVITY/GRADIENT _____ psig/ft PRESSURE AT MID-POINT OF PERFORATIONS _____ psig

OIL GRAVITY _____ GRADIENT _____ psig/ft DATUM DEPTH PRESSURE _____ psig

4. BUILD UP OR DRAWDOWN TEST (Attach Forms O-12A)

RESERVOIR/WELL PARAMETERS: ϕ _____ % Rw _____ ft H _____ ft Sw _____ %

C _____ 1/psi μ _____ cp B.H. TEMPERATURE _____ °F

GAS WELLS ONLY: Z _____ S.G. _____ OIL WELLS ONLY: P_g _____ psig B _____ RB/STB

DATE AND DESCRIPTION OF LAST WELLBORE TREATMENT: _____

CASING I.D. _____ ft TUBING I.D. _____ ft TUBING WEIGHT _____ lb/ft

WELL PRODUCING RATE, DURING/PRIOR TO TEST: OIL _____ bbl/d GAS _____ mcf/d WATER _____ bbl/d

TOTAL PRODUCTION – DURING/PRIOR TO TEST: OIL _____ bbls GAS _____ mcf WATER _____ bbls

5. CHART READINGS AND CALCULATIONS FOR STATIC TEST

DATE	DEPTH BELOW CF ft	TIME	DEFLECTION in/inches	CALCULATED PRESSURE psig	CORRECTION P ± PC psig	CORRECTED PRESSURE psig	GRADIENT psig/ft

REMARKS _____

SURVEY COMPANY _____ TEST BY _____ COMPUTED BY _____ CHECKED BY _____

ENERGY RESOURCES CONSERVATION BOARD
PROVINCE OF ALBERTA
SUBSURFACE PRESSURE MEASUREMENTS

COMPANY _____ WELL NAME _____

DATE OF TEST _____ LOCATION _____ PAGE _____ OF _____

CHART READINGS AND CALCULATIONS FOR BUILDUP OR DRAWDOWN TEST

DATE	DEPTH BELOW CF ft	TIME	DEFLECTION in/ inches	CALCULATED PRESSURE psig	CORRECTION P ± PC psig	CORRECTED PRESSURE psig	PRESSURE AT MID-POINT OF PERFORATIONS psig

REFERENCES

Abramowitz, M. and J. A. Stegun, eds. (1964). *Handbook of Mathematical Functions With Formulas, Graphs, and Mathematical Tables,* National Bureau of Standards, Wash., D.C.

Adams, A. R., H. J. Ramey, Jr. and R. J. Burgess (1968). Gas Well Testing in a Fractured Carbonate Reservoir, *J. Pet. Tech.,* 20, 1187-1193.

Agarwal, R. G., R. Al-Hussainy and H. J. Ramey, Jr. (1970). An Investigation of Wellbore Storage and Skin Effect in Unsteady Liquid Flow: I. Analytical Treatment, *Soc. Pet. Eng. J.,* 10, 279-290.

Agnew, B. G. (1966). Evaluation of Fracture Treatments With Temperature Surveys, *J. Pet. Tech.,* 18, 892-898.

Al-Hussainy, R. (1965). The Flow of Real Gases Through Porous Media, M. Sc. Thesis, Texas A. and M. Univ.

Al-Hussainy, R. (1967). Transient Flow of Ideal and Real Gases Through Porous Media, Ph.D. Thesis, Texas A. and M. Univ.

Al-Hussainy, R. and H. J. Ramey, Jr. (1966). Application of Real Gas Flow Theory to Well Testing and Deliverability Forecasting, *J. Pet. Tech.,* 18, 637-642.

Al-Hussainy, R., H. J. Ramey, Jr. and P. B. Crawford (1966). The Flow of Real Gases Through Porous Media, *J. Pet. Tech.,* 18. 624-636.

Aronofsky, J. S. and R. Jenkins (1954). A Simplified Analysis of Unsteady Radial Gas Flow, *Trans., AIME,* 201, 149-154.

Aziz, K. (1963). *Ways to Calculate Gas Flow and Static Head,* Handbook Reprint from Pet. Eng., Dallas, Tex.

Aziz, K. (1967a). Calculation of Bottom-Hole Pressure in Gas Wells, *J. Pet. Tech.,* 19, 897-899.

Aziz, K. (1967b). Theoretical Basis of Isochronal and Modified Isochronal Back-Pressure Testing of Gas Wells, *J. Can. Pet. Tech.,* 6(1), 20-22.

Aziz, K. and D. L. Flock (1963). Unsteady State Gas Flow--Use of Drawdown Data in the Prediction of Gas Well Behaviour, *J. Can. Pet. Tech.,* 2(1), 9-15.

Aziz, K., G. W. Govier and M. Fogarasi (1972). Pressure Drop in Wells Producing Oil and Gas, *J. Can. Pet. Tech.,* 11(3), 38-48.

Aziz, K., T. Kaneko, N. Mungan and A. Settari (1973). Some Practical Aspects of Coning Simulation, Paper presented 24th Technical Meeting of Pet. Soc. of C.I.M., May 8-11, Edmonton, Alta.

Aziz, K., L. Mattar, S. Ko and G. S. Brar (1975). Use of Pressure, Pressure-Squared or Pseudo-Pressure in the Analysis of Gas Well Data, submitted for publication in *J. Can. Pet. Tech.*

Beach, F. K. (1952). Geothermal Gradients in Canadian Plains, *Can. Oil and Gas Ind.*, 5(11), 43.

Bear, J. (1972). *Dynamics of Fluids in Porous Media*, Amer. Elsevier Publishing Co., Inc., New York.

Bennett, E. N. and C. D. Forgerson (1974). Predicting Reserves and Forecasting Flow Rates of Relatively Tight Gas Wells Using Limited Performance Data, Paper SPE 5058, 49th Fall Meeting of AIME, Houston, Tex.

Bird, R. B., W. E. Stewart and E. N. Lightfoot (1960). *Transport Phenomena*, John Wiley and Sons, Inc., New York.

Brauer, E. B. (1965). Simplification of the Superposition Principle for Pressure Analysis at Variable Rates, Paper SPE 1184, 40th Fall Meeting of AIME, Denver, Col.

Brown, G. G., D. L. Katz, G. G. Oberfell and R. C. Alden (1948). Natural Gasoline and the Volatile Hydrocarbons. Sponsored by NGAA, Tulsa, Okla.

Bruce, G. H., D. W. Peaceman, H. H. Rachford, Jr. and J. D. Rice (1953). Calculations of Unsteady-State Gas Flow Through Porous Media, *Trans., AIME*, 198, 79-92.

Carr, N. L., R. Kobayashi and D. B. Burrows (1954). Viscosity of Hydrocarbon Gases under Pressure, *Trans., AIME*, 201, 264-272.

Carslaw, H. S. and J. C. Jaeger (1959). *Conduction of Heat in Solids*, Oxford Univ. Press, London.

Carter, R. D. (1962). Solutions of Unsteady-State Radial Gas Flow, *J. Pet. Tech.*, 14, 549-554.

Carter, R. D. (1966). Performance Predictions for Gas Reservoirs Considering Two-Dimensional Unsteady-State Flow, *Soc. Pet. Eng. J.*, 6, 35-43.

Carter, R. D., S. C. Miller, Jr. and H. G. Riley (1963). Determination of Stabilized Gas Well Performance from Short Flow Tests, *J. Pet. Tech.*, 15, 651-658.

Clegg, M. W. (1968). The Flow of Real Gases in Porous Media, Paper SPE 2091, 43rd Fall Meeting of AIME, Houston, Tex.

Cobb, W. M., H. J. Ramey, Jr. and F. G. Miller (1972). Well-Test Analysis for Wells Producing Commingled Zones, *J. Pet. Tech.*, 29, 28-37.

Cobb, W. M. and J. T. Smith (1974). An Investigation of Pressure Buildup Tests in Bounded Reservoirs, Paper SPE 5133, 49th Fall Meeting of AIME, Houston, Tex.

Colebrook, C. F. (1939). Turbulent Flow in Pipes With Particular Reference to the Transition Region Between the Smooth and Rough Pipe Laws, *Inst. Civ. Eng. J.*, 11, 133.

Collins, R. E. (1961). *Flow of Fluids Through Porous Materials*, Reinhold Publishing Corp., New York.

Cornell, D. and D. L. Katz (1953). Flow of Gases Through Consolidated Porous Media, *Ind. Eng. Chem.*, 45(10), 2145-2152.

Cornelson, D. W. (1974). Analytical Prediction of Natural Gas Reservoir Recovery Factors, *J. Can. Pet. Tech.*, 13(4), 17-24.

Cornett, J. E. (1961). How to Locate Reservoir Limits, *Pet. Eng. J.*, 33, B19-B24.

Crawford, G. E., A. R. Hagedorn and A. E. Pierce (1973). Analysis of Pressure Buildup Tests in a Naturally Fractured Reservoir, Paper SPE 4558, 48th Fall Meeting of AIME, Las Vegas, Nev.

Cullender, M. H. and C. W. Binckley (1950). Adaptation of the Relative Roughness Correlation of the Coefficient of Friction to the Flow of Natural Gas in Gas Well Casing, Report presented to Railroad Commission of Texas.

Cullender, M. H. (1955). The Isochronal Performance Method of Determining the Flow Characteristics of Gas Wells, *Trans.*, AIME, 204, 137-142.

Cullender, M. H. and R. V. Smith (1956). Practical Solution of Gas-Flow Equations for Well and Pipelines with Large Temperature Gradients, *Trans.*, AIME, 207, 281-287.

Darcy, H. (1856). Determination des lois d'écoulement de l'eau à travers le sable, Les Fontaines Publiques de la Ville de Dijon, 590-594; as reprinted by Hubbert, M. King (1969). *The Theory of Ground-Water Motion and Related Papers*, Hafner Publishing Co., New York.

Davis, E. G., Jr. and M. F. Hawkins, Jr. (1963). Linear Fluid-Barrier Detection by Well Pressure Measurements, *J. Pet. Tech.*, 15, 1077-1079.

De Wiest, R. J. M., ed. (1969). *Flow Through Porous Media*, Academic Press, Inc., New York.

Dietz, D. N. (1965). Determination of Average Reservoir Pressure From Build-Up Surveys, *Trans., AIME*, 234, 955-959.

Dolan, J. P., C. A. Einarsen and G. A. Hill (1957). Special Applications of Drill-Stem Test Pressure Data, *Trans., AIME*, 210, 318-324.

Dranchuk, P. M. and J. G. Flores (1973). Non-Darcy Transient Radial Gas Flow Through Porous Media, Paper SPE 4595, 48th Fall Meeting of AIME, Las Vegas, Nev.

Dranchuk, P. M. and J. D. McFarland (1974). The Effect of the Time Rate of Change of Momentum on Bottom-Hole Pressure in Flowing Gas Wells, *J. Can. Pet. Tech.*, 13(2), 34-38.

Dranchuk, P. M., R. A. Purvis and D. B. Robinson (1974). Computer Calculation of Natural Gas Compressibility Factors Using the Standing and Katz Correlations, *Inst. of Pet. Tech.*, IP-74-008.

Dyes, A. B. and O. C. Johnston (1953). Spraberry Permeability from Build-up Curve Analyses, *Trans., AIME*, 198, 135-138.

Dykstra, H. (1961). Calculated Pressure Build-Up for a Low-Permeability Gas-Condensate Well, *J. Pet. Tech.*, 13, 1131-1134.

Earlougher, R. C., Jr. (1971). Estimating Drainage Shapes from Reservoir Limit Tests, *J. Pet. Tech.*, 23, 1266-1268.

Earlougher, R. C., Jr. (1972). Variable Flow Rate Reservoir Limit Testing, *J. Pet. Tech.*, 24, 1423-1430.

Earlougher, R. C., Jr. and H. J. Ramey, Jr. (1968). The Use of Interpolation to Obtain Shape Factors for Pressure Buildup Calculations, *J. Pet. Tech.*, 20, 449-450.

Earlougher, R. C., Jr., H. J. Ramey, Jr., F. G. Miller and T. D. Mueller (1968). Pressure Distributions in Rectangular Reservoirs, *J. Pet. Tech.*, 20, 199-208.

Earlougher, R. C., Jr. and H. J. Ramey, Jr. (1973). Interference Analysis in Bounded Systems, *J. Can. Pet. Tech.*, 12(4), 33-45.

Earlougher, R. C., Jr. and K. M. Kersch (1974). Analysis of Short-Time Transient Test Data by Type-Curve Matching, *J. Pet. Tech.*, 26, 793-800.

Earlougher, R. C., Jr., K. M. Kersch and W. J. Kunzman (1974). Some Characteristics of Pressure Buildup Behaviour in Bounded Multiple-Layered Reservoirs Without Crossflow, *J. Pet. Tech.*, 26, 1178-1186.

Edgington, A. N. and N. E. Cleland (1967). Gas Field Deliverability Predictions and Development Economics, *Australian Pet. Exploration Assoc. J.*, 7(2), 115-119.

Elenbaas, J. R. and D. L. Katz (1948). A Radial Turbulent Flow Formula, *Trans., AIME*, 174, 25-40.

Fancher, G. H. and J. A. Lewis (1933). Flow of Simple Fluids Through Porous Materials, *Ind. Eng. Chem.*, 25, 1139-1147.

Fetkovich, M. J. (1973). Decline Curve Analysis Using Type Curves, Paper SPE 4629, 48th Fall Meeting of AIME, Las Vegas, Nev.

Forchheimer, Ph. (1901). Wasserbewegung durch Boden, *Z. Ver. Deutsch. Ing.*, 45, 1781-1788.

Fraser, C. D. and B. E. Pettitt (1962). Results of a Field Test to Determine the Type and Orientation of a Hydraulically Induced Formation Fracture, *J. Pet. Tech.*, 14, 463-466.

Fussell, D. D. (1972). Single-Well Performance Predictions for Gas Condensate Reservoirs, Paper SPE 4072, 47th Fall Meeting of AIME, San Antonio, Tex.

Gibson, J. A. and A. T. Campbell, Jr. (1970). Calculating the Distance to a Discontinuity from D.S.T. Data, Paper SPE 3016, 45th Fall Meeting of AIME, Houston, Tex.

Gladfelter, R. E., G. W. Tracy and L.E. Wilsey (1955). Selecting Wells Which Will Respond to Production-Stimulation Treatment, *API Drill. and Prod. Practice*, 117-129.

Govier, G. W. (1961). Interpretation of the Results of Back Pressure Testing of Gas Wells, *Trans., AIME*, LXIV, 511-514.

Govier, G. W. and K. Aziz (1972). *The Flow of Complex Mixtures in Pipes*, Van Nostrand Reinhold Co., New York.

Govier, G. W. and M. Fogarasi (1975). Pressure Drop in Wells Producing Gas and Condensate, Paper presented at 26th Technical Meeting of Pet. Soc. of CIM, Banff, Alta.

Gray, K. E. (1965). Approximating Well-to-Fault Distance from Pressure Build-Up Tests, *J. Pet. Tech.*, 17, 761-767.

Gringarten, A. C. and H. J. Ramey, Jr. (1974). Unsteady-State Pressure Distributions Created by a Well With a Single Horizontal Fracture, Partial Penetration, or Restricted Entry, *Soc. Pet. Eng. J.*, 14, 413-426.

Gringarten, A. C., H. J. Ramey, Jr. and R. Raghavan (1974). Unsteady-State Pressure Distributions Created by a Well With a Single Infinite-Conductivity Vertical Fracture, *Soc. Pet. Eng. J.*, 14, 347-360.

Gringarten, A. C., H. J. Ramey, Jr. and R. Raghavan (1975). Applied Pressure Analysis for Fractured Wells, *J. Pet. Tech.*, 27, 887-892.

Hawkins, M. F., Jr. (1956). A Note on the Skin Effect, *Trans.*, *AIME*, 207, 356-357.

Horner, D. R. (1951). Pressure Build-Up in Wells, *Proceedings, Third World Pet. Congress--Sect. II*, 503-521.

Houpeurt, A. (1959). On the Flow of Gases in Porous Media, *Revue de L'Institut Francais du Petrole*, XIV(11), 1468-1684.

Hubbert, M. (1940). The Theory of Ground-Water Motion, *J. of Geol.*, 48(8), Part 1.

Hubbert, M. (1956). Darcy's Law and the Field Equations of Flow of Underground Fluids, *Trans.*, *AIME*, 207, 222-239.

Hurst, W., W. C. Goodson and R. E. Leeser (1963). Aspects of Gas Deliverability, *J. Pet. Tech.*, 15, 668-676.

Hurst, W., J. D. Clark and E. B. Brauer (1969). The Skin Effect in Producing Wells, *J. Pet. Tech.*, 21, 1483-1489.

Irmay, S. (1958). On the Theoretical Derivation of Darcy and Forchheimer Formulas, *Trans.*, *Amer. Geophysical Union*, 39(4), 702-707.

Ishteiwy, A. A. and H. K. Van Poollen (1967). Radius-of-Drainage Equation For Pressure Build-Up, Paper presented at Libyan Assoc. of Pet. Technologists' Meeting, Tripoli, Libya, Jan. 25-26.

Jahnke, E. and F. Emde (1945). *Tables of Functions With Formulae and Curves*, Dover Publications, New York, Fourth Edition.

Janicek, J. and D. L. Katz (1955). *Applications of Unsteady State Gas Flow Calculations*, Preprint, Univ. of Michigan Publishing Services, Ann Arbor, Mich.

Jones, L. G. (1961). An Approximate Method for Computing Nonsteady-State Flow of Gases in Porous Media, *Soc. Pet. Eng. J.*, 1, 264-276.

Jones, L. G. (1963). Reservoir Reserve Tests, *J. Pet. Tech.*, 15, 333-337.

Jones, P. (1962). Reservoir Limits Test on Gas Wells, *J. Pet. Tech.*, 14, 613-619.

Katz, D. L. (1942). High Pressure Gas Measurement, *Proceedings 21st Annual Convention, NGAA*, 44.

Katz, D. L. and D. Cornell (1955). Flow of Natural Gas from Reservoirs, Notes for intensive course, Univ. of Michigan Publishing Services, Ann Arbor, Mich.

Katz, D. L., D. Cornell, R. Kobayashi, F. H. Poettmann, J. A. Vary, J. R. Elenbaas and C. F. Weinaug (1959). *Handbook of Natural Gas Engineering*, McGraw-Hill Book Co., Inc., New York.

Katz, D. L. and D. K. Coats (1968). *Underground Storage of Fluid*, Ulrich's Books Inc., Ann Arbor, Mich.

Kay, W. B. (1936). Density of Hydrocarbon Gases and Vapors, *Ind. Eng. Chem.*, 28, 1014.

Kazemi, H. (1969). Pressure Transient Analysis of Naturally Fractured Reservoirs with Uniform Fracture Distribution, *Soc. Pet. Eng. J.*, 69, 451-462.

Kazemi, H. (1970). Pressure Buildup in Reservoir Limit Testing of Stratified Systems, *J. Pet. Tech.*, 22, 503-511.

Kazemi, H. (1974). Determining Average Reservoir Pressure from Pressure Buildup Tests, *Soc. Pet. Eng. J.*, 14, 55-62.

Kazemi, H. and M. S. Seth (1969). Effect of Anisotropy and Stratification on Pressure Transient Analysis of Wells With Restricted Flow Entry, *J. Pet. Tech.*, 21, 639-646.

Klinkenberg, L. J. (1941). The Permeability of Porous Media to Liquids and Gases, *API Drill. and Prod. Prac.*, 200-213.

Knudsen, J. G. and D. L. Katz (1958). *Fluid Dynamics and Heat Transfer*, McGraw-Hill Book Co., Inc., New York.

Kulczycki, W. (1955). New Method of Determination of the Output and the Absolute Open-Flow of Gas Wells, *Nafta*, 11(10), 233-237.

Larson, V. C. (1963). Understanding the Muskat Method of Analyzing Pressure Build-Up Curves, *J. Can. Pet. Tech.*, 2(3), 136-141.

Lee, A. L., M. H. Gonzalez and B. E. Eakin (1966). The Viscosity of Natural Gases, *J. Pet. Tech.*, 18, 997-1000.

Lee, W. J., R. R. Harrell and W. D. McCain, Jr. (1972). Evaluation of a Gas Well Testing Method, Paper SPE 3872, N. Plains Sect. Regional Meeting of AIME, Omaha, Neb.

Lefkovits, H. C., P. Hazebroek, E. E. Allen and C. S. Matthews (1961). A Study of the Behavior of Bounded Reservoirs Composed of Stratified Layers, *Soc. Pet. Eng. J.*, 1, 43-58.

Lesem, L. B., F. Greytock, F. Marotta and J. J. McKetta, Jr. (1957). A Method of Calculating the Distribution of Temperature in Flowing Gas Wells, *Trans.*, *AIME*, 210, 169-176.

Leshikar, A. G. (1961). How to Estimate Equivalent Gas Volume of Stock Tank Condensate, *World Oil*, 152(1), 108-109.

Letkeman, J. P. and R. L. Ridings (1970). A Numerical Coning Model, *Trans.*, *AIME*, 249, 418-424.

MacDonald, R. C. and K. H. Coats (1970). Methods for Numerical Simulation of Water and Gas Coning, *Soc. Pet. Eng. J.*, 10, 425-436.

Maer, N. K., Jr. (1974). Type Curves for Analysis of Afterflow-Dominated Gas Well Buildup Data, Paper SPE 5134, 49th Fall Meeting of AIME, Houston, Tex.

Martin, J. C. (1959). Simplified Equations of Flow in Gas Drive Reservoirs and the Theoretical Foundation of Multiphase Pressure Buildup Analyses, *Trans.*, *AIME*, 216, 309-311.

Mattar, L., G. S. Brar and K. Aziz (1975). Compressibility of Natural Gases. Accepted for publication in *J. Can. Pet. Tech.*

Matthews, C. S., F. Brons and P. Hazebroek (1954). A Method for Determination of Average Pressure in a Bounded Reservoir, *Trans.*, *AIME*, 201, 182-191.

Matthews, C. S. and H. C. Lefkovits (1955). Studies on Pressure Distribution in Bounded Reservoirs at Steady State, *Trans.*, *AIME*, 209, 182-189.

Matthews, C. S. and D. G. Russell (1967). *Pressure Buildup and Flow Tests in Wells*, AIME, Monograph Vol. 1, SPE-AIME, New York.

Miller, C. C., A. B. Dyes and C. A. Hutchinson (1950). The Estimation of Permeability and Reservoir Pressures from Bottom Hole Pressure Build-Up Characteristics, *Trans.*, *AIME*, 189, 91-104.

Millheim, K. K. and L. Cichowicz (1968). Testing and Analyzing Low-Permeability Fractured Gas Wells, *J. Pet. Tech.*, 20, 193-198.

Mueller, T. D. and P. A. Witherspoon (1965). Pressure Interference Effects Within Reservoirs and Aquifers, *J. Pet. Tech.*, 17, 471-474.

Muskat, M. (1936). Use of Data on the Build-Up of Bottom-Hole Pressures, Paper presented Fort Worth Meeting, Oct.

Muskat, M. (1937). *The Flow of Homogeneous Fluids Through Porous Media*, McGraw-Hill Book Co., Inc., New York.

McKinley, R. M. (1970). Wellbore Transmissibility From Afterflow-Dominated Pressure Buildup Data, Paper SPE 2416, 45th Fall Meeting of AIME, Houston, Tex.

McKinley, R. M. (1974). Estimating Flow Efficiency From Afterflow-Distorted Pressure Buildup Data, *J. Pet. Tech.*, 26(6), 696-697.

McMahon, J. J. (1961). Determination of Gas Well Stabilization Factors from Surface Flow Tests and Build-up Tests, Paper SPE 114, 36th Fall Meeting of AIME, Dallas, Tex.

Nikuradse, J. (1940). *VDI Forschungsheft*, No. 356, 1932; No. 361, 1938; *Pet. Eng.*, 11(6), 164.

Nisle, R. G. (1956). The Effect of a Short Term Shut-In on a Subsequent Pressure Build-Up Test on an Oil Well, *Trans.*, AIME, 207, 320-321.

Odeh, A. S. (1965). Unsteady-State Behaviour of Naturally Fractured Reservoirs, *Soc. Pet. Eng. J.*, 5, 60-66.

Odeh, A. S. (1969). Flow Test Analysis for a Well With Radial Discontinuity, *J. Pet. Tech.*, 21, 207-210.

Odeh, A. S. and F. Selig (1963). Pressure Build-Up Analysis, Variable-Rate Case, *J. Pet. Tech.*, 15, 790-794.

Odeh, A. S. and L. G. Jones (1965). Pressure Drawdown Analysis, Variable-Rate Case, *J. Pet. Tech.*, 17, 960-964.

Odeh, A. S. and G. W. Nabor (1966). The Effect of Production History on Determination of Formation Characteristics from Flow Tests, *J. Pet. Tech.*, 18, 1343-1350.

Odeh, A. S. and R. Al-Hussainy (1971). A Method for Determining the Static Pressure of a Well From Buildup Data, *J. Pet. Tech.*, 23, 621-624.

Perrine, R. L. (1956). Analysis of Pressure-buildup Curves, *API Drill. and Prod. Practice*, 482.

Pierce, H. R. and E. L. Rawlins (1929). *The Study of a Fundamental Basis for Controlling and Gauging Natural-Gas Wells*, U.S. Dept. of Commerce--Bureau of Mines, Serial 2929.

Pinson, A. E., Jr. (1972). Concerning the Value of Producing Time Used in Average Pressure Determinations from Pressure Buildup Analysis, *J. Pet. Tech.*, 1369-1370.

Pirson, R. S. and S. J. Pirson (1961). An Extension of the Pollard Analysis Method of Well Pressure Build-up and Drawdown Tests, Paper SPE 101, 36th Fall Meeting of AIME, Dallas, Tex.

Pitzer, S. C. (1964). Uses of Transient Pressure Tests, *API Drill. and Prod. Practice*, 115-130.

Pollard, P. (1959). Evaluation of Acid Treatments from Pressure Build-up Analysis, *Trans., AIME*, 216, 38-43.

Prasad, R. K. (1973). Pressure Transient Analysis in the Presence of Two Intersecting Boundaries, Paper SPE 4560, 48th Fall Meeting of AIME, Las Vegas, Nev.

Prats, M. (1961). Effect of Vertical Fractures on Reservoir Behavior-- Incompressible Fluid Case, *Soc. Pet. Eng. J.*, 6(1), 105.

Prats, M., P. Hazebroek and W. R. Strickler (1963). Effect of Vertical Fractures on Reservoir Behavior--Compressible Fluid Case, *Soc. Pet. Eng. J.*, 3, 87.

Prats, M. and J. S. Levine (1965). Effect of Vertical Fractures on Reservoir Behaviour--Results on Oil and Gas Flow, *Trans., AIME*, 228, 1119.

Quon, D., P. M. Dranchuk, S. R. Allada and P. K. Leung (1966). Application of the Alternating Direction Explicit Procedure to Two-Dimensional Natural Gas Reservoirs, *Soc. Pet. Eng. J.*, 6, 137-142.

Raghavan, R., G. V. Cady and H. J. Ramey, Jr. (1972). Well Test Analysis for Vertically Fractured Wells, *J. Pet. Tech.*, 24, 1014-1020.

Raghavan, R., H. N. Topaloglu, W. M. Cobb and H. J. Ramey, Jr. (1973). Well Test Analysis for Wells Producing from Two Commingled Zones of Unequal Thickness, Paper SPE 4559, 48th Fall Meeting of AIME, Las Vegas, Nev.

Ramey, H. J., Jr. (1965). Non-Darcy Flow and Wellbore Storage Effects in Pressure Build-Up and Drawdown of Gas Wells, *J. Pet. Tech.*, 7, 223-233.

Ramey, H. J., Jr. (1967). Application of the Line Source Solution to Flow in Porous Media--A Review, *Producers Monthly*, 31(5), 4-7 and 25-27.

Ramey, H. J., Jr. (1970). Short-Time Well Test Data Interpretation in the Presence of Skin Effect and Wellbore Storage, *J. Pet. Tech.*, 22, 97-104.

Ramey, H. J., Jr. and W. M. Cobb (1971). A general Pressure Buildup Theory for a Well in a Closed Drainage Area, *J. Pet. Tech.*, 23, 1493-1505.

Ramey, H. J., Jr., A. Kumar and M. S. Gulati (1973). *Gas Well Test Analysis Under Water-Drive Conditions*, Amer. Gas Assoc., Vir.

Rawlins, E. L. and M. A. Schellhardt (1936). *Backpressure Data on Natural Gas Wells and their Application to Procudtion Practices*, U.S. Bureau of Mines, Monograph 7.

Reid, R. C. and T. K. Sherwood (1966). *The Properties of Gases and Liquids*, McGraw-Hill Book Co., New York.

Riley, H. G. (1970). A Short Cut to Stabilized Gas Well Productivity, *J. Pet. Tech.*, 22, 537-542.

Robinson, D. B., C. A. Macrygeorgos and G. W. Govier (1960). The Volumetric Behavior of Natural Gases Containing Hydrogen Sulfide and Carbon Dioxide, *Trans.*, AIME, 219, 54.

Russell, D. G. (1963). Determination of Formation Characteristics from Two-Rate Flow Tests, *J. Pet. Tech.*, 15, 1317-1355.

Russell, D. G. (1966). Extensions of Pressure Build-Up Analysis Methods, *J. Pet. Tech.*, 18, 1624-1636.

Russell, D. G. and N. E. Truitt (1964). Transient Pressure Behaviour in Vertically Fractured Reservoirs, *J. Pet. Tech.*, 16, 1159-1170.

Russell, D. G., J. H. Goodrich, G. E. Perry and J. F. Bruskotter (1966). Methods for Predicting Gas Well Performance, *J. Pet. Tech.*, 18, 99-108.

Scott, J. O. (1963). The Effect of Vertical Fractures on Transient Pressure Behaviour of Wells, *J. Pet. Tech.*, 15, 1365-1369.

Settari, A. and K. Aziz (1973). Boundary Conditions in Coning Studies, Paper SPE 4285, 3rd Numerical Simulation of Reservoir Performance Symposium of AIME, Houston, Tex.

Slider, H. C. (1966). Application of Pseudo-Steady-State Flow to Pressure-Buildup Analysis, Paper SPE 1403, 41st Fall Meeting of AIME, Amarillo, Tex.

Slider, H. C. (1971). A Simplified Method of Pressure Analysis for a Stabilized Well, *J. Pet. Tech.*, 23, 1155-1160.

Smith, R. V. (1961). Unsteady-State Gas Flow into Gas Wells, *J. Pet. Tech.*, 13, 1151-1159.

Smith, R. V., R. H. Williams and R. H. Dewees (1954). Measurement of Resistance to Flow of Fluids in Natural Gas Wells, *Trans.*, AIME, 201, 279.

Smith, R. V., J. S. Miller and J. W. Ferguson (1956). *Flow of Natural Gas Through Experimental Pipe Lines and Transmission Lines*, U.S. Bureau of Mines, Monograph 9.

Standing, M. B. and D. L. Katz (1942). Density of Natural Gases, *Trans.*, AIME, 146, 140.

Stegemeier, G. L. and C. S. Matthews (1958). A Study of Anomalous Pressure Build-up Behavior, *Trans.*, AIME, 213, 43-50.

Swift, G. W. and O. G. Kiel (1962). The Prediction of Gas-Well Performance Including the Effect of Non-Darcy Flow, *J. Pet. Tech.*, 14, 791-798.

Tek, M. R., M. L. Grove and F. H. Poettmann (1957). Method of Predicting the Back-Pressure Behavior of Low Permeability Natural Gas Wells, *Trans.*, AIME, 210, 302-309.

Theis, C. V. (1935). The Relation Between the Lowering of the Piezometric Surface and the Rate and Duration of Discharge of a Well Using Ground-Water Storage, *Amer. Geophys. Union Trans.*, 16, 519-524.

Thomas, L. K., R. W. Hankinson and K. A. Phillips (1970). Determination of Acoustic Velocities for Natural Gas, *J. Pet. Tech.*, 22, 889-895.

Van Everdingen, A. F. and W. Hurst (1949). The Application of the Laplace Transformation to Flow Problems in Reservoirs, *Trans.*, AIME., 179, 305-324.

Van Everdingen, A. F. (1953). The Skin Effect and Its Influence on the Productive Capacity of a Well, *Trans.*, AIME, 198, 171-176.

Van Poollen, H. K. (1964). Radius-of-Drainage and Stabilization-Time Equations, *Oil and Gas J.*, 62, 138-146.

Van Poollen, H. K. (1965). Drawdown Curves Give Angle Between Intersecting Faults, *Oil and Gas J.*, 63(51), 71-75.

Von Karman, T. (1931). *NACA-TM* 611.

Warren, J. E. and P. J. Root (1963). The Behavior of Naturally Fractured Reservoirs, *Soc. Pet. Eng. J.*, 3, 245-255.

Wattenbarger, R. A. (1967). Effects of Turbulence, Wellbore Damage, Wellbore Storage and Vertical Fractures on Gas Well Testing, Ph.D. Thesis, Stanford Univ., Stanford, Calif.

Wattenbarger, R. A. and H. J. Ramey, Jr. (1968). Gas Well Testing With Turbulence, Damage, and Wellbore Storage, *J. Pet. Tech.*, 20, 877-887.

Wattenbarger, R. A. and H. J. Ramey, Jr. (1970). An Investigation of Wellbore Storage and Skin Effect in Unsteady Liquid Flow: II. Finite Difference Treatment, *Soc. Pet. Eng. J.*, 10, 291-297.

Wentink, J. J., J. G. Goemans and C. W. Hutchinson (1971). Deliverability Forecasting and Compressor Optimization for Gas Fields, *Oilweek*, 22(31), 50-54.

Wichert, E. and K. Aziz (1972). Calculate Z's for Sour Gases, *Hydrocarbon Processing*, 51(5), 119-122.

Wiley, C. R. (1960). *Advanced Engineering Mathematics*, McGraw-Hill Book Co., Inc., New York.

Willis, R. B. (1965). How to Simplify Gas-Well Test Analysis, *Pet. Eng. J.*, 37, 95-98.

Winestock, A. G. and G. P. Colpitts (1965). Advances in Estimating Gas Well Deliverability, *J. Can. Pet. Tech.*, 4(3), 111-119.

Wright, D. E. (1968). Nonlinear Flow Through Granular Media, *J. Hydraul. Div. Amer. Soc. Civ. Eng. Proceedings*, 94, (HY4), 851-872.

Wyckoff, R. D., H. G. Botset, M. Muskat and D. W. Reed (1934). Measurement of Permeability of Porous Media, *Amer. Assoc. of Pet. Geologists Bulletin*, 18(2), 161-190.

Young, K. L. (1967). Effect of Assumptions Used to Calculate Bottom-Hole Pressures in Gas Wells, *J. Pet. Tech.*, 19, 547-550.

Zana, E. T. and G. W. Thomas (1970). Some Effects of Contaminants on Real Gas Flow, *J. Pet. Tech.*, 22(9), 1157-1168.

Amer. Gas. Assoc. Natural Gas Dept., Gas Measurement Committee, Report No. 3 (1955). Orifice Metering of Natural Gas. Revised 1969, reprinted 1972.

Amer. Gas. Assoc. Natural Gas Dept. (1963). *Gas Measurement Manual*, First Edition.

Energy Resources Conservation Board (1974). *Guide for the Planning, Conducting and Reporting of Subsurface Pressure Tests.*

Gas Processors Suppliers Association, *Engineering Data Book*. Ninth Edition 1972, Revised 1974.

Interstate Oil Compact Commission (1962). *Manual of Back Pressure. Testing of Gas Wells.*

Kansas State Corporation Commission (1959). *Manual of Back Pressure Testing of Gas Wells.*

Railroad Commission of Texas (1950). *Back Pressure Test for Natural Gas Wells.* Revised Edition, 1951.

U.S. Bureau of Mines, Monograph 7 (1936). *Back-pressure Data on Natural Gas Wells and their Application to Production Practices,* E. L. Rawlins and M. A. Schellhardt.

UNITS CONVERSION

Conversion of Common Field Units to Metric (SI) Units

Base conditions: Field $60^\circ F$ 14.65 psia

Metric (SI) $15^\circ C$, 101.325 kPa

Field Unit	Multiplying Factor	Metric (SI) Unit Name	Symbol
acre	4.046 856 E+03	square metre	m^2
acre	4.046 856 E-01	hectare	ha
acre-foot	1.233 482 E+03	cubic metre	m^3
atmosphere	1.013 25 E+02	kilopascal	kPa
barrel (35 Imp. gal.)	1.589 873 E-01	cubic metre	m^3
BTU per standard cubic foot ($60^\circ F$, 14.65 psia)	8.799 136 E-01	kilojoule per mole	kJ/mol
centipoise	1.0 E+00	millipascal second	mPa·s
cubic foot	2.831 685 E-02	cubic metre	m^3
cubic foot gas per barrel ($60^\circ F$, 14.65 psia)	7.494 773 E+00	mole per cubic metre	mol/m^3
darcy	9.869 233 E-01	square micrometre	μm^2
degree Fahrenheit	($^\circ F$-32)5/9 E+00	degree Celsius	$^\circ C$
degree Rankine	5/9 E+00	kelvin	K
gallon (Cdn)	4.546 09 E-03	cubic metre	m^3
gallon (US)	3.785 412 E-03	cubic metre	m^3
gas constant	8.314 32 E+00	joule per mole kelvin	J/(mol·K)
Mcf (thousand cubic foot $60^\circ F$, 14.65 psia)	{ 1.191 574 E+00 2.826 231 E+01	kilo mole cubic metre (API)	kmol m^3API
millidarcy	9.869 233 E-04	square micrometre	μm^2
MMcf (million cubic foot $60^\circ F$, 14.65 psia)	{ 1.191 574 E+00 2.826 231 E+04	megamole cubic metre (API)	Mmol m^3API
pound-force per square inch (psi)	6.894 757 E+00	kilopascal	kPa
pound-mass	4.535 924 E-01	kilogram	kg
psi per foot	2.262 059 E+01	kilopascal per metre	kPa/m
section (640 acres)	2.589 988 E+06	square metre	m^2
section (640 acres)	2.589 988 E+02	hectare	ha
standard cubic foot ($60^\circ F$, 14.65 psia – ideal gas)	{ 1.191 574 E+00 2.826 231 E-02	mole cubic metre (API)	mol m^3API
Tcf (trillion cubic foot $60^\circ F$, 14.65 psia)	{ 1.191 574 E+00 2.826 231 E+10	teramole cubic metre (API)	Tmol m^3API
ton (US short – 2000 lb)	9.071 847 E-01	tonne	t
ton (UK long – 2240 lb)	1.016 047 E+00	tonne	t